TESIS DE DOCTORADO

ADVANCED NUMERICAL METHODS FOR WAVE PROPAGATION PROBLEMS: THE ARLEQUIN METHOD & POTENTIAL FORMULATION FOR ELASTODYNAMICS

Jorge Albella Martínez

ESCUELA DE DOCTORADO INTERNACIONAL

PROGRAMA DE DOCTORADO EN MÉTODOS MATEMÁTICOS Y SIMULACIÓN NUMÉRICA EN INGENIERÍA Y CIENCIAS APLICADAS

SANTIAGO DE COMPOSTELA

AÑO 2019

DECLARACIÓN DEL AUTOR DE LA TESIS

Advanced numerical methods for wave propagation problems: The Arlequin method & Potential formulation for elastodynamics

D. Jorge Albella Martínez

Presento mi tesis, siguiendo el procedimiento adecuado al Reglamento, y declaro que:

1) *La tesis abarca los resultados de la elaboración de mi trabajo.*
2) *En su caso, en la tesis se hace referencia a las colaboraciones que tuvo este trabajo.*
3) *La tesis es la versión definitiva presentada para su defensa y coincide con la versión enviada en formato electrónico.*
4) *Confirmo que la tesis no incurre en ningún tipo de plagio de otros autores ni de trabajos presentados por mí para la obtención de otros títulos.*

En Santiago de Compostela, 18 de diciembre de 2019.

Fdo. Jorge Albella Martínez

AUTORIZACIÓN DEL DIRECTOR DE LA TESIS

Advanced numerical methods for wave propagation problems: The Arlequin method & Potential formulation for elastodynamics

D. Jerónimo Rodríguez García

INFORMA:

Que la presente tesis, corresponde con el trabajo realizado por D. ***Jorge Albella Martínez****, bajo mi dirección, y autorizo su presentación, considerando que reúne los requisitos exigidos en el Reglamento de Estudios de Doctorado de la USC, y que como director de ésta no incurre en las causas de abstención establecidas en Ley 40/2015.*

En Santiago de Compostela, 18 de diciembre de 2019.

Fdo. Jerónimo Rodríguez García

AUTORIZACIÓN DEL DIRECTOR DE LA TESIS

Advanced numerical methods for wave propagation problems: The Arlequin method & Potential formulation for elastodynamics

D. Sébastien Imperiale

INFORMA:

Que la presente tesis, corresponde con el trabajo realizado por D. ***Jorge Albella Martínez****, bajo mi dirección, y autorizo su presentación, considerando que reúne los requisitos exigidos en el Reglamento de Estudios de Doctorado de la USC, y que como director de ésta no incurre en las causas de abstención establecidas en Ley 40/2015.*

En Santiago de Compostela, 18 de diciembre de 2019.

Fdo. Sébastien Imperiale

Agradecimientos

El trabajo que se presenta en este manuscrito, es el fruto de un largo esfuerzo en el que por suerte, he contado con la ayuda y apoyo de muchas personas a las cuales me gustaría dedicar unas palabras de profundo agradecimiento.

En primer lugar, siempre le estaré enormemente agradecido a Jerónimo Rodríguez por confiar en mí y ofrecerme la oportunidad de realizar este trabajo de principio a fin. Así mismo, quiero agradecerle también todo lo que me ha enseñado en estos años y todas las ideas y bromas que hemos compartido en interminables horas de despacho, que siempre empieza con "tienes un minuto" y que nunca sabes cuando terminan. Nada de este trabajo hubiese sido posible sin él y los kilos de tiza y paciencia que me ha dedicado.

I will also always be especially grateful to Sébastien Imperiale. Since the first time we met, he was always very generous to share with me all his knowledge and ideas. When he was not my advisor yet, I had the opportunity to make a stay abroad and he was very happy to receive me and include me in his research. He was very welcoming and I keep very good memories of that time. A big part of the thesis was developed in his office and I am very happy that he finally became one of my advisors.

I also want to thank to Patrick Joly for all his help in the second part of the thesis. This was his topic too and without his knowledge and experience this work would not have been the same.

From my time in Paris, I do not forget about all the people from MΞDISIM, they really make me feel part of the team. The time abroad is always complicated and a nice working environment can make the difference. Thank you for all the coffee breaks, the group meals, the raclette ...

También quiero acordarme ahora de todos los amigos que hice en el Colegio de España. Con los años es difícil mantener el contacto con todo el mundo, pero sin la gente que conocí allí, el tiempo que pasé en París hubiese sido mucho más complicado. Me resulta imposible nombrar a todo el mundo, así que espero que cada uno se sienta reconocido cuando doy las gracias por todos los desayunos compartidos, los agónicos viajes en RER, las noches en las cocinas, los viajes a la mina, las salidas a Nouvel, los juegos de mesa, las jornadas turísticas ...

En estos años, también ha sido muy importante el apoyo de todas las personas que me han acompañado en el día a día en la facultad de matemáticas. En especial le quiero dar las gracias a los amigos del café, a la tropa de las comidas y a todos los compañeros de despacho con los que he compartido tantas cosas durante estos años. Todos forman parte de varias generaciones de consejos de sabios sin los cuales no *hubiese sabido qué hacer en muchas ocasiones.*

Por otro lado, nadie se merece más mi agradecimiento que mi familia y amigos más cercanos. Ellos son los principales responsables de que yo sea hoy la persona que soy, y sin su cariño y apoyo nada de esto tendría sentido. Gracias en especial a mis padres, por darme la educación que me han dado y por haber confiado siempre en mí desde que un día decidí estudiar matemáticas. Pero sobre todo, les estoy muy agradecido a todos por estar siempre ahí y solo lamento no haber podido disfrutar más de ellos en estos años.

Finalmente, quiero darle las gracias a Vanessa, ella es la persona más importante de mi vida y durante estos años ha sufrido y celebrado conmigo en los buenos y en los malos momentos. Su compañía en este viaje ha sido fundamental para superar los momentos de más estrés y ayudarme a recordar que la vida es mucho más. Gracias por todo, te quiero.

En definitiva, cada una de estas personas ha ayudado a que el viaje fuese un poquito menos duro, poniendo así su granito de arena para que este trabajo fuese posible, y dejando de alguna manera su huella impresa en estas páginas. De modo que sin ellos nada de esto hubiese sido posible y por tanto siempre les estaré agradecido.

Contents

Preface

The thesis is divided in **two different parts** (with their own detailed introduction and conclusion) where we are interested in two independent questions leading to the development of two different techniques. In addition to the intellectual motivation, in both parts we are also driven by a common aim, the development of efficient techniques for the numerical resolution of wave propagation problems, and, in that context, the two developed techniques could be in principle combined. We refer the reader to the introductory chapter of each part, given later in this document, for the detailed descriptions and motivations of the questions that will be tackled. In this preface we only give a brief general overview of the overall work.

In the **first part** of the thesis, we aim to develop a domain decomposition method which is well adapted to the consideration of local scattering phenomena in acoustic problems. We will be particularly interested in the efficiency of the methodology in presence of local defects, such as cracks, holes or inclusions, that moreover might be surrounded by a damaged region as it happens in non destructive testing. In terms of modelling, the main difficulty of these problems lies in the discrepancy between the scale of the defects and the structure, which requires specially refined meshes that usually need to be generated for each new distribution of the defect. In practice, this approach is computationally expensive and therefore many works have been devoted to circumvent this issue. For instance, the fictitious domain methods (see [1, 2]) and the unfitted finite element methods on cut meshes (see [3, 4]) are useful in this context, although the first is not compatible with high order space discretizations, while for the second this is still an open question. Moreover, non-overlapping domain decomposition methods, such as mortar finite elements introduced in [5, 6, 7], may also be useful in this context, however as far as we know, there is not an automatic procedure for non-overlapping domain decomposition methods to treat different domain configurations without a re-meshing process, which we want to avoid for computational reasons. On the other hand, overlapping domain decomposition techniques should offer an interesting approach in this context. We expect that these methods allow to easily consider a patch that can be adapted for several positions of the obstacle (see Figure 0.1).

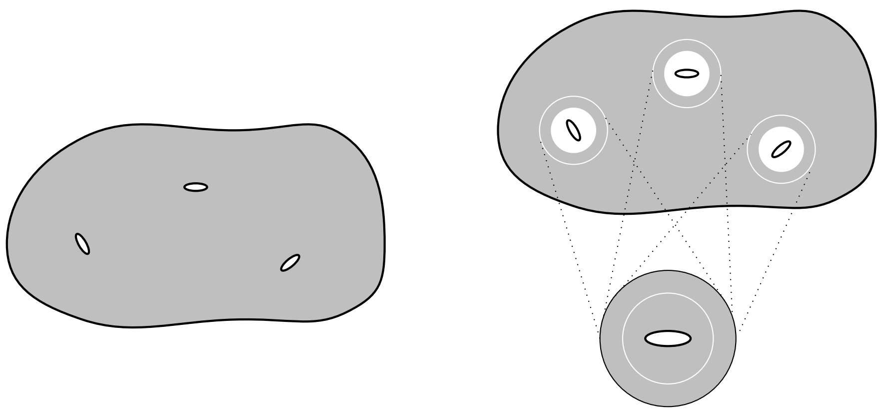

Figure 0.1: Sketch of the domain configuration and the domain decomposition we aim to consider in order to treat each position of the obstacle with a unique patch.

Among these methods, we will consider the Arlequin method (see [8, 9]) as a starting point. In particular, this technique imposes the matching of the solution in the overlapping region in a weak variational way. In consequence, the problem is partitioned in different variational problems and each of them needs to be corrected by means of a Lagrange multiplier which is defined on each overlapping region. This would allow for instance to consider a regular mesh of the background domain and a fine mesh for the patch and both can be easily adapted for a large family of positions of the defect (see Figure 0.2). After detailing why this method could suffer from a lack of flexibility (or either consistence), we present new families of Arlequin couplings – where the matching is performed only close to the boundaries of the overlapping region – that cures the lack of flexibility. The fully discrete transient and frequency case will be addressed paying special attention to stability and error analysis.

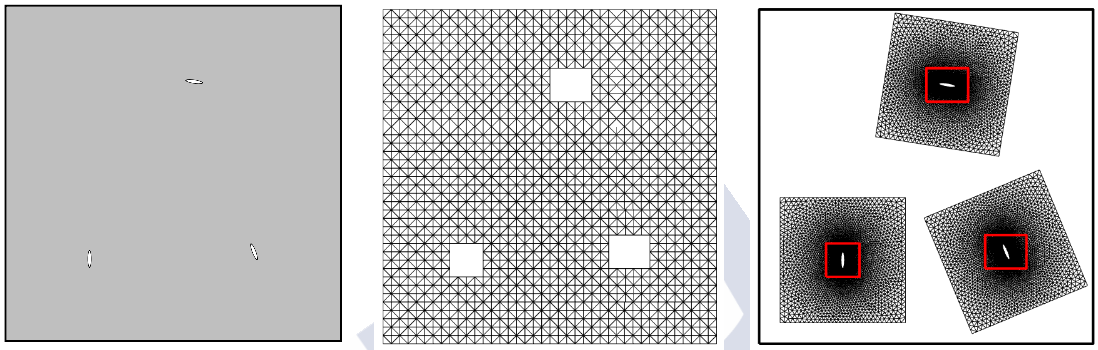

(a) Defected computational domain.

(b) Coarse mesh adapted for each position of the obstacle.

(c) Fine mesh adapted for each position of the obstacle.

Figure 0.2: Sketch of an Arlequin decomposition for a defected computational domain.

In the **second part** of the thesis we will revisit a very classical question, namely, the numerical solution of linear isotropic elastodynamics equations, which govern the propagation of waves in elastic isotropic solids. In this context, it is well-known that there are two different types of waves, usually called pressure waves and shear waves, that in the free space are known to propagate independently with different velocities V_P and V_S respectively (notice that $V_P > V_S$). In consequence, as we shall see, the classical space-time discretization techniques based in Lagrange finite elements (FE) in space and explicit finite differences (FD) in time are not efficient when $V_P >> V_S$ (see for instance [10, 11]). The cause of this lack of efficiency is that, for accuracy, the space step must be adapted to the smaller wavelength (which is proportional to the minimal velocity V_S), while the time step is constrained by a stability condition that involves the maximal velocity V_P , i.e.

$$h \approx V_S \quad \text{and} \quad \Delta t \approx \frac{h}{V_P} \approx \frac{V_S}{V_P}.$$

Therefore, classical explicit methods are only recommended when the pressure waves and the shear waves propagate with similar velocities, i.e. when the ratio V_P/V_S is low (see Figure 0.3). Thus a natural question arises: How do we proceed for higher values of the ratio V_P/V_S ? If the ratio V_P/V_S is large, then two cases must be distinguish. On the one hand, if V_S is bounded by below and V_P is very high, then the problem can be reasonably well approximated by its incompressible limit (see for instance [12, 13, 14, 15, 16]). On the other hand if V_P is bounded by above and V_S is very low, then the problem can be well approximated by a scalar acoustic problem (note that, in fact both phenomena are essentially the same time, only the time scale at which the system is observed will naturally “select” which approximation should be used).

However, it seems that very few works have been devoted to the treatment of an intermediate value of the ratio V_P/V_S, for which standard FE/FD explicit methods are penalizing and asymptotic methods are not accurate. In recent years, a new line of research has been opened concerning

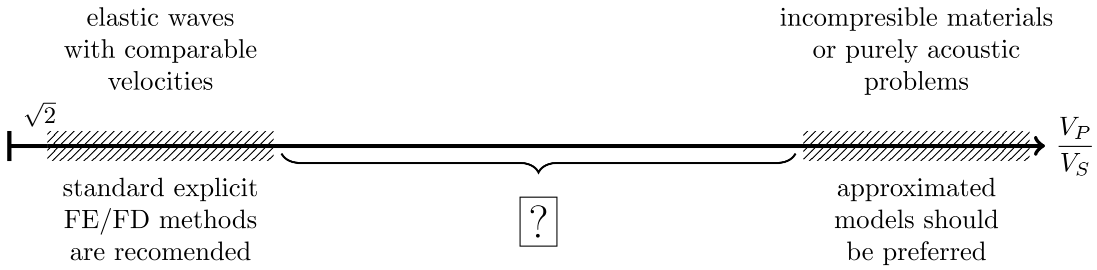

Figure 0.3: Diagram of the different regimes depending on the value of V_P/V_S and the correspondent choice of an efficient fully discretization method.

this question. This new approach is motivated by the classical techniques that consider the well known Helmholtz decomposition of vector fields that allows to write the displacement vector field as the sum of pressure waves and shear waves, and relates the elastodynamics equations to two scalar wave equations that are related to each type of wave. The resultant is a system of equations that in the free space is fully decoupled and better adapted for finite elements discretization. However the extension of this approach for the resolution of elastodynamics equations by using finite elements computations is very recent and incomplete. The difficulties arise when we consider a piecewise homogeneous bounded domain, since both types of waves are known to be coupled on boundaries and interfaces due to reflections and transmissions. In particular, in [17, 18] the technique has been introduced and applied to the case of isotropic homogeneous elastic media when the boundary is assumed to be clamped (usually called Dirichlet case). The authors have found that the treatment of the free boundary conditions (usually called Neumann case) rises severe difficulties, since the natural extension of the method provides an unstable numerical scheme when considering standard discretization techniques. From this starting point, in [19, 20] we have overcome these difficulties by being able to develop a stable and consistent alternative approach that we analysed up to the fully discrete level.

Part I

Wave scattering by obstacles with Arlequin method

Table of Contents

Chapter 1

Introduction

In this first part of the thesis, we are interested in the development and analysis of a domain decomposition method that avoids the generation of a well adapted global mesh of the domain. Among these methods we will focus in overlapping non-matching grid techniques which are commonly used in many large scale simulations where local mesh refinement is needed. Our aim is to present a methodology that reduces the cost of grid generation and allows easily to consider unstructured local grids and therefore corresponding fast solvers for the background medium. The procedure might be of interest in different physical contexts, however to show the promising potential of this approach we will consider acoustic problems where a local scattering phenomena might happen. For instance a change of the local behaviour in a globally simplified modelling of a given material, or the introduction of local defects (cracks, holes or inclusions), as in non destructive testing. In terms of modelling, the main difficulty lies in the discrepancy between the scale of the defects and the structure which requires specially refined meshes. Such meshes must be generated for each distribution of defects and the generation of one of them is almost always a time consuming and tedious task (see Figure 1.1). Moreover, in many applications we are interested in the resolution

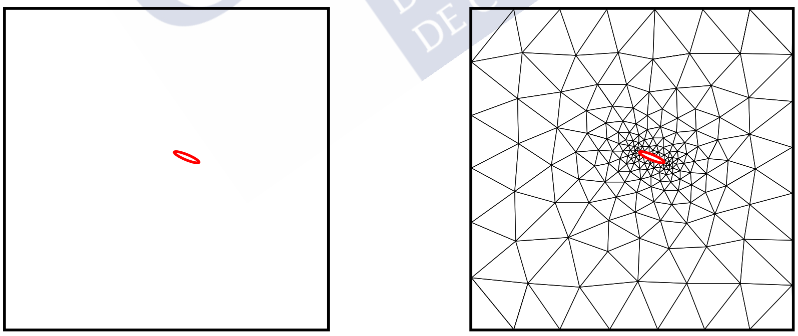

(a) Cracked domain. (b) Adapted mesh.

Figure 1.1: Global adapted mesh for a defected domain.

of the same problem for many different configurations, as it is the case of generic optimization procedures where the domain changes from one iteration to the next. This occurs for example in obstacle detection, where a scattering problem needs to be solved for each new position of the obstacle that is given by an optimization procedure. In such kind of situations re-meshing is needed and the computational cost may be very large. To circumvent all the mentioned difficulties we would like to consider a procedure that satisfies the following properties:

- Allow the use of **independent meshes**. It should be possible to consider independent meshes on each sub-domain of the decomposition. This would allow to easily introduce a **local refinement** to capture the sharp variation of parameters as well as the defect geometric properties. Moreover in many applications related to acoustics, it is optimal to use a coarse regular mesh for the background medium that only needs to be adapted to the smallest wavelength of the emitted waves.

- Preserve the **mesh quality**. The cut or modification of mesh elements should be avoided since it leads to poor meshes that penalizes the overall discretization process.
- Compatibility with **high order** discretization. High order methods for the resolution of wave scattering problems have proven to be really efficient (see [21, 22, 23, 24]).

Moreover, in the case of transient problems, the following properties are also important

- **Discrete energy preservation**. This is important for the numerical stability of the time scheme as well as for its convergence behaviour.
- **Compatibility with efficient time schemes**. It should be possible to consider, at least in regions far from the obstacle, efficient explicit time-stepping with quasi-optimal discretization parameters. This can be achieved with locally implicit time integration in the region next to the defect as in [25, 26, 27, 28].

In generic **optimization** procedures we are also interested in

- **Avoid the re-meshing** of any part of the computational domain when the optimization process leads to the treatment of a different domain configuration. If re-meshing were needed, it would imply not only a large computational cost, but also the evaluation of an optimization functional, which is difficult to analyse, since it would depend on the parameters of the continuous problem and also on the re-meshing procedure.

In the literature, there exist already some techniques especially developed to treat wave scattering by obstacles. However, there seems to be no method that verifies all the above properties:

- The **fictitious domain method** used in [1] is designed to take into account scattering by impenetrable obstacles. It preserves a discrete energy and allows the use of a time step adapted to the discretization properties of the background medium. However in [2] it is shown that it can not be compatible with high order space discretization.
- The **space-time refinement method** presented in [27, 28] is based upon local time stepping and boundary coupling by mortar elements. It satisfies all the mentioned properties but it is a non-overlapping domain decomposition method. In consequence it requires conformity between the geometry of the sub-domain boundaries, this can not be guaranteed in a generic optimization procedure where the position of a defect is not known exactly and changes between each simulation.
- **Enrichment methods** allow to introduce small defects, such as cracks, without modifying the coarse regular mesh of the background medium but instead by introducing additional test functions that capture the behaviour induced by the defect (e.g. discontinuity). Such methods enter in the framework of the eXtended Finite Element Method (XFEM, see [29] for a detailed review and [30] for an overview on the implementation). These methods are not extensively used for scattering wave propagation problems (see however [31]) but they potentially offer all the mentioned advantages. They can be seen as complementary methods since they can easily be combined with the strategy we present (see [32]).
- **Unfitted finite element methods on cut meshes**, as in [3] or [4], introduce, in the finite element space, basis functions restricted to sub-domains. By doing so, a transmission problem can be written between sub-domains. Then, one has to deal with the fact that the support of the basis functions at the interface can be arbitrarily small depending on the cut and the defect position. Although stabilization methods can be employed, it remains to be proven if the method is compatible with high order discretizations. A nice advance in that direction is provided in [33].

- The **Arlequin method** originally developed in [8, 9] for static problems and extended to dynamic problems in [34, 35] (see also [36]) is an overlapping domain decomposition technique that preserves discrete energy and allows the use of explicit time stepping methods far from the obstacle (see for instance [37]). It has many of the properties that we would like to achieve, however in principle a mesh of the intersection of the domain decomposition is needed, which in practice requires for each new domain configuration a re-meshing of the overlapping. In order to avoid the re-meshing of the overlapping region a penalised version of the method can be considered as in [38, 39] (later we will mention the drawback of the penalised version).

Our aim in this work is to construct and analyse some variants of the Arlequin method adapted to wave scattering that allow less constraints in the generation of the meshes and therefore satisfying all the mentioned properties. The strategy we propose has already been presented in [40] and consists in: **First** constructing a coarse structured mesh of the background domain (ignoring the obstacle) as in Figure 1.2a, and a local fine mesh of the neighbourhood of the obstacle, called the patch, as shown in Figure 1.2b. **Second** we remove from the mesh of the background domain the unnecessary elements (those that interact with the obstacle) as in Figures 1.3a and 1.4a. **Third** we adapt the patch to the actual position of the obstacle as represented in Figures 1.3b and 1.4b. **Fourth** we apply a matching on the intersection region that we denote by ω (see Figures 1.3c and 1.4c). The matching is applied by imposing the equality of the fields in a weak variational sense in ω, which requires the projection of one mesh on the other (see [41] for a projection algorithm of linear complexity). This implies also, in order to have a correct global energy balance, the partitioning of the two involved variational formulations in the overlapping region and a correction of them by means of a Lagrange multiplier. Therefore, the obtained method will be a mixed weak formulation.

In the following chapters, we first present the Arlequin procedure in the context of Helmholtz equation. This context also provides a simpler framework to develop the new variants of the method and it allows to discuss with detail their space discretization. Then, we detail the non trivial extension of the developed Arlequin methods to the case of transient wave equation. In this context we also discuss and motivate the importance of choosing an adequate time discretization. Finally, to conclude this first part of the thesis, we apply the developed technique to a generic optimization problem.

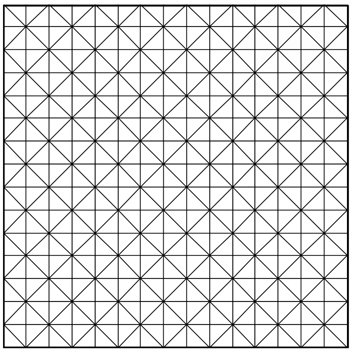

(a) Coarse homogeneous mesh of the non defected domain.

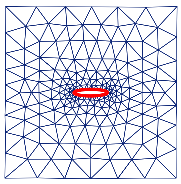

(b) Local fine mesh of a neighbourhood of the obstacle.

Figure 1.2: Meshes required for the Arlequin method.

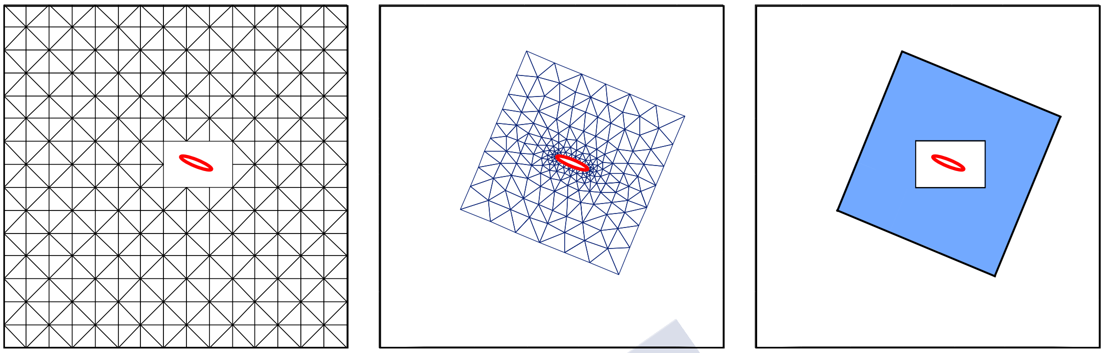

(a) Reduction of the coarse mesh for a given position of the obstacle.

(b) Fine mesh adapted for a given position of the obstacle.

(c) Overlapping region.

Figure 1.3: Sketch of an Arlequin decomposition for a given position of the obstacle.

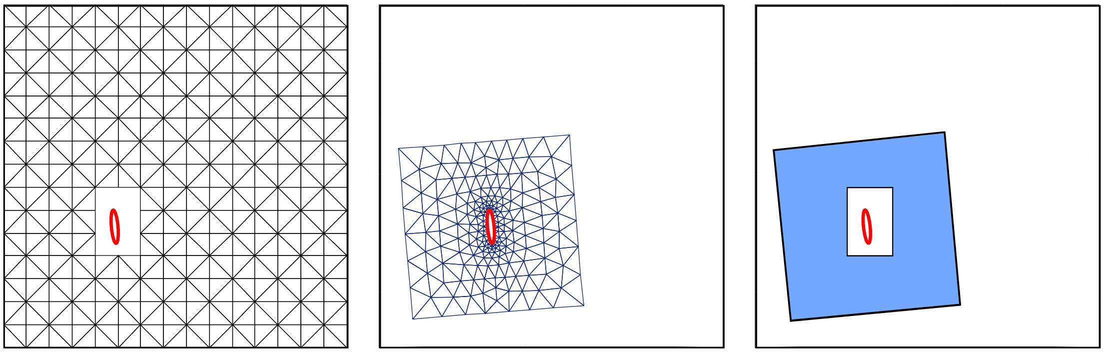

(a) Reduction of the coarse mesh for a new position of the obstacle.

(b) Fine mesh adapted for a new position of the obstacle.

(c) Overlapping region.

Figure 1.4: Sketch of an Arlequin decomposition for a given position of the obstacle.

Chapter 2

The Arlequin formulation for Helmholtz equation

Contents

In this chapter we are interested in the extension of the Arlequin method and its mathematical analysis for the Helmholtz equation, which is a relevant problem in the context of wave scattering problems. The Arlequin method has already been presented in [8, 9, 42] for elastostatic problems and recently integrated in an industrial computational platform in [36]. Note that the extension of the method to the Helmholtz equation is not straightforward since the problem is not coercive. In this framework we first present the method and exhibit some of its limitations. Then, we develop some variants that are better adapted to easily consider the introduction of local defects, such as cracks, holes or inclusions.

2.1 Preliminaries on Helmholtz equation

In this section we aim to provide a brief introduction of the model problem that we are going to consider along the chapter, thus we begin by recalling very basic elements concerning Helmholtz problem. As we are mainly interested in local defects, we will denote by $\Theta \subset \mathbb{R}^d$ the non-defected open domain that we assume to be bounded, homogeneous and Lipschitz regular and by $\mathcal{O}$ the defect (possibly empty) which is assumed to be compact and embedded in Θ. Finally we define the defected domain as the open set

$$\Omega = \Theta \setminus \overline{\mathcal{O}}.$$

Then, we look for the solution of the **Helmholtz equation** with a regular enough source term $f \in L^2(\Omega)$, and for the sake of simplicity, homogeneous Neumann boundary conditions:

$$\left\{ \begin{array}{rcll} -\,\ell^2\,\rho\,u \,-\, \mathrm{div}(\mu\,\nabla u) &=& f, & \text{in} \quad \Omega, \\ \nabla u \cdot \mathbf{n} &=& 0, & \text{on} \quad \partial\Omega, \end{array} \right. \tag{2.1}$$

where ℓ denotes the frequency and $(\rho, \mu) \in (L^\infty(\Omega))^2$ denote the physical coefficients of the problem that are assumed to be such that

$$\inf_{\boldsymbol{x}\in\Omega} \rho(\boldsymbol{x}) \geq \rho_0 > 0 \quad \text{and} \quad \inf_{\boldsymbol{x}\in\Omega} \mu(\boldsymbol{x}) \geq \mu_0 > 0.$$

The variational formulation associated to problem (2.1) is obtained by multiplying equation (2.1) with test function $v \in H^1(\Omega)$ and integrating over Ω.

$$\left\{ \begin{array}{l} \text{Find } u \in H^1(\Omega), \text{ such that} \\ -\,\ell^2\,(\rho\,u, v)_{L^2(\Omega)} + (\mu\,\nabla u, \nabla v)_{L^2(\Omega)} = (f, v)_{L^2(\Omega)} \quad \forall\, v \in H^1(\Omega), \end{array} \right. \tag{2.2}$$

where $(\cdot,\cdot)_{L^2(\Omega)}$ is the standard inner product in $L^2(\Omega)$. Notice, that the existence and uniqueness of solution for this problem can not be guaranteed by Lax-Milgram theorem since the bilinear form associated to the problem is not coercive. Indeed it is easy to verify that choosing $v_1 \in \mathbb{R} \subset H^1(\Omega)$

$$-\,\ell^2\,(\rho\,v_1, v_1)_{L^2(\Omega)} + (\mu\,\nabla v_1, \nabla v_1)_{L^2(\Omega)} = -\,\ell^2 \int_\Omega \rho \,\mathrm{d}\boldsymbol{x} \;<\; 0$$

while choosing $v_2 = e^{\alpha\,x_1}$ for large enough $\alpha \in \mathbb{R}$

$$-\,\ell^2\,(\rho\,v_2, v_2)_{L^2(\Omega)} + (\mu\,\nabla v_2, \nabla v_2)_{L^2(\Omega)} = \int_\Omega (-\rho\,\ell^2 + \mu\,\alpha^2)\,e^{2\,\alpha\,x_1}\mathrm{d}\boldsymbol{x} \;>\; 0.$$

Then, by continuity we can apply Bolzano's theorem and therefore it must exist $\beta \in (0,1)$ such that for $v = \beta\, v_1 + (1-\beta)\, v_2 \in H^1(\Omega)$ we have

$$-\,\ell^2\,(\rho\, v, v)_{L^2(\Omega)} + (\mu\,\nabla v, \nabla v)_{L^2(\Omega)} \;=\; 0,$$

thus, since $v \neq 0$ the bilinear form is not coercive. In consequence, we need to consider a different framework to discuss the well posedness of problem (2.2). In the literature, it is classical to consider the Fredholm's Alternative theorem (see section 11.5 in [43]) to analyse the existence of solution of problems of this type (compact perturbations of coercive problems). For our problem, this theorem reads

Theorem 2.1

Let us consider the eigenvalue problem

$$\left\{\begin{array}{l} \text{Find } \nu \in \mathbb{R} \text{ and } u \in H^1(\Omega)\backslash\{0\}, \text{ such that} \\[2ex] (\mu\,\nabla u, \nabla v)_{L^2(\Omega)} \;=\; \nu\;(\rho\, u, v)_{L^2(\Omega)} \quad \forall\, v \in H^1(\Omega), \end{array}\right. \tag{2.3}$$

then, problem (2.2) has a unique solution if and only if ℓ^2 is not an eigenvalue of (2.3). However, if ℓ^2 is an eigenvalue of (2.3) but $(f,v)_{L^2(\Omega)} = 0$ for all $v \in V_\ell$ where V_ℓ denotes the subspace of eigenfunctions associated to $\nu = \ell^2$, then there exists a solution which is unique up to an element of V_ℓ.

Finally, we also present a result concerning the regularity of the solution u of problem (2.2) depending on the regularity of the source f as well as the regularity of $\partial\Omega$. These results are classical and can be found in [44, 45].

Theorem 2.2

Let us consider $f \in H^s(\Omega)$ for $s \geq 0$ and ρ, μ smooth enough, then a solution u of problem (2.2) satisfies:

- *For any open set ϱ such that $\overline{\varrho} \subset \Omega$, we have $u \in H^{s+2}(\varrho)$.*
- *If $\partial\Omega \in \mathcal{C}^\infty$, we have $u \in H^{s+2}(\Omega)$.*
- *In 2D, if $\partial\Omega$ is polygonal which largest interior angle is $\frac{2\pi}{\kappa}$ for $\kappa > 1$, we have $u = u_s + u_\sigma$ where $u_s \in H^{s+2}(\Omega)$ and $u_\sigma \in H^\sigma(\Omega)$ for all $\sigma < 1 + \frac{\kappa}{2}$.*

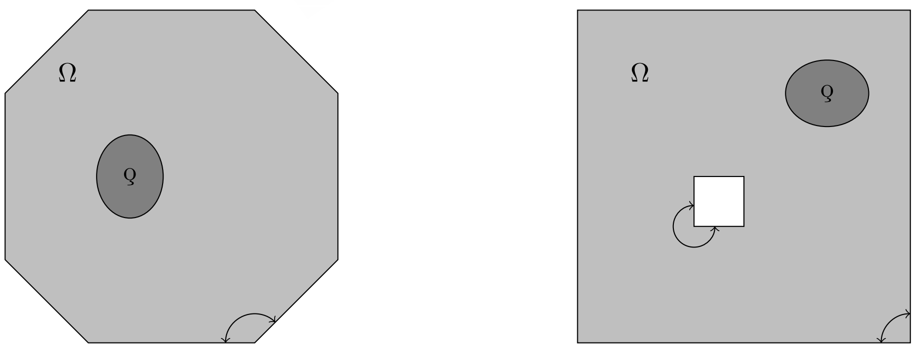

(a) Example of a polygonal domain which largest interior angle is $3\,\pi/4$ and therefore, according to Theorem 2.2, the solution belongs to $H^\sigma(\Omega)$ for all $\sigma < 7/3$.

(b) Example of a polygonal domain which largest interior angle is $3\,\pi/2$ and therefore, according to Theorem 2.2, the solution belongs to $H^\sigma(\Omega)$ for all $\sigma < 5/3$.

Figure 2.1: Examples of 2D polygonal domains which largest interior angle gives the regularity of a solution of problem (2.2).

2.2 Introduction to the Arlequin method

In this section we follow the work originally developed in [8] for elastostatic problems and we extend the Arlequin methodology to the treatment of problem (2.1). We first consider that the defected domain Ω is decomposed into two overlapping open sub-domains Ω_1 and Ω_2 such that their boundaries do not intersect and Ω is the union of these sub-domains (see Figure 2.2),

$$\Omega_j \subset \Omega \quad j \in \{1,2\}, \qquad \Omega = \Omega_1 \cup \Omega_2 \qquad \text{and} \qquad \partial\Omega_1 \cap \partial\Omega_2 = \emptyset.$$

Notice that this decomposition can be freely chosen attending to our interests. In practice, as we mentioned in the introduction, we will choose them to be conform with a given mesh of Θ and another one of a neighbourhood of the obstacle. Then, in the sequel, we will consider that Ω_1 is adapted to the background domain avoiding the defect, while Ω_2 is devoted to capture the obstacle properties (see Figure 2.2). In consequence, the boundary of Θ is assumed to be a subset

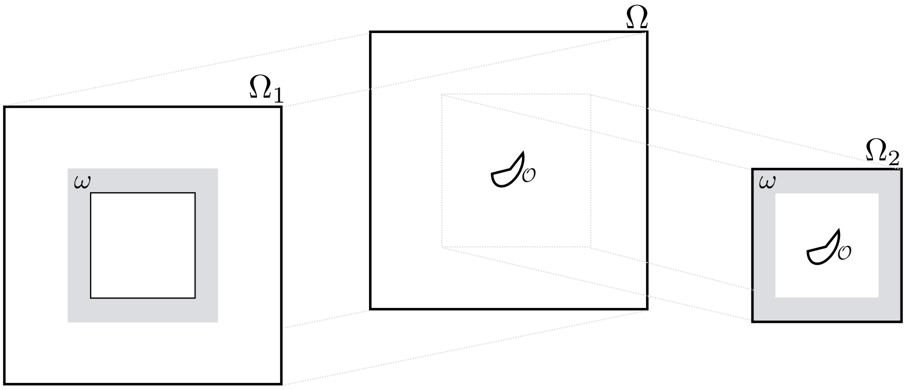

Figure 2.2: Typical configuration of a domain including a hole (a defect). The defect is captured by Ω_2 whereas the background medium is captured by Ω_1. The coupling domain ω is the overlapping region between Ω_1 and Ω_2.

of $\partial\Omega_1$, while the boundary of the hole $\mathcal{O}$ is assumed to be a subset of $\partial\Omega_2$, i.e.,

$$\partial\Theta \subset \partial\Omega_1 \quad \text{and} \quad \partial\mathcal{O} \subset \partial\Omega_2.$$

Moreover, since the overlapping region (that we denote ω) will correspond to the matching region, it is important to notice that

$$\omega = \Omega_1 \cap \Omega_2 \neq \emptyset \quad \text{and} \quad \overline{\omega} \cap \partial\Omega = \emptyset.$$

Now we introduce another assumption which is related to the source term that we consider. Our purpose is just to make things simpler and be more clear in the introduction of the technique. More precisely, we avoid the interaction of the source term with Ω_2 (especially to avoid the interaction with the matching region ω) by considering

$$f \text{ is compactly supported in } \Omega_1 \setminus \Omega_2.$$

This assumption is very reasonable when considering scattering problems. Moreover, the reader should notice that it is not restrictive and it is only made for pedagogical reasons. The treatment of a source that interacts also with Ω_2 would be similar to the one we detail bellow for the other terms following the Arlequin methodology developed in [8, 9].

2.2.1 Formulation in a constrained space

We look for a suitable continuous formulation that will allow a flexible non-conform discretization process of the two sub-domains Ω_1 and Ω_2. To do so, we first rewrite the equation in (2.2) by splitting the terms in the following way

$$
\begin{array}{l}
- \ \ell^2\,(\rho\,u, v)_{L^2(\Omega_1\setminus\omega)} \ - \ \ell^2\,(\rho\,u, v)_{L^2(\omega)} \ - \ \ell^2\,(\rho\,u, v)_{L^2(\Omega_2\setminus\omega)} \\
+ \ (\mu\,\nabla u, \nabla v)_{L^2(\Omega_1\setminus\omega)} \ + \ (\mu\,\nabla u, \nabla v)_{L^2(\omega)} \ + \ (\mu\,\nabla u, \nabla v)_{L^2(\Omega_2\setminus\omega)} \ = \ (f, v)_{L^2(\Omega_1\setminus\omega)}.
\end{array}
\tag{2.4}
$$

Then, we can distribute to each sub-domain the terms related to the overlapping region ω by introducing the following partitioning

$$
\sum_{j=1}^{2} \alpha_j = 1 \quad \text{and} \quad \sum_{j=1}^{2} \beta_j = 1, \quad \text{in} \quad \omega. \tag{2.5}
$$

In order to simplify the notation, we also consider that outside of the intersection region they are defined as

$$
\alpha_j = 1 \quad \text{and} \quad \beta_j = 1, \quad \text{in } \Omega_j \setminus \omega, \quad j \in \{1, 2\}. \tag{2.6}
$$

Moreover, in order to have enough regularity we also need to consider the following assumption.

Assumption I.1

We assume that the two couples of coefficients defined by equations (2.5) *and* (2.6) *are such that*

$$
(\alpha_j, \beta_j) \in L^\infty(\Omega_j)^2, \quad \textit{for } j \in \{1, 2\}.
$$

and there exists $(\alpha_0, \beta_0) \in \mathbb{R}^2$ *such that*

$$
\inf_{\boldsymbol{x}\in\Omega_j} \alpha_j(\boldsymbol{x}) \geq \alpha_0 > 0 \quad \textit{and} \quad \inf_{\boldsymbol{x}\in\Omega_j} \beta_j(\boldsymbol{x}) \geq \beta_0 > 0, \quad j \in \{1, 2\}.
$$

With this notation we can easily rephrase equation (2.4) as

$$
\begin{array}{l}
- \ \ell^2\,(\alpha_1\,\rho\,u, v)_{L^2(\Omega_1)} \ - \ \ell^2\,(\alpha_2\,\rho\,u, v)_{L^2(\Omega_2)} \\
+ \ (\beta_1\,\mu\,\nabla u, \nabla v)_{L^2(\Omega_1)} \ + \ (\beta_2\,\mu\,\nabla u, \nabla v)_{L^2(\Omega_2)} \ = \ (f, v)_{L^2(\Omega_1\setminus\omega)}.
\end{array}
\tag{2.7}
$$

Now, we introduce new variables that represent $u \in H^1(\Omega)$ but restricted to each sub-domain Ω_1 and Ω_2, we consider,

$$
u_1 = u_{|\Omega_1} \qquad \text{and} \qquad u_2 = u_{|\Omega_2} \tag{2.8}
$$

and we want to find a variational formulation for $\boldsymbol{u} = (u_1, u_2)$ which is equivalent to problem (2.2) (in the sense that the reconstruction of u from $\boldsymbol{u} = (u_1, u_2)$ should be also given by (2.8)). Notice, that to ensure $u \in H^1(\Omega)$ it is important to have $u_1 = u_2$ in ω. Moreover, this condition is also important for the test functions in order to complete the partitioning of (2.7). In consequence, we introduce the following functional space

$$
V = \{\boldsymbol{v} = (v_1, v_2) \in W \mid v_1 = v_2 \text{ in } \omega\}, \quad \text{with} \quad W = H^1(\Omega_1) \times H^1(\Omega_2). \tag{2.9}
$$

Notice that both are Hilbert spaces equipped with the scalar product and respective norm

$$
\begin{aligned}
(\boldsymbol{u}, \boldsymbol{v})_1 &= (u_1, v_1)_{H^1(\Omega_1)} + (u_2, v_2)_{H^1(\Omega_2)}, \\
\|\boldsymbol{u}\|_1 &= \sqrt{(\boldsymbol{u}, \boldsymbol{u})_1} = \sqrt{\|u_1\|^2_{H^1(\Omega_1)} + \|u_2\|^2_{H^1(\Omega_2)}}.
\end{aligned}
$$

We shall also introduce the following notation for the scalar product and respective norm in the space $L^2(\Omega_1) \times L^2(\Omega_2)$

$$
\begin{aligned}
(\boldsymbol{u}, \boldsymbol{v})_0 &= (u_1, v_1)_{L^2(\Omega_1)} + (u_2, v_2)_{L^2(\Omega_2)}, \\
\|\boldsymbol{u}\|_0 &= \sqrt{(\boldsymbol{u}, \boldsymbol{u})_0} = \sqrt{\|u_1\|^2_{L^2(\Omega_1)} + \|u_2\|^2_{L^2(\Omega_2)}}.
\end{aligned}
$$

Remark 2.3

The space V is isomorph to $H^1(\Omega)$ in the sense that any $v \in H^1(\Omega)$ is such that $(v_{|\Omega_1}, v_{|\Omega_2}) \in V$ and also for any $\boldsymbol{v} = (v_1, v_2) \in V$ we can define $v \in H^1(\Omega)$ by

$$v_{|\Omega_1} = v_1 \qquad \text{and} \qquad v_{|\Omega_2} = v_2.$$

Then, equation (2.7) gives for any test function $\boldsymbol{v} = (v_1, v_2) \in V$

$$\begin{aligned} &- \ \ell^2\,(\alpha_1\,\rho\,u_1, v_1)_{L^2(\Omega_1)} \ - \ \ell^2\,(\alpha_2\,\rho\,u_2, v_2)_{L^2(\Omega_2)} \\ &+ \ (\beta_1\,\mu\,\nabla u_1, \nabla v_1)_{L^2(\Omega_1)} \ + \ (\beta_2\,\mu\,\nabla u_2, \nabla v_2)_{L^2(\Omega_2)} \ = \ (f, v_1)_{L^2(\Omega_1 \setminus \omega)}. \end{aligned}$$

And it seems natural to rephrase problem (2.2) as:

$$\left\{ \begin{array}{l} \text{Find } \boldsymbol{u} \in V, \text{ such that } \forall\, \boldsymbol{v} \in V, \\[2ex] -\,\ell^2\, m(\boldsymbol{u}, \boldsymbol{v}) \ + \ a(\boldsymbol{u}, \boldsymbol{v}) \ = \ g(\boldsymbol{v}). \end{array} \right. \tag{2.10}$$

where we have introduced the following linear and bilinear forms

$$m : W \times W \longrightarrow \mathbb{R} \qquad \text{such that} \qquad m(\boldsymbol{u}, \boldsymbol{v}) = \sum_{j=1}^{2} (\alpha_j\, \rho\, u_j, v_j)_{L^2(\Omega_j)}, \tag{2.11}$$

$$a : W \times W \longrightarrow \mathbb{R} \qquad \text{such that} \qquad a(\boldsymbol{u}, \boldsymbol{v}) = \sum_{j=1}^{2} (\beta_j\, \mu\, \nabla u_j, \nabla v_j)_{L^2(\Omega_j)}, \tag{2.12}$$

$$g : W \longrightarrow \mathbb{R} \qquad \text{such that} \qquad g(\boldsymbol{v}) = (f, v_1)_{L^2(\Omega_1 \setminus \Omega_2)}. \tag{2.13}$$

It is easy to show the following results.

Proposition 2.4

If Assumption I.1 is satisfied, then the bilinear forms in (2.11), (2.12) and (2.13) are well defined and continuous, i.e. there exist positive constants K_m, K_a and K_g such that

$$\begin{aligned} |m(\boldsymbol{u}, \boldsymbol{v})| &\leq K_m \|\boldsymbol{u}\|_0 \|\boldsymbol{v}\|_0 && \text{for all} \quad \boldsymbol{u}, \boldsymbol{v} \in W, \\ |a(\boldsymbol{u}, \boldsymbol{v})| &\leq K_a \|\boldsymbol{u}\|_1 \|\boldsymbol{v}\|_1 && \text{for all} \quad \boldsymbol{u}, \boldsymbol{v} \in W, \\ |g(\boldsymbol{v})| &\leq K_g \|\boldsymbol{v}\|_1 && \text{for all} \quad \boldsymbol{v} \in W. \end{aligned}$$

Notice, that formulation (2.10) is still not well adapted for discretization since an internal approximation of V is needed. Therefore, basis functions that strongly satisfy the equality $u_1 = u_2$ in ω should be considered, which is rather difficult in practice and/or inefficient. Moreover it would not allow to consider independent meshes which is one of our main interests as we mentioned already in the introduction. However, for theoretical reasons we are interested in the equivalence of this formulation with respect to formulation (2.2), since it represents a first step to obtain the desired Arlequin formulation where we will finally impose the matching weakly.

Theorem 2.5

If Assumption I.1 is satisfied, then problems (2.2) and (2.10) are equivalent in the sense that

$$u \text{ is solution of } (2.2) \quad \Longleftrightarrow \quad \boldsymbol{u} = (u_{|\Omega_1}, u_{|\Omega_2}) \text{ is solution of } (2.10).$$

In consequence, existence and uniqueness of solution for problem (2.10) is given by Theorem 2.1.

Proof. Let u be solution of problem (2.2). Then it is clear that $\boldsymbol{u} = (u_{|\Omega_1}, u_{|\Omega_2}) \in V$ and we only have to check if it is solution of (2.10). So we take any $\boldsymbol{v} = (v_1, v_2) \in V$ and we consider in problem (2.2) the test function $v \in H^1(\Omega)$ defined as

$$v = v_1 \quad \text{in } \Omega_1 \backslash \omega, \quad v = v_2 \quad \text{in } \Omega_2 \backslash \omega \quad \text{and} \quad v = v_1 (= v_2) \quad \text{in } \omega. \tag{2.14}$$

This provides the equation

$$-\,\ell^2\,(\rho\, u, v)_{L^2(\Omega)} \;+\; (\mu\,\nabla u, \nabla v)_{L^2(\Omega)} \;=\; (f, v)_{L^2(\Omega)},$$

which we notice is equivalent to

$$-\,\ell^2\, m(\boldsymbol{u}, \boldsymbol{v}) \;+\; a(\boldsymbol{u}, \boldsymbol{v}) \;=\; -\,\ell^2\,(\rho\, u, v)_{L^2(\Omega)} \;+\; (\mu\,\nabla u, \nabla v)_{L^2(\Omega)} \;=\; g(\boldsymbol{v}).$$

Now, to prove the reverse, let $\boldsymbol{u} = (u_1, u_2)$ be solution of problem equation (2.10). Then, we can define $u \in H^1(\Omega)$ as

$$u = u_1 \quad \text{in } \Omega_1 \backslash \omega, \quad u = u_2 \quad \text{in } \Omega_2 \backslash \omega \quad \text{and} \quad u = u_1 (= u_2) \quad \text{in } \omega, \tag{2.15}$$

and we have to check if it is solution of (2.2). So we consider any $v \in H^1(\Omega)$ and we observe that, since $\boldsymbol{v} = (v_{|\Omega_1}, v_{|\Omega_2}) \in V$, we have

$$-\,\ell^2\,(\rho\, u, v)_{L^2(\Omega)} + (\mu\,\nabla u, \nabla v)_{L^2(\Omega)} = -\,\ell^2\, m(\boldsymbol{u}, \boldsymbol{v}) + a(\boldsymbol{u}, \boldsymbol{v}) = g(\boldsymbol{v}) = (f, v)_{L^2(\Omega_1 \backslash \omega)}.$$

■

The reader might notice that, as it is classical, the existence of solution of problem (2.10) could be analysed without relating it to problem (2.2). In that case, the reader must be careful since conditions (2.5) and (2.6) might seem unnecessary. And indeed they are, at least when it comes to the existence of solution of problem (2.10). However, as we have just seen in Theorem 2.5, they are important in order to guarantee that problems (2.10) and (2.2) are actually equivalent.

2.2.2 Mixed formulation of classic Arlequin method

To avoid the internal approximation of the space V, we choose to weakly impose the matching in the overlapping region ω. This is done by the introduction of a Lagrange multiplier as it is usual for treating equality constraints (e.g. [46, 47, 48]). Since solutions are in $H^1(\Omega)$, it seems natural to impose the equality constraint in the H^1-sense. Therefore, we choose to introduce

$$M = H^1(\omega) \quad \text{and} \quad b : W \times M \longrightarrow \mathbb{R} \quad \text{such that} \quad b(\boldsymbol{v}, m) = (v_1 - v_2, m)_{H^1(\omega)} \tag{2.16}$$

and notice that $b(\cdot,\cdot)$ is also a continuous bilinear form.

Proposition 2.6

The bilinear form defined in (2.16) *is continuous, i.e. there exists a positive constant K_b such that*

$$|b(\boldsymbol{v}, m)| \le K_b \|\boldsymbol{v}\|_1 \|m\|_M \quad \textit{for all} \quad (\boldsymbol{v}, m) \in W \times M.$$

We obtain in this way the **classic Arlequin formulation** which is given by the following mixed problem

$$\left\{\begin{array}{ll} \text{Find } (\boldsymbol{u}, \lambda) \in W \times M, \text{ such that} & \\ -\,\ell^2\, m(\boldsymbol{u}, \boldsymbol{v}) \;+\; a(\boldsymbol{u}, \boldsymbol{v}) \;+\; b(\boldsymbol{v}, \lambda) \;=\; g(\boldsymbol{v}), \quad \forall \boldsymbol{v} \in W, & \text{(2.17a)} \\ \qquad\qquad b(\boldsymbol{u}, m) \;=\; 0, \qquad \forall m \in M, & \text{(2.17b)} \end{array}\right.$$

which equivalence to problem (2.10), and consequently to problem (2.2), is given by Theorem 2.11 below which is based in the following lemmas that are crucial for the existence and uniqueness of the Lagrange multiplier.

Lemma 2.7

There exists a constant $\delta > 0$ such that the following Inf-Sup condition is satisfied

$$\inf_{m\in M} \sup_{\boldsymbol{v}\in W} \frac{|b(\boldsymbol{v},m)|}{\|m\|_M \ \|\boldsymbol{v}\|_1} \ \geq \ \delta. \tag{2.18}$$

Proof. We essentially reproduce here the proof presented in [9]. First notice that there exists a continuous extension operator $\mathtt{E}(\cdot)$ from $M = H^1(\omega)$ into $H^1_0(\Omega)$ (see Theorem 1.2 in [49]), then there exists a constant $K_{\mathtt{E}} > 0$ such that

$$\mathtt{E}(m)_{|\omega} = m \quad \text{and} \quad \|\mathtt{E}(m)\|_{H^1(\Omega)} \leq K_{\mathtt{E}}\|m\|_M, \quad \forall m \in M.$$

In consequence, for any $m \in M$ we can consider $\boldsymbol{v}^\star = (\mathtt{E}(m)_{|\Omega_1}, 0) \in W$ such that

$$\sup_{\boldsymbol{v}\in W} \frac{|b(\boldsymbol{v},m)|}{\|m\|_M \ \|\boldsymbol{v}\|_1} \ \geq \ \frac{|b(\boldsymbol{v}^\star,m)|}{\|m\|_M \ \|\boldsymbol{v}^\star\|_1} \ = \ \frac{(\mathtt{E}(m),m)_{H^1(\omega)}}{\|m\|_{H^1(\omega)} \ \|\mathtt{E}(m)\|_{H^1(\Omega_1)}} \ \geq \ \frac{1}{K_{\mathtt{E}}}.$$

Since the previous inequality holds for any $m \in M$, it leads to the claimed result. ■

Remark 2.8

The reader might wonder why we do not consider the coupling in the L^2-sense, i.e.

$$M = L^2(\omega) \quad \text{and} \quad b : W \times M \longrightarrow \mathbb{R} \quad \text{such that} \quad b(\boldsymbol{v},m) = (v_1 - v_2, m)_{L^2(\omega)}.$$

This question is treated on detail in Appendix A where we prove that in this case the Inf-Sup condition provided in Lemma 2.7 does not hold. Notice that, as we show in the following, the verification of the Inf-Sup condition is crucial for the existence and uniqueness of the Lagrange multiplier.

Moreover, since $b(\cdot,\cdot)$ is bilinear and continuous from $W \times M$ into $\mathbb{R}$, we notice that according to Riesz representation theorem (Theorem 5.5 in [50]), there exist linear continuous operators

$$\mathcal{B} : M \longrightarrow W \qquad \text{such that} \qquad (\mathcal{B}\,m, \boldsymbol{v})_1 = b(\boldsymbol{v},m) \quad \forall(\boldsymbol{v},m) \in W \times M,$$

$$\mathcal{B}^T : W \longrightarrow M \qquad \text{such that} \qquad (\mathcal{B}^T\boldsymbol{v}, m)_M = b(\boldsymbol{v},m) \quad \forall(\boldsymbol{v},m) \in W \times M.$$

Next, we prove that the *Inf-Sup condition* (also known as Babuška condition, Brezzi condition or LBB condition for Ladyzhenskaya, Babuška and Brezzi [51, 52]) is equivalent to the two following lemmas that are classical and included for completeness (Lemma 2.1 in [53]).

Lemma 2.9

The Inf-Sup condition (2.18) *is equivalent to say that $\mathcal{B}$ is a bijective operator from M into $\operatorname{Im}\mathcal{B}$ with continuous inverse. More precisely*

$$\|m\|_M \leq \frac{1}{\delta}\|\mathcal{B}\,m\|_1, \quad \forall m \in M, \tag{2.19}$$

where δ is the constant that appears in (2.18).

Proof. First notice that *Inf-Sup condition* (2.18) can also be written as

$$\sup_{\boldsymbol{v}\in W} \frac{|b(\boldsymbol{v},m)|}{\|\boldsymbol{v}\|_1} \ \geq \ \delta\,\|m\|_M, \quad \forall m \in M,$$

where the term on the left is exactly $\|\mathcal{B}\,m\|_1$. Then it is clear that $\|\mathcal{B}\,m\|_1 \geq \delta\,\|m\|_M$ for all $m \in M$. This trivially implies injectivity and since $\mathcal{B}$ is a surjective operator from M into $\operatorname{Im}\mathcal{B}$ we have the bijectivity from M into $\operatorname{Im}\mathcal{B}$.

Now, we prove that the inverse of $\mathcal{B}$ is also continuous by application of the open mapping theorem (see Corollary 2.12 in [54]). To fit into the hypothesis we just need to check if M and $\operatorname{Im}\mathcal{B}$ are Banach spaces. The first is a Banach space by definition, while for the second we prove it next. Let us consider $\{\mathcal{B}\, m_n\}_{n\in\mathbb{N}}$ a Cauchy sequence in $\operatorname{Im}\mathcal{B} \subset W$, we easily verify (using (2.19)) that $\{m_n\}_{n\in\mathbb{N}}$ is also a Cauchy sequence in M and since M is complete, then $\{m_n\}_{n\in\mathbb{N}}$ is convergent and therefore also $\{\mathcal{B}\, m_n\}_{n\in\mathbb{N}}$. Thus by application of the open mapping theorem $\mathcal{B}^{-1}$ is continuous. Finally, we remark that $\operatorname{Im}\mathcal{B} = \overline{\operatorname{Im}\mathcal{B}}$ since it is a Banach space.

■

Moreover, the following result also holds and represents a transpose version of previous lemma.

Lemma 2.10

Respectively, the Inf-Sup condition (2.18) *is also equivalent to say that* $\mathcal{B}^T$ *is a bijective operator from* $(\operatorname{Ker}\mathcal{B}^T)^\perp$ *into* M *with continuous inverse. More precisely*

$$\|\boldsymbol{v}\|_1 \leq \frac{1}{\delta}\|\mathcal{B}^T\,\boldsymbol{v}\|_M, \quad \forall \boldsymbol{v} \in (\operatorname{Ker}\mathcal{B}^T)^\perp, \tag{2.20}$$

where δ *is again the constant that appears in* (2.18).

Proof. We first remark that in general, for every linear continuous operator between two Hilbert spaces, we have that $(\operatorname{Ker}\mathcal{B}^T)^\perp = \overline{\operatorname{Im}\mathcal{B}}$. Then, if we consider $\boldsymbol{v} \in \overline{\operatorname{Im}\mathcal{B}}$, it is clear that

$$\|\boldsymbol{v}\|_1 = \sup_{\boldsymbol{w}\in\,(\operatorname{Ker}\mathcal{B}^T)^\perp} \frac{(\boldsymbol{v},\boldsymbol{w})_1}{\|\boldsymbol{w}\|_1} = \sup_{m\in M}\frac{(\boldsymbol{v},\mathcal{B}\,m)_1}{\|\mathcal{B}\,m\|_1}.$$

Now, considering (2.19) from previous lemma we obtain

$$\|\boldsymbol{v}\|_1 \leq \frac{1}{\delta}\sup_{m\in M}\frac{(\boldsymbol{v},\mathcal{B}\,m)_1}{\|m\|_M} = \frac{1}{\delta}\sup_{m\in M}\frac{(\mathcal{B}^T\,\boldsymbol{v},m)_M}{\|m\|_M} = \frac{1}{\delta}\|\mathcal{B}^T\,\boldsymbol{v}\|_M.$$

Thus we can conclude as in previous lemma.

■

Now, as it is the main objective of this section, we give an important result that relates formulation (2.17) to problem (2.10), and consequently to problem (2.2) (by Theorem 2.5).

Theorem 2.11

If Assumption I.1 is satisfied, then problems (2.10) *and* (2.17) *are equivalent in the sense that*

$$\boldsymbol{u} \text{ is a solution of } (2.10) \quad \Longleftrightarrow \quad \big(\boldsymbol{u},\lambda(\boldsymbol{u})\big) \text{ is a solution of } (2.17).$$

Moreover for any solution $\boldsymbol{u} \in V$*, the Lagrange multiplier* $\lambda(\boldsymbol{u}) \in M$ *is uniquely defined by* (2.17a)*. In consequence, existence and uniqueness of solution for problem* (2.17) *is given by Theorem 2.1.*

Proof. Let $(\boldsymbol{u},\lambda)$ be solution of (2.17) and notice that (2.17b) implies $\boldsymbol{u} \in V$. Then, we only have to check if it is solution of (2.10). But it is straightforward by considering in (2.17a) test functions $\boldsymbol{v} \in V \subset W$ since in that case $b(\boldsymbol{v},\lambda) = 0$.

The reverse implication is more complicated. Let $\boldsymbol{u}$ be solution of (2.10), then we proceed to check (2.17a) since (2.17b) is trivially satisfied just because $\boldsymbol{u} \in V$. First notice that since $m(\cdot,\cdot)$ and $a(\cdot,\cdot)$ are bilinear continuous forms from $W \times W$ into $\mathbb{R}$, by the Riesz representation theorem (Theorem 5.5 in [50]) there exist linear continuous operators

$$\mathcal{M} : W \longrightarrow W \qquad \text{such that} \qquad (\mathcal{M}\,\boldsymbol{u},\boldsymbol{v})_1 = m(\boldsymbol{u},\boldsymbol{v}) \quad \forall(\boldsymbol{u},\boldsymbol{v}) \in W \times W,$$

$$\mathcal{A} : W \longrightarrow W \qquad \text{such that} \qquad (\mathcal{A}\,\boldsymbol{u},\boldsymbol{v})_1 = a(\boldsymbol{u},\boldsymbol{v}) \quad \forall(\boldsymbol{u},\boldsymbol{v}) \in W \times W.$$

Moreover, by the linearity of $g(\cdot)$, there exists $\boldsymbol{f} \in W$ such that

$$g(\boldsymbol{v}) = (\boldsymbol{f}, \boldsymbol{v})_1 \quad \text{for all} \quad \boldsymbol{v} \in W.$$

Thus $\boldsymbol{u}$ must satisfy (since by definition $\operatorname{Ker}\mathcal{B}^T = V$)

$$-\,\ell^2\,(\mathcal{M}\,\boldsymbol{u}, \boldsymbol{v})_1 \;+\; (\mathcal{A}\,\boldsymbol{u}, \boldsymbol{v})_1 \;=\; (\boldsymbol{f}, \boldsymbol{v})_1, \quad \forall \boldsymbol{v} \in \operatorname{Ker}\mathcal{B}^T,$$

which is equivalent to say that $-\,\ell^2\,\mathcal{M}\,\boldsymbol{u} + \mathcal{A}\,\boldsymbol{u} - \boldsymbol{f} \in (\operatorname{Ker}\mathcal{B}^T)^\perp$. Now we recall that since $\mathcal{B}^T$ is a linear continuous operator between Hilbert spaces, we have that $\overline{\operatorname{Im}\mathcal{B}} = (\operatorname{Ker}\mathcal{B}^T)^\perp$. Then, since $\mathcal{B}$ is a bijective operator from M into $\overline{\operatorname{Im}\mathcal{B}}$ (see Lemma 2.9), there exists a unique $\lambda \in M$ such that $-\,\ell^2\,\mathcal{M}\,\boldsymbol{u} + \mathcal{A}\,\boldsymbol{u} - \boldsymbol{f} = -\mathcal{B}\lambda$, or equivalently

$$-\,\ell^2\,(\mathcal{M}\,\boldsymbol{u}, \boldsymbol{v})_1 \;+\; (\mathcal{A}\,\boldsymbol{u}, \boldsymbol{v})_1 \;+\; (\mathcal{B}\,\lambda, \boldsymbol{v})_1 \;=\; (\boldsymbol{f}, \boldsymbol{v})_1, \quad \forall \boldsymbol{v} \in W.$$

Finally notice that this concludes the proof. ■

Concerning the regularity of the solution $(\boldsymbol{u}, \lambda)$ of problem (2.17), we notice that the regularity of $\boldsymbol{u}$ is given by Theorem 2.2, however for the regularity of λ we first need to find a suitable interpretation of the Lagrange multiplier.

Proposition 2.12

If Assumption I.1 is satisfied and u is a solution of problem (2.2), then $\big((u_{|\Omega_1}, u_{|\Omega_2}), \lambda\big)$ is a solution of (2.17) where the Lagrange multiplier λ is the unique solution of the following variational problem:

$$\left\{\begin{aligned} &\text{Find } \lambda \in H^1(\omega), \text{ such that } \forall\, m \in H^1(\omega),\\ &2\,(\lambda, m)_{H^1(\omega)} = \; -\,\ell^2\,\big((\alpha_2 - \alpha_1)\rho\,u, m\big)_{L^2(\omega)} + \big((\beta_2 - \beta_1)\mu\,\nabla u, \nabla m\big)_{L^2(\omega)}\\ &\qquad\qquad + \langle m, \mu\,\partial_{\boldsymbol{n}} u\rangle_{\partial\omega\cap\partial\Omega_2} - \langle m, \mu\,\partial_{\boldsymbol{n}} u\rangle_{\partial\omega\cap\partial\Omega_1}, \end{aligned}\right. \tag{2.21}$$

where $\boldsymbol{n}$ denotes the outward normal to ω and $\langle\cdot,\cdot\rangle_\gamma$ stands for the duality product between $H^{\frac{1}{2}}(\gamma)$ and its dual.

Proof. First, we introduce the continuous extension operator $\mathtt{E}(\cdot)$ from $H^1(\omega)$ into $H^1_0(\Omega)$ (see Theorem 1.2 in [49]) such that for all $m \in H^1(\omega)$ we can consider in (2.17a) test functions $(v_1, v_2) = (\mathtt{E}(m)_{|\Omega_1}, -\mathtt{E}(m)_{|\Omega_2})$ and obtain

$$\begin{aligned} &-\,\ell^2\,(\rho\,u, \mathtt{E}(m))_{L^2(\Omega_1\setminus\omega)} + (\mu\,\nabla u, \nabla\mathtt{E}(m))_{L^2(\Omega_1\setminus\omega)} - \ell^2\,(\alpha_1\rho\,u, m)_{L^2(\omega)} + (\beta_1\mu\,\nabla u, \nabla m)_{L^2(\omega)}\\ &+\,\ell^2\,(\rho\,u, \mathtt{E}(m))_{L^2(\Omega_2\setminus\omega)} - (\mu\,\nabla u, \nabla\mathtt{E}(m))_{L^2(\Omega_2\setminus\omega)} + \ell^2\,(\alpha_2\rho\,u, m)_{L^2(\omega)} - (\beta_2\mu\,\nabla u, \nabla m)_{L^2(\omega)}\\ &\qquad\qquad + 2\,(m, \lambda)_{H^1(\omega)} = (f, \mathtt{E}(m))_{L^2(\Omega_1\setminus\omega)}. \end{aligned}$$

Now, since u is solution of problem (2.2), we have that $\operatorname{div}(\mu\,\nabla u) \in L^2(\Omega)$ and then we can apply Green's formula in $\Omega_1\setminus\omega$ to obtain

$$\begin{aligned} &-\,\ell^2\,(\rho\,u, \mathtt{E}(m))_{L^2(\Omega_1\setminus\omega)} + (\mu\,\nabla u, \nabla\mathtt{E}(m))_{L^2(\Omega_1\setminus\omega)}\\ &\quad = -\,\ell^2\,(\rho\,u, \mathtt{E}(m))_{L^2(\Omega_1\setminus\omega)} - (\operatorname{div}(\mu\,\nabla u), \mathtt{E}(m))_{L^2(\Omega_1\setminus\omega)} - \langle\mathtt{E}(m), \mu\,\partial_{\boldsymbol{n}} u\rangle_{\partial(\Omega_1\setminus\omega)}\\ &\quad = (f, \mathtt{E}(m))_{L^2(\Omega_1\setminus\omega)} - \langle\mathtt{E}(m), \mu\,\partial_{\boldsymbol{n}} u\rangle_{\partial\omega\cap\partial\Omega_2} \end{aligned}$$

where $\boldsymbol{n}$ denotes the outward normal to ω. Analogously

$$-\,\ell^2\,(\rho\,u, \mathtt{E}(m))_{L^2(\Omega_2\setminus\omega)} + (\mu\,\nabla u, \nabla\mathtt{E}(m))_{L^2(\Omega_2\setminus\omega)} = -\,\langle\mathtt{E}(m), \mu\,\partial_{\boldsymbol{n}} u\rangle_{\partial\omega\cap\partial\Omega_1}.$$

Thus combining the three previous equations we obtain the desired result

$$\begin{aligned} 2\,(\lambda, m)_{H^1(\omega)} = & -\ell^2\left((\alpha_2-\alpha_1)\rho\,\partial_t^2 u, m\right)_{L^2(\omega)} + \left((\beta_2-\beta_1)\mu\,\nabla u, \nabla m\right)_{L^2(\omega)} \\ & + \langle m, \mu\,\partial_{\boldsymbol{n}} u\rangle_{\partial\omega\cap\partial\Omega_2} - \langle m, \mu\,\partial_{\boldsymbol{n}} u\rangle_{\partial\omega\cap\partial\Omega_1} \qquad \forall m \in H^1(\omega). \end{aligned}$$

■

Corollary 2.13

Under the assumptions of Proposition 2.12, if $\operatorname{div}\big((\beta_2-\beta_1)\mu\,\nabla u\big) \in L^2(\omega)$, *then the Lagrange multiplier can be interpreted as the unique solution of problem*

$$\left\{\begin{array}{rcl} \multicolumn{3}{l}{\text{Find } \lambda \in H^1(\omega), \text{ such that}} \\ 2\,(\lambda - \Delta\lambda) & = & -\,\ell^2\,(\alpha_2-\alpha_1)\rho\,u - \operatorname{div}\big((\beta_2-\beta_1)\mu\,\nabla u\big) \quad \text{in } \omega, \\ \partial_{\boldsymbol{n}}\lambda & = & -\beta_{1|\omega}\,\partial_{\boldsymbol{n}} u \quad \text{on } \partial\omega\cap\partial\Omega_1, \\ \partial_{\boldsymbol{n}}\lambda & = & \beta_{2|\omega}\,\partial_{\boldsymbol{n}} u \quad \text{on } \partial\omega\cap\partial\Omega_2. \end{array}\right.$$

Finally, we complete this section with the following theorem concerning the regularity of a solution of problem (2.17) with respect to the regularity of the data, the computational domain and the overlapping region. These results are direct extensions of the classical results in [44, 45].

Theorem 2.14

Let us consider $f \in H^s(\Omega)$ *for* $s \geq 0$, ρ μ *smooth enough and a solution* $(\boldsymbol{u}, \lambda)$ *of problem* (2.17), *then the primal variable* $\boldsymbol{u}$ *has the regularity described in Theorem 2.2. Moreover, if* α_j *and* β_j *for* $j \in \{1, 2\}$ *are smooth enough, the Lagrange multiplier satisfies:*

- *For any open set* ϱ *such that* $\overline{\varrho} \subset \omega$, *we have* $\lambda \in H^{s+2}(\varrho)$.
- *If* $\partial\omega \in \mathcal{C}^\infty$, *we have* $\lambda \in H^{s+2}(\omega)$.
- *In 2D, if* $\partial\omega$ *is polygonal which largest interior angle is* $\frac{2\,\pi}{\kappa}$ *for* $\kappa > 1$, *we have* $\lambda = \lambda_s + \lambda_\sigma$ *where* $\lambda_s \in H^{s+2}(\omega)$ *and* $\lambda_\sigma \in H^\sigma(\omega)$ *for all* $\sigma < 1 + \frac{\kappa}{2}$.

Remark 2.15

Let us remark that the regularity of the primal variable $\boldsymbol{u}$ *and the Lagrange multiplier* λ *are independent. This is due to* $\overline{\omega} \subset \Omega$, *which according to Theorem 2.2 ensures that* $u_{|\omega} \in H^{s+2}(\omega)$ *and therefore in Corollary 2.13 the source term belongs to* $H^s(\omega)$ *and the Neumann data to* $H^{s+\frac{1}{2}}(\gamma)$ *for any smooth* $\gamma \subset \partial\omega$. *This is enough to fit in the hypothesis of Theorem 5.1.3.5 in [45] which provides the previous result.*

Remark 2.16

The reader should notice that the regularity of $\partial\omega$ *is not related to the regularity of* $\partial\Omega$ *bu to the regularity of* $\partial\Omega_1$ *and* $\partial\Omega_2$, *since* $\omega = \Omega_1 \cap \Omega_2$. *Therefore, the regularity of* λ *depends on the regularity of the source and the choice of the domain decomposition.*

2.3 Modified Arlequin formulations

In this section, we first explain a drawback of the classic Arlequin formulation (2.17), to then propose alternative formulations that are better adapted to the problem of scattering by a local defect. Let us illustrate this by considering a given mesh $\mathcal{T}_{1,h}$ of the non defected domain Θ (see Figure 1.2a) and another mesh $\mathcal{T}_{2,h}$ of a neighbourhood of the obstacle $\mathcal{O}$ (see Figure 1.2b). Then for every position of the obstacle $\mathcal{O}$, we have the freedom to chose Ω_1 as the domain defined by $\mathcal{T}_{1,h}$ after removing the elements that interact with $\mathcal{O}$ (see Figure 2.3a). On the other hand, we also have the freedom to chose Ω_2 as the domain defined by $\mathcal{T}_{2,h}$ after adapting it to the new position of the obstacle, with the only assumption that $\Omega_2 \subset \Theta$ (see Figure 2.3b). In this way, we have adequate meshes to discretize $H^1(\Omega_1)$ and $H^1(\Omega_2)$. However, a standard finite element discretization of problem (2.17) requires also the construction of an approximation of the Lagrange multipliers space $H^1(\omega)$ which is based on a mesh of the overlapping domain ω (see Figure 2.3c). This is a drawback of the method since for every new position of the obstacle $\mathcal{O}$ (see Figure 2.4),

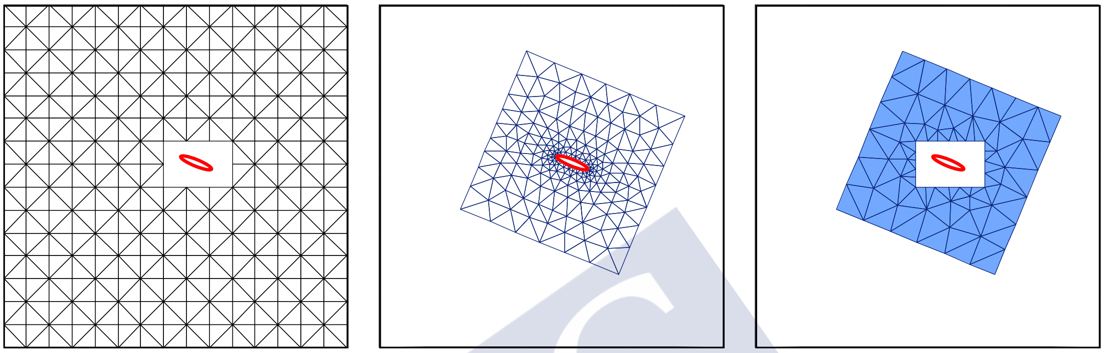

(a) Reduction of the coarse mesh for a given position of the obstacle.

(b) Fine mesh adapted to a given position of the obstacle.

(c) Mesh of the overlapping region.

Figure 2.3: Meshes adapted for a standard Arlequin decomposition of a given position of the obstacle.

we obtain a different overlapping region ω and therefore a new mesh of ω needs to be computed (see Figure 2.4c). There are several possible strategies to circumvent this issue:

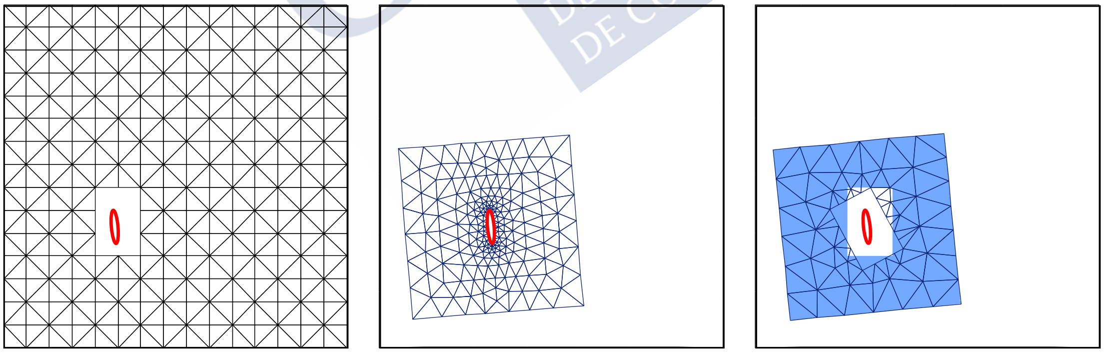

(a) Reduction of the coarse mesh for a new position of the obstacle.

(b) Fine mesh adapted to the new position of the obstacle.

(c) Mismatch between the overlapping region and the previous mesh of the overlapping region Figure 2.3c. Therefore re-meshing is needed.

Figure 2.4: Drawback of the standard Arlequin decomposition of a new position of the obstacle.

- The mesh elements of $\mathcal{T}_{1,h}$ or $\mathcal{T}_{2,h}$ can be cut or modified to be conform with the overlapping region ω (see Figure 2.5c). This corresponds to a re-meshing procedure that needs to be done for every new position of the obstacle $\mathcal{O}$. Moreover, it may lead to poor meshes in terms of quality that will require eventually a global re-meshing. In the end, it can be seen as the introduction of small or distorted elements in one mesh or the other. In consequence, the overall discretization process is penalized. Moreover, it is worth to note that in transient problems, if a explicit time scheme is considered, the mentioned penalization is critical.

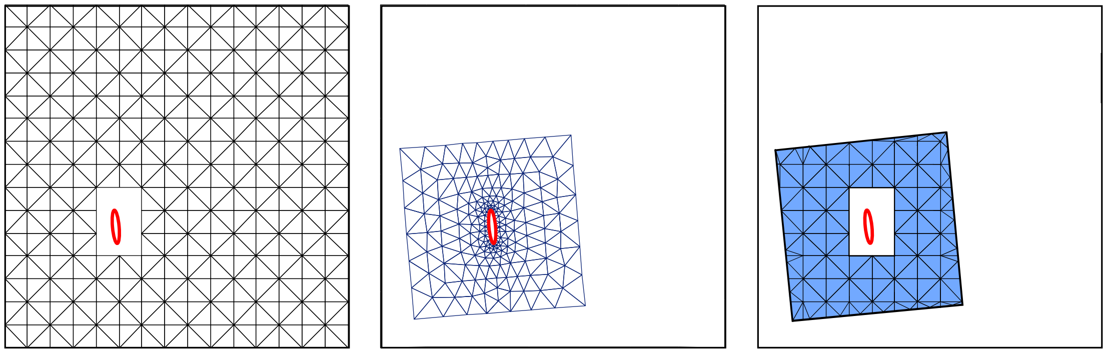

(a) Reduction of the coarse mesh for a new position of the obstacle.

(b) Fine mesh adapted to the new position of the obstacle.

(c) Mesh for the overlapping region obtained by cutting the coarse mesh.

Figure 2.5: Illustration of re-meshing procedure to obtain a valid mesh of the overlapping region when using standard Arlequin decomposition.

- The strategy classically used in the Arlequin method (see [32, 9, 38]) is to first consider that Ω_1 does no longer take into account the existence of the obstacle $\mathcal{O}$ (see Figure 2.6a). In consequence, it is meshed by the whole triangulation $\mathcal{T}_{1,h}$ of the non defected domain Θ and moreover, the resultant overlapping region ω is the whole Ω_2, thus the space of Lagrange multipliers can be discretized using $\mathcal{T}_{2,h}$ (see Figure 2.6c). This strategy clearly avoids any re-meshing as desired, however it does not fit in our developed framework since Ω_1 is no longer a sub-domain of $\Omega = \Theta \setminus \mathcal{O}$. The drawback of this approach is that, for consistency reasons, we must consider that the partitioning coefficients (α_1, β_1) vanish in $\mathcal{O}$. This is required to guarantee that the problem we solve is equivalent to the original problem, however it clearly spoils the uniqueness of solution of the continuous problem since any function with compact support inside of $\mathcal{O}$ would be solution of the problem with null source term. In consequence, even if at the discrete level a unique solution may exist (assuming that there is no basis function with compact support inside of $\mathcal{O}$), the problem would not be well adapted to develop the error analysis. Finally notice, that the degeneration of the coefficients could be considered in a larger region than $\mathcal{O}$, but in that case we still find the same drawbacks.

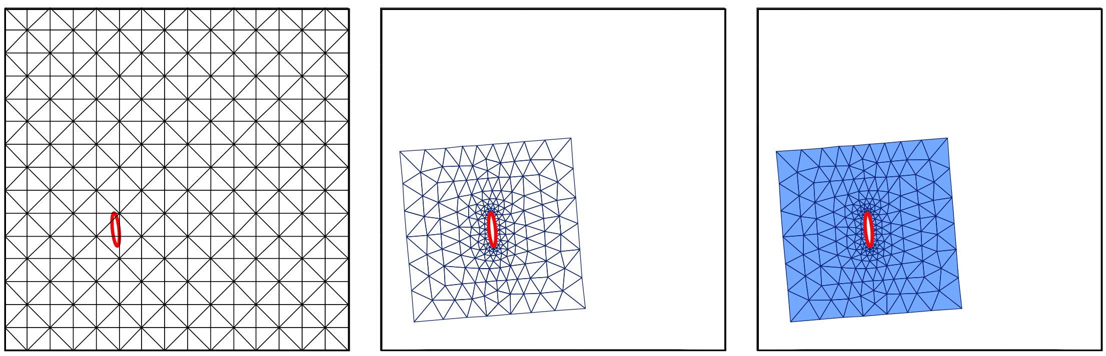

(a) Coarse mesh that ignores the existence of the obstacle.

(b) Fine mesh adapted to the position of the obstacle.

(c) The fine mesh is valid mesh for the overlapping region.

Figure 2.6: Illustration of the strategy classically used in the Arlequin method to avoid re-meshing.

- The approach we will propose to circumvent this issue is to couple the fine and coarse meshes only close to the boundaries of the overlapping region ω as we sketched in Figure 2.7. In

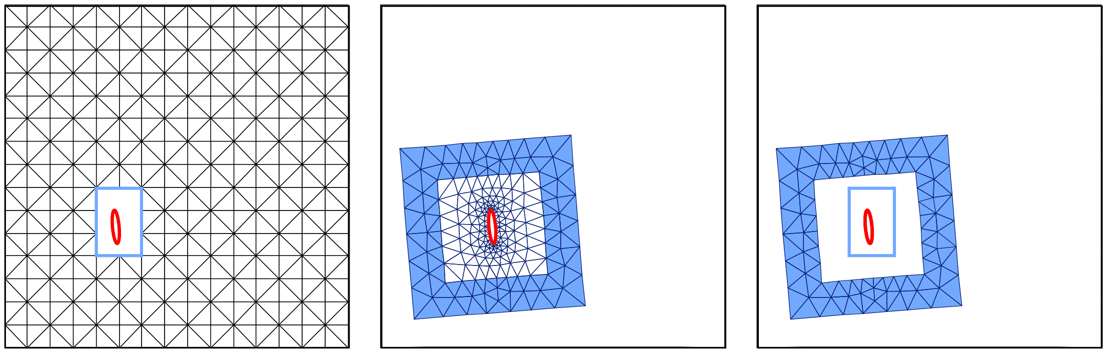

(a) Reduction of the coarse mesh for a new position of the obstacle. In blue we denote the boundary where the coupling occurs.

(b) Fine mesh adapted to the actual position of the obstacle. In blue we denote the region where the volume coupling occurs.

(c) The coupling regions can always be discretized with sub-meshes of the coarse and fine meshes respectively.

Figure 2.7: Illustration of the new decomposition strategy that we will propose to avoid re-meshing. Notice that in this way, the meshes can be easily adapted to any position of the obstacle that is far enough from the exterior boundary of the computational domain.

  this sense we can consider different options where we choose between a boundary coupling where we couple the traces of the solutions (similarly to mortar elements methods, see [5, 6, 7, 55, 56]) and a volume coupling where we impose that the solutions are equal on the volume. In this way we expect that the Lagrange multipliers associated to these constraints can be discretized using the trace (in case of coupling on the boundary) or the restriction (in case of coupling in a volume) of the corresponding coarse or fine meshes (see Figure 2.7). Thus any construction of a mesh of the overlapping region ω would be avoided.

The challenging task of the strategy we aim to introduce is to find suitable and reasonable hypothesis which guaranty that the resultant formulations (depending in the kind of coupling we choose) are all equivalent at the continuous level. Then, after discretization, we will obtain different numerical schemes that we expect to be more flexible in terms of mesh generation. The new schemes will clearly allow the use of independent meshes without modifying any of the meshes nor requiring any re-meshing procedure.

A first step in the pursuit of the desired formulation was given by the interpretation of the Lagrange multiplier presented in Proposition 2.12. Now, we look for suitable conditions that allow us to avoid the contribution of the Lagrange multiplier at least in a part of the matching region ω. Thus we take advantage of the freedom in the choice of the partitioning (only Assumption I.1 is needed) and we provide an extra assumption that simplifies the expression in (2.21). To do so, we introduce a new open sub-domain $\omega_c \subset \omega$ and assume that the two couples of coefficients (α_j, β_j) for $j = 1, 2$ are such that,

$$\alpha_2 - \alpha_1 \;=\; \beta_2 - \beta_1 \;=\; c \quad \text{in} \quad \omega_c, \tag{2.22}$$

for a constant $c \in (-1, 1)$ according to Assumption I.1. Under this assumption, we can compute, for all $m \in H^1(\omega_c)$,

$$\begin{aligned} &- \ell^2 \left((\alpha_2 - \alpha_1)\,\rho\;, u, m\right)_{L^2(\omega_c)} \;+\; \left((\beta_2 - \beta_1)\,\mu\,\nabla u, \nabla m\right)_{L^2(\omega_c)} \\ &\qquad = -\,c\,\ell^2 \left(\rho\, u + \operatorname{div}(\mu\,\nabla u)\;,\, m\right)_{L^2(\omega_c)} \;+\; c\,\langle m, \mu\,\partial_{\boldsymbol{n}_c} u\rangle_{\partial\omega_c} \;=\; c\,\langle m, \mu\,\partial_{\boldsymbol{n}_c} u\rangle_{\partial\omega_c}, \end{aligned} \tag{2.23}$$

where $\boldsymbol{n}_c$ is the outward normal to ω_c. In the following, we will refer to condition (2.22) by the following equivalent assumption (where $2\,C = 1 - c$)

Assumption I.2

We assume that there exists a constant $C \in (0,1)$ such that (α_1, β_1) and (α_2, β_2) satisfy

$$\alpha_1 = \beta_1 = C \quad \text{and} \quad \alpha_2 = \beta_2 = 1 - C \quad \text{in} \quad \omega_c.$$

Then, under this assumption, we can combine Proposition 2.12 and equation (2.23) to obtain an interpretation of the Lagrange multiplier which is independent of $u_{|\omega_c}$. More precisely, λ is solution of the following problem.

$$\left\{ \begin{array}{l} \text{Find } \lambda \in H^1(\omega), \text{ such that } \forall\, m \in H^1(\omega), \\ 2\,(\lambda, m)_{H^1(\omega)} = \; -\,\ell^2 \left((\alpha_2 - \alpha_1)\rho\, u, m\right)_{L^2(\omega\setminus\omega_c)} + \left((\beta_2 - \beta_1)\mu\, \nabla u, \nabla m\right)_{L^2(\omega\setminus\omega_c)} \\ \qquad\qquad + \langle m, \mu\, \partial_{\boldsymbol{n}} u\rangle_{\partial\omega\cap\partial\Omega_2} - \langle m, \mu\, \partial_{\boldsymbol{n}} u\rangle_{\partial\omega\cap\partial\Omega_1} + c\,\langle m, \mu\, \partial_{\boldsymbol{n}_c} u\rangle_{\partial\omega_c}. \end{array} \right. \tag{2.24}$$

This would motivate the introduction of new Lagrange multipliers that are defined inlying the region $\omega \setminus \omega_c$. In accordance, this will also imply a modification in the definition of $b(\cdot,\cdot)$ and therefore in the coupling condition. However, we expect that these changes lead us to new formulations that are equivalent to formulation (2.17). The reader may find this surprising since it seems that we will be just imposing $u_1 = u_2$ in $\omega \setminus \omega_c$ and we have already mentioned that it is important to ensure $u_1 = u_2$ in ω. This question will be addressed in detail for all the new variants later in Lemma 2.26, nevertheless we can already mention that the idea is to use Assumption I.2 to verify that u_1 and u_2 are solution of the same problem in ω_c and since they will be coupled in $\partial\omega_c$ we will obtain also that they are equal in ω_c and therefore in the whole ω. Next, we present the following result which is a consequence of (2.24) and is more convenient for our purposes.

Proposition 2.17

If assumptions I.1 and I.2 are satisfied and $(\boldsymbol{u}, \lambda)$ is a solution of (2.17), then the Lagrange multiplier $\lambda \in H^1(\omega)$ verifies in ω_c the following equality in a distributional sense:

$$\lambda - \Delta\lambda = 0 \qquad \text{in } [\mathcal{D}(\omega_c)]'.$$

Proof. Notice that we are in the hypothesis of Proposition 2.12 and since we are considering Assumption I.2, we can repeat the previous computations in order to obtain (2.24). Then, for any $\varphi \in \mathcal{D}(\omega_c)$ we can consider in problem (2.24) test functions

$$m = \left\{ \begin{array}{lll} 0 & \text{in} & \omega\setminus\omega_c, \\ \varphi & \text{in} & \omega_c, \end{array} \right.$$

and therefore the Lagrange multiplier satisfies $(\lambda, \varphi)_{H^1(\omega_c)} = 0$. In consequence, we obtain the result since

$$(\lambda, \varphi - \Delta\lambda, \varphi)_{L^2(\omega_c)} \;=\; 0, \quad \forall \varphi \in \mathcal{D}(\omega_c).$$

■

In what follows, as we have already mentioned, we will use the previous result to construct alternative formulations to problem (2.17) where the Lagrange multiplier will be related only to the region $\omega \setminus \omega_c$. In consequence, the resultant formulations will depend in the choice of ω_c and will imply the introduction of new Lagrange multipliers that will be related to different parts of ω. Therefore, we need to introduce some notations to clearly specify the decomposition of ω. We first define γ_i and γ_e as the interior and exterior boundaries of ω

$$\gamma_i = \partial\Omega_1 \cap \partial\omega \qquad \text{and} \qquad \gamma_e = \partial\Omega_2 \cap \partial\omega,$$

as well as two disjoint open sub-domains ω_i and ω_e (by disjoint we mean that they have no common boundary $\overline{\omega_i} \cap \overline{\omega_e} = \emptyset$) that represent two regions close to γ_i and γ_e respectively (see Figure 2.8).

These sets are either empty sets or satisfy

$$\gamma_i \subset \partial\omega_i \text{ (resp. } \gamma_e \subset \partial\omega_e) \qquad \text{and} \qquad \gamma_i \cap \overline{\partial\omega_i \backslash \gamma_i} = \emptyset \text{ (resp. } \gamma_e \cap \overline{\partial\omega_e \backslash \gamma_e} = \emptyset).$$

Thus, the already introduced region ω_c where Assumption I.2 must hold, is defined by

$$\omega_c = \omega \setminus \overline{\omega_i \cup \omega_e}.$$

Finally we deduce the alternative formulations that are obtained under Assumption I.2 for different

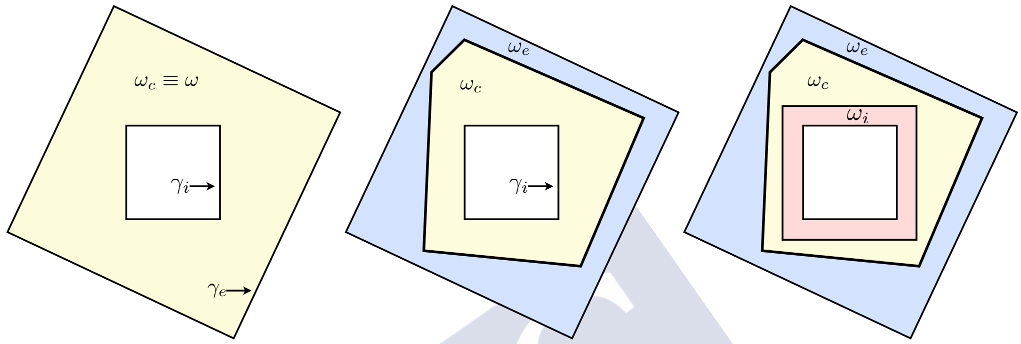

(a) Boundary-Boundary: when $\omega_i = \emptyset$ and $\omega_e = \emptyset$

(b) Boundary-Volume: when $\omega_i = \emptyset$ and $\omega_e \neq \emptyset$

(c) Volume-Volume: when $\omega_i \neq \emptyset$ and $\omega_e \neq \emptyset$

Figure 2.8: Representation of the typical domain decompositions considered for the overlapping region ω.

choices of ω_c. The common advantage of all of the new variants will be that a mesh of ω is not longer needed. Instead, we will need to consider meshes of γ_i, γ_e, ω_i or ω_e which is always possible, since we have the freedom to choose those regions to be conform with sub-meshes of Ω_1 or Ω_2.

2.3.1 Boundary - Boundary coupling (BB)

First of all we notice that in this case we consider

$$\omega_i = \emptyset, \quad \omega_e = \emptyset \quad \text{and} \quad \omega_c = \omega.$$

In consequence, according to Proposition 2.17, we deduce that $\Delta\lambda \in L^2(\omega)$, then the normal derivative of λ is well defined on $\partial\omega$ and also it is possible to use Green's formula. Therefore, for all $m \in H^1(\omega)$ we have that

$$(\lambda, m)_{H^1(\omega)} = (\lambda - \Delta\lambda, m)_{L^2(\omega)} + \langle m, \partial_{\boldsymbol{n}}\lambda\rangle_{\partial\omega} = \langle m, \partial_{\boldsymbol{n}}\lambda\rangle_{\gamma_i} + \langle m, \partial_{\boldsymbol{n}}\lambda\rangle_{\gamma_e},$$

where $\boldsymbol{n}$ is the outward normal to ω and $\langle\cdot,\cdot\rangle_\gamma$ stands for the duality product between $H^{\frac{1}{2}}(\gamma)$ and its dual. Then, since γ_i and γ_e are assumed to be closed and disjoint, one can choose to introduce

$$\lambda_i \equiv \partial_{\boldsymbol{n}}\lambda_{|\gamma_i} \in [H^{\frac{1}{2}}(\gamma_i)]' \quad \text{and} \quad \lambda_e \equiv \partial_{\boldsymbol{n}}\lambda_{|\gamma_e} \in [H^{\frac{1}{2}}(\gamma_e)]'$$

such that

$$(\lambda, m)_{H^1(\omega)} = \langle m, \lambda_i\rangle_{\gamma_i} + \langle m, \lambda_e\rangle_{\gamma_e} \quad \forall m \in H^1(\omega). \tag{2.25}$$

This motivates the modification of problem (2.17) by substituting M and $b(\cdot,\cdot)$ defined in (2.16) with the new couple

$$\begin{aligned} M_{BB} = [H^{\frac{1}{2}}(\gamma_i)]' \times [H^{\frac{1}{2}}(\gamma_e)]' \quad \text{and} \quad & b_{BB} : W \times M_{BB} \longrightarrow \mathbb{R} \quad \text{such that} \\ & b_{BB}(\boldsymbol{v}, \boldsymbol{m}) = \langle v_1 - v_2, m_i\rangle_{\gamma_i} + \langle v_1 - v_2, m_e\rangle_{\gamma_e}. \end{aligned} \tag{2.26}$$

Notice that the modification of (2.17a) is direct consequence of (2.25), while the modification of (2.17b) (that should ensure $u_1 = u_2$ in ω for equivalence with problem (2.17)) is more involved and will be addressed in Lemma 2.26. In the following, we will refer to this kind of coupling as **Boundary - Boundary coupling** and the equivalence of the resultant formulation with respect to formulation (2.17) will be provided later in Theorem 2.27.

Remark 2.18

If Assumptions I.1 and I.2 are satisfied and $(\boldsymbol{u}, \lambda)$ *is a solution of* (2.17)*, we can combine equations* (2.24) *and* (2.25) *to obtain*

$$\langle m, \lambda_e \rangle_{\gamma_e} + \langle m, \lambda_i \rangle_{\gamma_i} = (1-C)\,\langle m, \mu\,\partial_{\boldsymbol{n}} u \rangle_{\gamma_e} - C\,\langle m, \mu\,\partial_{\boldsymbol{n}} u \rangle_{\gamma_i} \qquad \forall m \in H^1(\omega).$$

Therefore, the new Lagrange multipliers are interpreted as

$$\lambda_i \equiv -C\,\mu\,\partial_{\boldsymbol{n}} u_{|\gamma_i} \in [H^{\frac{1}{2}}(\gamma_i)]' \quad \text{and} \quad \lambda_e \equiv (1-C)\,\mu\,\partial_{\boldsymbol{n}} u_{|\gamma_e} \in [H^{\frac{1}{2}}(\gamma_e)]'.$$

The reader may notice, that the resultant alternative formulation has many similarities with mortar techniques (see [5, 6, 7, 55, 56]). However, the main difference is that we present an overlapping domain decomposition technique while in the mortar context overlapping is not considered.

2.3.2 Boundary - Volume coupling (BV)

We proceed in a similar way to the previous case by considering

$$\omega_i = \emptyset, \quad \omega_e \neq \emptyset \quad \text{and} \quad \omega_c = \omega \setminus \omega_e.$$

In consequence, this time Proposition 2.17 allows us to compute for all $m \in H^1(\omega)$ the following equality

$$\begin{aligned}(\lambda, m)_{H^1(\omega)} &= (\lambda, m)_{H^1(\omega_e)} + (\lambda - \Delta\lambda, m)_{L^2(\omega_c)} + \langle m, \partial_{\boldsymbol{n}_c}\lambda \rangle_{\partial\omega_c} \\ &= (\lambda, m)_{H^1(\omega_e)} + \langle m, \partial_{\boldsymbol{n}_c}\lambda \rangle_{\partial\omega_e \setminus \gamma_e} + \langle m, \partial_{\boldsymbol{n}_c}\lambda \rangle_{\gamma_i},\end{aligned}$$

where $\boldsymbol{n}_c$ is the outward normal to ω_c. Then, one can choose to introduce again

$$\lambda_i \equiv \partial_{\boldsymbol{n}_c}\lambda_{|\gamma_i} \in [H^{\frac{1}{2}}(\gamma_i)]' \qquad (\text{notice } \boldsymbol{n} = \boldsymbol{n}_c \text{ on } \gamma_i)$$

and a new $\lambda_e \in H^1(\omega_e)$ which is the unique solution of

$$(\lambda_e, m_e)_{H^1(\omega_e)} = (\lambda, m_e)_{H^1(\omega_e)} + \langle m_e, \partial_{\boldsymbol{n}_c}\lambda \rangle_{\partial\omega_e \setminus \gamma_e} \quad \forall m_e \in H^1(\omega_e).$$

In consequence

$$(\lambda, m)_{H^1(\omega)} = \langle m, \lambda_i \rangle_{\gamma_i} + (\lambda_e, m)_{H^1(\omega_e)} \quad \forall m \in H^1(\omega) \tag{2.27}$$

and this motivates the modification of problem (2.17) by substituting M and $b(\cdot,\cdot)$ defined by (2.16) with the new couple

$$\begin{aligned}&M_{BV} = [H^{\frac{1}{2}}(\gamma_i)]' \times H^1(\omega_e) \quad \text{and} \quad b_{BV} : W \times M_{BV} \longrightarrow \mathbb{R} \quad \text{such that} \\ &\qquad\qquad b_{BV}(\boldsymbol{v}, \boldsymbol{m}) = \langle v_1 - v_2, m_i \rangle_{\gamma_i} + (v_1 - v_2, m_e)_{H^1(\omega_e)}.\end{aligned} \tag{2.28}$$

Notice that the modification of (2.17a) is direct consequence of (2.27), while the modification of (2.17b) (that should ensure $u_1 = u_2$ in ω for equivalence with problem (2.17)) is more involved and will be addressed in Lemma 2.26. In the following, we will refer to this kind of coupling as **Boundary - Volume coupling** and the equivalence of the resultant formulation with respect to formulation (2.17) will be provided later in Theorem 2.27.

Remark 2.19

If Assumptions I.1 and I.2 are satisfied and $(\boldsymbol{u}, \lambda)$ *is a solution of* (2.17)*, we can combine* *equations (2.24) and (2.27) to obtain*

$$2(\lambda_e, m)_{H^1(\omega_e)} + 2\langle\lambda_i, m\rangle_{\gamma_i} = -\,\ell^2\left((\alpha_2-\alpha_1)\,\rho\,u, m\right)_{L^2(\omega_e)} + \left((\beta_2-\beta_1)\,\mu\,\nabla u, \nabla m\right)_{L^2(\omega_e)}$$
$$+\langle m, \mu\,\partial_{\boldsymbol{n}} u\rangle_{\gamma_e} + (1-2\,C)\langle m, \mu\,\partial_{\boldsymbol{n}_c} u\rangle_{\partial\omega_e\setminus\gamma_e} - 2\,C\,\langle m, \mu\,\partial_{\boldsymbol{n}} u\rangle_{\gamma_i}, \qquad \forall m \in H^1(\omega)$$

where $\boldsymbol{n}$ and $\boldsymbol{n}_c$ are the outward normals of ω and ω_c respectively. Therefore the new Lagrange multipliers are interpreted as $\lambda_i \equiv -C\,\mu\,\partial_{\boldsymbol{n}} u_{|\gamma_i} \in [H^{\frac{1}{2}}(\gamma_i)]'$ and $\lambda_e \in H^1(\omega_e)$ satisfying

$$\begin{aligned}2(\lambda_e, m_e)_{H^1(\omega_e)} = &-\,\ell^2\left((\alpha_2-\alpha_1)\,\rho\,u, m_e\right)_{L^2(\omega_e)} + \left((\beta_2-\beta_1)\,\mu\,\nabla u, \nabla m_e\right)_{L^2(\omega_e)}\\ &+\langle m_e, \mu\,\partial_{\boldsymbol{n}} u\rangle_{\gamma_e} + (1-2\,C)\langle m_e, \mu\,\partial_{\boldsymbol{n}_c} u\rangle_{\partial\omega_e\setminus\gamma_e}, \qquad \forall m_e \in H^1(\omega_e).\end{aligned} \tag{2.29}$$

Notice that in the previous remark and similarly to Corollary 2.13, the interpretation of the Lagrange multiplier λ_e could be further developed in those situations where $\operatorname{div}\big((\beta_2-\beta_1)\mu\,\nabla u\big)$ belongs to $L^2(\omega_e)$, which allows to apply Green's formula in (2.29).

2.3.3 Volume - Boundary coupling (VB)

Notice that in the previous case we have arbitrarily chosen $\omega_e \neq \emptyset$ and $\omega_i = \emptyset$. However, a similar treatment can be done when

$$\omega_i \neq \emptyset, \quad \omega_e = \emptyset \quad \text{and} \quad \omega_c = \omega \setminus \omega_i.$$

In consequence in this case, problem (2.17) should be modified by substituting M and $b(\cdot,\cdot)$ defined by (2.16) with the new couple

$$\begin{aligned}M_{VB} = H^1(\omega_i) \times [H^{\frac{1}{2}}(\gamma_e)]' \quad \text{and} \quad & b_{VB} : W \times M_{VB} \longrightarrow \mathbb{R} \quad \text{such that}\\ & b_{VB}(\boldsymbol{v}, \boldsymbol{m}) = (v_1 - v_2, m_i)_{H^1(\omega_i)} + \langle v_1 - v_2, m_e\rangle_{\gamma_e}.\end{aligned} \tag{2.30}$$

In the following, we will refer to this kind of coupling as **Volume - Boundary coupling** and the equivalence of the resultant formulation with respect to formulation (2.17) will be addressed later in Theorem 2.27.

Remark 2.20

If Assumptions I.1 and I.2 are satisfied and $(\boldsymbol{u}, \lambda)$ is a solution of (2.17), we can interpret the new Lagrange multipliers as $\lambda_e \equiv (1-C)\,\mu\,\partial_{\boldsymbol{n}} u_{|\gamma_e} \in [H^{\frac{1}{2}}(\gamma_e)]'$ and $\lambda_i \in H^1(\omega_i)$ satisfying

$$\begin{aligned}2(\lambda_i, m_i)_{H^1(\omega_i)} = &-\,\ell^2\left((\alpha_2-\alpha_1)\,\rho\,u, m_i\right)_{L^2(\omega_i)} + \left((\beta_2-\beta_1)\,\mu\,\nabla u, \nabla m_i\right)_{L^2(\omega_i)}\\ &-\langle m_i, \mu\,\partial_{\boldsymbol{n}} u\rangle_{\gamma_i} + (1-2\,C)\langle m_i, \mu\,\partial_{\boldsymbol{n}_c} u\rangle_{\partial\omega_i\setminus\gamma_i}, \qquad \forall m_i \in H^1(\omega_i).\end{aligned} \tag{2.31}$$

As we have mentioned after Remark 2.19, when $\operatorname{div}\big((\beta_2-\beta_1)\mu\,\nabla u\big) \in L^2(\omega_i)$, Greens formula can be applied to (2.31) and thus an interpretation of λ_i is derived similarly to Corollary 2.13.

2.3.4 Volume - Volume coupling (VV)

Finally we consider the case when

$$\omega_i \neq \emptyset, \quad \omega_e \neq \emptyset \quad \text{and} \quad \omega_c = \omega \setminus (\omega_i \cup \omega_e).$$

Then, similar ideas lead to the introduction of $(\lambda_i, \lambda_e) \in H^1(\omega_i) \times H^1(\omega_e)$ and to the modification of problem (2.17) by substituting M and $b(\cdot,\cdot)$ defined by (2.16) with the new couple

$$\begin{aligned}M_{VV} = H^1(\omega_i) \times H^1(\omega_e) \quad \text{and} \quad & b_{VV} : W \times M_{VV} \longrightarrow \mathbb{R} \quad \text{such that}\\ & b_{VV}(\boldsymbol{v}, \boldsymbol{m}) = (v_1 - v_2, m_i)_{H^1(\omega_i)} + (v_1 - v_2, m_e)_{H^1(\omega_e)}.\end{aligned} \tag{2.32}$$

In the following, we will refer to this kind of coupling as **Volume - Volume coupling** and the equivalence of the resultant formulation with respect to problem (2.17) will be addressed later in Theorem 2.27.

Remark 2.21

If Assumptions I.1 and I.2 are satisfied and $(\boldsymbol{u}, \lambda)$ *is a solution of* (2.17)*, we can interpret the new Lagrange multipliers as* $\lambda_e \in H^1(\omega_e)$ *satisfying equation* (2.29) *and* $\lambda_i \in H^1(\omega_i)$ *satisfying equation* (2.31).

2.3.5 Abstract analysis of new Arlequin formulations

Next, we unify the notation and give an abstract setting that embrace all the Arlequin variants. With this purpose we consider the kind of formulation used in problem (2.17) but, in order to distinguish between the different kind of couplings that we have presented up to now, we choose to introduce the subscript C that refers to the applied coupling. Thus, all the formulations presented fit in the following abstract setting

$$\left\{\begin{aligned} &\text{Find } (\boldsymbol{u},\boldsymbol{\lambda}) \in W \times M_C, \text{ such that} \\ &-\ell^2\, m(\boldsymbol{u},\boldsymbol{v}) \;+\; a(\boldsymbol{u},\boldsymbol{v}) \;+\; b_C(\boldsymbol{v},\boldsymbol{\lambda}) \;=\; g(\boldsymbol{v}), \qquad \forall \boldsymbol{v}\in W, && (2.33\text{a}) \\ &\qquad\qquad\qquad\qquad\qquad\quad b_C(\boldsymbol{u},\boldsymbol{m}) \;=\; 0, \qquad \forall \boldsymbol{m} \in M_C, && (2.33\text{b}) \end{aligned}\right.$$

where the functional space $W = H^1(\Omega_1) \times H^1(\Omega_2)$ (already defined in (2.9)) does not depend in the type of coupling, as well as the mass and stiffness bilinear forms and the source term (already defined in (2.11), (2.12) and (2.13))

$$m : W \times W \longrightarrow \mathbb{R} \qquad \text{such that} \qquad m(\boldsymbol{u},\boldsymbol{v}) = \sum_{j=1}^{2} (\alpha_j\, \rho\, u_j, v_j)_{L^2(\Omega_j)}, \tag{2.34}$$

$$a : W \times W \longrightarrow \mathbb{R} \qquad \text{such that} \qquad a(\boldsymbol{u},\boldsymbol{v}) = \sum_{j=1}^{2} (\beta_j\, \mu\, \nabla u_j, \nabla v_j)_{L^2(\Omega_j)}, \tag{2.35}$$

$$g : W \longrightarrow \mathbb{R} \qquad \text{such that} \qquad g(\boldsymbol{v}) = (f, v_1)_{L^2(\Omega_1 \setminus \Omega_2)}. \tag{2.36}$$

Then, the only novelties lie in the definition of the Lagrange multiplier space M_C and the coupling bilinear form

$$b_C : W \times M_C \longrightarrow \mathbb{R} \tag{2.37}$$

which actually distinguish between the couplings. The different choices have been presented already in (2.26), (2.28), (2.30) and (2.32), however we recast here their definition in order to summarize

$$M_{BB} = [H^{\frac{1}{2}}(\gamma_i)]' \times [H^{\frac{1}{2}}(\gamma_e)]', \qquad b_{BB}(\boldsymbol{v},\boldsymbol{m}) = \langle v_1 - v_2, m_i\rangle_{\gamma_i} + \langle v_1 - v_2, m_e\rangle_{\gamma_e}.$$

$$M_{BV} = [H^{\frac{1}{2}}(\gamma_i)]' \times H^1(\omega_e), \qquad b_{BV}(\boldsymbol{v},\boldsymbol{m}) = \langle v_1 - v_2, m_i\rangle_{\gamma_i} + (v_1 - v_2, m_e)_{H^1(\omega_e)}.$$

$$M_{VB} = H^1(\omega_i) \times [H^{\frac{1}{2}}(\gamma_e)]', \qquad b_{VB}(\boldsymbol{v},\boldsymbol{m}) = (v_1 - v_2, m_i)_{H^1(\omega_i)} + \langle v_1 - v_2, m_e\rangle_{\gamma_e}.$$

$$M_{VV} = H^1(\omega_i) \times H^1(\omega_e), \qquad b_{VV}(\boldsymbol{v},\boldsymbol{m}) = (v_1 - v_2, m_i)_{H^1(\omega_i)} + (v_1 - v_2, m_e)_{H^1(\omega_e)}.$$

It should be clear that the notation does not specify the definition of the partitioning (α_j, β_j), neither the decomposition of ω, but according to the kind of coupling we want to use there are some restrictions (see Assumptions I.1 and I.2 and Figure 2.8). Notice that, in order to include also the classic Arlequin formulation into this abstract framework, we may also introduce (considering definition (2.16))

$$M_V = M = H^1(\omega), \qquad b_V(\boldsymbol{v}, \boldsymbol{m}) = b(\boldsymbol{v}, \boldsymbol{m}) = (v_1 - v_2, m)_{H^1(\omega)},$$

where we have made a small abuse of notation since in that case $\boldsymbol{\lambda}$ and $\boldsymbol{m}$ represent scalar fields (instead of vector fields). We shall also remark that these new bilinear forms are all continuous.

Proposition 2.22

The bilinear forms $b_C(\cdot,\cdot)$ are continuous, this is to say that there exist positive constants $K_{b,C}$ such that

$$|b_C(\boldsymbol{v}, \boldsymbol{m})| \leq K_{b,C} \|\boldsymbol{v}\|_1 \|\boldsymbol{m}\|_{M_C} \quad \textit{for all} \quad (\boldsymbol{v}, \boldsymbol{m}) \in W \times M_C.$$

Finally, we analyse the existence of solution of problem (2.33) by relating it to problem (2.17). This time, unlike in previous results (theorems 2.5 and 2.11), we need to introduce the following assumption.

Assumption I.3

We assume that ℓ^2 is not an eigenvalue of the eigenvalue problem

$$\left\{ \begin{array}{l} \textit{Find } \nu \in \mathbb{R} \textit{ and } u \in H^1_0(\omega_c)\backslash\{0\}, \textit{ such that} \\[2ex] (\mu \nabla u, \nabla v)_{L^2(\omega_c)} \;=\; \nu \; (\rho\, u, v)_{L^2(\omega_c)} \quad \forall\, v \in H^1_0(\omega_c). \end{array} \right. \tag{2.38}$$

Remark 2.23

Notice that in the case we consider the classical Arlequin coupling, the region ω_c is considered to be empty and therefore Assumption I.3 is not restrictive.

Remark 2.24

The reader should notice that Assumption I.3 is restrictive compared to classical techniques. However, we remark that Assumption I.3 would not be required for a coercive problem and will not have an equivalent in Chapter 3 where we extend the Arlequin methods to the case of the transient wave equation.

To remark that the introduction of Assumption I.3 is essential, we show in the following result that if a solution of problem (2.38) exists, then we can build a non trivial solution of problem (2.33) with vanishing source term.

Theorem 2.25

If Assumption I.3 does not hold, then there exist non trivial solutions of problem (2.33) *with vanishing source term.*

Proof. Let us begin, by noticing that if Assumption I.3 does not hold, then there exists an eigenpair (ℓ^2, u_c) solution of problem (2.38) and to conclude we show how we can build a non trivial solution $(\boldsymbol{u}^\star, \boldsymbol{\lambda}^\star)$ of problem (2.33) with vanishing source term. To do so, we first define $\boldsymbol{\lambda}^\star = (\lambda_i^\star, \lambda_e^\star) \in M_C$ such that, for $j \in \{i, e\}$ and $\boldsymbol{n}_c$ the outward normal to ω_c:

$$\text{if} \quad \omega_j = \emptyset: \quad \lambda_j^\star \in [H^{\frac{1}{2}}(\gamma_j)]' \quad \text{defined as} \quad \lambda_j^\star = -\,\mu\,\partial_{\boldsymbol{n}_c} u_c,$$

$$\text{if} \quad \omega_j \neq \emptyset: \quad \lambda_j^\star \in H^1(\omega_j) \quad \text{solution of} \quad (\lambda_j^\star, w)_{H^1(\omega_j)} = -\,\langle w, \mu\,\partial_{\boldsymbol{n}_c} u_c\rangle_{\partial\omega_j \cap \partial\omega_c}, \quad \forall w \in H^1(\omega_j).$$

In consequence, notice that

$$b_C(\boldsymbol{v}, \boldsymbol{\lambda}^\star) = -\,\langle v_1 - v_2, \mu\,\partial_{\boldsymbol{n}_c} u_c\rangle_{\partial\omega_c}, \qquad \forall \boldsymbol{v} \in W.$$

Then, if we denote again $\mathtt{E}(\cdot)$ the trivial extension by zero to Ω, we can simply define $\boldsymbol{u}^\star = (u_1^\star, u_2^\star)$ as

$$u_1^\star = \frac{\mathtt{E}(u_c)_{|\Omega_1}}{C} \qquad \text{and} \qquad u_2^\star = -\frac{\mathtt{E}(u_c)_{|\Omega_2}}{1-C} \qquad \text{with } C \text{ given by Assumption I.2.}$$

Thus, it is clear that (2.33b) holds (since u_c is supported in ω_c) and only remains to check if also (2.33a) holds. To do so we consider any test function $\boldsymbol{v} \in W$ and compute

$$\begin{aligned} -\ell^2\, m(\boldsymbol{u}^\star, \boldsymbol{v}) + a(\boldsymbol{u}^\star, \boldsymbol{v}) \quad &= \quad -\ell^2(\rho\, u_c, v_1)_{L^2(\omega_c)} + (\mu\, \nabla u_c, \nabla v_1)_{L^2(\omega_c)} \\ &\quad\; + \ell^2(\rho\, u_c, v_2)_{L^2(\omega_c)} - (\mu\, \nabla u_c, \nabla v_2)_{L^2(\omega_c)}. \end{aligned}$$

Then, integrating by parts in ω_c and using that (ℓ^2, u_c) is solution of problem (2.38) we obtain

$$-\ell^2\, m(\boldsymbol{u}^\star, \boldsymbol{v}) + a(\boldsymbol{u}^\star, \boldsymbol{v}) = \langle v_1, \mu\, \nabla u_c \cdot \boldsymbol{n}_c \rangle_{\partial\omega_c} - \langle v_2, \mu\, \nabla u_c \cdot \boldsymbol{n}_c \rangle_{\partial\omega_c} = -\, b_C(\boldsymbol{v}, \boldsymbol{\lambda}^\star).$$

Thus $(\boldsymbol{u}^\star, \boldsymbol{\lambda}^\star)$ is solution of problem (2.33) with vanishing source term.

■

Now that we have justified the introduction of Assumption I.3, let us present the following lemma which verifies that the new formulations are enough to guarantee the coupling in the whole overlapping region ω.

Lemma 2.26

If Assumptions I.1, I.2 and I.3 are satisfied and $(\boldsymbol{u}, \boldsymbol{\lambda})$ *is a solution of problem* (2.33)*, then we have that* $u_1 = u_2$ *in the whole overlapping region* ω*.*

Proof. First notice that in any case, equation (2.33b) implies that $u_1 = u_2$ in the region $\omega \setminus \omega_c$ and since both functions have a trace, the equality holds up to the boundary. Moreover, taking into account Assumption I.2, we can choose test functions in (2.33a) such that $v_1 = w/C \in H_0^1(\omega_c)$ and $v_2 = -w/(1-C) \in H_0^1(\omega_c)$, thus we obtain

$$-\,\ell^2\left(\rho\,(u_1 - u_2), w\right)_{L^2(\omega_c)} \;+\; \left(\mu\,\nabla(u_1 - u_2), \nabla w\right)_{L^2(\omega_c)} \;=\; 0, \quad \forall w \in H_0^1(\omega_c)$$

which implies that $u_1 - u_2$ is identically 0 in the region ω_c since otherwise ℓ^2 would be an eigenvalue of problem (2.38) and by Assumption I.3 this is not possible. Thus we have $u_1 = u_2$ also in the region ω_c and the proof is concluded since $\boldsymbol{u} \in H^1(\Omega_1) \times H^1(\Omega_2)$.

■

Then, we proceed to analyse the existence of solution of problem (2.33). Notice that we could proceed similarly to the classic Arlequin coupling (see Theorem 2.11) by proving for each new coupling an adequate *Inf-Sup condition* as in Lemma 2.7. However, we prefer to provide a different approach where we take advantage of the relation with respect to problem (2.17).

Theorem 2.27

If Assumptions I.1, I.2 and I.3 are satisfied, then problems (2.17) *and* (2.33) *are equivalent in the sense that*

$$(\boldsymbol{u}, \lambda(\boldsymbol{u})) \text{ is a solution of } (2.17) \quad \Longleftrightarrow \quad (\boldsymbol{u}, \boldsymbol{\lambda}(\boldsymbol{u})) \text{ is a solution of } (2.33),$$

where $\lambda(\boldsymbol{u})$ *and* $\boldsymbol{\lambda}(\boldsymbol{u})$ *are uniquely defined by* (2.17a) *and* (2.33a) *respectively. In consequence, existence and uniqueness of solution for problem* (2.33) *is given by Theorem 2.1.*

Proof. Let $(\boldsymbol{u}, \lambda)$ be solution of problem (2.17). Then, it is clear that $\boldsymbol{u}$ satisfies equation (2.33b). Moreover, we can define $\boldsymbol{\lambda} = (\lambda_i, \lambda_e) \in M_C$ where $\lambda_i = \partial_{\boldsymbol{n}} \lambda_{|\gamma_i}$ (respectively $\lambda_e = \partial_{\boldsymbol{n}} \lambda_{|\gamma_e}$) if the coupling is of boundary type or, in case the coupling is of volume type, as $\lambda_i \in H^1(\omega_i)$

(respectively $\lambda_e \in H^1(\omega_e)$) the unique solution of

$$\begin{aligned} (\lambda_i, m_i)_{H^1(\omega_i)} &= (\lambda, m_i)_{H^1(\omega_i)} + \langle m_i, \partial_{\boldsymbol{n}_c}\lambda\rangle_{\partial\omega_i\setminus\gamma_i}, \quad \forall m_i \in H^1(\omega_i), \\ \text{(respectively)} \quad (\lambda_e, m_e)_{H^1(\omega_e)} &= (\lambda, m_e)_{H^1(\omega_e)} + \langle m_e, \partial_{\boldsymbol{n}_c}\lambda\rangle_{\partial\omega_e\setminus\gamma_e}, \quad \forall m_e \in H^1(\omega_e), \end{aligned}$$

where $\boldsymbol{n}_c$ is the outward normal to ω_c. Then, due to the Assumptions I.1 and I.2 we can consider Proposition 2.17 and therefore integrating by parts in ω_c we obtain

$$b(\boldsymbol{v}, \lambda) = (v_1 - v_2, \lambda)_{H^1(\omega)} = (v_1 - v_2, \lambda)_{H^1(\omega\setminus\omega_c)} + \langle v_1 - v_2, \partial_{\boldsymbol{n}_c}\lambda\rangle_{\partial\omega_c}, \qquad \forall \boldsymbol{v} \in W.$$

Now, it is important to notice that depending on the kind of coupling, we obtain

$$\begin{aligned} b(\boldsymbol{v}, \lambda) &= \langle v_1 - v_2, \lambda_i\rangle_{\gamma_i} + \langle v_1 - v_2, \lambda_e\rangle_{\gamma_e} &&= b_{BB}(\boldsymbol{v}, \boldsymbol{\lambda}) \\ b(\boldsymbol{v}, \lambda) &= \langle v_1 - v_2, \lambda_i\rangle_{\gamma_i} + (v_1 - v_2, \lambda_e)_{H^1(\omega_e)} &&= b_{BV}(\boldsymbol{v}, \boldsymbol{\lambda}) \\ b(\boldsymbol{v}, \lambda) &= (v_1 - v_2, \lambda_i)_{H^1(\omega_i)} + \langle v_1 - v_2, \lambda_e\rangle_{\gamma_e} &&= b_{VB}(\boldsymbol{v}, \boldsymbol{\lambda}) \\ b(\boldsymbol{v}, \lambda) &= (v_1 - v_2, \lambda_i)_{H^1(\omega_i)} + (v_1 - v_2, \lambda_e)_{H^1(\omega_e)} &&= b_{VV}(\boldsymbol{v}, \boldsymbol{\lambda}). \end{aligned}$$

In consequence, equation (2.33a) becomes exactly equation (2.17a) and then $(\boldsymbol{u}, \boldsymbol{\lambda})$ is solution of problem (2.33).

Now, to prove the reverse, let $(\boldsymbol{u}, \boldsymbol{\lambda})$ be solution of problem (2.33). Then, according to Lemma 2.26 we have that $u_1 = u_2$ in the whole overlapping region ω. Thus $\boldsymbol{u}$ satisfies equation (2.17b). Moreover, we can find $\lambda \in H^1(\omega)$ such that (notice $b_C(\cdot, \cdot)$ depends in $(v_1 - v_2)_{|\omega\setminus\omega_c}$)

$$(\lambda, v_1 - v_2)_{H^1(\omega)} = b_C(\boldsymbol{v}, \boldsymbol{\lambda}) \qquad \forall \boldsymbol{v} \in W$$

and in consequence equation (2.17a) becomes exactly equation (2.33a). And therefore $(\boldsymbol{u}, \lambda)$ is solution of problem (2.17).

■

We provide not the regularity result of the solutions of problems (2.33). These results depend on the regularity of the data and the regularity of the different domains involved. Notice that, for the primal variable $\boldsymbol{u}$, as well as the volume multipliers, the regularity we presented is a consequence of the classical results in [44, 45]. On the other hand, for the boundary multipliers, the regularity is consequence of the regularity of the primal variable as well as the normal vector (for the regularity in polygonal domains, where boundary multipliers may be discontinuous, we refer to [57]).

Theorem 2.28

Let us consider $f \in H^s(\Omega)$ for $s \geq 0$, ρ, μ smooth enough and a solution $(\boldsymbol{u}, \lambda)$ of problem (2.33), then the primal variable $\boldsymbol{u}$ has the regularity described in Theorem 2.2 while for the Lagrange multipliers we shall distinguish between boundary type or volume type:

- *When $\omega_j = \emptyset$ for $j \in \{i, e\}$*
  - *If $\gamma_j \in \mathcal{C}^\infty$, we have $\lambda_j \in H^{s+\frac{1}{2}}(\gamma_j)$.*
  - *If γ_j is polygonal, we have $\lambda_j \in H^{\frac{1}{2}-\varepsilon}(\gamma_j)$ for $\varepsilon > 0$.*
- *When $\omega_j \neq \emptyset$ for $j \in \{i, e\}$ and α_k, β_k for $k \in \{1, 2\}$ smooth enough, then:*
  - *For any open set ϱ such that $\overline{\varrho} \subset \omega_j$, we have $\lambda_j \in H^{s+2}(\varrho)$.*
  - *If $\partial\omega_j \in \mathcal{C}^\infty$, we have $\lambda_j \in H^{s+2}(\omega_j)$.*
  - *In 2D, if $\partial\omega_j$ is polygonal which largest interior angle is $\frac{2\pi}{\kappa}$ for $\kappa > 1$, we have $\lambda_j = \lambda_{s,j} + \lambda_{\sigma,j}$ where $\lambda_{s,j} \in H^{s+2}(\omega_j)$ and $\lambda_{\sigma,j} \in H^\sigma(\omega_j)$ for all $\sigma < 1 + \frac{\kappa}{2}$.*

Remark 2.29

Let us recall remarks 2.15 and 2.16 in order note that in a similar way, the regularity of the new Lagrange multipliers depends only on the regularity of the source and the choice of the domain decomposition.

Notice that, as we commented after Theorem 2.5, if we choose an approach where we do not use the relation between problem (2.33) and problem (2.17), then conditions (2.5) and (2.6) as well as Assumption I.2 might seem unnecessary. However, as we have already seen, they are important in order to guarantee that the formulations we have presented are actually equivalent. Moreover, it might also seem that with such approach Assumption I.3 is not necessary, but in fact, it will be implicitly considered in the first step of the two steps procedure that we sketch next:
Setp 1: We must first analyse the existence of solution of the following problem (notice it is a modification of (2.10))

$$\begin{cases} \text{Find } \boldsymbol{u} \in V_C, \text{ such that } \forall\, \boldsymbol{v} \in V_C, \\ \\ -\,\ell^2\, m(\boldsymbol{u},\boldsymbol{v}) \;+\; a(\boldsymbol{u},\boldsymbol{v}) \;=\; g(\boldsymbol{v}), \end{cases} \tag{2.39}$$

in the constrained space (modification of (2.9))

$$V_C = \{\boldsymbol{v} \in W \;/\; b_C(\boldsymbol{v},\boldsymbol{m}) = 0,\ \forall \boldsymbol{m} \in M_C\}. \tag{2.40}$$

This is classically done by application of Fredholm's Alternative as we show in the next theorem. It should be clear that the eigenvalues mentioned in Assumption I.3 would also be eigenvalues of the following eigenvalue problem set in V_C.

Theorem 2.30

Let us consider the eigenvalue problem

$$\begin{cases} \text{Find } \nu \in \mathbb{R} \text{ and } \boldsymbol{u} \in V_C\backslash\{0\}, \text{ such that} \\ \\ a(\boldsymbol{u},\boldsymbol{v}) \;=\; \nu\, m(\boldsymbol{u},\boldsymbol{v}) \quad \forall\, \boldsymbol{v} \in V_C, \end{cases} \tag{2.41}$$

then, problem (2.39) *has a unique solution in* V_C*, if and only if,* ℓ^2 *is not an eigenvalue of* (2.41)*. However, if* ℓ^2 *is an eigenvalue of* (2.41) *but* $(f,\boldsymbol{v})_{L^2(\Omega)} = 0$ *for all* $\boldsymbol{v} \in V_C^\ell$ *where* V_C^ℓ *denotes the subspace of eigenfunctions associated to* $\nu = \ell^2$*, then there exists a solution which is unique up to an element of* V_C^ℓ*.*

Step 2: Then, the second step would be to find $\boldsymbol{\lambda}$ uniquely defined by $\boldsymbol{u}$. This is similar to what we have already done in Theorem 2.11 and requires for each $b_C(\cdot,\cdot)$ the verification of an *Inf-Sup condition* like the one in Lemma 2.7. This is the approach we choose to follow in the next section for the discrete formulations since the resultant discrete roblems will no longer be equivalent. Therefore we can not analyse the existence of solution by relating it directly to the solution of the discretized Helmholtz problem.

Remark 2.31

Notice that we have analysed problem (2.33) *by relating it to problem* (2.17) *instead of using the process we have sketched above. Therefore, for the new choices of* M_C *and* $b_C(\cdot,\cdot)$*, we have avoided the verification of an Inf-Sup condition like the one in Lemma 2.7. Nevertheless, it is interesting to remark that an adequate Inf-Sup condition holds also for this new couplings.*

2.4 The Arlequin discrete formulation

This section is devoted to the development and analysis of a Galerkin discretization of all the different variants of the Arlequin method that we have presented up to now. For the sake of compactness we will focus on the abstract formulation (2.33). However, we should notice that after discretization, each kind of coupling will provide a different discrete scheme. In order to simplify the analysis and since our main interest is to study the Arlequin couplings, we assume that all the forms introduced are exactly evaluated although the proposed approach is compatible with quadrature rules. The interest of considering quadrature rules is related on the one hand to the evaluation of the source term and on the other hand to provide mass lumping at least far of the overlapping region ω. Notice that the compatibility with mass lumping techniques applied also in the overlapping region seems not possible since we must capture the jumps of the coefficients ($\alpha_1, \alpha_2, \beta_1$ and β_2). For a detailed analysis concerning the use of quadrature rules we refer to [21, 22, 24, 58] and the references therein.

2.4.1 Galerkin discretization

The consideration of adequate discretizations of the problems that fit into the Arlequin abstract formulation (2.33) relies first in the introduction of finite dimensional approximations of the spaces W and M_C that will be denoted by W_h and $M_{C,h}$. Then we obtain the following discrete scheme of the problems that fit into the Arlequin abstract formulation (2.33).

$$\begin{cases} \text{Find } (\boldsymbol{u}_h, \boldsymbol{\lambda}_h) \in W_h \times M_{C,h}, \quad \text{such that} \\ -\,\ell^2\, m(\boldsymbol{u}_h, \boldsymbol{v}_h) \;+\; a(\boldsymbol{u}_h, \boldsymbol{v}_h) \;+\; b_C(\boldsymbol{v}_h, \boldsymbol{\lambda}_h) \;=\; g(\boldsymbol{v}_h), \quad \forall \boldsymbol{v}_h \in W_h, & \text{(2.42a)} \\ \qquad\qquad b_C(\boldsymbol{u}_h, \boldsymbol{m}_h) \;=\; 0, \qquad \forall \boldsymbol{m}_h \in M_{C,h}. & \text{(2.42b)} \end{cases}$$

However, the choice of these spaces must provide an adequate framework to analyse the existence of solution of the previous problem as well as its convergence to problem (2.33). These questions are linked to the following properties.

(P.1) We consider $W_h \subset W$ such that it provides a good approximation in the sense that for all $\boldsymbol{v} \in W$ there exists a sequence $(\boldsymbol{v}_h)_h \subset W$ that for each h we have $\boldsymbol{v}_h \in W_h$ and the sequence verifies

$$\lim_{h \to 0} \|\boldsymbol{v} - \boldsymbol{v}_h\|_1 = 0.$$

(P.2) Similarly, we consider $M_{C,h} \subset M_C$ such that for all $\boldsymbol{m} \in M_C$ there exists a sequence $(\boldsymbol{m}_h)_h \subset M_C$ that for each h we have $\boldsymbol{m}_h \in M_{C,h}$ and the sequence verifies

$$\lim_{h \to 0} \|\boldsymbol{m} - \boldsymbol{m}_h\|_{M_C} = 0.$$

(P.3) An uniform *discrete Inf-Sup condition* is satisfied: there exists a constant $\delta > 0$ independent of h and such that

$$\inf_{\boldsymbol{m}_h \in M_{C,h}} \sup_{\boldsymbol{v}_h \in W_h} \frac{|b_C(\boldsymbol{v}_h, \boldsymbol{m}_h)|}{\|\boldsymbol{m}_h\|_{M_C}\ \|\boldsymbol{v}_h\|_1} \;\geq\; \delta \;>\; 0.$$

In order to justify their importance and before we provide the specific choices that we have made to build the discrete spaces W_h and $M_{C,h}$, we will just assume that these conditions hold to then exhibit that they actually provide a good framework for the numerical analysis of the method.

2.4.2 Well posedness of the discrete problems

In this section we analyse the existence of solution of problem (2.42) assuming that the property **(P.3)** is satisfied. We will proceed in the classical way described at the end of Section 2.3. In consequence, we will first analyse the existence of solution in a discrete version of problem (2.39), that is to say, the existence of solution of the following discrete problem

$$\begin{cases} \text{Find } \boldsymbol{u}_h \in V_{C,h}, \text{ such that } \forall\, \boldsymbol{v}_h \in V_{C,h}, \\ -\,\ell^2\, m(\boldsymbol{u}_h, \boldsymbol{v}_h) \;+\; a(\boldsymbol{u}_h, \boldsymbol{v}_h) \;=\; g(\boldsymbol{v}_h), \end{cases} \tag{2.43}$$

which is set in the constrained space

$$V_{C,h} = \{\boldsymbol{v}_h \in W_h \ / \ b_C(\boldsymbol{v}_h, \boldsymbol{m}_h) = 0, \ \forall \boldsymbol{m}_h \in M_{C,h}\}. \tag{2.44}$$

Notice that this space is not a subspace of the constrained continuous space V_C defined in (2.40), then the analysis of existence of solution is not given by Theorem 2.30. However, we can consider again Fredholm's Alternative to obtain the following result.

Theorem 2.32

Let us consider the discrete eigenvalue problem

$$\left\{\begin{array}{l} \text{Find } \nu \in \mathbb{R} \text{ and } \boldsymbol{u}_h \in V_{C,h}\backslash\{0\}, \text{ such that} \\ \\ a(\boldsymbol{u}_h, \boldsymbol{v}_h) \ = \ \nu \, m(\boldsymbol{u}_h, \boldsymbol{v}_h) \quad \forall \, \boldsymbol{v}_h \in V_{C,h}, \end{array}\right. \tag{2.45}$$

then, problem (2.43) has a unique solution in $V_{C,h}$, if and only if, ℓ^2 is not an eigenvalue of (2.45). However, if ℓ^2 is an eigenvalue of (2.45) but $(f, \boldsymbol{v}_h)_{L^2(\Omega)} = 0$ for all $\boldsymbol{v}_h \in V_{C,h}^{\ell}$ where $V_{C,h}^{\ell}$ denotes the subspace of eigenfunctions associated to $\nu = \ell^2$, then there exists a solution which is unique up to an element of $V_{C,h}^{\ell}$.

Then, as in Theorem 2.11, we want to provide a result that relates formulation (2.42) to problem (2.43) by using the *discrete Inf-Sup condition* (**P.3**). Notice that to do so, we used Lemma 2.9 where the *continuous Inf-Sup condition* (2.18) was proven to be equivalent to the bijectivity of the operator $\mathcal{B}$. Thus we need to prove here an equivalent at the discrete level. Notice, that since we are considering $W_h \subset W$ and $M_{C,h} \subset M_C$, the bilinear form $b_C(\cdot,\cdot)$ is continuous from W_h into $M_{C,h}$ with the scalar products $(\cdot,\cdot)_1$ and $(\cdot,\cdot)_{M_C}$, then we know by Riesz representation theorem (Theorem 5.5 in [50]) that there exist continuous linear operators

$$\mathcal{B}_{C,h} : M_{C,h} \longrightarrow W_h \quad \text{such that} \quad (\mathcal{B}_{C,h}\, \boldsymbol{m}_h, \boldsymbol{v}_h)_1 = b_C(\boldsymbol{v}_h, \boldsymbol{m}_h), \qquad \forall (\boldsymbol{v}_h, \boldsymbol{m}_h) \in W_h \times M_{C,h},$$

$$\mathcal{B}_{C,h}^T : W_h \longrightarrow M_{C,h} \quad \text{such that} \quad (\mathcal{B}_{C,h}^T\, \boldsymbol{v}_h, \boldsymbol{m}_h)_{M_C} = b_C(\boldsymbol{v}_h, \boldsymbol{m}_h), \quad \forall (\boldsymbol{v}_h, \boldsymbol{m}_h) \in W_h \times M_{C,h}.$$

Moreover, we can prove that the following results holds just reproducing the proofs in Lemma 2.9 and Lemma 2.10.

Lemma 2.33

The discrete Inf-Sup condition (**P.3**) *is equivalent to say that $\mathcal{B}_{C,h}$ is bijective operator from $M_{C,h}$ into $\overline{\operatorname{Im} \mathcal{B}_{C,h}}$ with continuous inverse. More precisely*

$$\|\boldsymbol{m}\|_{M_C} \leq \frac{1}{\delta} \|\mathcal{B}_{C,h}\, \boldsymbol{m}\|_1, \quad \forall \boldsymbol{m} \in M_{C,h}, \tag{2.46}$$

where δ is the constant that appears in (**P.3**).

Lemma 2.34

Respectively, the discrete Inf-Sup condition (**P.3**) *is also equivalent to say that $\mathcal{B}_{C,h}^T$ is bijective operator from $(\operatorname{Ker} \mathcal{B}_{C,h}^T)^{\perp}$ into $M_{C,h}$ with continuous inverse. More precisely*

$$\|\boldsymbol{v}_h\|_1 \leq \frac{1}{\delta} \|\mathcal{B}_{C,h}^T\, \boldsymbol{v}_h\|_{M_C}, \quad \forall \boldsymbol{v}_h \in (\operatorname{Ker} \mathcal{B}_{C,h}^T)^{\perp}, \tag{2.47}$$

where δ is again the constant that appears in (**P.3**).

Finally we conclude this section by giving also a discrete equivalent of Theorem 2.11. The proof is not given since it is a reproduction of the one in Theorem 2.11.

Theorem 2.35

If property **(P.3)** *is satisfied, then problems* (2.43) *and* (2.42) *are equivalent in the sense that*

$$\boldsymbol{u}_h \text{ is a solution of (2.43)} \iff \big(\boldsymbol{u}_h, \boldsymbol{\lambda}_h(\boldsymbol{u}_h)\big) \text{ is a solution of (2.42).}$$

Moreover, for any solution $\boldsymbol{u}_h \in V_{C,h}$*, the Lagrange multiplier* $\boldsymbol{\lambda}_h(\boldsymbol{u}_h) \in M_{C,h}$ *is uniquely defined by* (2.42a)*. In consequence, existence and uniqueness of solution for problem* (2.42) *is given by Theorem 2.32.*

2.4.3 Error analysis

In this section we provide an analogue to Cea's lemma (Proposition 3.1 in [59]) to show that the error of the method is bounded by the best approximation error, i.e. the distance between the exact solution $(\boldsymbol{u}, \boldsymbol{\lambda})$ and the approximation spaces $W_h \times M_{C,h}$. As it is natural, this analysis will be developed only considering the situations where both problems (continuous (2.33) and discrete (2.42)) have a unique solution. This is to say, that we are under the following assumption.

Assumption I.4

We assume that there exist a unique solution of continuous problem (2.33) *and a unique solution of the discrete problem* (2.42)*. Equivalently,* ℓ^2 *is not an eigenvalue of the continuous eigenvalue problem* (2.41)*, neither of the discrete eigenvalue problem* (2.45)*.*

Remark 2.36

In consequence Assumption I.3 is no longer needed since the eigenvalues of problem (2.38) *(set in* $H_0^1(\omega_c)$*) are also eigenvalues of problem* (2.41) *(set in* V_C*). Indeed, if we consider that* (ℓ^2, u_c) *is an eigenpair of problem* (2.38) *and we denote again* $\mathtt{E}(\cdot)$ *the trivial extension by zero to* Ω*, we can simply define* $\boldsymbol{u} = (u_1, u_2)$ *as*

$$u_1 = \frac{\mathtt{E}(u_c)_{|\Omega_1}}{C} \quad \text{and} \quad u_2 = -\frac{\mathtt{E}(u_c)_{|\Omega_2}}{1-C} \quad \text{with } C \text{ given by Assumption I.2.}$$

Then, noticing that for all $\boldsymbol{v} \in V_C$ *we have that* $v_1 - v_2 \in H_0^1(\omega_c)$*, we observe that (note that* $\alpha_1 = \beta_1 = C$ *and* $\alpha_2 = \beta_2 = (1-C)$ *due to Assumption I.2)*

$$a(\boldsymbol{u}, \boldsymbol{v}) \;=\; (\mu \nabla u_c, \nabla(v_1 - v_2))_{L^2(\omega_c)} \;=\; \ell^2 (\rho\, u_c, v_1 - v_2)_{L^2(\omega_c)} \;=\; \ell^2 m(\boldsymbol{u}, \boldsymbol{v}).$$

Thus $(\ell^2, \boldsymbol{u})$ *is an eigenpair of problem* (2.38)*.*

Remark 2.37

We expect that in Assumption I.4, the condition that ℓ^2 *is not an eigenvalue of the continuous eigenvalue problem* (2.41) *implies, for small enough* h*, that* ℓ^2 *is not an eigenvalue of the discrete eigenvalue problem* (2.45)*. The verification of this requires the development of an adequate convergence analysis between problems* (2.41) *and* (2.45) *and has not been carried out.*

The procedure we will present is similar to the classical techniques developed for the error analysis of mixed coercive problems (see [52]), although our problem is not coercive. Therefore, to overcome the lack of coercivity, we will base ourselves in the classical techniques for the error analysis of Helmholtz problem (see Theorem 1.6 in [53]). To do so, we will make use of the coercivity of $m(\cdot,\cdot) + a(\cdot,\cdot)$ in W that we introduce in the following lemma which is a direct consequence of Assumption I.1.

Lemma 2.38

If Assumption I.1 is satisfied, there exists $K_e > 0$ *such that for any* $\boldsymbol{v} \in W$ *we have*

$$m(\boldsymbol{v}, \boldsymbol{v}) + a(\boldsymbol{v}, \boldsymbol{v}) \geq K_e \|\boldsymbol{v}\|_1^2.$$

With all these ingredients we proceed to bound the error in three different steps. First we bound the error by the distance of the exact solution with respect to the space $V_{C,h} \times M_{C,h}$.

Proposition 2.39

*If Assumptions I.1, I.2 and I.4 are satisfied and conditions (**P.1**) and (**P.2**) hold, then for h sufficiently small we have*

$$\|\boldsymbol{u} - \boldsymbol{u}_h\|_1 \le K\Big(\inf_{\boldsymbol{v}_h \in V_{C,h}} \|\boldsymbol{u} - \boldsymbol{v}_h\|_1 + \inf_{\boldsymbol{m}_h \in M_{C,h}} \|\boldsymbol{\lambda} - \boldsymbol{m}_h\|_{M_C}\Big) \tag{2.48}$$

where $K > 0$ is a constant independent of h, and the pairs $(\boldsymbol{u}, \boldsymbol{\lambda})$ and $(\boldsymbol{u}_h, \boldsymbol{\lambda}_h)$ are the unique solutions of the continuous and discrete problems (2.33) *and* (2.42) *respectively.*

Proof. Notice that, since $W_h \times M_{C,h} \subset W \times M_C$, we can consider in both problems (continuous (2.33) and discrete (2.42)) test functions $(\boldsymbol{v}_h, \boldsymbol{m}_h) \in W_h \times M_{C,h}$ to obtain

$$\begin{cases} -\,\ell^2\, m(\boldsymbol{u} - \boldsymbol{u}_h, \boldsymbol{v}_h) \,+\, a(\boldsymbol{u} - \boldsymbol{u}_h, \boldsymbol{v}_h) \,+\, b_C(\boldsymbol{v}_h, \boldsymbol{\lambda} - \boldsymbol{\lambda}_h) \,=\, 0, \quad \forall \boldsymbol{v}_h \in W_h, & \text{(2.49a)} \\ b_C(\boldsymbol{u} - \boldsymbol{u}_h, \boldsymbol{m}_h) \,=\, 0, \quad \forall \boldsymbol{m}_h \in M_{C,h}. & \text{(2.49b)} \end{cases}$$

Now, notice that due to (2.49a) we obtain for any $\boldsymbol{v}_h \in W_h$

$$\begin{aligned} \mathcal{E}_h \;&:=\; -\,\ell^2 m(\boldsymbol{u} - \boldsymbol{u}_h, \boldsymbol{u} - \boldsymbol{u}_h) \,+\, a(\boldsymbol{u} - \boldsymbol{u}_h, \boldsymbol{u} - \boldsymbol{u}_h) \,+\, b_C(\boldsymbol{u} - \boldsymbol{u}_h, \boldsymbol{\lambda} - \boldsymbol{\lambda}_h) \\ &=\; -\,\ell^2 m(\boldsymbol{u} - \boldsymbol{u}_h, \boldsymbol{u}) \,+\, a(\boldsymbol{u} - \boldsymbol{u}_h, \boldsymbol{u}) \,+\, b_C(\boldsymbol{u}, \boldsymbol{\lambda} - \boldsymbol{\lambda}_h). \\ &=\; -\,\ell^2 m(\boldsymbol{u} - \boldsymbol{u}_h, \boldsymbol{u} - \boldsymbol{v}_h) \,+\, a(\boldsymbol{u} - \boldsymbol{u}_h, \boldsymbol{u} - \boldsymbol{v}_h) \,+\, b_C(\boldsymbol{u} - \boldsymbol{v}_h, \boldsymbol{\lambda} - \boldsymbol{\lambda}_h). \end{aligned} \tag{2.50}$$

On the other hand, since $M_{C,h} \subset M_C$, we can also consider in the continuous problem discrete test functions $\boldsymbol{m}_h \in M_{C,h}$ and we obtain

$$b_C(\boldsymbol{u}, \boldsymbol{m}_h) \,=\, 0.$$

Therefore, if we consider $\boldsymbol{v}_h \in V_{C,h}$, we can similarly substitute in (2.50) the discrete multiplier $\boldsymbol{\lambda}_h$ by any $\boldsymbol{m}_h \in M_{C,h}$ and obtain

$$\mathcal{E}_h = -\ell^2 m(\boldsymbol{u} - \boldsymbol{u}_h, \boldsymbol{u} - \boldsymbol{v}_h) + a(\boldsymbol{u} - \boldsymbol{u}_h, \boldsymbol{u} - \boldsymbol{v}_h) + b_C(\boldsymbol{u} - \boldsymbol{v}_h, \boldsymbol{\lambda} - \boldsymbol{m}_h). \tag{2.51}$$

Thus by continuity of the bilinear forms (propositions 2.4 and 2.22) we obtain the bound

$$\mathcal{E}_h \le \big(\ell^2 K_m + K_a + K_{b,C}\big)\big(\|\boldsymbol{u} - \boldsymbol{u}_h\|_1 + \|\boldsymbol{\lambda} - \boldsymbol{m}_h\|_{M_C}\big)\|\boldsymbol{u} - \boldsymbol{v}_h\|_1 \tag{2.52}$$

which holds for all $(\boldsymbol{v}_h, \boldsymbol{m}_h) \in V_{C,h} \times M_{C,h}$. Now, the challenging task is the treatment of the negative term. For that purpose, let us assume that $\boldsymbol{u} \neq \boldsymbol{u}_h$ for all h (otherwise the result holds immediately). Then we introduce the auxiliary sequence in W defined by

$$\widehat{\boldsymbol{u}}_h = \frac{\boldsymbol{u} - \boldsymbol{u}_h}{\|\boldsymbol{u} - \boldsymbol{u}_h\|_1} \tag{2.53}$$

which is bounded by construction in the space W which is a Hilbert space compactly embedded in $L^2(\Omega_1) \times L^2(\Omega_2)$ (by Rellich-Kondrachov theorem, see Theorem 6.3 in [60]). Therefore, there exists a sub-sequence (that we denote $(\widehat{\boldsymbol{u}}_h)_h$) which converges weakly in W and strongly in $L^2(\Omega_1) \times L^2(\Omega_2)$. This is to say

$$\exists\, \widehat{\boldsymbol{u}} \in W \quad \text{s.t.} \quad \lim_{h\to 0} \|\widehat{\boldsymbol{u}} - \widehat{\boldsymbol{u}}_h\|_0 = 0 \quad \text{and} \quad \lim_{h\to 0} (\widehat{\boldsymbol{u}} - \widehat{\boldsymbol{u}}_h, \boldsymbol{v})_1 = 0, \quad \forall \boldsymbol{v} \in W.$$

Next, we want to show that $\widehat{\boldsymbol{u}} = \boldsymbol{0}$ and to do so, we proceed by proving that it is solution of the continuous problem (2.41) with $\nu = \ell^2$ which is not an eigenvalue due to Assumption I.4. Since this problem is set in the constrained space V_C, we first verify that $\widehat{\boldsymbol{u}} \in V_C$. Let us consider any $\boldsymbol{m} \in M_C$ and compute

$$b_C(\widehat{\boldsymbol{u}}, \boldsymbol{m}) = b_C(\widehat{\boldsymbol{u}} - \widehat{\boldsymbol{u}}_h, \boldsymbol{m}) + b_C(\widehat{\boldsymbol{u}}_h, \boldsymbol{m}). \tag{2.54}$$

Then, we notice that on the one hand, the first term of the right hand side tends to zero since there exists $\boldsymbol{v}^\star \in W$ such that $(\boldsymbol{v}^\star, \boldsymbol{v})_1 = b_C(\boldsymbol{v}, \boldsymbol{m})$ for all $\boldsymbol{v} \in W$ and therefore

$$\lim_{h \to 0} b_C(\widehat{\boldsymbol{u}} - \widehat{\boldsymbol{u}}_h, \boldsymbol{m}) = \lim_{h \to 0} (\widehat{\boldsymbol{u}} - \widehat{\boldsymbol{u}}_h, \boldsymbol{v}^\star)_1 = 0.$$

Now we make use of the condition (**P.2**), that gives us a sequence $(\boldsymbol{m}_h)_h \subset M_{C,h}$ such that

$$\lim_{h \to 0} \|\boldsymbol{m} - \boldsymbol{m}_h\|_{M_C} = 0,$$

and we observe, that on the other hand (notice $b_C(\widehat{\boldsymbol{u}}_h, \boldsymbol{m}_h) = 0$ by (2.49b))

$$\lim_{h \to 0} b_C(\widehat{\boldsymbol{u}}_h, \boldsymbol{m}) = \lim_{h \to 0} b_C(\widehat{\boldsymbol{u}}_h, \boldsymbol{m} - \boldsymbol{m}_h).$$

In consequence, from (2.54) we deduce that $b_C(\widehat{\boldsymbol{u}}, \boldsymbol{m}) = 0$ (thus $\widehat{\boldsymbol{u}} \in V_C$) since it is not h dependent, but we have just proved that it tends to zero. Second, we proceed to verify that $\widehat{\boldsymbol{u}}$ is actually solution of problem (2.41). Let us consider any $\boldsymbol{v} \in V_C$ (notice that $b_C(\boldsymbol{v}, \boldsymbol{m}) = 0$ for any $\boldsymbol{m} \in M_C$), then for $\boldsymbol{m} \in M_C$ (specified latter) we have

$$\begin{aligned} -\ell^2 m(\widehat{\boldsymbol{u}}, \boldsymbol{v}) + a(\widehat{\boldsymbol{u}}, \boldsymbol{v}) \quad = \quad & -\ell^2 m(\widehat{\boldsymbol{u}} - \widehat{\boldsymbol{u}}_h, \boldsymbol{v}) \quad + \quad a(\widehat{\boldsymbol{u}} - \widehat{\boldsymbol{u}}_h, \boldsymbol{v}) \\ & -\ell^2 m(\widehat{\boldsymbol{u}}_h, \boldsymbol{v}) \quad + \quad a(\widehat{\boldsymbol{u}}_h, \boldsymbol{v}) \quad + \quad b_C(\boldsymbol{v}, \boldsymbol{m}). \end{aligned}$$

Now we make use of condition (**P.1**), but this time to obtain a sequence $(\boldsymbol{v}_h)_h \subset W_h$ such that

$$\lim_{h \to 0} \|\boldsymbol{v} - \boldsymbol{v}_h\|_1 = 0,$$

and we compute for every h

$$\begin{aligned} -\ell^2 m(\widehat{\boldsymbol{u}}, \boldsymbol{v}) + a(\widehat{\boldsymbol{u}}, \boldsymbol{v}) \quad = \quad & -\ell^2 m(\widehat{\boldsymbol{u}} - \widehat{\boldsymbol{u}}_h, \boldsymbol{v}) \quad + \quad a(\widehat{\boldsymbol{u}} - \widehat{\boldsymbol{u}}_h, \boldsymbol{v}) \\ & -\ell^2 m(\widehat{\boldsymbol{u}}_h, \boldsymbol{v} - \boldsymbol{v}_h) \quad + \quad a(\widehat{\boldsymbol{u}}_h, \boldsymbol{v} - \boldsymbol{v}_h) \quad + \quad b_C(\boldsymbol{v} - \boldsymbol{v}_h, \boldsymbol{m}) \\ & -\ell^2 m(\widehat{\boldsymbol{u}}_h, \boldsymbol{v}_h) \quad + \quad a(\widehat{\boldsymbol{u}}_h, \boldsymbol{v}_h) \quad + \quad b_C(\boldsymbol{v}_h, \boldsymbol{m}). \end{aligned}$$

Notice that the term in the left hand side is not h dependent while in the right hand side the two first rows vanish when h tends to zero. Then if we consider definition (2.53) of $\widehat{\boldsymbol{u}}_h$, it is clear, choosing

$$\boldsymbol{m} = \frac{\boldsymbol{\lambda} - \boldsymbol{\lambda}_h}{\|\boldsymbol{u} - \boldsymbol{u}_h\|_1} \in M_C,$$

that in the third row we obtain equation (2.49a) and then $\widehat{\boldsymbol{u}} \in V_C$ is solution of

$$-\ell^2 m(\widehat{\boldsymbol{u}}, \boldsymbol{v}) + a(\widehat{\boldsymbol{u}}, \boldsymbol{v}) = 0, \quad \forall \boldsymbol{v} \in V_C.$$

Thus $\widehat{\boldsymbol{u}} = \boldsymbol{0}$, since ℓ^2 is not an eigenvalue of problem (2.41) due to assumption I.4. In consequence, by the definition of convergence, we know that

$$\forall \varepsilon > 0,\ \exists h_\varepsilon \ \text{ such that } \ \forall h < h_\varepsilon \ \text{ we have } \ \|\widehat{\boldsymbol{u}}_h\|_0 \le \varepsilon \quad \big(\text{by (2.53) } \|\boldsymbol{u} - \boldsymbol{u}_h\|_0 \le \varepsilon \|\boldsymbol{u} - \boldsymbol{u}_h\|_1\big).$$

As desired, this allows us to handle the negative term by choosing the appropriate ε. First notice that

$$\|\boldsymbol{u} - \boldsymbol{u}_h\|_1^2 \ \le \ 2\|\boldsymbol{u} - \boldsymbol{u}_h\|_1^2 - \varepsilon^{-1}\|\boldsymbol{u} - \boldsymbol{u}_h\|_1 \|\boldsymbol{u} - \boldsymbol{u}_h\|_0 \ \le \ 2\|\boldsymbol{u} - \boldsymbol{u}_h\|_1^2 - \varepsilon^{-1}\|\boldsymbol{u} - \boldsymbol{u}_h\|_0^2,$$

then we use the coercivity of $m(\cdot,\cdot)+a(\cdot,\cdot)$ (Lemma 2.38) and continuity of $m(\cdot,\cdot)$ (Proposition 2.4)

$$\begin{aligned}\|\boldsymbol{u}-\boldsymbol{u}_h\|_1^2 &\leq 2\,K_e^{-1}\big(m(\boldsymbol{u}-\boldsymbol{u}_h,\boldsymbol{u}-\boldsymbol{u}_h)+a(\boldsymbol{u}-\boldsymbol{u}_h,\boldsymbol{u}-\boldsymbol{u}_h)\big)-(\varepsilon\,K_m)^{-1}m(\boldsymbol{u}-\boldsymbol{u}_h,\boldsymbol{u}-\boldsymbol{u}_h)\\ &= \big(2\,K_e^{-1}-(\varepsilon\,K_m)^{-1}\big)\;m(\boldsymbol{u}-\boldsymbol{u}_h,\boldsymbol{u}-\boldsymbol{u}_h)+2\,K_e^{-1}\;a(\boldsymbol{u}-\boldsymbol{u}_h,\boldsymbol{u}-\boldsymbol{u}_h).\end{aligned}$$

Thus, to combine this with (2.52) we need to chose ε such that $2\,K_e^{-1}-(\varepsilon\,K_m)^{-1}=-2\,\ell^2\,K_e^{-1}$ and make appear $b_C(\cdot,\cdot)$. Then we choose $\varepsilon=K_e\,\big(2\,K_m(1+\ell^2)\,\big)^{-1}$ and write

$$\begin{aligned}\|\boldsymbol{u}-\boldsymbol{u}_h\|_1^2 &\leq 2\,K_e^{-1}\big(-\ell^2 m(\boldsymbol{u}-\boldsymbol{u}_h,\boldsymbol{u}-\boldsymbol{u}_h)+a(\boldsymbol{u}-\boldsymbol{u}_h,\boldsymbol{u}-\boldsymbol{u}_h)+b_C(\boldsymbol{u}-\boldsymbol{u}_h,\boldsymbol{\lambda}-\boldsymbol{\lambda}_h)\,\big)\\ &- 2\,K_e^{-1}\,b_C(\boldsymbol{u}-\boldsymbol{u}_h,\boldsymbol{\lambda}-\boldsymbol{\lambda}_h)\\ &= 2\,K_e^{-1}\mathcal{E}_h\;-\;2\,K_e^{-1}\,b_C(\boldsymbol{u}-\boldsymbol{u}_h,\boldsymbol{\lambda}-\boldsymbol{\lambda}_h).\end{aligned}$$

Then applying (2.52) we obtain

$$\begin{aligned}\|\boldsymbol{u}-\boldsymbol{u}_h\|_1^2 &\leq 2\,K_e^{-1}\big(\ell^2 K_m+K_a+K_{b,C}\big)\big(\|\boldsymbol{u}-\boldsymbol{u}_h\|_1+\|\boldsymbol{\lambda}-\boldsymbol{m}_h\|_{M_C}\big)\|\boldsymbol{u}-\boldsymbol{v}_h\|_1\\ &- 2\,K_e^{-1}\,b_C(\boldsymbol{u}-\boldsymbol{u}_h,\boldsymbol{\lambda}-\boldsymbol{\lambda}_h).\end{aligned}$$

and notice that this implies due to (2.49b)

$$\begin{aligned}&\|\boldsymbol{u}-\boldsymbol{u}_h\|_1\;\big(\|\boldsymbol{u}-\boldsymbol{u}_h\|_1+\|\boldsymbol{\lambda}-\boldsymbol{m}_h\|_{M_C}\big)\leq\\ &\qquad 2\,K_e^{-1}\big(\ell^2 K_m+K_a+K_{b,C}\big)\big(\|\boldsymbol{u}-\boldsymbol{u}_h\|_1+\|\boldsymbol{\lambda}-\boldsymbol{m}_h\|_{M_C}\big)\|\boldsymbol{u}-\boldsymbol{v}_h\|_1\\ &\qquad -2\,K_e^{-1}\,b_C(\boldsymbol{u}-\boldsymbol{u}_h,\boldsymbol{\lambda}-\boldsymbol{m}_h)+\|\boldsymbol{u}-\boldsymbol{u}_h\|_1\|\boldsymbol{\lambda}-\boldsymbol{m}_h\|_{M_C}.\end{aligned}$$

Finally by continuity of $b_C(\cdot,\cdot)$ (Proposition 2.22)

$$\begin{aligned}&\|\boldsymbol{u}-\boldsymbol{u}_h\|_1\;\big(\|\boldsymbol{u}-\boldsymbol{u}_h\|_1+\|\boldsymbol{\lambda}-\boldsymbol{m}_h\|_{M_C}\big)\leq\\ &\qquad 2\,K_e^{-1}\big(\ell^2 K_m+K_a+K_{b,C}\big)\big(\|\boldsymbol{u}-\boldsymbol{u}_h\|_1+\|\boldsymbol{\lambda}-\boldsymbol{m}_h\|_{M_C}\big)\|\boldsymbol{u}-\boldsymbol{v}_h\|_1\\ &\qquad +\big(2\,K_e^{-1}\,K_{b,C}+1\big)\|\boldsymbol{u}-\boldsymbol{u}_h\|_1\|\boldsymbol{\lambda}-\boldsymbol{m}_h\|_{M_C}\end{aligned}$$

which gives the result since for all $(\boldsymbol{v}_h,\boldsymbol{m}_h)\in V_{C,h}\times M_{C,h}$ we deduce

$$\|\boldsymbol{u}-\boldsymbol{u}_h\|_1\leq 2\,K_e^{-1}\big(\ell^2 K_m+K_a+K_{b,C}\big)\|\boldsymbol{u}-\boldsymbol{v}_h\|_1+\big(2\,K_e^{-1}\,K_{b,C}+1\big)\|\boldsymbol{\lambda}-\boldsymbol{m}_h\|_{M_C}.$$

■

Now, to extend the previous result to any $\boldsymbol{v}_h\in W_h$, we need first to introduce the orthogonal projection $\Pi_{C,h}$ from M_C into $M_{C,h}$ that for every $\boldsymbol{m}\in M_C$ assigns $\Pi_{C,h}\boldsymbol{m}\in M_{C,h}$ satisfying

$$(\Pi_{C,h}\boldsymbol{m},\boldsymbol{m}_h)_{M_C}=(\boldsymbol{m},\boldsymbol{m}_h)_{M_C},\quad\forall\boldsymbol{m}_h\in M_{C,h}. \tag{2.55}$$

Notice, that $\Pi_{C,h}$ is uniformly continuous in the sense of the following lemma.

Lemma 2.40

The operator $\Pi_{C,h}$ from M_C into $M_{C,h}$ defined by (2.55) *is such that*

$$\|\Pi_{C,h}\boldsymbol{m}\|_{M_C}\leq\|\boldsymbol{m}\|_{M_C},\quad\forall\boldsymbol{m}\in M_C.$$

Then, we make use of the previous operator and its properties, as well as the uniform *discrete Inf-Sup condition* (**P.3**) (more precisely the subsequent Lemma 2.34) to provide the following result.

Theorem 2.41

If Assumptions I.1, I.2 and I.4 are satisfied and conditions (**P.1**), (**P.2**) *and* (**P.3**) *hold, then for h sufficiently small we have*

$$\|\boldsymbol{u}-\boldsymbol{u}_h\|_1 \leq K\Big(\inf_{\boldsymbol{w}_h\in W_h}\|\boldsymbol{u}-\boldsymbol{w}_h\|_1+\inf_{\boldsymbol{m}_h\in M_{C,h}}\|\boldsymbol{\lambda}-\boldsymbol{m}_h\|_{M_C}\Big)$$

where $K>0$ is a constant independent of h, and the pairs $(\boldsymbol{u},\boldsymbol{\lambda})$ and $(\boldsymbol{u}_h,\boldsymbol{\lambda}_h)$ are the unique solutions of the continuous and discrete problems (2.33) *and* (2.42).

Proof. First of all, we notice that we are in the hypothesis of Proposition 2.39 and therefore estimate (2.48) holds. Then, it is enough to find an appropriate bound for $\|\boldsymbol{u}-\boldsymbol{v}_h\|_1$ for some well chosen $\boldsymbol{v}_h\in V_{C,h}$ that we compute below. Let us begin considering $\boldsymbol{w}_h\in W_h$ and notice that $\mathcal{B}_C^T(\boldsymbol{u}-\boldsymbol{w}_h)\in M_C$ is such that $\Pi_{C,h}(\mathcal{B}_C^T(\boldsymbol{u}-\boldsymbol{w}_h))\in M_{C,h}$. Moreover, since $\mathcal{B}_{C,h}^T$ is bijective (Lemma 2.34) we know that there exists $\boldsymbol{z}_h\in(\operatorname{Ker}\mathcal{B}_{C,h}^T)^\perp$ such that $\mathcal{B}_{C,h}^T\boldsymbol{z}_h=\Pi_{C,h}(\mathcal{B}_C^T(\boldsymbol{u}-\boldsymbol{w}_h))\in M_{C,h}$ and

$$\|\boldsymbol{z}_h\|_1\leq\frac{1}{\delta}\|\mathcal{B}_{C,h}^T\boldsymbol{z}_h\|_{M_C}=\frac{1}{\delta}\|\Pi_{C,h}(\mathcal{B}_C^T(\boldsymbol{u}-\boldsymbol{w}_h))\|_{M_C}.$$

Then, the continuity of the projection $\Pi_{C,h}$ (Lemma 2.40) and the continuity of $b_C(\cdot,\cdot)$ (proposition 2.22) give

$$\|\boldsymbol{z}_h\|_1\leq\frac{1}{\delta}\|\mathcal{B}_C^T(\boldsymbol{u}-\boldsymbol{w}_h)\|_{M_C}\leq\frac{K_{b,C}}{\delta}\|\boldsymbol{u}-\boldsymbol{w}_h\|_1.$$

Now, since in general any linear continuous operator between two Hilbert spaces is such that $\overline{\operatorname{Im}\mathcal{B}_{C,h}}=(\operatorname{Ker}\mathcal{B}_{C,h}^T)^\perp$, we compute

$$\mathcal{B}_{C,h}^T(\boldsymbol{z}_h+\boldsymbol{w}_h)=\Pi_{C,h}(\mathcal{B}_C^T(\boldsymbol{u}-\boldsymbol{w}_h))+\mathcal{B}_{C,h}^T\boldsymbol{w}_h=\Pi_{C,h}(\mathcal{B}_C^T\boldsymbol{u})-\Pi_{C,h}(\mathcal{B}_C^T\boldsymbol{w}_h)+\mathcal{B}_{C,h}^T\boldsymbol{w}_h.$$

Moreover, we remark that $\Pi_{C,h}(\mathcal{B}_C^T\boldsymbol{w}_h)=\mathcal{B}_{C,h}^T\boldsymbol{w}_h$ since

$$(\mathcal{B}_{C,h}^T\boldsymbol{w}_h,\boldsymbol{m}_h)_{M_{C,h}}=b_C(\boldsymbol{w}_h,\boldsymbol{m}_h)=(\mathcal{B}_C^T\boldsymbol{w}_h,\boldsymbol{m}_h)_{M_C},\quad\forall\boldsymbol{m}_h\in M_{C,h}.$$

Thus, since $\boldsymbol{u}\in\operatorname{Ker}\mathcal{B}_C^T$, we get $\mathcal{B}_{C,h}^T(\boldsymbol{z}_h+\boldsymbol{w}_h)=0$ and we choose in (2.48) $\boldsymbol{v}_h=\boldsymbol{z}_h+\boldsymbol{w}_h$ that belongs to $\operatorname{Ker}\mathcal{B}_{C,h}^T=V_{C,h}$. Finally, notice that the following inequality holds for all $\boldsymbol{w}_h\in W_h$

$$\|\boldsymbol{u}-\boldsymbol{v}_h\|_1\leq\|\boldsymbol{u}-\boldsymbol{w}_h\|_1+\|\boldsymbol{z}_h\|_1\leq\big(1+\frac{K_{b,C}}{\delta}\big)\|\boldsymbol{u}-\boldsymbol{w}_h\|_1,$$

and then the proof is concluded. ∎

Finally, we want to provide also an estimate for the error of the Lagrange multiplier. To do so we will make use again of the uniform *discrete Inf-Sup condition* (**P.3**).

Theorem 2.42

If Assumptions I.1, I.2 and I.4 are satisfied and conditions (**P.1**), (**P.2**) *and* (**P.3**) *hold, then for h sufficiently small we have*

$$\|\boldsymbol{\lambda}-\boldsymbol{\lambda}_h\|_{M_C}\leq K\Big(\|\boldsymbol{u}-\boldsymbol{u}_h\|_1+\inf_{\boldsymbol{m}_h\in M_{C,h}}\|\boldsymbol{\lambda}-\boldsymbol{m}_h\|_{M_C}\Big)$$

where $K>0$ is a constant independent of h, and the pairs $(\boldsymbol{u},\boldsymbol{\lambda})$ and $(\boldsymbol{u}_h,\boldsymbol{\lambda}_h)$ are the unique solutions of the continuous and discrete problems (2.33) *and* (2.42).

Proof. Let us consider any $\boldsymbol{m}_h$ and notice that

$$\|\boldsymbol{\lambda}-\boldsymbol{\lambda}_h\|_{M_C}\leq\|\boldsymbol{\lambda}-\boldsymbol{m}_h\|_{M_C}+\|\boldsymbol{m}_h-\boldsymbol{\lambda}_h\|_{M_C}$$

then it will be enough to find an adequate bound for the last term. To do so, we first consider the uniform *discrete Inf-Sup condition* (**P.3**) to compute

$$\|\boldsymbol{m}_h - \boldsymbol{\lambda}_h\|_{M_C} \leq \frac{1}{\delta} \sup_{\boldsymbol{v}_h \in W_h} \frac{|b_C(\boldsymbol{v}_h, \boldsymbol{m}_h - \boldsymbol{\lambda}_h)|}{\|\boldsymbol{v}_h\|_1}. \tag{2.56}$$

Now, we remark that in this context (2.49a) holds and then

$$b_C(\boldsymbol{v}_h, \boldsymbol{\lambda} - \boldsymbol{\lambda}_h) = \ell^2\, m(\boldsymbol{u} - \boldsymbol{u}_h, \boldsymbol{v}_h) \, - \, a(\boldsymbol{u} - \boldsymbol{u}_h, \boldsymbol{v}_h)$$

which allows us to compute (considering also the continuity of the bilinear forms (propositions 2.4 and 2.22))

$$\begin{aligned}
b_C(\boldsymbol{v}_h, \boldsymbol{m}_h - \boldsymbol{\lambda}_h) &= b_C(\boldsymbol{v}_h, \boldsymbol{m}_h - \boldsymbol{\lambda}) + b_C(\boldsymbol{v}_h, \boldsymbol{\lambda} - \boldsymbol{\lambda}_h) \\
&= b_C(\boldsymbol{v}_h, \boldsymbol{m}_h - \boldsymbol{\lambda}) + \ell^2\, m(\boldsymbol{u} - \boldsymbol{u}_h, \boldsymbol{v}_h) - a(\boldsymbol{u} - \boldsymbol{u}_h, \boldsymbol{v}_h) \\
&\leq \|\boldsymbol{v}_h\|_1 \Big(K_{b,C} \|\boldsymbol{m}_h - \boldsymbol{\lambda}\|_{M_C} + (\ell^2 K_m + K_a) \|\boldsymbol{u} - \boldsymbol{u}_h\|_1 \Big).
\end{aligned}$$

Thus, we conclude the result combining this with equation (2.56)

$$\|\boldsymbol{m}_h - \boldsymbol{\lambda}_h\|_{M_C} \leq \frac{1}{\delta} \Big(K_{b,C} \|\boldsymbol{m}_h - \boldsymbol{\lambda}\|_{M_C} + (\ell^2 K_m + K_a) \|\boldsymbol{u} - \boldsymbol{u}_h\|_1 \Big).$$

■

2.5 Discretization by Lagrange finite elements

In this section, we are going to provide an explicit choice for the approximation spaces W_h and $M_{C,h}$, such that the properties we have introduced in Section 2.4.1 are satisfied. However, the reader should notice that there might be some other possibilities that also provide an adequate framework. Our choices will be based in the standard Lagrange finite elements spaces of order p

$$X_p(\mathcal{T}_h) = \Big\{ v_h \in \mathcal{C}^0\big(\bigcup_{\kappa \in \mathcal{T}_h} \kappa \big) \text{ s.t. } \forall \kappa \in \mathcal{T}_h,\ v_{h|\kappa} \in \mathcal{P}_p \Big\} \tag{2.57}$$

where $\mathcal{T}_h$ is a quasi-uniform triangulation of affine triangles in 2D or straight edges in 1D and $\mathcal{P}_p$ denotes the space of polynomials of order $p \geq 1$.

Remark 2.43

Let us recall that a family of triangulations $\mathcal{T}_h$ is said to be quasi-uniform, if there exists a constant $\varrho > 0$ (usually called the quasi-uniformity factor) independent of h and such that $\forall \kappa \in \mathcal{T}_h$ we have that $\varrho_\kappa \geq \varrho\, h$ where ϱ_κ is the radius of the largest disk included in κ.

In consequence, we shall consider $\mathcal{T}_{1,h}$ (respectively $\mathcal{T}_{2,h}$) a triangulation of Ω_1 (respectively Ω_2), depending on the parameter h_1 (respectively h_2). Then, the space W_h will be naturally sought in the form

$$W_h = W_{1,h} \times W_{2,h} \subset W, \quad \text{where} \quad W_{j,h} = X_{p_j}(\mathcal{T}_{j,h}), \quad \text{for } j \in \{1,2\}.$$

Similarly, we shall also consider $\mathcal{G}_h$ a triangulation of ω depending on the parameter h as well as $\mathcal{G}_{i,h}$ (respectively $\mathcal{G}_{e,h}$) that may represent either a triangulation of ω_i (respectively ω_e) or a 1D mesh of the closed boundary γ_i (respectively γ_e), depending on the parameter h_i (respectively h_e). Then, depending on the kind of coupling we are using, we introduce the spaces $M_{C,h}$ defined by (see in Section 2.3.5 the definition of M_C for each type of coupling)

$$M_{V,h} = X_{p_c}(\mathcal{G}_h) \subset M_V \quad \text{or} \quad M_{C,h} = X_{p_i}(\mathcal{G}_{i,h}) \times X_{p_e}(\mathcal{G}_{e,h}) \subset M_C. \tag{2.58}$$

Next we proceed to investigate under what hypothesis these spaces provide an adequate framework to automatically verify both, the approximation property (**P.1**) as well as the uniform *discrete Inf-Sup condition* (**P.2**).

2.5.1 Approximation property

The Lagrange finite elements spaces defined in (2.57) are widely studied in the literature [61, 62, 63, 64] and provide a good approximation of Sobolev spaces in the sense of the following proposition which is classical (see for instance Corollary 1.128 in [64]).

Proposition 2.44

Let us consider a bounded domain Λ and a family of conforming quasi-uniform triangulations $\mathcal{T}_h$. Then, the spaces $X_p(\mathcal{T}_h)$ are such that exists a constant $K>0$ independent of h that for any $s\in[0,1]$ and any $\sigma\in[s,p+1]$ we have

$$\inf_{v_h\in X_p(\mathcal{T}_h)}\|v-v_h\|_{H^s(\Lambda)}\le Kh^{\sigma-s}\|v\|_{H^\sigma(\Lambda)},\quad \forall v\in H^\sigma(\Lambda).$$

Moreover, we shall also remark that this result can be extended to the dual Sobolev spaces $[H^s(\Lambda)]'$ with $s\in(0,1]$ in the following sense.

Corollary 2.45

Let us consider a bounded domain Λ and a family of conforming quasi-uniform triangulations $\mathcal{T}_h$. Then, the spaces $X_p(\mathcal{T}_h)$ are such that exists a constant $K>0$ independent of h that for any $s\in(0,1]$ and any $\sigma\in[0,p+1]$ we have

$$\inf_{v_h\in X_p(\mathcal{T}_h)}\|v-v_h\|_{[H^s(\Lambda)]'}\le Kh^{\sigma+s}\|v\|_{H^\sigma(\Lambda)},\quad \forall v\in H^\sigma(\Lambda).$$

Proof. Let us consider $v\in H^\sigma(\Lambda)$ and find its L^2–orthogonal projection $v_h^\star\in X_p(\mathcal{T}_h)$ such that

$$(v-v_h^\star,w_h)_{L^2(\Lambda)}=0,\quad \forall w_h\in X_p(\mathcal{T}_h).\tag{2.59}$$

First notice that the approximation property given in Proposition 2.44 (with $s=0$) provides

$$\|v-v_h^\star\|_{L^2(\Lambda)}=\inf_{v_h\in X_p(\mathcal{T}_h)}\|v-v_h\|_{L^2(\Lambda)}\le Kh^\sigma\|v\|_{H^\sigma(\Lambda)}.\tag{2.60}$$

Then, by definition of dual norm and denoting by $\langle\cdot,\cdot\rangle_s$ the duality pairing between $H^s(\Lambda)$ and $[H^s(\Lambda)]'$ which is an extension of the scalar product in $L^2(\Lambda)$ we have

$$\inf_{v_h\in X_p(\mathcal{T}_h)}\|v-v_h\|_{[H^s(\Lambda)]'}\le\|v-v_h^\star\|_{[H^s(\Lambda)]'}=\sup_{w\in H^s(\Lambda)}\frac{\langle w,v-v_h^\star\rangle_s}{\|w\|_{H^s(\Lambda)}}=\sup_{w\in H^s(\Lambda)}\frac{(w,v-v_h^\star)_{L^2(\Lambda)}}{\|w\|_{H^s(\Lambda)}}.$$

Now, we consider (2.59) and Cauchy-Schwartz inequality, thus for any $w_h\in X_p(\mathcal{T}_h)$

$$\inf_{v_h\in X_p(\mathcal{T}_h)}\|v-v_h\|_{[H^s(\Lambda)]'}\le\sup_{w\in H^s(\Lambda)}\frac{(w-w_h,v-v_h^\star)_{L^2(\Lambda)}}{\|w\|_{H^s(\Lambda)}}\le\sup_{w\in H^s(\Lambda)}\frac{\|w-w_h\|_{L^2(\Lambda)}\|v-v_h^\star\|_{L^2(\Lambda)}}{\|w\|_{H^s(\Lambda)}}.$$

Finally, we consider (2.60) and we take the infimum in $w_h\in X_p(\mathcal{T}_h)$ to obtain

$$\begin{aligned}\inf_{v_h\in X_p(\mathcal{T}_h)}\|v-v_h\|_{[H^s(\Lambda)]'}&\le\|v-v_h^\star\|_{L^2(\Lambda)}\sup_{w\in H^s(\Lambda)}\inf_{w_h\in X_p(\mathcal{T}_h)}\frac{\|w-w_h\|_{L^2(\Lambda)}}{\|w\|_{H^s(\Lambda)}}\\&\le Kh^\sigma\|v\|_{H^\sigma(\Lambda)}\sup_{w\in H^s(\Lambda)}\frac{Kh^s\|w\|_{H^s(\Lambda)}}{\|w\|_{H^s(\Lambda)}}=K^2h^{\sigma+s}\|v\|_{H^\sigma(\Lambda)}.\end{aligned}$$

■

Now, in order to verify that the previous result imply that properties (**P.1**) and (**P.2**) hold, we first introduce the following classical density result (see for instance [65]).

Lemma 2.46

For any bounded domain Λ, the space $\mathcal{D}(\overline{\Lambda})$ is dense in $[H^s(\Lambda)]'$ for all $s \in (0, \infty)$.

Then, we show that the spaces $X_p(\mathcal{T}_h)$ verify properties **(P.1)** and **(P.2)**.

Corollary 2.47

Let us consider a bounded domain Λ and a family of conforming quasi-uniform triangulations $\mathcal{T}_h$ of Λ. Then

- *For any $r \in H^s(\Lambda)$ with $s \in [0,1]$, there exists a sequence $(r_h)_h \subset H^s(\Lambda)$ such that*

$$r_h \in X_p(\mathcal{T}_h), \quad \text{and} \quad \lim_{h\to 0} \|r - r_h\|_{H^s(\Lambda)} = 0.$$

- *For any $v \in [H^s(\Lambda)]'$ with $s \in (0, \infty)$, there exists a sequence $(v_h)_h \subset [H^s(\Lambda)]'$ such that*

$$v_h \in X_p(\mathcal{T}_h), \quad \text{and} \quad \lim_{h\to 0} \|v - v_h\|_{[H^s(\Lambda)]'} = 0.$$

Proof. Let us first notice that we do the proof only for $[H^s(\Lambda)]'$ since the other case is analogous. Then we consider $v \in [H^s(\Lambda)]'$ and notice that $H^2(\Lambda)$ is dense in $[H^s(\Lambda)]'$ due to Lemma 2.46. Then there exists a sequence

$$(v_k)_k \subset H^2(\Lambda), \quad \text{such that} \quad \lim_{k\to\infty} \|v - v_k\|_{[H^s(\Lambda)]'} = 0.$$

Moreover, by Proposition 2.44, there exist for each k a sequence $(v_k^h)_h \subset [H^s(\Lambda)]'$ such that

$$v_k^h \in X_p(\mathcal{T}_h), \quad \text{and} \quad \|v_k - v_k^h\|_{H^1(\Lambda)} = \inf_{v_h \in X_p(\mathcal{T}_h)} \|v_k - v_h\|_{H^1(\Lambda)} \leq Kh\|v_k\|_{H^2(\Lambda)}.$$

Thus, noticing that $\|\cdot\|_{[H^s(\Lambda)]'} \leq \|\cdot\|_{H^1(\Lambda)}$, the result is obtain since

$$\lim_{k\to\infty}\lim_{h\to 0} \|v - v_k^h\|_{[H^s(\Lambda)]'} \leq \lim_{k\to\infty} \|v - v_k\|_{[H^s(\Lambda)]'} + \lim_{k\to\infty}\lim_{h\to 0} \|v_k - v_k^h\|_{H^1(\Lambda)} = 0.$$

■

This results confirms that Lagrange finite elements spaces provide an adequate framework to introduce approximation spaces W_h and $M_{C,h}$ such that properties **(P.1)** and **(P.2)** are automatically satisfied. However, we still need to confirm that the uniform *discrete Inf-Sup condition* **(P.3)** is also satisfied.

2.5.2 Discrete Inf-Sup condition

In this section, our aim is to introduce some assumptions depending on the kind of coupling we are considering, so that the uniform *discrete Inf-Sup condition* **(P.3)** is automatically satisfied. Therefore, in the following we will proceed separately for each variant of the method. We will begin with the analysis of the **classic Arlequin coupling** which has already been treated in [9]. Then, following the same philosophy we present how the technique can be extended to the treatment of the **Volume - Volume coupling**. Next, we will also show how to proceed for the **Boundary - Boundary coupling**, which treatment is significantly different. Finally, we will combine the ideas in order to extend the presented techniques for the analysis of **Volume - Boundary coupling** and **Boundary - Volume coupling** which is not straightforward.

As we shall see in the following analysis, we will make use of an adequate lifting operator that we present in the following lemma which is included for completeness. Notice that the proof is adapted from Theorem 2 in [9] where a similar lifting operator was introduced in the context of the classical Arlequin method. Moreover, we also remark that a more general result can be found in Theorem 5.1 in [63].

Lemma 2.48

Let us consider a bounded domain Λ and a family of conforming triangulations $\mathcal{D}_h$ of Λ and let us denote by $\mathcal{F}_h$ a 1D mesh of a closed boundary $\vartheta \subset \partial\Lambda$ which is made of edges in $\mathcal{D}_h$. Then, there exists a discrete lifting operator

$$\begin{array}{rclll} L^h_\Lambda : X_p(\mathcal{F}_h) & \longrightarrow & X_p(\mathcal{D}_h) & \text{such that} & (L^h_\Lambda(\mu_h), v_h)_{H^1(\Lambda)} = 0, \quad \forall v_h \in X_p(\mathcal{D}_h) \cap H^1_0(\Lambda), \\ \mu_h & \mapsto & L^h_\Lambda(\mu_h) & & L^h_\Lambda(\mu_h)_{|\vartheta} = \mu_h \quad \text{and} \quad L^h_\Lambda(\mu_h)_{\partial\Lambda\setminus\vartheta} = 0. \end{array}$$

Moreover, this lifting is uniformly continuous, i.e., there exists a constant $K_\Lambda > 0$ independent of h and such that

$$\|L^h_\Lambda(\mu_h)\|_{H^1(\Lambda)} \leq K_\Lambda \|\mu_h\|_{H^{\frac{1}{2}}(\vartheta)}.$$

Proof. Let us consider any $\mu_h \in X_p(\mathcal{F}_h)$ and notice that $L^h_\Lambda(\mu_h)$ is a finite elements approximation of $L_\Lambda(\mu_h) \in H^1(\Lambda)$ such that

$$\begin{array}{rcll} L_\Lambda(\mu_h) - \Delta L_\Lambda(\mu_h) & = & 0, & \text{in} \quad \Lambda, \\ L_\Lambda(\mu_h) & = & \mu_h, & \text{on} \quad \vartheta, \\ L_\Lambda(\mu_h) & = & 0, & \text{on} \quad \partial\Lambda \setminus \vartheta. \end{array}$$

In consequence, there exist two constants $K_1 > 0$ and $K_2 > 0$ independent of h and such that

$$\|L_\Lambda(\mu_h)\|_{H^1(\Lambda)} \leq K_1 \|\mu_h\|_{H^{\frac{1}{2}}(\vartheta)} \quad \text{and} \quad \|L_\Lambda(\mu_h) - L^h_\Lambda(\mu_h)\|_{H^1(\Lambda)} \leq K_2 \|L_\Lambda(\mu_h)\|_{H^1(\Lambda)}.$$

Thus we can combine both to obtain the result

$$\|L^h_\Lambda(\mu_h)\|_{H^1(\Lambda)} \leq \|L_\Lambda(\mu_h)\|_{H^1(\Lambda)} + \|L_\Lambda(\mu_h) - L^h_\Lambda(\mu_h)\|_{H^1(\Lambda)} \leq K_1(1 + K_2)\|\mu_h\|_{H^{\frac{1}{2}}(\vartheta)}.$$

■

Moreover, when a boundary coupling is considered in any of the sides and since in that case the space of multipliers is a dual Sobolev space of the type $[H^{\frac{1}{2}}(\vartheta)]'$, we are going to need also the following lemma concerning the properties of the orthogonal projection operator from $L^2(\vartheta)$ into $X_p(\mathcal{F}_h)$.

Lemma 2.49

Let us consider a closed boundary ϑ and let us denote by $\mathcal{F}_h$ a conforming quasi-uniform 1D mesh of ϑ. Thus we can define the orthogonal projection operator P^h_ϑ from $L^2(\vartheta)$ into $X_p(\mathcal{F}_h)$ that for every $\phi \in L^2(\vartheta)$ assigns $P^h_\vartheta \phi \in X_p(\mathcal{F}_h)$ satisfying

$$(P^h_\vartheta \phi, v_h)_{L^2(\vartheta)} = (\phi, v_h)_{L^2(\vartheta)}, \quad \forall v_h \in X_p(\mathcal{F}_h) \quad \text{and} \quad \|P^h_\vartheta \phi\|_{L^2(\vartheta)} \leq \|\phi\|_{L^2(\vartheta)}.$$

This operator is such that for all $\phi \in H^{\frac{1}{2}}(\vartheta)$ there exist two constants $K_\vartheta > 0$ and $K^\star_\vartheta > 0$ independent of h and such that

$$\|P^h_\vartheta \phi\|_{H^{\frac{1}{2}}(\vartheta)} \leq K_\vartheta \, \|\phi\|_{H^{\frac{1}{2}}(\vartheta)} \quad \text{and} \quad \|\phi - P^h_\vartheta \phi\|_{L^2(\vartheta)} \leq K^\star_\vartheta \, h^{\frac{1}{2}} \|\phi\|_{H^{\frac{1}{2}}(\vartheta)}.$$

Proof. On the one hand, we first refer to Theorem 3.2 in [66] for a proof of stability of the L^2-projection in any fractional Sobolev space $H^s(\vartheta)$ with $s \in (0, 1]$. On the other hand, we notice that $(\phi - P^h_\vartheta \phi, v_h)_{L^2(\vartheta)} = 0$ for all $v_h \in X_p(\mathcal{F}_h)$, thus considering Cauchy-Schwartz inequality

$$\|\phi - P^h_\vartheta \phi\|^2_{L^2(\vartheta)} = (\phi - P^h_\vartheta \phi, \phi - v_h)_{L^2(\vartheta)} \leq \|\phi - P^h_\vartheta \phi\|_{L^2(\vartheta)} \|\phi - v_h\|_{L^2(\vartheta)}, \quad \forall v_h \in X_p(\mathcal{F}_h).$$

Then, for all $\phi \in H^{\frac{1}{2}}(\vartheta)$ we can apply the approximation property given in Proposition 2.44 (with $s = 0$ and $\sigma = 1/2$) to obtain

$$\|\phi - P_\vartheta^h \phi\|_{L^2(\vartheta)} = \inf_{v_h \in X_p(\mathcal{F}_h)} \|\phi - v_h\|_{L^2(\vartheta)} \leq K_\vartheta^\star \, h^{\frac{1}{2}} \|\phi\|_{H^{\frac{1}{2}}(\vartheta)}.$$

■

Details on why we need this operators are given later. But we can already mention that in order to make use of L_Λ^h and P_ϑ^h, it is necessary to make some conformity assumptions between the meshes of $\mathcal{G}_h$, $\mathcal{G}_{i,h}$ and $\mathcal{G}_{e,h}$ (depending on the type of coupling considered) with respect to $\mathcal{T}_{1,h}$ and $\mathcal{T}_{2,h}$. Next, we proceed in detail for each variant of the method.

2.5.2.1 Classic Arlequin coupling (V)

For the **classic Arlequin coupling**, this question has already been treated in previous works (see [9]) under the consideration of the following assumption.

Assumption I.5

We assume that there exists $j \in \{1, 2\}$ such that $\mathcal{T}_{j,h}$ is conform with ω. Thus we consider that the triangulation $\mathcal{G}_h$ of ω is made of triangles of $\mathcal{T}_{j,h}$

$$\mathcal{G}_h = \{\kappa \in \mathcal{T}_{j,h} \text{ s.t. } \kappa \subset \overline{\omega}\} \tag{2.61}$$

and that the finite elements are of the same order, i.e. $p_c = p_j$.

First, we remark that the other mesh, that we denote $\mathcal{T}_{k,h}$ with $k \in \{1, 2\} \setminus \{j\}$, may be conform or not with ω. Moreover, if Assumption I.5 holds, we notice that we are in the hypothesis of Lemma 2.48 and we can introduce the operator $L_{\Omega_j \setminus \omega}^h$ (with $\vartheta = \partial\Lambda \cap \partial\omega$). Furthermore, the discrete Lagrange multipliers space $M_{V,h}$ is then the restrictions of functions in $W_{j,h}$ to ω

$$M_{V,h} = \{v_{j,h|\omega} \text{ such that } v_{j,h} \in W_{j,h}\}.$$

We shall also remark that Assumption I.5 is even more restrictive that the situation described at the beginning of Section 2.3, where we have explained the drawbacks of the need of a particular mesh for the overlapping region ω. In consequence, those drawbacks are still here and we remark that our purpose is to avoid this type of coupling and use any of the other variants. However, as we shall see now, Assumption I.5 allows to have a systematic approach so that the uniform *discrete Inf-Sup condition* (**P.3**) is automatically satisfied and thus it will provide some intuition on how to proceed for the new variants of the method.

Theorem 2.50

*If Assumption I.5 is verified, then $b_V(\cdot,\cdot)$ satisfies the uniform discrete Inf-Sup condition (**P.3**).*

Proof. First notice that due to Assumption I.5 we can consider in Lemma 2.48, $\Lambda = \Omega_j \setminus \omega$, $\vartheta = \partial\Lambda \cap \partial\omega$ and the lifting operator

$$L_\Lambda^h : X_{p_j}(\mathcal{F}_h) \longrightarrow X_{p_j}(\mathcal{D}_h), \quad \text{where} \quad \mathcal{D}_h = \{\kappa \in \mathcal{T}_{j,h} \text{ s.t. } \kappa \subset \overline{\Lambda}\}$$
$$\text{and} \quad \mathcal{F}_h = \{e = \kappa \cap \partial\Lambda \text{ s.t. } \kappa \in \mathcal{T}_{j,h}\}.$$

Then, for any $m_h \in M_{V,h}$ notice that $m_{h|\vartheta} \in X_{p_j}(\mathcal{F}_h)$ and $L_\Lambda^h(m_{h|\vartheta}) \in X_{p_j}(\mathcal{D}_h)$. Thus for every $m_h \in M_{V,h}$ we can define (see Assumption I.5 and the following comments for the choice of j and k and note that if $j = 1$ then $k = 2$ and vice versa)

$$\boldsymbol{v}_h^\star = (v_{1,h}^\star, v_{2,h}^\star) \in W_h \quad \text{such that} \quad v_{k,h}^\star = 0,\ v_{j,h|\Lambda}^\star = L_\Lambda^h(m_{h|\vartheta}) \quad \text{and} \quad v_{j,h|\omega}^\star = m_h.$$

In consequence, on the one hand it is straightforward to verify

$$b_V(\boldsymbol{v}_h^\star, m_h) = (v_{j,h}^\star, m_h)_{H^1(\omega)} = (m_h, m_h)_{H^1(\omega)} = \|m_h\|_{M_V}^2. \tag{2.62}$$

While on the other hand, considering the continuity of the lifting operator L_Λ^h and the continuity of the trace, we can also obtain

$$\begin{aligned} \|\boldsymbol{v}_h^\star\|_1^2 &= \|v_{j,h|\Lambda}^\star\|_{H^1(\Lambda)}^2 + \|m_h\|_{H^1(\omega)}^2 \\ &\le K_\Lambda \|m_h\|_{H^{\frac{1}{2}}(\vartheta)}^2 + \|m_h\|_{H^1(\omega)}^2 \le K\|m_h\|_{M_V}^2. \end{aligned} \tag{2.63}$$

Finally notice that we can easily combine (2.63) and (2.62) as follows

$$\sup_{\boldsymbol{v}_h \in W_h} \frac{|b_V(\boldsymbol{v}_h, m_h)|}{\|m_h\|_{M_V}\ \|\boldsymbol{v}_h\|_1} \ge \frac{|b_V(\boldsymbol{v}_h^\star, m_h)|}{\|m_h\|_{M_V}\ \|\boldsymbol{v}_h^\star\|_1} \ \ge\ \frac{1}{\sqrt{K}}\ >\ 0$$

and since this holds for any $m_h \in M_{V,h}$, it also holds for the infimum and thus the proof is concluded.

■

In consequence, the following convergence result holds for regular enough solutions.

Corollary 2.51

If $\boldsymbol{u} \in H^{s_1}(\Omega_1) \times H^{s_2}(\Omega_2)$ for $s_1, s_2 > 1$ and $\lambda \in H^\sigma(\omega)$ for $\sigma > 1$, then

$$\|\boldsymbol{u} - \boldsymbol{u}_h\|_1 + \|\lambda - \lambda_h\|_{M_V} \le K\, h^q$$

where $q = \min\limits_{1\le j\le 2} \{p_j, s_j - 1, \sigma - 1\}$.

Remark 2.52

According to the interpretation of the Lagrange multiplier λ (see Corollary 2.13), we expect in Corollary 2.51 that $\sigma \le s_\star$ where $s_\star$ gives the regularity of the primal variable $\boldsymbol{u}$ in the overlapping region ω, i.e. $\boldsymbol{u}_{|\omega} \in H^{s_\star}(\omega) \times H^{s_\star}(\omega)$. More details on the expected regularity of the primal variable $\boldsymbol{u}$ and the Lagrange multiplier λ are provided in Theorem 2.14.

2.5.2.2 Volume - Volume coupling (VV)

Now, our aim is to treat the **Volume - Volume coupling** by following the ideas presented for the classic Arlequin coupling but considering assumptions that are less restrictive than Assumption I.5 although they may be more elaborated. Notice first, that in this case we have two independent coupling regions ω_i and ω_e. Therefore, in order facilitate the verification of an analogous property to (2.62), we want to define two lifting operators, each of them associated to one side of the coupling and such that it does not interact with the other side. Thus, we introduce (see Figure 2.9)

$$\omega_{ci} \subset \omega_c, \quad \text{such that} \quad \gamma_{ci} := \partial\omega_{ci} \cap \partial\omega_i \neq \emptyset \quad \text{closed and} \quad \gamma_{ci} \cap \overline{(\partial\omega_{ci} \setminus \gamma_{ci})} = \emptyset, \tag{2.64}$$

$$\text{and} \quad \omega_{ce} \subset \omega_c, \quad \text{such that} \quad \gamma_{ce} := \partial\omega_{ce} \cap \partial\omega_e \neq \emptyset \quad \text{closed and} \quad \gamma_{ce} \cap \overline{(\partial\omega_{ce} \setminus \gamma_{ce})} = \emptyset. \tag{2.65}$$

Then, our purpose is to extend the elements in $M_{VV,h} = X_{p_i}(\mathcal{G}_{i,h}) \times X_{p_e}(\mathcal{G}_{e,h})$ by considering twice Lemma 2.48 in order to introduce lifting operators $L_{\omega_{ci}}^h$ and $L_{\omega_{ce}}^h$ (with $\vartheta = \gamma_{ci}$ and $\vartheta = \gamma_{ce}$ respectively) such that

$$\omega_e \cap \operatorname{supp} L_{\omega_{ci}}^h(\mu_h) = \emptyset \quad \text{and} \quad \omega_i \cap \operatorname{supp} L_{\omega_{ce}}^h(\mu_h) = \emptyset \quad \text{(details in Theorem 2.53).}$$

Thus, in order to fulfil this requirement in a way that the resultant lifting operators are independent of h, it is natural to consider the following two assumptions, each of them related to one side of the coupling.

Assumption I.6

We assume that ω_i and ω_{ci} are independent of h and that $\mathcal{T}_{1,h}$ is conform with them (see Figure 2.9a). Thus we consider that the triangulations $\mathcal{G}_{i,h}$ and $\mathcal{D}_{i,h}$ of ω_i and ω_{ci} are made of triangles of $\mathcal{T}_{1,h}$

$$\mathcal{G}_{i,h} = \{\kappa \in \mathcal{T}_{1,h} \text{ s.t. } \kappa \subset \overline{\omega}_i\} \quad \text{and} \quad \mathcal{D}_{i,h} = \{\kappa \in \mathcal{T}_{1,h} \text{ s.t. } \kappa \subset \overline{\omega}_{ci}\}, \tag{2.66}$$

and that the finite elements are of the same order, i.e. $p_i = p_1$.

Assumption I.7

We assume that ω_e and ω_{ce} are independent of h and that $\mathcal{T}_{2,h}$ is conform with them (see Figure 2.9b). Thus we consider that the triangulations $\mathcal{G}_{e,h}$ and $\mathcal{D}_{e,h}$ of ω_e and ω_{ce} are made of triangles of $\mathcal{T}_{2,h}$

$$\mathcal{G}_{e,h} = \{\kappa \in \mathcal{T}_{2,h} \text{ s.t. } \kappa \subset \overline{\omega}_e\} \quad \text{and} \quad \mathcal{D}_{e,h} = \{\kappa \in \mathcal{T}_{2,h} \text{ s.t. } \kappa \subset \overline{\omega}_{ce}\}, \tag{2.67}$$

and that the finite elements are of the same order, i.e. $p_e = p_2$.

If assumptions I.6 and I.7 hold, we notice that the hypothesis of Lemma 2.48 are satisfied and we can introduce the operators $L^h_{\omega_{ci}}$ and $L^h_{\omega_{ce}}$ (with $\vartheta = \gamma_{ci}$ and $\vartheta = \gamma_{ce}$ respectively). Moreover, we also notice that

$$X_{p_i}(\mathcal{G}_{i,h}) = \{v_{1,h|\omega_i} \text{ s.t. } v_{1,h} \in W_{1,h}\} \quad \text{and} \quad X_{p_e}(\mathcal{G}_{e,h}) = \{v_{2,h|\omega_e} \text{ s.t. } v_{2,h} \in W_{2,h}\}.$$

We point out that it might be possible that assumptions I.6 and I.7 are not necessary in practice,

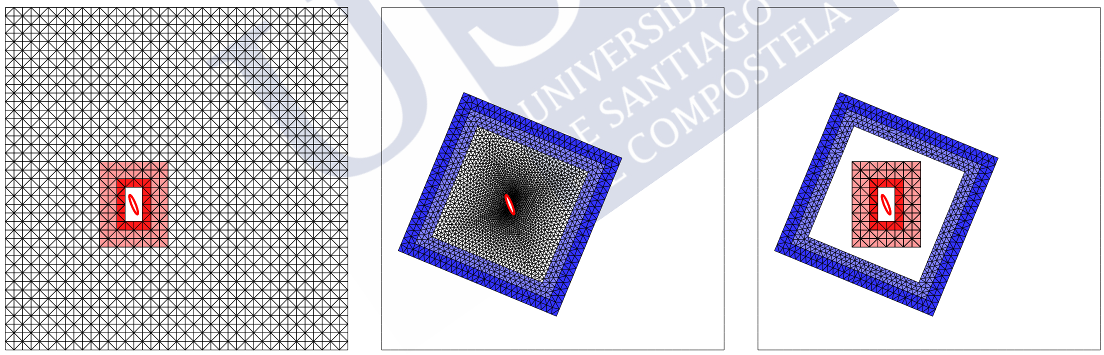

(a) Triangulation $\mathcal{T}_{1,h}$ of Ω_1 and its sub-triangulations $\mathcal{G}_{i,h}$ of ω_i (in dark red) and $\mathcal{D}_{ci,h}$ of ω_{ci} (in light red)

(b) Triangulation $\mathcal{T}_{2,h}$ of Ω_2 and its sub-triangulations $\mathcal{G}_{e,h}$ of ω_e (in dark blue) and $\mathcal{D}_{ce,h}$ of ω_{ce} (in light blue)

(c) Triangulations in ω. Notice that $\mathcal{D}_{ce,h}$ and $\mathcal{D}_{ci,h}$ could intersect. However $\mathcal{D}_{ce,h}$ and $\mathcal{G}_{i,h}$ can not neither $\mathcal{D}_{ci,h}$ and $\mathcal{G}_{e,h}$.

Figure 2.9: Standard triangulations so that the *Inf-Sup condition* is satisfied.

but we need them in order to introduce suitable lifting operators. The reader should notice that these assumptions are not very restrictive although they look very elaborated. The only restriction is that they must be satisfied independently of h. Indeed, for a given pair of triangulations $\mathcal{T}_{1,h}$ and $\mathcal{T}_{2,h}$ that are fine enough, the verification of assumptions I.6 and I.7 is always possible since we have the freedom to chose the coupling regions ω_i and ω_e to be conform with the respective meshes, while for ω_{ci} and ω_{ce} is enough to have a strip of elements. However, if we would not consider that both assumptions hold (i.e. ω_{ci} and ω_{ce} independent of h), then the *discrete Inf-Sup condition* (**P.3**) that we prove next would not be uniform.

Theorem 2.53

If assumptions I.6 and I.7 are verified, then $b_{VV}(\cdot,\cdot)$ satisfies the uniform discrete Inf-Sup *condition* (**P.3**).

Proof. First notice that due to assumptions I.6 and I.7 we can consider twice Lemma 2.48 (first with $\Lambda = \omega_{ci}$ and $\vartheta = \gamma_{ci}$, and second with $\Lambda = \omega_{ce}$ and $\vartheta = \gamma_{ce}$) to introduce the lifting operators

$$\begin{aligned} L^h_{\omega_{ci}} : X_{p_1}(\mathcal{F}_{i,h}) \longrightarrow X_{p_1}(\mathcal{D}_{i,h}), \quad &\text{where} \quad \mathcal{D}_{i,h} \quad \text{is given in (2.66)} \\ &\text{and} \quad \mathcal{F}_{i,h} = \{e = \kappa \cap \gamma_{ci} \text{ s.t. } \kappa \in \mathcal{T}_{1,h}\} \end{aligned} \tag{2.68}$$

$$\begin{aligned} L^h_{\omega_{ce}} : X_{p_2}(\mathcal{F}_{e,h}) \longrightarrow X_{p_2}(\mathcal{D}_{e,h}), \quad &\text{where} \quad \mathcal{D}_{e,h} \quad \text{is given in (2.67)} \\ &\text{and} \quad \mathcal{F}_{e,h} = \{e = \kappa \cap \gamma_{ce} \text{ s.t. } \kappa \in \mathcal{T}_{2,h}\}. \end{aligned} \tag{2.69}$$

Then, for any $\boldsymbol{m}_h \in M_{VV,h}$ notice that on the one hand

$$m_{i,h|\gamma_{ci}} \in X_{p_1}(\mathcal{F}_{i,h}) \quad \text{and} \quad L^h_{\omega_{ci}}(m_{i,h|\gamma_{ci}}) \in X_{p_1}(\mathcal{D}_{i,h}),$$

while on the other hand

$$m_{e,h|\gamma_{ce}} \in X_{p_2}(\mathcal{F}_{e,h}) \quad \text{and} \quad L^h_{\omega_{ce}}(m_{e,h|\gamma_{ce}}) \in X_{p_2}(\mathcal{D}_{e,h}).$$

Thus, for any $\boldsymbol{m}_h \in M_{VV,h}$ we can define

$$\begin{aligned} \boldsymbol{v}^\star_h \in W_h \quad \text{such that} \quad & v^\star_{1,h|\Omega_1\setminus(\omega_i\cup\omega_{ci})} = 0, \quad v^\star_{1,h|\omega_{ci}} = L^h_{\omega_{ci}}(m_{i,h|\gamma_{ci}}), \quad v^\star_{1,h|\omega_i} = m_{i,h} \\ \text{and} \quad & v^\star_{2,h|\Omega_2\setminus(\omega_e\cup\omega_{ce})} = 0, \quad v^\star_{2,h|\omega_{ce}} = -L^h_{\omega_{ce}}(m_{e,h|\gamma_{ce}}), \quad v^\star_{2,h|\omega_e} = -m_{e,h}. \end{aligned}$$

In consequence, on the one hand it is straightforward to verify

$$\begin{aligned} b_{VV}(\boldsymbol{v}^\star_h, \boldsymbol{m}_h) &= (v^\star_{1,h} - v^\star_{2,h}, m_{i,h})_{H^1(\omega_i)} + (v^\star_{1,h} - v^\star_{2,h}, m_{e,h})_{H^1(\omega_e)} \\ &= (m_{i,h}, m_{i,h})_{H^1(\omega_i)} + (m_{e,h}, m_{e,h})_{H^1(\omega_e)} = \|\boldsymbol{m}_h\|^2_{M_{VV}}. \end{aligned} \tag{2.70}$$

While on the other hand, considering the continuity of the lifting operators $L^h_{\omega_{ci}}$ and $L^h_{\omega_{ce}}$ and the continuity of the traces, we can also obtain

$$\|v^\star_{1,h}\|^2_{H^1(\Omega_1)} \le K^2_{\omega_{ci}} \|m_{i,h}\|^2_{H^{\frac{1}{2}}(\gamma_{ci})} + \|m_{i,h}\|^2_{H^1(\omega_i)} \le K_1 \|m_{i,h}\|^2_{H^1(\omega_i)} \tag{2.71}$$

$$\text{and} \quad \|v^\star_{2,h}\|^2_{H^1(\Omega_2)} \le K^2_{\omega_{ce}} \|m_{e,h}\|^2_{H^{\frac{1}{2}}(\gamma_{ce})} + \|m_{e,h}\|^2_{H^1(\omega_e)} \le K_2 \|m_{e,h}\|^2_{H^1(\omega_e)}. \tag{2.72}$$

where K_1 and K_2 are positive constants independent of h. Finally, we can easily combine (2.70), (2.71) and (2.72) to find a constant $K = \max\{K_1, K_2\} > 0$ independent of h and such that

$$\sup_{\boldsymbol{v}_h \in W_h} \frac{|b_{VV}(\boldsymbol{v}_h, \boldsymbol{m}_h)|}{\|\boldsymbol{m}_h\|_{M_{VV}} \ \|\boldsymbol{v}_h\|_1} \ge \frac{|b_{VV}(\boldsymbol{v}^\star_h, \boldsymbol{m}_h)|}{\|\boldsymbol{m}_h\|_{M_{VV}} \ \|\boldsymbol{v}^\star_h\|_1} \ge \frac{1}{\sqrt{K}} > 0$$

and since this holds for any $\boldsymbol{m}_h \in M_{VV,h}$, it also holds for the infimum and thus the proof is concluded.

■

In consequence, the following convergence result holds for regular enough solutions.

Corollary 2.54

If $\boldsymbol{u} \in H^{s_1}(\Omega_1) \times H^{s_2}(\Omega_2)$ *for* $s_1, s_2 > 1$ *and* $\boldsymbol{\lambda} \in H^{\sigma_i}(\omega_i) \times H^{\sigma_e}(\omega_e)$ *for* $\sigma_i, \sigma_e > 1$, *then*

$$\|\boldsymbol{u} - \boldsymbol{u}_h\|_1 + \|\boldsymbol{\lambda} - \boldsymbol{\lambda}_h\|_{M_{VV}} \le K\, h^q$$

where $q = \min\big\{ \min_{1\le j\le 2} \{p_j, s_j - 1\}, \min_{k\in\{i,e\}} \{\sigma_k - 1\} \big\}$.

Remark 2.55

According to the interpretation of the Lagrange multiplier $\boldsymbol{\lambda}$ (see Remark 2.21), we expect in Corollary 2.54 that $\sigma_k \leq s_\star$ for $k \in \{i, e\}$ and $s_\star$ given by the regularity of the primal variable $\boldsymbol{u}$ in the coupling region ω_k, i.e. $\boldsymbol{u}_{|\omega_k} \in H^{s_\star}(\omega_k) \times H^{s_\star}(\omega_k)$. More details on the expected regularity of the primal variable $\boldsymbol{u}$ and the Lagrange multiplier $\boldsymbol{\lambda}$ are provided in Theorem 2.28.

2.5.2.3 Boundary - Boundary coupling (BB)

Now, for the treatment of the **Boundary - Boundary coupling** the procedure is significantly different since the space of multipliers is $M_{BB} = [H^{\frac{1}{2}}(\gamma_i)]' \times [H^{\frac{1}{2}}(\gamma_e)]'$. It seems complicated to find, as we have done in previous cases, for each $\boldsymbol{m}_h \in M_{BB,h}$ an adequate $\boldsymbol{v}_h^\star \in W_h$ such that

$$\|\boldsymbol{v}_h^\star\|_1 \leq K_1 \|\boldsymbol{m}_h\|_{M_{BB}} \quad \text{and} \quad b_{BB}(\boldsymbol{v}_h^\star, \boldsymbol{m}_h) \geq K_2 \|\boldsymbol{m}_h\|^2_{M_{BB}}.$$

However, as we shall see later, there is a different way to proceed by combining Lemmas 2.48 and 2.49 and using the definition of the dual norm. Thus, in order to adapt to the hypothesis of these lemmas, we still need to consider similar assumptions to the previous case. In consequence, in the first steps we proceed very similarly, but notice that now both ω_i and ω_e are empty. Thus γ_i and γ_e will take their own role as well as the the role of γ_{ci} and γ_{ce} (with this we mean that formally $\gamma_j = \gamma_{cj}$ for $j \in \{i, e\}$ in the proof of the *Inf-Sup*). More precisely, this means that on the one hand when introducing the regions ω_{ci} and ω_{ce} instead of considering (2.64) and (2.65) we introduce them as follows (see Figure 2.10)

$$\omega_{ci} \subset \omega_c, \quad \text{such that} \quad \gamma_i \subset \partial\omega_{ci} \quad \text{and} \quad \gamma_i \cap \overline{(\partial\omega_{ci} \setminus \gamma_i)} = \emptyset, \tag{2.73}$$

$$\text{and} \quad \omega_{ce} \subset \omega_c, \quad \text{such that} \quad \gamma_e \subset \partial\omega_{ce} \quad \text{and} \quad \gamma_e \cap \overline{(\partial\omega_{ce} \setminus \gamma_e)} = \emptyset. \tag{2.74}$$

While on the other hand, in order to introduce lifting operators that are independent of h, it is natural to reformulate the assumptions in following way. Notice that still each of them is related to one side of the coupling.

Assumption I.8

We assume that γ_i and ω_{ci} are independent of h and that $\mathcal{T}_{1,h}$ is conform with them (see Figure 2.10a). Thus we consider that the 1D mesh $\mathcal{G}_{i,h}$ of γ_i and the triangulation $\mathcal{D}_{i,h}$ of ω_{ci} are made of edges and triangles of $\mathcal{T}_{1,h}$ respectively

$$\mathcal{G}_{i,h} = \{e = \kappa \cap \gamma_i \text{ s.t. } \kappa \in \mathcal{T}_{1,h}\} \quad \text{and} \quad \mathcal{D}_{i,h} = \{\kappa \in \mathcal{T}_{1,h} \text{ s.t. } \kappa \subset \overline{\omega}_{ci}\}, \tag{2.75}$$

and that the finite elements are of the same order, i.e. $p_i = p_1$.

Assumption I.9

We assume that γ_e and ω_{ce} are independent of h and that $\mathcal{T}_{2,h}$ is conform with them (see Figure 2.10b). Thus we consider that the 1D mesh $\mathcal{G}_{e,h}$ of γ_e and the triangulation $\mathcal{D}_{e,h}$ of ω_{ce} are made of edges and triangles of $\mathcal{T}_{2,h}$ respectively

$$\mathcal{G}_{e,h} = \{e = \kappa \cap \gamma_e \text{ s.t. } \kappa \in \mathcal{T}_{2,h}\} \quad \text{and} \quad \mathcal{D}_{e,h} = \{\kappa \in \mathcal{T}_{2,h} \text{ s.t. } \kappa \subset \overline{\omega}_{ce}\}, \tag{2.76}$$

and that the finite elements are of the same order, i.e. $p_e = p_2$.

If assumptions I.8 and I.9 hold, we notice that we are in the hypothesis of Lemma 2.48 to introduce the operators $L^h_{\omega_{ci}}$ and $L^h_{\omega_{ce}}$ (using $\vartheta = \gamma_i$ and $\vartheta = \gamma_e$ respectively). Moreover, we also notice that

$$X_{p_i}(\mathcal{G}_{i,h}) = \{v_{1,h|\gamma_i} \text{ s.t. } v_{1,h} \in W_{1,h}\} \quad \text{and} \quad X_{p_e}(\mathcal{G}_{e,h}) = \{v_{2,h|\gamma_e} \text{ s.t. } v_{2,h} \in W_{2,h}\}.$$

We remark that the comments we have made about the importance of the assumptions in the

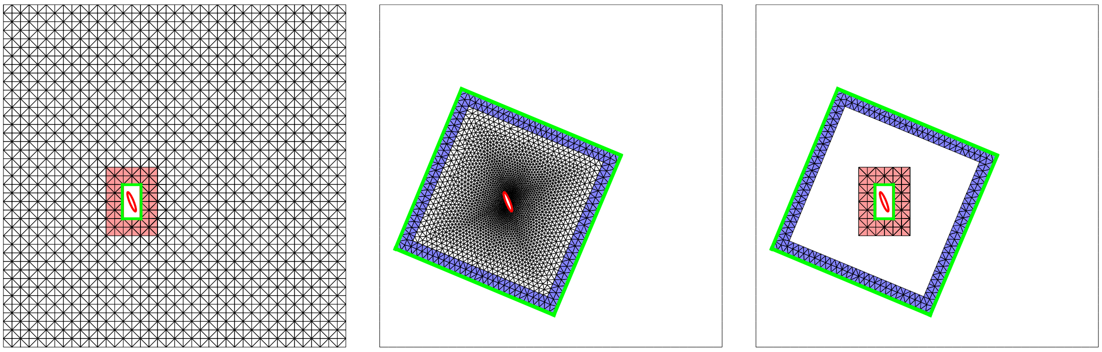

(a) Triangulation $\mathcal{T}_{1,h}$ of Ω_1 and its sub-meshes $\mathcal{G}_{i,h}$ of γ_i (in green) and $\mathcal{D}_{ci,h}$ of ω_{ci} (in light red)

(b) Triangulation $\mathcal{T}_{2,h}$ of Ω_2 and its sub-meshes $\mathcal{G}_{e,h}$ of γ_e (in green) and $\mathcal{D}_{ce,h}$ of ω_{ce} (in light blue)

(c) Meshes in ω. Notice that $\mathcal{D}_{ce,h}$ and $\mathcal{D}_{ci,h}$ could intersect. However $\mathcal{D}_{ce,h}$ and $\mathcal{G}_{i,h}$ can not neither $\mathcal{D}_{ci,h}$ and $\mathcal{G}_{e,h}$.

Figure 2.10: Standard triangulations so that the *Inf-Sup condition* is satisfied.

previous section (just before Theorem 2.53) are still valid in this case. Moreover, we also remark that the proof of the uniform *discrete Inf-Sup condition* (**P.3)** below is not analogous to the previous cases. Instead, we are inspired by the results in mortar finite elements (see for instance [56]).

Theorem 2.56

*If assumptions I.8 and I.9 are verified, then $b_{BB}(\cdot,\cdot)$ satisfies the uniform discrete Inf-Sup condition (**P.3**).*

Proof. First notice that due to assumptions I.8 and I.9 we can consider twice Lemma 2.48 (first with $\Lambda = \omega_{ci}$ and $\vartheta = \gamma_i$, and second with $\Lambda = \omega_{ce}$ and $\vartheta = \gamma_e$) to introduce the lifting operators

$$L^h_{\omega_{ci}} : X_{p_1}(\mathcal{G}_{i,h}) \longrightarrow X_{p_1}(\mathcal{D}_{i,h}), \quad \text{where} \quad \mathcal{D}_{i,h} \quad \text{and} \quad \mathcal{G}_{i,h} \quad \text{are given in (2.75)}$$

$$L^h_{\omega_{ce}} : X_{p_2}(\mathcal{G}_{e,h}) \longrightarrow X_{p_2}(\mathcal{D}_{e,h}), \quad \text{where} \quad \mathcal{D}_{e,h} \quad \text{and} \quad \mathcal{G}_{e,h} \quad \text{are given in (2.76).}$$

Moreover, notice that we can also consider twice Lemma 2.49 to introduce the orthogonal projections

$$P^h_{\gamma_i} : L^2(\gamma_i) \longrightarrow X_{p_1}(\mathcal{G}_{i,h}), \quad \text{such that} \quad \|P^h_{\gamma_i}\phi\|_{H^{\frac{1}{2}}(\gamma_i)} \leq K_{\gamma_i} \|\phi\|_{H^{\frac{1}{2}}(\gamma_i)} \quad \forall \phi \in H^{\frac{1}{2}}(\gamma_i)$$

$$P^h_{\gamma_e} : L^2(\gamma_e) \longrightarrow X_{p_2}(\mathcal{G}_{e,h}), \quad \text{such that} \quad \|P^h_{\gamma_e}\phi\|_{H^{\frac{1}{2}}(\gamma_e)} \leq K_{\gamma_e} \|\phi\|_{H^{\frac{1}{2}}(\gamma_e)} \quad \forall \phi \in H^{\frac{1}{2}}(\gamma_e).$$

Then, for any $\boldsymbol{m}_h \in M_{BB,h}$ we proceed separately for $m_{i,h} \in [H^{\frac{1}{2}}(\gamma_i)]'$ and $m_{e,h} \in [H^{\frac{1}{2}}(\gamma_e)]'$. On the one hand by the definition of the dual norm, taking into account that the duality paring is an extension of the scalar product in $L^2(\gamma_i)$ and the stability of $P^h_{\gamma_i}$, we obtain

$$\|m_{i,h}\|_{[H^{\frac{1}{2}}(\gamma_i)]'} = \sup_{\phi \in H^{\frac{1}{2}}(\gamma_i)} \frac{\langle \phi, m_{i,h}\rangle_{\gamma_i}}{\|\phi\|_{H^{\frac{1}{2}}(\gamma_i)}} \leq K_{\gamma_i} \sup_{\phi \in H^{\frac{1}{2}}(\gamma_i)} \frac{(P^h_{\gamma_i}(\phi), m_{i,h})_{L^2(\gamma_i)}}{\|P^h_{\gamma_i}(\phi)\|_{H^{\frac{1}{2}}(\gamma_i)}}. \tag{2.77}$$

Now notice that $L^h_{\omega_{ci}}(P^h_{\gamma_i}(\phi))_{|\gamma_i} = P^h_{\gamma_i}(\phi)$, that $L^h_{\omega_{ci}}$ is continuous with constant $K_{\omega_{ci}}$ and that $L^h_{\omega_{ci}}(P^h_{\gamma_i}(\phi)) \in X_{p_1}(\mathcal{D}_{i,h})$, therefore

$$\|m_{i,h}\|_{[H^{\frac{1}{2}}(\gamma_i)]'} \leq K_{\gamma_i} K_{\omega_{ci}} \sup_{\phi \in H^{\frac{1}{2}}(\gamma_i)} \frac{(L^h_{\omega_{ci}}(P^h_{\gamma_i}(\phi)), m_{i,h})_{L^2(\gamma_i)}}{\|L^h_{\omega_{ci}}(P^h_{\gamma_i}(\phi))\|_{H^1(\omega_{ci})}}.$$

Next, we denote by $\mathtt{E}_1^h$ the extension by zero to the whole Ω_1 and we remark that in that case $(\mathtt{E}_1^h(L_{\omega_{ci}}^h(P_{\gamma_i}^h(\phi))), m_{e,h})_{L^2(\gamma_e)} = 0$, thus if we denote $\mathtt{G}_1^h = \mathtt{E}_1^h \circ L_{\omega_{ci}}^h \circ P_{\gamma_i}^h$

$$\|m_{i,h}\|_{[H^{\frac{1}{2}}(\gamma_i)]'} \leq K_{\gamma_i} K_{\omega_{ci}} \sup_{\phi \in H^{\frac{1}{2}}(\gamma_i)} \frac{(\mathtt{G}_1^h(\phi), m_{i,h})_{L^2(\gamma_i)} + (\mathtt{G}_1^h(\phi), m_{e,h})_{L^2(\gamma_e)}}{\|\mathtt{G}_1^h(\phi)\|_{H^1(\Omega_1)}}.$$

And to obtain the adequate bound, we shall notice that in the previous inequality we can consider the supremum in W_h since $(\mathtt{G}_1^h(\phi), 0) \in W_h$, thus we are considering a bigger space with therefore a larger supreme. Then we obtain

$$\|m_{i,h}\|_{[H^{\frac{1}{2}}(\gamma_i)]'} \leq K_{\gamma_i} K_{\omega_{ci}} \sup_{\boldsymbol{v}_h \in W_h} \frac{(v_{1,h} - v_{2,h}, m_{i,h})_{L^2(\gamma_i)} + (v_{1,h} - v_{2,h}, m_{e,h})_{L^2(\gamma_e)}}{\|\boldsymbol{v}_h\|_1}. \tag{2.78}$$

On the other hand, it is analogous to verify that

$$\|m_{e,h}\|_{[H^{\frac{1}{2}}(\gamma_e)]'} \leq K_{\gamma_e} K_{\omega_{ce}} \sup_{\boldsymbol{v}_h \in W_h} \frac{(v_{1,h} - v_{2,h}, m_{i,h})_{L^2(\gamma_i)} + (v_{1,h} - v_{2,h}, m_{e,h})_{L^2(\gamma_e)}}{\|\boldsymbol{v}_h\|_1}. \tag{2.79}$$

Now we consider $K = K_{\gamma_i} K_{\omega_{ci}} + K_{\gamma_e} K_{\omega_{ce}}$ and we take into account that the duality pairing is an extension of the scalar product in L^2 to obtain

$$\|\boldsymbol{m}_h\|_{M_{BB}} \leq \|m_{i,h}\|_{[H^{\frac{1}{2}}(\gamma_i)]'} + \|m_{e,h}\|_{[H^{\frac{1}{2}}(\gamma_e)]'} \leq K \sup_{\boldsymbol{v}_h \in W_h} \frac{b_{BB}(\boldsymbol{v}_h, \boldsymbol{m}_h)}{\|\boldsymbol{v}_h\|_1}.$$

Finally, since this holds for any $\boldsymbol{m}_h \in M_{BB,h}$, it also holds for the infimum and thus the proof is concluded.

■

In consequence, the following convergence result holds for regular enough solutions (note that for γ closed $H^{-\sigma}(\gamma) = [H^\sigma(\gamma)]'$).

Corollary 2.57

If $\boldsymbol{u} \in H^{s_1}(\Omega_1) \times H^{s_2}(\Omega_2)$ for $s_1, s_2 > 1$ and $\boldsymbol{\lambda} \in H^{\sigma_i}(\gamma_i) \times H^{\sigma_e}(\gamma_e)$ for $\sigma_i, \sigma_e > -\frac{1}{2}$, then

$$\|\boldsymbol{u} - \boldsymbol{u}_h\|_1 + \|\boldsymbol{\lambda} - \boldsymbol{\lambda}_h\|_{M_{BB}} \leq K\, h^q$$

where $q = \min\big\{ \min_{1 \leq j \leq 2} \{p_j, s_j - 1\}, \min_{k \in \{i,e\}} \{\sigma_k + \frac{1}{2}\} \big\}$.

Remark 2.58

According to the interpretation of the Lagrange multiplier $\boldsymbol{\lambda}$ (see Remark 2.18), we expect for Corollary 2.57 that $\sigma_k \leq s_\star - \frac{3}{2}$ for $k \in \{i, e\}$ and $s_\star$ given by the regularity of the primal variable $\boldsymbol{u}$ in the region ω_c, i.e. $\boldsymbol{u}_{|\omega_c} \in H^{s_\star}(\omega_c) \times H^{s_\star}(\omega_c)$. More details on the expected regularity of the primal variable $\boldsymbol{u}$ and the Lagrange multiplier $\boldsymbol{\lambda}$ are provided in Theorem 2.28.

2.5.2.4 Volume - Boundary coupling (VB)

Next, we treat the **Volume - Boundary coupling** by combining the ideas developed for Volume - Volume and Boundary - Boundary couplings.

Theorem 2.59

*If assumptions I.6 and I.9 are verified, then $b_{VB}(\cdot, \cdot)$ satisfies the uniform discrete Inf-Sup condition (**P.3**).*

Proof. Let us consider $\boldsymbol{m}_h \in M_{VB,h}$ and we proceed separately for $m_{i,h} \in H^1(\omega_i)$ and $m_{e,h} \in [H^{\frac{1}{2}}(\gamma_e)]'$. On the one hand notice that due to assumption I.6 we can consider Lemma 2.48 as we did in (2.68) to introduce

$$\boldsymbol{v}^\star_{1,h} \in W_{1,h} \text{ such that } v^\star_{1,h|\Omega_1\setminus(\omega_i\cup\omega_{ci})} = 0,\ v^\star_{1,h|\omega_{ci}} = L^h_{\omega_{ci}}(m_{i,h|\gamma_{ci}}),\ v^\star_{1,h|\omega_i} = m_{i,h}.$$

Then it is straightforward to verify that (as in (2.70) and (2.71))

$$(v^\star_{1,h}, m_{i,h})_{H^1(\omega_i)} = \|m_{i,h}\|^2_{H^1(\omega_i)} \quad \text{and} \quad \|v^\star_{1,h}\|^2_{H^1(\Omega_1)} \le K_1 \|m_{i,h}\|^2_{H^1(\omega_i)}.$$

Moreover, we also notice that $\langle v^\star_{1,h}, m_{e,h}\rangle_{\gamma_e} = 0$ thus

$$\|m_{i,h}\|_{H^1(\omega_i)} \le \sqrt{K_1}\frac{(v^\star_{1,h}, m_{i,h})_{H^1(\omega_i)}}{\|v^\star_{1,h}\|_{H^1(\Omega_1)}} = \sqrt{K_1}\frac{(v^\star_{1,h}, m_{i,h})_{H^1(\omega_i)} + \langle v^\star_{1,h}, m_{e,h}\rangle_{\gamma_e}}{\|v^\star_{1,h}\|_{H^1(\Omega_1)}}.$$

And to obtain the adequate bound, we shall notice that we can consider the supremum in W_h since $(v^\star_{1,h}, 0) \in W_h$.Then we obtain

$$\|m_{i,h}\|_{H^1(\omega_i)} \le \sqrt{K_1} \sup_{\boldsymbol{v}_h \in W_h} \frac{(v_{1,h} - v_{2,h}, m_{i,h})_{H^1(\omega_i)} + \langle v_{1,h} - v_{2,h}, m_{e,h}\rangle_{\gamma_e}}{\|\boldsymbol{v}_h\|_1}.$$

On the other hand, as we did to obtain (2.78) and (2.79), we can also obtain

$$\|m_{e,h}\|_{[H^{\frac{1}{2}}(\gamma_e)]'} \le \sqrt{K_2} \sup_{\boldsymbol{v}_h \in W_h} \frac{(v_{1,h} - v_{2,h}, m_{i,h})_{H^1(\omega_i)} + (v_{1,h} - v_{2,h}, m_{e,h})_{L^2(\gamma_e)}}{\|\boldsymbol{v}_h\|_1}.$$

Thus we consider $K = \sqrt{K_1} + \sqrt{K_2}$ and we take into account that the duality pairing is an extension of the scalar product in L^2 to obtain

$$\|\boldsymbol{m}_h\|_{M_{VB}} \le \|m_{i,h}\|_{H^1(\omega_i)} + \|m_{e,h}\|_{[H^{\frac{1}{2}}(\gamma_e)]'} \le K \sup_{\boldsymbol{v}_h \in W_h} \frac{b_{VB}(\boldsymbol{v}_h, \boldsymbol{m}_h)}{\|\boldsymbol{v}_h\|_1}.$$

Finally, since this holds for any $\boldsymbol{m}_h \in M_{VB,h}$, it also holds for the infimum and thus the proof is concluded. ■

Corollary 2.60

If $\boldsymbol{u} \in H^{s_1}(\Omega_1) \times H^{s_2}(\Omega_2)$ for $s_1, s_2 > 1$ and $\boldsymbol{\lambda} \in H^{\sigma_i}(\omega_i) \times H^{\sigma_e}(\gamma_e)$ for $\sigma_1 > 1$ and $\sigma_e > -\frac{1}{2}$, then

$$\|\boldsymbol{u} - \boldsymbol{u}_h\|_1 + \|\boldsymbol{\lambda} - \boldsymbol{\lambda}_h\|_{M_{VB}} \le K\, h^q$$

where $q = \min_{1\le j\le 2}\{p_j, s_j - 1, \sigma_i - 1, \sigma_e + \frac{1}{2}\}$.

Remark 2.61

See Remark 2.55 and Remark 2.58 concerning the expected values of σ_i and σ_e in Corollary 2.60 according to the interpretation of the Lagrange multiplier $\boldsymbol{\lambda}$ which was presented in Remark 2.20.

2.5.2.5 Boundary - Volume coupling (BV)

Finally notice that the treatment of the **Boundary - Volume coupling** is totally analogous to the Volume - Boundary coupling. Thus we do not reply the proof but we give the result in order to remark the assumptions that are needed in this case.

Theorem 2.62

If assumptions I.7 and I.8 are verified, then $b_{BV}(\cdot,\cdot)$ satisfies the uniform discrete Inf-Sup *condition* (**P.3**).

Corollary 2.63

If $\boldsymbol{u} \in H^{s_1}(\Omega_1) \times H^{s_2}(\Omega_2)$ *for* $s_1, s_2 > 1$ *and* $\boldsymbol{\lambda} \in H^{\sigma_i}(\gamma_i) \times H^{\sigma_e}(\omega_e)$ *for* $\sigma_i > -\frac{1}{2}$ *and* $\sigma_e > 1$, *then*

$$\|\boldsymbol{u} - \boldsymbol{u}_h\|_1 + \|\boldsymbol{\lambda} - \boldsymbol{\lambda}_h\|_{M_{BV}} \leq K\, h^q$$

where $q = \min_{1\leq j\leq 2}\{p_j, s_j - 1, \sigma_i + \frac{1}{2}, \sigma_e - 1\}$.

Remark 2.64

See Remark 2.55 and Remark 2.58 concerning the expected values of σ_i *and* σ_e *in Corollary 2.63 according to the interpretation of the Lagrange multiplier* $\boldsymbol{\lambda}$ *which was presented in Remark 2.19.*

2.5.3 Algebraic system and computational aspects

Finally, we complete this section by deducing the algebraic version of the discrete problem (2.42). In the following, we consider the vectors $\boldsymbol{U}_h^T = (\boldsymbol{U}_{1,h}^T, \boldsymbol{U}_{2,h}^T)$ and $\boldsymbol{\Lambda}_h^T = (\boldsymbol{\Lambda}_{i,h}^T, \boldsymbol{\Lambda}_{e,h}^T)$ of the Lagrange degrees of freedom representing respectively the decompositions of $\boldsymbol{u}_h \in W_h$ and $\boldsymbol{\lambda}_h \in M_{C,h}$. Then we obtain

$$\left\{\begin{array}{rcl} (-\,\ell^2\, \mathbb{M}_h + \mathbb{A}_h)\, \boldsymbol{U}_h \;+\; \mathbb{B}_h\, \boldsymbol{\Lambda}_h &=& \boldsymbol{G}_h, \\ \mathbb{B}_h^T\, \boldsymbol{U}_h &=& \boldsymbol{0}, \end{array}\right. \tag{2.80}$$

where the embeddings $W_h \subset W$ and $M_{C,h} \subset M_C$ authorizes the use of the exact bilinear forms to compute (note $\mathbb{O}$ refers to null matrices of the respective size)

$$\mathbb{M}_h = \begin{pmatrix} \mathbb{M}_{1,h} & \mathbb{O} \\ \mathbb{O} & \mathbb{M}_{2,h} \end{pmatrix}, \quad \mathbb{A}_h = \begin{pmatrix} \mathbb{A}_{1,h} & \mathbb{O} \\ \mathbb{O} & \mathbb{A}_{2,h} \end{pmatrix}, \quad \mathbb{B}_h = \begin{pmatrix} \mathbb{B}_{1,h}^i & \mathbb{B}_{1,h}^e \\ \mathbb{B}_{2,h}^i & \mathbb{B}_{2,h}^e \end{pmatrix} \quad \text{and} \quad \boldsymbol{G}_h = \begin{pmatrix} \boldsymbol{G}_{1,h} \\ \boldsymbol{0} \end{pmatrix}.$$

Remark 2.65

Notice that the classic Arlequin coupling is also included in this framework. In that case $\boldsymbol{\Lambda}_h^T = \boldsymbol{\Lambda}_{j,h}^T$ *and* $(\mathbb{B}_h)^T = ((\mathbb{B}_{1,h}^j)^T, (\mathbb{B}_{2,h}^j)^T)$ *for some* $j \in \{i, e\}$ *depending on the choice of* $M_{V,h}$ *as the restriction to* ω *of* $W_{1,h}$ *or* $W_{2,h}$ *respectively (see Assumption I.5).*

It is important to remark that the computation of these matrices is not standard. Concerning the mass and stiffness matrices, if we denote by $\{\psi_j^k\}_{k=1}^{K_j}$ the set of Lagrange basis functions of $W_{j,h}$ for $j \in \{1, 2\}$, we have to compute

$$(\mathbb{M}_{j,h})_{k,l} = (\alpha_j\, \rho\, \psi_j^k, \psi_j^l)_{L^2(\Omega_j)} \quad \text{and} \quad (\mathbb{A}_{j,h})_{k,l} = (\beta_j\, \mu\, \nabla\psi_j^k, \nabla\psi_j^l)_{L^2(\Omega_j)},$$

where the discontinuities of the two couples of coefficients (α_j, β_j) for $j \in \{1, 2\}$, should be taken into account. On the other hand, the computation of the coupling matrices is more complicated. Let us denote by $\{\xi_i^l\}_{l=1}^{L_i}$ and $\{\xi_e^l\}_{l=1}^{L_e}$ the sets of Lagrange basis functions in which $M_{C,h}$ is decomposed. Then we have to compute

$$(\mathbb{B}_{1,h}^i)_{k,l} = b_C\big((\psi_1^k, 0), (\xi_i^l, 0)\big), \qquad (\mathbb{B}_{1,h}^e)_{k,l} = b_C\big((\psi_1^k, 0), (0, \xi_e^l)\big),$$

$$(\mathbb{B}_{2,h}^i)_{k,l} = b_C\big((0, \psi_2^k), (\xi_i^l, 0)\big) \quad \text{and} \quad (\mathbb{B}_{2,h}^e)_{k,l} = b_C\big((0, \psi_2^k), (0, \xi_e^l)\big).$$

These computations imply the intersection between the meshes chosen to build W_h and $M_{C,h}$. However, since we have chosen the meshes for $M_{C,h}$ to be sub-meshes of W_h, the computation of $\mathbb{B}_{1,h}^i$ and $\mathbb{B}_{2,h}^e$ are simple. This is not the case for the computation of $\mathbb{B}_{1,h}^e$ and $\mathbb{B}_{2,h}^i$. An intersection algorithm with linear complexity to perform projections between 2d and 3d non-matching grids was presented in [41]. Following the ideas presented there, similar algorithms can be developed to perform projections between 1d and 2d non-matching grids. Finally, let us remark that the solution of problem (2.80) is given by the invertibility of the matrix

$$\begin{pmatrix} -\,\ell^2\ \mathbb{M}_h + \mathbb{A}_h & \mathbb{B}_h \\ \\ \mathbb{B}_h^T & \mathbb{O} \end{pmatrix}.$$

This questions is equivalent to Theorem 2.35 where by making use of the *discrete Inf-Sup condition* (**P.3**), it was related to Theorem 2.32. In consequence, the uniqueness of solution and therefore the invertibility of the previous matrix will depend on whether ℓ^2 is or not an eigenvalue of the discrete eigenvalue problem (2.41). More precisely it is related to the existence of $\boldsymbol{U}_h \in \operatorname{Ker}\mathbb{B}_h^T$ such that

$$(-\,\ell^2\ \mathbb{M}_h + \mathbb{A}_h)\,\boldsymbol{U}_h = \mathbf{0}.$$

2.6 First numerical results

In this section we present some numerical results to exhibit the convergence properties of the method. Notice that the examples we provide are all developed for a fixed domain configuration and therefore the classic Arlequin formulation can always be used by considering adequate meshes that satisfy Assumption I.5. However, as explained in Section 2.3, the classic Arlequin method can only deal with that precise domain configuration without re-meshing while the new Arlequin couplings we propose allow to consider the same meshes for a large family of domain configurations. We remark that this gain is not visible in this section, where we focus in the convergence analysis of each coupling and therefore we fix the domain configuration. Moreover, we shall also mention that we use first and second order Lagrange finite elements with exact integration, although if the solution is regular enough, the proposed approach is fully compatible with high order spectral elements (see [22, 23, 24] for more details on spectral elements) that provide mass lumping using some quadrature rule (see [21, 22, 24, 58] and the references therein).

2.6.1 1D convergence test

Notice that in 1D configurations the consideration of an obstacle $\mathcal{O} \subset \Theta$ has not a particular interest and moreover, the consideration of fine meshes is not a time consuming task. Therefore in this context the methodology we have presented may not be of interest. However, for academic reasons it is interesting to show 1D numerical convergence analysis, since it allows to consider much finer meshes with reasonable computational time. Therefore, in the following we propose a numerical test in an unbounded domain in order to have uniqueness of solution for any value of ℓ.

Continuous equations. We look for $u(x)$ solution of the one-dimensional scalar Helmholtz equation (2.1),

$$-\ell^2\,\rho\,u - \partial_x\,\mu\,\partial_x u = 0, \quad x \in [0,\infty),$$

with inhomogeneous Dirichlet boundary condition at $x = 0$. In practice, the unbounded domain is simulated by considering absorbing boundary conditions at $x = 3$, which are known to be perfectly transparent in 1D settings if ρ and μ are constants for $x > 3$. Thus we consider the bounded domain $\Omega = (0, 3)$ and we set the boundary conditions (notice $\mathbb{i} = \sqrt{-1}$)

$$u(0) = 1 \quad \text{and} \quad -\,\mathbb{i}\ell\,u(3) + \sqrt{\frac{\mu(3)}{\rho(3)}}\,\partial_x u(3) = 0.$$

Notice that in this framework, it is known that there exists a unique solution for any value of ℓ and we choose $\ell = 10$.

Arlequin formulation. Now, in order to fit in the framework of the different couplings, we choose to decompose the computational domain $\Omega = (0, 3)$ into

$$\Omega_1 = \left(0, \frac{9}{4}\right) \quad \text{and} \quad \Omega_2 = \left(\frac{3}{4}, 3\right), \text{ thus } \gamma_e = \frac{3}{4},\ \gamma_i = \frac{9}{4} \ \text{ and } \ \omega = \left(\frac{3}{4}, \frac{9}{4}\right).$$

Then, to introduce the coupling domains ω_i and ω_e we first introduce two auxiliary regions that are defined up to an element of the different meshes considered (see Figure 2.11)

$$\omega_1 = \left(\frac{3}{4}, \frac{21}{16} + O(h_2)\right) \quad \text{and} \quad \omega_2 = \left(\frac{27}{16} + O(h_1), \frac{9}{4}\right),$$

where h_1 and h_2 stand for the space-step of the discretizations in Ω_1 and Ω_2 respectively. These

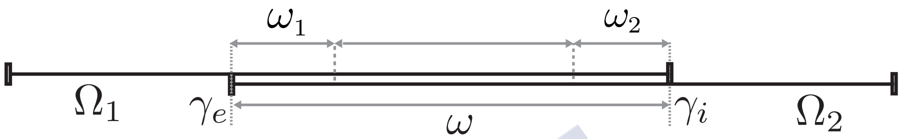

Figure 2.11: Representation of the configuration and geometry of the problem considered.

auxiliary regions help us to introduce ω_i and ω_e (remember $\omega_c = \omega \backslash \overline{(\omega_i \cup \omega_e)}$) depending in the variant of the coupling we want to consider:

VV: $\omega_i = \omega_2,\quad \omega_e = \omega_1.$ **VB:** $\omega_i = \omega_2,\quad \omega_e = \emptyset.$ **V:** $\omega_i = \emptyset,\quad \omega_e = \omega.$

BB: $\omega_i = \emptyset,\quad \omega_e = \emptyset.$ **BV:** $\omega_i = \emptyset,\quad \omega_e = \omega_1.$

Space discretization. We assume on the one hand, that the domain Ω_1 represents a coarse region. Therefore, to study the convergence of our algorithms, we use a uniform mesh of Ω_1 with space step $h_1 = |\Omega_1|/N_1$, where N_1 represents the number of elements and takes values in $\{12, 24, 48, 96, 192, 384, 768\}$. On the other hand, we assume that the domain Ω_2 represents a region where heterogeneities are supported in. To take into account these properties we use non uniform meshes built as follows: given a refinement factor $R = 5$ we start from a uniform mesh with space step $h_2 = \frac{|\Omega_2|}{N_2}$, where $N_2 = N_1 \times R$ represents the number of elements. Then every vertex ϑ_2 of the mesh of Ω_2 is slightly shifted in order to avoid effects related to mesh-uniformity. More precisely we set

$$\vartheta_2 \leftarrow \vartheta_2 + \frac{h_2}{3} \sin\left(\frac{N_2 + 2}{2}\,\pi\, \frac{\vartheta_2 - \min \vartheta_2}{\max \vartheta_2 - \min \vartheta_2}\right),$$

so that the end points of Ω_2 are not modified. Moreover, we shall also considered that γ_e is a vertex of the meshes for Ω_1 in such a way that the classical Arlequin method can also be used (and compared with the new variants introduced). In that case, the mesh for the multiplier is constructed as a restriction of the coarse mesh of Ω_1 to the overlapping region ω.

Physical coefficients and partitioning. In a preliminary example we consider **constant** physical coefficients as well as the simplest choice of **partitioning**

$$\rho = \mu = 1 \quad \text{and} \quad \alpha_1 = \alpha_2 = \beta_1 = \beta_2 = 1/2.$$

In a second example, we consider **non constant** physical coefficients. Our objective is to take into account a case where close to a given position (here $x = 9/4$), the speed of waves (given by $c(x) = \sqrt{\mu(x)/\rho(x)}$) sharply decreases up to approximately five times its base value. Such configuration is supposed to model a softer area close to a defect. Therefore we choose

$$\rho(x) = 1, \quad \mu(x) = \left(1 + 10\, e^{\frac{500\cdot 6^2}{\left(x+\frac{3}{4}\right)\left(x-\frac{21}{4}\right)} + 4\cdot 500}\right)^{-1},$$

and a **partitioning** given by

$$\alpha_1 = \begin{cases} \dfrac{3}{4} & \text{in } \omega_i \cup \omega_e \\ \dfrac{1}{2} & \text{in } \omega_c \end{cases}, \quad \beta_1 = \begin{cases} \dfrac{0.05}{\mu} & \text{in } \omega_i \cup \omega_e \\ \dfrac{1}{2} & \text{in } \omega_c \end{cases}$$

with $\alpha_2 = 1 - \alpha_1$ and $\beta_2 = 1 - \beta_1$ in ω. This choice of the coefficients is done in order to capture in the region $\omega_i \cup \omega_e$ the strong variation of the physical coefficients with the finest mesh. In Figure 2.12 we illustrate the decomposition of $\mu(\cdot)$ for the **VV** formulation. Moreover, we remark that the **V**, **VV** and **VB** couplings allow to capture with the fine mesh of Ω_2 the strong variation of μ, since it happens in a region where we are considering a volume coupling and therefore $\beta_1\mu = 0.05$ and $\beta_2\mu = \mu - 0.05$. This is not the case for the **BB** and **BV** couplings since in both cases $\omega_i = \emptyset$ and then the strong variation of μ happens inside of ω_c where $\beta_1\mu = \beta_2\mu = \mu/2$.

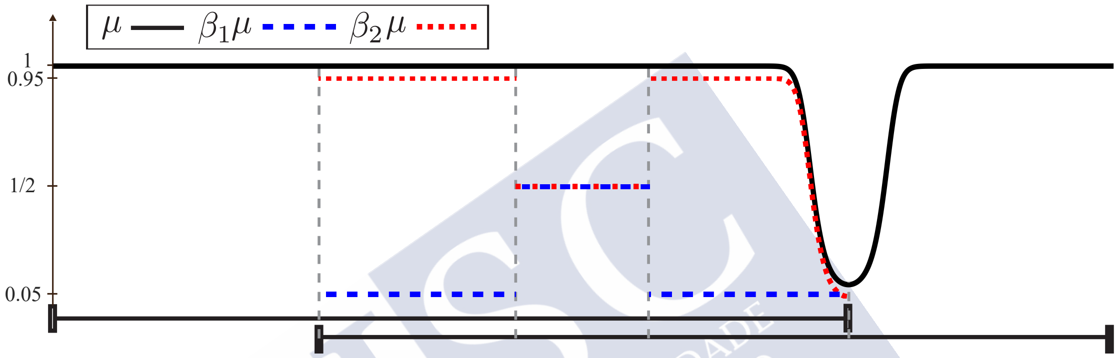

Figure 2.12: Parameters of the 1D experiment in the heterogeneous case when the volume-volume coupling (**VV**) is used.

Regularity of the solution. Notice that in this context and according to Theorem 2.28 the primal variable $\boldsymbol{u}$ belongs to $\mathcal{C}^\infty(\Omega_1) \times \mathcal{C}^\infty(\Omega_2)$ while the Lagrange multipliers are also very regular. More precisely, if the multiplier λ_j with $j \in \{i, e\}$ is of boundary type $\lambda_j \in \mathcal{C}^\infty(\gamma_j)$ and if the multiplier λ_j with $j \in \{i, e\}$ is of volume type $\lambda_j \in \mathcal{C}^\infty(\omega_j)$.

Convergence results First notice that according to the regularity of the solution $(\boldsymbol{u}, \boldsymbol{\lambda})$ and taking into account the corollaries in Section 2.5.2, we expect optimal convergence rates when considering Lagrange finite elements approximation of any order. In order to exhibit this property of the method, we provide in tables (2.1), (2.2), (2.3), (2.3) and (2.4) and figures 2.13, 2.14, 2.15 and 2.16, the relative errors for each component of the solution, i.e.

$$\|e_1\| := \frac{\|u_{|\Omega_1} - u_{1,h}\|_{H^1(\Omega_1)}}{\|u_{|\Omega_1}\|_{H^1(\Omega_1)}} \quad \text{and} \quad \|e_2\| := \frac{\|u_{|\Omega_2} - u_{2,h}\|_{H^1(\Omega_2)}}{\|u_{|\Omega_2}\|_{H^1(\Omega_2)}}. \tag{2.81}$$

Notice that the exact solution u can only be computed analytically when the physical coefficients are constant. Thus, when the physical coefficients vary we consider u as the numerical solution obtained by a classical finite elements method on a fine grid. Numerical results presented in tables (2.1), (2.2), (2.3), (2.3) and (2.4) show that all variants keep the appropriate convergence rate. Indeed, in many cases the results are better than expected, specially for the errors in Ω_1. In consequence we observe that in many situations the error in Ω_1 is lower than the error in Ω_2 even if the mesh considered is coarser. This may be a consequence of the mesh regularity and it is convenient for our purposes since in the applications, we are frequently interested in the value of the solutions on the external boundary of the computational domain. We also compare in figures 2.13, 2.14, 2.15 and 2.16, the results obtained for the different couplings and we observe that in many cases, the classical Arlequin coupling provides the lowest error, however we should notice that the use of the new couplings is plenty justified by the computational time saved due to the flexibility on the mesh generation and the reduction of degrees of freedom of the Lagrange multiplier used to impose the matching on the overlapping region. Finally, we remark that similar results are obtained when considering different ratio between the meshes involved and also when γ_e is not a vertex of the mesh for Ω_1. This situation is not shown since it is not compatible with the standard Arlequin method.

	V		**VV**		**VB**		**BV**		**BB**	
h_1	$\|e_1\|$	Slope	$\|e_1\|$	Slope	$\|e_1\|$	Slope	$\|e_1\|$	Slope	$\|e_1\|$	Slope
0.188	0.9400		1.1038		0.7910		1.1377		0.9711	
0.094	0.3126	1.59	0.3628	1.61	0.4191	0.92	0.4280	1.41	0.3310	1.55
0.047	0.0847	1.88	0.0950	1.93	0.1980	1.08	0.1584	1.43	0.1009	1.71
0.023	0.0217	1.97	0.0242	1.97	0.0738	1.42	0.0601	1.40	0.0266	1.92
0.012	0.0055	1.99	0.0061	1.98	0.0218	1.76	0.0192	1.64	0.0068	1.98
0.006	0.0014	1.99	0.0016	1.96	0.0058	1.91	0.0055	1.82	0.0017	1.99
0.003	0.0003	1.98	0.0004	1.87	0.0015	1.97	0.0015	1.90	0.0004	2.00
h_1	$\|e_2\|$	Slope	$\|e_2\|$	Slope	$\|e_2\|$	Slope	$\|e_2\|$	Slope	$\|e_2\|$	Slope
0.188	1.2197		1.3500		1.0080		1.5977		1.0950	
0.094	0.4175	1.54	0.4940	1.44	0.4614	1.12	0.5210	1.61	0.4054	1.43
0.047	0.1132	1.88	0.1389	1.83	0.1982	1.22	0.1800	1.53	0.1191	1.76
0.023	0.0290	1.96	0.0425	1.71	0.0729	1.44	0.0667	1.43	0.0310	1.94
0.012	0.0074	1.97	0.0159	1.41	0.0216	1.75	0.0235	1.51	0.0078	1.98
0.006	0.0019	1.94	0.0071	1.16	0.0058	1.89	0.0086	1.44	0.0020	2.00
0.003	0.0006	1.79	0.0035	1.05	0.0016	1.88	0.0037	1.24	0.0005	2.00

Table 2.1: 1D Convergence table when considering **constant** coefficients and **first order** Lagrange finite elements.

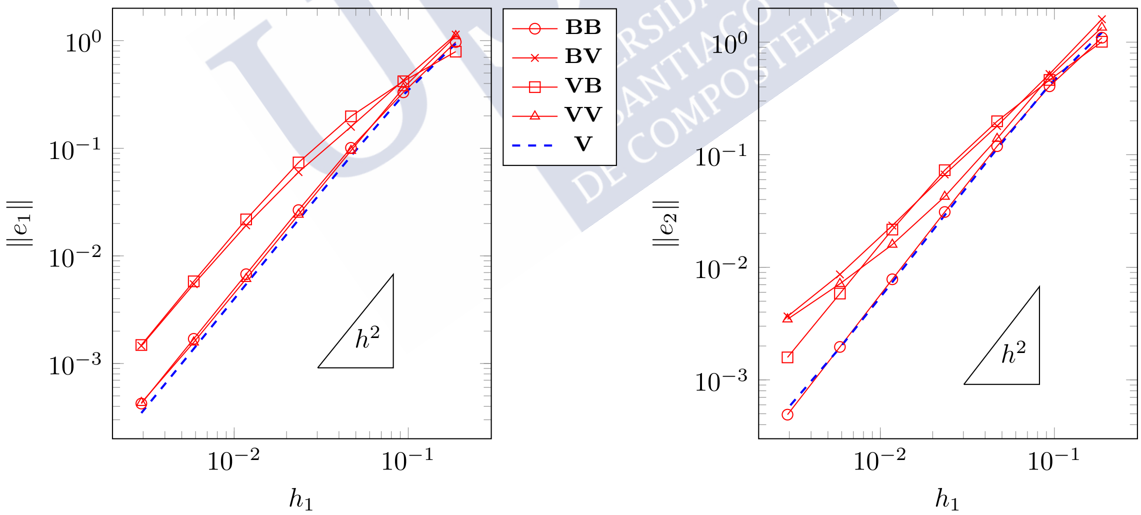

(a) Error in Ω_1.

(b) Error in Ω_2.

Figure 2.13: 1D Convergence curves when considering **constant** coefficients and **first order** Lagrange finite elements.

	V		**VV**		**VB**		**BV**		**BB**	
h_1	$\|e_1\|$	Slope	$\|e_1\|$	Slope	$\|e_1\|$	Slope	$\|e_1\|$	Slope	$\|e_1\|$	Slope
0.188	0.07311508		0.08218405		0.17722290		0.23518313		0.08512613	
0.094	0.00527151	3.79	0.00610804	3.75	0.01899307	3.22	0.01614512	3.86	0.00641142	3.73
0.047	0.00035762	3.88	0.00054219	3.49	0.00126332	3.91	0.00247285	2.71	0.00042985	3.90
0.023	0.00002733	3.71	0.00005828	3.22	0.00008018	3.98	0.00033095	2.90	0.00003019	3.83
0.012	0.00000311	3.14	0.00000868	2.75	0.00000496	4.01	0.00004363	2.92	0.00000252	3.58
0.006	0.00000057	2.44	0.00000156	2.48	0.00000043	3.52	0.00000572	2.93	0.00000026	3.27
0.003	0.00000013	2.12	0.00000031	2.32	0.00000008	2.42	0.00000076	2.92	0.00000003	3.07
h_1	$\|e_2\|$	Slope	$\|e_2\|$	Slope	$\|e_2\|$	Slope	$\|e_2\|$	Slope	$\|e_2\|$	Slope
0.188	0.09527930		0.12404066		0.18608250		0.22725247		0.10025012	
0.094	0.00677510	3.79	0.01737508	2.82	0.01914480	3.26	0.02053839	3.45	0.00727621	3.76
0.047	0.00044125	3.93	0.00406224	2.09	0.00126467	3.91	0.00466064	2.13	0.00046947	3.94
0.023	0.00003159	3.80	0.00101261	2.00	0.00007927	3.99	0.00106040	2.13	0.00002944	3.99
0.012	0.00000424	2.89	0.00025319	2.00	0.00000479	4.04	0.00025659	2.05	0.00000183	4.00
0.006	0.00000097	2.12	0.00006329	2.00	0.00000049	3.28	0.00006351	2.01	0.00000012	3.98
0.003	0.00000024	2.01	0.00001582	2.00	0.00000011	2.13	0.00001583	2.00	0.00000001	3.34

Table 2.2: 1D Convergence table when considering **constant** coefficients and **second order** Lagrange finite elements.

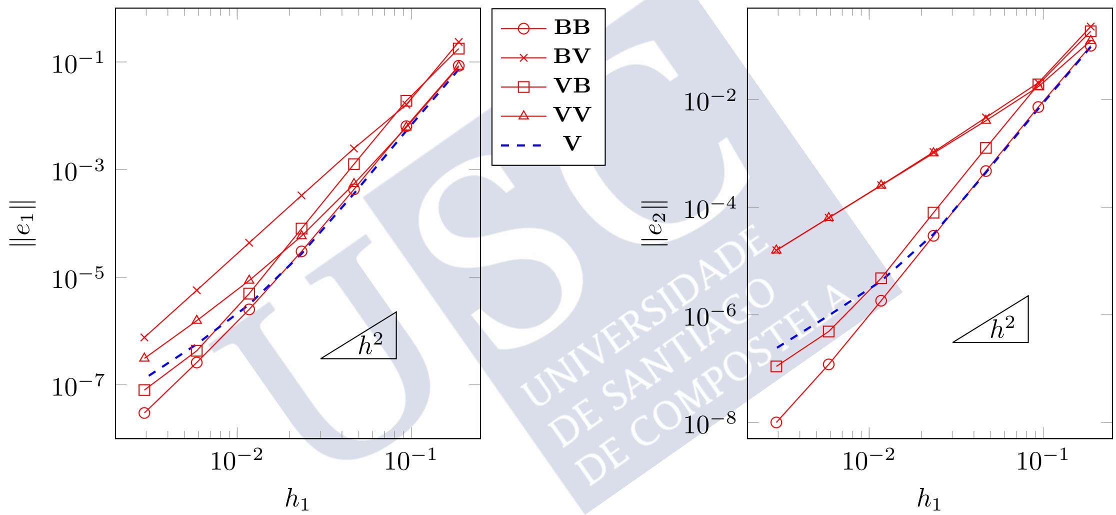

(a) Error in Ω_1.

(b) Error in Ω_2.

Figure 2.14: 1D Convergence curves when considering **constant** coefficients and **second order** Lagrange finite elements.

	V		**VV**		**VB**		**BV**		**BB**	
h_1	$\|e_1\|$	Slope	$\|e_1\|$	Slope	$\|e_1\|$	Slope	$\|e_1\|$	Slope	$\|e_1\|$	Slope
0.188	0.9400		1.3994		1.4821		1.3578		1.1321	
0.094	0.3126	1.59	0.6178	1.18	0.4481	1.73	1.0794	0.33	4.6708	2.04
0.047	0.0847	1.88	0.1250	2.30	0.1752	1.35	0.1442	2.90	0.2261	4.37
0.023	0.0217	1.97	0.0310	2.01	0.0631	1.47	0.0362	1.99	0.0509	2.15
0.012	0.0055	1.99	0.0081	1.94	0.0190	1.73	0.0091	1.99	0.0123	2.05
0.006	0.0014	1.99	0.0023	1.84	0.0052	1.88	0.0023	1.96	0.0030	2.02
0.003	0.0003	1.98	0.0008	1.58	0.0014	1.89	0.0007	1.85	0.0008	2.01
h_1	$\|e_2\|$	Slope	$\|e_2\|$	Slope	$\|e_2\|$	Slope	$\|e_2\|$	Slope	$\|e_2\|$	Slope
0.188	1.2197		1.5463		1.7334		0.7579		1.1788	
0.094	0.4175	1.54	0.5859	1.39	0.6490	1.41	0.6374	0.25	2.7903	1.24
0.047	0.1132	1.88	0.1978	1.56	0.2448	1.40	0.1253	2.34	0.1719	4.01
0.023	0.0290	1.96	0.0658	1.59	0.0866	1.50	0.0367	1.77	0.0416	2.04
0.012	0.0074	1.97	0.0279	1.24	0.0318	1.44	0.0125	1.55	0.0104	2.00
0.006	0.0019	1.94	0.0133	1.07	0.0133	1.26	0.0053	1.25	0.0026	2.00
0.003	0.0006	1.79	0.0066	1.02	0.0062	1.10	0.0025	1.08	0.0007	1.99

Table 2.3: 1D Convergence table when considering **non constant** coefficients and **first order** Lagrange finite elements.

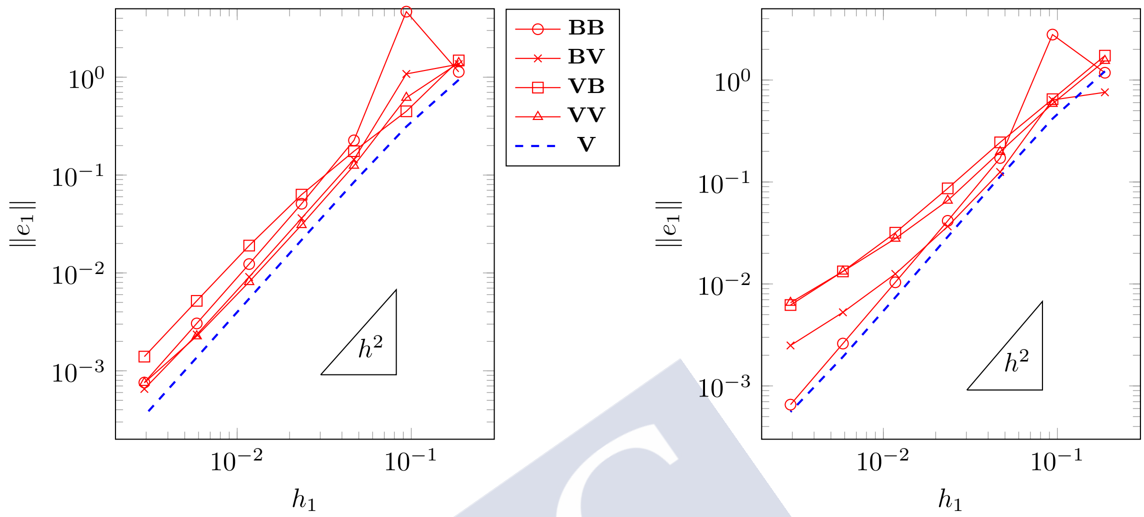

(a) Error in Ω_1. (b) Error in Ω_2.

Figure 2.15: 1D Convergence curves when considering **non constant** coefficients and **first order** Lagrange finite elements.

	V		**VV**		**VB**		**BV**		**BB**	
h_1	$\|e_1\|$	Slope	$\|e_1\|$	Slope	$\|e_1\|$	Slope	$\|e_1\|$	Slope	$\|e_1\|$	Slope
0.188	0.0731151		0.2079332		0.2952978		0.1974475		0.5420031	
0.094	0.0052715	3.79	0.0680007	1.61	0.0710451	2.06	0.0741031	1.41	0.0647866	3.06
0.047	0.0003576	3.88	0.0072167	3.24	0.0072401	3.29	0.0110510	2.75	0.0117974	2.46
0.023	0.0000273	3.71	0.0008437	3.10	0.0008499	3.09	0.0012470	3.15	0.0012466	3.24
0.012	0.0000031	3.14	0.0001136	2.89	0.0001139	2.90	0.0001517	3.04	0.0001513	3.04
0.006	0.0000006	2.45	0.0000174	2.70	0.0000174	2.71	0.0000189	3.01	0.0000188	3.01
0.003	0.0000001	2.11	0.0000029	2.61	0.0000028	2.62	0.0000024	2.98	0.0000023	3.00
h_1	$\|e_2\|$	Slope	$\|e_2\|$	Slope	$\|e_2\|$	Slope	$\|e_2\|$	Slope	$\|e_2\|$	Slope
0.188	0.0952797		0.3423520		0.3533975		0.1334319		0.4670175	
0.094	0.0067751	3.79	0.1395433	1.29	0.1407663	1.32	0.0546393	1.28	0.0622007	2.89
0.047	0.0004413	3.93	0.0195170	2.83	0.0194531	2.85	0.0052051	3.38	0.0063078	3.29
0.023	0.0000318	3.79	0.0054113	1.85	0.0053694	1.85	0.0007398	2.81	0.0003902	4.01
0.012	0.0000046	2.79	0.0013904	1.96	0.0013796	1.96	0.0001748	2.08	0.0000259	3.91
0.006	0.0000013	1.81	0.0003508	1.99	0.0003481	1.99	0.0000435	2.01	0.0000030	3.11
0.003	0.0000005	1.39	0.0000879	2.00	0.0000873	2.00	0.0000109	2.00	0.0000011	1.50

Table 2.4: 1D Convergence table when considering **non constant** coefficients and **second order** Lagrange finite elements.

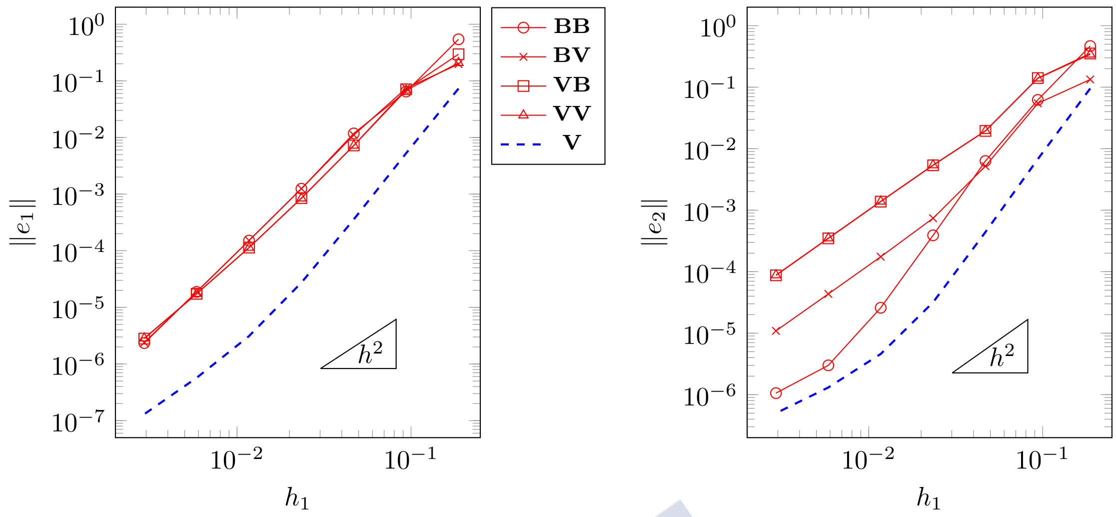

(a) Error in Ω_1.

(b) Error in Ω_2.

Figure 2.16: 1D Convergence curves when considering **non constant** coefficients and **second order** Lagrange finite elements.

2.6.2 2D convergence test

Now our purpose is to develop a similar analysis to exhibit the convergence properties of the method in 2D configurations. However in 2D configurations the computation of an exact solution is usually not a simple task, even when physical coefficients are constant. Thus we propose a very specific numerical test where the expression of the exact solution is known and moreover, the regularity of the solution is enough to expect at least quadratic convergence when second order Lagrange finite elements are applied.

Continuous equations. First, we recap some classical material related to the exact solution of the Helmholtz equation (2.1) in unbounded domains. Let us denote the Dirac's distribution at the origin by $\delta_{\boldsymbol{x}=\boldsymbol{0}}$ and the *Green's function* in dimension two by (see [67])

$$G(\boldsymbol{x}) = \frac{\mathbb{i}}{4} H_0^{(1)}(\ell|\boldsymbol{x}|), \quad \text{where } H_0^{(1)} \text{ is the Hankel function.}$$

Thus, it is known that this function is the unique solution of the following problem in a distributional sense (notice we are considering $\rho = \mu = 1$)

$$\left\{ \begin{array}{rcll} -\,\ell^2\, u \,-\, \operatorname{div}(\nabla u) & = & \delta_{\boldsymbol{x}=\boldsymbol{0}} & \text{in} \quad \mathbb{R}^2, \\ \lim\limits_{|\boldsymbol{x}|\to\infty} \left| \mathbb{i}\,\ell\, u(\boldsymbol{x}) + \partial_{\boldsymbol{n}} u(\boldsymbol{x}) \right| & = & 0. & \end{array} \right.$$

Attending to these considerations, we propose a numerical test such that we know G is the exact solution but set in a domain where the singularity that occurs at the origin is avoided. Thus we consider $\mathcal{O} = [-0.4, 0.4] \times [-0.2, 0.2]$, $\ell = 1$ and we set the problem of finding u such that

$$\left\{ \begin{array}{rcll} -\,\ell^2\, u \,-\, \operatorname{div}(\nabla u) & = & 0 & \text{in} \quad \mathbb{R}^2 \setminus \mathcal{O}, \\ u & = & G & \text{on} \quad \partial\mathcal{O}. \end{array} \right.$$

Moreover, we simulate the unbounded domain by using a Perfect Matching Layer from the literature [68]. Thus in the following we consider the bounded computational domain

$$\Omega = ([-4, 4] \times [-4, 4]) \setminus ([-0.4, 0.4] \times [-0.2, 0.2]).$$

Arlequin formulation. Now, in order to fit in the framework of the different couplings, we chose to decompose the computational domain Ω into the two overlapping regions

$$\begin{aligned} \Omega_1 &= ([-4,4]\times[-4,4]) \setminus ([-0.8,0.8]\times[-0.4,0.4]),\\ \Omega_2 &= ([-2.4,2.4]\times[-2,2]) \setminus ([-0.4,0.4]\times[-0.2,0.2]). \end{aligned}$$

In consequence, the overlapping region is defined by

$$\omega = ([-2.4,2.4]\times[-2,2]) \setminus ([-0.8,0.8]\times[-0.4,0.4])$$

and before providing its decomposition we introduce first (see Figure 2.17)

$$\begin{aligned} \omega_1 &= ([-2.4,2.4]\times[-2,2]) \setminus ([-1.9,1.9]\times[-1.5,1.5])\\ \text{and} \quad \omega_2 &= ([-1.4,1.4]\times[-1,1]) \setminus ([-0.8,0.8]\times[-0.4,0.4]). \end{aligned}$$

Therefore ω_i and ω_e (remember $\omega_c = \omega\setminus\overline{(\omega_i \cup \omega_e)}$) are defined for each variant by:

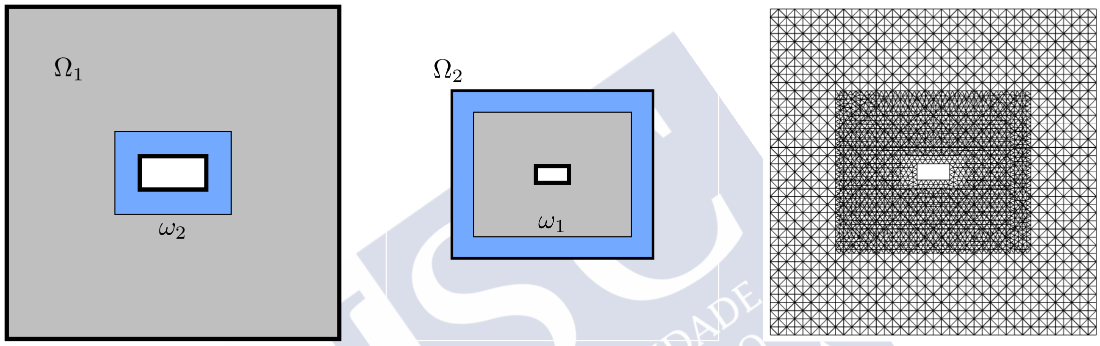

(a) Background media Ω_1 and region ω_2.

(b) The patch.

(c) Plot of the first triangulations of Ω_1 and Ω_2.

Figure 2.17: Specific choice of the domain decomposition for numerical test in Section 2.6.2.

VV: $\omega_i = \omega_2, \quad \omega_e = \omega_1.$ **VB:** $\omega_i = \omega_2, \quad \omega_e = \emptyset.$ **V:** $\omega_i = \emptyset, \quad \omega_e = \omega.$

BB: $\omega_i = \emptyset, \quad \omega_e = \emptyset.$ **BV:** $\omega_i = \emptyset, \quad \omega_e = \omega_1.$

Partitioning. In this occasion, as we have already mentioned, we only consider the case of **constant** physical coefficients as well as the simplest choice of the **partitioning**, i.e.

$$\rho = \mu = 1 \quad \text{and} \quad \alpha_1 = \alpha_2 = \beta_1 = \beta_2 = 1/2.$$

Space discretization. Since we are interested in a general configuration where the domain Ω_1 represents a coarse region, we chose to use a family of three coarse regular meshes where the size of the edges are divided by two from one mesh to the next. On the other hand, the domain Ω_2 is the one that is supposed to capture the shape of the domain in the general case. Thus we chose finer meshes that are obtained using a mesh generator of the literature [69] with mesh size parameter $h_k^\star = 0.12/2^k$ for $k \in \{0,1,2\}$ (see Figure 2.17c for a plot of the first pair of meshes). Notice that the maximum edge length for each pair of meshes is given by

$$\text{Case 1: } h_1 \simeq 0.28,\ h_2 \simeq 0.17, \quad \text{Case 2: } h_1 \simeq 0.14,\ h_2 \simeq 0.09, \quad \text{Case 3: } h_1 \simeq 0.07,\ h_2 \simeq 0.04.$$

In order to compare all the formulations, the meshes we use are also chosen to satisfy some conformity properties that allow to use the same meshes for all the different variants of the method. More precisely, we have chosen the meshes for Ω_2 to be conform with ω_2 while the meshes for Ω_1 are conform with both ω_1 and ω in such a way that the classic Arlequin method can also be used. In this way, as explained in Section 2.5 the spaces of multipliers are build with sub-meshes of the meshes of Ω_1 and Ω_2 and thus the uniform *discrete Inf-Sup condition* is automatically satisfied.

Regularity of the solution. Notice that the primal variable $\boldsymbol{u} = (G_{|\Omega_1}, G_{|\Omega_2})$ belongs to $\mathcal{C}^\infty(\Omega_1) \times \mathcal{C}^\infty(\Omega_2)$, however the regularity of the Lagrange multiplier will be low due to the corners introduced on its domain of definition. More precisely, according to Theorem 2.28, if the multiplier λ_j with $j \in \{i, e\}$ is of boundary type, we can not expect better than $\lambda_j \in H^{\frac{1}{2}-\varepsilon}(\gamma_j)$ for $\varepsilon > 0$ and if the multiplier λ_j with $j \in \{i, e\}$ is of volume type, we can not expect better than $\lambda_j \in H^\sigma(\omega_j)$ for all $\sigma < \frac{5}{3}$.

Convergence results Notice that according to the regularity of the solution $(\boldsymbol{u}, \boldsymbol{\lambda})$ and taking into account the corollaries in Section 2.5.2, we can not guaranty optimal convergence rates even when first order Lagrange finite elements are considered. However we do not know precisely the regularity of the Lagrange multiplier and we can not say a priory the expected convergence rate. Thus, we analyse the behaviour of the relative error of the solution by comparing it with respect to the exact solution which is known. Notice that we consider the notation introduced in (2.81) in order to analyse the convergence behaviour of the relative error separately for each component of the solution. Numerical results presented in Table 2.5 and Figure 2.18 show that all variants keep the appropriate convergence rate when first order finite elements are applied. Indeed, we observe that the error in Ω_1 behaves similarly to $\mathcal{O}(h^{1.5})$ for all the couplings, which is better than expected. Moreover, we notice that for the error in Ω_2 this effect is only observed for the boundary-boundary coupling where we observe a behaviour similar to $\mathcal{O}(h^{1.6})$ while all the other couplings behave like $\mathcal{O}(h)$. However, as we show in Table 2.6 and Figure 2.19, when second order finite elements are considered, the results are not optimal. We observe that the error in Ω_1 behaves as $\mathcal{O}(h^2)$, but the error in Ω_2 is suboptimal and behaves as $\mathcal{O}(h^{1.3})$ in the best case. In the next section we discuss the cause of this sub-optimality and we propose alternative formulations to overcome this drawback.

	V		**VV**		**VB**		**BV**		**BB**	
h_1	$\|e_1\|$	Slope	$\|e_1\|$	Slope	$\|e_1\|$	Slope	$\|e_1\|$	Slope	$\|e_1\|$	Slope
0.28	0.0192		0.0192		0.0190		0.0215		0.0213	
0.14	0.0065	1.57	0.0065	1.57	0.0064	1.56	0.0071	1.60	0.0070	1.60
0.07	0.0023	1.48	0.0023	1.48	0.0023	1.48	0.0024	1.54	0.0024	1.54
h_1	$\|e_2\|$	Slope	$\|e_2\|$	Slope	$\|e_2\|$	Slope	$\|e_2\|$	Slope	$\|e_2\|$	Slope
0.28	0.0302		0.0316		0.0276		0.0179		0.0090	
0.14	0.0156	0.96	0.0166	0.93	0.0149	0.89	0.0078	1.20	0.0028	1.71
0.07	0.0083	0.91	0.0085	0.96	0.0077	0.95	0.0037	1.07	0.0009	1.66

Table 2.5: 2D Convergence table when considering **constant** coefficients and **first order** Lagrange finite elements.

	V		**VV**		**VB**		**BV**		**BB**	
h_1	$\|e_1\|$	Slope	$\|e_1\|$	Slope	$\|e_1\|$	Slope	$\|e_1\|$	Slope	$\|e_1\|$	Slope
0.28	0.00310		0.00310		0.00310		0.00303		0.00303	
0.14	0.00072	2.11	0.00072	2.11	0.00072	2.11	0.00070	2.13	0.00070	2.13
0.07	0.00018	1.99	0.00018	1.99	0.00018	1.99	0.00017	2.01	0.00017	2.01
h_1	$\|e_2\|$	Slope	$\|e_2\|$	Slope	$\|e_2\|$	Slope	$\|e_2\|$	Slope	$\|e_2\|$	Slope
0.28	0.00370		0.00381		0.00376		0.00137		0.00124	
0.14	0.00157	1.24	0.00159	1.26	0.00158	1.25	0.00049	1.49	0.00047	1.41
0.07	0.00073	1.09	0.00074	1.11	0.00074	1.10	0.00019	1.35	0.00019	1.32

Table 2.6: 2D Convergence table when considering **constant** coefficients and **second order** Lagrange finite elements.

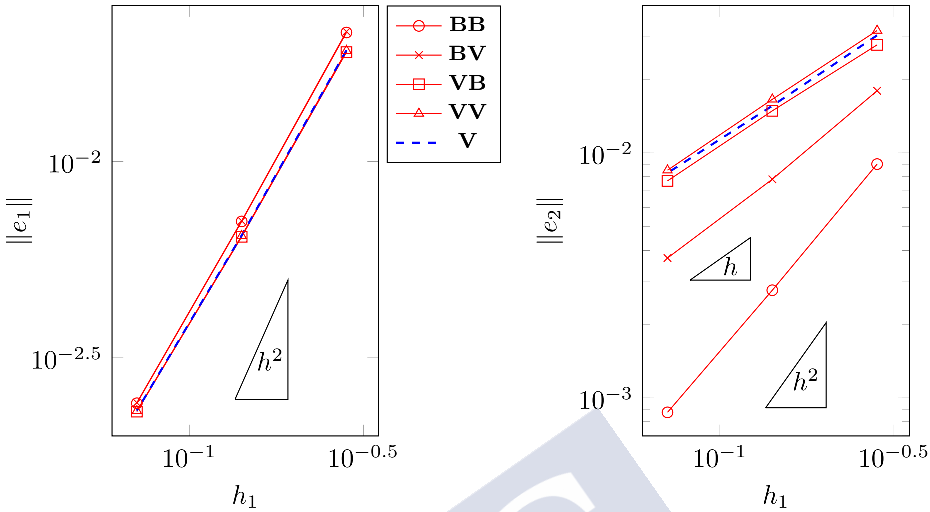

(a) Error in Ω_1.

(b) Error in Ω_2.

Figure 2.18: 2D Convergence curves when considering **constant** coefficients and **first order** Lagrange finite elements.

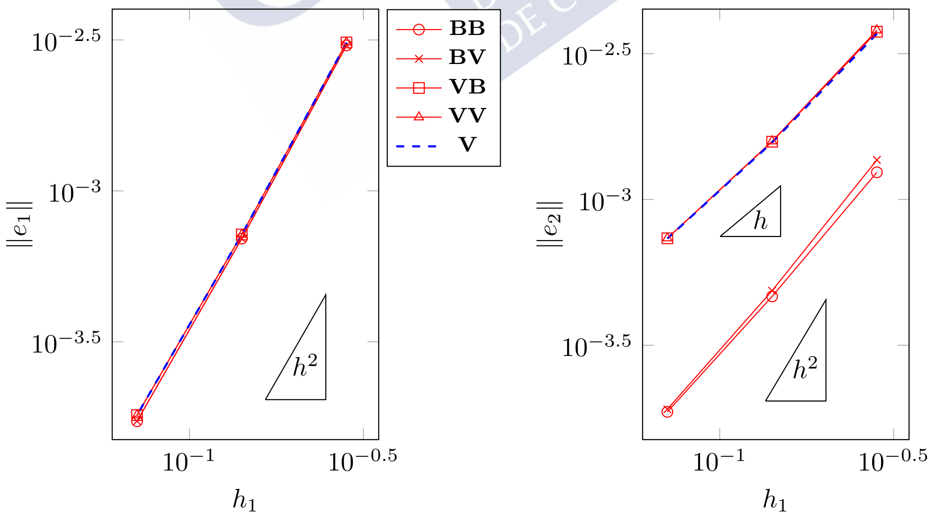

(a) Error in Ω_1.

(b) Error in Ω_2.

Figure 2.19: 2D Convergence curves when considering **constant** coefficients and **second order** Lagrange finite elements.

2.7 Improved Arlequin formulations for polygonal overlapping regions

In this section, our purpose is to first analyse the cause of the sub-optimality observed in the previous section to then propose an alternative approach that improves the numerical scheme. In principle, the formulations that we have proposed are totally compatible with high order discretizations. Indeed in the 1D configuration we have observed optimal convergence for the proposed numerical test. However, the reader should notice that attending to Theorem 2.41, the convergence in the primal variable $\boldsymbol{u}$ is affected by the convergence of the Lagrange multiplier $\boldsymbol{\lambda}$. Thus, the lack of regularity on the Lagrange multiplier is the responsible of the sub-optimality observed due to the approximation properties of the discrete Lagrange multipliers spaces (see Proposition 2.44 and Corollary 2.45).

- On the one hand, when a **volume multiplier** is considered (even in classic Arlequin), we observe that it can be interpreted as the solution of a Laplace like problem (see Section 2.3) where the source depends in the primal variable $\boldsymbol{u}$ and the choice of the partitioning. Thus, if both the partitioning and the primal solution are regular in the coupling region, the regularity of the Lagrange multiplier only depends on the geometry of the coupling region (see Theorems 2.14 and 2.28). However, we notice that we are choosing a geometry for the volume Lagrange multiplier that has corners (some of them reentrant). In consequence, it is known that the regularity will be low and also the order of convergence (see corollaries in Section 2.5.2).
- On the other hand, when a **boundary multiplier** is considered, the Lagrange multiplier is interpreted as the normal derivative of the solution (see Section 2.3). Thus, also due to the existence of corners where the normal vector $\boldsymbol{n}$ jumps, we can not expect the boundary multiplier to be more regular than $H^{\frac{1}{2}-\varepsilon}(\gamma)$ for $\varepsilon > 0$ on any closed boundary γ (see Theorem 2.28). In consequence, the order of convergence is also penalised (see corollaries in Section 2.5.2).

These considerations not only explain the sub-optimality observed in Figure 2.19b, but also why this effect is not observed in the 1D case, where these phenomena are not present. Moreover, we remark that this effect is somehow artificial, since it is due to the Lagrange multipliers and not to the primal variable $\boldsymbol{u}$ which we are interested in. Thus a different choice in the introduction of the Lagrange multipliers and their approximation spaces may help to overcome this drawback of the method.

A first naive idea would be to simply avoid the existence of corners in the coupling regions. Notice that this is always possible since the corners we want to avoid are not the corners of Ω but the corners of ω and ω_c. Thus, for instance in the example described in Section 2.6.2, we could consider

$$\begin{aligned} \Omega_1 &= ([-4,4]\times[-4,4]) \setminus \mathcal{D}(\mathbf{0},0.6), \\ \Omega_2 &= \mathcal{D}(\mathbf{0},2) \setminus ([-0.4,0.4]\times[-0.2,0.2]), \end{aligned}$$

where $\mathcal{D}(\boldsymbol{x}, r)$ denotes the disc of radius r and centred at $\boldsymbol{x}$. With this decomposition, we first notice that we avoid the existence of any corner in the overlapping region $\omega = \mathcal{D}(\mathbf{0},2)\setminus\mathcal{D}(\mathbf{0},0.5)$, as well as on its boundaries γ_i and γ_e. Moreover, in order to avoid also the existence of corners in ω_c (and thus in ω_i and ω_e) we decompose ω, as we did in Section 2.6.2, by introducing (see Figure 2.20)

$$\begin{aligned} \omega_1 &= \mathcal{D}(\mathbf{0},2) \setminus \mathcal{D}(\mathbf{0},1.6) \\ \text{and} \quad \omega_2 &= \mathcal{D}(\mathbf{0},1) \setminus \mathcal{D}(\mathbf{0},0.6). \end{aligned}$$

Next we remark that with this approach, we should reconsider the spaces of finite elements we have introduced in Section 2.5 and provide a different framework to treat with optimality the consideration of curved domains. This question has already been treated in the literature for different problems by considering isoparametric finite elements (see for instance [64]). However,

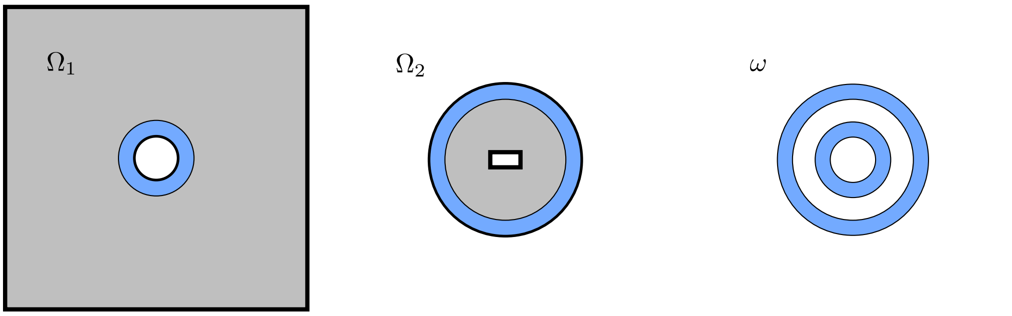

(a) Background media. (b) The patch. (c) Decomposition of the overlapping region.

Figure 2.20: Sketch of a choice of domain decomposition that avoids corners in ω_c.

we do not consider this approach since it has two main drawbacks related to our context of application. The first is technical and related to the intersection algorithms we consider [41], which are not easy to extend for curved finite elements. The second is related to the interest of the methods we propose. As we have already mentioned, one of our main objectives is to provide a framework where we can solve a large family of problems without re-meshing. However, with this choice of the domain decomposition, it is not clear how to proceed in order to have from a mesh of the background media Θ, a systematic approach to obtain a mesh for Ω_1 for each new configuration.

In the following, we develop a different approach where, under reasonable assumptions, we are able to improve the convergence properties of the resultant numerical scheme without losing any flexibility of the method. We remark that we will proceed very differently when the coupling is of boundary type than when it is of volume type. In the case of boundary couplings we provide a different approximation space (based in mortar finite elements, see for instance [56]) that provides optimal convergence properties for the method (if the data is regular). However, in the case of volume couplings we modify the formulation in order to obtain more regular Lagrange multipliers, as a result, we will present a numerical scheme which is optimal at least when second order finite elements are considered (if the data is regular).

2.7.1 Boundary-Boundary coupling

In this section our purpose is to provide a better choice for the approximation of the space $M_{BB} = [H^{\frac{1}{2}}(\gamma_i)]' \times [H^{\frac{1}{2}}(\gamma_e)]'$ in presence of corners. In order to motivate the introduction of the new choice, we first point out the main drawback of considering $M_{BB,h} = X_{p_1}(\mathcal{G}_{i,h}) \times X_{p_2}(\mathcal{G}_{e,h})$ as we have introduced in (2.58). For that purpose, we first introduce the sets χ_i and χ_e of corners that separate both γ_i and γ_e respectively into two families of **smooth** curves (see Figure 2.21)

$$\{\gamma_{i,k}\}_{k=1}^{s_i} \quad \text{such that} \quad \gamma_i = \bigcup_{k=1}^{s_i} \gamma_{i,k} \quad \text{and} \quad \gamma_{i,k} \cap \gamma_{i,j} \in \chi_i \quad \text{if} \quad k \neq j, \tag{2.82}$$

$$\{\gamma_{e,k}\}_{k=1}^{s_e} \quad \text{such that} \quad \gamma_e = \bigcup_{k=1}^{s_e} \gamma_{e,k} \quad \text{and} \quad \gamma_{e,k} \cap \gamma_{e,j} \in \chi_e \quad \text{if} \quad k \neq j. \tag{2.83}$$

Thus notice that in this context, if the primal variable $\boldsymbol{u}$ is regular (for instance, $\boldsymbol{u} \in H^\sigma(\Omega_1) \times H^\sigma(\Omega_2)$, with $\sigma \geq 2$), then, each Lagrange multiplier λ_j with $j \in \{i, e\}$ is also regular on the respective $\gamma_{j,k}$ with $k \in \{1, \ldots, s_j\}$ (indeed $\lambda_{j|\gamma_{j,k}} \in H^{\sigma-\frac{3}{2}}(\gamma_{j,k})$), even if they are not so regular on the total γ_j, since $\boldsymbol{n}$ is discontinuous on corners (note that in any case $\lambda_j \in H^{\frac{1}{2}-\varepsilon}(\gamma_j) \subset L^2(\gamma_j)$)

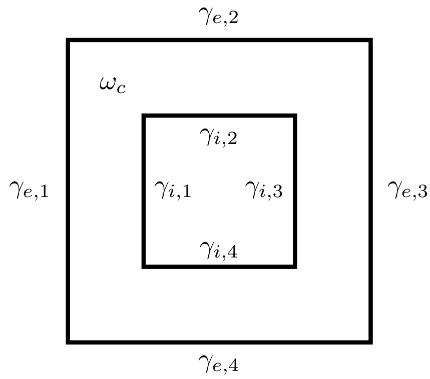

Figure 2.21: Sketch of the decomposition of the boundaries γ_i and γ_e.

for $\varepsilon > 0$). In this context, we also notice that for all $\boldsymbol{m}_h \in M_{BB,h}$ we have (for $j \in \{i, e\}$)

$$\begin{aligned}
\|\lambda_j - m_{j,h}\|_{[H^{\frac{1}{2}}(\gamma_j)]'} &= \sup_{\phi \in H^{\frac{1}{2}}(\gamma_j)} \frac{(\phi, \lambda_j - m_{j,h})_{L^2(\gamma_j)}}{\|\phi\|_{H^{\frac{1}{2}}(\gamma_j)}} \leq \sup_{\phi \in H^{\frac{1}{2}}(\gamma_j)} \sum_{k=1}^{s_j} \frac{(\phi, \lambda_j - m_{j,h})_{L^2(\gamma_{j,k})}}{\|\phi\|_{H^{\frac{1}{2}}(\gamma_{j,k})}} \\
&\leq \sum_{k=1}^{s_j} \sup_{\phi \in H^{\frac{1}{2}}(\gamma_j)} \frac{(\phi, \lambda_j - m_{j,h})_{L^2(\gamma_{j,k})}}{\|\phi\|_{H^{\frac{1}{2}}(\gamma_{j,k})}} = \sum_{k=1}^{s_j} \|\lambda_j - m_{j,h}\|_{[H^{\frac{1}{2}}(\gamma_{j,k})]'}
\end{aligned}$$

and therefore, for all $\boldsymbol{m}_h \in M_{BB,h}$ we have that

$$\begin{aligned}
\|\boldsymbol{\lambda} - \boldsymbol{m}_h\|_{M_{BB}} &\leq \|\lambda_i - m_{i,h}\|_{[H^{\frac{1}{2}}(\gamma_i)]'} + \|\lambda_e - m_{e,h}\|_{[H^{\frac{1}{2}}(\gamma_e)]'} \\
&\leq \sum_{k=1}^{s_i} \|\lambda_i - m_{i,h}\|_{[H^{\frac{1}{2}}(\gamma_{i,k})]'} + \sum_{k=1}^{s_e} \|\lambda_e - m_{e,h}\|_{[H^{\frac{1}{2}}(\gamma_{e,k})]'}.
\end{aligned}$$

However, in general, due to continuity of $m_{i,h}$ and $m_{e,h}$

$$\begin{aligned}
\inf_{\boldsymbol{m}_h \in M_{BB,h}} \|\boldsymbol{\lambda} - \boldsymbol{m}_h\| \not\leq & \sum_{k=1}^{s_i} \inf_{m_{i,h} \in X_{p_1}(\mathcal{G}_{i,h})} \|\lambda_i - m_{i,h}\|_{[H^{\frac{1}{2}}((\gamma_{i,k}))]'} \\
&+ \sum_{k=1}^{s_e} \inf_{m_{e,h} \in X_{p_2}(\mathcal{G}_{e,h})} \|\lambda_e - m_{e,h}\|_{[H^{\frac{1}{2}}((\gamma_{e,k}))]'}.
\end{aligned} \tag{2.84}$$

Thus, we can not bound the error of the Lagrange multiplier by its error on each part of the boundary, where the Lagrange multiplier may be regular if the primal variable $\boldsymbol{u}$ is regular. This is the main reason of the suboptimal convergence of the Lagrange multiplier and the subsequent suboptimal convergence of the primal variable. Thus, our purpose is to provide a new approximation space $M_{BB,h}$ that allows discontinuities on corners (thus the previous inequality trivially holds) while keeping the good approximation properties in the sense of Corollary 2.45.

2.7.1.1 New approximation space

The reader may notice that similar difficulties arise in other contexts such as the theory of mortar finite elements (see [56] for a monograph). Therefore, we will follow the same ideas in order to introduce new approximation spaces for the Lagrange multipliers. Note, that in mortar finite elements two different approaches are usually used and in the following we will refer to them as *classic* (see [5, 6, 7, 55]) or *dual* (see [70, 71, 72, 73, 74, 75]). Thus we choose to introduce as approximation space for the Lagrange multipliers (note *op* refers to the option, *cl* for *classic* or *du* for *dual*)

$$M_{BB,h} = M_{B_i,h} \times M_{B_e,h},$$

$$\text{with} \quad M_{B_j,h} = \{m_{j,h} \ / \ m_{j,h|\gamma_{j,k}} \in Y_{p_j}^{op}(\mathcal{G}_{j,k}),\ 1 \leq k \leq s_j\}, \quad \text{for } j \in \{i,e\} \text{ and } op \in \{cl, du\},$$

where we denote by $\mathcal{G}_{j,k}$ the restrictions to $\gamma_{j,k}$ of the 1D mesh $\mathcal{G}_{j,h}$ (defined in Assumptions I.8 and I.9) and we have introduced the spaces $Y_{p_j}^{op}(\mathcal{G}_{j,k})$ that we define next depending in the option we consider:

For the *classic* approach $op = cl$ (see [5, 6, 7, 55]) we choose to introduce the mortar finite elements spaces (see Figure 2.22)

$$\begin{aligned} Y_{p_j}^{cl}(\mathcal{G}_{j,k}) = \{m_h \in \mathcal{C}^0(\gamma_{j,k}) \quad \text{such that} \quad & \forall \kappa \in \mathcal{G}_{j,k},\ m_{h|\kappa} \in \mathcal{P}_{p_j} \\ \text{and} \quad & m_{h|\kappa} \in \mathcal{P}_{p_j - 1} \text{ if } \kappa \cap \chi_j \neq \emptyset\}. \end{aligned} \tag{2.85}$$

(a) When considering **first order** finite elements. (b) When considering **second order** finite elements.

Figure 2.22: Basis functions of $M_{B_j,h}^{cl}$ in the interior and at the corner. Notice that ■ denotes the vertex in the corner while each • denotes a degree of freedom.

For the *dual* approach $op = du$ (see [70, 71, 72, 73, 74, 75]) the introduction of the spaces $Y_{p_j}^{du}(\mathcal{G}_{j,k})$ is more involved, therefore in this document we restrict ourselves to first and second order finite elements (see Figure 2.23) and refer to [71] for the general order. We will introduce the spaces by providing the respective basis functions, thus we consider the boundary $\gamma_{j,k}$ to be parametrized by $\boldsymbol{x}(s)$ where $s \in [0, |\gamma_{j,k}|]$ is the abscissa along $\gamma_{j,k}$. Moreover, we denote by $\{\vartheta_l\}_{l=0}^{L+1}$ the set of values of s such that $\{\boldsymbol{x}(\vartheta_l)\}_{l=0}^{L+1}$ is a vertex of $\mathcal{G}_{i,k}$ (note that $\vartheta_0 = 0$ and $\vartheta_{L+1} = |\gamma_{j,k}|$ represent the corners $\boldsymbol{x}(\vartheta_0)$ and $\boldsymbol{x}(\vartheta_{L+1})$ in χ_j). Then, for the first order finite elements we denote by $\{\zeta_1^l\}_{l=1}^{L}$ the basis of the space $Y_1^{cl}(\mathcal{G}_{j,k})$ (see Figure 2.22a) and we introduce the space (see Figure 2.23a)

$$Y_1^{du}(\mathcal{G}_{j,k}) = \operatorname*{span}_{1 \leq l \leq L} \{\xi_1^l\} \quad \text{where}$$

$$\xi_1^1(s) = \begin{cases} 1,\ s \in [0, \vartheta_1], \\ 0,\ \text{elsewhere}, \end{cases} \quad \xi_1^L(s) = \begin{cases} 1,\ s \in [\vartheta_L, \vartheta_{L+1}], \\ 0,\ \text{elsewhere}, \end{cases} \quad \xi_1^l(s) = \begin{cases} 2\zeta_1^l(s) - \zeta_1^{l-1}(s),\ s \in [\vartheta_{l-1}, \vartheta_l], \\ 2\zeta_1^l(s) - \zeta_1^{l+1}(s),\ s \in [\vartheta_l, \vartheta_{l+1}], \\ 0,\ \text{elsewhere}. \end{cases}$$

Now, for the second order finite elements we denote by $\{\zeta_2^l\}_{l=1}^{2L+1}$ the basis of the space $Y_2^{cl}(\mathcal{G}_{j,k})$ (see Figure 2.22b) and we introduce the space (see Figure 2.23b)

$$Y_2^{du}(\mathcal{G}_{j,k}) = \operatorname*{span}_{1 \leq l \leq 2L+1} \{\xi_2^l\} \quad \text{where} \tag{2.86}$$

$$\xi_2^1(s) = \begin{cases} 2\frac{\vartheta_1 - s}{\vartheta_1}, & s \in [0, \vartheta_1], \\ 0, & \text{elsewhere}, \end{cases} \qquad \xi_2^2(s) = \begin{cases} \frac{2s-\vartheta_1}{\vartheta_1}, & s \in [0, \vartheta_1], \\ \zeta_2^2(s) - \frac{3}{4}\zeta_2^3(s) + \frac{1}{2}, & s \in [\vartheta_1, \vartheta_2], \\ 0, & \text{elsewhere}, \end{cases}$$

$$\xi_2^{2L+1}(s) = \begin{cases} 2\frac{s-\vartheta_L}{\vartheta_{L+1}-\vartheta_L}, & s \in [\vartheta_L, \vartheta_{L+1}], \\ 0, & \text{elsewhere}, \end{cases} \qquad \xi_2^{2L}(s) = \begin{cases} \zeta_2^{2L}(s) - \frac{3}{4}\zeta_2^{2L-1}(s) + \frac{1}{2}, & s \in [\vartheta_{L-1}, \vartheta_L], \\ \frac{2s-\vartheta_L-\vartheta_{L+1}}{\vartheta_L-\vartheta_{L+1}}, & s \in [\vartheta_L, \vartheta_{L+1}], \\ 0, & \text{elsewhere}, \end{cases}$$

$$\xi_2^{2l+1}(s) = \begin{cases} \frac{5}{2}\zeta_2^{2l+1}(s) - 1, & s \in [\vartheta_l, \vartheta_{l+1}], \\ 0, & \text{elsewhere}, \end{cases} \qquad \xi_2^{2l}(s) = \begin{cases} \zeta_2^{2l}(s) - \frac{3}{4}\zeta_2^{2l-1}(s) + \frac{1}{2}, & s \in [\vartheta_{l-1}, \vartheta_l], \\ \zeta_2^{2l}(s) - \frac{3}{4}\zeta_2^{2l+1}(s) + \frac{1}{2}, & s \in [\vartheta_l, \vartheta_{l+1}], \\ 0, & \text{elsewhere}. \end{cases}$$

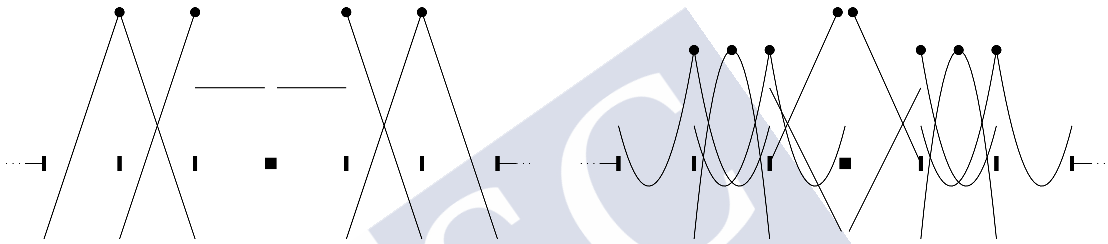

(a) When considering **first order** finite elements. (b) When considering **second order** finite elements.

Figure 2.23: Basis functions of $M^{du}_{B_j,h}$ in the interior and at the corner. Notice that ■ denotes the vertex in the corner while each • denotes a degree of freedom.

In both cases, the spaces $Y_p^{op}(\cdot)$ for $op \in \{cl, du\}$ and arbitrary order p, are known to satisfy adequate approximations properties as we present in the following result.

Theorem 2.66

Let us consider a family of 1D quasi-uniform meshes $\mathcal{F}_h$ conform with a given region ϑ. Then, the spaces $Y_p^{op}(\mathcal{F}_h)$ for $op \in \{cl, du\}$ are such that there exist constants $K_1 > 0$ and $K_2 > 0$ independent of h such that if $v \in H^\sigma(\vartheta)$

$$\text{for } \sigma \in [0,p] \text{ then } \quad \inf_{v_h \in Y_p^{op}(\mathcal{F}_h)} \|v - v_h\|_{[H^{\frac{1}{2}}(\vartheta)]'} \quad \leq \quad K_1 h^{\sigma+\frac{1}{2}} \|v\|_{H^\sigma(\vartheta)}.$$

Proof. On the one hand, for the case $op = cl$ we refer to (17) in [7] for the precise result. On the other hand, for the case $op = du$ we refer to (Sb) in [56] where the author shows that

$$\text{for } \sigma \in [0,p] \text{ then } \quad \inf_{v_h \in Y_p^{du}(\mathcal{F}_h)} \|v - v_h\|_{L^2(\vartheta)} \quad \leq \quad K_0 h^\sigma \|v\|_{H^\sigma(\vartheta)}.$$

Then, we can conclude with the same arguments we have used in Corollary 2.45.

■

As we have already mentioned, the discontinuities in corners allow (2.84) to hold and combined with the previous theorem we obtain the following approximation property.

Corollary 2.67

There exists a constant $K > 0$ independent of h such that, for $\boldsymbol{\lambda}$ satisfying $\lambda_{j|\gamma_{j,k}} \in H^\sigma(\gamma_{j,k})$

for $j \in \{i, e\}$, $k \in \{1, \ldots, s_j\}$ *and* $\sigma \in [0, \min\{p_i, p_e\}]$, *then*

$$\inf_{\boldsymbol{m}_h \in M_{BB,h}} \|\boldsymbol{\lambda} - \boldsymbol{m}_h\|_{[H^{\frac{1}{2}}(\gamma_i)]' \times [H^{\frac{1}{2}}(\gamma_e)]'} \leq K h^{\sigma + \frac{1}{2}} \max_{j,k} \|\lambda_j\|_{H^{\sigma}(\gamma_{j,k})}.$$

Moreover we remark that, similarly to Corollary 2.47, we can prove that Corollary 2.67 implies the verification of the approximation property (**P.2**).

2.7.1.2 Discrete Inf-Sup condition

Notice that in the definition of the space $M_{BB,h}$ we also reduce one order the degree of the polynomials in the elements intersecting corners. This consideration is technical and it is related to the verification of uniform *discrete Inf-Sup condition* (**P.3**). A close look to the proof we have given in Theorem 2.56, reveals that with the new choice of $M_{BB,h}$ inequality (2.77) is no longer true (since now $m_{j,h} \in M_{B_j,h}$ for $j \in \{i, e\}$ are discontinuous and do not belong to $X_{p_j}(\mathcal{G}_{j,h})$). In consequence, we require the introduction of different projection operators than $P^h_{\gamma_j}$ for $j \in \{i, e\}$ such that the proof in Theorem 2.56 is still valid. More precisely, we need a projection from $L^2(\gamma_i)$ into $X_{p_j}(\mathcal{G}_{j,h})$ (or at least a subspace) which considers $M_{B_j,h}$ as the space of test functions and moreover the projection should be stable in the norm of $H^{\frac{1}{2}}(\gamma_j)$.

In the context of mortar finite elements, this issue is treated by the introduction of the usually called mortar projection (for $j \in \{i, e\}$)

$$Q^h_{\gamma_j} : L^2(\gamma_j) \to X^0_{p_j}(\mathcal{G}_{j,h}) = \{v_h \in X_{p_j}(\mathcal{G}_{j,h}) \text{ such that } v_h(\boldsymbol{x}) = 0 \ \forall \boldsymbol{x} \in \chi_j\},$$

that for every $\phi \in L^2(\gamma_j)$ assigns $Q^h_{\gamma_j}\phi \in X^0_{p_j}(\mathcal{G}_{j,h})$ satisfying

$$(Q^h_{\gamma_j}\phi, m_h)_{L^2(\gamma_j)} = (\phi, m_h)_{L^2(\gamma_j)}, \quad \forall m_h \in M_{B_j,h}.$$

We remark that, for $j \in \{i, e\}$, these operators project into $X^0_{p_j}(\mathcal{G}_{j,h})$ which under Assumptions I.8 and I.9 are subspaces of the traces of the $W_{1,h}$ and $W_{2,h}$ respectively, which allows a later extension to the whole domain. Moreover, we also note that the spaces $M_{B_j,h}$ and $X^0_{p_j}(\mathcal{G}_{j,h})$ (for $j \in \{i, e\}$) have the same dimension, this is not enough to ensure that $Q^h_{\gamma_j}$ is well defined, however it simplifies the analysis (see Proposition 2.21 in [64]). For a detailed proof of the well definition of the mortar projection $Q^h_{\gamma_j}$, we refer to Lemma 1.3 in [56] where moreover, it is proved to be L^2-stable and H^1_0-stable. However, as we mentioned before, in Theorem 2.56, the stability of $P^h_{\gamma_j}$ (that we want to substitute by $Q^h_{\gamma_j}$) in the norm of $H^{\frac{1}{2}}(\gamma_j)$ plays an important role in the proof of uniform *discrete Inf-Sup condition*. In consequence, in the literature of mortar finite elements, the resultant uniform *discrete Inf-Sup conditions* are usually obtained considering different norms for the Lagrange multipliers.

See [55] for a proof with the norm defined by $\quad \|\lambda_j\|^2 = \sum_{k=1}^{N_j} \|\lambda_j\|^2_{[H^{\frac{1}{2}}_{00}(\gamma_{j,k})]'}$.

See [76] for a proof with the mesh dependent L^2-norm defined by $\quad \|\lambda_j\|^2 = \sum_{\kappa \in \mathcal{G}_{j,h}} h_\kappa \|\lambda_j\|^2_{L^2(\kappa)}$.

However, in [75] we can find a proof of uniform *discrete Inf-Sup condition* for the dual norm $\|\cdot\|_{[H^{\frac{1}{2}}(\gamma_j)]'}$ in a context which is not general for the mortar framework and where the Lagrange multipliers space is built considering the *dual* spaces $Y^{du}_{p_j}(\mathcal{G}_{j,k})$ (defined in (2.7.1.1) and (2.86)). Since our framework is also different than the general mortar, we are able here to adapt the technique. The analysis is based in the introduction of slightly different projection operators (for $j \in \{i, e\}$)

$$\widetilde{Q}^h_{\gamma_j} : L^2(\gamma_j) \to \widetilde{X}_{p_j}(\mathcal{G}_{j,h}), \quad \text{where } \widetilde{X}_{p_j}(\mathcal{G}_{j,h}) \subset X_{p_j}(\mathcal{G}_{j,h}) \text{ and } \dim(\widetilde{X}_{p_j}(\mathcal{G}_{j,h})) = \dim(M_{B_j,h}).$$

We note that the spaces $\widetilde{X}_{p_j}(\mathcal{G}_{j,h})$ have the standard approximation properties in the sense of Proposition 2.44, since only the basis functions associated with a node adjacent to a corner are modified. In particular, if we denote by ξ_0 a basis function of $X_{p_j}(\mathcal{G}_{j,h})$ associated to a corner and by ξ_1 the adjacent basis function, then $\widetilde{X}_{p_j}(\mathcal{G}_{j,h})$ does not have a basis function associated to the corner and the adjacent basis function is defined by $\widetilde{\xi}_1 = \xi_1 + 0.5\,\xi_0$ (see Figure 2.24). Thus, for

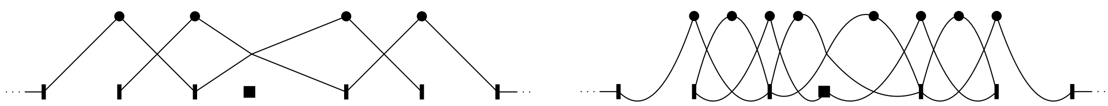

(a) When considering **first order** finite elements. (b) When considering **second order** finite elements.

Figure 2.24: Basis functions of $\widetilde{X}_{p_j}(\mathcal{G}_{j,h})$ in the interior and next to the corner. Notice that $\blacksquare$ denotes the node in the corner while each $\bullet$ denotes a degree of freedom.

every $\phi \in L^2(\gamma_j)$ we assign $\widetilde{Q}^h_{\gamma_j}\phi \in \widetilde{X}_{p_j}(\mathcal{G}_{j,h})$ satisfying

$$(\widetilde{Q}^h_{\gamma_j}\phi, m_h)_{L^2(\gamma_j)} = (\phi, m_h)_{L^2(\gamma_j)}, \quad \forall m_h \in M_{B_j,h}. \tag{2.87}$$

We remark that for $j \in \{i, e\}$, these operators project into $\widetilde{X}_{p_j}(\mathcal{G}_{j,h})$, which under Assumptions I.8 and I.9 are also subspaces of the traces of the $W_{1,h}$ and $W_{2,h}$ on γ_i and γ_e respectively, which allows a later extension to the whole domain.

Moreover, in [75] for the particular case of the *dual* Lagrange multipliers spaces $Y^{du}_{p_j}(\mathcal{G}_{j,k})$, the operators $\widetilde{Q}^h_{\gamma_j}$ are proved to be well defined and L^2-stable. However, the verification of this question for the particular case of the *classic* Lagrange multipliers spaces $Y^{cl}_{p_j}(\mathcal{G}_{j,k})$ remains open up to our knowledge, although we believe it holds under reasonable mesh regularity assumptions. Thus in the following we consider the next assumption (that could be seen as a conjecture; note it is not required for the *dual* approach however we include it in order to proceed in general).

Assumption I.10

We assume that for any $j \in \{i, e\}$, any order p_j and any $op \in \{cl, du\}$, the projection operators $\widetilde{Q}^h_{\gamma_j}$ defined by (2.87) are well defined and L^2-stable, i.e.

$$\|\widetilde{Q}^h_{\gamma_j}\phi\|_{L^2(\gamma_j)} \leq K_Q\|\phi\|_{L^2(\gamma_j)}, \quad \forall \phi \in L^2(\gamma_j),$$

where $K_Q > 0$ is a constant independent of h.

Next, we verify that under Assumption I.10 the projection operators $\widetilde{Q}^h_{\gamma_j}$ are also $H^{\frac{1}{2}}$-stable and we recall that this property will be important in Theorem 2.69 where we prove the uniform *discrete Inf-Sup condition* (**P.3**) when considering the new choices of $M_{BB,h}$.

Lemma 2.68

If Assumption I.10 holds, then for any $j \in \{i, e\}$, any order p_j and any $op \in \{cl, du\}$, there exists a constant $K > 0$ independent of h and such that

$$\|\widetilde{Q}^h_{\gamma_j}\phi\|_{H^{\frac{1}{2}}(\gamma_j)} \leq K\|\phi\|_{H^{\frac{1}{2}}(\gamma_j)} \quad \forall \phi \in H^{\frac{1}{2}}(\gamma_j). \tag{2.88}$$

Proof. First, as in Lemma 2.49, we introduce an orthogonal projection $\widetilde{P}^h_{\gamma_j}$ from $L^2(\gamma_j)$ into $\widetilde{X}_p(\mathcal{G}_{j,h})$. Thus, for all $\phi \in L^2(\gamma_j)$ we have $\|\widetilde{P}^h_{\gamma_j}\phi\|_{L^2(\gamma_j)} \leq \|\phi\|_{L^2(\gamma_j)}$, while for all $\phi \in H^{\frac{1}{2}}(\gamma_j)$ there exist two constants $K^\star > 0$ and $\widetilde{K} > 0$ independent of h and such that

$$\|\phi - \widetilde{P}^h_{\gamma_j}\phi\|_{L^2(\gamma_j)} \leq K^\star\, h^{\frac{1}{2}}\,\|\phi\|_{H^{\frac{1}{2}}(\gamma_j)} \quad \text{and} \quad \|\widetilde{P}^h_{\gamma_j}\phi\|_{H^{\frac{1}{2}}(\gamma_j)} \leq \widetilde{K}\,\|\phi\|_{H^{\frac{1}{2}}(\gamma_j)}.$$

Moreover, we notice that $\widetilde{Q}^h_{\gamma_j}\widetilde{P}^h_{\gamma_j}\phi = \widetilde{P}^h_{\gamma_j}\phi$ for all $\phi \in L^2(\gamma_j)$, then considering inverse inequality (see II.6.8 in [77]) and the continuity of $\widetilde{Q}^h_{\gamma_j}$, we obtain

$$\begin{aligned}\|\widetilde{Q}^h_{\gamma_j}\phi - \widetilde{P}^h_{\gamma_j}\phi\|_{H^{\frac12}(\gamma_j)} &\le c\,h^{-\frac12}\|\widetilde{Q}^h_{\gamma_j}\phi - \widetilde{P}^h_{\gamma_j}\phi\|_{L^2(\gamma_j)}\\ &\le c\,K_Q\,h^{-\frac12}\|\phi - \widetilde{P}^h_{\gamma_j}\phi\|_{L^2(\gamma_j)} \;\le\; c\,K_Q\,K^\star\|\phi\|_{H^{\frac12}(\gamma_j)}.\end{aligned}$$

Thus, for any $\phi \in H^{\frac12}(\gamma_j)$ we observe

$$\|\widetilde{Q}^h_{\gamma_j}\phi\|_{H^{\frac12}(\gamma_j)} \le \|\widetilde{Q}^h_{\gamma_j}\phi - \widetilde{P}^h_{\gamma_j}\phi\|_{H^{\frac12}(\gamma_j)} + \|\widetilde{P}^h_{\gamma_j}\phi\|_{H^{\frac12}(\gamma_j)} \le (c\,K_Q\,K^\star + \widetilde{K})\,\|\phi\|_{H^{\frac12}(\gamma_j)}.$$

■

Finally, we conclude this section by verifying the uniform *discrete Inf-Sup condition* (**P.3**). Notice that the proof is essentially a reproduction of the one in Theorem 2.56 and the assumptions required are the same plus Assumption I.10.

Theorem 2.69

If Assumptions I.8, I.9 and I.10 are verified, then for both $op \in \{cl, du\}$, the bilinear form $b_{BB}(\cdot,\cdot)$ satisfies the uniform discrete Inf-Sup condition (**P.3**).

Proof. First of all, we notice that due to assumptions I.8 and I.9 we can still consider twice Lemma 2.48 to introduce the lifting operators (the same as in Theorem 2.56)

$$L^h_{\omega_{ci}} : X_{p_1}(\mathcal{G}_{i,h}) \longrightarrow X_{p_1}(\mathcal{D}_{i,h}), \quad \text{where} \quad \mathcal{D}_{i,h} \;\text{ and }\; \mathcal{G}_{i,h} \;\text{ are given in (2.75)}$$

$$L^h_{\omega_{ce}} : X_{p_2}(\mathcal{G}_{e,h}) \longrightarrow X_{p_2}(\mathcal{D}_{e,h}), \quad \text{where} \quad \mathcal{D}_{e,h} \;\text{ and }\; \mathcal{G}_{e,h} \;\text{ are given in (2.76)}.$$

Next, attending to (2.87) and Lemma 2.68 we introduce

$$\widetilde{Q}^h_{\gamma_i} : L^2(\gamma_i) \longrightarrow \widetilde{X}_{p_1}(\mathcal{G}_{i,h}), \quad \text{such that} \quad \|\widetilde{Q}^h_{\gamma_i}\phi\|_{H^{\frac12}(\gamma_i)} \le K_{\gamma_i}\,\|\phi\|_{H^{\frac12}(\gamma_i)} \quad \forall\phi \in H^{\frac12}(\gamma_i),$$

$$\widetilde{Q}^h_{\gamma_e} : L^2(\gamma_e) \longrightarrow \widetilde{X}_{p_2}(\mathcal{G}_{e,h}), \quad \text{such that} \quad \|\widetilde{Q}^h_{\gamma_e}\phi\|_{H^{\frac12}(\gamma_e)} \le K_{\gamma_e}\,\|\phi\|_{H^{\frac12}(\gamma_e)} \quad \forall\phi \in H^{\frac12}(\gamma_e).$$

Notice, that the introduction of these projections is the main difference with respect to the proof of Theorem 2.56. We also remark that $\widetilde{X}_{p_1}(\mathcal{G}_{i,h}) \subset X_{p_1}(\mathcal{G}_{i,h})$ and $\widetilde{X}_{p_2}(\mathcal{G}_{e,h}) \subset X_{p_2}(\mathcal{G}_{e,h})$. Then, for any $\boldsymbol{m}_h \in M_{BB,h}$ we proceed separately for $m_{i,h} \in [H^{\frac12}(\gamma_i)]'$ and $m_{e,h} \in [H^{\frac12}(\gamma_e)]'$. On the one hand by the definition of the dual norm, taking into account that the duality paring is an extension of the scalar product in $L^2(\gamma_i)$ and the stability of $\widetilde{Q}^h_{\gamma_i}$, we obtain

$$\|m_{i,h}\|_{[H^{\frac12}(\gamma_i)]'} = \sup_{\phi\in H^{\frac12}(\gamma_i)} \frac{\langle\phi, m_{i,h}\rangle_{\gamma_i}}{\|\phi\|_{H^{\frac12}(\gamma_i)}} \le K_i \sup_{\phi\in H^{\frac12}(\gamma_i)} \frac{(\widetilde{Q}^h_{\gamma_i}(\phi), m_{i,h})_{L^2(\gamma_i)}}{\|\widetilde{Q}^h_{\gamma_i}(\phi)\|_{H^{\frac12}(\gamma_i)}}.$$

Now notice that $L^h_{\omega_{ci}}(\widetilde{Q}^h_{\gamma_i}(\phi))_{|\gamma_i} = \widetilde{Q}^h_{\gamma_i}(\phi)$, that $L^h_{\omega_{ci}}$ is continuous with constant $K_{\omega_{ci}}$ and that $L^h_{\omega_{ci}}(\widetilde{Q}^h_{\gamma_i}(\phi)) \in X_{p_1}(\mathcal{D}_{i,h})$, therefore

$$\|m_{i,h}\|_{[H^{\frac12}(\gamma_i)]'} \le K_i K_{\omega_{ci}} \sup_{\phi\in H^{\frac12}(\gamma_i)} \frac{(L^h_{\omega_{ci}}(\widetilde{Q}^h_{\gamma_i}(\phi)), m_{i,h})_{L^2(\gamma_i)}}{\|L^h_{\omega_{ci}}(\widetilde{Q}^h_{\gamma_i}(\phi))\|_{H^1(\omega_{ci})}}.$$

Next, we denote by $\mathtt{E}^h_1$ the extension by zero to the whole Ω_1 and we remark that in that case $\mathtt{E}^h_1(L^h_{\omega_{ci}}(\widetilde{Q}^h_{\gamma_i}(\phi))), m_{e,h})_{L^2(\gamma_e)} = 0$, thus if we denote $\mathtt{G}^h_1 = \mathtt{E}^h_1 \circ L^h_{\omega_{ci}} \circ \widetilde{Q}^h_{\gamma_i}$

$$\|m_{i,h}\|_{[H^{\frac12}(\gamma_i)]'} \le K_i K_{\omega_{ci}} \sup_{\phi\in H^{\frac12}(\gamma_i)} \frac{(\mathtt{G}^h_1(\phi), m_{i,h})_{L^2(\gamma_i)} + (\mathtt{G}^h_1(\phi), m_{e,h})_{L^2(\gamma_e)}}{\|\mathtt{G}^h_1(\phi)\|_{H^1(\Omega_1)}}.$$

To obtain the adequate bound, we shall notice that in the previous inequality we can consider the supremum in W_h since $(\mathtt{G}_1^h(\phi), 0) \in W_h$, thus we are considering a bigger space with therefore a larger supremum. Then we obtain

$$\|m_{i,h}\|_{[H^{\frac{1}{2}}(\gamma_i)]'} \leq K_i K_{\omega_{ci}} \sup_{\boldsymbol{v}_h \in W_h} \frac{(v_{1,h} - v_{2,h}, m_{i,h})_{L^2(\gamma_i)} + (v_{1,h} - v_{2,h}, m_{e,h})_{L^2(\gamma_e)}}{\|\boldsymbol{v}_h\|_1}.$$

On the other hand, it is analogous to verify that

$$\|m_{e,h}\|_{[H^{\frac{1}{2}}(\gamma_e)]'} \leq K_e K_{\omega_{ce}} \sup_{\boldsymbol{v}_h \in W_h} \frac{(v_{1,h} - v_{2,h}, m_{i,h})_{L^2(\gamma_i)} + (v_{1,h} - v_{2,h}, m_{e,h})_{L^2(\gamma_e)}}{\|\boldsymbol{v}_h\|_1}.$$

Now we consider $K = K_i K_{\omega_{ci}} + K_e K_{\omega_{ce}}$ and we take again into account that the duality pairing is an extension of the scalar product in L^2 to obtain

$$\|\boldsymbol{m}_h\|_{M_{BB}} \leq \|m_{i,h}\|_{[H^{\frac{1}{2}}(\gamma_i)]'} + \|m_{e,h}\|_{[H^{\frac{1}{2}}(\gamma_e)]'} \leq K \sup_{\boldsymbol{v}_h \in W_h} \frac{b_{BB}(\boldsymbol{v}_h, \boldsymbol{m}_h)}{\|\boldsymbol{v}_h\|_1}.$$

Finally, since this holds for any $\boldsymbol{m}_h \in M_{BB,h}$, it also holds for the infimum and thus the proof is concluded.

■

Corollary 2.70

If $\boldsymbol{u} \in H^\sigma(\Omega_1) \times H^\sigma(\Omega_2)$ for $\sigma > 1$, then $\lambda_{j|\gamma_{j,k}} \in H^{\sigma - \frac{3}{2}}(\gamma_{j,k})$ for $j \in \{i, e\}$, $k \in \{1, \dots, s_j\}$ and

$$\|\boldsymbol{u} - \boldsymbol{u}_h\|_1 + \|\boldsymbol{\lambda} - \boldsymbol{\lambda}_h\|_{M_{BB}} \leq K\, h^q$$

where $q = \min\{p_1, p_2, \sigma - 1\}$.

2.7.2 Volume-Volume coupling

In this section we develop a different approach. We modify the introduction of the coupling in order to obtain a more regular Lagrange multiplier when volume couplings are considered. The idea is to reduce the order of the singularities of the Lagrange multipliers that are associated to regions with corners, but instead of considering curved interfaces (we have already discussed that this approach is not well adapted to our purposes), we will split each volume coupling region in order to reduce the interior angle on the corners. Let us remark that this approach is technical and implies the introduction of involved notation in order to refer to the different parts of ω_i and ω_e. Moreover, we note that contrary to the boundary coupling case, this approach does not provide an optimal numerical scheme for high order (larger than two) Lagrange finite elements, but it helps us to improve the convergence properties of the method.

2.7.2.1 Reformulation of the coupling and continuous Inf-Sup

First of all, we recall that for a Lagrange multiplier λ_j with $j \in \{i, e\}$ of volume type, which is defined in a polygonal region ω_j, we can not ensure more regularity than $\lambda_j \in H^\sigma(\omega_j)$ for all $\sigma < 1 + \frac{\kappa}{2}$ where $\frac{2\pi}{\kappa}$ is the largest interior angle of ω_j (see Theorem 2.28). In consequence, it is possible to improve the regularity of the volume multipliers by reducing the interior angles of the regions where they are defined. However, to ensure $\lambda_j \in H^2(\omega_j)$, which is required for optimality when considering first order Lagrange finite elements, we need to provide a domain decomposition which largest possible interior angle is smaller than π, which seems not possible if ω_j is polygonal and non simply connected. Thus our aim is to provide a new formulation where the coupling is performed separately on each region of a domain decomposition of ω_j which is given by

$$\{\omega_{j,k}\}_{k=1}^{N_j} \quad \text{where } \omega_{j,k} \text{ are disjoint open subset of } \omega_j \text{ such that } \bigcup_{k=1}^{N_j} \overline{\omega_{j,k}} = \overline{\omega_j}. \tag{2.89}$$

With this new coupling, it will be possible to provide domain decompositions where both, ω_i and ω_e, are rectangular frame shape domains such that the largest interior angle of the regions $\omega_{j,k}$ is $\pi/2$ (see Figure 2.25). Notice, that with this choice we expect to obtain (quasi-) optimality when considering second order Lagrange finite elements.

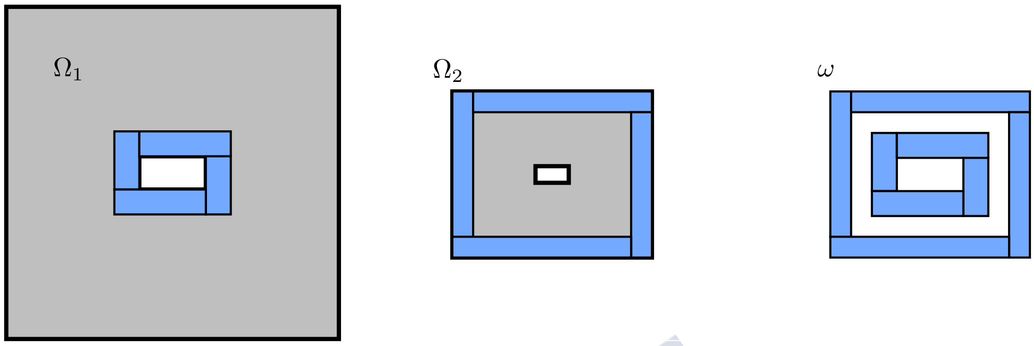

(a) The background media Ω_1 and the regions $\omega_{i,k}$ that decompose ω_i.

(b) The patch Ω_2 and the regions $\omega_{e,k}$ that decompose ω_e.

(c) Decomposition of the overlapping region.

Figure 2.25: Sketch of the proposed decomposition of the overlapping region in order to obtain more regular multipliers.

Remark 2.71

Notice that, as we show in Figure 2.26, it is also possible to provide a domain decomposition where the largest interior angle of the regions $\omega_{j,k}$ is $\pi/3$, which provides (quasi-) optimality when considering third order Lagrange finite elements. However in practice this approach is more involved and for simplicity, we consider the domain decomposition in Figure 2.25.

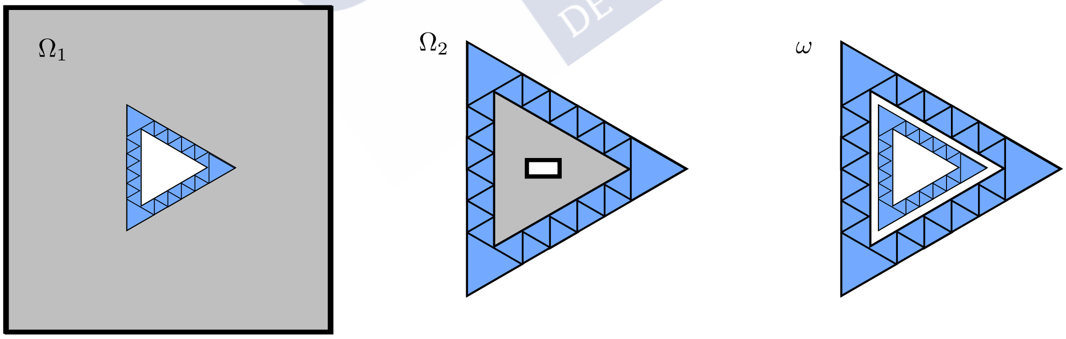

(a) The background media Ω_1 and the regions $\omega_{i,k}$ that decompose ω_i.

(b) The patch Ω_2 and the regions $\omega_{e,k}$ that decompose ω_e.

(c) Decomposition of the overlapping region.

Figure 2.26: Sketch of the proposed decomposition of the overlapping region in order to obtain more regular multipliers.

In this context, it is not trivial how the coupling needs to be imposed and thus how the Lagrange multipliers are introduced in order to obtain an equivalent formulation, i.e., if we consider the abstract problem (2.33), we need to find an adequate choice of M_{VV} and $b_{VV}(\cdot,\cdot)$. Notice, that in order to analyse existence and uniqueness of solution of the resultant problem, we could proceed similarly to Theorem 2.11, i.e. we could relate the new formulation to problem (2.10), and consequently to problem (2.2) (by Theorem 2.5). Thus, following the proof of Theorem 2.11, it is enough to find an adequate choice of M_{VV} and $b_{VV}(\cdot,\cdot)$ such that first

$$b_{VV}(\boldsymbol{v},\boldsymbol{m}) = 0 \quad \forall \boldsymbol{m} \in M_{VV} \quad \text{implies} \quad u_1 = u_2 \quad \text{in} \quad \omega, \tag{2.90}$$

and second, there exists a constant $\delta > 0$ such that the following Inf-Sup condition holds

$$\inf_{m \in M_{VV}} \sup_{\boldsymbol{v} \in W} \frac{|b_{VV}(\boldsymbol{v}, m)|}{\|m\|_{M_{VV}} \ \|\boldsymbol{v}\|_1} \ \geq \ \delta. \tag{2.91}$$

Thus, the proof in Theorem 2.11 could be repeated here. A first approach would be to consider problem (2.33) with the choice

$$M_{VV} = \prod_{k=1}^{N_i} H^1(\omega_{i,k}) \times \prod_{k=1}^{N_e} H^1(\omega_{e,k})$$
$$b_{VV}(\boldsymbol{v},\boldsymbol{m}) = \sum_{k=1}^{N_i} (v_1 - v_2, m_{i,k})_{H^1(\omega_{i,k})} + \sum_{k=1}^{N_e} (v_1 - v_2, m_{e,k})_{H^1(\omega_{e,k})}.$$

Thus requirement (2.90) is satisfied as a consequence of Lemma 2.26, however we prove next that requirement (2.91) is not verified.

Proposition 2.72

There exists $\boldsymbol{m} \in M_{VV}$ such that $b_{VV}(\boldsymbol{v},\boldsymbol{m}) = 0$ for all $\boldsymbol{v} \in W$.

Proof. Let us assume, without loss of generality, that there exists $\gamma_{1,2} = \partial\omega_{i,1} \cap \partial\omega_{i,2}$. Thus, we consider any $\phi \in [H^{\frac{1}{2}}(\gamma_{1,2})]'$ and we find

$$\begin{array}{lll} m_{i,1} \in H^1(\omega_{i,1}) \quad \text{such that} \quad (m_{i,1}, w)_{H^1(\omega_{i,1})} & = & \langle \phi, w\rangle_{\gamma_{1,2}} \quad \forall w \in H^1(\omega_{i,1}), \\ m_{i,2} \in H^1(\omega_{i,2}) \quad \text{such that} \quad (m_{i,2}, w)_{H^1(\omega_{i,2})} & = & -\langle \phi, w\rangle_{\gamma_{1,2}} \quad \forall w \in H^1(\omega_{i,2}). \end{array}$$

Thus, if we set $m_{i,k} = 0$ for all $k \in \{3, \ldots, N_i\}$ and $m_{e,k} = 0$ for all $k \in \{1, \ldots, N_j\}$ we can compute for all $\boldsymbol{v} \in W$

$$\begin{aligned} b_{VV}(\boldsymbol{v},\boldsymbol{m}) &= (m_{i,1}, v_1 - v_2)_{H^1(\omega_{i,1})} + (m_{i,2}, v_1 - v_2)_{H^1(\omega_{i,2})} \\ &= \langle \phi, v_1 - v_2\rangle_{\gamma_{1,2}} - \langle \phi, v_1 - v_2\rangle_{\gamma_{1,2}} = 0. \end{aligned}$$

■

Notice that in the previous proof, we exploit the fact that the coupling on $\gamma_{1,2}$ is in some sense duplicated. Thus in the following, in order to avoid this effect, we provide a different approach where the coupling is performed separately in the interior of the regions $\omega_{j,k}$ and on the skeleton of the decomposition. Then we first introduce for $j \in \{i, e\}$

$$\mathcal{S}_j = \bigcup_{k=1}^{N_j} \partial\omega_{j,k}$$

and we consider problem (2.33) with the choices

$$M_{VV} = [H^{\frac{1}{2}}(\mathcal{S}_i)]' \times \prod_{k=1}^{N_i} H^1_0(\omega_{i,k}) \times [H^{\frac{1}{2}}(\mathcal{S}_e)]' \times \prod_{k=1}^{N_e} H^1_0(\omega_{e,k}), \tag{2.92}$$

$$\begin{aligned} b_{VV}(\boldsymbol{v},\boldsymbol{m}) \;=\; & \langle v_1 - v_2, m_{\mathcal{S}_i}\rangle_{\mathcal{S}_i} + \sum_{k=1}^{N_i} (v_1 - v_2, m_{i,k})_{H^1(\omega_{i,k})} \\ + \; & \langle v_1 - v_2, m_{\mathcal{S}_e}\rangle_{\mathcal{S}_e} + \sum_{k=1}^{N_e} (v_1 - v_2, m_{e,k})_{H^1(\omega_{e,k})}. \end{aligned} \tag{2.93}$$

Thus requirement (2.90) is still satisfied as a consequence of Lemma 2.26, while requirement (2.91) is proved next.

Theorem 2.73

There exists a constant $\delta > 0$ such that the following Inf-Sup condition is satisfied

$$\inf_{\boldsymbol{m}\in M_{VV}} \sup_{\boldsymbol{v}\in W} \frac{|b_{VV}(\boldsymbol{v},\boldsymbol{m})|}{\|\boldsymbol{m}\|_{M_{VV}}\ \|\boldsymbol{v}\|_1} \ \geq\ \delta.$$

Proof. Let us consider any $\boldsymbol{m} \in M_{VV}$ and we proceed separately for each component. First, for $m_{\mathcal{S}_i}$ we introduce a continuous lifting operator L_i from $H^{\frac{1}{2}}(\mathcal{S}_i)$ into $H^1(\Omega_1)$ that for every $\phi \in H^{\frac{1}{2}}(\mathcal{S}_i)$ assigns $L_i(\phi) \in H^1(\Omega_1)$ such that $L_i(\phi) = 0$ in $\Omega_1 \setminus (\omega_i \cup \omega_c)$ and

$$\begin{aligned} L_i(\phi) - \Delta L_i(\phi) &= 0 \quad \text{in} \quad \omega_{i,k}, \\ L_i(\phi) &= \phi \quad \text{on} \quad \partial\omega_{i,k}, \end{aligned} \qquad \begin{aligned} L_i(\phi) - \Delta L_i(\phi) &= 0 \quad \text{in} \quad \omega_c, \\ L_i(\phi) &= \phi \quad \text{on} \quad \partial\omega_c \cap \partial\omega_i, \\ L_i(\phi) &= 0 \quad \text{on} \quad \partial\omega_c \cap \partial\omega_e. \end{aligned}$$

Notice, that this operator is continuous (with constant K_i) thus

$$\|m_{\mathcal{S}_i}\|_{[H^{\frac{1}{2}}(\mathcal{S}_i)]'} = \sup_{\phi\in H^{\frac{1}{2}}(\mathcal{S}_i)} \frac{\langle \phi, m_{\mathcal{S}_i}\rangle_{\mathcal{S}_i}}{\|\phi\|_{H^{\frac{1}{2}}(\mathcal{S}_i)}} \leq K_i \sup_{\phi\in H^{\frac{1}{2}}(\mathcal{S}_i)} \frac{\langle L_i(\phi), m_{\mathcal{S}_i}\rangle_{\mathcal{S}_i}}{\|L_i(\phi)\|_{H^1(\Omega_i)}}.$$

Moreover, for all $k \in \{1,\dots,N_i\}$ by definition $(w, L_i(\phi))_{H^1(\omega_{i,k})} = 0$ for all $w \in H^1_0(\omega_{i,k})$. Thus, since $m_{i,k} \in H^1_0(\omega_{i,k})$ and $L_i(\phi) = 0$ in $\overline{\omega_e}$

$$\|m_{\mathcal{S}_i}\|_{[H^{\frac{1}{2}}(\mathcal{S}_i)]'} \leq K_i \sup_{\phi\in H^{\frac{1}{2}}(\mathcal{S}_i)} \frac{b_{VV}((L_i(\phi),0),\boldsymbol{m})}{\|(L_i(\phi),0)\|_1} \leq K_i \sup_{\boldsymbol{v}\in W} \frac{b_{VV}(\boldsymbol{v},\boldsymbol{m})}{\|\boldsymbol{v}\|_1}.$$

It is analogous to prove that

$$\|m_{\mathcal{S}_e}\|_{[H^{\frac{1}{2}}(\mathcal{S}_e)]'} \leq K_e \sup_{\boldsymbol{v}\in W} \frac{b_{VV}(\boldsymbol{v},\boldsymbol{m})}{\|\boldsymbol{v}\|_1}.$$

Next, to find a bound for $m_{i,k} \in H^1_0(\omega_{i,k})$ with $k \in \{1,\dots,N_i\}$, we consider $\boldsymbol{v} = (\mathtt{E}_1(m_{i,k}), 0)$ where $\mathtt{E}_1$ denotes the extension by zero to the whole Ω_1 and we observe that

$$\|m_{i,k}\|_{H^1(\omega_{i,k})} = \frac{b_{VV}(\boldsymbol{v},\boldsymbol{m})}{\|\boldsymbol{v}\|_1} \leq \sup_{\boldsymbol{v}\in W} \frac{b_{VV}(\boldsymbol{v},\boldsymbol{m})}{\|\boldsymbol{v}\|_1}.$$

Notice that it is analogous to prove for $k \in \{1,\dots,N_j\}$, that

$$\|m_{e,k}\|_{H^1(\omega_{i,k})} \leq \sup_{\boldsymbol{v}\in W} \frac{b_{VV}(\boldsymbol{v},\boldsymbol{m})}{\|\boldsymbol{v}\|_1}.$$

Now, we combine the previous inequalities to obtain

$$\begin{aligned} \|\boldsymbol{m}\|_{M_{VV}} &\leq \|m_{\mathcal{S}_i}\|_{[H^{\frac{1}{2}}(\mathcal{S}_i)]'} + \sum_{k=1}^{N_i} \|m_{i,k}\|_{H^1(\omega_{i,k})} + \|m_{\mathcal{S}_e}\|_{[H^{\frac{1}{2}}(\mathcal{S}_e)]'} + \sum_{k=1}^{N_e} \|m_{e,k}\|_{H^1(\omega_{e,k})} \\ &\leq (2 + K_i + K_e) \sup_{\boldsymbol{v}\in W} \frac{b_{VV}(\boldsymbol{v},\boldsymbol{m})}{\|\boldsymbol{v}\|_1}. \end{aligned}$$

Finally, since this holds for any $\boldsymbol{m} \in M_{VV}$, it also holds for the infimum and thus the proof is concluded.

■

Thus, as we mentioned before, this new coupling that fits into the framework of the abstract problem (2.33) can be analysed by reproducing the proof in Theorem 2.11. In consequence, the regularity of $\boldsymbol{u}$ is given by Theorem 2.2 however, for the regularity of $\boldsymbol{\lambda}$ we need to find a suitable interpretation of the Lagrange multiplier. Thus we provide the following result which is obtained proceeding similarly to Proposition 2.12.

Proposition 2.74

If Assumptions I.1 to I.3 are satisfied and u is a solution of problem (2.2), then a solution of problem (2.33) with the choices (2.92) and (2.93) is given by $\big((u_{|\Omega_1}, u_{|\Omega_2}), \boldsymbol{\lambda}\big)$ where the Lagrange multiplier $\boldsymbol{\lambda}$ is uniquely defined by u. Moreover, if we assume that $div\big((\beta_2-\beta_1)\mu\,\nabla u\big) \in L^2(\omega_{j,k})$ for all $j \in \{i,e\}$ and $k, \widehat{k} \in \{1,\dots,N_j\}$ such that $k \neq \widehat{k}$, the Lagrange multiplier $\boldsymbol{\lambda}$ is given by:

(i) *For all $j \in \{i,e\}$ and $k \in \{1,\dots,N_j\}$*

$$\begin{aligned} 2(\lambda_{j,k} - \Delta\lambda_{j,k}) &= -\,\ell^2(\alpha_2-\alpha_1)\rho\,u - div\big((\beta_2-\beta_1)\mu\,\nabla u\big) \quad in \quad \omega_{j,k},\\ \lambda_{j,k} &= 0 \qquad on \quad \partial\omega_{j,k}. \end{aligned}$$

(ii) *For $\gamma = \partial\omega_{e,k}\cap\gamma_e$, we have $\lambda_{\mathcal{S}_e} = \beta_2\,\mu\,\partial_{\boldsymbol{n}_k}u - \partial_{\boldsymbol{n}_k}\lambda_{e,k}$ in $[H^{\frac12}_{00}(\gamma)]'$.*

(iii) *For $\gamma = \partial\omega_{i,k}\cap\gamma_i$, we have $\lambda_{\mathcal{S}_i} = -\beta_1\,\mu\,\partial_{\boldsymbol{n}_k}u - \partial_{\boldsymbol{n}_k}\lambda_{i,k}$ in $[H^{\frac12}_{00}(\gamma)]'$.*

(iv) *For $\gamma = \partial\omega_{j,k}\cap\partial\omega_c$ we have $\lambda_{\mathcal{S}_j} = (C-\beta_1)\,\mu\,\partial_{\boldsymbol{n}_k}u - \partial_{\boldsymbol{n}_k}\lambda_{j,k}$ in $[H^{\frac12}_{00}(\gamma)]'$.*

(v) *For $\gamma = \partial\omega_{j,k}\cap\partial\omega_{j,\widehat{k}}$ we have $\lambda_{\mathcal{S}_j} = [\beta_1]\,\mu\,\partial_{\boldsymbol{n}_k}u + \partial_{\boldsymbol{n}_k}\lambda_{j,\widehat{k}} - \partial_{\boldsymbol{n}_k}\lambda_{j,k}$ in $[H^{\frac12}_{00}(\gamma)]'$.*

Notice that $\boldsymbol{n}_k$ denotes the outward normal to $\omega_{j,k}$ and $[\beta_1] = (\beta_{1|\omega_{j,\widehat{k}}} - \beta_{1|\omega_{j,k}})_{|\gamma}$.

Proof. (**i**) First, we introduce the continuous extension operator $\mathtt{E}_{j,k}(\cdot)$ from $H^1_0(\omega_{j,k})$ into $H^1(\Omega)$ that extends by zero to the whole Ω the functions of $H^1_0(\omega_{j,k})$. Thus, for all $m \in H^1_0(\omega_{j,k})$ we can consider in (2.33a) test functions $(v_1,v_2) = (\mathtt{E}_{j,k}(m)_{|\Omega_1}, -\mathtt{E}_{j,k}(m)_{|\Omega_2})$ and obtain

$$2\,(m,\lambda_{j,k})_{H^1(\omega_{j,k})} = -\ell^2\,((\alpha_2-\alpha_1)\rho\,u, m)_{L^2(\omega_{j,k})} + ((\beta_2-\beta_1)\mu\,\nabla u, \nabla m)_{L^2(\omega_{j,k})}.$$

(**ii**) Next, for $\gamma = \partial\omega_{e,k}\cap\partial\gamma_e$ let us introduce Λ as a neighbourhood of γ such that $\gamma = \Lambda\cap\mathcal{S}_e$ (see Figure 2.27) and consider a continuous extension operator $\mathtt{E}_\gamma(\cdot)$ from $H^{\frac12}_{00}(\gamma)$ into $H^1(\Omega)$ that first extends to $H^1_0(\Lambda)$ and then extends by zero to the whole Ω. Thus, for all $m \in H^{\frac12}_{00}(\gamma)$ we can consider in (2.33a) test functions $(v_1,v_2) = (\mathtt{E}_\gamma(m)_{|\Omega_1}, -\mathtt{E}_\gamma(m)_{|\Omega_2})$ and obtain

$$\begin{aligned} &-\ \ell^2\,(\rho\,u, \mathtt{E}_\gamma(m))_{L^2(\Lambda\setminus\omega_{e,k})} \ +\ (\mu\,\nabla u, \nabla\mathtt{E}_\gamma(m))_{L^2(\Lambda\setminus\omega_{e,k})}\\ &-\ \ell^2\,((\alpha_1-\alpha_2)\,\rho\,u, \mathtt{E}_\gamma(m))_{L^2(\Lambda\cap\omega_{e,k})} \ +\ ((\beta_1-\beta_2)\mu\,\nabla u, \nabla\mathtt{E}_\gamma(m))_{L^2(\Lambda\cap\omega_{e,k})}\\ &+\ 2\,(\lambda_{e,k}, \mathtt{E}_\gamma(m))_{H^1(\Lambda\cap\omega_{e,k})} \ +\ 2\langle m, \lambda_{\mathcal{S}_e}\rangle_\gamma \ =\ (f, \mathtt{E}_\gamma(m))_{L^2(\Lambda\setminus\omega_{e,k})}. \end{aligned}$$

Now, we recall that on the one hand $-\ell^2\rho\,u - \mathrm{div}(\mu\nabla u) = f$, while on the other hand $\lambda_{e,k}$ satisfies the partial differential equation in case (**i**). Then we apply Green's formula separately in $\Lambda\setminus\omega_{e,k}$ and $\Lambda\cap\omega_{e,k}$ to obtain that for all $m \in H^{\frac12}_{00}(\gamma)$ we have

$$2\langle m, \lambda_{\mathcal{S}_e}\rangle_\gamma \ =\ \langle m, \mu\,\partial_{\boldsymbol{n}_k}u\rangle_\gamma \ -\ \langle m, (\beta_1-\beta_2)\mu\,\partial_{\boldsymbol{n}_k}u\rangle_\gamma \ -\ 2\,\langle m, \partial_{\boldsymbol{n}_k}\lambda_{e,k}\rangle_\gamma.$$

Thus, since $\beta_1+\beta_2 = 1$, we have $\lambda_{\mathcal{S}_e} = \beta_2\,\mu\,\partial_{\boldsymbol{n}_k}u - \partial_{\boldsymbol{n}_k}\lambda_{e,k}$ in $[H^{\frac12}_{00}(\gamma)]'$.
(**iii**) Next we proceed in an analogous way for $\gamma = \partial\omega_{i,k}\cap\partial\gamma_i$. Then we introduce Λ as a neighbourhood of γ such that $\gamma = \Lambda\cap\mathcal{S}_i$ (see Figure 2.27) and consider a continuous extension operator $\mathtt{E}_\gamma(\cdot)$ from $H^{\frac12}_{00}(\gamma)$ into $H^1(\Omega)$ that first extends to $H^1_0(\Lambda)$ and then extends by zero to the whole Ω. Thus, for all $m \in H^{\frac12}_{00}(\gamma)$ we can consider in (2.33a) test functions $(v_1,v_2) =$

$(\mathtt{E}_\gamma(m)_{|\Omega_1}, -\mathtt{E}_\gamma(m)_{|\Omega_2})$ and this time we obtain

$$\begin{aligned} & \ell^2\,(\rho\, u, \mathtt{E}_\gamma(m))_{L^2(\Lambda\setminus\omega_{i,k})} \;-\; (\mu\,\nabla u, \nabla\mathtt{E}_\gamma(m))_{L^2(\Lambda\setminus\omega_{i,k})} \\ - \;& \ell^2\,((\alpha_1-\alpha_2)\,\rho\, u, \mathtt{E}_\gamma(m))_{L^2(\Lambda\cap\omega_{i,k})} \;+\; ((\beta_1-\beta_2)\mu\,\nabla u, \nabla\mathtt{E}_\gamma(m))_{L^2(\Lambda\cap\omega_{i,k})} \\ + \;& 2\,(\lambda_{i,k}, \mathtt{E}_\gamma(m))_{H^1(\Lambda\cap\omega_{i,k})} \;+\; 2\langle m, \lambda_{\mathcal{S}_i}\rangle_\gamma \;=\; 0. \end{aligned}$$

Then, since $-\ell^2\rho\, u - \operatorname{div}(\mu\nabla u) = f$ and $\lambda_{i,k}$ satisfies the partial differential equation in case (**i**), we apply Green's formula separately in $\Lambda\setminus\omega_{i,k}$ and $\Lambda\cap\omega_{i,k}$ to obtain that for all $m \in H^{\frac{1}{2}}_{00}(\gamma)$ we have

$$2\langle m, \lambda_{\mathcal{S}_i}\rangle_\gamma \;=\; -\,\langle m, \mu\,\partial_{\boldsymbol{n}_k} u\rangle_\gamma \;-\; \langle m, (\beta_1-\beta_2)\mu\,\partial_{\boldsymbol{n}_k} u\rangle_\gamma \;-\; 2\,\langle m, \partial_{\boldsymbol{n}_k}\lambda_{i,k}\rangle_\gamma.$$

Thus, since $\beta_1+\beta_2 = 1$, we have $\lambda_{\mathcal{S}_i} = -\beta_1\,\mu\,\partial_{\boldsymbol{n}_k} u - \partial_{\boldsymbol{n}_k}\lambda_{i,k}$ in $[H^{\frac{1}{2}}_{00}(\gamma)]'$.

iv) Similarly, for $\gamma = \partial\omega_{j,k}\cap\partial\omega_c$ we redefine the extension operator $\mathtt{E}_\gamma(\cdot)$. Thus, for all $m \in H^{\frac{1}{2}}_{00}(\gamma)$ we can consider in (2.33a) test functions $(v_1, v_2) = (\mathtt{E}_\gamma(m)_{|\Omega_1}, -\mathtt{E}_\gamma(m)_{|\Omega_2})$ and obtain (notice the constant comes from Assumption I.2)

$$\begin{aligned} - \;& \ell^2\,((2C-1)\,\rho\, u, \mathtt{E}_\gamma(m))_{L^2(\Lambda\setminus\omega_{j,k})} \;+\; ((2C-1)\,\mu\,\nabla u, \nabla\mathtt{E}_\gamma(m))_{L^2(\Lambda\setminus\omega_{j,k})} \\ - \;& \ell^2\,((\alpha_1-\alpha_2)\rho\, u, \mathtt{E}_\gamma(m))_{L^2(\Lambda\cap\omega_{j,k})} \;+\; ((\beta_1-\beta_2)\mu\,\nabla u, \nabla\mathtt{E}_\gamma(m))_{L^2(\Lambda\cap\omega_{j,k})} \\ + \;& 2\,(\lambda_{j,k}, \mathtt{E}_\gamma(m))_{H^1(\Lambda\cap\omega_{j,k})} \;+\; 2\langle m, \lambda_{\mathcal{S}_j}\rangle_\gamma \;=\; 0. \end{aligned}$$

Then we apply Green's formula separately in $\Lambda\setminus\omega_{j,k}$ and $\Lambda\cap\omega_{j,k}$ to obtain that for all $m \in H^{\frac{1}{2}}_{00}(\gamma)$ we have

$$2\langle m, \lambda_{\mathcal{S}_j}\rangle_\gamma \;=\; \langle m, (2C-1)\,\mu\,\partial_{\boldsymbol{n}_k} u\rangle_\gamma \;-\; \langle m, (\beta_1-\beta_2)\mu\,\partial_{\boldsymbol{n}_k} u\rangle_\gamma \;-\; 2\,\langle m, \partial_{\boldsymbol{n}_k}\lambda_{j,k}\rangle_\gamma.$$

Thus, since $\beta_1+\beta_2 = 1$, we have $\lambda_{\mathcal{S}_j} = (C-\beta_1)\,\mu\,\partial_{\boldsymbol{n}_k} u - \partial_{\boldsymbol{n}_k}\lambda_{j,k}$ in $[H^{\frac{1}{2}}_{00}(\gamma)]'$.

v) Finally, for $\gamma = \partial\omega_{j,k}\cap\partial\omega_{j,\widehat{k}}$, we redefine the extension operator $\mathtt{E}_\gamma(\cdot)$. Thus, for all $m \in H^{\frac{1}{2}}_{00}(\gamma)$ we can consider in (2.33a) test functions $(v_1, v_2) = (\mathtt{E}_\gamma(m)_{|\Omega_1}, -\mathtt{E}_\gamma(m)_{|\Omega_2})$ and obtain

$$\begin{aligned} - \;& \ell^2\,((\alpha_1-\alpha_2)\rho\, u, \mathtt{E}_\gamma(m))_{L^2(\Lambda\setminus\omega_{j,k})} + ((\beta_1-\beta_2)\mu\,\nabla u, \nabla\mathtt{E}_\gamma(m))_{L^2(\Lambda\setminus\omega_{j,k})} \\ - \;& \ell^2\,((\alpha_1-\alpha_2)\rho\, u, \mathtt{E}_\gamma(m))_{L^2(\Lambda\cap\omega_{j,k})} + ((\beta_1-\beta_2)\mu\,\nabla u, \nabla\mathtt{E}_\gamma(m))_{L^2(\Lambda\cap\omega_{j,k})} \\ + \;& 2\,(\lambda_{j,\widehat{k}}, \mathtt{E}_\gamma(m))_{H^1(\Lambda\setminus\omega_{j,k})} \;+\; 2\,(\lambda_{j,k}, \mathtt{E}_\gamma(m))_{H^1(\Lambda\cap\omega_{j,k})} \;+\; 2\langle m, \lambda_{\mathcal{S}_j}\rangle_\gamma \;=\; 0. \end{aligned}$$

Then we apply Green's formula separately in $\Lambda\setminus\omega_{j,k}$ and $\Lambda\cap\omega_{j,k}$ to obtain that for all $m \in H^{\frac{1}{2}}_{00}(\gamma)$ we have

$$\begin{aligned} 2\langle m, \lambda_{\mathcal{S}_j}\rangle_\gamma \;&=\; \langle m, (\beta_1-\beta_2)_{|\omega_{j,\widehat{k}}}\mu\,\partial_{\boldsymbol{n}_k} u\rangle_\gamma \;-\; \langle m, (\beta_1-\beta_2)_{|\omega_{j,k}}\mu\,\partial_{\boldsymbol{n}_k} u\rangle_\gamma \\ &\quad + 2\,\langle m, \partial_{\boldsymbol{n}_k}\lambda_{j,\widehat{k}}\rangle_\gamma \;-\; 2\,\langle m, \partial_{\boldsymbol{n}_k}\lambda_{j,k}\rangle_\gamma. \end{aligned}$$

Thus, since $\beta_1+\beta_2 = 1$, we have $\lambda_{\mathcal{S}_j} = [\beta_1]\,\mu\,\partial_{\boldsymbol{n}_k} u + \partial_{\boldsymbol{n}_k}\lambda_{j,\widehat{k}} - \partial_{\boldsymbol{n}_k}\lambda_{j,k}$ in $[H^{\frac{1}{2}}_{00}(\gamma)]'$.

■

In consequence, we provide the following result (which extends Theorem 2.28 to the new formulation) concerning the regularity of the Lagrange multiplier with respect to the regularity of the primal variable when considering polygonal coupling regions.

Theorem 2.75

Let us consider in 2D a solution of problem (2.2) given by $u \in H^s(\Omega)$ for $s \geq 1$. Then, if α_i,

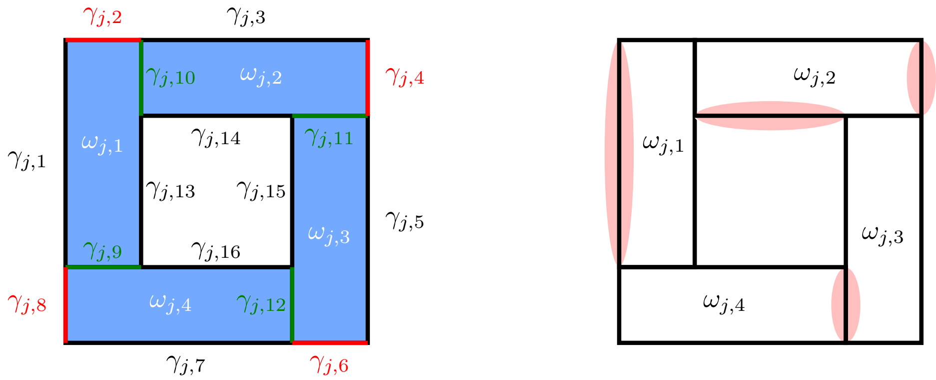

Figure 2.27: Sketch of the decomposition of the skeleton $\mathcal{S}_j$ with $j \in \{i, e\}$ and representation of a neighbourhood of each type of $\gamma_{j,k}$ that do not interact with $\mathcal{S}_j \setminus \gamma_{j,k}$.

β_i for $i \in \{1, 2\}$ are smooth enough in the regions $\omega_{j,k}$ for $j \in \{i, e\}$ and $k \in \{1, \ldots, N_j\}$ and the largest interior angle of the regions $\omega_{j,k}$ is given by $\frac{2\pi}{\kappa}$ for $\kappa > 1$, the Lagrange multiplier satisfies:

- *$\lambda_{j,k} \in H^\sigma(\omega_{j,k})$ for all $\sigma < \min\{s, 1 + \frac{\kappa}{2}\}$.*
- *$\lambda_{\mathcal{S}_j|\gamma} \in H^{\sigma-\frac{3}{2}}(\gamma)$ for all the choices of γ considered in Proposition 2.74.*

Remark 2.76

Let us recall remarks 2.15, 2.16 and 2.29 in order to note that in a similar way, the regularity of the new Lagrange multipliers depends only on the regularity of the source and the choice of the domain decomposition.

Notice that, as it was our purpose, if we consider a domain decomposition as in Figure 2.25, then the regularity of the volume multipliers is improved since $\kappa = 4$. However, in order to guarantee optimality for first and second order Lagrange finite elements approximations, we still need to provide an adequate choice for $M_{VV,h}$ that satisfies a suitable approximation property and which is well adapted for the verification of the uniform *discrete Inf-Sup condition* (**P.3**).

2.7.2.2 New approximation space and discrete Inf-Sup

We complete this section providing also an adequate choice for $M_{VV,h}$ such that the approximation property (**P.2**) and the uniform *discrete Inf-Sup condition* (**P.3**) are both automatically satisfied. First, let us remind the introduction of ω_{ci}, γ_{ci}, ω_{ce} and γ_{ce} given by (2.64) and (2.65). Then, we also introduce the sets χ_i and χ_e of corners that separate both $\mathcal{S}_i$ and $\mathcal{S}_e$ respectively into two families of **smooth** curves (see Figure 2.27)

$$\{\gamma_{i,k}\}_{k=1}^{s_i} \quad \text{such that} \quad \mathcal{S}_i = \bigcup_{k=1}^{s_i} \gamma_{i,k} \quad \text{and} \quad \gamma_{i,k} \cap \gamma_{i,j} \in \chi_i \quad \text{if} \quad k \neq j, \tag{2.94}$$

$$\{\gamma_{e,k}\}_{k=1}^{s_e} \quad \text{such that} \quad \mathcal{S}_e = \bigcup_{k=1}^{s_e} \gamma_{e,k} \quad \text{and} \quad \gamma_{e,k} \cap \gamma_{e,j} \in \chi_e \quad \text{if} \quad k \neq j. \tag{2.95}$$

And we consider the following two assumptions, each of them related to one side of the coupling.

Assumption I.11

We assume that $\omega_{c,i}$ and $\omega_{i,k}$ for all $k \in \{1, \ldots, N_i\}$ are independent of h and that $\mathcal{T}_{1,h}$ is *conform with them. Thus we consider that the triangulations $\mathcal{D}_{i,h}$ of ω_{ci} and $\mathcal{G}_{i,k}$ of $\omega_{i,k}$ for $k \in \{1, \dots, N_i\}$ are made of triangles of $\mathcal{T}_{1,h}$*

$$\mathcal{G}_{i,k} = \{\kappa \in \mathcal{T}_{1,h} \text{ s.t. } \kappa \subset \omega_{i,k}\} \quad \text{and} \quad \mathcal{D}_{i,h} = \{\kappa \in \mathcal{T}_{1,h} \text{ s.t. } \kappa \subset \omega_{ci}\}. \tag{2.96}$$

We also consider that the 1D meshes $\mathcal{F}_{i,k}$ of $\gamma_{i,k}$ for $k \in \{1, \dots, s_i\}$ are made of edges of $\mathcal{T}_{1,h}$

$$\mathcal{F}_{i,k} = \{e = \kappa \cap \gamma_{i,k} \text{ s.t. } \kappa \in \mathcal{T}_{1,h}\}. \tag{2.97}$$

And the finite elements are considered of the same order, i.e. $p_i = p_1$.

Assumption I.12

We assume that $\omega_{c,e}$ and $\omega_{e,k}$ for all $k \in \{1, \dots, N_e\}$ are independent of h and that $\mathcal{T}_{2,h}$ is conform with them. Thus we consider that the triangulations $\mathcal{D}_{e,h}$ of ω_{ce} and $\mathcal{G}_{e,k}$ of $\omega_{e,k}$ for $k \in \{1, \dots, N_e\}$ are made of triangles of $\mathcal{T}_{2,h}$

$$\mathcal{G}_{e,k} = \{\kappa \in \mathcal{T}_{2,h} \text{ s.t. } \kappa \subset \omega_{e,k}\} \quad \text{and} \quad \mathcal{D}_{e,h} = \{\kappa \in \mathcal{T}_{2,h} \text{ s.t. } \kappa \subset \omega_{ce}\}. \tag{2.98}$$

We also consider that the 1D meshes $\mathcal{F}_{e,k}$ of $\gamma_{e,k}$ for $k \in \{1, \dots, s_e\}$ are made of edges of $\mathcal{T}_{2,h}$

$$\mathcal{F}_{e,k} = \{e = \kappa \cap \gamma_{e,k} \text{ s.t. } \kappa \in \mathcal{T}_{2,h}\}. \tag{2.99}$$

And the finite elements are considered of the same order, i.e. $p_e = p_2$.

Thus, under these assumptions we chose to introduce

$$M_{VV,h} = M_{\mathcal{S}_i,h} \times \prod_{k=1}^{N_i} M_{V_{i,k},h} \times M_{\mathcal{S}_e,h} \times \prod_{k=1}^{N_e} M_{V_{e,k},h},$$

where we have introduced for $j \in \{i, e\}$

$$\begin{aligned} M_{\mathcal{S}_j,h} &= \{m_{\mathcal{S}_j,h} \ / \ m_{\mathcal{S}_j,h|\gamma_{j,k}} \in Y_{p_j}^{op}(\mathcal{F}_{j,k}),\ 1 \le k \le s_j\}, \\ \text{and} \quad M_{V_{j,k},h} &= X_{p_j}(\mathcal{G}_{j,k}) \cap H_0^1(\omega_{j,k}) \quad \text{for} \quad k \in \{1, \dots, N_j\}. \end{aligned}$$

Notice, that an adequate approximation property (which similarly to Corollary 2.47 can be proven to imply (**P.2)**) is obtained by combining Proposition 2.44 for the approximation of the volume multipliers and Theorem 2.66 for the approximation of the boundary multipliers.

Thus, it only remains to prove that the uniform *discrete Inf-Sup condition* (**P.3)** is also satisfied. For that purpose and similarly to the **BB** case (see Theorem 2.69) we require the introduction of a projection operator $\widetilde{Q}^h_{\mathcal{S}_j}$ for $j \in \{i, e\}$, with similar properties that $\widetilde{Q}^h_{\gamma_j}$ introduced in (2.87). Notice that the main difference now is that there exist corners in χ_j where three different curves $\gamma_{j,k}$ with $k \in \{1, \dots, s_j\}$ intersect (see Figure 2.27). Therefore, we generalize the introduction of the space $\widetilde{X}_{p_j}(\cdot)$ to take into account this situation (notice that we keep the same notation since it is a generalization). We consider

$$\widetilde{X}_{p_j}\big(\bigcup_{k=1}^{s_j} \mathcal{F}_{j,k}\big) \subset X_{p_j}\big(\bigcup_{k=1}^{s_j} \mathcal{F}_{j,k}\big) \quad \text{such that} \quad \dim\Big(\widetilde{X}_{p_j}\big(\bigcup_{k=1}^{s_j} \mathcal{F}_{j,k}\big)\Big) = \dim(M_{\mathcal{S}_j,h}),$$

and we note that the spaces $\widetilde{X}_{p_j}(\cup \mathcal{F}_{j,k})$ have the standard approximation properties in the sense of Proposition 2.44, since only the basis functions associated with a node adjacent to a corner are modified. In particular, if we denote by ξ_0 a basis function of $X_{p_j}(\cup \mathcal{F}_{j,k})$ associated to a corner and by ξ_1 the adjacent basis function, then $\widetilde{X}_{p_j}(\cup \mathcal{F}_{j,k})$ does not have a basis function associated to the corner and the adjacent basis function is defined by $\widetilde{\xi}_1 = \xi_1 + \frac{1}{N_0}\,\xi_0$ where $N_0 \in \{2, 3\}$ is the number of curves $\gamma_{j,k}$ that meet in that corner. Then we introduce the projection operator $\widetilde{Q}^h_{\mathcal{S}_j}$ from $L^2(\mathcal{S}_j)$ into $\widetilde{X}_{p_j}(\cup\mathcal{F}_{j,k})$ that for every $\phi \in L^2(\gamma_j)$ assigns $\widetilde{Q}^h_{\gamma_j}\phi \in \widetilde{X}_{p_j}(\cup\mathcal{F}_{j,k})$ satisfying

$$(\widetilde{Q}^h_{\mathcal{S}_j}\phi, m_h)_{L^2(\gamma_j)} = (\phi, m_h)_{L^2(\gamma_j)}, \quad \forall m_h \in M_{\mathcal{S}_j,h}. \tag{2.100}$$

We remark that for $j \in \{i, e\}$, these operators project into $\widetilde{X}_{p_j}(\cup\mathcal{F}_{j,k})$, which under Assumptions I.11 and I.12 are also subspaces of the traces of the $W_{1,h}$ and $W_{2,h}$ on $\mathcal{S}_i$ and $\mathcal{S}_e$ respectively, which allows a later extension to the hole domain.

Next, similarly to the case of **BB** coupling we consider the following assumption that we believe to hold under reasonable mesh regularity assumptions.

Assumption I.13

We assume that for any $j \in \{i, e\}$, any order p_j and any $op \in \{cl, du\}$, the projection operators $\widetilde{Q}^h_{\mathcal{S}_j}$ defined by (2.100) are well defined and L^2-stable, i.e.

$$\|\widetilde{Q}^h_{\mathcal{S}_j}\phi\|_{L^2(\mathcal{S}_j)} \leq K_Q\|\phi\|_{L^2(\mathcal{S}_j)}, \quad \forall \phi \in L^2(\mathcal{S}_j),$$

where $K_Q > 0$ is a constant independent of h.

Next, we provide under Assumption I.13 the following $H^{\frac{1}{2}}$-stability property of the projection operators $\widetilde{Q}^h_{\mathcal{S}_j}$, which is analogous to Lemma 2.68 and thus the proof is not included. Notice that this property will be important in Theorem 2.78 where we prove the uniform *discrete Inf-Sup condition* (**P.3**) when considering the new choice $M_{VV,h}$.

Lemma 2.77

If Assumption I.13 holds, then for any $j \in \{i, e\}$, any order p_j and any $op \in \{cl, du\}$, there exists a constant $K > 0$ independent of h and such that

$$\|\widetilde{Q}^h_{\mathcal{S}_j}\phi\|_{H^{\frac{1}{2}}(\mathcal{S}_j)} \leq K_j\|\phi\|_{H^{\frac{1}{2}}(\mathcal{S}_j)} \quad \forall \phi \in H^{\frac{1}{2}}(\mathcal{S}_j). \tag{2.101}$$

Now we proceed to verify that the uniform *discrete Inf-Sup condition* (**P.3**) is verified when considering the new choice $M_{VV,h}$.

Theorem 2.78

*If Assumptions I.11, I.12 and I.13 are verified, then for both $op \in \{cl, du\}$ the bilinear form $b_{VV}(\cdot,\cdot)$ satisfies the uniform discrete Inf-Sup condition (**P.3**).*

Proof. First of all, attending to (2.100) and Lemma 2.77 we introduce for $j \in \{i, e\}$ the following projection operators

$$\widetilde{Q}^h_{\mathcal{S}_j} : L^2(\mathcal{S}_j) \longrightarrow \widetilde{X}_{p_j}(\bigcup_{k=1}^{s_j}\mathcal{F}_{j,k}), \quad \text{such that} \quad \|\widetilde{Q}^h_{\mathcal{S}_j}\phi\|_{H^{\frac{1}{2}}(\mathcal{S}_j)} \leq K_j\,\|\phi\|_{H^{\frac{1}{2}}(\mathcal{S}_j)} \quad \forall \phi \in H^{\frac{1}{2}}(\mathcal{S}_j),$$

where the constants $K_j > 0$ are independent of h. Moreover, we shall also introduce for all $j \in \{i, e\}$ and all $k \in \{1, \dots, N_j\}$ the lifting operators given by

$$\begin{array}{rcl} L^h_{\omega_{j,k}} : \widetilde{X}_{p_j}(\bigcup_{k=1}^{s_j}\mathcal{F}_{j,k}) & \longrightarrow & X_{p_j}(\mathcal{G}_{j,k}), \\ \mu_h & \mapsto & L^h_{\omega_{j,k}}(\mu_h) \end{array} \quad \text{and} \quad \begin{array}{rcl} L^h_{\omega_{cj}} : \widetilde{X}_{p_j}(\bigcup_{k=1}^{s_j}\mathcal{F}_{j,k}) & \longrightarrow & X_{p_j}(\mathcal{D}_{j,h}), \\ \mu_h & \mapsto & L^h_{\omega_{cj}}(\mu_h) \end{array}$$

where $L^h_{\omega_{j,k}}(\mu_h) \in X_{p_j}(\mathcal{G}_{j,k})$ is such that $L^h_{\omega_{j,k}}(\mu_h)_{|\partial\omega_{j,k}} = \mu_{h|\partial\omega_{j,k}}$ and

$$(L^h_{\omega_{j,k}}(\mu_h), w_h)_{H^1(\omega_{j,k})} = 0, \quad \forall w_h \in M_{V_{j,k},h},$$

while $L^h_{\omega_{cj}}(\mu_h) \in X_{p_j}(\mathcal{D}_{j,h})$ is such that $L^h_{\omega_{cj}}(\mu_h)_{|\gamma_{cj}} = \mu_{h|\gamma_{cj}}$, $L^h_{\omega_{cj}}(\mu_h)_{|\partial\omega_{cj}\setminus\gamma_{cj}} = 0$ and

$$(L^h_{\omega_{cj}}(\mu_h), w_h)_{H^1(\omega_{cj})} = 0, \quad \forall w_h \in X_{p_j}(\mathcal{D}_{j,h}) \cap H^1_0(\omega_{cj}).$$

And we remark that due to Lemma 2.48 (first with $\Lambda = \omega_{jk}$ and $\vartheta = \partial\omega_{jk}$, and second with $\Lambda = \omega_{cj}$ and $\vartheta = \gamma_{cj}$), there exist constants $K_{j,k} > 0$ and $K_{cj} > 0$ independent of h and such that

$$\|L^h_{\omega_{j,k}}(\mu_h)\|_{H^1(\omega_{j,k})} \le K_{j,k}\|\mu_h\|_{H^{\frac{1}{2}}(\partial\omega_{j,k})} \quad \text{and} \quad \|L^h_{\omega_{cj}}(\mu_h)\|_{H^1(\omega_{cj})} \le K_{cj}\|\mu_h\|_{H^{\frac{1}{2}}(\gamma_{cj})}.$$

Next, let us consider any $\boldsymbol{m}_h \in M_{VV,h}$ and we proceed separately for each component. First for $m_{\mathcal{S}_i,h}$ we notice that for all $\phi \in H^{\frac{1}{2}}(\mathcal{S}_i)$ we can combine the previous operators to continuously define $\mathtt{G}^h_1(\phi) \in W_{1,h}$ (with constant $\widetilde{K}_1$) such that

$$\mathtt{G}^h_1(\phi)_{|\Omega_1\setminus(\omega_{ci}\cup\omega_i)} = 0, \quad \mathtt{G}^h_1(\phi)_{|\omega_{ci}} = L_{\omega_{ci}}(\widetilde{Q}^h_{\mathcal{S}_i}(\phi)) \quad \text{and} \quad \mathtt{G}^h_1(\phi)_{|\omega_{i,k}} = L_{\omega_{i,k}}(\widetilde{Q}^h_{\mathcal{S}_i}(\phi)).$$

Therefore we obtain

$$\|m_{\mathcal{S}_i,h}\|_{[H^{\frac{1}{2}}(\mathcal{S}_i)]'} = \sup_{\phi\in H^{\frac{1}{2}}(\mathcal{S}_i)} \frac{\langle\phi, m_{\mathcal{S}_i,h}\rangle_{\mathcal{S}_i}}{\|\phi\|_{H^{\frac{1}{2}}(\mathcal{S}_i)}} \le \widetilde{K}_1 \sup_{\phi\in H^{\frac{1}{2}}(\mathcal{S}_i)} \frac{(\mathtt{G}^h_1(\phi), m_{\mathcal{S}_i,h})_{L^2(\mathcal{S}_i)}}{\|\mathtt{G}^h_1(\phi)\|_{H^{\frac{1}{2}}(\mathcal{S}_i)}}.$$

Moreover, for all $k \in \{1, \dots, N_i\}$ since $m_{i,k} \in M_{V_{i,k},h}$ and $\mathtt{G}^h_1(\phi) = 0$ in $\overline{\omega_e}$

$$\|m_{\mathcal{S}_i,h}\|_{[H^{\frac{1}{2}}(\mathcal{S}_i)]'} \le \widetilde{K}_1 \sup_{\phi\in H^{\frac{1}{2}}(\mathcal{S}_i)} \frac{b_{VV}((\mathtt{G}^h_1(\phi),0),\boldsymbol{m})}{\|(\mathtt{G}^h_1(\phi),0)\|_1} \le \widetilde{K}_1 \sup_{\boldsymbol{v}_h\in W_h} \frac{b_{VV}(\boldsymbol{v}_h,\boldsymbol{m}_h)}{\|\boldsymbol{v}_h\|_1}.$$

It is analogous to prove that

$$\|m_{\mathcal{S}_e,h}\|_{[H^{\frac{1}{2}}(\mathcal{S}_e)]'} \le K_e \sup_{\boldsymbol{v}_h\in W_h} \frac{b_{VV}(\boldsymbol{v}_h,\boldsymbol{m}_h)}{\|\boldsymbol{v}_h\|_1}.$$

Finally, notice that the rest of the proof is done adapting the proof of Theorem 2.73.

■

Finally, we provide the following convergence result for regular enough solutions. Notice that, as it was the purpose of this section, this result guarantees optimality for first and second order Lagrange finite elements approximations when considering a domain decomposition as in Figure 2.25.

Corollary 2.79

If $\boldsymbol{u} \in H^s(\Omega_1) \times H^s(\Omega_2)$ for $s > 1$, then $\lambda_{j,k} \in H^\sigma(\omega_{j,k})$ for all $\sigma < \min\{s, 1 + \frac{\kappa}{2}\}$, $\lambda_{\mathcal{S}_j|\gamma_{j,k}} \in H^{\sigma-\frac{3}{2}}(\gamma_{j,k})$ and

$$\|\boldsymbol{u} - \boldsymbol{u}_h\|_1 + \|\boldsymbol{\lambda} - \boldsymbol{\lambda}_h\|_{M_{VV}} \le K\, h^q$$

where $q = \min\{p_1, p_2, s-1, \sigma-1\}$.

2.7.3 Boundary-Volume and Volume-Boundary couplings

Finally notice that the treatment of the **Boundary - Volume** and **Volume - Boundary** couplings are derived from the previous sections. Thus we do not reply the analysis here, however for completeness we provide the specific choices and assumptions that need to be considered.

In the case of **Boundary - Volume** coupling, we consider ω_e decomposed by (2.89) and we introduce

$$M_{BV} = [H^{\frac{1}{2}}(\gamma_i)]' \times [H^{\frac{1}{2}}(\mathcal{S}_e)]' \times \prod_{k=1}^{N_e} H^1_0(\omega_{e,k})$$

$$b_{BV}(\boldsymbol{v},\boldsymbol{m}) = \langle v_1 - v_2, m_i\rangle_{\gamma_i} + \langle v_1 - v_2, m_{\mathcal{S}_e}\rangle_{\mathcal{S}_e} + \sum_{k=1}^{N_e}(v_1 - v_2, m_{e,k})_{H^1(\omega_{e,k})}.$$

Moreover, for discretization we shall also consider γ_i decomposed by (2.82), $\mathcal{S}_e$ decomposed by (2.95) and that Assumptions I.8, I.10, I.12 and I.13 are verified. Thus we introduce

$$M_{BV,h} = M_{B_i,h} \times M_{\mathcal{S}_e,h} \times \prod_{k=1}^{N_e} M_{V_{e,k},h}.$$

In the case of **Volume - Boundary** coupling, we consider ω_i decomposed by (2.89) and we introduce

$$M_{VB} = [H^{\frac{1}{2}}(\mathcal{S}_i)]' \times \prod_{k=1}^{N_i} H_0^1(\omega_{i,k}) \times [H^{\frac{1}{2}}(\gamma_e)]'$$

$$b_{VB}(\boldsymbol{v}, \boldsymbol{m}) = \langle v_1 - v_2, m_{\mathcal{S}_i}\rangle_{\mathcal{S}_i} + \sum_{k=1}^{N_i}(v_1 - v_2, m_{i,k})_{H^1(\omega_{i,k})} + \langle v_1 - v_2, m_e\rangle_{\gamma_e}.$$

Moreover, for discretization we shall also consider γ_e decomposed by (2.83), $\mathcal{S}_i$ decomposed by (2.94) and that Assumptions I.9, I.10, I.11 and I.13 are verified. Thus we introduce

$$M_{VB,h} = M_{\mathcal{S}_i,h} \times \prod_{k=1}^{N_i} M_{V_{i,k},h} \times M_{B_e,h}.$$

2.8 Second numerical results

In this section, we recover the numerical test presented in Section 2.6.2 in order to exhibit that the formulations introduced in the previous section provide optimal convergence curves for first and second order Lagrange finite elements when considering for the approximation of the boundary multipliers either the *classic* or the *dual* approach. In consequence, we consider the same continuous equations and the same computational domain Ω. Concerning the Arlequin formulation, we also consider the same choices for regions Ω_1, Ω_2, ω, ω_i and ω_e (depending on the variant) and we only need to specify the choices for $\omega_{j,k}$ and $\gamma_{j,k}$ for $j \in \{i, e\}$ and $k \in \{1, \ldots, s_j\}$. However for simplicity, instead of giving their definitions, and since it is possible to deduce them from the definition of ω_i and ω_e, we just refer to Figures 2.21 and 2.27 for a sketch of the decomposition of the overlapping region. We also consider the same physical coefficients as well as the same partitioning as those in Section 2.6.2. Finally, concerning the space discretization we compute new meshes (of similar size) in order to satisfy Assumptions I.11 and I.12. Moreover we also choose the meshes for Ω_1 to be conform with ω in such a way that the classic Arlequin method can also be used. In this way, as explained in Section 2.7 the spaces of multipliers are build with sub-meshes of the meshes of Ω_1 and Ω_2 and thus the uniform *discrete Inf-Sup conditions* are automatically satisfied.

2.8.1 2D convergence test

We consider the notation introduced in (2.81) in order to analyse the convergence behaviour of the relative error separately for each component of the solution. We first observe that the numerical results presented in Tables 2.7, 2.8, 2.9 and 2.10 and Figures 2.28, 2.29, 2.30 and 2.31 show that all the variants of the method keep the appropriate convergence rate for first and second order Lagrange finite elements when considering for the approximation of the boundary multipliers either the *classic* or the *dual* approach. It is also interesting to compare the results with those obtained in Section 2.6.2. We observe that the results in Figures 2.28a, 2.29a, 2.30a and 2.31a are essentially the same as in Figures 2.18a and 2.19a, i.e. we do not observe an improvement in the error in Ω_1 where the convergence was already with optimal order. However, this is not the case for the error in Ω_2 which convergence was suboptimal in Figures 2.18b and 2.19b. With the new schemes, we observe in Figures 2.28b, 2.29b, 2.30b and 2.31b, not only an improvement in the order of convergence when second order Lagrange finite elements are considered, but also an improvement in the value of the error when first order Lagrange finite elements are applied.

	V		VV		VB		BV		BB	
h_1	$\Vert e_1\Vert$	Slope	$\Vert e_1\Vert$	Slope	$\Vert e_1\Vert$	Slope	$\Vert e_1\Vert$	Slope	$\Vert e_1\Vert$	Slope
0.28	0.0192		0.0217		0.0214		0.0217		0.0215	
0.14	0.0065	1.57	0.0070	1.62	0.0070	1.61	0.0071	1.62	0.0071	1.61
0.07	0.0023	1.48	0.0024	1.54	0.0024	1.54	0.0024	1.55	0.0024	1.54
h_1	$\Vert e_2\Vert$	Slope	$\Vert e_2\Vert$	Slope	$\Vert e_2\Vert$	Slope	$\Vert e_2\Vert$	Slope	$\Vert e_2\Vert$	Slope
0.28	0.0302		0.0190		0.0094		0.0189		0.0091	
0.14	0.0156	0.96	0.0077	1.30	0.0028	1.75	0.0077	1.30	0.0027	1.76
0.07	0.0083	0.91	0.0037	1.07	0.0008	1.74	0.0037	1.07	0.0008	1.78

Table 2.7: 2D Convergence table when considering **constant** coefficients and **first order** Lagrange finite elements with the *classic* approach for the approximation of the boundary multipliers.

	VV		VB		BV		BB	
h_1	$\Vert e_1\Vert$	Slope	$\Vert e_1\Vert$	Slope	$\Vert e_1\Vert$	Slope	$\Vert e_1\Vert$	Slope
0.28	0.0217		0.0215		0.0218		0.0217	
0.14	0.0071	1.62	0.0070	1.61	0.0071	1.62	0.0071	1.61
0.07	0.0024	1.54	0.0024	1.54	0.0024	1.55	0.0024	1.55
h_1	$\Vert e_2\Vert$	Slope	$\Vert e_2\Vert$	Slope	$\Vert e_2\Vert$	Slope	$\Vert e_2\Vert$	Slope
0.28	0.0190		0.0100		0.0188		0.0096	
0.14	0.0078	1.28	0.0030	1.73	0.0078	1.28	0.0029	1.74
0.07	0.0037	1.08	0.0009	1.73	0.0037	1.07	0.0009	1.75

Table 2.8: 2D Convergence table when considering **constant** coefficients and **first order** Lagrange finite elements with the *dual* approach for the approximation of the boundary multipliers.

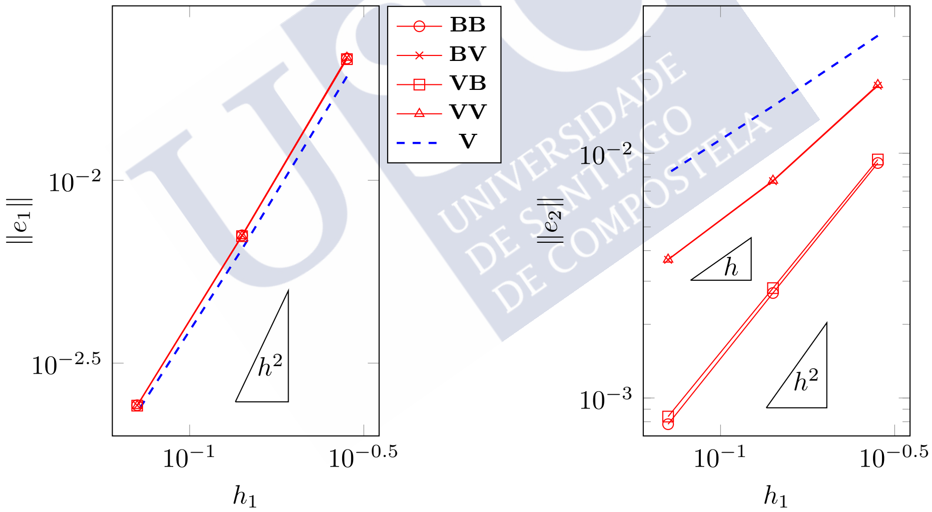

(a) Error in Ω_1.

(b) Error in Ω_2.

Figure 2.28: 2D Convergence curves when considering **constant** coefficients and **first order** Lagrange finite elements with the *classic* approach for the approximation of the boundary multipliers.

	V		VV		VB		BV		BB	
h_1	$\Vert e_1\Vert$	Slope	$\Vert e_1\Vert$	Slope	$\Vert e_1\Vert$	Slope	$\Vert e_1\Vert$	Slope	$\Vert e_1\Vert$	Slope
0.28	0.00310		0.00304		0.00304		0.00303		0.00303	
0.14	0.00072	2.11	0.00070	2.13	0.00070	2.13	0.00070	2.13	0.00070	2.13
0.07	0.00018	1.99	0.00017	2.01	0.00017	2.01	0.00017	2.01	0.00017	2.01
h_1	$\Vert e_2\Vert$	Slope	$\Vert e_2\Vert$	Slope	$\Vert e_2\Vert$	Slope	$\Vert e_2\Vert$	Slope	$\Vert e_2\Vert$	Slope
0.28	0.00370		0.00114		0.00098		0.00114		0.00097	
0.14	0.00157	1.24	0.00027	2.07	0.00023	2.08	0.00027	2.06	0.00023	2.06
0.07	0.00073	1.09	0.00007	2.04	0.00006	2.05	0.00007	2.04	0.00006	2.06

Table 2.9: 2D Convergence table when considering **constant** coefficients and **second order** Lagrange finite elements with the *classic* approach for the approximation of the boundary multipliers.

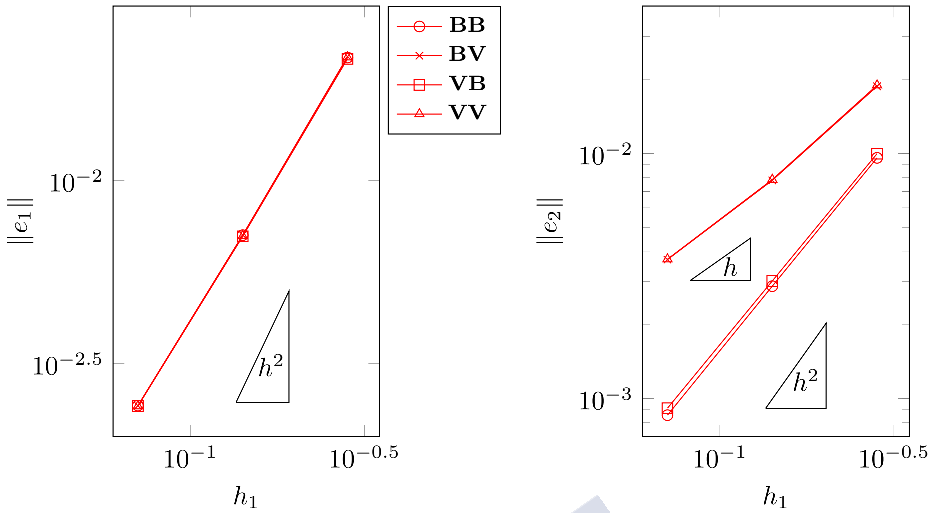

(a) Error in Ω_1.

(b) Error in Ω_2.

Figure 2.29: 2D Convergence curves when considering **constant** coefficients and **first order** Lagrange finite elements with the *dual* approach for the approximation of the boundary multipliers.

	VV		VB		BV		BB	
h_1	$\|e_1\|$	Slope	$\|e_1\|$	Slope	$\|e_1\|$	Slope	$\|e_1\|$	Slope
0.28	0.00303		0.00303		0.00302		0.00302	
0.14	0.00069	2.12	0.00069	2.12	0.00069	2.12	0.00069	2.12
0.07	0.00017	2.01	0.00017	2.01	0.00017	2.01	0.00017	2.01
h_1	$\|e_2\|$	Slope	$\|e_2\|$	Slope	$\|e_2\|$	Slope	$\|e_2\|$	Slope
0.28	0.00117		0.00101		0.00116		0.00101	
0.14	0.00028	2.08	0.00024	2.09	0.00028	2.07	0.00024	2.08
0.07	0.00007	2.05	0.00006	2.07	0.00007	2.06	0.00006	2.08

Table 2.10: 2D Convergence table when considering **constant** coefficients and **second order** Lagrange finite elements with the *dual* approach for the approximation of the boundary multipliers.

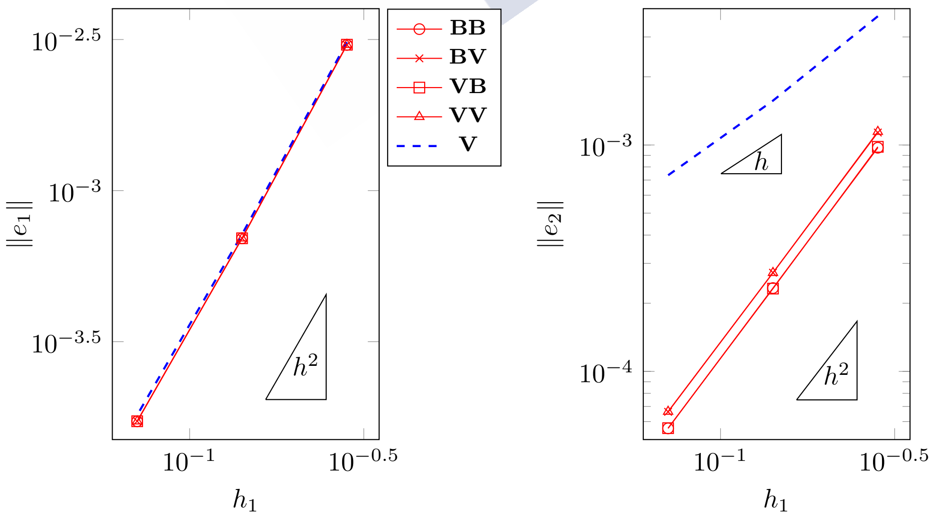

(a) Error in Ω_1.

(b) Error in Ω_2.

Figure 2.30: 2D Convergence curves when considering **constant** coefficients and **second order** Lagrange finite elements with the *classic* approach for the approximation of the boundary multipliers.

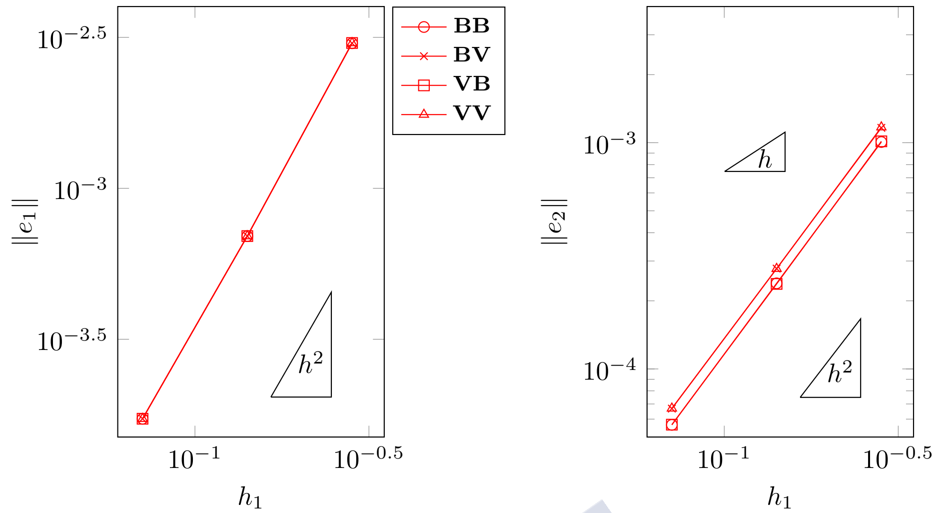

(a) Error in Ω_1. (b) Error in Ω_2.

Figure 2.31: 2D Convergence curves when considering **constant** coefficients and **second order** Lagrange finite elements with the *dual* approach for the approximation of the boundary multipliers.

2.8.2 Application to a more realistic problem

In this section, our aim is to solve a more realistic problem where we consider an elliptic obstacle $\mathcal{O}$ surrounded by a damaged region. In this context an exact solution is not known, therefore in order to validate the results, we compare with respect to a solution computed with a classical method. This section has also the purpose to exhibit the advantages of Arlequin methods compared to the classical ones when solving the same problem for different positions of the obstacle.

Continuous equations. We look for the solution of the following Helmholtz problem

$$\left\{\begin{aligned} -\,9\,u - \operatorname{div}(\mu\,\nabla u) &= f \quad \text{in} \quad \mathbb{R}^2\setminus\mathcal{O},\\ \partial_{\boldsymbol{n}}\,u &= 0 \quad \text{on} \quad \partial\mathcal{O},\\ \lim_{|\boldsymbol{x}|\to\infty}\left|\mathbb{i}\,\ell\,u(\boldsymbol{x}) + \partial_{\boldsymbol{n}} u(\boldsymbol{x})\right| &= 0, \end{aligned}\right. \tag{2.102}$$

where the medium is excited by the source (see Figure 2.32b)

$$f(\boldsymbol{x}) = \exp\left(1 + \frac{1}{|2\,\boldsymbol{x}|^2 - 1}\right), \quad \text{if} \quad |\boldsymbol{x}| < 0.5, \quad f(\boldsymbol{x}) = 0, \quad \text{elsewhere.}$$

We also consider the medium to be defected by an obstacle that is assumed to be represented by an ellipse

$$\mathcal{O}(\boldsymbol{x}_0,\theta) = \begin{pmatrix} \cos(\theta) & \sin(\theta)\\ -\sin(\theta) & \cos(\theta)\end{pmatrix}\mathcal{O}_0 + \boldsymbol{x}_0,$$

where the pair $(\boldsymbol{x}_0,\theta)$ provides the centre and rotation of the obstacle and $\mathcal{O}_0$ denotes an ellipse centred at the origin, with semi-major and semi-minor axes aligned with the Cartesian axes and which length are given by 0.2 and 0.04 respectively. We also assume that a damaged region surrounds the obstacle and we model this effect by considering (see Figure 2.32a)

$$\mu(\boldsymbol{x}) = \left(1 + 10\,e^{-10|\boldsymbol{x}-\boldsymbol{x}_0|^2}\right)^{-1}, \quad \boldsymbol{x}\in\mathbb{R}^2\setminus\mathcal{O}(\boldsymbol{x}_0,\theta).$$

Moreover, Perfectly Matched Layers (see [68]) are used to simulate the unbounded medium, leading to the following bounded computational domain

$$\Omega = \Theta \setminus \mathcal{O}(\boldsymbol{x}_0, \theta), \quad \text{where} \quad \Theta = [-4, 4] \times [-4, 4].$$

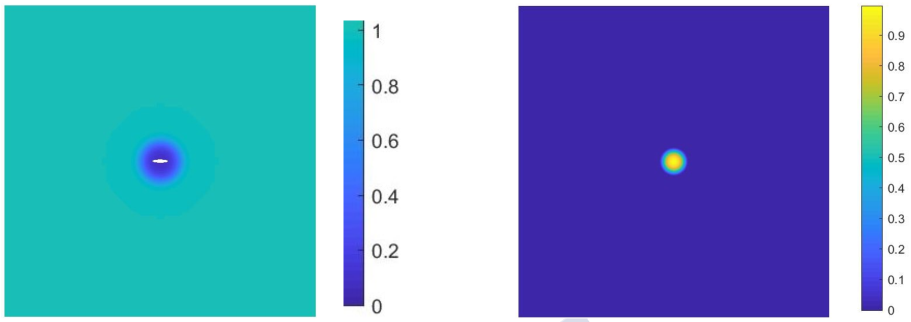

(a) Plot of μ in $\Theta \setminus \mathcal{O}_0$.

(b) Plot of f in Θ.

Figure 2.32: Graphic representation of the source term and the physical coefficient μ for a given pair $(\boldsymbol{x}_0, \theta)$.

Arlequin formulation. We consider **boundary-boundary** coupling to solve problem (2.102). The computational domain Ω is decomposed into two overlapping sub-domains Ω_1 and Ω_2 (s.t. $\Omega = \Omega_1 \cap \Omega_2$) which definition depends on the position of the obstacle and the mesh considered for the background media Θ. In particular, in order to capture the strong variations of the physical coefficients with Ω_2, we consider

$$\Omega_1 = \Theta \setminus S_{\mathcal{O}}^h \quad \text{and} \quad \Omega_2 = \begin{pmatrix} \cos(\theta) & \sin(\theta) \\ -\sin(\theta) & \cos(\theta) \end{pmatrix} \Omega_2^0 + \boldsymbol{x}_0,$$

where $\Omega_2^0 := [-1.5, 1.5] \times [-1.5, 1.5] \setminus \mathcal{O}_0$ and $S_{\mathcal{O}}^h$ denotes an area surrounding the obstacle and conform with the mesh considered for the background media Θ, thus it is detailed later for each specific configuration. Finally, in order to satisfy Assumption I.2, we choose the partitioning to be given by the simplest choice

$$\alpha_1 = \alpha_2 = \beta_1 = \beta_2 = \frac{1}{2} \quad \text{in } \omega.$$

Space discretization. We choose to use **second** order finite elements and for the approximation of the boundary multipliers we consider the *classic* approach. Moreover, we use a coarse regular mesh for the background media Θ and a fine mesh for Ω_2^0 (see Figure 2.33). Notice that the mesh for Ω_2^0 is refined close the ellipse in order to capture the geometry of the obstacle as well as the strong variation of the physical coefficient μ.

Numerical results. We consider three different experiments where the only physical modification concerns the choice of the pair $(\boldsymbol{x}_0, \theta)$ that characterizes the position of the obstacle and its surrounding damaged region. Moreover, according to the choice of $(\boldsymbol{x}_0, \theta)$ we also specify the region $S_{\mathcal{O}}^h$ that surrounds the obstacle and must be conform with the mesh of the background media Θ.

Case 1 :	Case 2 :	Case 3 :
$(\boldsymbol{x}_0, \theta) = \left((-2, -2), \frac{\pi}{2}\right),$	$(\boldsymbol{x}_0, \theta) = \left((0.5, 2.2), \frac{\pi}{20}\right),$	$(\boldsymbol{x}_0, \theta) = \left((1.5, -1.8), \frac{3\pi}{8}\right),$
$S_{\mathcal{O}}^h = [-2.4, -1.6] \times [-2.4, -1.6],$	$S_{\mathcal{O}}^h = [0, 1] \times [1.8, 2.6],$	$S_{\mathcal{O}}^h = [1, 2] \times [-2.2, -1.4].$

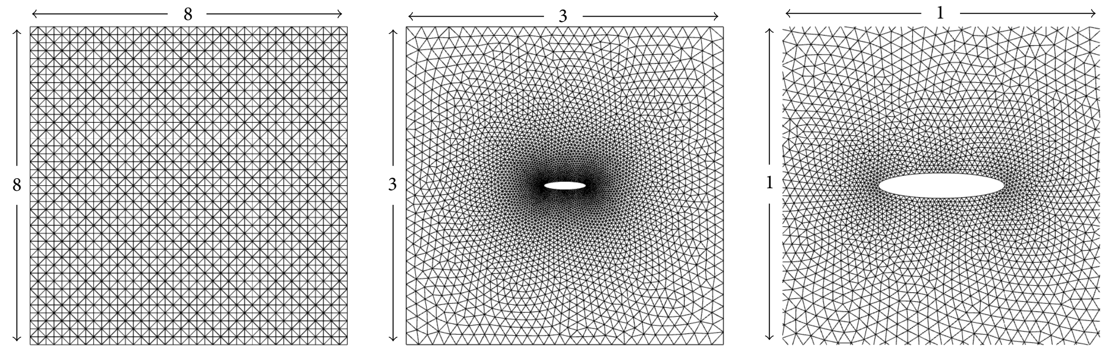

(a) Coarse homogeneous mesh of the non defected domain Θ.

(b) Fine mesh of Ω_2^0 refined in a neighbourhood of the obstacle.

(c) Zoom of a neighbourhood of the obstacle.

Figure 2.33: Meshes considered for the Arlequin decomposition.

In consequence, the resultant meshes that we consider when solving problem (2.102) with **boundary-boundary** coupling are plotted in figures 2.34, 2.35 and 2.36. Moreover, in figures 2.37, 2.38 and 2.39 we compare the results with respect to a solution obtained by a standard finite element method. Notice that we also consider a second order finite elements method and the meshes considered have a number of nodes which is comparable to the sum of the number of nodes of the meshes considered for Ω_1 and Ω_2 (see figures 2.34, 2.35 and 2.36).

Finally, we remark that figures 2.37, 2.38 and 2.39 show a good agreement between the numerical solutions obtained with the Arlequin method and the classical method. The reader should notice that the advantage of the Arlequin method is that the re-meshing procedure required to generate meshes of Ω for the classical method, has been replaced by the adjustment of the meshes of Θ (which moreover is structured) and Ω_2^0 which is more efficient.

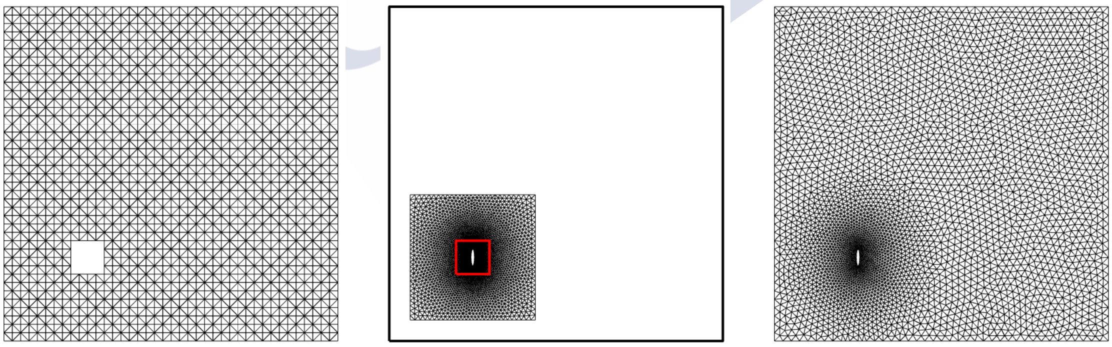

Figure 2.34: Comparison between meshes considered in case 1.

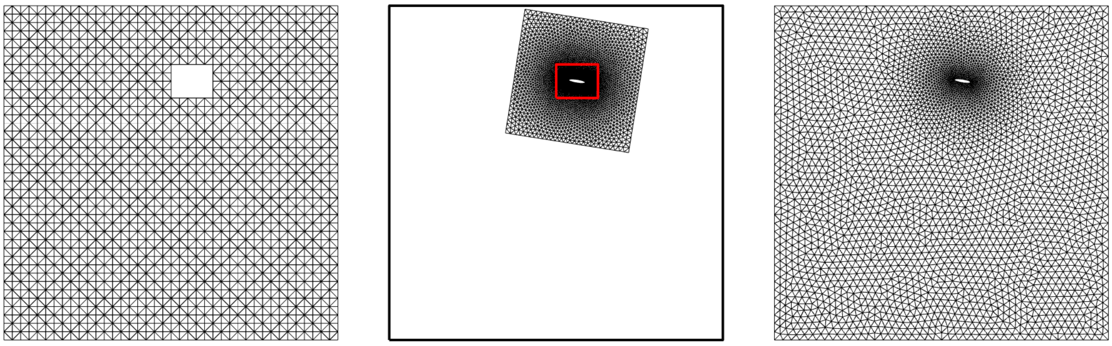

Figure 2.35: Comparison between meshes considered in case 2.

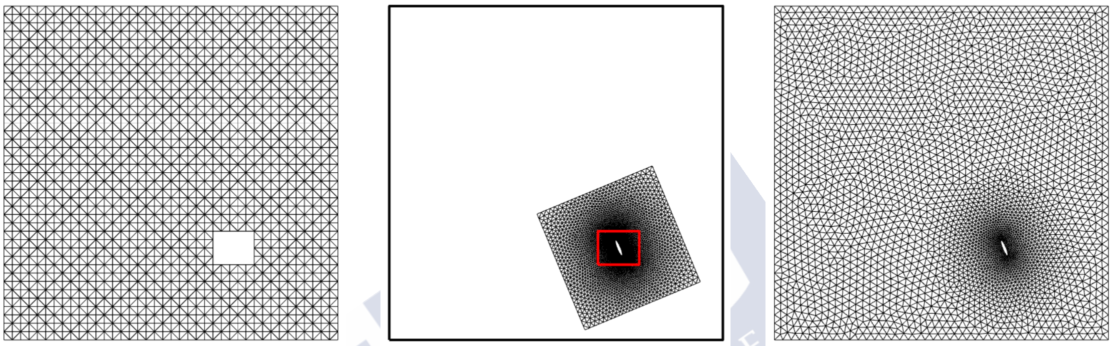

Figure 2.36: Comparison between meshes considered in case 3.

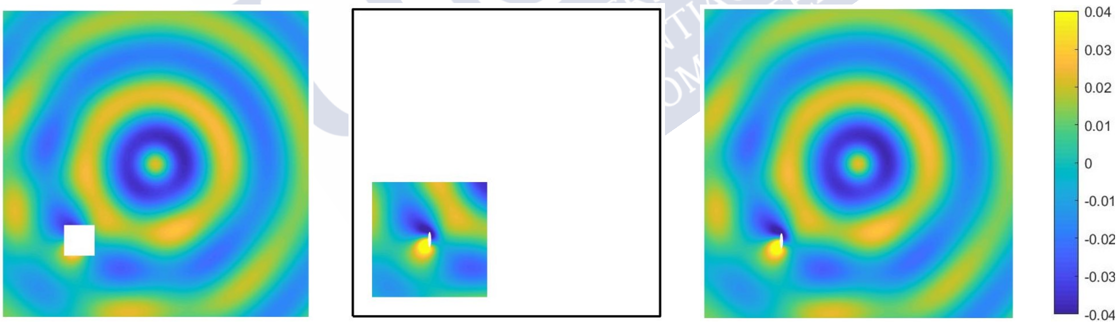

Figure 2.37: Solution of problem (2.102) in case 1. Comparison between the solution obtained with classic finite elements and with **boundary-boundary** Arlequin coupling.

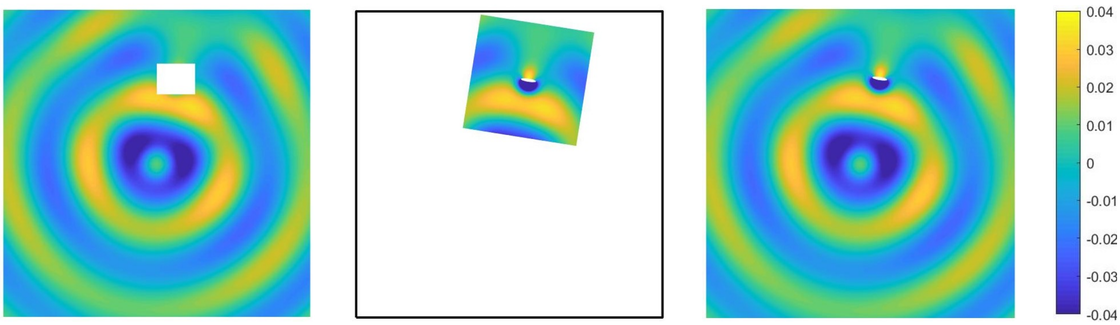

Figure 2.38: Solution of problem (2.102) in case 2. Comparison between the solution obtained with classic finite elements and with **boundary-boundary** Arlequin coupling.

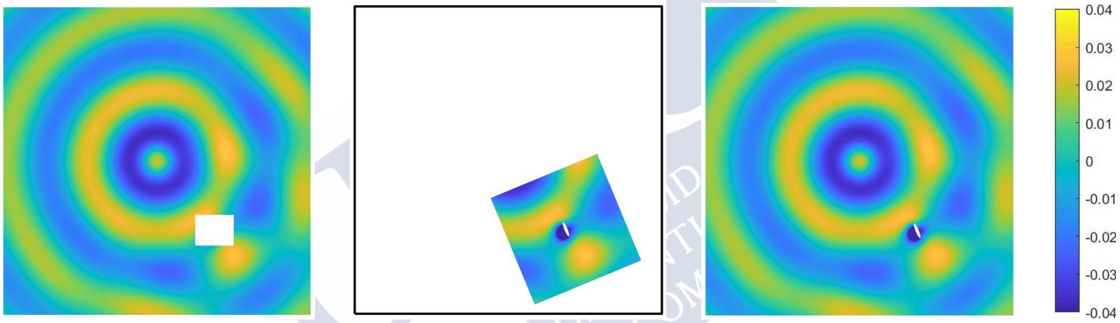

Figure 2.39: Solution of problem (2.102) in case 3. Comparison between the solution obtained with classic finite elements and with **boundary-boundary** Arlequin coupling.

Chapter 3

The Arlequin formulation for transient wave equation

Contents

In this chapter we extend the formulation and mathematical analysis of the Arlequin methods presented in previous chapter to the problem of wave propagation in the context of transient wave scattering by obstacles. The resultant formulations, as for the Helmholtz problem, allow to solve wave propagation problems considering non-conforming and overlapping meshes, one for the background propagating medium and another for a local patch surrounding the obstacle. The formulation of the method at the continuous level is rather straightforward, however the mathematical analysis of the resultant formulations as well as the adequate choice of efficient time schemes that guarantee the numerical stability of the method is not trivial.

3.1 Preliminaries on transient wave equation

Let us begin by a brief introduction of the model problem we consider. As in previous chapter we are mainly interested in local defects, thus we recall some notations of Chapter 2. We consider the defected domain defined by

$$\Omega = \Theta \setminus \overline{\mathcal{O}},$$

where $\Theta \subset \mathbb{R}^d$ denotes a non-defected open domain that we assume to be bounded, homogeneous and Lipschitz regular while $\mathcal{O}$ (possibly empty) denotes the defect which is assumed to be compactly embedded in Θ. Moreover, we also denote by $(\rho, \mu) \in L^\infty(\Omega)^2$ the physical coefficients of the wave propagation problem that are assumed to satisfy

$$\inf_{\boldsymbol{x}\in\Omega} \rho(\boldsymbol{x}) \geq \rho_0 > 0 \quad \text{and} \quad \inf_{\boldsymbol{x}\in\Omega} \mu(\boldsymbol{x}) \geq \mu_0 > 0. \tag{3.1}$$

Then, we look for the solution of the **transient wave equation** with regular enough source term $f \in \mathcal{C}^1([0,T]; L^2(\Omega))$, and for the sake of simplicity, homogeneous Neumann boundary conditions:

$$\begin{cases} \rho\, \partial_t^2 u \,-\, \operatorname{div}(\mu\, \nabla u) = f, & \text{in } \Omega, \quad t \in [0,T], \\ \nabla u \cdot \mathbf{n} = 0, & \text{on } \partial\Omega, \quad t \in [0,T]. \end{cases} \tag{3.2}$$

We also consider for simplicity, that the system (3.2) is completed with vanishing initial data and we assume that the source term vanishes at the initial time

$$u(\cdot, 0) = 0, \quad \partial_t u(\cdot, 0) = 0, \quad f(\cdot, 0) = 0 \quad \text{in } \Omega. \tag{3.3}$$

Notice that the derivation of the variational formulation associated to problem (3.2)-(3.3) can be obtained by classical techniques. Thus we obtain:

$$\begin{cases} \text{Find } u(t) : [0,T] \longrightarrow H^1(\Omega) \text{ such that } (u, \partial_t u)(t=0) = (0,0) \text{ and} \\ (\rho\, \partial_t^2 u, v)_{L^2(\Omega)} + (\mu\, \nabla u, \nabla v)_{L^2(\Omega)} = (f, v)_{L^2(\Omega)} \quad \forall\, v \in H^1(\Omega). \end{cases} \tag{3.4}$$

We shall also remark that the existence and uniqueness of solution of problem (3.4) is classical (for instance, from standard Hille-Yosida's theory for evolution problems, see [78]) and it verifies that

$$u \in \mathcal{C}^2([0,T]; L^2(\Omega)) \cap \mathcal{C}^1([0,T]; H^1(\Omega)).$$

3.2 The Arlequin formulations

In this section, we present the Arlequin formulations when applied to problem (3.2). In consequence, as in previous chapter we consider that the defected domain Ω is decomposed into Ω_1 and Ω_2 that are two overlapping open sub-domains such that

$$\Omega_j \subset \Omega \quad j \in \{1,2\}, \qquad \Omega = \Omega_1 \cup \Omega_2 \qquad \text{and} \qquad \partial\Omega_1 \cap \partial\Omega_2 = \emptyset.$$

We also recall that in practice, Ω_1 will be adapted to the background domain avoiding the defect, while Ω_2 will be devoted to capture the obstacle properties. In consequence, we consider

$$\partial\Theta \subset \partial\Omega_1 \quad \text{and} \quad \partial\mathcal{O} \subset \partial\Omega_2.$$

Moreover, it is important to notice that

$$\omega = \Omega_1 \cap \Omega_2 \neq \emptyset \quad \text{and} \quad \overline{\omega} \cap \partial\Omega = \emptyset$$

and recall the introduction of the decomposition of ω as it was presented in Chapter 2 (see Figure 3.1). Thus we denote by γ_i and γ_e the internal and external boundaries of ω

$$\gamma_i := \partial\Omega_1 \cap \partial\omega \qquad \text{and} \qquad \gamma_e := \partial\Omega_2 \cap \partial\omega,$$

and we introduce two open sub-domains ω_i and ω_e that represent two disjoint regions close to γ_i and γ_e respectively (by disjoint we mean $\overline{\omega_i} \cap \overline{\omega_e} = \emptyset$). These sets are either empty sets or satisfy

$$\gamma_i \subset \partial\omega_i \text{ (resp. } \gamma_e \subset \partial\omega_e) \qquad \text{and} \qquad \gamma_i \cap \overline{\partial\omega_i \backslash \gamma_i} = \emptyset \text{ (resp. } \gamma_e \cap \overline{\partial\omega_e \backslash \gamma_e} = \emptyset).$$

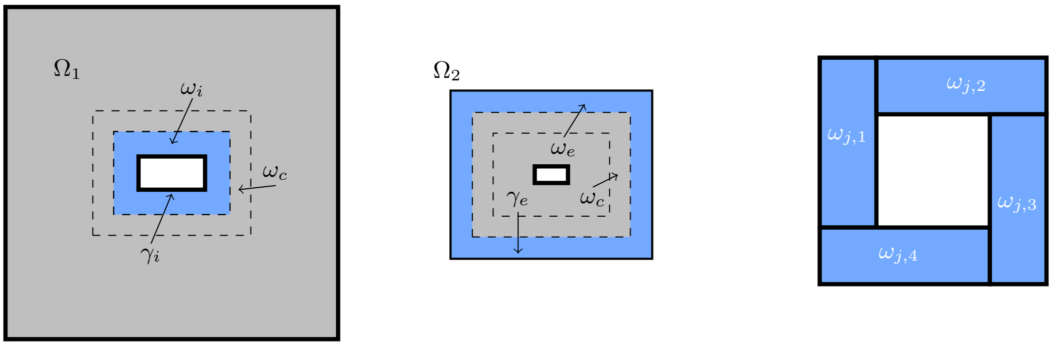

(a) The background media Ω_1 and the regions γ_i, ω_i and ω_c.

(b) The patch Ω_2 and the regions γ_e, ω_e and ω_c.

(c) Decomposition of ω_j for $j \in \{i, e\}$ into the regions $\{\omega_{j,k}\}_{k=1}^{N_j}$.

Figure 3.1: Sketch of the proposed decomposition of the overlapping region in order to obtain more regular multipliers.

We shall also denote the region that is between ω_i and ω_e by (see in Figure 3.1)

$$\omega_c = \omega \setminus \overline{\omega_i \cup \omega_e}.$$

Moreover, following the decomposition introduced in Chapter 2, we consider for $j \in \{i, e\}$ a domain decomposition of ω_j which is given by (see Figure 3.1 right),

$$\{\omega_{j,k}\}_{k=1}^{N_j} \quad \text{where } \omega_{j,k} \text{ are disjoint open subset of } \omega_j \text{ such that} \quad \bigcup_{k=1}^{N_j} \overline{\omega_{j,k}} = \overline{\omega_j},$$

which in practice is chosen in order to reduce the size of the largest interior angle of ω_i and ω_e and therefore improve the regularity of the resultant Lagrange multipliers. Note, that we also introduce the notation for the skeleton

$$\mathcal{S}_j = \bigcup_{k=1}^{N_j} \partial\omega_{j,k}, \quad \text{for} \quad j \in \{i, e\}.$$

Furthermore, in order to simplify notation, as in Chapter 2 we avoid the interaction of the source term with Ω_2 by considering

$$f \text{ is compactly supported in } \Omega_1 \setminus \Omega_2, \quad f \in \mathcal{C}^1([0,T]; L^2(\Omega_1 \setminus \Omega_2)). \tag{3.5}$$

Then, we follow the methodology presented in previous chapter to develop the Arlequin formulations of problem (3.4). Thus we first recall the definition of the partitioning (that we consider to satisfy Assumptions I.1 and I.2)

$$\sum_{j=1}^{2} \alpha_j = \sum_{j=1}^{2} \beta_j = 1, \quad \text{in} \quad \omega, \quad \text{and} \quad \alpha_j = \beta_j = 1, \quad \text{in } \Omega_j \setminus \omega, \quad j \in \{1, 2\},$$

as well as the functional space $W = H^1(\Omega_1) \times H^1(\Omega_2)$, and the forms

$$m : W \times W \longrightarrow \mathbb{R} \qquad \text{such that} \qquad m(\boldsymbol{u}, \boldsymbol{v}) = \sum_{j=1}^{2} (\alpha_j \, \rho \, u_j, v_j)_{L^2(\Omega_j)},$$

$$a : W \times W \longrightarrow \mathbb{R} \qquad \text{such that} \qquad a(\boldsymbol{u}, \boldsymbol{v}) = \sum_{j=1}^{2} (\beta_j \, \mu \, \nabla u_j, \nabla v_j)_{L^2(\Omega_j)},$$

$$g : W \longrightarrow \mathbb{R} \qquad \text{such that} \qquad g(\boldsymbol{v}) = (f, v_1)_{L^2(\Omega_1 \setminus \Omega_2)},$$

that are well defined and continuous under Assumption I.1 (see Proposition 2.4). Then, we shall also recall the introduction of the Lagrange multiplier spaces M_C and the coupling bilinear forms

$$b_C : W \times M_C \longrightarrow \mathbb{R}$$

which distinguish between the type of coupling we want to apply. Thus in the following we denote the functional spaces

$$\begin{aligned}
M_{BB} &= [H^{\frac{1}{2}}(\gamma_i)]' \times [H^{\frac{1}{2}}(\gamma_e)]', \\
M_{BV} &= [H^{\frac{1}{2}}(\gamma_i)]' \times [H^{\frac{1}{2}}(\mathcal{S}_e)]' \times \prod_{k=1}^{N_e} H_0^1(\omega_{e,k}), \\
M_{VB} &= [H^{\frac{1}{2}}(\mathcal{S}_i)]' \times \prod_{k=1}^{N_i} H_0^1(\omega_{i,k}) \times [H^{\frac{1}{2}}(\gamma_e)]', \\
M_{VV} &= [H^{\frac{1}{2}}(\mathcal{S}_i)]' \times \prod_{k=1}^{N_i} H_0^1(\omega_{i,k}) \times [H^{\frac{1}{2}}(\mathcal{S}_e)]' \times \prod_{k=1}^{N_e} H_0^1(\omega_{e,k}),
\end{aligned}$$

as well as the continuous bilinear forms

$$\begin{aligned}
b_{BB}(\boldsymbol{v}, \boldsymbol{m}) &= \langle v_1 - v_2, m_i \rangle_{\gamma_i} + \langle v_1 - v_2, m_e \rangle_{\gamma_e}, \\
b_{BV}(\boldsymbol{v}, \boldsymbol{m}) &= \langle v_1 - v_2, m_i \rangle_{\gamma_i} + \langle v_1 - v_2, m_{\mathcal{S}_e} \rangle_{\mathcal{S}_e} + \sum_{k=1}^{N_e} (v_1 - v_2, m_{e,k})_{H^1(\omega_{e,k})}, \\
b_{VB}(\boldsymbol{v}, \boldsymbol{m}) &= \langle v_1 - v_2, m_{\mathcal{S}_i} \rangle_{\mathcal{S}_i} + \sum_{k=1}^{N_i} (v_1 - v_2, m_{i,k})_{H^1(\omega_{i,k})} + \langle v_1 - v_2, m_e \rangle_{\gamma_e}, \\
b_{VV}(\boldsymbol{v}, \boldsymbol{m}) &= \langle v_1 - v_2, m_{\mathcal{S}_i} \rangle_{\mathcal{S}_i} + \sum_{k=1}^{N_i} (v_1 - v_2, m_{i,k})_{H^1(\omega_{i,k})} \\
&+ \langle v_1 - v_2, m_{\mathcal{S}_e} \rangle_{\mathcal{S}_e} + \sum_{k=1}^{N_e} (v_1 - v_2, m_{e,k})_{H^1(\omega_{e,k})}.
\end{aligned}$$

Finally, notice that the methodology we developed in Chapter 2 provides the following Arlequin formulations of problem (3.4), that we present in an abstract framework where the subscript C denotes the kind of coupling that we want to apply:

$$\left\{\begin{array}{l}
\text{Find } (\boldsymbol{u}(t), \boldsymbol{\lambda}(t)) : [0,T] \longrightarrow W \times M_C \text{ such that } (\boldsymbol{u}, \partial_t \boldsymbol{u})(t=0) = (\boldsymbol{0}, \boldsymbol{0}) \text{ and} \\
\dfrac{\mathrm{d}^2}{\mathrm{d}t^2} m(\boldsymbol{u}, \boldsymbol{v}) \ + \ a(\boldsymbol{u}, \boldsymbol{v}) \ + \ b_C(\boldsymbol{v}, \boldsymbol{\lambda}) \ = \ g(\boldsymbol{v}), \qquad \forall \boldsymbol{v} \in W, \qquad (3.6a) \\
\qquad\qquad\qquad\qquad b_C(\boldsymbol{u}, \boldsymbol{m}) \ = \ 0, \qquad \forall \boldsymbol{m} \in M_C. \qquad (3.6b)
\end{array}\right.$$

The equivalence of problem (3.6) with respect to problem (3.4) is given by the following theorem.

Theorem 3.1

If assumptions I.1 and I.2 are satisfied and if (according to (3.5))

$$f \in W^{1,1}([0,T]; L^2(\Omega_1 \setminus \omega)) \quad \big(\supset \mathcal{C}^1([0,T]; L^2(\Omega_1 \setminus \omega)) \big),$$

then, problem (3.6) has a unique solution such that

$$(u_1, u_2, \boldsymbol{\lambda}) \ \in \ \prod_{j=1}^{2} \big(\mathcal{C}^2([0,T]; L^2(\Omega_j)) \cap \mathcal{C}^1([0,T]; H^1(\Omega_j)) \big) \ \times \ \mathcal{C}^0([0,T]; M_C). \qquad (3.7)$$

Moreover, if we denote by u the unique solution of (3.4), we have that

$$u_{|\Omega_1} = u_1 \quad \text{and} \quad u_{|\Omega_2} = u_2. \tag{3.8}$$

Proof. We begin by proving the last part of the statement, thus let us assume that there exists $(\boldsymbol{u}, \boldsymbol{\lambda})$ solution of (3.6) with the regularity given in (3.7). Then, equation (3.6b) clearly implies that $u_1 = u_2$ in $\omega \backslash \omega_c$ and also on $\partial\omega_c$. Moreover, taking into account Assumption I.2, we can choose test functions in (3.6a) such that $v_1 = w/C \in H_0^1(\omega_c)$ and $v_2 = -w/(1-C) \in H_0^1(\omega_c)$, thus we obtain

$$\big(\rho\,\partial_t^2\,(u_1 - u_2), w\big)_{L^2(\omega_c)} \;+\; \big(\mu\,\nabla(u_1-u_2), \nabla w\big)_{L^2(\omega_c)} \;=\; 0, \quad \forall w \in H_0^1(\omega_c),$$

which implies that $u_1 - u_2$ is identically 0 in ω_c due to the vanishing initial conditions. In consequence, $u(t)$ defined by (3.8) belongs to $H^1(\Omega)$, more precisely

$$u \in \mathcal{C}^2([0,T]; L^2(\Omega)) \cap \mathcal{C}^1([0,T]; H^1(\Omega))$$

and if we choose in (3.6a) test functions such that $v_1 = v_2$ in ω_c, we obtain

$$(\rho\,\partial_t^2 u, v)_{L^2(\Omega)} + (\mu\,\nabla u, \nabla v)_{L^2(\Omega)} = (f, v)_{L^2(\Omega\backslash\Omega_2)} \quad \forall v \in H^1(\Omega).$$

The rest of the proof is dedicated to prove the existence, uniqueness and regularity of the solution of problem (3.6). The proof is based ib Laplace transform and is presented in several steps.

Step 1: Extension of the source term.
We denote by $f_e \in W^{1,1}(\mathbb{R}^+; L^2(\Omega_1 \setminus \omega))$ an extension of the source term $f(\cdot, t)$ for $t > T$ such that $f_e(\cdot, t) = 0$ for $t > 2T$ (see Section 5.2.2 in [21]). Note that with both f_e or f, the solutions should coincide for $t \leq T$. Therefore existence, uniqueness and estimates will be obtained with source term f_e. To obtain a preliminary result we assume that $f_e \in \mathcal{C}_0^\infty(\mathbb{R}^+; L^2(\Omega_1 \setminus \omega))$.

Step 2: Existence, uniqueness and estimations in Laplace domain.
We introduce the Laplace transform $\mathcal{L}$ of any time dependent function h as

$$\mathcal{L}(h(t)) = \widehat{h}(s) = \int_0^{+\infty} h(t)\, e^{-st}\, \mathrm{d}t, \quad s = \mathbb{i}\,\xi + \eta, \quad \eta > 0.$$

where $\mathbb{i} = \sqrt{-1}$, $\eta \in \mathbb{R}^+$ is assumed fixed and $\xi \in \mathbb{R}$ is usually called the *frequency variable*. Note that $\boldsymbol{u}$ and its first two derivatives vanish at $t = 0$, hence $\mathcal{L}(\partial_t^2 u) = s^2\,\widehat{u}$. Then, after transformation in Laplace domain, the variational formulation of (3.6) written for $t \in \mathbb{R}^+$ becomes

$$\left\{\begin{array}{ll} \text{Find } (\widehat{\boldsymbol{u}}, \widehat{\boldsymbol{\lambda}}) \in W \times M_C, \text{ such that} & \\[2mm] m^\star(s; \widehat{\boldsymbol{u}}, \widehat{\boldsymbol{v}}) \;+\; a^\star(s; \widehat{\boldsymbol{u}}, \widehat{\boldsymbol{v}}) \;+\; b_C^\star(s; \widehat{\boldsymbol{v}}, \widehat{\boldsymbol{\lambda}}) \;=\; g^\star(s; \widehat{\boldsymbol{v}}), & \forall\,\widehat{\boldsymbol{v}} \in W, \quad (3.9a) \\[2mm] b_C^\star(s; \widehat{\boldsymbol{u}}, \widehat{\boldsymbol{m}}) \;=\; 0, & \forall\,\widehat{\boldsymbol{m}} \in M_C. \quad (3.9b) \end{array}\right.$$

where all the forms are defined by considering the respective **complex hermitian** inner products:

$$\begin{array}{lll} m^\star(s) : W \times W \longrightarrow \mathbb{C} & \text{such that} & m^\star(s; \widehat{\boldsymbol{u}}, \widehat{\boldsymbol{v}}) = \overline{s}\; s^2\; m(\widehat{\boldsymbol{u}}, \widehat{\boldsymbol{v}}), \\ a^\star(s) : W \times W \longrightarrow \mathbb{C} & \text{such that} & a^\star(s; \widehat{\boldsymbol{u}}, \widehat{\boldsymbol{v}}) = \overline{s}\; a(\widehat{\boldsymbol{u}}, \widehat{\boldsymbol{v}}), \\ b_C^\star(s) : W \times M_C \longrightarrow \mathbb{C} & \text{such that} & b_C^\star(s; \widehat{\boldsymbol{v}}, \widehat{\boldsymbol{m}}) = \overline{s}\; b_C(\widehat{\boldsymbol{v}}, \widehat{\boldsymbol{m}}), \\ g^\star(s) : W \longrightarrow \mathbb{C} & \text{such that} & g^\star(s; \widehat{\boldsymbol{v}}) = \overline{s}\; g(\widehat{\boldsymbol{v}}). \end{array}$$

Now notice that, to guarantee the existence and uniqueness of solution of problem (3.9), we need to check for adequate norms, the continuity of the previous forms, the coercivity of $m^\star(s) + a^\star(s)$ and an adequate *inf-sup condition.* To do so, as in [21], we define the s-dependent H^1-like norm,

$$\|\widehat{v}_j\|_{\Omega_j}^2 = |s|^2\, \|\widehat{v}_j\|_{L^2(\Omega_j)}^2 + \|\nabla\,\widehat{v}_j\|_{L^2(\Omega_j)}^2,$$

and notice that it is easy to verify that there exist positive constants C_m, C_a, C_b, C_g and C_e only depending in the L^∞ norm of ρ, μ, α_j and β_j such that

$$\begin{array}{rcl} |m^\star(s;\widehat{\boldsymbol{u}},\widehat{\boldsymbol{v}})| & \leq & C_m\ |s|\ (\ \|\widehat{u}_1\|^2_{\Omega_1}+\|\widehat{u}_2\|^2_{\Omega_2}\ )^{\frac{1}{2}}\ (\|\widehat{v}_1\|^2_{\Omega_1}+\|\widehat{v}_2\|^2_{\Omega_2}\ )^{\frac{1}{2}}, \\ |a^\star(s;\widehat{\boldsymbol{u}},\widehat{\boldsymbol{v}})| & \leq & C_a\ |s|\ (\ \|\widehat{u}_1\|^2_{\Omega_1}+\|\widehat{u}_2\|^2_{\Omega_2}\ )^{\frac{1}{2}}\ (\|\widehat{v}_1\|^2_{\Omega_1}+\|\widehat{v}_2\|^2_{\Omega_2}\ )^{\frac{1}{2}}, \\ |b^\star_C(s;\widehat{\boldsymbol{v}},\widehat{\boldsymbol{m}})| & \leq & C_b\ |s|\ (\ \|\widehat{v}_1\|^2_{\Omega_1}+\|\widehat{v}_2\|^2_{\Omega_2}\ )^{\frac{1}{2}}\ \|\widehat{\boldsymbol{m}}\|_{M_C}, \\ |g^\star(s;\widehat{\boldsymbol{v}})| & \leq & C_g\ |s|\ (\ \|\widehat{v}_1\|^2_{\Omega_1}+\|\widehat{v}_2\|^2_{\Omega_2}\ )^{\frac{1}{2}}, \\ |m^\star(s;\widehat{\boldsymbol{u}},\widehat{\boldsymbol{u}})+a^\star(s;\widehat{\boldsymbol{u}},\widehat{\boldsymbol{u}})| & \geq & C_e\ \eta\ (\ \|\widehat{u}_1\|^2_{\Omega_1}+\|\widehat{u}_2\|^2_{\Omega_2}\ ). \end{array}$$

Thus it only remains to prove an adequate *inf-sup condition*, i.e, we need to find an adequate positive constant δ such that

$$\sup_{\widehat{\boldsymbol{v}}\in W}\frac{|b^\star_C(s;\widehat{\boldsymbol{v}},\widehat{\boldsymbol{m}})|}{(\ \|\widehat{v}_1\|^2_{\Omega_1}+\|\widehat{v}_2\|^2_{\Omega_2}\ )^{\frac{1}{2}}}\ \geq\ \delta\,\|\widehat{\boldsymbol{m}}\|_{M_C}. \tag{3.10}$$

To do so, we recall Theorem 2.73 where we proved an *inf-sup condition* for $C = VV$ and notice that it can be easily adapted to the complex case and also for the other couplings. Therefore, there exists a positive constant δ_0 such that

$$\sup_{\widehat{\boldsymbol{v}}\in W}\frac{|b_C(\widehat{\boldsymbol{v}},\widehat{\boldsymbol{m}})|}{\|\widehat{\boldsymbol{v}}\|_1}\ \geq\ \delta_0\,\|\widehat{\boldsymbol{m}}\|_{M_C}.$$

Moreover, we shall also notice that

$$(\ \|\widehat{v}_1\|^2_{\Omega_1}+\|\widehat{v}_2\|^2_{\Omega_2}\ )^{\frac{1}{2}}\leq\max\{1,|s|\}\|\boldsymbol{v}\|_1,\quad\text{and}\quad |b^\star_C(s;\widehat{\boldsymbol{v}},\widehat{\boldsymbol{m}})|=|s|\ |b_C(\widehat{\boldsymbol{v}},\widehat{\boldsymbol{m}})|.$$

In consequence

$$\sup_{\widehat{\boldsymbol{v}}\in W}\frac{|b^\star_C(s;\widehat{\boldsymbol{v}},\widehat{\boldsymbol{m}})|}{(\ \|\widehat{v}_1\|^2_{\Omega_1}+\|\widehat{v}_2\|^2_{\Omega_2}\ )^{\frac{1}{2}}}\ \geq\ \frac{|s|\ \delta_0\ \|\widehat{\boldsymbol{m}}\|_{M_C}}{\max\{1,|s|\}}\ =\ \min\{1,|s|\}\ \delta_0\ \|\widehat{\boldsymbol{m}}\|_{M_C},$$

and if we notice that $|s| = \sqrt{\xi^2+\eta^2} \geq \eta$, and that η is a strictly positive fixed constant, thus (3.10) is verified for

$$\delta = \delta_0 \min\{1,\eta\}.$$

Hence, existence and uniqueness of solution of problem (3.9) is guaranteed, and using standard results on mixed problems (see [79]), it can be shown that the solution $(\widehat{\boldsymbol{u}},\widehat{\boldsymbol{\lambda}})$ of problem (3.9) satisfies the estimates

$$\sqrt{\|\widehat{u}_1\|^2_{\Omega_1}+\|\widehat{u}_2\|^2_{\Omega_2}}\leq\frac{\|\widehat{f}_e\|_{L^2(\Omega_1\setminus\omega)}}{C_e\,\eta},\quad \|\widehat{\boldsymbol{\lambda}}\|_{M_C}\leq\frac{1}{\delta(\eta)}\Big(1+\frac{(C_m+C_a)|s|}{C_e\,\eta}\Big)\|\widehat{f}_e\|_{L^2(\Omega_1\setminus\omega)}. \tag{3.11}$$

Step 3: Existence and uniqueness in time domain.
Estimate (3.11) is the key estimate to obtain existence and uniqueness of the solution in time domain. Following the standard arguments of [80] Chap. XVI, we observe that for any causal time dependent function $h(t)$ which n first derivatives vanish at the origin, we have

$$s^n\,\widehat{h} = \mathcal{F}(e^{-\eta\,t}\,\partial_t^n\,h(t)),$$

where $\mathcal{F}$ is the Fourier transform from the *time variable* t to the *frequency variable* ξ and η is assume fixed and strictly positive. Now, since by assumption f_e is smooth and compactly supported, we have

$$\|e^{-\eta\,t}\,f_e(t)\|_{L^2(\Omega_1\setminus\omega)}\in L^2(\mathbb{R}^+),\quad \|e^{-\eta\,t}\,\partial_t\,f_e(t)\|_{L^2(\Omega_1\setminus\omega)}\in L^2(\mathbb{R}^+)$$

and since f_e and $\partial_t f_e$ vanish at the origin we have by application of Plancherel theorem

$$\int_{\mathbb{R}} \| \widehat{f}_e \|^2_{L^2(\Omega_1\setminus\omega)} \,\mathrm{d}\xi < +\infty \quad \text{and} \quad \int_{\mathbb{R}} \| s\, \widehat{f}_e \|^2_{L^2(\Omega_1\setminus\omega)} \,\mathrm{d}\xi < +\infty. \tag{3.12}$$

Therefore from estimates (3.11) and (3.12), we see that $\|\widehat{u}_j(s)\|_{\Omega_j}$ and $\| \widehat{\boldsymbol{\lambda}} \|_{M_C}$ are square integrable functions of ξ:

$$\begin{aligned}
\int_{\mathbb{R}} (|s|^2 + |s|^4)\, \|\widehat{u}_j(s)\|^2_{L^2(\Omega_j)} \,\mathrm{d}\xi &< +\infty, \\
\int_{\mathbb{R}} (1 + |s|^2)\, \|\nabla\widehat{u}_j(s)\|^2_{L^2(\Omega_j)} \,\mathrm{d}\xi &< +\infty, \\
\int_{\mathbb{R}} \|\widehat{\boldsymbol{\lambda}}(s)\|^2_{M_C} \,\mathrm{d}\xi &< +\infty.
\end{aligned}$$

Using Plancherel theorem we find that the unique solution $(\boldsymbol{u}, \boldsymbol{\lambda})$ of (3.6) satisfies for $n \in \{0, 1\}$,

$$\|e^{-\eta\, t}\partial_t^{n+1} u_j(t)\|_{L^2(\Omega_j)} \in L^2(\mathbb{R}^+),\ \|e^{-\eta\, t}\partial_t^{n}\nabla u_j(t)\|_{L^2(\Omega_j)} \in L^2(\mathbb{R}^+) \text{ and } \|e^{-\eta\, t}\boldsymbol{\lambda}\|_{M_C} \in L^2(\mathbb{R}^+).$$

This implies in particular

$$\partial_t u_j \in L^2\big([0,T]; L^2(\Omega_j)\big), \quad u_j \in L^2\big([0,T]; H^1(\Omega_j)\big) \quad \text{and} \quad \boldsymbol{\lambda} \in L^2\big([0,T]; M_C\big),$$

as well as

$$\partial_t^2 u_j \in L^2\big([0,T]; L^2(\Omega_j)\big) \quad \text{and} \quad \partial_t u_j \in L^2\big([0,T]; H^1(\Omega_j)\big).$$

Moreover, we can deduce by injection (see [80] Chap. XVIII) that

$$\boldsymbol{u} \in \prod_{j=1}^{2} \big(\mathcal{C}^1([0,T]; L^2(\Omega_j)) \cap \mathcal{C}^0([0,T]; H^1(\Omega_j))\big).$$

Now, since $f_e \in \mathcal{C}_0^\infty(\mathbb{R}^+; L^2(\Omega_1 \setminus \omega))$, notice that we can repeat the same arguments after differentiating in time the problem (3.6), and observing that

$$\|e^{-\eta\, t}\, \partial_t^2\, f_e(t)\|_{L^2(\Omega_1\setminus\omega)} \in L^2(\mathbb{R}^+)$$

we can also show that

$$\boldsymbol{u} \in \prod_{j=1}^{2} \big(\mathcal{C}^2([0,T]; L^2(\Omega_j)) \cap \mathcal{C}^1([0,T]; H^1(\Omega_j))\big) \quad \text{and} \quad \boldsymbol{\lambda} \in H^1\big([0,T]; M_C\big).$$

Note that the last relation implies $\boldsymbol{\lambda} \in \mathcal{C}^0\big([0,T]; M_C\big)$.

Step 4: Source terms with minimal regularity.

We now show that there exists a unique solution of problem (3.6) with the adequate regularity without assuming that f_e is in $\mathcal{C}_0^\infty(\mathbb{R}^+; L^2(\Omega_1\setminus\omega))$. By density, there exists a sequence of compactly supported functions $f_e^m \in \mathcal{C}_0^\infty(\mathbb{R}^+; L^2(\Omega_1 \setminus \omega))$ such that $f_e^m \to f_e$ in $W^{1,1}(\mathbb{R}^+; L^2(\Omega_1 \setminus \omega))$ with $f_e(\cdot, 0) = 0$. The associated solutions are denoted $(\boldsymbol{u}^m, \boldsymbol{\lambda}^m)$, and satisfy, as shown previously

$$\boldsymbol{u}^m \in \prod_{j=1}^{2} \big(\mathcal{C}^2([0,T]; L^2(\Omega_j)) \cap \mathcal{C}^1([0,T]; H^1(\Omega_j))\big) \quad \text{and} \quad \boldsymbol{\lambda}^m \in H^1\big([0,T]; M_C\big).$$

Next, to derive an estimate for $\boldsymbol{u}^m$, let us choose in problem (3.6a) the test function $\boldsymbol{v} = \partial_t \boldsymbol{u}^m$. Then, since (3.6b) implies for $k \in \{0, 1\}$ that $\partial_t^k u_1^m = \partial_t^k u_2^m$ in ω, we obtain that $u^m \in H^1(\Omega)$ defined by $u^m_{|\Omega_j} = u_j^m$ for $j \in \{1, 2\}$ is such that

$$(\rho\, \partial_t^2 u^m, \partial_t u^m)_{L^2(\Omega)} \ + \ (\mu\, \nabla u^m, \nabla \partial_t u^m)_{L^2(\Omega)} \ = \ (f_e^m, \partial_t u^m)_{L^2(\Omega_1\setminus\omega)}.$$

This is equivalent to say

$$\frac{\mathrm{d}}{\mathrm{d}t}\mathcal{E}(t) = (f_e^m, \partial_t u^m)_{L^2(\Omega_1\setminus\omega)} \quad \text{where} \quad \mathcal{E}(t) = \frac{1}{2}\,(\rho\,\partial_t u^m, \partial_t u^m)_{L^2(\Omega)} \;+\; \frac{1}{2}\,(\mu\,\nabla u^m, \nabla u^m)_{L^2(\Omega)}.$$

Moreover, notice that considering the chain rule and Cauchy-Schwartz inequality we obtain

$$\begin{aligned}\frac{\mathrm{d}}{\mathrm{d}t}\sqrt{\mathcal{E}(t)} \;&=\; \frac{1}{2\sqrt{\mathcal{E}(t)}}\frac{\mathrm{d}}{\mathrm{d}t}\mathcal{E}(t) \;\le\; \frac{\|f_e^m\|_{L^2(\Omega_1\setminus\omega)}\,\|\partial_t u^m\|_{L^2(\Omega_1\setminus\omega)}}{2\sqrt{\mathcal{E}(t)}}\\ &\le\; \frac{\|f_e^m\|_{L^2(\Omega_1\setminus\omega)}\sqrt{2\,\mathcal{E}(t)}}{2\sqrt{\rho_0}\,\sqrt{\mathcal{E}(t)}} \;\le\; \frac{\|f_e^m\|_{L^2(\Omega_1\setminus\omega)}}{\sqrt{2}\,\rho_0},\end{aligned}$$

where ρ_0 is the strictly positive constant introduced in (3.1). Thus, for $j \in \{1,2\}$, we obtain the estimates

$$\begin{aligned}\|\partial_t u_j^m\|_{L^2(\Omega_j)} \;+\; \|\nabla u_j^m\|_{L^2(\Omega_j)} \;&\le\; \|\partial_t u^m\|_{L^2(\Omega)} \;+\; \|\nabla u^m\|_{L^2(\Omega)}\\ &\le\; \frac{\sqrt{2\,\mathcal{E}(t)}}{\sqrt{\min\{\rho_0,\mu_0\}}} \;\le\; \int_0^t \frac{\|f_e^m(s)\|_{L^2(\Omega_1\setminus\omega)}}{\min\{\rho_0,\sqrt{\rho_0\,\mu_0}\}}\mathrm{d}s.\end{aligned} \tag{3.13}$$

Now, if we differentiate in time problem (3.6) and we perform an analogous reasoning, we obtain for $j \in \{1,2\}$ the estimates

$$\|\partial_t^2 u_j^m\|_{L^2(\Omega_j)} \;+\; \|\nabla\partial_t u_j^m\|_{L^2(\Omega_j)} \;\le\; \int_0^t \frac{\|\partial_t f_e^m(s)\|_{L^2(\Omega_1\setminus\omega)}}{\min\{\rho_0,\sqrt{\rho_0\,\mu_0}\}}\mathrm{d}s. \tag{3.14}$$

To obtain also an estimate for the Lagrange multiplier $\boldsymbol{\lambda}^m$, we first notice that due to *Inf-Sup condition* and taking into account (3.6a) we have that

$$\|\boldsymbol{\lambda}^m\|_{M_C} \le \frac{1}{\delta_0}\sup_{\boldsymbol{v}\in W}\frac{|b_C(\boldsymbol{v},\boldsymbol{\lambda}^m)|}{\|\boldsymbol{v}\|_1} = \frac{1}{\delta_0}\sup_{\boldsymbol{v}\in W}\frac{|-\partial_t^2\, m(\boldsymbol{u}^m,\boldsymbol{v}) - a(\boldsymbol{u}^m,\boldsymbol{v}) + g(\boldsymbol{v})|}{\|\boldsymbol{v}\|_1},$$

and thus considering again Cauchy-Schwartz inequality we obtain

$$\|\boldsymbol{\lambda}^m\|_{M_C} \le \frac{C_0}{\delta_0}\Big(\sum_{j=1}^2\|\partial_t^2 u_j^m\|_{L^2(\Omega_j)} + \sum_{j=1}^2\|\nabla u_j^m\|_{L^2(\Omega_j)} + \|f_e^m\|_{L^2(\Omega_1\setminus\omega)}\Big), \tag{3.15}$$

where C_0 is a strictly positive constant only depending in the L^∞ norm of ρ, μ, α_j and β_j. This implies the following estimate on the Lagrange multiplier

$$\|\boldsymbol{\lambda}^m(t)\|_{M_C} \le \frac{C_0}{\delta_0}\;\Big(\;\|f_e^m(t)\|_{L^2(\Omega_1\setminus\omega)} + \sum_{k=0}^1\int_0^t\frac{\|\partial_t^k f_e^m(s)\|_{L^2(\Omega_1\setminus\omega)}}{\min\{\rho_0,\sqrt{\rho_0\,\mu_0}\}}\mathrm{d}s\Big).$$

Now, we construct a sequence $(\boldsymbol{u}^m - \boldsymbol{u}^n, \boldsymbol{\lambda}^m - \boldsymbol{\lambda}^n)$ in the space

$$A_0 = \{(\boldsymbol{u},\boldsymbol{\lambda}) \in A \;/\; u_1 = 0,\; u_2 = 0,\; \partial_t u_1 = 0,\; \partial_t u_2 = 0,\; \text{at } t = 0\;\}$$

where we have introduced the notation

$$A = \prod_{j=1}^2\big(C^2([0,T];L^2(\Omega_j)) \cap C^1([0,T];H^1(\Omega_j))\big) \;\times\; C^0([0,T];M_C).$$

Notice that A_0 is a Banach space equipped with the norm

$$\|(\boldsymbol{u},\boldsymbol{\lambda})\|_{A_0} = \sup_{t\in[0,T]}\Big(\sum_{k=0}^1\sum_{j=1}^2\|\partial_t^{k+1}u_j(t)\|_{L^2(\Omega_j)} + \sum_{k=0}^1\sum_{j=1}^2\|\nabla\partial_t^k u_j(t)\|_{L^2(\Omega_j)} + \|\boldsymbol{\lambda}(t)\|_{M_C}\Big).$$

Therefore, considering previous estimates (3.13), (3.14) and (3.15), we have

$$\|(\boldsymbol{u}^m-\boldsymbol{u}^n, \boldsymbol{\lambda}^m-\boldsymbol{\lambda}^n)\|_{A_0} \leq C_1 \sup_{t\in[0,T]} \Big(\|(f_e^m-f_e^n)(t)\|_{L^2(\Omega_1\setminus\omega)} + \sum_{k=0}^{1} \int_0^t \|\partial_t^k (f_e^m-f_e^n)(s)\|_{L^2(\Omega_1\setminus\omega)} ds \Big),$$

where C_1 depends in C_0, δ_0, ρ_0 and μ_0. Now, notice that this implies that our sequence is a Cauchy sequence since the right hand side of the previous equation is also a Cauchy sequence ($f_e^m \to f_e$ in $W^{1,1}(\mathbb{R}^+; L^2(\Omega_1 \setminus \omega))$) and according to Sobolev embedding theorem (see Corollary 9.11 in [50])

$$\sup_{t\in[0,T]} \|(f_e^m - f_e^n)(t)\|_{L^2(\Omega_1\setminus\omega)} \leq C_2 \|f_e^m - f_e^n\|_{W^{1,1}(\mathbb{R}^+;L^2(\Omega_1\setminus\omega))}.$$

In consequence we have that $(\boldsymbol{u}^m, \boldsymbol{\lambda}^m) \to (\boldsymbol{u}, \boldsymbol{\lambda})$ in A_0 and finally one can show that $(\boldsymbol{u}, \boldsymbol{\lambda})$ is indeed solution of (3.6) by writing (3.6) for $(\boldsymbol{u}^m, \boldsymbol{\lambda}^m)$ and going to the weak limit when $m \to +\infty$.

■

Remark 3.2

Let us remark, that if we consider a source which is more regular and compactly supported in time, i.e.

$$f \in \mathcal{C}_0^{k+1}([0,T]; L^2(\Omega_1 \setminus \omega)), \quad \textit{which implies} \quad \partial_t^k f \in \mathcal{C}_0^1([0,T]; L^2(\Omega_1 \setminus \omega)),$$

then we can differentiate k times with respect to time problem (3.6). *In consequence, by application of Theorem 3.1, we obtain extra regularity for the solution*

$$(u_1, u_2, \boldsymbol{\lambda}) \in \prod_{j=1}^{2} \big(\mathcal{C}^{k+2}([0,T]; L^2(\Omega_j)) \cap \mathcal{C}^{k+1}([0,T]; H^1(\Omega_j)) \big) \times \mathcal{C}^k([0,T]; M_C).$$

3.3 Space discretization

In this section we aim to present adequate finite dimensional spaces W_h and $M_{C,h}$ that perform internal approximation of the space W and M_C respectively. Notice that the introduction of these spaces is enough to present the following semi-discrete scheme of problem (3.6).

$$\begin{cases} \text{Find } (\boldsymbol{u}_h(t), \boldsymbol{\lambda}_h(t)) : [0,T] \longrightarrow W_h \times M_{C,h} \text{ such that } (\boldsymbol{u}_h, \partial_t \boldsymbol{u}_h)(t=0) = (\mathbf{0}, \mathbf{0}) \text{ and} \\ \dfrac{\mathrm{d}^2}{\mathrm{d}t^2} m(\boldsymbol{u}_h, \boldsymbol{v}_h) + a(\boldsymbol{u}_h, \boldsymbol{v}_h) + b_C(\boldsymbol{v}_h, \boldsymbol{\lambda}_h) = g(\boldsymbol{v}_h), \quad \forall \boldsymbol{v}_h \in W_h, \qquad (3.16a) \\ b_C(\boldsymbol{u}_h, \boldsymbol{m}_h) = 0, \qquad \boldsymbol{m}_h \in M_{C,h}. \qquad (3.16b) \end{cases}$$

Moreover, the difficulties that arise concerning approximation properties and *Inf-Sup conditions* are the same as in the previous chapter. In consequence, we merely recap the discretization choices we make and we refer to the analysis developed in previous chapter for details.

3.3.1 Discretization by Lagrange finite elements

Let us consider for Ω_1 and Ω_2, two quasi-uniform triangulations $\mathcal{T}_{1,h}$ and $\mathcal{T}_{2,h}$ depending on the parameters h_1 and h_2 respectively (affine triangles in 2D or straight edges in 1D). Then, on the one hand, the space W will be approximated by W_h which is naturally sought in the form (see (2.57) for definition of $X_p(\cdot)$)

$$W_h = W_{1,h} \times W_{2,h} \subset W, \quad \text{where} \quad W_{j,h} = X_{p_j}(\mathcal{T}_{j,h}), \quad \text{for } j \in \{1, 2\}.$$

On the other hand, the choice of the space $M_{C,h}$ that approximates the multipliers space M_C is more complicated and depends in the coupling we consider. Moreover we shall also recall that $M_{C,h}$ needs to be build considering meshes that are conform with $\mathcal{T}_{1,h}$ or $\mathcal{T}_{2,h}$ in order to automatically satisfy the uniform *discrete Inf-Sup condition* (**P.3**). Thus depending on the kind of coupling we consider, some conformity assumptions are required. Next, we briefly recall the introduction of $M_{C,h}$ and the mentioned assumptions and refer to Section 2.7 for more details.

Boundary-Boundary coupling. Let us consider that the assumptions I.8 and I.9 are verified and we introduce the sets χ_i and χ_e of corners that separate both γ_i and γ_e respectively into two families of **smooth** curves (see Figure 2.21)

$$\{\gamma_{i,k}\}_{k=1}^{s_i} \quad \text{such that} \quad \gamma_i = \bigcup_{k=1}^{s_i} \gamma_{i,k} \quad \text{and} \quad \gamma_{i,k} \cap \gamma_{i,j} \in \chi_i \quad \text{if} \quad k \neq j, \tag{3.17}$$

$$\{\gamma_{e,k}\}_{k=1}^{s_e} \quad \text{such that} \quad \gamma_e = \bigcup_{k=1}^{s_e} \gamma_{e,k} \quad \text{and} \quad \gamma_{e,k} \cap \gamma_{e,j} \in \chi_e \quad \text{if} \quad k \neq j. \tag{3.18}$$

Then we chose to introduce as approximation space for the Lagrange multipliers (for $j \in \{i, e\}$)

$$M_{BB,h} = M_{B_i,h} \times M_{B_e,h} \subset M_{BB},$$

$$\text{with} \quad M_{B_j,h} = \{m_{j,h} \ / \ m_{j,h|\gamma_{j,k}} \in Y_{p_j}^{cl}(\mathcal{G}_{j,k}),\ 1 \leq k \leq s_j\}, \quad \text{for } j \in \{i, e\},$$

where we denote by $\mathcal{G}_{j,k}$ the restrictions to $\gamma_{j,k}$ of the 1D mesh $\mathcal{G}_{j,h}$ (defined in Assumptions I.8 and I.9) and where we have introduced the mortar finite elements spaces (see Figure 2.22)

$$\begin{aligned} Y_{p_j}^{cl}(\mathcal{G}_{j,k}) = \{m_h \in \mathcal{C}^0(\gamma_{j,k}) \quad \text{such that} \quad & \forall \kappa \in \mathcal{G}_{j,k},\ m_{h|\kappa} \in \mathcal{P}_{p_j} \\ & \text{and} \quad m_{h|\kappa} \in \mathcal{P}_{p_j-1} \text{ if } \kappa \cap \chi_j \neq \emptyset\}. \end{aligned}$$

Volume-Volume coupling. Let us begin by introducing the sets χ_i and χ_e of corners that separate both $\mathcal{S}_i$ and $\mathcal{S}_e$ respectively into two families of **smooth** curves (see Figure 2.27)

$$\{\gamma_{i,k}\}_{k=1}^{s_i} \quad \text{such that} \quad \mathcal{S}_i = \bigcup_{k=1}^{s_i} \gamma_{i,k} \quad \text{and} \quad \gamma_{i,k} \cap \gamma_{i,j} \in \chi_i \quad \text{if} \quad k \neq j, \tag{3.19}$$

$$\{\gamma_{e,k}\}_{k=1}^{s_e} \quad \text{such that} \quad \mathcal{S}_e = \bigcup_{k=1}^{s_e} \gamma_{e,k} \quad \text{and} \quad \gamma_{e,k} \cap \gamma_{e,j} \in \chi_e \quad \text{if} \quad k \neq j. \tag{3.20}$$

Then under assumptions I.11 and I.12 we chose to introduce

$$M_{VV,h} = M_{\mathcal{S}_i,h} \times \prod_{k=1}^{N_i} M_{V_{i,k},h} \times M_{\mathcal{S}_e,h} \times \prod_{k=1}^{N_e} M_{V_{e,k},h} \subset M_{VV}$$

where we have introduced for $j \in \{i, e\}$

$$\begin{aligned} M_{\mathcal{S}_j,h} &= \{m_{\mathcal{S}_j,h} \ / \ m_{\mathcal{S}_j,h|\gamma_{j,k}} \in Y_{p_j}^{cl}(\mathcal{F}_{j,k}),\ 1 \leq k \leq s_j\}, \\ \text{and} \quad M_{V_{j,k},h} &= X_{p_j}(\mathcal{G}_{j,k}) \cap H_0^1(\omega_{j,k}), \quad \text{for} \quad k \in \{1, \dots, N_j\}. \end{aligned}$$

Boundary-Volume coupling. We consider γ_i decomposed by (3.17), $\mathcal{S}_e$ decomposed by (3.20) and that the assumptions I.8 and I.12 are verified. Thus we introduce

$$M_{BV,h} = M_{B_i,h} \times M_{\mathcal{S}_e,h} \times \prod_{k=1}^{N_e} M_{V_{e,k},h} \subset M_{BV}.$$

Volume-Boundary coupling. we consider γ_e decomposed by (3.18), $\mathcal{S}_i$ decomposed by (3.19) and that the assumptions I.9 and I.11 are verified. Thus we introduce

$$M_{VB,h} = M_{\mathcal{S}_i,h} \times \prod_{k=1}^{N_i} M_{V_{i,k},h} \times M_{B_e,h} \subset M_{VB}.$$

Remark 3.3

*Let us remark that the choices of W_h, $M_{C,h}$ and $b_C(\cdot,\cdot)$ are consistent with the analysis developed in Section 2.7 In consequence, we automatically satisfy the approximation properties (**P.1**) and (**P.2**), as well as the uniform discrete Inf-Sup condition (**P.3**). Moreover, concerning the approximation properties we also recall that the results presented in Proposition 2.44 and Corollary 2.67 guarantee the optimal best approximation error for regular enough solutions.*

Algebraic system. We complete this section providing, similarly to Section 2.5.3, the algebraic version of the semi-discrete variational problem (3.16). Note that the linear and bilinear forms, as well as the finite elements spaces involved are the same as in previous chapter. Thus we keep the notation $\boldsymbol{U}_h^T = (\boldsymbol{U}_{1,h}^T, \boldsymbol{U}_{2,h}^T)$ and $\boldsymbol{\Lambda}_h^T = (\boldsymbol{\Lambda}_{i,h}^T, \boldsymbol{\Lambda}_{e,h}^T)$ for the time-dependent vector of the Lagrange degrees of freedom representing respectively the decompositions of $\boldsymbol{u}_h \in W_h$ and $\boldsymbol{\lambda}_h \in M_{C,h}$. We shall also keep the same notation for the matrices involved and we refer to Section 2.5.3 for details concerning definitions and computational aspects. Then we obtain the following semi-discrete algebraic system:

$$\begin{cases} \mathbb{M}_h \dfrac{\mathrm{d}^2}{\mathrm{d}t^2} \boldsymbol{U}_h \;+\; \mathbb{A}_h \boldsymbol{U}_h \;+\; \mathbb{B}_h \boldsymbol{\Lambda}_h \;=\; \boldsymbol{G}_h, & \text{(3.21a)} \\ \mathbb{B}_h^T \boldsymbol{U}_h \;=\; \boldsymbol{0}, & \text{(3.21b)} \end{cases}$$

which is completed with vanishing initial condition $\boldsymbol{U}_h(0) = \dfrac{\mathrm{d}}{\mathrm{d}t}\boldsymbol{U}_h(0) = \boldsymbol{0}$.

3.3.2 Well-posedness and stability of the semi-discrete problem

In this section we show that the well-posedness and stability of the semi-discrete problem (3.16) (or equivalently the algebraic system (3.21)) is consequence of the coercivity of $m(\cdot,\cdot)$ as well as the uniform *discrete Inf-Sup condition* (**P.3**). Let us begin with the following theorem concerning the well-posedness of the problem.

Theorem 3.4

If Assumptions I.1 and I.2 are satisfied, conditions (**P.1**), (**P.2**) *and* (**P.3**) *hold and if (according to* (3.5)*)*

$$f \in \mathcal{C}^0([0,T]; L^2(\Omega_1 \setminus \omega)) \quad \big(\supset \mathcal{C}^1([0,T]; L^2(\Omega_1 \setminus \omega))\big),$$

then, the semi-discrete problem (3.16) *has a unique solution such that*

$$(\boldsymbol{u}_h, \boldsymbol{\lambda}_h) \;\in\; \mathcal{C}^2([0,T]; W_h) \;\times\; \mathcal{C}^0([0,T]; M_{C,h}).$$

Proof. We proceed by analysing the algebraic form (3.21) of the semi-discrete problem, therefore let us denote by $K_W = \dim(W_h)$ and $K_M = \dim(M_C)$ and notice that $\boldsymbol{G}_h \in \mathcal{C}^0([0,T]; \mathbb{R}^{K_W})$. Then, we remark that the bilinear form $m(\cdot,\cdot)$ is coercive and therefore the matrix $\mathbb{M}_h$ is positive definite. In consequence we can multiply (3.21a) by the matrix $\mathbb{B}_h^T \mathbb{M}_h^{-1}$ and obtain

$$\mathbb{B}_h^T \mathbb{M}_h^{-1} \mathbb{B}_h \boldsymbol{\Lambda}_h \;=\; \mathbb{B}_h^T \mathbb{M}_h^{-1} (\boldsymbol{G}_h \;-\; \mathbb{A}_h \boldsymbol{U}_h). \tag{3.22}$$

Moreover, we note that, as pointed out in [28], the invertibility of the matrix $\mathbb{B}_h^T\,\mathbb{M}_h^{-1}\,\mathbb{B}_h$ is ensured by the *discrete Inf-Sup condition* (**P.3)** which implies $\operatorname{Ker}\mathbb{B}_h = \{\mathbf{0}\}$. Therefore, there exists a unique solution $\boldsymbol{\Lambda}_h(t)$ of (3.22), that we can introduce in (3.21a) to obtain

$$\mathbb{M}_h\,\frac{\mathrm{d}^2}{\mathrm{d}t^2}\,\boldsymbol{U}_h \;+\; \mathbb{A}_h\,\boldsymbol{U}_h \;-\; \mathbb{B}_h\,(\mathbb{B}_h^T\,\mathbb{M}_h^{-1}\,\mathbb{B}_h)^{-1}\mathbb{B}_h^T\,\mathbb{M}_h^{-1}\,\mathbb{A}_h\,\boldsymbol{U}_h$$
$$= \boldsymbol{G}_h \;-\; \mathbb{B}_h\,(\mathbb{B}_h^T\,\mathbb{M}_h^{-1}\,\mathbb{B}_h)^{-1}\mathbb{B}_h^T\,\mathbb{M}_h^{-1}\,\boldsymbol{G}_h.$$

Now, since $\boldsymbol{G}_h \in \mathcal{C}^0([0,T];\mathbb{R}^{K_W})$, we notice that previous problem has a unique solution $\boldsymbol{U}_h \in \mathcal{C}^2([0,T];\mathbb{R}^{K_W})$ and thus, according to (3.22) we also have that $\boldsymbol{\Lambda}_h \in \mathcal{C}^0([0,T],\mathbb{R}^{K_M})$. Finally, if we introduce in previous equation (3.22) we notice that $(\boldsymbol{U}_h, \boldsymbol{\Lambda}_h)$ satisfies the algebraic form (3.21) of the semi-discrete problem (3.16), thus the proof is concluded.

■

Next, we verify the stability of the semi-discrete problem by considering classical energy techniques. Thus we begin by providing the following estimate for the semi-discrete energy.

Theorem 3.5

The energy associated to the semi-discrete problem (3.16) *is given by*

$$\mathcal{E}_h(t) := \frac{1}{2}\,m(\partial_t\boldsymbol{u}_h, \partial_t\boldsymbol{u}_h) \;+\; \frac{1}{2}\,a(\boldsymbol{u}_h, \boldsymbol{u}_h)$$

and it is such that

$$\frac{d}{dt}\mathcal{E}_h(t) = (f, \partial_t u_{1,h})_{L^2(\Omega_1\setminus\omega)} \quad \textit{and} \quad \sqrt{\mathcal{E}_h(t)} \;\le\; \frac{1}{\sqrt{2\,\rho_0}}\int_0^t \|f(s)\|_{L^2(\Omega_1\setminus\omega)}ds,$$

where $\rho_0 > 0$ is the h-independent constant introduced in (3.1).

Proof. Let us begin noticing that since $\boldsymbol{u}_h \in \mathcal{C}^2([0,T];W_h)$, we can differentiate with respect to time (3.16b), thus we obtain

$$b_C(\partial_t\boldsymbol{u}_h, \boldsymbol{m}_h) = 0, \quad \forall \boldsymbol{m}_h \in M_{C,h}.$$

Therefore, if we consider in (3.16a) the test function $\boldsymbol{v}_h = \partial_t\boldsymbol{u}_h$, we obtain

$$m(\partial_t^2\boldsymbol{u}_h, \partial_t\boldsymbol{u}_h) \;+\; a(\boldsymbol{u}_h, \partial_t\boldsymbol{u}_h) \;=\; (f, \partial_t\boldsymbol{u}_h)_{L^2(\Omega_1\setminus\omega)}.$$

Notice that this is equivalent to

$$\frac{\mathrm{d}}{\mathrm{d}t}\mathcal{E}_h(t) = (f, \partial_t u_{1,h})_{L^2(\Omega_1\setminus\omega)}.$$

Moreover, considering the chain rule and Cauchy-Schwartz inequality we obtain

$$\frac{\mathrm{d}}{\mathrm{d}t}\sqrt{\mathcal{E}_h(t)} \;=\; \frac{1}{2\sqrt{\mathcal{E}_h(t)}}\frac{\mathrm{d}}{\mathrm{d}t}\mathcal{E}_h(t) \;\le\; \frac{\|f\|_{L^2(\Omega_1\setminus\omega)}\,\|\partial_t u_{1,h}\|_{L^2(\Omega_1\setminus\omega)}}{2\sqrt{\mathcal{E}_h(t)}}$$
$$\le\; \frac{\|f\|_{L^2(\Omega_1\setminus\omega)}\sqrt{2\,\mathcal{E}_h(t)}}{2\,\sqrt{\rho_0}\,\sqrt{\mathcal{E}_h(t)}} \;\le\; \frac{\|f\|_{L^2(\Omega_1\setminus\omega)}}{\sqrt{2\,\rho_0}}.$$

Finally integrating in time we estimate

$$\sqrt{\mathcal{E}_h(t)} \;\le\; \frac{1}{\sqrt{2\,\rho_0}}\int_0^t \|f(s)\|_{L^2(\Omega_1\setminus\omega)}\mathrm{d}s.$$

■

A direct consequence of the two previous results is provided in the following corollary that guarantees the stability of the semi-discrete problem (3.16).

Remark 3.6

If we consider a source which is more regular and compactly supported in time, i.e.

$$f \in \mathcal{C}_0^k([0,T]; L^2(\Omega_1 \setminus \omega)), \quad \textit{which implies} \quad \partial_t^k f \in \mathcal{C}_0^0([0,T]; L^2(\Omega_1 \setminus \omega)),$$

then we can differentiate k times with respect to time the semi-discrete problem (3.16). *In consequence, by application of Theorem 3.4, we obtain extra regularity for the solution*

$$(\boldsymbol{u}_h, \boldsymbol{\lambda}_h) \in \mathcal{C}^{k+2}([0,T]; W_h) \ \times \ \mathcal{C}^k([0,T]; M_{C,h}).$$

Moreover by application of Theorem 3.5, we also obtain the estimates

$$\begin{aligned} \sqrt{a\big(\partial_t^k \boldsymbol{u}_h(t), \partial_t^k \boldsymbol{u}_h(t)\big)} \quad &\leq \quad \frac{1}{\sqrt{\rho_0}} \int_0^t \|\partial_t^k f(s)\|_{L^2(\Omega_1\setminus\omega)}\, ds, \\ \sqrt{m\big(\partial_t^{k+1} \boldsymbol{u}_h(t), \partial_t^{k+1} \boldsymbol{u}_h(t)\big)} \quad &\leq \quad \frac{1}{\sqrt{\rho_0}} \int_0^t \|\partial_t^k f(s)\|_{L^2(\Omega_1\setminus\omega)}\, ds. \end{aligned}$$

Remark 3.7

Notice that $\boldsymbol{u}_h \in \mathcal{C}^{k+2}([0,T]; W_h)$ is not enough to estimate $\sqrt{m(\partial_t^{k+2}\boldsymbol{u}_h, \partial_t^{k+2}\boldsymbol{u}_h)}$ since it may happen that $\lim\limits_{h\to 0} \|\partial_t^{k+2}\boldsymbol{u}_h(t)\|_0 = +\infty$.

3.3.3 Error estimates for the semi-discrete problem

Now, we deduce an error estimate for the difference between $(\boldsymbol{u}, \boldsymbol{\lambda})$ solution of the continuous problem (3.6) and $(\boldsymbol{u}_h, \boldsymbol{\lambda}_h)$ solution of the discrete problem (3.16). We will proceed as in [2] by finding an adequate $(\widetilde{\boldsymbol{u}}_h, \widetilde{\boldsymbol{\lambda}}_h) \in W_h \times M_{C,h}$ such that we can estimate separately $(\boldsymbol{u}_h - \widetilde{\boldsymbol{u}}_h, \boldsymbol{\lambda}_h - \widetilde{\boldsymbol{\lambda}}_h)$ and $(\boldsymbol{u} - \widetilde{\boldsymbol{u}}_h, \boldsymbol{\lambda} - \widetilde{\boldsymbol{\lambda}}_h)$ to then conclude by considering the triangular inequality. Therefore, as it is classical, we introduce the usually called *elliptic projection*, that for every $(\boldsymbol{u}, \boldsymbol{\lambda}) \in W \times M_C$ assigns $(\widetilde{\boldsymbol{u}}_h, \widetilde{\boldsymbol{\lambda}}_h) \in W_h \times M_{C,h}$ solution of the following problem

$$\left\{ \begin{array}{l} \text{Find } (\widetilde{\boldsymbol{u}}_h, \widetilde{\boldsymbol{\lambda}}_h) \in W_h \times M_{C,h}, \text{ such that} \\[2ex] m(\widetilde{\boldsymbol{u}}_h - \boldsymbol{u}, \boldsymbol{v}_h) \ + \ a(\widetilde{\boldsymbol{u}}_h - \boldsymbol{u}, \boldsymbol{v}_h) \ + \ b_C(\boldsymbol{v}_h, \widetilde{\boldsymbol{\lambda}}_h - \boldsymbol{\lambda}) \ = \ 0, \quad \forall \boldsymbol{v}_h \in W_h, \qquad (3.23\text{a}) \\[2ex] \hfill b_C(\widetilde{\boldsymbol{u}}_h - \boldsymbol{u}, \boldsymbol{m}_h) \ = \ 0, \quad \boldsymbol{m}_h \in M_{C,h}. \qquad (3.23\text{b}) \end{array} \right.$$

Notice that this operator can be analysed proceeding similarly to Chapter 2, however in this occasion, since problem (3.23) is coercive, the analysis fits in the classical theory of mixed finite elements. In consequence we do not develop the analysis for the *elliptic projection* (3.23) and we refer to [79] for details. We only remark that, Assumption I.1 implies the coercivity of $m(\cdot,\cdot) + a(\cdot,\cdot)$, while $b_C(\cdot,\cdot)$ satisfies an adequate *Inf-Sup condition* under the correspondent assumptions mentioned in previous sections. Both conditions guarantee the existence and uniqueness of a solution of problem (3.23) and thus the well posedness of the *elliptic projection* (notice that in this context Assumption I.3 and Assumption I.4 are no longer required). Moreover it also provides the following error estimates.

Theorem 3.8

If Assumptions I.1 and I.2 are satisfied and conditions (**P.1**), (**P.2**) *and* (**P.3**) *hold, then*

$$\|\boldsymbol{u} - \widetilde{\boldsymbol{u}}_h\|_1 \leq K_0 \Big(\inf_{\boldsymbol{v}_h \in W_h} \|\boldsymbol{u} - \boldsymbol{v}_h\|_1 + \inf_{\boldsymbol{m}_h \in M_{C,h}} \|\boldsymbol{\lambda} - \boldsymbol{m}_h\|_{M_C} \Big),$$

$$\|\boldsymbol{\lambda}-\widetilde{\boldsymbol{\lambda}}_h\|_{M_C} \le K_1\Big(\|\boldsymbol{u}-\widetilde{\boldsymbol{u}}_h\|_1 + \inf_{\boldsymbol{m}_h\in M_{C,h}} \|\boldsymbol{\lambda}-\boldsymbol{m}_h\|_{M_C}\Big),$$

where K_0 and K_1 are strictly positive constants independent of h, and the pairs $(\boldsymbol{u},\boldsymbol{\lambda})$ and $(\widetilde{\boldsymbol{u}}_h,\widetilde{\boldsymbol{\lambda}}_h)$ are the unique solutions problems (3.6) and (3.23).

Next, we estimate the difference between the solutions of the continuous problem (3.6) and the discrete problem (3.16) with the energy norm

$$\|\boldsymbol{v}\|_E = \Big(\sum_{j=1}^{2}\|v_j\|^2_{E,\Omega_j}\Big)^{\frac12} \quad \text{where} \quad \|v_j\|_{E,\Omega_j} = \big(\|\partial_t v_j\|^2_{L^2(\Omega_j)} + \|\nabla v_j\|^2_{L^2(\Omega_j)}\big)^{\frac12}.$$

This is provided in the following result where, as we mentioned before, we make use of the *elliptic projection* as well as Theorem 3.8.

Theorem 3.9

*If Assumptions I.1 and I.2 are satisfied, conditions (**P.1**), (**P.2**) and (**P.3**) hold and we consider $f\in\mathcal{C}^3_0([0,T];L^2(\Omega_1\setminus\omega))$, then for h sufficiently small we have*

$$\begin{aligned}
\sup_{t\in[0,T]}\|\boldsymbol{u}-\boldsymbol{u}_h\|_E &\le K(T)\sup_{t\in[0,T]}\sum_{k=0}^{2}\Big(\inf_{\boldsymbol{v}_h\in W_h}\|\partial_t^k\boldsymbol{u}-\boldsymbol{v}_h\|_1 + \inf_{\boldsymbol{m}_h\in M_{C,h}}\|\partial_t^k\boldsymbol{\lambda}-\boldsymbol{m}_h\|_{M_C}\Big),\\
\sup_{t\in[0,T]}\|\boldsymbol{\lambda}-\boldsymbol{\lambda}_h\|_{M_C} &\le \widetilde{K}(T)\sup_{t\in[0,T]}\sum_{k=0}^{2}\Big(\inf_{\boldsymbol{v}_h\in W_h}\|\partial_t^k\boldsymbol{u}-\boldsymbol{v}_h\|_1 + \inf_{\boldsymbol{m}_h\in M_{C,h}}\|\partial_t^k\boldsymbol{\lambda}-\boldsymbol{m}_h\|_{M_C}\Big),
\end{aligned}$$

where $K(T)$ and $\widetilde{K}(T)$ are strictly positive constants independent of h.

Proof. Let us first notice, that we can consider the elliptic projection $(\widetilde{\boldsymbol{u}}_h,\widetilde{\boldsymbol{\lambda}}_h)$ defined by (3.23) and therefore by triangular inequality we have that

$$\|\boldsymbol{u}-\boldsymbol{u}_h\|_E \le \|\boldsymbol{u}-\widetilde{\boldsymbol{u}}_h\|_E + \|\widetilde{\boldsymbol{u}}_h-\boldsymbol{u}_h\|_E, \tag{3.24}$$

$$\|\boldsymbol{\lambda}-\boldsymbol{\lambda}_h\|_{M_C} \le \|\boldsymbol{\lambda}-\widetilde{\boldsymbol{\lambda}}_h\|_{M_C} + \|\widetilde{\boldsymbol{\lambda}}_h-\boldsymbol{\lambda}_h\|_{M_C}. \tag{3.25}$$

Thus, we will proceed separately to estimate $(\boldsymbol{u}-\widetilde{\boldsymbol{u}}_h,\boldsymbol{\lambda}-\widetilde{\boldsymbol{\lambda}}_h)$ and $(\boldsymbol{u}_h-\widetilde{\boldsymbol{u}}_h,\boldsymbol{\lambda}_h-\widetilde{\boldsymbol{\lambda}}_h)$. We begin by providing an adequate bound for $(\boldsymbol{u}_h-\widetilde{\boldsymbol{u}}_h,\boldsymbol{\lambda}_h-\widetilde{\boldsymbol{\lambda}}_h)$. To do so, we first notice that subtracting (3.6) to (3.16), both with test functions $(\boldsymbol{v}_h,\boldsymbol{m}_h)$, we obtain

$$\left\{\begin{aligned}
\partial_t^2 m(\boldsymbol{u}_h-\boldsymbol{u},\boldsymbol{v}_h) + a(\boldsymbol{u}_h-\boldsymbol{u},\boldsymbol{v}_h) + b_C(\boldsymbol{v}_h,\boldsymbol{\lambda}_h-\boldsymbol{\lambda}) &= 0, \quad \forall\boldsymbol{v}_h\in W_h, && (3.26a)\\
b_C(\boldsymbol{u}_h-\boldsymbol{u},\boldsymbol{m}_h) &= 0, \quad \boldsymbol{m}_h\in M_{C,h}. && (3.26b)
\end{aligned}\right.$$

Then, on the one hand, we can combine (3.23a) and (3.26a) to obtain for all $\boldsymbol{v}_h\in W_h$

$$\begin{aligned}
&\partial_t^2 m(\widetilde{\boldsymbol{u}}_h-\boldsymbol{u}_h,\boldsymbol{v}_h) + a(\widetilde{\boldsymbol{u}}_h-\boldsymbol{u}_h,\boldsymbol{v}_h) + b_C(\boldsymbol{v}_h,\widetilde{\boldsymbol{\lambda}}_h-\boldsymbol{\lambda}_h)\\
&\qquad = \partial_t^2 m(\widetilde{\boldsymbol{u}}_h-\boldsymbol{u},\boldsymbol{v}_h) + a(\widetilde{\boldsymbol{u}}_h-\boldsymbol{u},\boldsymbol{v}_h) + b_C(\boldsymbol{v}_h,\widetilde{\boldsymbol{\lambda}}_h-\boldsymbol{\lambda})\\
&\qquad + \partial_t^2 m(\boldsymbol{u}-\boldsymbol{u}_h,\boldsymbol{v}_h) + a(\boldsymbol{u}-\boldsymbol{u}_h,\boldsymbol{v}_h) + b_C(\boldsymbol{v}_h,\boldsymbol{\lambda}-\boldsymbol{\lambda}_h)\\
&\qquad = \partial_t^2 m(\widetilde{\boldsymbol{u}}_h-\boldsymbol{u},\boldsymbol{v}_h) - m(\widetilde{\boldsymbol{u}}_h-\boldsymbol{u},\boldsymbol{v}_h),
\end{aligned}\tag{3.27}$$

while on the other hand, we combine (3.23b) and (3.26b) to obtain for all $\boldsymbol{m}_h\in M_{C,h}$

$$b_C(\widetilde{\boldsymbol{u}}_h-\boldsymbol{u}_h,\boldsymbol{m}_h) = b_C(\widetilde{\boldsymbol{u}}_h-\boldsymbol{u},\boldsymbol{m}_h) + b_C(\boldsymbol{u}-\boldsymbol{u}_h,\boldsymbol{m}_h) = 0.$$

Notice that previous equality also holds for the time derivative, then if we choose $\boldsymbol{v}_h = \partial_t(\widetilde{\boldsymbol{u}}_h - \boldsymbol{u}_h)$ in (3.27) we find that

$$\begin{aligned} m\big(\partial_t^2(\widetilde{\boldsymbol{u}}_h - \boldsymbol{u}_h), \partial_t(\widetilde{\boldsymbol{u}}_h - \boldsymbol{u}_h)\big) \;+\; a\big(\widetilde{\boldsymbol{u}}_h - \boldsymbol{u}_h, \partial_t(\widetilde{\boldsymbol{u}}_h - \boldsymbol{u}_h)\big) \\ = \; m\big(\partial_t^2(\widetilde{\boldsymbol{u}}_h - \boldsymbol{u}), \partial_t(\widetilde{\boldsymbol{u}}_h - \boldsymbol{u}_h)\big) \;-\; m\big(\widetilde{\boldsymbol{u}}_h - \boldsymbol{u}, \partial_t(\widetilde{\boldsymbol{u}}_h - \boldsymbol{u}_h)\big). \end{aligned} \tag{3.28}$$

Now, considering the energy norm and applying Cauchy-Schwartz inequality in (3.28), we deduce that there exists a positive constant K_2 independent of h and such that

$$\frac{\mathrm{d}}{\mathrm{d}t}\|\widetilde{\boldsymbol{u}}_h - \boldsymbol{u}_h\|_E^2 \;\leq\; K_2\|\partial_t(\widetilde{\boldsymbol{u}}_h - \boldsymbol{u}_h)\|_0 \,\big(\|\partial_t^2(\widetilde{\boldsymbol{u}}_h - \boldsymbol{u})\|_0 + \|\widetilde{\boldsymbol{u}}_h - \boldsymbol{u}\|_0\big).$$

Moreover, noticing that by the chain rule

$$\frac{\mathrm{d}}{\mathrm{d}t}\|\widetilde{\boldsymbol{u}}_h - \boldsymbol{u}_h\|_E^2 = 2\;\|\widetilde{\boldsymbol{u}}_h - \boldsymbol{u}_h\|_E\;\frac{\mathrm{d}}{\mathrm{d}t}\|\widetilde{\boldsymbol{u}}_h - \boldsymbol{u}_h\|_E$$

and since $\|\partial_t \boldsymbol{v}_h\|_0 \leq \|\boldsymbol{v}_h\|_E$, we obtain

$$\|\widetilde{\boldsymbol{u}}_h - \boldsymbol{u}_h\|_E \leq \frac{K_2}{2}\int_0^t \big(\|\partial_t^2(\widetilde{\boldsymbol{u}}_h - \boldsymbol{u})\|_0 + \|\widetilde{\boldsymbol{u}}_h - \boldsymbol{u}\|_0\big)\mathrm{d}s. \tag{3.29}$$

Next, to find a bound for $\widetilde{\boldsymbol{\lambda}}_h - \boldsymbol{\lambda}_h$, we first notice that due to (3.27)

$$b_C(\boldsymbol{v}_h, \widetilde{\boldsymbol{\lambda}}_h - \boldsymbol{\lambda}_h) \;=\; \partial_t^2 m(\widetilde{\boldsymbol{u}}_h - \boldsymbol{u}, \boldsymbol{v}_h) \;-\; m(\widetilde{\boldsymbol{u}}_h - \boldsymbol{u}, \boldsymbol{v}_h) \;-\; a(\widetilde{\boldsymbol{u}}_h - \boldsymbol{u}_h, \boldsymbol{v}_h), \quad \forall \boldsymbol{v}_h \in W_h,$$

and thanks to the the uniform *discrete Inf-Sup condition* (**P.3**), we deduce that

$$\|\widetilde{\boldsymbol{\lambda}}_h - \boldsymbol{\lambda}_h\|_{M_C} \leq \frac{K_3}{\delta}\big(\|\partial_t^2(\widetilde{\boldsymbol{u}}_h - \boldsymbol{u})\|_0 + \|\widetilde{\boldsymbol{u}}_h - \boldsymbol{u}\|_0 + \|\nabla(\widetilde{\boldsymbol{u}}_h - \boldsymbol{u}_h)\|_0\big), \tag{3.30}$$

where K_3 is a strictly positive constant independent of h (note that the last term is bounded by (3.29)).

Now, we go back to inequalities (3.24) and (3.25). We recall that we still need to find adequate estimates for

$$\|\boldsymbol{u} - \widetilde{\boldsymbol{u}}_h\|_E \quad \text{and} \quad \|\boldsymbol{\lambda} - \boldsymbol{\lambda}_h\|_{M_C},$$

but according to (3.29) and (3.30), we also need to find adequate estimates for

$$\|\boldsymbol{u} - \widetilde{\boldsymbol{u}}_h\|_0 \quad \text{and} \quad \|\partial_t^2(\boldsymbol{u} - \widetilde{\boldsymbol{u}}_h)\|_0.$$

For this purpose, we have considered the regularity assumption $f \in \mathcal{C}_0^3([0,T]; L^2(\Omega_1))$ which according to Remark 3.2 provides extra regularity for the solution, in particular

$$(u_1, u_2, \boldsymbol{\lambda}) \in \prod_{j=1}^{2}\big(\mathcal{C}^4([0,T]; L^2(\Omega_j)) \cap \mathcal{C}^3([0,T]; H^1(\Omega_j))\big) \;\times\; \big(\mathcal{C}^2([0,T]; M_C)\big).$$

This extra regularity allows to differentiate twice with respect to time problem (3.23) and thus by Theorem 3.8, we have for $k \in \{0,1,2\}$, that

$$\|\partial_t^k(\boldsymbol{u} - \widetilde{\boldsymbol{u}}_h)\|_1 \quad\leq\quad K_0\big(\inf_{\boldsymbol{v}_h \in W_h}\|\partial_t^k\boldsymbol{u} - \boldsymbol{v}_h\|_1 + \inf_{\boldsymbol{m}_h \in M_{C,h}}\|\partial_t^k\boldsymbol{\lambda} - \boldsymbol{m}_h\|_{M_C}\big), \tag{3.31}$$

$$\|\partial_t^k(\boldsymbol{\lambda} - \widetilde{\boldsymbol{\lambda}}_h)\|_{M_C} \quad\leq\quad K_1\big(\|\boldsymbol{u} - \widetilde{\boldsymbol{u}}_h\|_1 + \inf_{\boldsymbol{m}_h \in M_{C,h}}\|\boldsymbol{\lambda} - \boldsymbol{m}_h\|_{M_C}\big). \tag{3.32}$$

Finally, we combine inequalities (3.24) and (3.25) with estimates (3.29), (3.30), (3.31) and (3.32) to obtain

$$\sup_{t\in[0,T]} \|\boldsymbol{u}-\boldsymbol{u}_h\|_E \leq K(T) \sup_{t\in[0,T]} \sum_{k=0}^{2} \Big(\inf_{\boldsymbol{v}_h\in W_h} \|\partial_t^k \boldsymbol{u}-\boldsymbol{v}_h\|_1 + \inf_{\boldsymbol{m}_h\in M_{C,h}} \|\partial_t^k \boldsymbol{\lambda}-\boldsymbol{m}_h\|_{M_C}\Big),$$

$$\sup_{t\in[0,T]} \|\boldsymbol{\lambda}-\boldsymbol{\lambda}_h\|_{M_C} \leq \widetilde{K}(T) \sup_{t\in[0,T]} \sum_{k=0}^{2} \Big(\inf_{\boldsymbol{v}_h\in W_h} \|\partial_t^k \boldsymbol{u}-\boldsymbol{v}_h\|_1 + \inf_{\boldsymbol{m}_h\in M_{C,h}} \|\partial_t^k \boldsymbol{\lambda}-\boldsymbol{m}_h\|_{M_C}\Big),$$

where $K(T)$ and $\widetilde{K}(T)$ are strictly positive constants independent of h.

■

We remark that the error depends only on the best approximation errors of the time derivatives of the primal variable $\partial_t^k \boldsymbol{u}$ and the Lagrange multiplier $\partial_t^k \boldsymbol{\lambda}$ for $k \in \{0,1,2\}$. In consequence, we expect high order convergence results when both $\boldsymbol{u}$ and $\boldsymbol{\lambda}$ are regular enough. Moreover, we shall also remark that estimates in the L^2-norm can also be deduced using the technique introduced in [81].

3.4 Time discretization

In this section we present a time discretization of the semi-discrete algebraic system (3.21). We choose a uniform finite difference discretization of the time derivative, therefore for a fixed time step Δt, the unknowns $\boldsymbol{U}_h^T = (\boldsymbol{U}_{1,h}^T, \boldsymbol{U}_{2,h}^T)$ and $\boldsymbol{\Lambda}_h^T = (\boldsymbol{\Lambda}_{i,h}^T, \boldsymbol{\Lambda}_{e,h}^T)$ at each time $t^n = n\Delta t$ for $n \in \{0,\ldots,N\} \subset \mathbb{N}$ (note $T = t^N$) are approximated by $(\boldsymbol{U}_h^n)^T = ((\boldsymbol{U}_{1,h}^n)^T, (\boldsymbol{U}_{2,h}^n)^T)$ and $(\boldsymbol{\Lambda}_h^n)^T = ((\boldsymbol{\Lambda}_{i,h}^n)^T, (\boldsymbol{\Lambda}_{e,h}^n)^T)$ respectively. The time discretization we suggest relies on the conservative Neumark scheme family. We use centred second order approximation of the second order time derivative as well as centred approximation for the term $\mathbb{A}_{1,h}\boldsymbol{U}_{1,h}$ and $\mathbb{A}_{2,h}\boldsymbol{U}_{2,h}$. These approximations are parametrized by θ_1 and θ_2 respectively and corresponds to so called theta-schemes. Then we consider vanishing initial data $\boldsymbol{U}_{j,h}^0 = \boldsymbol{U}_{j,h}^1 = \boldsymbol{0}$ for $j \in \{1,2\}$ and for all $n \in \{1,\ldots,N-1\}$ the following algebraic system of equations:

$$\left\{\begin{array}{ll}
\mathbb{M}_{1,h}\dfrac{\boldsymbol{U}_{1,h}^{n+1}-2\boldsymbol{U}_{1,h}^{n}+\boldsymbol{U}_{1,h}^{n-1}}{\Delta t^2} & \\
\quad + \mathbb{A}_{1,h}\big(\theta_1\boldsymbol{U}_{1,h}^{n+1}+(1-2\theta_1)\boldsymbol{U}_{1,h}^{n}+\theta_1\boldsymbol{U}_{1,h}^{n-1}\big) + \mathbb{B}_{1,h}\boldsymbol{\Lambda}_h^n = \boldsymbol{G}_{1,h}^n, & (3.33a)\\[2ex]
\mathbb{M}_{2,h}\dfrac{\boldsymbol{U}_{2,h}^{n+1}-2\boldsymbol{U}_{2,h}^{n}+\boldsymbol{U}_{2,h}^{n-1}}{\Delta t^2} & \\
\quad + \mathbb{A}_{2,h}\big(\theta_2\boldsymbol{U}_{2,h}^{n+1}+(1-2\theta_2)\boldsymbol{U}_{2,h}^{n}+\theta_2\boldsymbol{U}_{2,h}^{n-1}\big) + \mathbb{B}_{2,h}\boldsymbol{\Lambda}_h^n = \boldsymbol{0}, & (3.33b)\\[2ex]
\mathbb{B}_{1,h}^T\boldsymbol{U}_{1,h}^{n+1} + \mathbb{B}_{2,h}^T\boldsymbol{U}_{2,h}^{n+1} = \boldsymbol{0}, & (3.33c)
\end{array}\right.$$

where we have introduced the notation $\mathbb{B}_{j,h} = (\mathbb{B}_{j,h}^i, \mathbb{B}_{j,h}^e)$ for $j \in \{1,2\}$ (see Section 2.5.3 for details concerning definitions and computational aspects).

Remark 3.10

Notice that for $j \in \{1,2\}$, the choice $\boldsymbol{U}_{j,h}^0 = \boldsymbol{0}$ is exact since we are considering $\boldsymbol{u}_{j,h}(0) = 0$. This is not true in general for the choice $\boldsymbol{U}_{j,h}^1 = \boldsymbol{0}$ since assuming $\boldsymbol{u}_{j,h} \in \mathcal{C}^k([0,T];W_h)$ the Taylor expansion gives

$$\boldsymbol{u}_{j,h}(\Delta t) = \sum_{m=0}^{k-1} \frac{\Delta t^m}{m!}\frac{d^m}{dt^m}\boldsymbol{u}_{j,h}(0) + \frac{\Delta t^k}{k!}\frac{d^k}{dt^k}\boldsymbol{u}_{j,h}(s) \quad \textit{for a given} \quad s \in [0,\Delta t].$$

However, since we are considering $(\boldsymbol{u}_{j,h}, \partial_t \boldsymbol{u}_{j,h})(t=0) = (0,0)$, the second order accuracy is ensured ($k = 2$ above). Moreover, we also remark that if we assume for instance that the source $\boldsymbol{f}(t)$ is compactly supported in $[0, T]$, the initial conditions are exact for Δt small enough.

In practice, the parameters θ_1 and θ_2 are chosen to be 0 (explicit case) or strictly positive (implicit case). Notice that theta-schemes are widely studied in the literature, for instance we refer to [82] for an stability analysis in absence of coupling. There, the authors show that when $\theta < 1/4$, the resultant scheme has a time step that is constrained by a CFL type condition (see (3.39) for the details), while in the case that $\theta \geq 1/4$ the integrator is unconditionally stable (no restriction on Δt is imposed by the stability). We expect a similar property for scheme (3.33) where the coupling is considered (the analysis is developed in (3.39)). For our interests, this property of the theta-schemes can be very helpful since we are interested on the treatment of situations where the domain contains a defect $\mathcal{O}$ which is small compared to the size of the background media Θ. Thus in practice, on the one hand we will consider a coarse mesh for a large domain Ω_1 that avoids the defect $\mathcal{O}$, while on the other hand, we will consider a fine mesh for a small domain Ω_2 which represents a neighbourhood of the defect $\mathcal{O}$. In consequence, it will be preferable to use an explicit integrator in the coarse domain Ω_1 (with a time step imposed by a CFL related to the coarse mesh) and use an implicit (and unconditionally stable) discretization in the small domain Ω_2. Therefore, a natural choice would be for instance $\theta_1 = 0$ and $\theta_2 \geq 1/4$.

In what follows, we present a detailed stability analysis of system (3.33). Notice that the analysis is non trivial since the parameters α_j and β_j jump on the boundaries of the coupling domains and, as shown in what follows, such jumps may reduce the maximum time step allowed in the case of an explicit discretization.

3.4.1 Algorithm

Let us assume that $(\boldsymbol{U}^n_{1,h}, \boldsymbol{U}^{n-1}_{1,h})$ and $(\boldsymbol{U}^n_{2,h}, \boldsymbol{U}^{n-1}_{2,h})$ are given, then the next iterants $\boldsymbol{U}^{n+1}_{1,h}$, $\boldsymbol{U}^{n+1}_{2,h}$ and $\boldsymbol{\Lambda}^n_h$ are computed by solving the saddle point problem (note $\mathbb{O}$ refers to null matrices of the respective size)

$$\begin{pmatrix} \frac{1}{\Delta t^2}\mathbb{M}_{1,h} + \theta_1 \mathbb{A}_{1,h} & \mathbb{O} & \mathbb{B}_{1,h} \\ \mathbb{O} & \frac{1}{\Delta t^2}\mathbb{M}_{2,h} + \theta_2 \mathbb{A}_{2,h} & \mathbb{B}_{2,h} \\ \mathbb{B}^T_{1,h} & \mathbb{B}^T_{2,h} & \mathbb{O} \end{pmatrix} \begin{pmatrix} \boldsymbol{U}^{n+1}_{1,h} \\ \boldsymbol{U}^{n+1}_{2,h} \\ \boldsymbol{\Lambda}^n_h \end{pmatrix} = \begin{pmatrix} \boldsymbol{S}^{n+1}_{1,h} \\ \boldsymbol{S}^{n+1}_{2,h} \\ \mathbf{0} \end{pmatrix} \tag{3.34}$$

where the terms $(\boldsymbol{S}^{n+1}_{1,h}, \boldsymbol{S}^{n+1}_{2,h})$ on the right hand side only depend on known data. Notice that system (3.34) can be solved using a Schur complement strategy (see for instance [83]). We simply consider the third equation of the system to eliminate $\boldsymbol{U}^{n+1}_{1,h}$ and $\boldsymbol{U}^{n+1}_{2,h}$ thus we obtain an equation only for the Lagrange multiplier

$$\mathbb{K}_h \boldsymbol{\Lambda}^n_h = \boldsymbol{L}^{n+1}_h \quad \text{where} \quad \mathbb{K}_h := \mathbb{B}^T_{1,h}\big(\mathbb{M}_{1,h} + \theta_1 \Delta t^2 \mathbb{A}_{1,h}\big)^{-1}\mathbb{B}_{1,h} + \mathbb{B}^T_{2,h}\big(\mathbb{M}_{2,h} + \theta_2 \Delta t^2 \mathbb{A}_{2,h}\big)^{-1}\mathbb{B}_{2,h},$$

and $\boldsymbol{L}^{n+1}_h$ depends only on $\boldsymbol{S}^{n+1}_{1,h}$ and $\boldsymbol{S}^{n+1}_{2,h}$. Notice, as pointed out in [28], that the invertibility of the matrix $\mathbb{K}_h$ is ensured by

$$\mathrm{Ker}\,(\mathbb{B}_{1,h}) \cap \mathrm{Ker}\,(\mathbb{B}_{2,h}) = \{\mathbf{0}\},$$

which is implied by the uniform *discrete Inf-Sup condition.* In consequence, we can compute $\boldsymbol{\Lambda}^n_h$ and then use that information to compute $\boldsymbol{U}^{n+1}_{1,h}$ and $\boldsymbol{U}^{n+1}_{2,h}$ using respectively the first and second equations of (3.34).

In practice, we observe that the conditioning of the matrix $\mathbb{K}_h$ is not good when volume coupling is used in ω_j with $j \in \{i, e\}$ (compared to the boundary coupling). To explain this, let us consider the particular case of **Volume - Boundary** coupling for which the involved bilinear form is given by

$$b_{VB}(\boldsymbol{v},\boldsymbol{m}) = \langle v_1 - v_2, m_{\mathcal{S}_i}\rangle_{\mathcal{S}_i} + \sum_{k=1}^{N_i}(v_1 - v_2, m_{i,k})_{H_0^1(\omega_{i,k})} + \langle v_1 - v_2, m_e\rangle_{\gamma_e},$$

while the correspondent space of multipliers is defined by

$$M_{VB,h} \;=\; M_{\mathcal{S}_i,h} \times \prod_{k=1}^{N_i} M_{V_{i,k},h} \times M_{B_e,h} \;\subset\; [H^{\frac{1}{2}}(\mathcal{S}_i)]' \times \prod_{k=1}^{N_i} H_0^1(\omega_{i,k}) \times [H^{\frac{1}{2}}(\gamma_e)]'.$$

Then, if we denote by $\{\xi_{\mathcal{S}_i}^\ell\}_{\ell=1}^{L_i}$, $\{\xi_0^\ell\}_{\ell=1}^{L_0}$ and $\{\xi_{\gamma_e}^\ell\}_{\ell=1}^{L_e}$ the sets of Lagrange basis functions which are used to build $M_{S_i,h}$, $\prod M_{V_{i,k},h}$ and $M_{B_e,h}$ respectively and by $\{\psi_j^k\}_{k=1}^{K_j}$ the set of Lagrange basis functions which are used to build $W_{j,h}$ for $j \in \{1,2\}$, we can rewrite the coupling matrices as

$$\mathbb{B}_{1,h} = (\mathbb{B}_{1,h}^{\mathcal{S}_i}, \mathbb{B}_{1,h}^{0}, \mathbb{B}_{1,h}^{\gamma_e}) \quad \text{and} \quad \mathbb{B}_{2,h} = (\mathbb{B}_{2,h}^{\mathcal{S}_i}, \mathbb{B}_{2,h}^{0}, \mathbb{B}_{2,h}^{\gamma_e}).$$

where, in order to distinguish between the different parts of the coupling, we have introduced the matrices

$$(\mathbb{B}_{1,h}^{\mathcal{S}_i})_{s,\ell} = \langle \psi_1^s, \xi_{\mathcal{S}_i}^\ell\rangle_{\mathcal{S}_i}, \quad (\mathbb{B}_{1,h}^{0})_{s,\ell} = \sum_{k=1}^{N_i}(\psi_1^s, \xi_0^\ell)_{H^1(\omega_{i,k})}, \quad (\mathbb{B}_{1,h}^{\gamma_e})_{s,\ell} = \langle \psi_1^s, \xi_{\gamma_e}^\ell\rangle_{\gamma_e},$$
$$(\mathbb{B}_{2,h}^{\mathcal{S}_i})_{s,\ell} = -\langle \psi_2^s, \xi_{\mathcal{S}_i}^\ell\rangle_{\mathcal{S}_i}, \quad (\mathbb{B}_{2,h}^{0})_{s,\ell} = -\sum_{k=1}^{N_i}(\psi_2^s, \xi_0^\ell)_{H^1(\omega_{i,k})}, \quad (\mathbb{B}_{2,h}^{\gamma_e})_{s,\ell} = -\langle \psi_2^s, \xi_{\gamma_e}^\ell\rangle_{\gamma_e}.$$

In consequence, since the matrices $\mathbb{B}_{j,h}^0$ for $j \in \{1,2\}$ correspond to the $H_0^1(\omega_{i,k})$ scalar product for $k \in \{1,\dots,N_i\}$, we expect (and have observed) that the conditioning number of the matrix $\mathbb{K}_h$ behaves as $O(h^{-4})$. However, the system may be easily preconditioned (see [83] for classical techniques). To do so, we first introduce the matrices

$$(\mathbb{D}_h^{\mathcal{S}_i})_{s,\ell} = \langle \xi_\ell^{\mathcal{S}_i}, \xi_s^{\mathcal{S}_i}\rangle_{\mathcal{S}_i}, \quad (\mathbb{D}_h^{0})_{s,\ell} = \sum_{k=1}^{N_i}(\xi_\ell^0, \xi_s^0)_{H^1(\omega_{i,k})}, \quad (\mathbb{D}_h^{\gamma_e})_{s,\ell} = \langle \xi_\ell^{\gamma_e}, \xi_s^{\gamma_e}\rangle_{\gamma_e}$$

$$\text{and} \quad \mathbb{D}_h = \begin{pmatrix} \mathbb{D}_h^{\mathcal{S}_i} & \mathbb{O} & \mathbb{O} \\ \mathbb{O} & \mathbb{D}_h^0 & \mathbb{O} \\ \mathbb{O} & \mathbb{O} & \mathbb{D}_h^{\gamma_e} \end{pmatrix},$$

and notice that $\mathbb{D}_h$ is an invertible matrix with a conditioning number that behaves as $\mathcal{O}(h^{-2})$. Thus we use $\mathbb{D}_h^{-1}$ as a left preconditioner since this provides a conditioning number for $(\mathbb{D}_h^{-1}\mathbb{K}_h)$ that should behave as $\mathcal{O}(h^{-2})$. Therefore, we find $\boldsymbol{\Lambda}_h^n$ by solving

$$(\mathbb{D}_h^{-1}\mathbb{K}_h)\boldsymbol{\Lambda}_h^n \;=\; \mathbb{D}_h^{-1}\boldsymbol{L}_h^{n+1}.$$

Finally, as mentioned before, we use $\boldsymbol{\Lambda}_h^n$ to compute $\boldsymbol{U}_{1,h}^{n+1}$ and $\boldsymbol{U}_{2,h}^{n+1}$ using respectively the first and second equations of (3.34).

3.4.2 Discrete energy identity

The stability of the numerical scheme (3.33) is classically analysed considering energy techniques. Thus, we begin by providing a discrete energy identity to then show that the scheme is stable in those cases where the energy is positive. First, for compactness, let us introduce the notation

$$\|\boldsymbol{V}\|_{\mathbb{S}} := \sqrt{\mathbb{S}\,\boldsymbol{V}\cdot\boldsymbol{V}}, \quad \text{for any symmetric positive semi-definite matrix } \mathbb{S},$$

as well as the matrices

$$\widetilde{\mathbb{M}}_{j,h} \;:=\; \mathbb{M}_{j,h} - \frac{(1-4\,\theta_j)}{4}\,\Delta t^2\,\mathbb{A}_{j,h}, \quad \text{for} \quad j \in \{1,2\}. \tag{3.35}$$

Then, we notice that (3.33) can be rewritten as: $\boldsymbol{U}^0_{j,h} = \boldsymbol{U}^1_{j,h} = \boldsymbol{0}$ for $j \in \{1,2\}$ while for all $n \in \{1,\ldots,N-1\}$

$$\begin{cases} \widetilde{\mathbb{M}}_{1,h}\dfrac{\boldsymbol{U}^{n+1}_{1,h} - 2\boldsymbol{U}^{n}_{1,h} + \boldsymbol{U}^{n-1}_{1,h}}{\Delta t^2} \\ \quad + \mathbb{A}_{1,h}\dfrac{\boldsymbol{U}^{n+1}_{1,h} + 2\boldsymbol{U}^{n}_{1,h} + \boldsymbol{U}^{n-1}_{1,h}}{4} + \mathbb{B}_{1,h}\boldsymbol{\Lambda}^n_h = \boldsymbol{G}^n_{1,h}, & (3.36a) \\ \widetilde{\mathbb{M}}_{2,h}\dfrac{\boldsymbol{U}^{n+1}_{2,h} - 2\boldsymbol{U}^{n}_{2,h} + \boldsymbol{U}^{n-1}_{2,h}}{\Delta t^2} \\ \quad + \mathbb{A}_{2,h}\dfrac{\boldsymbol{U}^{n+1}_{2,h} + 2\boldsymbol{U}^{n}_{2,h} + \boldsymbol{U}^{n-1}_{2,h}}{4} + \mathbb{B}_{2,h}\boldsymbol{\Lambda}^n_h = \boldsymbol{0}, & (3.36b) \\ \mathbb{B}^T_{1,h}\boldsymbol{U}^{n+1}_{1,h} + \mathbb{B}^T_{2,h}\boldsymbol{U}^{n+1}_{2,h} = \boldsymbol{0}. & (3.36c) \end{cases}$$

Now, following classical techniques, we first multiply (3.36a) by $\big(\boldsymbol{U}^{n+1}_{1,h} - \boldsymbol{U}^{n-1}_{1,h}\big)/2\Delta t$ and (3.36b) by $\big(\boldsymbol{U}^{n+1}_{2,h} - \boldsymbol{U}^{n-1}_{2,h}\big)/2\Delta t$. Then, we sum up the resultant equations and therefore, according to (3.36c) the terms involving the Lagrange multipliers vanish and we obtain

$$\begin{aligned} &\sum_{j=1}^{2}\widetilde{\mathbb{M}}_{j,h}\frac{\boldsymbol{U}^{n+1}_{j,h} - 2\boldsymbol{U}^{n}_{j,h} + \boldsymbol{U}^{n-1}_{j,h}}{\Delta t^2}\cdot\frac{\boldsymbol{U}^{n+1}_{j,h} - \boldsymbol{U}^{n-1}_{j,h}}{2\Delta t} \\ &+ \sum_{j=1}^{2}\mathbb{A}_{j,h}\frac{\boldsymbol{U}^{n+1}_{j,h} + 2\boldsymbol{U}^{n}_{j,h} + \boldsymbol{U}^{n-1}_{j,h}}{4}\cdot\frac{\boldsymbol{U}^{n+1}_{j,h} - \boldsymbol{U}^{n-1}_{j,h}}{2\Delta t} = \boldsymbol{G}^n_{1,h}\cdot\frac{\boldsymbol{U}^{n+1}_{1,h} - \boldsymbol{U}^{n-1}_{1,h}}{2\Delta t}. \end{aligned}$$

Notice that, although the terms related to the Lagrange multipliers are removed, the previous equation is still affected by the coupling since the matrices $\mathbb{M}_{j,h}$ and $\mathbb{A}_{j,h}$ are computed considering the partitioning (α_j,β_j). Next, we consider the equality

$$\boldsymbol{U}^{n+1}_{j,h} \pm 2\boldsymbol{U}^{n}_{j,h} + \boldsymbol{U}^{n-1}_{j,h} \;=\; (\boldsymbol{U}^{n+1}_{j,h} \pm \boldsymbol{U}^{n}_{j,h}) \pm (\boldsymbol{U}^{n}_{j,h} \pm \boldsymbol{U}^{n-1}_{j,h}),$$

and with some straightforward computations we get

$$\begin{aligned} &\frac{1}{\Delta t}\sum_{j=1}^{2}\frac{\widetilde{\mathbb{M}}_{j,h}}{2}\,\frac{\boldsymbol{U}^{n+1}_{j,h} - \boldsymbol{U}^{n}_{j,h}}{\Delta t}\cdot\frac{\boldsymbol{U}^{n+1}_{j,h} - \boldsymbol{U}^{n}_{j,h}}{\Delta t} \\ &+ \frac{1}{\Delta t}\sum_{j=1}^{2}\frac{\mathbb{A}_{j,h}}{2}\,\frac{(\boldsymbol{U}^{n+1}_{j,h} + \boldsymbol{U}^{n}_{j,h})}{2}\cdot\frac{(\boldsymbol{U}^{n+1}_{j,h} + \boldsymbol{U}^{n}_{j,h})}{2} \\ &- \frac{1}{\Delta t}\sum_{j=1}^{2}\frac{\widetilde{\mathbb{M}}_{j,h}}{2}\,\frac{\boldsymbol{U}^{n}_{j,h} - \boldsymbol{U}^{n-1}_{j,h}}{\Delta t}\cdot\frac{\boldsymbol{U}^{n}_{j,h} - \boldsymbol{U}^{n-1}_{j,h}}{\Delta t} \\ &- \frac{1}{\Delta t}\sum_{j=1}^{2}\frac{\mathbb{A}_{j,h}}{2}\,\frac{(\boldsymbol{U}^{n}_{j,h} + \boldsymbol{U}^{n-1}_{j,h})}{2}\cdot\frac{(\boldsymbol{U}^{n}_{j,h} + \boldsymbol{U}^{n-1}_{j,h})}{2} \;=\; \boldsymbol{G}^n_{1,h}\cdot\frac{\boldsymbol{U}^{n+1}_{1,h} - \boldsymbol{U}^{n-1}_{1,h}}{2\Delta t}. \end{aligned}$$

Therefore, if we introduce the notation $\boldsymbol{U}^{n+\frac{1}{2}}_{j,h} := \frac{1}{2}(\boldsymbol{U}^{n+1}_{j,h} + \boldsymbol{U}^{n}_{j,h})$ and define the following discrete energy associated to the region Ω_j,

$$\mathcal{E}^{n+\frac{1}{2}}_j = \frac{1}{2}\Big(\Big\|\frac{\boldsymbol{U}^{n+1}_{j,h} - \boldsymbol{U}^{n}_{j,h}}{\Delta t}\Big\|^2_{\widetilde{\mathbb{M}}_{j,h}} + \|\boldsymbol{U}^{n+\frac{1}{2}}_{j,h}\|^2_{\mathbb{A}_{j,h}}\Big) \quad \text{for} \quad n \in \{0,\ldots,N-1\},$$

we obtain the discrete energy relation

$$\sum_{j=1}^{2} \frac{\mathcal{E}_j^{n+\frac{1}{2}} - \mathcal{E}_j^{n-\frac{1}{2}}}{\Delta t} \;=\; \boldsymbol{G}_{1,h}^n \cdot \frac{\boldsymbol{U}_{1,h}^{n+1} - \boldsymbol{U}_{1,h}^{n-1}}{2\Delta t}. \tag{3.37}$$

3.4.3 Stability of the fully-discrete scheme: CFL condition

In this section, our aim is to show that the stability of the numerical scheme (3.33) is guaranteed if $\mathcal{E}_j^{n+\frac{1}{2}}$ is positive. Thus we first remark that the discrete energy is positive if the following condition is fulfilled for $j \in \{1,2\}$:

$$\widetilde{\mathbb{M}}_{j,h} \;=\; \mathbb{M}_{j,h} - \frac{(1-4\,\theta_j)}{4}\,\Delta t^2\,\mathbb{A}_{j,h} \quad \text{is positive definite.} \tag{3.38}$$

This condition is usually called CFL condition and notice that it is trivially satisfied if $\theta_j \geq 1/4$ while for $\theta_j < 1/4$ it requires that

$$\Delta t^2 < \frac{4}{1-4\theta_j}\left(\sup_{\boldsymbol{V}\neq \boldsymbol{0}} \frac{\mathbb{M}_{j,h}^{-1}\,\mathbb{A}_{j,h}\,\boldsymbol{V}\cdot\boldsymbol{V}}{\boldsymbol{V}\cdot\boldsymbol{V}}\right)^{-1}. \tag{3.39}$$

In practice, in order to fulfil the previous condition when $\theta_j < 1/4$, we denote by Δt_j the maximal limit time step allowed in previous inequality (3.39) and we choose

$$\Delta t \;=\; \xi \min_{\substack{1\,\leq\, j\,\leq\, 2\\ \text{s.t. }\ \theta_j\,<\,1/4}} \{\Delta t_j\} \quad \text{where} \quad \xi < 1. \tag{3.40}$$

This choice allows to easily prove the following result which is going to be very useful in the following.

Lemma 3.11

We assume $\Delta t > 0$ if $\min\{\theta_1,\theta_2\} \geq 1/4$ or Δt given by (3.40) if $\min\{\theta_1,\theta_2\} < 1/4$. Then, for $j \in \{1,2\}$ we have that

$$\|\boldsymbol{V}\|_{\mathbb{M}_{j,h}} \;\leq\; K_{\xi,j}\|\boldsymbol{V}\|_{\widetilde{\mathbb{M}}_{j,h}} \quad \textit{where} \quad K_{\xi,j} = \begin{cases} 1 & \textit{if} \quad \theta_j \geq 1/4, \\ \dfrac{1}{\sqrt{1-\xi^2}} & \textit{if} \quad \theta_j < 1/4. \end{cases}$$

Proof. The case $\theta_j \geq 1/4$ is trivial since $(1-4\theta_j) < 0$ and $\mathbb{A}_{j,h}$ is positive semi-definite. Thus

$$\|\boldsymbol{V}\|^2_{\mathbb{M}_{j,h}} \;=\; \mathbb{M}_{j,h}\boldsymbol{V}\cdot\boldsymbol{V} \;\leq\; \widetilde{\mathbb{M}}_{j,h}\boldsymbol{V}\cdot\boldsymbol{V} \;\leq\; \|\boldsymbol{V}\|^2_{\widetilde{\mathbb{M}}_{j,h}}.$$

The case $\theta_j < 1/4$ is consequence of the choice $\Delta t = \xi \min\limits_{\theta_j<1/4}\{\Delta t_j\}$ where Δt_j is the maximal time step allowed in (3.39). Indeed, notice

$$\|\boldsymbol{V}\|^2_{\mathbb{M}_{j,h}} \;=\; \|\boldsymbol{V}\|^2_{\widetilde{\mathbb{M}}_{j,h}} + \frac{1-4\,\theta_j}{4}\Delta t^2\|\boldsymbol{V}\|^2_{\mathbb{A}_{j,h}} \;\leq\; \|\boldsymbol{V}\|^2_{\widetilde{\mathbb{M}}_{j,h}} + \xi^2\,\frac{1-4\,\theta_j}{4}\Delta t_j^2\|\boldsymbol{V}\|^2_{\mathbb{A}_{j,h}},$$

while according to the choice of Δt_j we also have

$$\frac{1-\theta_j}{4}\Delta_j^2\|\boldsymbol{V}\|^2_{\mathbb{A}_{j,h}} \;\leq\; \|\boldsymbol{V}\|^2_{\mathbb{M}_{j,h}}.$$

Thus we have that $\|\boldsymbol{V}\|^2_{\mathbb{M}_{j,h}} \leq \|\boldsymbol{V}\|^2_{\widetilde{\mathbb{M}}_{j,h}} + \xi^2\;\|\boldsymbol{V}\|^2_{\mathbb{M}_{j,h}}$ which implies

$$\|\boldsymbol{V}\|_{\mathbb{M}_{j,h}} \;\leq\; \frac{1}{\sqrt{1-\xi^2}}\;\|\boldsymbol{V}\|_{\widetilde{\mathbb{M}}_{j,h}}. \tag{3.41}$$

■

Next, we proceed to prove that the positivity of the discrete energy implies the stability of the numerical scheme (3.33).

Theorem 3.12

If the discrete energies $\mathcal{E}_1^{n+\frac{1}{2}}$ *and* $\mathcal{E}_2^{n+\frac{1}{2}}$ *are positive for all* $0 \le n \le N-1$, *then*

$$\Big(\sum_{j=1}^{2} \mathcal{E}_j^{n+\frac{1}{2}}\Big)^{\frac{1}{2}} \;\le\; \frac{K_\xi\,\Delta t}{\sqrt{2}\,\rho_0}\sum_{k=1}^{n}\|f(t^k)\|_{L^2(\Omega_1\setminus\omega)},$$

where $\rho_0 > 0$ *is the* h*-independent constant introduced in* (3.1), *while* $K_\xi = 1$ *if* $\min\{\theta_1,\theta_2\} \ge 1/4$ *and* $K_\xi = 1/\sqrt{1-\xi^2}$ *if* $\min\{\theta_1,\theta_2\} < 1/4$. *Moreover, the numerical solution of the fully-discrete scheme* (3.33) *is such that*

$$\Big(\sum_{j=1}^{2}\|\boldsymbol{U}_{j,h}^{n+1}\|^2_{\mathbb{M}_{j,h}}\Big)^{\frac{1}{2}} \;\le\; \frac{K_\xi^2\,\Delta t^2}{\sqrt{\rho_0}}\sum_{s=1}^{n}\sum_{k=1}^{s}\|f(t^k)\|_{L^2(\Omega_1\setminus\omega)},$$

$$\Big(\sum_{j=1}^{2}\|\boldsymbol{U}_{j,h}^{n+\frac{1}{2}}\|^2_{\mathbb{A}_{j,h}}\Big)^{\frac{1}{2}} \;\le\; \frac{K_\xi\,\Delta t}{\sqrt{\rho_0}}\sum_{k=1}^{n}\|f(t^k)\|_{L^2(\Omega_1\setminus\omega)}.$$

Proof. We begin by noticing that considering Cauchy Schwartz inequality in (3.37), we obtain

$$\sum_{j=1}^{2}\frac{\mathcal{E}_j^{n+\frac{1}{2}}-\mathcal{E}_j^{n-\frac{1}{2}}}{\Delta t} \;\le\; \frac{\|f(t^n)\|_{L^2(\Omega_1\setminus\omega)}}{2\sqrt{\rho_0}}\Big(\Big\|\frac{\boldsymbol{U}_{1,h}^{n+1}-\boldsymbol{U}_{1,h}^{n}}{\Delta t}\Big\|_{\mathbb{M}_{1,h}}+\Big\|\frac{\boldsymbol{U}_{1,h}^{n}-\boldsymbol{U}_{1,h}^{n-1}}{\Delta t}\Big\|_{\mathbb{M}_{1,h}}\Big).$$

Moreover, according to Lemma 3.11 and the definition of $\mathcal{E}_j^{n+\frac{1}{2}}$, we observe that

$$\Big\|\frac{\boldsymbol{U}_{j,h}^{n+1}-\boldsymbol{U}_{j,h}^{n}}{\Delta t}\Big\|_{\mathbb{M}_{j,h}} \;\le\; K_{\xi,j}\Big\|\frac{\boldsymbol{U}_{j,h}^{n+1}-\boldsymbol{U}_{j,h}^{n}}{\Delta t}\Big\|_{\widetilde{\mathbb{M}}_{j,h}} \;\le\; K_{\xi,j}\sqrt{2\,\mathcal{E}_j^{n+\frac{1}{2}}}. \tag{3.42}$$

Then we deduce

$$\sum_{j=1}^{2}\frac{\mathcal{E}_j^{n+\frac{1}{2}}-\mathcal{E}_j^{n-\frac{1}{2}}}{\Delta t} \;\le\; K_{\xi,1}\,\frac{\|f(t^n)\|_{L^2(\Omega_1\setminus\omega)}}{2\sqrt{\rho_0}}\Big(\sqrt{2\,\mathcal{E}_1^{n+\frac{1}{2}}}+\sqrt{2\,\mathcal{E}_1^{n-\frac{1}{2}}}\Big),$$

which implies that

$$\sqrt{\mathcal{E}_1^{n+\frac{1}{2}}+\mathcal{E}_2^{n+\frac{1}{2}}}-\sqrt{\mathcal{E}_1^{n-\frac{1}{2}}+\mathcal{E}_2^{n-\frac{1}{2}}} \;\le\; \frac{K_{\xi,1}\,\Delta t}{\sqrt{2}\,\rho_0}\,\|f(t^n)\|_{L^2(\Omega_1\setminus\omega)},$$

and consequently

$$\sqrt{\mathcal{E}_1^{n+\frac{1}{2}}+\mathcal{E}_2^{n+\frac{1}{2}}} \;\le\; \sqrt{\mathcal{E}_1^{n-\frac{1}{2}}+\mathcal{E}_2^{n-\frac{1}{2}}} \;+\; \frac{K_{\xi,1}\,\Delta t}{\sqrt{2}\,\rho_0}\,\|f(t^n)\|_{L^2(\Omega_1\setminus\omega)}.$$

And by recursion up to $n=1$ and noticing that $\mathcal{E}_j^{\frac{1}{2}}=0$, we obtain

$$\sqrt{\mathcal{E}_1^{n+\frac{1}{2}}+\mathcal{E}_2^{n+\frac{1}{2}}} \;\le\; \frac{K_{\xi,1}\,\Delta t}{\sqrt{2}\,\rho_0}\sum_{k=1}^{n}\|f(t^k)\|_{L^2(\Omega_1\setminus\omega)}. \tag{3.43}$$

Now, to estimate $\boldsymbol{U}_{j,h}^{n+1}$ we first consider triangular inequality

$$\|\boldsymbol{U}_{j,h}^{n+1}\|^2_{\mathbb{M}_{j,h}} \;\le\; \|\boldsymbol{U}_{j,h}^{n+1}-\boldsymbol{U}_{j,h}^{n}\|^2_{\mathbb{M}_{j,h}} \;+\; \|\boldsymbol{U}_{j,h}^{n}\|^2_{\mathbb{M}_{j,h}}$$

and then, we apply again (3.42), considering $K_\xi = \max\{K_{\xi,1}, K_{\xi,2}\}$, to obtain

$$\|\boldsymbol{U}_{j,h}^{n+1}\|^2_{\mathbb{M}_{j,h}} \;\leq\; \|\boldsymbol{U}_{j,h}^{n}\|^2_{\mathbb{M}_{j,h}} \;+\; 2\,K_\xi^2\,\Delta t^2\;\mathcal{E}_j^{n+\frac{1}{2}}.$$

Again by recursion up to $n = 1$, considering the vanishing initial conditions and (3.43)

$$\Big(\sum_{j=1}^{2}\|\boldsymbol{U}_{j,h}^{n+1}\|^2_{\mathbb{M}_{j,h}}\Big)^{\frac{1}{2}} \;\leq\; \sqrt{2}\,K_\xi\,\Delta t\;\sum_{s=1}^{n}\Big(\sum_{j=1}^{2}\mathcal{E}_j^{s+\frac{1}{2}}\Big)^{\frac{1}{2}} \;\leq\; \frac{K_\xi^2\,\Delta t^2}{\sqrt{\rho_0}}\;\sum_{s=1}^{n}\sum_{k=1}^{s}\|f(t^k)\|_{L^2(\Omega_1\setminus\omega)}.$$

Finally, we can also estimate

$$\Big(\sum_{j=1}^{2}\|\boldsymbol{U}_{j,h}^{n+\frac{1}{2}}\|^2_{\mathbb{A}_{j,h}}\Big)^{\frac{1}{2}} \;\leq\; \sqrt{2}\,\Big(\sum_{j=1}^{2}\mathcal{E}_j^{s+\frac{1}{2}}\Big)^{\frac{1}{2}} \;\leq\; \frac{K_\xi\,\Delta t}{\sqrt{\rho_0}}\;\sum_{k=1}^{n}\|f(t^k)\|_{L^2(\Omega_1\setminus\omega)}.$$

■

Attending to previous theorem, the hypothesis that both discrete energies are positive seems non-optimal since theoretically only the positivity of $\mathcal{E}_1^{n+\frac{1}{2}} + \mathcal{E}_2^{n+\frac{1}{2}}$ has to be ensured. However the solutions are imposed to be equal in the coupling domain in a weak way, thus some pathologies may develop. It is also interesting to notice that K_ξ blows up when ξ tends to 1 (see Lemma 3.11). In absence of coupling, similar estimates to those in Theorem 3.12 can be obtained with a different technique based on a spectral decomposition that allows to consider $\xi = 1$. However, the extension of such results is not obvious in the cases presented here (see [82]). We shall also remark that in [82] it is shown that the choice $\theta_j = 1/12$ provides a fourth order scheme and that the consistency error constantly growths with values of θ_j larger and larger than $1/12$. Such observations motivate the choice $\theta_j = 1/4$ since it yields the unconditional stable scheme with the minimum consistency error (among the family of second order two time-steps schemes).

3.4.4 Local estimate of the CFL condition

In what follows, we focus on practical aspects and we consider the specific case of $\theta_1 = 0$ and $\theta_2 \geq 1/4$, which corresponds to an explicit/implicit coupling and we give a more detailed analysis of the stability condition equation (3.39), which in this case corresponds only to check the positivity of $\mathcal{E}_1^{n+\frac{1}{2}}$. Moreover, attending to equation (3.39) it may seem that the time step restriction is computed independently of the coupling process, however this is not true. As mentioned before, the parameters α_1 and β_1 vary (even jump) and this may decrease the CFL condition compared to the maximum time step allowed in the case where no coupling is considered (i.e. $\alpha_1 = \beta_1 = 1$ in the stability analysis). Then notice that the positivity of $\mathcal{E}_1^{n+\frac{1}{2}}$ is equivalent to

$$\Delta t^2 < 4\,\Big(\sup_{\boldsymbol{V}\neq\boldsymbol{0}}\frac{\mathbb{M}_{1,h}^{-1}\,\mathbb{A}_{1,h}\,\boldsymbol{V}\cdot\boldsymbol{V}}{\boldsymbol{V}\cdot\boldsymbol{V}}\Big)^{-1}, \tag{3.44}$$

which corresponds to check the positivity of

$$(\alpha_1\,\rho\,v_{1,h}, v_{1,h})_{L^2(\Omega_1)} - \frac{\Delta t^2}{4}(\beta_1\,\mu\,\nabla v_{1,h}, \nabla v_{1,h})_{L^2(\Omega_1)}, \quad v_{1,h} \in W_{1,h} \subset H^1(\Omega_1). \tag{3.45}$$

Notice that according to (3.44), the computation of the maximal time step allowed in (3.45) involves the computation of the largest eigenvalue of $\mathbb{M}_{1,h}^{-1}\,\mathbb{A}_{1,h}$, which might be expensive. In consequence, we aim to provide an alternative approach to choose an adequate Δt that satisfies (3.45). To do so, we follow the technique firstly introduced in [84] and recently used in [85], and we present a local analysis of the CFL condition based on local estimates. Let us begin by considering that the triangulation of Ω_1 (introduced in Section 3.3.1) is given by $\mathcal{T}_{1,h} = \{\kappa_k\}$ where the union of the triangles κ_k recovers Ω_1. Then we define element-wise scalars quantities $\Delta\tau_k$ as

$$\Delta\tau_k := \sup\Big\{\delta\tau \in \mathbb{R}^+ \;/\; (\rho\,v_{1,h}, v_{1,h})_{L^2(\kappa_k)} - \frac{\delta\tau^2}{4}(\mu\,\nabla v_{1,h}, \nabla v_{1,h})_{L^2(\kappa_k)} \geq 0,\; \forall\, v_{1,h} \in W_{1,h}\Big\}.$$

In absence of coupling, it is proven in [84] that a sufficient condition to satisfy the usual CFL condition is

$$\Delta t < \min_k \{\Delta\tau_k\}. \tag{3.46}$$

We now define the element-wise scalar Δt_k as

$$\Delta t_k := \max \Big\{ \delta t \in \mathbb{R}^+ \;/\; (\alpha_1\, \rho\, v_{1,h}, v_{1,h})_{L^2(\kappa_k)} - \frac{\delta t^2}{4} (\beta_1\, \mu\, \nabla v_{1,h}, \nabla v_{1,h})_{L^2(\kappa_k)} \geq 0,\ \forall\, v_{1,h} \in W_{1,h} \Big\}.$$

Then, using the same arguments, we deduce that by selecting the time step such that

$$\Delta t < \min_k \{\Delta t_k\}, \tag{3.47}$$

the CFL condition (3.45) holds leading to the stability of the coupled problem. We now study the relation between Δt_k and $\Delta\tau_k$ to obtain a local estimate of the influence of the coupling on the CFL. To do so, we remark that, for all k and all positive δt,

$$\begin{aligned} &(\alpha_1\, \rho\, v_{1,h}, v_{1,h})_{L^2(\kappa_k)} - \frac{\delta t^2}{4} (\beta_1\, \mu\, \nabla v_{1,h}, \nabla v_{1,h})_{L^2(\kappa_k)} \\ &\qquad\qquad \geq \big(\inf_{\boldsymbol{x}\in\kappa_k} \alpha_1\big)\, \|\rho^{\frac{1}{2}} v_{1,h}\|^2_{L^2(\kappa_k)} - \big(\sup_{\boldsymbol{x}\in\kappa_k} \beta_1\big) \frac{\delta t^2}{4} \|\mu^{\frac{1}{2}}\, \nabla v_{1,h}\|^2_{L^2(\kappa_k)}, \end{aligned}$$

from which we deduce that

$$\Delta t_k \;\geq\; \Delta\tau_k \sqrt{\frac{\inf_{\boldsymbol{x}\in\kappa_k} \alpha_1}{\sup_{\boldsymbol{x}\in\kappa_k} \beta_1}}. \tag{3.48}$$

This estimate suggests that we could take advantage of the freedom when choosing the values of α_1 and β_1 in the overlapping region ω in order to improve locally Δt_k (this will be exhibited in Section 3.5.1 for a 1D numerical example). This is useful in situations where, due to the variations of the physical coefficients ρ and μ, the smaller $\Delta\tau_k$ is inside of the coupling region ω. We shall also remark, that on $\partial\omega$, where the coefficients α_1 and β_1 jump, the local CFL will be always slightly penalised by the coupling procedure since $\sup\beta_1 = 1$ and $\inf\alpha_1 < 1$. However, the penalization should be low since for instance, if we simply chose $\alpha_1 = 1/2$ in the overlapping region ω, then the local CFL (3.47) obtained considering the coupling gives a time step which is $1/\sqrt{2} \simeq 0.7$ times smaller than the one given by the estimate (3.46) obtained without coupling. This reinforces the assumption that α_1 should not degenerate, since the time step would also degenerate. However, notice that it is possible to obtain an estimate of the stability condition independent of α_1 and β_1 by using an implicit scheme only for the elements that are penalized. This idea was presented in [86] for the case of the Maxwell equation and it can be seen as θ-scheme where the parameter θ depends on the space variable and allows to locally implicit the scheme. In next section we show how this technique can be applied to our problem.

3.4.5 Locally implicit scheme

First, we recall that we are considering $\theta_1 = 0$ and $\theta_2 \geq 1/4$, which corresponds to an explicit/implicit scheme. Thus our aim is to improve the stability properties of the scheme of Section 3.4 using a locally implicit scheme to compute $\boldsymbol{U}^n_{1,h}$. Therefore we obtain an estimate of the stability condition independent of α_1 and β_1. To do so we can introduce an implicit scheme only for the penalizing elements (see [86]). More precisely, let us rewrite the stiffness matrix as follows

$$\mathbb{A}_{1,h} = \widetilde{\mathbb{A}}_{1,h} + (\mathbb{A}_{1,h} - \widetilde{\mathbb{A}}_{1,h})$$

where $\widetilde{\mathbb{A}}_{1,h}$ is the stiffness matrix computed using a standard finite element procedure but only with the elements in $\widetilde{\mathcal{T}}_{1,h} \subset \mathcal{T}_{1,h}$ where $\widetilde{\mathcal{T}}_{1,h}$ is the triangulation of a sub-domain of Ω_1 where

$\alpha_1 = \beta_1 = 1$. Then, equation (3.33a) can be replaced by

$$\mathbb{M}_{1,h}\frac{\boldsymbol{U}_{1,h}^{n+1} - 2\boldsymbol{U}_{1,h}^{n} + \boldsymbol{U}_{1,h}^{n-1}}{\Delta t^2} \ + \ \widetilde{\mathbb{A}}_{1,h}\boldsymbol{U}_{1,h}^{n}$$
$$+ \left(\mathbb{A}_{1,h} - \widetilde{\mathbb{A}}_{1,h}\right)\frac{\boldsymbol{U}_{1,h}^{n+1} + 2\,\boldsymbol{U}_{1,h}^{n} + \boldsymbol{U}_{1,h}^{n-1}}{4} \ + \ \mathbb{B}_{1,h}\boldsymbol{\Lambda}_h^{n+1} \ = \ \boldsymbol{G}_{1,h}^{n}.$$

Note that the energy preservation relation (3.37) still holds with $\mathcal{E}_1^{n+\frac{1}{2}}$ now defined by

$$\mathcal{E}_1^{n+\frac{1}{2}} \quad = \quad \frac{1}{2}\left(\mathbb{M}_{1,h} - \frac{1}{4}\,\Delta t^2\,\widetilde{\mathbb{A}}_{1,h}\right)\frac{\boldsymbol{U}_{1,h}^{n+1} - \boldsymbol{U}_{1,h}^{n}}{\Delta t}\cdot\frac{\boldsymbol{U}_{1,h}^{n+1} - \boldsymbol{U}_{1,h}^{n}}{\Delta t}$$
$$+\frac{\mathbb{A}_{1,h}}{2}\,\frac{\boldsymbol{U}_{1,h}^{n+1} + \boldsymbol{U}_{1,h}^{n}}{2}\cdot\frac{\boldsymbol{U}_{1,h}^{n+1} + \boldsymbol{U}_{1,h}^{n}}{2}.$$

Then, since $\alpha_1 = \beta_1 = 1$ for each element $\kappa_k \in \widetilde{\mathcal{T}}_{1,h}$, we have $\Delta\tau_k = \Delta t_k$ and the CFL condition (3.47) now reads

$$\Delta t < \min_{\kappa_k \in \widetilde{\mathcal{T}}_{1,h}} \{\Delta t_k\}, \tag{3.49}$$

which corresponds to a CFL condition that depends only on the discretization parameters of the coarse mesh and thus independent of the coupling procedure.

3.4.6 Error estimate for the fully-discrete scheme

In this section we estimate the error caused by the time discretization, i.e. between the algebraic version of the semi-discrete problem (3.21) and the fully-discrete problem (3.33). Notice, that this analysis can be easily combined with the error estimation in Section 3.3.3 in order to provide estimates for the error of the fully-discrete scheme. Thus, we first subtract (3.21) evaluated at time t^n by (3.33) for $j \in \{1,2\}$ and $n \in \{1,\dots,N-1\}$

$$\mathbb{M}_{j,h}\Big(\frac{\mathrm{d}^2}{\mathrm{d}t^2}\,\boldsymbol{U}_{j,h}(t^n) \ - \ \frac{\boldsymbol{U}_{j,h}^{n+1} - 2\boldsymbol{U}_{j,h}^{n} + \boldsymbol{U}_{j,h}^{n-1}}{\Delta t^2}\Big)$$
$$+ \ \mathbb{A}_{j,h}\Big(\boldsymbol{U}_{j,h}(t^n) \ - \ \big(\theta_j\,\boldsymbol{U}_{j,h}^{n+1} + (1-2\theta_j)\boldsymbol{U}_{j,h}^{n} + \theta_j\,\boldsymbol{U}_{j,h}^{n-1}\big)\Big) \ + \mathbb{B}_{j,h}\Big(\boldsymbol{\Lambda}_h(t^n) \ - \ \boldsymbol{\Lambda}_h^{n}\Big) \ = \ \boldsymbol{0},$$

$$\mathbb{B}_{1,h}^T\Big(\boldsymbol{U}_{1,h}(t^{n+1}) - \boldsymbol{U}_{1,h}^{n+1}\Big) \ + \ \mathbb{B}_{2,h}^T\Big(\boldsymbol{U}_{2,h}(t^{n+1}) - \boldsymbol{U}_{2,h}^{n+1}\Big) \ = \ \boldsymbol{0}.$$

Then, we introduce the notation $\boldsymbol{E}_{j,h}^{n} = \boldsymbol{U}_{j,h}(t^n) - \boldsymbol{U}_{j,h}^{n}$ and $\boldsymbol{\Phi}_h^{n} = \boldsymbol{\Lambda}_h(t^n) \ - \ \boldsymbol{\Lambda}_h^{n}$ and we obtain the following algebraic system of equations: $\boldsymbol{E}_{j,h}^{0} = \boldsymbol{0}$ and $\boldsymbol{E}_{j,h}^{1} = \boldsymbol{U}_{j,h}(t^1)$ for $j \in \{1,2\}$, while for all $n \in \{1,\dots,N-1\}$

$$\begin{aligned}
&\mathbb{M}_{j,h}\frac{\boldsymbol{E}_{j,h}^{n+1} - 2\boldsymbol{E}_{j,h}^{n} + \boldsymbol{E}_{j,h}^{n-1}}{\Delta t^2}\\
&+ \mathbb{A}_{j,h}\big(\theta_j\,\boldsymbol{E}_{j,h}^{n+1} + (1-2\theta_j)\boldsymbol{E}_{j,h}^{n} + \theta_j\,\boldsymbol{E}_{j,h}^{n-1}\big) \ + \mathbb{B}_{j,h}\boldsymbol{\Phi}_h^{n}\\
&\quad = \ \mathbb{M}_{j,h}\Big(\frac{\boldsymbol{U}_{j,h}(t^{n+1}) - 2\boldsymbol{U}_{j,h}(t^n) + \boldsymbol{U}_{j,h}(t^{n-1})}{\Delta t^2} \ - \ \frac{\mathrm{d}^2}{\mathrm{d}t^2}\,\boldsymbol{U}_{j,h}(t^n)\Big)\\
&\qquad + \mathbb{A}_{j,h}\Big(\big(\theta_j\,\boldsymbol{U}_{j,h}(t^{n+1}) + (1-2\theta_j)\boldsymbol{U}_{j,h}(t^n) + \theta_j\,\boldsymbol{U}_{j,h}(t^{n-1})\big) \ - \ \boldsymbol{U}_{j,h}(t^n)\Big),\\
&\mathbb{B}_{1,h}^T\boldsymbol{E}_{1,h}^{n+1} \ + \ \mathbb{B}_{2,h}^T\boldsymbol{E}_{2,h}^{n+1} \ = \ \boldsymbol{0}.
\end{aligned} \tag{3.50}$$

Notice that this problem is like (3.36) with a different source term, thus we proceed in a similar way in order to obtain an equivalent to Theorem 3.12 that provides an estimate for $\boldsymbol{E}_{j,h}^{n+1}$. In the process, we will make use of the following lemma which is a discrete version of Gronwall's lemma.

Lemma 3.13

For any real positive sequence $\{v_n\}_{n\in\mathbb{N}}$ and any positive scalar numbers A and B, we have for all $n \geq 0$ (considering $\sum_{k=1}^{0}\sqrt{v_k} = 0$)

$$v_n \;\leq\; A \;+\; B\sum_{k=1}^{n}\sqrt{v_k} \quad\Longrightarrow\quad \sqrt{v_n} \;\leq\; \sqrt{A} \;+\; n\,B.$$

Proof. We begin by introducing the sequence $\{w_n\}_{n\in\mathbb{N}}$ defined by

$$w_n \;\coloneqq\; A \;+\; B\sum_{k=1}^{n}\sqrt{v_k}.$$

Then, we notice that $(w_n - w_{n-1}) = B\sqrt{v_n} \leq B(\sqrt{w_n} + \sqrt{w_{n-1}}\,)$ which gives $(\sqrt{w_n} - \sqrt{w_{n-1}}\,) \leq B$ and summing by recursion up to $n = 1$

$$\sqrt{v_n} \;\leq\; \sqrt{w_n} \;\leq\; n\,B \;+\; \sqrt{w_0} \;=\; n\,B \;+\; \sqrt{A}.$$

■

Next, considering some time regularity assumption, we provide estimates for the error between the fully-discrete scheme and the semi-discrete scheme.

Theorem 3.14

*If Assumptions I.1 and I.2 are satisfied, conditions (**P.1**), (**P.2**) and (**P.3**) hold and we consider $f \in \mathcal{C}_0^3([0,T]; L^2(\Omega_1 \setminus \omega))$, then we have for all $n \in \{0,\ldots,N-1\}$*

$$\begin{aligned}\Big(\sum_{j=1}^{2}\|\boldsymbol{E}_{j,h}^{n+1}\|^2_{\mathbb{M}_{j,h}}\Big)^{\frac{1}{2}} \quad&\leq\quad K_0\,\Delta t^2\sum_{k=2}^{3}\|\partial_t^k f\|_{L^1([0,T];L^2(\Omega_1\setminus\omega))}\\ \Big(\sum_{j=1}^{2}\|\boldsymbol{E}_{j,h}^{n+\frac{1}{2}}\|^2_{\mathbb{A}_{j,h}}\Big)^{\frac{1}{2}} \quad&\leq\quad K_1\,\Delta t^2\sum_{k=2}^{3}\|\partial_t^k f\|_{L^1([0,T];L^2(\Omega_1\setminus\omega))},\end{aligned}$$

where K_0 and K_1 are positive constants only depending in T and ξ (introduced in (3.40)).

Proof. *Step 1: Energy relation.*
The first part of the proof consists in proving an energy relation as in (3.37). Since the computations are very similar, we skip some of the details. As a result, we obtain the following discrete energy relation

$$\begin{aligned}&\sum_{j=1}^{2}\frac{\mathcal{E}_{\boldsymbol{E},j}^{n+\frac{1}{2}} - \mathcal{E}_{\boldsymbol{E},j}^{n-\frac{1}{2}}}{\Delta t}\\ &\;= \sum_{j=1}^{2}\mathbb{M}_{j,h}\Big(\frac{\boldsymbol{U}_{j,h}(t^{n+1}) - 2\boldsymbol{U}_{j,h}(t^n) + \boldsymbol{U}_{j,h}(t^{n-1})}{\Delta t^2} \;-\; \frac{\mathrm{d}^2}{\mathrm{d}t^2}\boldsymbol{U}_{j,h}(t^n)\Big)\cdot\frac{\boldsymbol{E}_{j,h}^{n+1} - \boldsymbol{E}_{j,h}^{n-1}}{2\Delta t}\\ &\;+ \sum_{j=1}^{2}\theta_j\mathbb{A}_{j,h}\Big(\boldsymbol{U}_{j,h}(t^{n+1}) - 2\,\boldsymbol{U}_{j,h}(t^n) + \boldsymbol{U}_{j,h}(t^{n-1})\Big)\cdot\frac{\boldsymbol{E}_{j,h}^{n+1} - \boldsymbol{E}_{j,h}^{n-1}}{2\Delta t},\end{aligned}\tag{3.51}$$

where each $\mathcal{E}_{\boldsymbol{E},j}^{n+\frac{1}{2}}$ is defined by (see (3.35) for definition of $\widetilde{\mathbb{M}}_{j,h}$ and notice $\boldsymbol{E}_{j,h}^{n+\frac{1}{2}} \coloneqq \frac{1}{2}(\boldsymbol{E}_{j,h}^{n+1} + \boldsymbol{E}_{j,h}^{n})$)

$$\mathcal{E}_{\boldsymbol{E},j}^{n+\frac{1}{2}} \;=\; \frac{1}{2}\Big(\Big\|\frac{\boldsymbol{E}_{j,h}^{n+1} - \boldsymbol{E}_{j,h}^{n}}{\Delta t}\Big\|^2_{\widetilde{\mathbb{M}}_{j,h}} + \|\boldsymbol{E}_{j,h}^{n+\frac{1}{2}}\|^2_{\mathbb{A}_{j,h}}\Big), \quad \text{for all} \quad n \in \{0,\ldots,N-1\}.$$

Then, when we sum (3.51) by recursion up to $n = 1$, we obtain (notice $\mathcal{E}_{\boldsymbol{E},j}^{\frac{1}{2}} \neq 0$ see Remark 3.10)

$$\begin{aligned} \sum_{j=1}^{2} \left(\mathcal{E}_{\boldsymbol{E},j}^{n+\frac{1}{2}} - \mathcal{E}_{\boldsymbol{E},j}^{\frac{1}{2}}\right) &= \Delta t \sum_{k=1}^{n}\sum_{j=1}^{2} \mathbb{M}_{j,h}\boldsymbol{e}_{j,h}^{k} \cdot \frac{\boldsymbol{E}_{j,h}^{k+1} - \boldsymbol{E}_{j,h}^{k-1}}{2\Delta t} \\ &+ \Delta t \sum_{k=1}^{n}\sum_{j=1}^{2} \theta_j \mathbb{A}_{j,h}\widetilde{\boldsymbol{e}}_{j,h}^{k} \cdot \frac{\boldsymbol{E}_{j,h}^{k+1} - \boldsymbol{E}_{j,h}^{k-1}}{2\Delta t}, \end{aligned} \tag{3.52}$$

where, for compactness, we have introduced the following notations for $k \in \{1, \dots, N-1\}$:

$$\begin{aligned} \boldsymbol{e}_{j,h}^{k} &:= \frac{\boldsymbol{U}_{j,h}(t^{k+1}) - 2\boldsymbol{U}_{j,h}(t^{k}) + \boldsymbol{U}_{j,h}(t^{k-1})}{\Delta t^2} - \frac{\mathrm{d}^2}{\mathrm{d}t^2}\boldsymbol{U}_{j,h}(t^k), \\ \widetilde{\boldsymbol{e}}_{j,h}^{k} &:= \boldsymbol{U}_{j,h}(t^{k+1}) - 2\boldsymbol{U}_{j,h}(t^{k}) + \boldsymbol{U}_{j,h}(t^{k-1}). \end{aligned}$$

Next, in order to estimate $\mathcal{E}_{\boldsymbol{E},j}^{n+\frac{1}{2}}$, we proceed separately for each term in (3.52).
Step 2: Estimate for the first term in (3.52).
Notice that considering Cauchy Schwartz inequality, the first term in (3.52) can be bounded by

$$\begin{aligned} &\Delta t \sum_{k=1}^{n}\sum_{j=1}^{2} \mathbb{M}_{j,h}\boldsymbol{e}_{j,h}^{k} \cdot \frac{\boldsymbol{E}_{j,h}^{k+1} - \boldsymbol{E}_{j,h}^{k-1}}{2\Delta t} \\ &\qquad \leq \Delta t \sum_{k=1}^{n}\sum_{j=1}^{2} \frac{1}{2}\|\boldsymbol{e}_{j,h}^{k}\|_{\mathbb{M}_{j,h}} \cdot \left(\left\|\frac{\boldsymbol{E}_{j,h}^{k+1} - \boldsymbol{E}_{j,h}^{k}}{\Delta t}\right\|_{\mathbb{M}_{j,h}} + \left\|\frac{\boldsymbol{E}_{j,h}^{k} - \boldsymbol{E}_{j,h}^{k-1}}{\Delta t}\right\|_{\mathbb{M}_{j,h}}\right). \end{aligned}$$

Moreover, according to Lemma 3.11 and the definition of $\mathcal{E}_{\boldsymbol{E},j}^{n+\frac{1}{2}}$, we observe that

$$\left\|\frac{\boldsymbol{E}_{j,h}^{k+1} - \boldsymbol{E}_{j,h}^{k}}{\Delta t}\right\|_{\mathbb{M}_{j,h}} \leq K_{\xi,j}\left\|\frac{\boldsymbol{E}_{j,h}^{k+1} - \boldsymbol{E}_{j,h}^{k}}{\Delta t}\right\|_{\widetilde{\mathbb{M}}_{j,h}} \leq K_{\xi,j}\sqrt{2\,\mathcal{E}_{\boldsymbol{E},j}^{k+\frac{1}{2}}}. \tag{3.53}$$

Thus, we consider $K_\xi = \max\{K_{\xi,1}, K_{\xi,2}\}$ and estimate

$$\Delta t \sum_{k=1}^{n}\sum_{j=1}^{2} \mathbb{M}_{j,h}\boldsymbol{e}_{j,h}^{k} \cdot \frac{\boldsymbol{E}_{j,h}^{k+1} - \boldsymbol{E}_{j,h}^{k-1}}{2\Delta t} \leq \frac{K_\xi\,\Delta t}{\sqrt{2}} \max_{\substack{1\,\leq\, j\,\leq\, 2\\ 1\,\leq\, k\,\leq\, n}}\{\|\boldsymbol{e}_{j,h}^{k}\|_{\mathbb{M}_{j,h}}\} \sum_{k=1}^{n}\sum_{j=1}^{2}\left(\sqrt{\mathcal{E}_{\boldsymbol{E},j}^{k+\frac{1}{2}}} + \sqrt{\mathcal{E}_{\boldsymbol{E},j}^{k-\frac{1}{2}}}\right).$$

Now, we notice that

$$\begin{aligned} \sum_{k=1}^{n}\sum_{j=1}^{2}\left(\sqrt{\mathcal{E}_{\boldsymbol{E},j}^{k+\frac{1}{2}}} + \sqrt{\mathcal{E}_{\boldsymbol{E},j}^{k-\frac{1}{2}}}\right) &\leq 2\sum_{k=1}^{n}\left(\left(\sum_{j=1}^{2}\mathcal{E}_{\boldsymbol{E},j}^{k+\frac{1}{2}}\right)^{\frac{1}{2}} + \left(\sum_{j=1}^{2}\mathcal{E}_{\boldsymbol{E},j}^{k-\frac{1}{2}}\right)^{\frac{1}{2}}\right) \\ &\leq 4\sum_{k=1}^{n}\left(\sum_{j=1}^{2}\mathcal{E}_{\boldsymbol{E},j}^{k+\frac{1}{2}}\right)^{\frac{1}{2}}. \end{aligned}$$

In consequence we have the following bound for the first term in (3.52)

$$\Delta t \sum_{k=1}^{n}\sum_{j=1}^{2} \mathbb{M}_{j,h}\boldsymbol{e}_{j,h}^{k} \cdot \frac{\boldsymbol{E}_{j,h}^{k+1} - \boldsymbol{E}_{j,h}^{k-1}}{2\Delta t} \leq \sqrt{8}\,K_\xi\,\Delta t \max_{\substack{1\,\leq\, j\,\leq\, 2\\ 1\,\leq\, k\,\leq\, n}}\{\|\boldsymbol{e}_{j,h}^{k}\|_{\mathbb{M}_{j,h}}\} \sum_{k=1}^{n}\left(\sum_{j=1}^{2}\mathcal{E}_{\boldsymbol{E},j}^{k+\frac{1}{2}}\right)^{\frac{1}{2}}.$$

Step 3: Estimate for the second term in (3.52).

Let us begin noticing that we can rewrite the second term in (3.52) as

$$\begin{aligned}\Delta t\sum_{k=1}^{n}\sum_{j=1}^{2}\theta_j\mathbb{A}_{j,h}\widetilde{\boldsymbol{e}}^{k}_{j,h}\cdot\frac{\boldsymbol{E}^{k+1}_{j,h}-\boldsymbol{E}^{k-1}_{j,h}}{2\Delta t} \;=\; & -\Delta t\sum_{k=1}^{n-1}\sum_{j=1}^{2}\theta_j\mathbb{A}_{j,h}\frac{\widetilde{\boldsymbol{e}}^{k+1}_{j,h}-\widetilde{\boldsymbol{e}}^{k}_{j,h}}{\Delta t}\cdot\boldsymbol{E}^{k+\frac12}_{j,h}\\ & +\Delta t\sum_{j=1}^{2}\theta_j\mathbb{A}_{j,h}\widetilde{\boldsymbol{e}}^{n}_{j,h}\cdot\boldsymbol{E}^{n+\frac12}_{j,h}\\ & -\Delta t\sum_{j=1}^{2}\theta_j\mathbb{A}_{j,h}\widetilde{\boldsymbol{e}}^{1}_{j,h}\cdot\boldsymbol{E}^{\frac12}_{j,h}.\end{aligned}$$

Now we consider Cauchy Schwartz inequality and the definition of $\mathcal{E}^{n+\frac12}_{\boldsymbol{E},j}$ to obtain the estimate

$$\begin{aligned}\Delta t\sum_{k=1}^{n}\sum_{j=1}^{2}\theta_j\mathbb{A}_{j,h}\widetilde{\boldsymbol{e}}^{k}_{j,h}\cdot\frac{\boldsymbol{E}^{k+1}_{j,h}-\boldsymbol{E}^{k-1}_{j,h}}{2\Delta t} \;\le\; & \Delta t\sum_{k=1}^{n-1}\sum_{j=1}^{2}\theta_j\left\|\frac{\widetilde{\boldsymbol{e}}^{k+1}_{j,h}-\widetilde{\boldsymbol{e}}^{k}_{j,h}}{\Delta t}\right\|_{\mathbb{A}_{j,h}}\sqrt{2\,\mathcal{E}^{k+\frac12}_{\boldsymbol{E},j}}\\ + & \;\Delta t\sum_{j=1}^{2}\theta_j\|\widetilde{\boldsymbol{e}}^{n}_{j,h}\|_{\mathbb{A}_{j,h}}\sqrt{2\,\mathcal{E}^{n+\frac12}_{\boldsymbol{E},j}}\\ + & \;\Delta t\sum_{j=1}^{2}\theta_j\|\widetilde{\boldsymbol{e}}^{1}_{j,h}\|_{\mathbb{A}_{j,h}}\sqrt{2\,\mathcal{E}^{\frac12}_{\boldsymbol{E},j}}.\end{aligned}$$

In consequence we have the following bound for the second term in (3.52)

$$\begin{aligned}\Delta t\sum_{k=1}^{n}\sum_{j=1}^{2}\theta_j\mathbb{A}_{j,h}\widetilde{\boldsymbol{e}}^{k}_{j,h}\cdot\frac{\boldsymbol{E}^{k+1}_{j,h}-\boldsymbol{E}^{k-1}_{j,h}}{2\Delta t} \;\le\; & \sqrt{8}\max_{\substack{1\le j\le 2\\ 1\le k\le n-1}}\left\{\theta_j\left\|\frac{\widetilde{\boldsymbol{e}}^{k+1}_{j,h}-\widetilde{\boldsymbol{e}}^{k}_{j,h}}{\Delta t}\right\|_{\mathbb{A}_{j,h}}\right\}\sum_{k=1}^{n-1}\Big(\sum_{j=1}^{2}\mathcal{E}^{k+\frac12}_{\boldsymbol{E},j}\Big)^{\frac12}\\ & +\sqrt{8}\,\Delta t\max_{1\le j\le 2}\{\theta_j\|\widetilde{\boldsymbol{e}}^{n}_{j,h}\|_{\mathbb{A}_{j,h}}\}\Big(\sum_{j=1}^{2}\mathcal{E}^{n+\frac12}_{\boldsymbol{E},j}\Big)^{\frac12}\\ & +\sqrt{8}\,\Delta t\max_{1\le j\le 2}\{\theta_j\|\widetilde{\boldsymbol{e}}^{1}_{j,h}\|_{\mathbb{A}_{j,h}}\}\Big(\sum_{j=1}^{2}\mathcal{E}^{\frac12}_{\boldsymbol{E},j}\Big)^{\frac12}.\end{aligned}$$

Step 4: Estimate for the energy.
Now, we notice that *Step 2* and *Step 3* can be combined to obtain from (3.52)

$$\sum_{j=1}^{2}\mathcal{E}^{n+\frac12}_{\boldsymbol{E},j}\;\le\;\sum_{j=1}^{2}\mathcal{E}^{\frac12}_{\boldsymbol{E},j}\;+\;\Delta t\,b(\Delta t)\sum_{k=1}^{n}\Big(\sum_{j=1}^{2}\mathcal{E}^{k+\frac12}_{\boldsymbol{E},j}\Big)^{\frac12}$$

where we have introduced

$$\begin{aligned}b(\Delta t)\;=\;\sqrt{8}\max_{\substack{1\le j\le 2\\ 1\le k\le n-1}}\Big\{& K_\xi\,\|\boldsymbol{e}^{k}_{j,h}\|_{\mathbb{M}_{j,h}}\;,\;K_\xi\,\|\boldsymbol{e}^{n}_{j,h}\|_{\mathbb{M}_{j,h}}\\ & ,\;\theta_j\left\|\frac{\widetilde{\boldsymbol{e}}^{k+1}_{j,h}-\widetilde{\boldsymbol{e}}^{k}_{j,h}}{\Delta t}\right\|_{\mathbb{A}_{j,h}}\;,\;\theta_j\|\widetilde{\boldsymbol{e}}^{1}_{j,h}\|_{\mathbb{A}_{j,h}}\;,\;\theta_j\|\widetilde{\boldsymbol{e}}^{n}_{j,h}\|_{\mathbb{A}_{j,h}}\Big\}.\end{aligned}$$

Then, considering the discrete Gronwall's inequality (see Lemma 3.13), we have that

$$\Big(\sum_{j=1}^{2}\mathcal{E}^{n+\frac12}_{\boldsymbol{E},j}\Big)^{\frac12}\;\le\;\Big(\sum_{j=1}^{2}\mathcal{E}^{\frac12}_{\boldsymbol{E},j}\Big)^{\frac12}\;+\;t^n\,b(\Delta t).\qquad(3.54)$$

Step 5: Estimate for $\mathcal{E}^{\frac12}_{\boldsymbol{E},j}$.

We are assuming that $f \in \mathcal{C}_0^3([0,T];L^2(\Omega_1 \setminus \omega))$, then according to Remark 3.6 we have that $\boldsymbol{u}_h \in \mathcal{C}_0^5([0,T];W_h)$. Moreover, if we recall the Taylor expansion in Remark 3.10, we can consider

$$\boldsymbol{U}_{j,h}(\Delta t) \;=\; \frac{\Delta t^3}{6}\,\frac{\mathrm{d}^3}{\mathrm{d}t^3}\boldsymbol{U}_{j,h}(s) \quad \text{and} \quad \boldsymbol{U}_{j,h}(\Delta t) \;=\; \frac{\Delta t^2}{2}\,\frac{\mathrm{d}^2}{\mathrm{d}t^2}\boldsymbol{U}_{j,h}(\widetilde{s}) \quad \text{for given} \quad s,\widetilde{s}\in[0,\Delta t].$$

Therefore, noticing that $\boldsymbol{E}^0_{j,h}=\boldsymbol{0}$ and $\boldsymbol{E}^1_{j,h}=\boldsymbol{U}_{j,h}(\Delta t)$, we find that (note $\|\cdot\|_{\widetilde{\mathbb{M}}_{j,h}} \le \|\cdot\|_{\mathbb{M}_{j,h}}$)

$$\begin{aligned}\mathcal{E}^{\frac12}_{\boldsymbol{E},j} \;&=\; \frac12\Big(\Big\|\frac{\boldsymbol{E}^1_{j,h}}{\Delta t}\Big\|^2_{\widetilde{\mathbb{M}}_{j,h}} + \Big\|\frac{\boldsymbol{E}^1_{j,h}}{2}\Big\|^2_{\mathbb{A}_{j,h}}\Big)\\ &\le\; K_0\;\Delta t^4\;\Big(\max_{t\in[0,\Delta t]}\Big\|\frac{\mathrm{d}^3}{\mathrm{d}t^3}\boldsymbol{U}_{j,h}(t)\Big\|^2_{\mathbb{M}_{j,h}} + \max_{t\in[0,\Delta t]}\Big\|\frac{\mathrm{d}^2}{\mathrm{d}t^2}\boldsymbol{U}_{j,h}(t)\Big\|^2_{\mathbb{A}_{j,h}}\Big).\end{aligned}$$

where $K_0>0$ is a constant independent of h and Δt. This provides the following estimate (note $[0,\Delta t]\subset[0,T]$)

$$\Big(\sum_{j=1}^{2}\mathcal{E}^{\frac12}_{\boldsymbol{E},j}\Big)^{\frac12} \;\le\; K_1\,\Delta t^2\,\Big(\max_{t\in[0,T]}\sqrt{m\big(\partial_t^3\boldsymbol{u}_h(t),\partial_t^3\boldsymbol{u}_h(t)\big)} \;+\; \max_{t\in[0,T]}\sqrt{a\big(\partial_t^2\boldsymbol{u}_h(t),\partial_t^2\boldsymbol{u}_h(t)\big)}\Big),$$

where $K_1>0$ is a constant independent of h and Δt.
Step 6: Estimate for $b(\Delta t)$.
As we explain at the beginning of the previous step, we are under the hypothesis that $\boldsymbol{u}_h \in \mathcal{C}^5([0,T];W_h)$. Then, we can consider the Taylor expansion, that gives for some $s_-\in[t^{k-1},t^k]$ and $s_+\in[t^k,t^{k+1}]$

$$\boldsymbol{U}_{j,h}(t^{k\pm1}) = \boldsymbol{U}_{j,h}(t^k) \pm \Delta t\,\frac{\mathrm{d}}{\mathrm{d}t}\boldsymbol{U}_{j,h}(t^k) + \frac{\Delta t^2}{2}\frac{\mathrm{d}^2}{\mathrm{d}t^2}\boldsymbol{U}_{j,h}(t^k) \pm \frac{\Delta t^3}{6}\frac{\mathrm{d}^3}{\mathrm{d}t^3}\boldsymbol{U}_{j,h}(t^k) + \frac{\Delta t^4}{24}\frac{\mathrm{d}^4}{\mathrm{d}t^4}\boldsymbol{U}_{j,h}(s_\pm).$$

In consequence, we can rewrite

$$\boldsymbol{e}^k_{j,h} = \frac{\boldsymbol{U}_{j,h}(t^{k+1}) - 2\boldsymbol{U}_{j,h}(t^k) + \boldsymbol{U}_{j,h}(t^{k-1})}{\Delta t^2} - \frac{\mathrm{d}^2}{\mathrm{d}t^2}\boldsymbol{U}_{j,h}(t^k) = \frac{\Delta t^2}{24}\Big(\frac{\mathrm{d}^4}{\mathrm{d}t^4}\boldsymbol{U}_{j,h}(s_+) + \frac{\mathrm{d}^4}{\mathrm{d}t^4}\boldsymbol{U}_{j,h}(s_-)\Big).$$

Then, we obtain the estimate (note $[0,t^{n+1}]\subset[0,T]$)

$$\max_{1\le k\le n}\{\|\boldsymbol{e}^k_{j,h}\|_{\mathbb{M}_{j,h}}\} \;\le\; \frac{\Delta t^2}{12}\max_{t\in[0,t^{n+1}]}\Big\|\frac{\mathrm{d}^4}{\mathrm{d}t^4}\boldsymbol{U}_{j,h}(t)\Big\|_{\mathbb{M}_{j,h}} \;\le\; \frac{\Delta t^2}{12}\max_{t\in[0,T]}\sqrt{m\big(\partial_t^4\boldsymbol{u}_h(t),\partial_t^4\boldsymbol{u}_h(t)\big)}.$$

Moreover, we can proceed similarly to show that for some $\widetilde{s}_+\in[t^n,t^{n+1}]$ and $\widetilde{s}_-\in[t^{n-1},t^n]$

$$\widetilde{\boldsymbol{e}}^n_{j,h} = \boldsymbol{U}_{j,h}(t^{n+1}) - 2\boldsymbol{U}_{j,h}(t^n) + \boldsymbol{U}_{j,h}(t^{n-1}) = \frac{\Delta t^2}{2}\Big(\frac{\mathrm{d}^2}{\mathrm{d}t^2}\boldsymbol{U}_{j,h}(\widetilde{s}_+) + \frac{\mathrm{d}^2}{\mathrm{d}t^2}\boldsymbol{U}_{j,h}(\widetilde{s}_-)\Big).$$

Then, we obtain the estimate (note $[t^{n-1},t^{n+1}]\subset[0,T]$)

$$\|\boldsymbol{e}^n_{j,h}\|_{\mathbb{A}_{j,h}} \;\le\; \frac{\Delta t^2}{2}\max_{t\in[t^{n-1},t^{n+1}]}\Big\|\frac{\mathrm{d}^2}{\mathrm{d}t^2}\boldsymbol{U}_{j,h}(t)\Big\|_{\mathbb{A}_{j,h}} \;\le\; \frac{\Delta t^2}{2}\max_{t\in[0,T]}\sqrt{a\big(\partial_t^2\boldsymbol{u}_h(t),\partial_t^2\boldsymbol{u}_h(t)\big)}.$$

Moreover, we notice that we have the analogous for the case $n=1$. Next, we notice that we can also rewrite for give $s_0\in[t^{k-1},t^k]$, $s_1\in[t^k,t^{k+1}]$ and $s_2\in[t^k,t^{k+2}]$

$$\frac{\widetilde{\boldsymbol{e}}^{k+1}_{j,h} - \widetilde{\boldsymbol{e}}^k_{j,h}}{\Delta t} \;=\; \frac{\Delta t^2}{6}\Big(8\,\frac{\mathrm{d}^3}{\mathrm{d}t^3}\boldsymbol{U}_{j,h}(s_2) - 3\,\frac{\mathrm{d}^3}{\mathrm{d}t^3}\boldsymbol{U}_{j,h}(s_1) + \frac{\mathrm{d}^3}{\mathrm{d}t^3}\boldsymbol{U}_{j,h}(s_0)\Big).$$

Then, we obtain the estimate (note $[0,t^{n+1}]\subset[0,T]$)

$$\begin{aligned}\max_{1\le k\le n-1}\Big\{\Big\|\frac{\widetilde{\boldsymbol{e}}^{k+1}_{j,h} - \widetilde{\boldsymbol{e}}^k_{j,h}}{\Delta t}\Big\|_{\mathbb{A}_{j,h}}\Big\} \;&\le\; 2\,\Delta t^2\max_{t\in[0,t^{n+1}]}\Big\|\frac{\mathrm{d}^3}{\mathrm{d}t^3}\boldsymbol{U}_{j,h}(t)\Big\|_{\mathbb{A}_{j,h}}\\ &\le\; 2\,\Delta t^2\max_{t\in[0,T]}\sqrt{a\big(\partial_t^3\boldsymbol{u}_h(t),\partial_t^3\boldsymbol{u}_h(t)\big)}.\end{aligned}$$

In consequence, we can combine previous estimates to obtain

$$b(\Delta t) \;\leq\; K_2\,\Delta t^2 \Big(\max_{t\in[0,T]} \sqrt{m\big(\partial_t^4 \boldsymbol{u}_h(t), \partial_t^4 \boldsymbol{u}_h(t)\big)} \;+\; \max_{t\in[0,T]} \sqrt{a\big(\partial_t^2 \boldsymbol{u}_h(t), \partial_t^2 \boldsymbol{u}_h(t)\big)} \;+\; \max_{t\in[0,T]} \sqrt{a\big(\partial_t^3 \boldsymbol{u}_h(t), \partial_t^3 \boldsymbol{u}_h(t)\big)}\Big),$$

where $K_2 > 0$ is a constant independent of h and Δt.
Step 7: Estimate for the error.
In order to estimate the error, we apply triangular inequality and consider (3.53) to obtain

$$\|\boldsymbol{E}_{j,h}^{n+1}\|^2_{\mathbb{M}_{j,h}} \;\leq\; \|\boldsymbol{E}_{j,h}^{n}\|^2_{\mathbb{M}_{j,h}} + \|\boldsymbol{E}_{j,h}^{n+1} - \boldsymbol{E}_{j,h}^{n}\|^2_{\mathbb{M}_{j,h}} \;\leq\; \|\boldsymbol{E}_{j,h}^{n}\|^2_{\mathbb{M}_{j,h}} + 2\,\Delta t^2\,K_{\xi,j}^2\,\mathcal{E}_{\boldsymbol{E},j}^{n+\frac{1}{2}}.$$

Therefore, if we sum by recursion up to $n = 0$ and consider estimate (3.54), we have that (notice $\boldsymbol{E}_{j,h}^0 = \boldsymbol{0}$)

$$\begin{aligned}\Big(\sum_{j=1}^{2} \|\boldsymbol{E}_{j,h}^{n+1}\|^2_{\mathbb{M}_{j,h}}\Big)^{\frac{1}{2}} \;&\leq\; \sqrt{2}\,\Delta t\,K_\xi \sum_{k=0}^{n} \Big(\sum_{j=1}^{2} \mathcal{E}_{\boldsymbol{E},j}^{k+\frac{1}{2}}\Big)^{\frac{1}{2}} \\ &\leq\; \sqrt{2}\,t^{n+1}\,K_\xi \Big(\sum_{j=1}^{2} \mathcal{E}_{\boldsymbol{E},j}^{\frac{1}{2}}\Big)^{\frac{1}{2}} \;+\; \sqrt{2}\,(t^{n+1})^2\,K_\xi\,b(\Delta t).\end{aligned}$$

Now, we consider the estimates provided in *Step 5* and *Step 6*, there exists a constant $K_3 > 0$ only depending in ξ and T, such that

$$\begin{aligned}\Big(\sum_{j=1}^{2} \|\boldsymbol{E}_{j,h}^{n+1}\|^2_{\mathbb{M}_{j,h}}\Big)^{\frac{1}{2}} \;\leq\; K_3\,\Delta t^2 \Big(& \max_{t\in[0,T]} \sqrt{m\big(\partial_t^4 \boldsymbol{u}_h(t), \partial_t^4 \boldsymbol{u}_h(t)\big)} \;+\; \max_{t\in[0,T]} \sqrt{m\big(\partial_t^3 \boldsymbol{u}_h(t), \partial_t^3 \boldsymbol{u}_h(t)\big)} \\ &+\; \max_{t\in[0,T]} \sqrt{a\big(\partial_t^3 \boldsymbol{u}_h(t), \partial_t^3 \boldsymbol{u}_h(t)\big)} \;+\; \max_{t\in[0,T]} \sqrt{a\big(\partial_t^2 \boldsymbol{u}_h(t), \partial_t^2 \boldsymbol{u}_h(t)\big)}\Big).\end{aligned}$$

On the other hand, we also have that (considering definition of $\mathcal{E}_{\boldsymbol{E},j}^{n+\frac{1}{2}}$ and estimate (3.54))

$$\Big(\sum_{j=1}^{2} \|\boldsymbol{E}_{j,h}^{n+\frac{1}{2}}\|^2_{\mathbb{A}_{j,h}}\Big)^{\frac{1}{2}} \;\leq\; \sqrt{2}\Big(\sum_{j=1}^{2} \mathcal{E}_{\boldsymbol{E},j}^{n+\frac{1}{2}}\Big)^{\frac{1}{2}} \;\leq\; \sqrt{2}\Big(\sum_{j=1}^{2} \mathcal{E}_{\boldsymbol{E},j}^{\frac{1}{2}}\Big)^{\frac{1}{2}} \;+\; \sqrt{2}\,t^n\,b(\Delta t).$$

Thus, considering the estimates provided in *Step 5* and *Step 6*, there exists a constant $K_4 > 0$ only depending in ξ and T, such that

$$\begin{aligned}\Big(\sum_{j=1}^{2} \|\boldsymbol{E}_{j,h}^{n+\frac{1}{2}}\|^2_{\mathbb{A}_{j,h}}\Big)^{\frac{1}{2}} \;\leq\; K_4\,\Delta t^2 \Big(& \max_{t\in[0,T]} \sqrt{m\big(\partial_t^4 \boldsymbol{u}_h(t), \partial_t^4 \boldsymbol{u}_h(t)\big)} \;+\; \max_{t\in[0,T]} \sqrt{m\big(\partial_t^3 \boldsymbol{u}_h(t), \partial_t^3 \boldsymbol{u}_h(t)\big)} \\ &+\; \max_{t\in[0,T]} \sqrt{a\big(\partial_t^3 \boldsymbol{u}_h(t), \partial_t^3 \boldsymbol{u}_h(t)\big)} \;+\; \max_{t\in[0,T]} \sqrt{a\big(\partial_t^2 \boldsymbol{u}_h(t), \partial_t^2 \boldsymbol{u}_h(t)\big)}\Big).\end{aligned}$$

Finally, we remark that since $f \in \mathcal{C}_0^3([0,T]; L^2(\Omega_1 \setminus \omega))$ and according to Remark 3.6, we have

$$\begin{aligned}\Big(\sum_{j=1}^{2} \|\boldsymbol{E}_{j,h}^{n+1}\|^2_{\mathbb{M}_{j,h}}\Big)^{\frac{1}{2}} \;&\leq\; \frac{K_3\,\Delta t^2}{\sqrt{\rho_0}} \sum_{k=2}^{3} \|\partial_t^k f\|_{L^1([0,T];L^2(\Omega_1\setminus\omega))}, \\ \Big(\sum_{j=1}^{2} \|\boldsymbol{E}_{j,h}^{n+\frac{1}{2}}\|^2_{\mathbb{A}_{j,h}}\Big)^{\frac{1}{2}} \;&\leq\; \frac{K_4\,\Delta t^2}{\sqrt{\rho_0}} \sum_{k=2}^{3} \|\partial_t^k f\|_{L^1([0,T];L^2(\Omega_1\setminus\omega))}.\end{aligned}$$

■

3.5 Numerical results

In this section we present some numerical results to exhibit the good properties of the method. We first show 1D numerical space-time convergence analysis as well as a numerical illustration of the local CFL condition when considering constant and non constant physical coefficients. Then, we present an illustrative 2D numerical example where we exhibit the good behaviour of the method in a more realistic situation.

3.5.1 1D convergence test

We begin by recalling Section 2.6.1 where a similar set up was developed for the 1D Helmholtz equation. Here we consider the same definition for the computational domain as well as the same choices for the regions involved in the Arlequin formulations and their respective meshes. In the following we detail the differences relative to the continuous equations, physical coefficients and the choice of partitioning. Moreover, we also specify the information concerning time discretization.

Continuous equations. We look for $u(x,t)$, solution of the one-dimensional wave equation

$$\rho\, \partial_t^2 u - \partial_x \cdot \mu\, \partial_x u = 0, \quad x \in [0,\infty), \quad t > 0,$$

with zero initial data and inhomogeneous Dirichlet boundary condition at $x = 0$. Moreover, we simulate the unbounded domain by considering outgoing boundary conditions which are known to be exact in 1D settings. Therefore, in the bounded domain $\Omega = [0,3]$, we consider

$$u(0,t) = u_D(t) \quad \text{and} \quad \partial_t u(3,t) + \sqrt{\frac{\mu(3)}{\rho(3)}}\, \partial_x u(3,t) = 0 \quad \text{for all} \quad t > 0.$$

Notice that in the case of constant coefficients, this problem represents a smooth pulse travelling from left to right since its solution can be easily computed by

$$u(x,t) = u_D\big(t - \sqrt{\frac{\rho}{\mu}}\, x\big), \quad x \in (0,3), \quad t \in [0,T]. \tag{3.55}$$

In the following, we shall consider the time bounded by $T = 15$ and the Dirichlet data given by (see Figure 3.2)

$$u_D(t) = 1_{[0,7.5)} \frac{200 \cdot 12^2\,(3 - 2\,t)}{2\left(t + \frac{9}{2}\right)^2 \left(t - \frac{15}{2}\right)^2} \quad e^{\frac{200\cdot 12^2}{\left(t+\frac{9}{2}\right)\left(t-\frac{15}{2}\right)} + 200\cdot 4}.$$

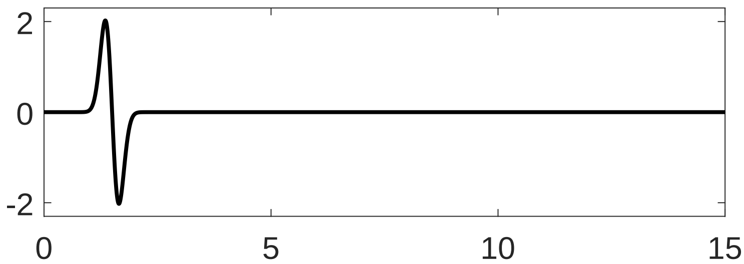

Figure 3.2: Dirichlet data $u_D(t)$, $t \in [0,15]$ for the 1D convergence test.

Physical coefficients and partitioning. We consider two different cases, one with **constant** physical coefficients $\rho = \mu = 1$ and another with the **non constant** physical coefficients given by

$$\rho = 1 - \frac{\sin(\frac{8\pi x}{3})}{10}, \quad \text{and} \quad \mu = 1 + 10\, e^{\frac{500\cdot 6^2}{(x+\frac{3}{4})(x-\frac{21}{4})}+4\cdot 500}.$$

In both cases, we consider the partitioning defined by

$$\alpha_1 = \begin{cases} \dfrac{3}{4\,\rho} & \text{in } \omega_i \cup \omega_e \\ \dfrac{1}{2} & \text{in } \omega_c \end{cases}, \quad \beta_1 = \begin{cases} \dfrac{1}{4\,\mu} & \text{in } \omega_i \cup \omega_e \\ \dfrac{1}{2} & \text{in } \omega_c \end{cases}, \quad \alpha_2 = 1 - \alpha_1, \quad \beta_2 = 1 - \beta_1,$$

as illustrated in Figure 3.3 for the volume-volume coupling. Notice that the choice of the partitioning is made to alleviate the time step restriction in the case we choose an explicit scheme in Ω_1 (see equation (3.48)).

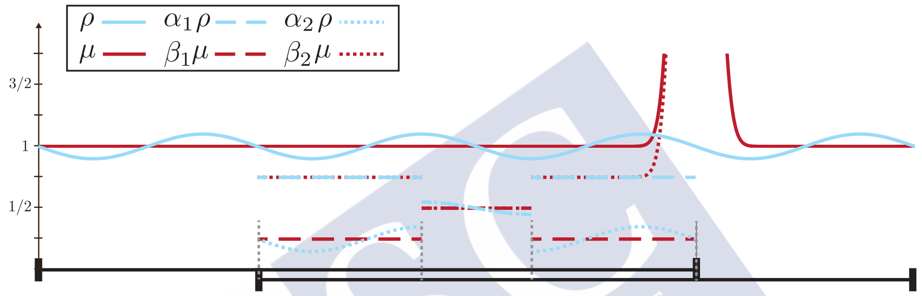

Figure 3.3: Parameters of the 1D experiment in the inhomogeneous case when volume-volume coupling is used.

Time discretization. We use the algorithm presented in Section 3.4.1 with

$$\theta_1 = 0 \quad \text{and} \quad \theta_2 = \frac{1}{4}.$$

Therefore, as explained in Section 3.4.4 the time step restriction depends only in the properties of the matrices $\mathbb{M}_{1,h}$ and $\mathbb{A}_{1,h}$ that are relative to the space discretization in the coarse region. Moreover, the time step Δt can be estimated locally by (3.47), thus we choose $\Delta t = \min \Delta t_k$.

Numerical illustration of the local CFL. It is interesting to compare the computations of $\Delta\tau_k$ and Δt_k (defined in Section 3.4.4). In Figures 3.4 and 3.5 we show the comparison for **constant** and **non constant** coefficients respectively when second order finite elements are used. One can see that in both cases the local CFL is improved when the Arlequin method is considered. However, it is important to notice that this may not have an impact in the local estimates (3.46) and (3.47) since the time step is considered as the minimum. For instance, in the case of **constant** coefficients the sufficient condition (3.47) remains the same with and without coupling. On the other hand, in the case of **non constant** coefficients the improvement of condition (3.47) is substantial. Finally, we should also notice that in the case of **boundary-boundary** coupling and **boundary-volume** coupling the heterogeneities happen inside of ω_c, thus Δt_k is also penalised and the maximum time step would be very restrictive. However, in order to circumvent this issue we have presented in Section 3.4.5 a locally implicit scheme that would allow to consider a time step such that

$$\Delta t < \min_{\kappa_k \in \widetilde{\mathcal{T}}_{1,h}} \{\Delta t_k\},$$

where $\widetilde{\mathcal{T}}_{1,h} \subset \mathcal{T}_{1,h}$ where $\widetilde{\mathcal{T}}_{1,h}$ is the triangulation of a sub-domain of $\Omega_1 \setminus \omega_c$ (note that ω_c may not be conform with $\mathcal{T}_{1,h}$).

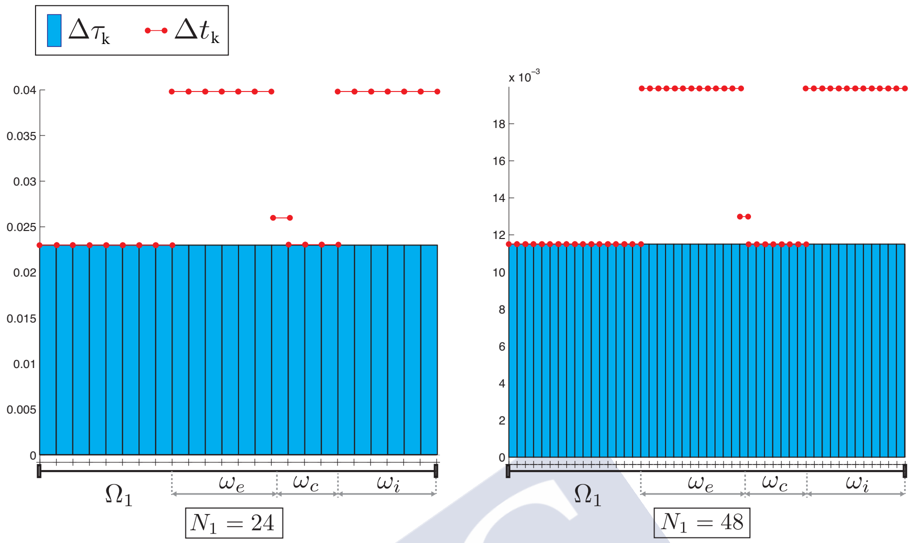

Figure 3.4: Histogram representing the local estimation of the CFL for each element of the mesh with second order elements in the case of **constant** physical coefficients.

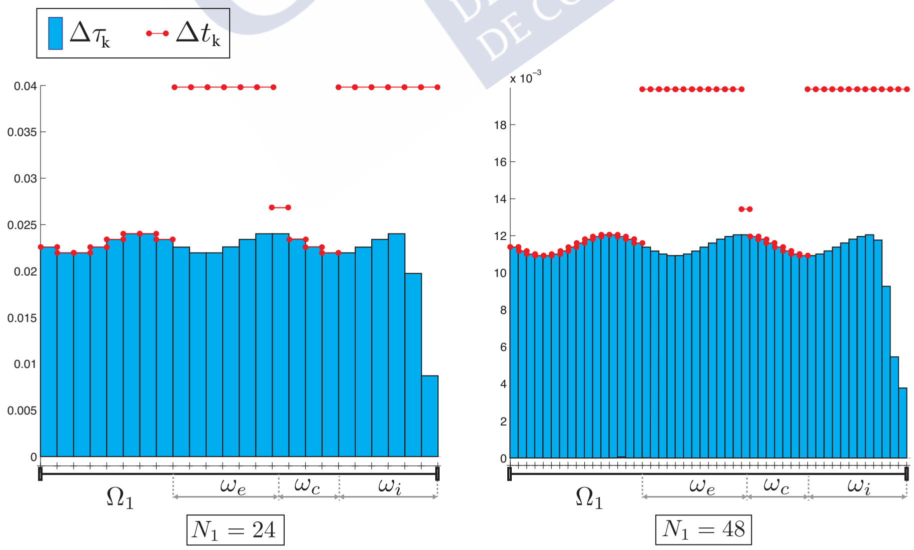

Figure 3.5: Histogram representing the local estimate of the CFL for each element of the mesh with second order elements in the case of **non constant** physical coefficients.

Convergence results. We study the space-time convergence behaviour of the volume unknown u_1 and u_2 in the following norm

$$\|e_1\| := \frac{\|u_{|\Omega_1} - u_{1,h}\|_{L^2(0,T;H^1(\Omega_1))}}{\|u_{|\Omega_1}\|_{L^2(0,T;H^1(\Omega_1))}} \quad \text{and} \quad \|e_2\| := \frac{\|u_{|\Omega_2} - u_{2,h}\|_{L^2(0,T;H^1(\Omega_2))}}{\|u_{|\Omega_2}\|_{L^2(0,T;H^1(\Omega_2))}},$$

where the solution u is given by (3.55) in the case of **constant** coefficients and it is computed numerically on a fine grid for the case of **non constant** coefficients. Numerical results presented in tables 3.1, 3.2, 3.3 and 3.9 and figures 3.6, 3.7, 3.8 and 3.9 show that all variants keep the appropriate convergence rate. Indeed, we observe that the results are better than expected when considering first order Lagrange finite elements. Moreover, we also compare the results obtained for the different couplings. Thus notice that in the case of **constant** coefficients we observe a slight increase of the error for the new variants compared to classic Arlequin. However, this lost of accuracy is justified by the computational time saved due to the flexibility on the mesh generation and the reduction of degrees of freedom of the Lagrange multiplier used to impose the matching on the overlapping region. Moreover, we remark that this effect does not appear to be general since in the case of **non constant** coefficients it is not observed. Let us also remark that in the case of **non constant** physical coefficients, the convergence curves for **BB** and **BV** couplings are not really comparable to the other variants since the time step is much smaller. This is due to the CFL condition (3.5) which, on those cases when the strong variation of the physical coefficients happens inside of ω_c, leads to a more restrictive condition and therefore a smaller time step. Finally, notice that all the new variants provide similar numerical results (not shown) when we consider a different ratio between the meshes involved or when γ_e is not forced to be a node of the mesh for Ω_1, situation which is not compatible with standard Arlequin method.

		V		**VV**		**VB**		**BV**		**BB**	
h_1	Δt	$\|e_1\|$	Slope	$\|e_1\|$	Slope	$\|e_1\|$	Slope	$\|e_1\|$	Slope	$\|e_1\|$	Slope
0.188	0.1027	1.0926		1.4881		1.7165		1.8110		1.7679	
0.094	0.0514	0.5079	1.11	0.6744	1.14	0.9206	0.90	1.0277	0.82	1.2519	0.50
0.047	0.0257	0.1677	1.60	0.2179	1.63	0.3310	1.48	0.3394	1.60	0.4887	1.36
0.023	0.0129	0.0450	1.90	0.0613	1.83	0.0976	1.76	0.0990	1.78	0.1436	1.77
0.012	0.0064	0.0114	1.98	0.0157	1.97	0.0252	1.96	0.0254	1.96	0.0371	1.95
0.006	0.0032	0.0029	1.99	0.0040	1.99	0.0063	1.99	0.0064	1.99	0.0093	1.99
h_1	Δt	$\|e_2\|$	Slope	$\|e_2\|$	Slope	$\|e_2\|$	Slope	$\|e_2\|$	Slope	$\|e_2\|$	Slope
0.188	0.1027	1.3319		1.5931		1.6914		1.7273		1.7214	
0.094	0.0514	0.6165	1.11	0.7708	1.05	0.8461	1.00	0.9331	0.89	1.1050	0.64
0.047	0.0257	0.2010	1.62	0.2559	1.59	0.3234	1.39	0.3433	1.44	0.4418	1.32
0.023	0.0129	0.0538	1.90	0.0740	1.79	0.0956	1.76	0.0998	1.78	0.1325	1.74
0.012	0.0064	0.0138	1.96	0.0225	1.72	0.0245	1.96	0.0282	1.82	0.0340	1.96
0.006	0.0032	0.0036	1.94	0.0084	1.42	0.0062	1.98	0.0094	1.59	0.0085	2.00

Table 3.1: 1D Convergence table when considering **constant** coefficients and **first order** Lagrange finite elements.

		V		**VV**		**VB**		**BV**		**BB**	
h_1	Δt	$\|e_1\|$	Slope	$\|e_1\|$	Slope	$\|e_1\|$	Slope	$\|e_1\|$	Slope	$\|e_1\|$	Slope
0.188	0.0459	0.2507		0.3895		0.5534		0.6558		0.8612	
0.094	0.0230	0.0363	2.79	0.0675	2.53	0.1498	1.89	0.1448	2.18	0.2319	1.89
0.047	0.0115	0.0057	2.66	0.0161	2.07	0.0354	2.08	0.0357	2.02	0.0552	2.07
0.023	0.0057	0.0012	2.23	0.0037	2.12	0.0086	2.05	0.0085	2.07	0.0134	2.05
0.012	0.0029	0.0003	2.06	0.0009	2.05	0.0021	2.01	0.0021	2.03	0.0033	2.01
0.006	0.0014	0.0001	2.02	0.0002	2.02	0.0005	2.00	0.0005	2.01	0.0008	2.00
h_1	Δt	$\|e_2\|$	Slope	$\|e_2\|$	Slope	$\|e_2\|$	Slope	$\|e_2\|$	Slope	$\|e_2\|$	Slope
0.188	0.0459	0.2638		0.4230		0.5823		0.6338		0.8123	
0.094	0.0230	0.0357	2.89	0.0715	2.57	0.1498	1.96	0.1453	2.12	0.2273	1.84
0.047	0.0115	0.0065	2.45	0.0169	2.08	0.0349	2.10	0.0358	2.02	0.0545	2.06
0.023	0.0057	0.0016	2.02	0.0040	2.08	0.0084	2.05	0.0086	2.07	0.0132	2.04
0.012	0.0029	0.0004	1.99	0.0010	2.03	0.0021	2.01	0.0021	2.02	0.0033	2.01
0.006	0.0014	0.0001	2.00	0.0002	2.01	0.0005	2.00	0.0005	2.01	0.0008	2.00

Table 3.2: 1D Convergence table when considering **constant** coefficients and **second order** Lagrange finite elements.

		V		VV		VB			BV		BB	
h_1	Δt	$\Vert e_1\Vert$	Slope	$\Vert e_1\Vert$	Slope	$\Vert e_1\Vert$	Slope	Δt	$\Vert e_1\Vert$	Slope	$\Vert e_1\Vert$	Slope
0.188	0.1042	1.2626		1.3571		1.4679		0.0644	1.5213		1.5757	
0.094	0.0507	1.0381	0.28	1.0248	0.41	1.0696	0.46	0.0249	1.0780	0.50	1.2201	0.37
0.047	0.0250	0.6125	0.76	0.5428	0.92	0.6130	0.80	0.0102	0.6167	0.81	0.6684	0.87
0.023	0.0124	0.2072	1.56	0.1734	1.65	0.2029	1.60	0.0045	0.2013	1.61	0.2124	1.65
0.012	0.0062	0.0542	1.93	0.0450	1.94	0.0528	1.94	0.0021	0.0519	1.96	0.0546	1.96
0.006	0.0031	0.0137	1.99	0.0114	1.99	0.0133	1.99	0.0010	0.0130	1.99	0.0137	2.00
h_1	Δt	$\Vert e_2\Vert$	Slope	$\Vert e_2\Vert$	Slope	$\Vert e_2\Vert$	Slope	Δt	$\Vert e_2\Vert$	Slope	$\Vert e_2\Vert$	Slope
0.188	0.1042	1.3601		1.3926		1.5624		0.0644	1.4528		1.3504	
0.094	0.0507	1.0584	0.36	1.0544	0.40	0.9962	0.65	0.0249	1.0451	0.48	0.9961	0.44
0.047	0.0250	0.6061	0.80	0.5421	0.96	0.5615	0.83	0.0102	0.5508	0.92	0.5366	0.89
0.023	0.0124	0.2034	1.58	0.1725	1.65	0.1819	1.63	0.0045	0.1738	1.66	0.1676	1.68
0.012	0.0062	0.0553	1.88	0.0477	1.85	0.0479	1.92	0.0021	0.0470	1.89	0.0427	1.97
0.006	0.0031	0.0159	1.79	0.0147	1.70	0.0128	1.91	0.0010	0.0139	1.76	0.0107	2.00

Table 3.3: 1D Convergence table when considering **non constant** coefficients and **first order** Lagrange finite elements.

		V		VV		VB			BV		BB	
h_1	Δt	$\Vert e_1\Vert$	Slope	$\Vert e_1\Vert$	Slope	$\Vert e_1\Vert$	Slope	Δt	$\Vert e_1\Vert$	Slope	$\Vert e_1\Vert$	Slope
0.188	0.0459	0.6108		0.5935		0.7309		0.0213	0.7358		0.8157	
0.094	0.0225	0.0528	3.53	0.0644	3.20	0.1809	2.01	0.0095	0.1460	2.33	0.1707	2.26
0.047	0.0111	0.0187	1.50	0.0144	2.16	0.0358	2.34	0.0042	0.0134	3.44	0.0156	3.45
0.023	0.0055	0.0059	1.65	0.0046	1.66	0.0085	2.07	0.0019	0.0016	3.05	0.0021	2.87
0.012	0.0027	0.0016	1.93	0.0012	1.93	0.0021	2.03	0.0009	0.0003	2.51	0.0004	2.37
0.006	0.0014	0.0004	1.99	0.0003	1.99	0.0005	2.01	0.0004	0.0001	2.22	0.0001	2.14
h_1	Δt	$\Vert e_2\Vert$	Slope	$\Vert e_2\Vert$	Slope	$\Vert e_2\Vert$	Slope	Δt	$\Vert e_2\Vert$	Slope	$\Vert e_2\Vert$	Slope
0.188	0.0459	0.5727		0.6027		0.6973		0.0213	0.6161		0.6056	
0.094	0.0225	0.0574	3.32	0.0692	3.12	0.1805	1.95	0.0095	0.1233	2.32	0.1358	2.16
0.047	0.0111	0.0202	1.51	0.0165	2.07	0.0415	2.12	0.0042	0.0135	3.19	0.0134	3.34
0.023	0.0055	0.0062	1.70	0.0050	1.73	0.0101	2.04	0.0019	0.0023	2.53	0.0021	2.68
0.012	0.0027	0.0016	1.94	0.0013	1.94	0.0025	2.02	0.0009	0.0005	2.16	0.0004	2.26
0.006	0.0014	0.0004	1.99	0.0003	1.99	0.0006	2.01	0.0004	0.0001	2.06	0.0001	2.10

Table 3.4: 1D Convergence table when considering **non constant** coefficients and **second order** Lagrange finite elements.

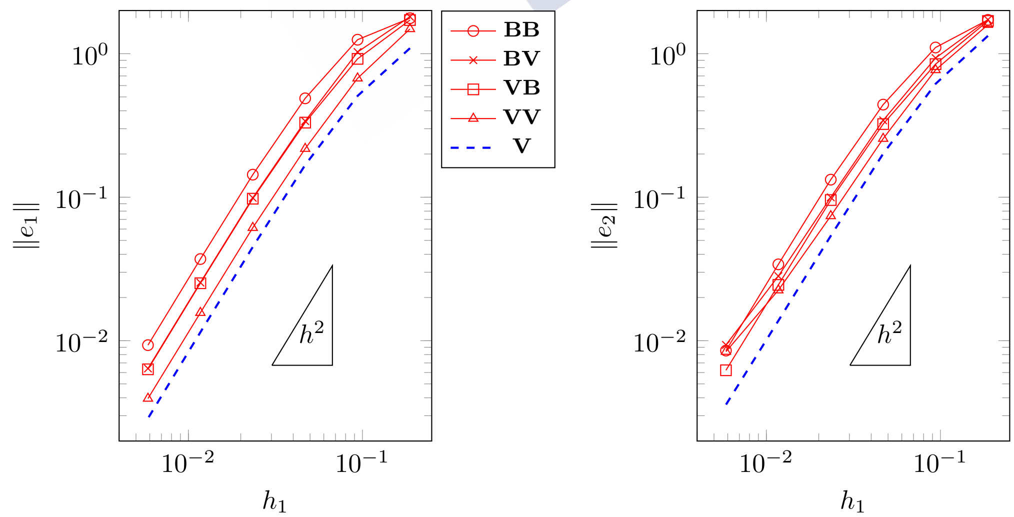

(a) Error in Ω_1. (b) Error in Ω_2.

Figure 3.6: 1D Convergence curves when considering **constant** coefficients and **first order** Lagrange finite elements.

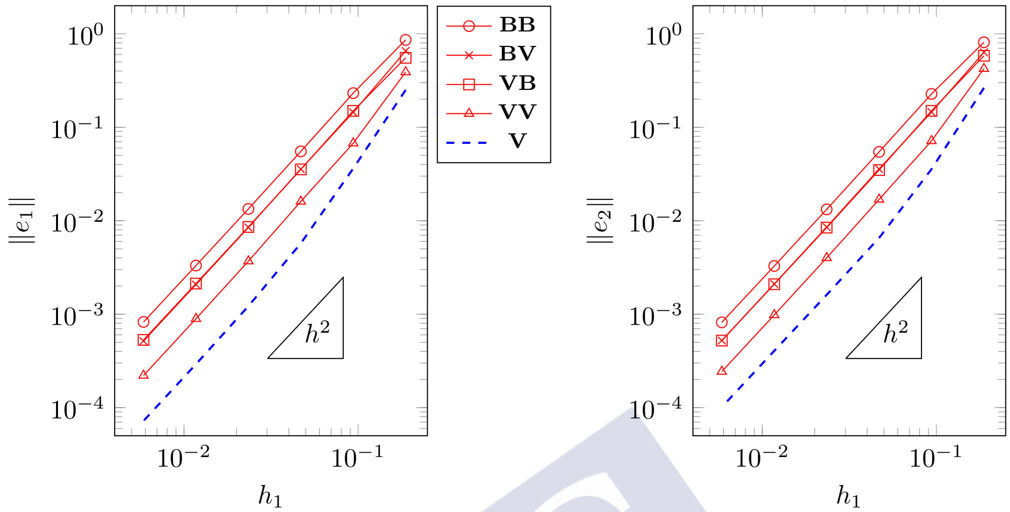

(a) Error in Ω_1. (b) Error in Ω_2.

Figure 3.7: 1D Convergence curves when considering **constant** coefficients and **second order** Lagrange finite elements.

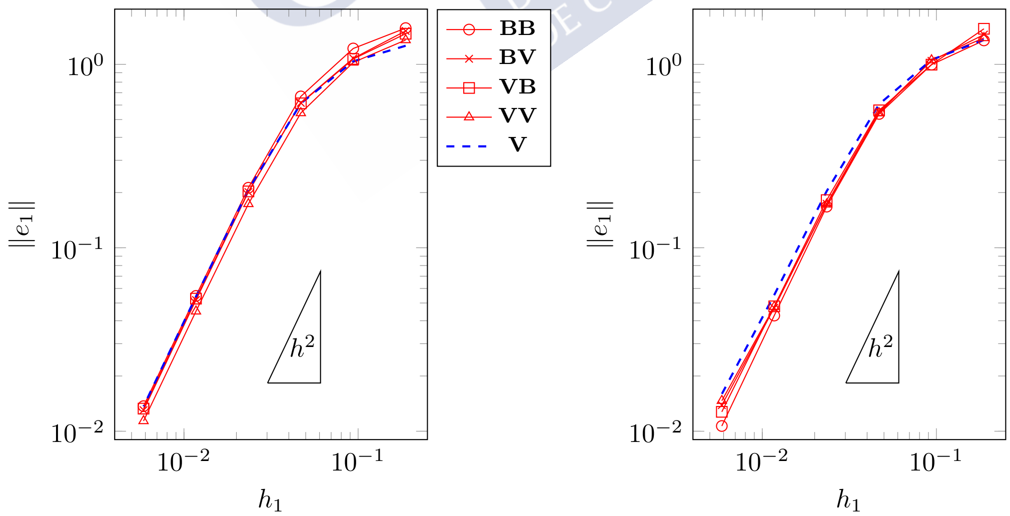

(a) Error in Ω_1. (b) Error in Ω_2.

Figure 3.8: 1D Convergence curves when considering **non constant** coefficients and **first order** Lagrange finite elements.

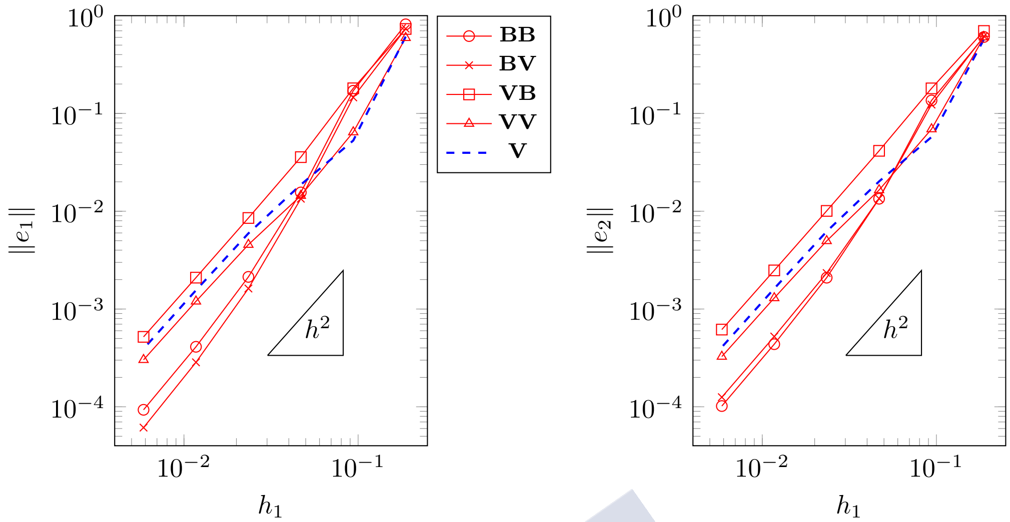

(a) Error in Ω_1.

(b) Error in Ω_2.

Figure 3.9: 1D Convergence curves when considering **non constant** coefficients and **second order** Lagrange finite elements.

3.5.2 2D numerical example in a more realistic situation

In this section, similarly to what we have presented in Section 2.8.2, we solve a more realistic problem where we consider an elliptic obstacle $\mathcal{O}$ surrounded by a damaged region. We consider the same type of computational domains, as well as the same choices for the regions involved in the Arlequin formulations and their respective meshes. In the following, we detail the differences relative to the continuous equations, physical coefficients, type of coupling and the choice of partitioning. Moreover, we also specify the information concerning time discretization.

Continuous equations. The example we provide corresponds to a transient wave scattered by an obstacle $\mathcal{O}$ in an unbounded medium. Thus we look for $u(\boldsymbol{x}, t)$ solution of the following wave equation (completed with vanishing initial data)

$$\left\{ \begin{array}{rcll} \rho\, \partial_t^2 u - \nabla \cdot \mu \nabla u & = & f & \text{in} \quad \mathbb{R}^2 \setminus \mathcal{O}, \\ \nabla u \cdot \mathbf{n} & = & 0 & \text{on} \quad \partial\mathcal{O}, \end{array} \right. \tag{3.56}$$

where the time is bounded by $T = 15$ and the medium is excited by a source expressed by (see figures 3.10a and 3.10b)

$$f(\boldsymbol{x}, t) = \frac{f_t(t) f_{\boldsymbol{x}}(\boldsymbol{x})}{\sup\limits_{s \in [0,T]} f_t(s)} \quad \text{where} \quad f_t(t) = 36(t - 1.5)e^{-36(t-1.5)^2} \quad \text{and} \quad f_{\boldsymbol{x}}(\boldsymbol{x}) = e^{-10|\boldsymbol{x}|^2}.$$

Notice that the obstacle $\mathcal{O}$ is defined as in Section 2.8.2 by the ellipse

$$\mathcal{O}(\boldsymbol{x}_0, \theta) = \begin{pmatrix} \cos(\theta) & \sin(\theta) \\ -\sin(\theta) & \cos(\theta) \end{pmatrix} \mathcal{O}_0 + \boldsymbol{x}_0,$$

where the pair $(\boldsymbol{x}_0, \theta)$ provides the centre and rotation of the obstacle and $\mathcal{O}_0$ denotes an ellipse centred at the origin, with semi-major and semi-minor axes aligned with the Cartesian axes and which length are given by 0.4 and 0.08 respectively. We also assume that a damaged region surrounds the obstacle and we model this effect by considering (see Figure 3.10c)

$$\rho(\boldsymbol{x}) = 1 \quad \text{and} \quad \mu(\boldsymbol{x}) = 1 + 10\, e^{-20|\boldsymbol{x}-\boldsymbol{x}_0|^2} \quad \text{for all} \quad \boldsymbol{x} \in \mathbb{R}^2 \setminus \mathcal{O}(\boldsymbol{x}_0, \theta).$$

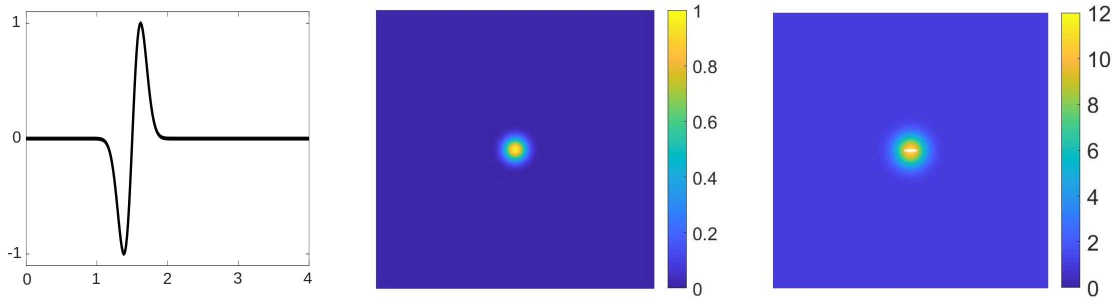

(a) Plot of $f_t(t)$, $t \in [0,4]$. (b) Plot of $f_{\boldsymbol{x}}$ in Θ. (c) Plot of μ in $\Theta \setminus \mathcal{O}_0$.

Figure 3.10: Graphic representation of the source term and the physical coefficient μ.

Moreover, Perfectly Matched Layers (see [68]) are used to simulate the unbounded medium, leading to the following bounded computational domain

$$\Omega = \Theta \setminus \mathcal{O}(\boldsymbol{x}_0, \theta), \quad \text{where} \quad \Theta = [-4,4] \times [-4,4].$$

Arlequin formulation. We choose to use the **volume-boundary** coupling (i.e. $\omega_i \neq \emptyset$ and $\omega_e = \emptyset$) to solve problem (3.56) considering the domain Ω decomposed as in Section 2.8.2. Notice that now, due to the type of coupling we are considering, we need also to specify the choice of the region ω_i. This region will also depend on the position we choose for the obstacle $\mathcal{O}(\boldsymbol{x}_0, \theta)$ and we recall that it must be conform with the mesh considered for the background media Θ, thus it is detailed later for each specific configuration. Finally, in order verify Assumption I.2 as well as capture the strong variations of the physical coefficients with Ω_2, we choose the partitioning in the overlapping region ω to be given by

$$\alpha_1 = \frac{1}{2}, \quad \beta_1 = \begin{cases} \dfrac{1}{4\,\mu} & \text{in } \omega_i \\ \dfrac{1}{2} & \text{in } \omega_c \end{cases} \quad \text{and} \quad \alpha_2 = 1 - \alpha_1, \quad \beta_2 = 1 - \beta_1.$$

Notice that this choice of the partitioning is made to alleviate the time step restriction in the case we choose an explicit scheme in Ω_1 (see equation (3.48)).

Time discretization. We use the algorithm presented in Section 3.4.1 with

$$\theta_1 = 0 \quad \text{and} \quad \theta_2 = \frac{1}{4}.$$

Therefore, as explained in Section 3.4.4 the time step restriction depends only in the properties of the matrices $\mathbb{M}_{1,h}$ and $\mathbb{A}_{1,h}$ that are relative to the space discretization in the coarse region. Moreover, the time step Δt can be estimated locally by (3.47), thus we choose $\Delta t = \min \Delta t_k$. In order to justify the use of the **volume-boundary** coupling, we compare in Figure 3.11 the computations of $\Delta \tau_k$ and Δt_k for one specific configuration.

Numerical results. We consider the three particular cases presented in Section 2.8.2. Therefore, we use the meshes plotted in figures 2.34, 2.35 and 2.36. Moreover, we choose ω_i as the first three rows of elements surrounding the region $\mathcal{S}^h_{\mathcal{O}}$, thus it is automatically conform with the mesh

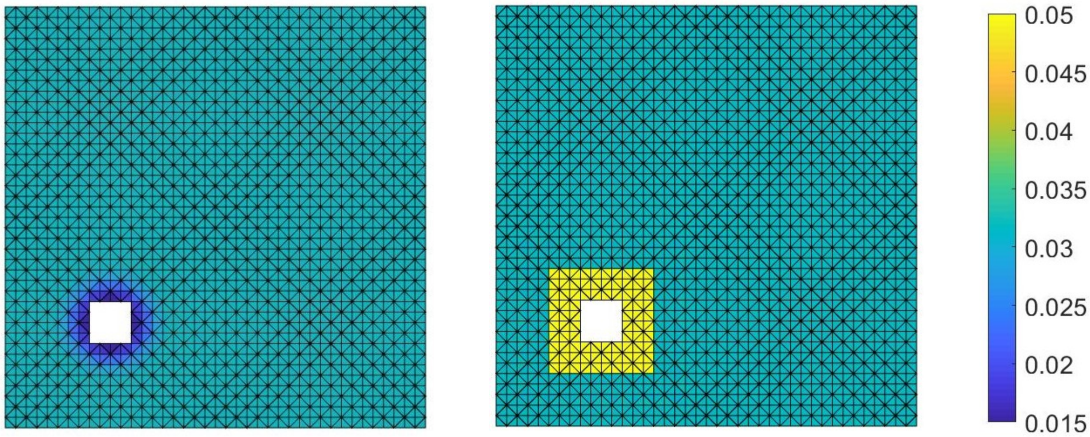

Figure 3.11: Representation of the local estimation of the CFL for each element of the mesh in case 1. On the left we see $\Delta\tau_k$ and on the right we plot Δt_k.

of the background media Θ. In consequence:

$$\begin{array}{lll}
\underline{\text{Case 1}}: & \underline{\text{Case 2}}: & \underline{\text{Case 3}}: \\
(\boldsymbol{x}_0,\theta) = \left((-2,-2), \dfrac{\pi}{2}\right), & (\boldsymbol{x}_0,\theta) = \left((0.5,2.2), \dfrac{\pi}{20}\right), & (\boldsymbol{x}_0,\theta) = \left((1.5,-1.8), \dfrac{3\,\pi}{8}\right), \\
S^h_{\mathcal{O}} = [-2.4,-1.6]\times[-2.4,-1.6], & S^h_{\mathcal{O}} = [0,1]\times[1.8,2.6], & S^h_{\mathcal{O}} = [1,2]\times[-2.2,-1.4], \\
\omega_i = [-3,-1]\times[-3,-1], & \omega_i = [-0.6,1.6]\times[1.2,3.2], & \omega_i = [0.4,2.6]\times[-2.8,-0.8].
\end{array}$$

Moreover, in figures 3.12, 3.13 and 3.14 we compare the results with respect to a solution obtained by a standard finite element method considering second order finite elements in space and a second order implicit time discretization. We recall that the meshes considered have a number of nodes which is comparable to the sum of the number of nodes of the meshes considered for Ω_1 and Ω_2 (see figures 2.34, 2.35 and 2.36).

Finally, we observe that figures 3.12, 3.13 and 3.14 show a good agreement between the numerical solutions obtained with the Arlequin method and the classical method. The reader should notice that the advantage of the Arlequin method is that the re-meshing procedure required to generate meshes of Ω for the classical method, has been replaced by the adjustment of the meshes of Θ (which moreover is structured) and Ω_2^0 which is more efficient.

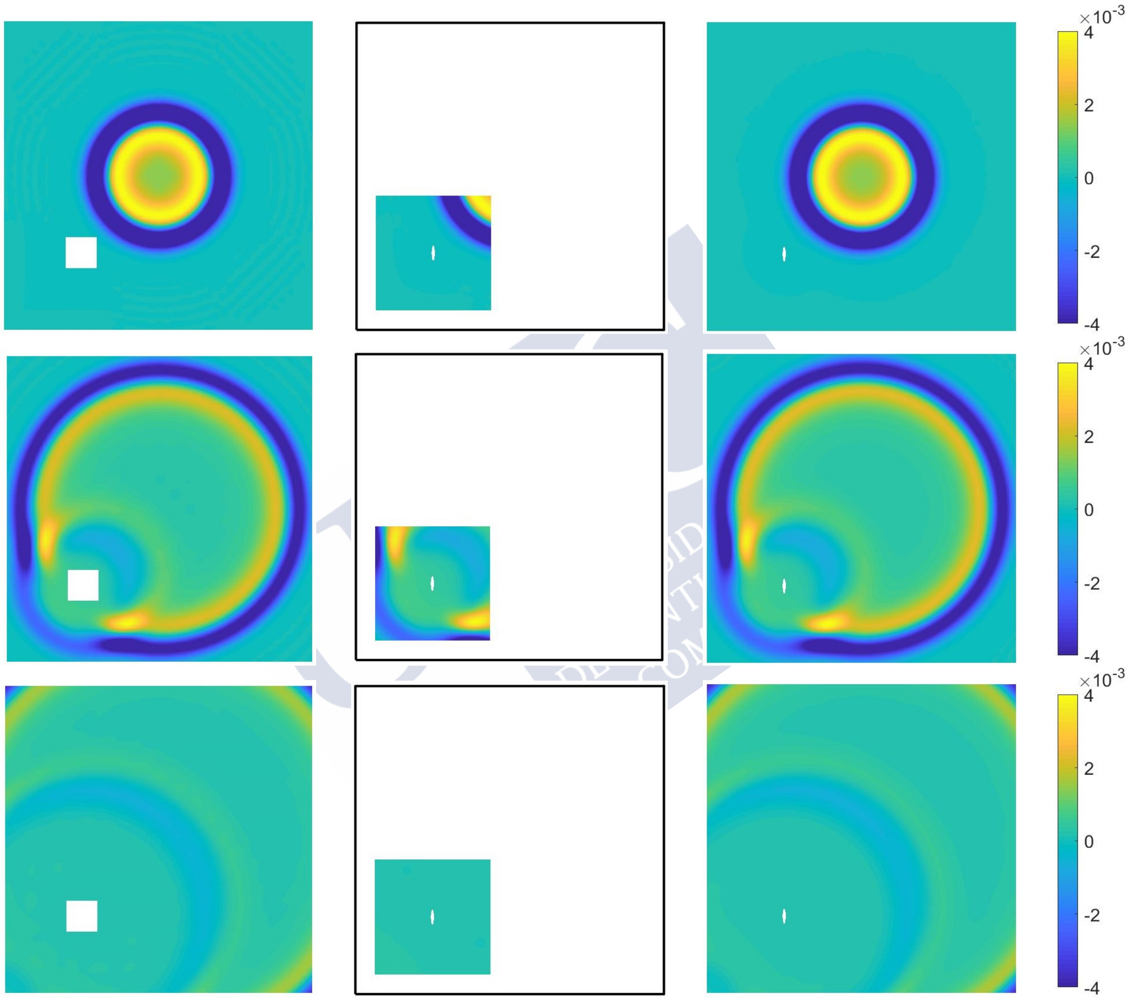

Figure 3.12: Snapshots at tree different times ($t = 3$, $t = 5$ and $t = 7$) of the solution of problem (3.56) in case 1. Comparison between the solution obtained with classic finite elements and with **volume-boundary** Arlequin coupling.

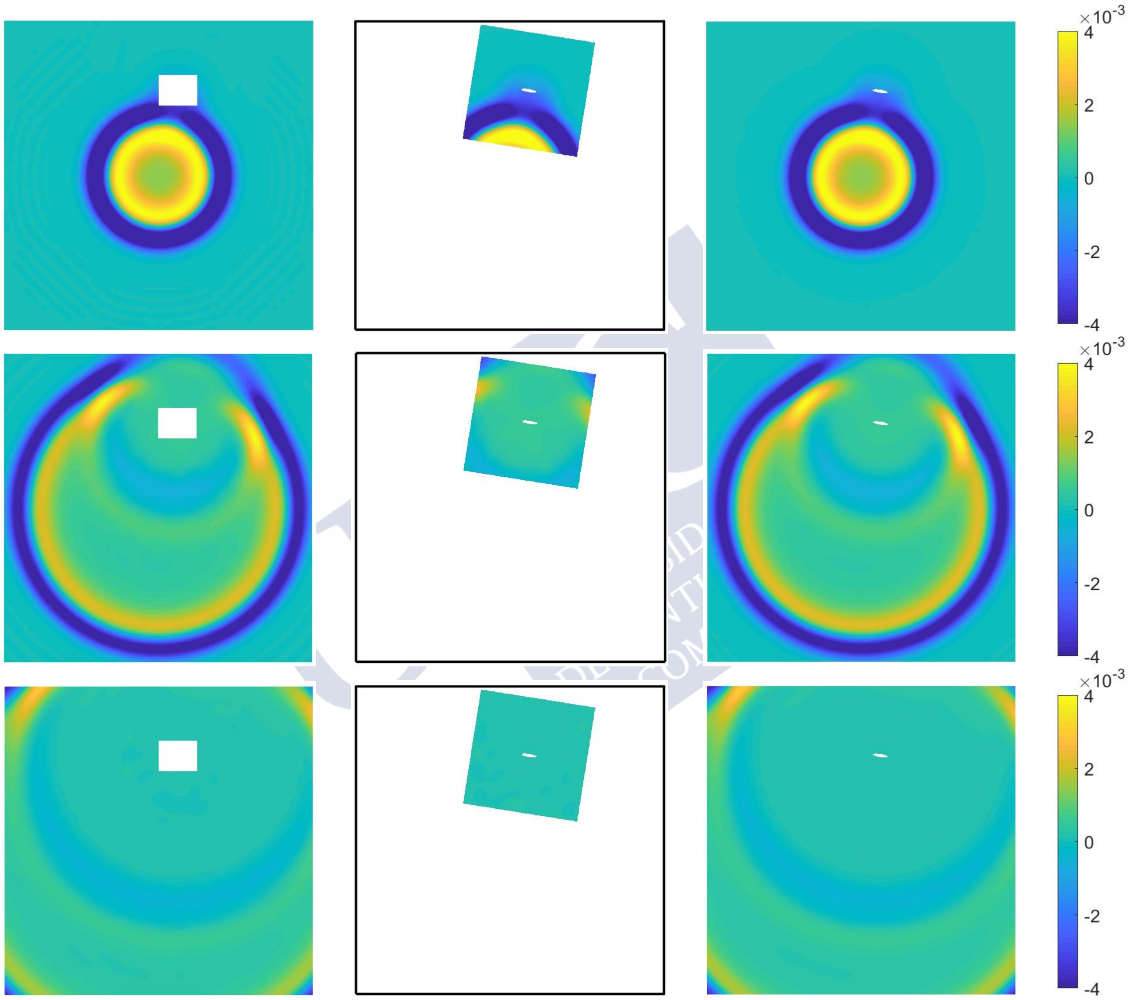

Figure 3.13: Snapshots at tree different times ($t = 3$, $t = 5$ and $t = 7$) of the solution of problem (3.56) in case 2. Comparison between the solution obtained with classic finite elements and with **volume-boundary** Arlequin coupling.

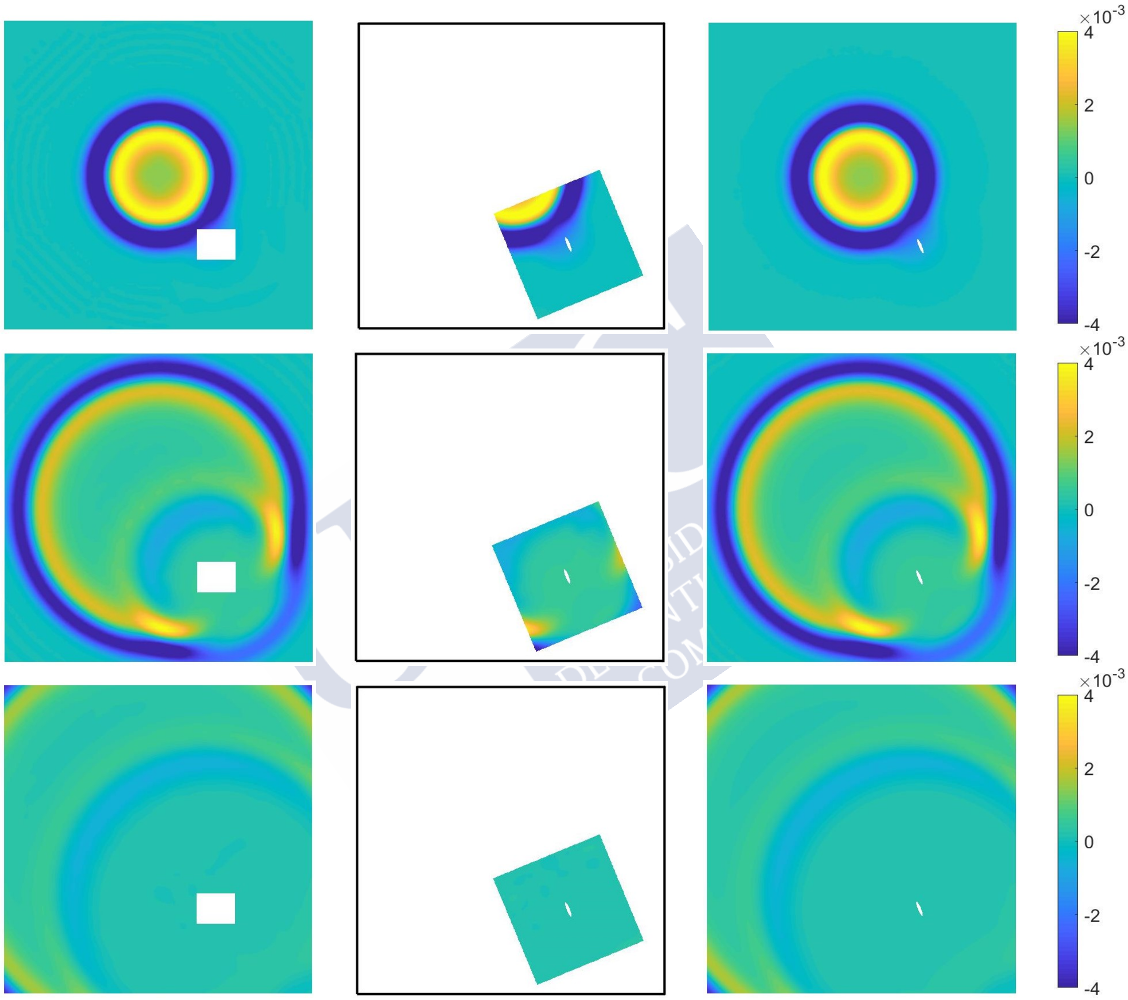

Figure 3.14: Snapshots at tree different times ($t = 3$, $t = 5$ and $t = 7$) of the solution of problem (3.56) in case 3. Comparison between the solution obtained with classic finite elements and with **volume-boundary** Arlequin coupling.

3.5.3 Application to obstacle detection

The aim of this section is to show, as we have mentioned in the introduction of this part of the thesis, that the Arlequin methods can be specially useful in generic optimization procedures where the domain changes from one iteration to the next. The details concerning advanced optimization algorithms are out of the scope of this manuscript, thus we only propose a naive example in order to show the advantages that the Arlequin methods offer for this kind of problems. In particular, we propose the naive example of finding an obstacle $\mathcal{O}$ (an ellipse) which is characterize by the parameters $(\boldsymbol{x}_c^\star, \theta^\star)$ (centre and orientation of the actual position) and embedded in a certain domain Θ. In particular, we assume that we have access to a part of the boundary of the domain $\Gamma_A \subset \partial\Theta$, thus we send a pulse from Γ_A imposing $\partial_{\boldsymbol{n}}\mathcal{U}_{|\Gamma_A} = g$ (Neumann data) and measure the response $\mathcal{U}_{|\Gamma_A}$ (Dirichlet data) up to a certain time T (see Figure 3.16). Then, we set an inverse problem designed to localize the obstacle by minimizing the functional

$$J(\boldsymbol{x}_c, \theta) = \int_0^T \int_{\Gamma_A} (\mathcal{U} - u_h(\boldsymbol{x}_c, \theta))^2 \,\mathrm{d}\gamma\,\mathrm{d}t,$$

where $u_h(\boldsymbol{x}_c, \theta)$ is the numerical solution of problem (completed with vanishing initial data)

$$\left\{\begin{array}{rcll} \partial_t^2 u - \operatorname{div}(\nabla u) &=& 0 & \text{in} \quad \Omega = \Theta \setminus \mathcal{O}(\boldsymbol{x}_c, \theta), \\ \partial_{\boldsymbol{n}} u &=& g & \text{on} \quad \Gamma_A, \\ \partial_{\boldsymbol{n}} u &=& 0 & \text{on} \quad \partial\Omega\backslash\Gamma_A, \end{array}\right.$$

and notice that $\mathcal{U} = u(\boldsymbol{x}_c^\star, \theta^\star)$. Usually, when minimizing the functional $J(\boldsymbol{x}_c, \theta)$, the numerical solution $u_h(\boldsymbol{x}_c, \theta)$ needs to be computed several times for different values of $(\boldsymbol{x}_c, \theta)$. In consequence, if a classic approach is used to compute $u_h(\boldsymbol{x}_c, \theta)$, a well-adapted global mesh of the domain needs to be recomputed for every new set of parameters (see Figure 3.15). However, if we compute

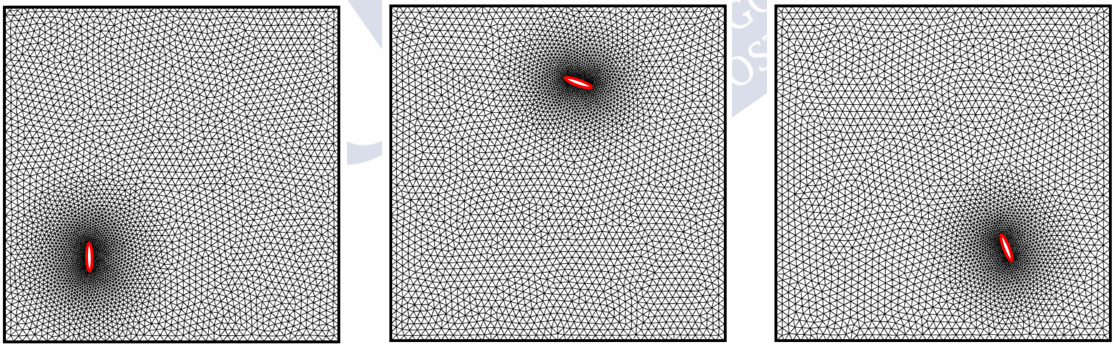

Figure 3.15: Meshes adapted for different positions of the obstacle.

$u_h(\boldsymbol{x}_c, \theta)$ considering the Arlequin technique this drawback can be avoided.

Physical data. We consider the background domain defined as $\Theta = [-2, 2] \times [-2, 2]$ while the obstacle $\mathcal{O}$, which depends on the parameters $(\boldsymbol{x}_c, \theta)$, is given by

$$\mathcal{O}(\boldsymbol{x}_c, \theta) = \begin{pmatrix} \cos(\theta) & \sin(\theta) \\ -\sin(\theta) & \cos(\theta) \end{pmatrix} \mathcal{O}_0 + \boldsymbol{x}_c,$$

where $\mathcal{O}_0$ denotes an ellipse centred at the origin, with semi-major and semi-minor axes aligned with the Cartesian axes and which length are given by 0.2 and 0.04 respectively. The boundary we have access to is given by $\Gamma_A = -2 \times [-2, 2]$ and we consider the pulse (see Figure 3.16)

$$g(x_2, t) = \frac{g_t(t) g_2(x_2)}{\sup\limits_{s\in[0,T]} g_t(s)} \quad \text{where} \quad g_t(t) = 9(t-2)e^{-9(t-2)^2} \quad \text{and} \quad g_2(x_2) = 0.01\, e^{10\, x_2^2}.$$

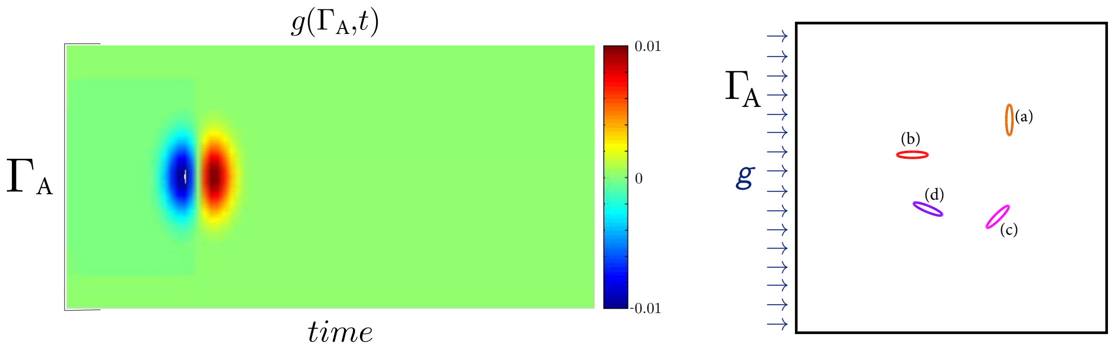

Figure 3.16: Representation of the boundary Γ_A to which we have access and the pulse g that is sent in order to localize de obstacle $\mathcal{O}$. We also plot the actual position of the obstacle in the different cases that we treat.

Arlequin formulation. We choose to use **boundary-boundary** coupling and the computational domain Ω to be decomposed into two overlapping sub-domains which definition depends on the parameters $(\boldsymbol{x}_c, \theta)$ and the mesh considered for the background media Θ. In particular we consider

$$\Omega_1 = \Theta \setminus \mathcal{S}_h(\boldsymbol{x}_c, \theta) \quad \text{and} \quad \Omega_2 = \begin{pmatrix} \cos(\theta) & -\sin(\theta) \\ \sin(\theta) & \cos(\theta) \end{pmatrix} \Omega_2^0 + \boldsymbol{x}_c,$$

where $\Omega_2^0 := [-1,1] \times [-1,1] \setminus \mathcal{O}_0$ and $S_h(\boldsymbol{x}_c, \theta)$ denotes an area surrounding the obstacle and conform with the mesh considered for the background media Θ. Finally, we choose the partitioning to be given by the simplest choice

$$\alpha_1 = \alpha_2 = \beta_1 = \beta_2 = \frac{1}{2} \quad \text{in } \omega.$$

Space-time discretization. We use the algorithm presented in Section 3.4.1 considering **first** order finite elements for the space discretization and the time discretization given by the parameters $\theta_1 = 0$ and $\theta_2 = \frac{1}{4}$. Moreover, we choose a coarse regular mesh for the background media Θ and a fine meshes for Ω_2^0 (see Figure 3.17). Notice that the mesh for Ω_2^0 is refined close to the ellipse in order to capture the geometry of the obstacle. In consequence, the time step Δt only

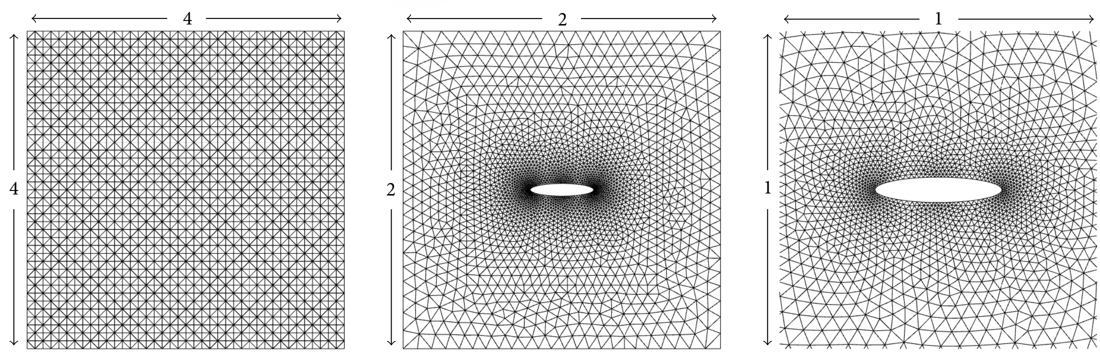

(a) Coarse homogeneous mesh of the non defected domain Θ.

(b) Fine mesh of Ω_2^0 refined in a neighbourhood of the obstacle.

(c) Zoom of a neighbourhood of the obstacle.

Figure 3.17: Meshes considered for the Arlequin decomposition.

depends on the properties of the coarse mesh and can be estimated locally by (3.47), thus we choose $\Delta t = \min \Delta t_k$.

Optimization algorithm. In order to minimize the functional $J(\boldsymbol{x}_c, \theta)$ we consider a multi-start gradient method, where we approximate the gradient by finite differences and compute the step using Armijo's rule. In particular, we begin with a random set of parameters $(\boldsymbol{x}_0, \theta_0)$ and we compute the gradient as

$$\big(\nabla J(\boldsymbol{x}_0, \theta_0)\big)_j = \frac{J(\boldsymbol{x}_0, \theta_0) - J\big((\boldsymbol{x}_0, \theta_0) + \boldsymbol{h}_j\big)}{||\boldsymbol{h}_j||_2}, \quad \text{for} \quad j \in \{1, 2, 3\} \quad \text{and} \quad \begin{array}{l} \boldsymbol{h}_1 = (4, 0, 0)/400, \\ \boldsymbol{h}_2 = (0, 4, 0)/400, \\ \boldsymbol{h}_3 = (0, 0, \pi)/400. \end{array}$$

Notice that this implies the computation of u_h for three different positions of the obstacle. Then, to considerate the next iterant $(\boldsymbol{x}_1, \theta_1)$, we compute

$$(\boldsymbol{x}_{1,0}, \theta_{1,0}) = (\boldsymbol{x}_0, \theta_0) - \frac{1}{2^0} \nabla J(\boldsymbol{x}_0, \theta_0) \quad \text{and check if} \quad J(\boldsymbol{x}_{1,0}, \theta_{1,0}) < J(\boldsymbol{x}_0, \theta_0) - \frac{1}{2^0} \frac{\|J(\boldsymbol{x}_0, \theta_0)\|_2^2}{10}.$$

If this holds, we consider $(\boldsymbol{x}_1, \theta_1) = (\boldsymbol{x}_{1,0}, \theta_{1,0})$, otherwise we continue iteratively the process until we find the smaller $s \in \mathbb{N}$ such that

$$(\boldsymbol{x}_{1,s}, \theta_{1,s}) = (\boldsymbol{x}_0, \theta_0) - \frac{1}{2^s} \nabla J(\boldsymbol{x}_0, \theta_0) \quad \text{verifies} \quad J(\boldsymbol{x}_{1,s}, \theta_{1,s}) < J(\boldsymbol{x}_0, \theta_0) - \frac{1}{2^s} \frac{\|J(\boldsymbol{x}_0, \theta_0)\|_2^2}{10}.$$

Then, we consider the next iterant as $(\boldsymbol{x}_1, \theta_1) = (\boldsymbol{x}_{1,s}, \theta_{1,s})$. Notice that this process implies the computation of u_h for $s+1$ different positions of the obstacle. With this algorithm, we can compute a sequence $(\boldsymbol{x}_n, \theta_n)_{n \in \mathbb{N}}$ that we expect to converge to $(\boldsymbol{x}_c^\star, \theta^\star)$. Finally, we choose to stop the algorithm when $\nabla J(\boldsymbol{x}_n, \theta_n) < 10^{-5}$.

Examples. Let us begin noticing that we use as data $\mathcal{U}_{|\Gamma_A}$ a numerical solution obtained for a specific position of the obstacle and considering a classical finite elements method in a refined mesh. In particular, we have considered different examples given by

(a) Case:	(b) Case:	(c) Case:	(d) Case:
$\boldsymbol{x}_c^\star = (0.75, 0.75)$,	$\boldsymbol{x}_c^\star = (-0.5, 0.3)$,	$\boldsymbol{x}_c^\star = (0.6, -0.5)$,	$\boldsymbol{x}_c^\star = (-0.3, -0.4)$,
$\theta^\star = \frac{\pi}{2}$,	$\theta^\star = 0$,	$\theta^\star = \frac{3\,\pi}{4}$,	$\theta^\star = \frac{\pi}{8}$.

Then, in Figure 3.18 we observe the evolution of the sequence that is provided by the presented optimization algorithm. The results show for all the cases a good agreement between the optimal position and the actual position of the obstacle. Moreover, we remark that thanks to the use of the Arlequin methodology, the optimization process has not required any re-meshing procedure. In consequence, the reader should notice that a large computational cost has been saved compared to the use of a classical finite elements approach.

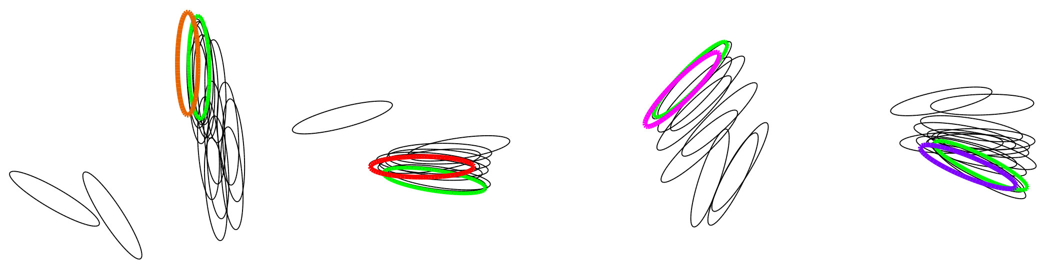

(a) Case (b) Case (c) Case (d) Case

Figure 3.18: Representation of the evolution of the algorithm when applied to the different cases we treat. In green we plot the optimal location and in the respective colours the actual position of each case.

Chapter 4

Conclusions and perspectives

In this first part of the thesis, we have analysed and extended the so called Arlequin method which is an overlapping domain decomposition method. The technique considers the computational domain Ω to be decomposed into two sub-domains Ω_1 and Ω_2 (such that $\Omega_1 \cup \Omega_2 = \Omega$, $\Omega_1 \cap \Omega_2 = \omega \neq \emptyset$ and $\partial\Omega_1 \cup \partial\Omega_2 = \emptyset$) and imposes the matching of u_1 and u_2 (that represents the solution of the sub-domains Ω_1 and Ω_2 respectively) in the overlapping region ω in a weak variational sense. This implies for consistency, the partitioning of the two involved variational formulations in the overlapping region and a correction of them by means of a Lagrange multiplier λ defined in the region ω.

From this starting point, we have developed new variants of the method where the solutions in Ω_1 and Ω_2 are coupled only close to the boundaries of the overlapping region ω, either with a boundary or with a volume coupling in a neighbourhood of the boundary (see Figure 4.1). Therefore, we avoid the introduction of a Lagrange multiplier in a region $\omega_c \subset \omega$ and we obtain a methodology that avoids the generation of a global mesh of the domain $\Omega = \Omega_1 \cup \Omega_2$, as well as a mesh of the complete overlapping region ω. This allows in practice to easily consider independent

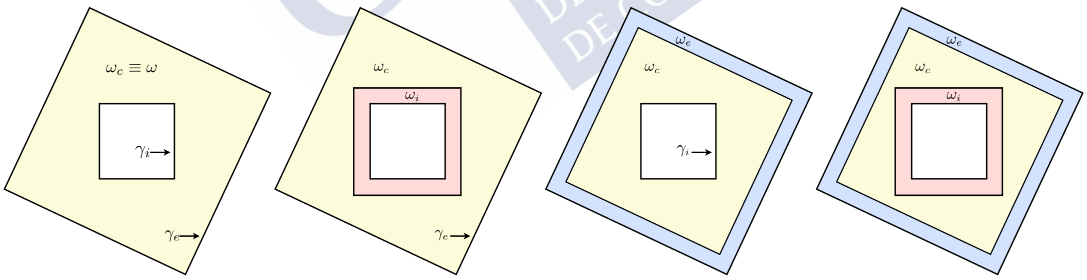

BB Boundary-Boundary: The coupling is performed in γ_i and γ_e.

BV Boundary-Volume: The coupling is performed in ω_i and γ_e.

VB Volume-Boundary: The coupling is performed in γ_i and ω_e.

VV Volume-Volume: The coupling is performed in ω_i and ω_e.

Figure 4.1: Representation of the regions of $\omega = \Omega_1 \cap \Omega_2$ where the new Arlequin formulations impose the coupling.

meshes for Ω_1 and Ω_2 that can also be used to discretize the Lagrange multipliers ensuring uniform *discrete Inf-Sup* conditions (therefore the stability of the space-discretization) under reasonable (not very restrictive) assumptions. In consequence, we have obtained new formulations that are more flexible in terms of mesh generation, allowing to use structured meshes (compatible with fast solvers) for the background medium, and to easily consider unstructured local grids around the defects.

In Chapter 2, we have introduced the original Arlequin method, as well as the new variants, for the particular case of the **Helmholtz equation**. Moreover, we have also discussed in detail the consideration of an adequate space discretization of the method and developed a complete convergence analysis for Galerkin discretizations satisfying adequate approximation properties, as well as an uniform discrete *Inf-Sup condition*.

A special attention has been devoted to the particular case of Lagrange finite elements ensuring the optimality of the method for regular enough solutions $(\boldsymbol{u}, \boldsymbol{\lambda})$. However in 2D configurations, we are restricted to the case of polygonal domains (unless isoparametric finite elements are used, which will be considered in future works) and therefore overlapping regions with corners, hence the regularity of the Lagrange multiplier $\boldsymbol{\lambda}$ may be low (depending on the coupling we consider) and consequently the convergence. Thus, in this context we have shown that the original Arlequin formulation may be suboptimal even for first order Lagrange finite elements, the volume couplings (**VV**, **VB** and **BV**) are optimal for first and second order Lagrange finite elements and only the boundary-boundary coupling (**BB**) is compatible with arbitrary high order Lagrange finite elements. Numerical results that support the theoretical analysis have been exhibited and moreover, we have also presented a more realistic numerical example, where we consider an elliptic obstacle surrounded by a damaged region (in particular the domain is bounded by a PML) in order to show the potential of the Arlequin methodology when treating the same problem for several positions of the obstacle.

In Chapter 3, we have presented the extension of Arlequin methodology for the particular case of the **transient wave equation**. The space discretization of the method has been briefly introduced according to the analysis developed for the Helmholtz equation and we have also analysed the stability and convergence of the resultant semi-discrete scheme (with the same conclusion as in Helmholtz equation concerning optimality).

Then, we have focussed in the choice of adequate second order time discretizations of the method and presented a detailed stability and error analysis of the resultant fully-discrete schemes. These guarantee second order convergence of the overall numerical scheme when the data is regular enough and the space discretization compatible with second order Lagrange finite elements.

We shall also remark, that a special effort has been devoted to guarantee that the fully discrete formulation is well adapted for a efficient treatment of local defects surrounded by damaged regions. In particular, if Ω_1 represents the background media and Ω_2 the patch that captures the geometry of the obstacle, we have analysed in detail the stability of an explicit-implicit time discretization (explicit for u_1 in Ω_1 and implicit for u_2 in Ω_2) which efficiency is ensured if the speed of waves do not strongly increase in ω_c (i.e. if a volume coupling is considered in the regions of ω where the speed of waves increases strongly). This would be a drawback for the boundary couplings (since $\omega_c = \omega$), however we have circumvented this issue by considering a time discretization which is also locally implicit for u_1 in ω_c or even only where the speed of waves increases strongly. In consequence, we have presented an efficient time discretization for all the variants of Arlequin method.

Numerical results that support the theoretical analysis have been exhibited. We have also developed a numerical example in a more realistic situation (in particular the domain is bounded by a PML), where we have shown the potential of the method. Moreover, as we have used as motivation in many parts of the document, we have also considered the optimization problem of finding an obstacle and we have exhibited how the Arlequin methods can save a large computational cost.

In conclusion, and according to the analysis developed in this first part of the thesis, we provide the following recommendations. In cases where the speed of waves do not present strong variations close to the defects (the complexity would only be related to the geometry) we suggest to consider the **boundary - boundary** coupling with and explicit-implicit time discretization, since it is compatible with arbitrary order (other variants are only compatible with first and second order) and it offers more flexibility in terms of mesh generation, since the overlap between Ω_1 and Ω_2 can be smaller (hence a smaller patch can be used). In presence of defects surrounded by regions with a strong decrease on the speed of waves (thus on the wavelength), we recommend to capture the regions with a low speed of waves with $\Omega_2 \setminus \Omega_1$, otherwise for accuracy we should consider a mesh for Ω_1 which is also adapted to the small wavelength. For the contrary, when the defects are surrounded by regions with a strong increase on the speed of waves, it is advised to capture the regions with a high speed of waves with $\Omega_2 \setminus \omega_c$ (note that this requires a volume coupling in the regions of ω where the speed of waves is high) and tune the partition coefficients in $\omega \setminus \omega_c$ accordingly, in order to avoid a restriction of the time step due the CFL condition. As we have mentioned before, another way to avoid this drawback but still using the **boundary-boundary** coupling (compatible with arbitrary order) would be to use a locally-implicit time discretization in Ω_1 (only implicit in some localized regions where the speed of waves is high). Moreover, we also remark that in cases where there is no particular preference among the different variants (for instance second order finite elements and constant speed of waves) we have observed in practice that all the variants provide similar numerical results.

The reader should also notice that there are some questions that remain open (that we intend to address in the future) and that we recapitulate next:

- In the case of the Helmholtz, we have presented a detailed analysis of the convergence assuming uniqueness of solution for both, continuous and discrete problems, i.e. assuming that the frequency of the problem is not an eigenvalue of the associated continuous nor discrete eigenvalue problems (2.41) and (2.45) (notice this is not an assumption for the transient wave equation). However, we expect to be enough that the frequency is not an eigenvalue of the continuous eigenvalue problem (2.41) (at least for h small enough). Note that the verification of this requires a complete convergence analysis for the mentioned continuous and discrete eigenvalue problems, which has not been developed an remains as an **open** question.

- We have used two different choices for the discretization of the Lagrange multipliers spaces that we have called *classic* and *dual*. Then, for the analysis, we have conjectured the L^2-stability of certain projection operator. We know that this result holds for boundary Lagrange multipliers spaces discretized with the *dual* spaces. However, this question remains **open** for the other cases although numerical results are encouraging.

- For the case of the transient wave equation, we have presented an algorithm where in the case of volume coupling a left preconditioner has been introduced for the efficient pre-computation of the Lagrange multiplier on each time step (through a Schur complement strategy). Note that the consideration of an adequate preconditioner has not been analysed in detail and remains as a an **open** question.

Finally, we are also interested in further developments of the method that we enumerate in the following list of perspectives:

- It would be very interesting to extend the analysis of the space discretization of the method to the case of isoparametric finite elements. However, as we have mentioned in Section 2.7, two main difficulties arise in this context. The first one is related to the intersection algorithms that are required to correctly impose the matching in the overlapping region and that are not well adapted for curved finite elements. The second concerns the automatic approach in order to adapt the mesh of the background for each configuration, since removing elements of a regular mesh leads to an overlapping region with re-entrant corners, which is precisely what we want to avoid. Thus we should also develop an efficient and automatic approach in order to circumvent this issue.

- The analysis of different techniques that may improve the efficiency of the pre-computation of the volume Lagrange multipliers. For instance the analysis of other preconditioners, but also new alternative formulations. In particular the introduction of a new term that performs an L^2-coupling of the velocity in the volume coupling regions may provide such an improvement. The analysis of the resultant formulation would be an interesting extension of the Arlequin methodology.

- In this first part of the thesis, the Arlequin methodology has been presented and analysed in detail for the Helmholtz equation and the transient wave equation. However, in principle it can be also considered for the treatment of different problems and other physical contexts such as solid mechanics or fluid dynamics.

- The extension of the Arlequin methodology to 3D configurations is also a relevant question concerning applications. However, the extension is not trivial due to the discretization of the boundary multipliers in polyedric overlapping regions. As in 2D configurations, similar difficulties arise also in the context of mortar finite elements and we expect that similar techniques can be adapted to the Arlequin methodology.

Part II

Linear isotropic elastodynamics by means of potentials

Table of Contents

Chapter 5

Introduction

Contents

In this second part of the thesis, our goal is to revisit a very classical question, namely, the numerical solution of **linear isotropic elastodynamics equations**, which govern the propagation of waves in elastic isotropic solids. For simplicity, we restrict our analysis to the **2D** case, while the extension to higher dimensions remains open and will be the object of further developments.

5.1 Linear isotropic elastodynamics equations

In the following, let us denote by $\boldsymbol{u}$ the displacement field that is known to be governed by the fundamental law in mechanics

$$\rho\, \partial_t^2 \boldsymbol{u} \,-\, \mathbf{div}\, \underline{\boldsymbol{\sigma}}(\boldsymbol{u}) \,=\, \boldsymbol{f}, \tag{5.1}$$

where the source $\boldsymbol{f}$ is given, as well as the density of the body $\rho(\boldsymbol{x}) \geq \rho_0 > 0$, that might depend on the $\boldsymbol{x}$ variable for heterogeneous media, while $\underline{\boldsymbol{\sigma}} = ((\sigma_{ij}))$ denotes the stress tensor that represents the internal efforts inside the body and $\mathbf{div}\, \underline{\boldsymbol{\sigma}}$ is the vector field defined by (with *Einstein's convention* for summation over the repeated indices)

$$\big(\mathbf{div}\, \underline{\boldsymbol{\sigma}}\big)_i = \partial_j \sigma_{ij}(\boldsymbol{u}).$$

Notice, that equation (5.1) must be completed by constitutive laws that relate the stress tensor $\underline{\boldsymbol{\sigma}}$ and the strain tensor $\underline{\boldsymbol{\varepsilon}} = ((\varepsilon_{ij}))$. In purely elastics materials the strain tensor can be expressed as

$$\underline{\boldsymbol{\varepsilon}}(\boldsymbol{u}) = \big((\varepsilon_{ij}(\boldsymbol{u}))\big), \quad \text{where} \quad \varepsilon_{ij}(\boldsymbol{u}) \,=\, \frac{1}{2}\Big(\partial_i u_j + \partial_j u_i\Big),\ 1 \leq i, j \leq 2,$$

and moreover the constitutive law is given by **Hooke's law** which linearly relates the components of the stress tensor $\underline{\boldsymbol{\sigma}}$ and the components of the strain tensor $\underline{\boldsymbol{\varepsilon}}$ in the following way

$$\underline{\boldsymbol{\sigma}}(\boldsymbol{u}) = \underline{\boldsymbol{C}}\, \underline{\boldsymbol{\varepsilon}}(\boldsymbol{u}),$$

where $\underline{\boldsymbol{C}}$ denotes the fourth order elasticity tensor that for an **isotropic** material is given by

$$C_{ijkl} = \lambda\, \delta_{ij}\, \delta_{kl} + \mu\, (\delta_{ik}\, \delta_{jl} + \delta_{il}\, \delta_{jk}),$$

where $\lambda(\boldsymbol{x})$ and $\mu(\boldsymbol{x})$ are the Lamé parameters that we assume such that

$$\lambda(\boldsymbol{x}) \geq \lambda_0 > 0 \quad \text{and} \quad \mu(\boldsymbol{x}) \geq \mu_0 > 0.$$

Thus, if we consider the identity tensor $\underline{\boldsymbol{I}}$ and the divergence operator $\operatorname{div}\boldsymbol{u} = \partial_1 u_1 + \partial_2 u_2$, we can directly relate the stress tensor to the displacement field by the equation

$$\underline{\boldsymbol{\sigma}}(\boldsymbol{u}) = \lambda \operatorname{div}\boldsymbol{u}\,\underline{\boldsymbol{I}} + 2\,\mu\,\underline{\boldsymbol{\varepsilon}}(\boldsymbol{u}). \tag{5.2}$$

Hence, we can eliminate the unknown $\underline{\boldsymbol{\sigma}}(\boldsymbol{u})$ from (5.1) by substituting with (5.2) and obtain a second order hyperbolic system in $\boldsymbol{u}$, which in case we assume the medium to be **homogeneous** reads as follows (see [87, 88] for instance)

$$\rho\,\partial_t^2 \boldsymbol{u} \,-\, (\lambda + 2\mu)\,\nabla \operatorname{div}\boldsymbol{u} + \mu\,\mathbf{curl}\left(\operatorname{curl}\boldsymbol{u}\right) \;=\; \boldsymbol{f}, \tag{5.3}$$

where we have introduced the curl operators in 2D defined by

$$\begin{aligned} \operatorname{curl}\boldsymbol{u} &\coloneqq \partial_1 u_2 - \partial_2 u_1, && \text{for the scalar curl of a vector field } \boldsymbol{u},\\ \mathbf{curl}\,\varphi &\coloneqq \big(\partial_2\varphi, -\partial_1\varphi\big), && \text{for the vector curl of a scalar field } \varphi. \end{aligned}$$

For the sake of simplicity, the problem is completed with vanishing initial conditions

$$\boldsymbol{u}(t=0) = \mathbf{0} \qquad \text{and} \qquad \partial_t \boldsymbol{u}(t=0) = \mathbf{0}, \tag{5.4}$$

and, in the presence of boundaries, with conditions

$$\begin{array}{ll} \underline{\textbf{Clamped}\text{ boundary }\Gamma:} & \underline{\textbf{Free}\text{ boundary }\Gamma:} \\ \boldsymbol{u} = \mathbf{0} \quad \text{on} \quad \Gamma. & \underline{\boldsymbol{\sigma}}(\boldsymbol{u})\boldsymbol{n} = 0 \quad \text{on} \quad \Gamma. \end{array} \tag{5.5}$$

As a matter of fact, there exist already many numerical methods for solving problem ((5.3), (5.4), (5.5)). For instance, we can consider conforming finite elements methods in space (possibly of high order) and finite differences in time (see [10]). It is also classical to consider the equivalent velocity-stress formulation of the same system (first order differential system) discretized using mixed finite element methods in space (see [11, 1]) and again finite differences in time. In both cases, assuming we use an explicit time integration, the stability of the resultant numerical scheme is subject to a CFL condition which may be very penalising as we explain next.

5.2 Drawback of standard space-time discretization methods

Let us begin by considering a d-dimensional isotropic homogeneous elastic medium of characteristic length L on each direction, subject to a source term involving a *minimal* time scale $T_\star$. This source is known to generate two different types of waves, usually called **pressure waves** (P-waves) and **shear waves** (S-waves), that in the free space are known to propagate independently with different velocities V_P and V_S respectively, where (notice $V_P > V_S$)

$$V_P \;=\; \sqrt{\frac{\lambda + 2\,\mu}{\rho}} \qquad \text{and} \qquad V_S \;=\; \sqrt{\frac{\mu}{\rho}}.$$

In consequence, each type of wave propagates also with a different wavelength $\lambda_P = T_\star\, V_P$ and $\lambda_S = T_\star\, V_S$. Moreover, if on the one hand we consider Lagrange finite elements on a mesh (either triangular or quadrilateral) of step size h that we assume to be quasi-uniform (see Remark 2.43), we notice that for accuracy reasons h should be chosen proportional to the *minimal* wavelength λ_S, i.e.

$$h \;=\; \frac{\lambda_S}{N_\star},$$

for a fixed $N_\star$ that denotes the number of mesh points that we want to consider per wavelength. On the other hand, if we consider the leap-frog scheme for the time discretization, then the time step is constrained by a stability condition that involves the *maximal* velocity V_P, i.e.

$$\Delta t \;\approx\; \frac{h}{V_P} \;=\; \frac{T_\star}{N_\star}\,\frac{V_S}{V_P},$$

where the equality holds up to a positive constant only depending on the order of the finite elements considered and the quasi-uniformity factor of the meshes. Thus for a time interval integration $[0,T]$, the number of time steps is $T/\Delta t$ and since the scheme is explicit, the cost of each iteration is proportional to the number of degrees of freedom, that behaves like L^d/h^d. In consequence, we can roughly estimate the overall computational cost by

$$\text{Cost} \;\propto\; \frac{L^d}{h^d}\,\frac{T}{\Delta t} \;\approx\; N_\star^{d+1}\,\frac{L^d}{\lambda_S^d}\,\frac{T}{T_\star}\,\frac{V_P}{V_S}.$$

It is then clear, that the resultant numerical scheme would be penalised by the factor V_P/V_S which can be very high for instance when we consider a nearly incompressible material, such as soft tissues, in which the P-waves propagate much faster than the S-waves. Finally, notice that the penalizing factor would not appear if we could solve separately each type of wave, since we could consider different meshes for each type of wave and adapt each of them to the respective wavelength, i.e.

$$h_P \;=\; \frac{\lambda_P}{N_\star} \quad \text{and} \quad h_S \;=\; \frac{\lambda_S}{N_\star}.$$

Then, we expect to obtain for each wave, a stability condition which is given by

$$\Delta t_P \;\approx\; \frac{h_P}{V_P} \;=\; \frac{T_\star}{N_\star} \quad \text{and} \quad \Delta t_S \;\approx\; \frac{h_S}{V_S} \;=\; \frac{T_\star}{N_\star}.$$

Thus the stability condition of the overall scheme, would avoid the penalising factor V_P/V_S. More precisely, we expect

$$\Delta t \;=\; \min\{\Delta t_P, \Delta t_S\} \;\approx\; \frac{T_\star}{N_\star},$$

and therefore an estimate for the computational cost given by

$$\text{Cost} \;\propto\; \Big(\frac{L^d}{h_P^d} + \frac{L^d}{h_S^d}\Big)\frac{T}{\Delta t} \;\approx\; N_\star^{d+1}\Big(\frac{L^d}{\lambda_P^d} + \frac{L^d}{\lambda_S^d}\Big)\,\frac{T}{T_\star},$$

hence this shows that the cost is not penalised by the factor V_P/V_S.

5.3 Potentials decomposition in the free space

It is classical to use the well known Helmholtz decomposition of vector fields (write a vector field as the sum of a gradient and a curl) to compute analytical solutions in isotropic homogeneous media (see [89, 90, 91]). Such a decomposition relates elastodynamics equations (5.3), which do not distinguish between both types of waves, to two wave equations and enlightens the decomposition of the displacement field $\boldsymbol{u}$ as the sum of pressure waves (P-waves, that are gradients of a pressure potential that we denote φ_P) and shear waves (S-waves, that are curls of a shear potential that we denote φ_S) that, as mentioned, propagate independently with different velocities V_P and V_S respectively. In the 2D case, to which we restrict ourselves, we define both pressure and shear potentials as the scalar fields obtained when solving the ordinary differential equations

$$\rho\,\partial_t\varphi_P = (\lambda + 2\mu)\,\mathrm{div}\,\boldsymbol{u} \qquad \text{and} \qquad \rho\,\partial_t\varphi_S = -\mu\,\mathrm{curl}\,\boldsymbol{u}, \tag{5.6}$$

both completed with vanishing initial conditions (compatible with (5.4))

$$\varphi_P(t=0) = 0 \qquad \text{and} \qquad \varphi_S(t=0) = 0. \tag{5.7}$$

Thus we substitute (5.6) into (5.3) to obtain $\partial_t\big(\partial_t\boldsymbol{u} - \nabla\,\varphi_P - \mathbf{curl}\,\varphi_S - \boldsymbol{g}\big) = 0$ where

$$\boldsymbol{g}(t) = \frac{1}{\rho}\int_0^t \boldsymbol{f}(s)\,ds \qquad (\text{notice } \boldsymbol{g}(0) = 0) \tag{5.8}$$

and since $\partial_t \boldsymbol{u}(t=0) = \boldsymbol{0}$ and $(\varphi_P, \varphi_S)(t=0) = \boldsymbol{0}$, we deduce that

$$\partial_t \boldsymbol{u} = \nabla \varphi_P + \mathbf{curl}\, \varphi_S + \boldsymbol{g}. \tag{5.9}$$

This means that φ_P and φ_S provide a *Helmholtz decomposition* [92] of the vector field $\partial_t \boldsymbol{u}$ when $\boldsymbol{g}$ vanishes.

Remark 5.1

The reader should notice that we could have considered in (5.7) *different initial conditions for the potentials, however this may introduce in* (5.9) *the additional term* $\nabla\varphi_P(0) + \mathbf{curl}\,\varphi_S(0)$ *that should be handled in the following. Thus for simplicity we have avoided that term by considering vanishing initial conditions.*

To obtain the equations satisfied by the potentials, we simply substitute (5.9) into the two equations in (5.6) and after differentiating in time, we get two scalar wave equations for φ_P and φ_S

$$\frac{1}{V_P^2}\,\partial_t^2 \varphi_P - \Delta\varphi_P = \operatorname{div} \boldsymbol{g} \qquad \text{and} \qquad \frac{1}{V_S^2}\,\partial_t^2 \varphi_S - \Delta\varphi_S = -\operatorname{curl} \boldsymbol{g}. \tag{5.10}$$

Both equations are then completed with the initial condition for the potentials (5.7) and also with the initial conditions for the time derivative of the potentials (according to (5.4) and (5.6))

$$\partial_t \varphi_P(t=0) = 0 \qquad \text{and} \qquad \partial_t \varphi_S(t=0) = 0. \tag{5.11}$$

This results in a system of equations for the potentials that in the free space (in absence of any boundary) are fully decoupled. Therefore, not only the computational cost is reduced for large values of V_P/V_S (as we have discussed in Section 5.2), but also one can benefit of well known techniques for the numerical treatment of the standard scalar wave equation, such as for example the use of perfectly matched layers (PMLs) for the treatment of unbounded domains. Indeed long time stable implementations of PMLs for isotropic elastodynamics equations raise some difficulties especially if the ratio V_P/V_S is large (even though the so-called C-PML solve the long time stability issue as shown in [93]). However, we shall also remark that in a piecewise homogeneous media, previous approach is valid only locally and the different types of waves, which propagate independently in the interior of the computational domain, are recoupled on boundaries and interfaces due to reflections and transmissions (the so-called conversion of modes). As the reader can expect, this is the main source of complexity of the propagation process because, contrary to the interior equations, boundary and transmission conditions (5.5) are not easily expressed in terms of potentials.

Notice that in the literature, it seems that very few works have been devoted on the exploitation of this idea for finite element computations. For instance one can find a few references concerning finite differences computations in space and time, see [94] in which a numerical scheme is constructed with approximation properties independent of the ratio V_P/V_S. However, this approach has proved to be useful in other domains of physics, in particular in fluid mechanics (current-vorticity formulations [49], chapter 2, [95], [96] and [97]).

In the following chapters, we present how the potentials are coupled on boundaries depending on the nature of the conditions (5.5) satisfied by the displacement field. Then, we discuss in detail how to obtain a suitable variational formulation which stability can be guaranteed and which is well adapted for discretization. In the process, we will guide ourselves by two main interests. The first being an intellectual curiosity: Can we use potentials to solve linear isotropic elastodynamics in bounded homogeneous media considering finite elements? The second is more related to applications: Can we still reduce the computational cost by avoiding the penalising factor V_P/V_S? We recall that for this question, it is important that we can consider independent meshes for the pressure waves and the shear waves, but we shall also pay special attention to the correspondent CFL condition after time discretization, which may be affected by the treatment of boundary conditions.

Remark 5.2

Note that, for convenience, we have chosen potentials which provide a Helmholtz decomposition of the velocity field. We could have chosen the potentials to provide a Helmholtz decomposition of the displacement field or acceleration field. In both cases, the result would be equivalent, only affecting computations related to the relation between potentials and displacements.

It is also possible to consider a Helmholtz decomposition of the source term and include it in the definition of the potentials. Thus we obtain a Helmholtz decomposition of the displacement at any time. However, this approach has the drawback that we are forced to pre-compute the Helmholtz decomposition of the source term.

In previous works [17, 18], the authors successfully addressed these questions for the case of an isotropic homogeneous elastic media which is bounded by a clamped boundary (usually known as Dirichlet problem). However, when treating the case of a media bounded by a free boundary (usually known as Neumann problem), the authors found that the natural extension of the technique provides a variational formulation which is not compatible with finite elements discretization due to severe time instabilities. From this starting point, in [19, 20] we have presented an alternative approach for the treatment of the Neumann boundary conditions. In the following chapters, we first revisit the case of Dirichlet boundary conditions (enlightened by treatment of the Neumann problem), then we analyse in detail the difficulties of the Neumann case and present the alternative approach. As we shall see, with this new approach, we are able to treat the difficulties of the Neumann boundary conditions and to solve the problem up to the fully discrete level.

Chapter 6

The case of clamped boundary conditions

Contents

In this chapter, we address the case of an isotropic homogeneous elastic medium in 2D, which we assume to be bounded by a clamped boundary, that is to say, the case of Dirichlet boundary condition. This case was firstly treated in [17, 18] and we revisit it here (enlightened by the treatment of the free surface boundary conditions) for making the work self contained and for preparing the forthcoming chapters.

6.1 Decomposition into potentials in a clamped domain

Let us begin by considering that the 2D homogeneous isotropic elastic domain Ω is connected, Lipschitz regular and bounded by $\Gamma = \partial\Omega$, that in the following we assume to be clamped. In consequence, the displacement problem ((5.3), (5.4)) is now formulated in $\Omega \times [0, T]$, where T denotes the final computational time and the problem is completed with the Dirichlet boundary conditions

$$\left\{\begin{array}{ll}\text{Find } \boldsymbol{u}(\boldsymbol{x},t) : \Omega \times [0,T] \longrightarrow \mathbb{R}^2, \text{ such that } (\boldsymbol{u}, \partial_t \boldsymbol{u})(t=0) = (0,0) \text{ and} & \\ \partial_t^2 \boldsymbol{u} \,-\, V_P^2 \,\nabla \operatorname{div} \boldsymbol{u} \,+\, V_S^2 \,\mathbf{curl}\left(\operatorname{curl} \boldsymbol{u}\right) \,=\, \boldsymbol{f}/\rho, \quad \text{in } \Omega \times [0,T], & (6.1a)\\ \boldsymbol{u}(\boldsymbol{x},t) \,=\, \mathbf{0}, \quad \text{on } \Gamma \times [0,T]. & (6.1b)\end{array}\right.$$

Moreover, to state a result concerning the existence, uniqueness and regularity of the solution of problem (6.1), we shall first introduce the following spaces of displacement fields:

$$\begin{array}{rcl}\boldsymbol{D} & := & \left\{\boldsymbol{w} \in H^1(\Omega)^2 \,/\, -V_P^2\,\nabla(\operatorname{div}\boldsymbol{w}) + V_S^2\,\mathbf{curl}\,(\operatorname{curl}\boldsymbol{w}) \in L^2(\Omega)^2\right\},\\ \text{and} \quad \boldsymbol{D}_D & := & \left\{\boldsymbol{w} \in \boldsymbol{D} \,/\, \boldsymbol{w} = 0 \text{ on } \Gamma\right\} \quad \text{(subscript } D \text{ holds for Dirichlet).}\end{array} \qquad (6.2)$$

We shall remark that $\boldsymbol{D}$ is a Hilbert space when equipped with the natural graph norm while $\boldsymbol{D}_D$ is a closed subspace of it. Then, we can state the following classical theorem that results, for instance, from the application of standard Hille-Yosida's theory for evolution problems (see [78]).

Theorem 6.1

Assume that $\boldsymbol{f} \in \mathcal{C}^1\big([0,T];L^2(\Omega)^2\big)$. *Then, problem* (6.1) *admits a unique solution:*

$$\boldsymbol{u} \in \mathcal{C}^2([0,T];L^2(\Omega)^2) \cap \mathcal{C}^1\big([0,T];H^1(\Omega)^2\big) \cap \mathcal{C}^0\big([0,T];\boldsymbol{D}_D\big).$$

Then, in the same way we presented in Section 5.3, we can introduce the scalar potentials φ_P (pressure potential) and φ_S (shear potential) via equations (5.6), i.e.

$$\rho\,\partial_t\varphi_P = (\lambda+2\mu)\operatorname{div}\boldsymbol{u} \qquad \text{and} \qquad \rho\,\partial_t\varphi_S = -\mu\operatorname{curl}\boldsymbol{u}, \tag{6.3}$$

both completed with the vanishing initial conditions (5.7)

$$\varphi_P(t=0) = 0 \qquad \text{and} \qquad \varphi_S(t=0)=0. \tag{6.4}$$

Therefore, we can deduce again that the decomposition (5.9) holds in the interior of the computational domain Ω, so that φ_P and φ_S provide a *Helmholtz decomposition* [92] of the velocity field $\partial_t\boldsymbol{u}$ when the source vanishes

$$\partial_t\boldsymbol{u} = \nabla\,\varphi_P + \mathbf{curl}\,\varphi_S + \boldsymbol{g} \quad \text{where we recall} \quad \boldsymbol{g}(t) = \frac{1}{\rho}\int_0^t \boldsymbol{f}(s)\,ds. \tag{6.5}$$

In consequence, if we introduce the decomposition (6.5) into the equations (6.3) and differentiate in time, we obtain that the potentials satisfy the scalar wave equations in (5.10),

$$\frac{1}{V_P^2}\,\partial_t^2\varphi_P - \Delta\varphi_P = \operatorname{div}\boldsymbol{g} \qquad \text{and} \qquad \frac{1}{V_S^2}\,\partial_t^2\varphi_S - \Delta\varphi_S = -\operatorname{curl}\boldsymbol{g}, \tag{6.6}$$

which are completed with the initial condition (6.4) and also with the initial conditions for the time derivative of the potentials (as in (5.11))

$$\partial_t\varphi_P(t=0) = 0 \qquad \text{and} \qquad \partial_t\varphi_S(t=0)=0. \tag{6.7}$$

Moreover, we notice that according to Theorem 6.1, the vector of potentials

$$\boldsymbol{\varphi} := (\varphi_P,\varphi_S) \quad \text{belongs to} \quad \mathcal{C}^2([0,T];L^2(\Omega)^2)\cap\mathcal{C}^1(0,T;\boldsymbol{V}) \tag{6.8}$$

where we have introduced the functional space

$$\boldsymbol{V} := \big\{\boldsymbol{\varphi} = (\varphi_P,\varphi_S)\in L^2(\Omega)^2 \text{ such that } \nabla\varphi_P + \mathbf{curl}\,\varphi_S \in L^2(\Omega)^2\big\}.$$

Moreover, it is interesting to notice that

$$\nabla\varphi_P + \mathbf{curl}\,\varphi_S = \begin{pmatrix} \operatorname{div}\boldsymbol{\varphi} \\ -\operatorname{curl}\boldsymbol{\varphi}\end{pmatrix} \tag{6.9}$$

in such a way that the space $\boldsymbol{V}$ can be alternatively characterized as

$$\boldsymbol{V} = H(\mathrm{div},\Omega)\cap H(\mathrm{curl},\Omega), \tag{6.10}$$

which is a Hilbert space equipped with the scalar product and the associated norm

$$(\boldsymbol{\varphi},\boldsymbol{\psi})_{\boldsymbol{V}} = \int_\Omega (\boldsymbol{\varphi}\cdot\boldsymbol{\psi} + \operatorname{div}\boldsymbol{\varphi}\operatorname{div}\boldsymbol{\psi} + \operatorname{curl}\boldsymbol{\varphi}\operatorname{curl}\boldsymbol{\psi})\,\mathrm{d}\boldsymbol{x} \quad \text{and} \quad \|\boldsymbol{\varphi}\|_{\boldsymbol{V}} = \sqrt{(\boldsymbol{\varphi},\boldsymbol{\varphi})_{\boldsymbol{V}}}. \tag{6.11}$$

This space is very well known from the theory of Maxwell's equations [92, 98] and clearly contains $[H^1(\Omega)]^2$. Moreover, it is known (see [99]) that for any bounded, connected and Lipschitz regular domain

$$\text{the space } \mathcal{D}(\overline{\Omega})^2 \text{ (and thus, the space } H^1(\Omega)^2) \text{ is dense in } \boldsymbol{V}. \tag{6.12}$$

In fact, it is worthy to remark that the functions in $[H^1(\Omega)]^2$ and $\boldsymbol{V}$ only differ close to the boundaries, i.e., each function in $\boldsymbol{V}$ belongs to $H^1(\omega)^2$ for any open set ω such that $\overline{\omega} \subset \Omega$. The reader should notice that property (6.12) will be of capital importance for the later discretization process since it ensures the good approximation properties of standard Lagrange finite element spaces when discretizing the space $\boldsymbol{V}$.

Finally, notice that problem (6.6) with the vanishing initial conditions (6.4) and (6.7) needs to be completed with adequate boundary conditions translating (6.1b). For this purpose, we first notice that since $\partial_t \boldsymbol{u} \in H^1(\Omega)^2$, we can apply trace operator to equation (6.5) and therefore considering (6.1b), we obtain

$$\nabla \varphi_P + \mathbf{curl}\, \varphi_S + \boldsymbol{g} = \mathbf{0} \qquad \text{on} \quad \Gamma \times [0,T] \tag{6.13}$$

which considering (6.9) can also be written as (notice we consider $\boldsymbol{g} = (g_1, g_2)$)

$$\operatorname{div} \boldsymbol{\varphi} + g_1 = 0 \quad \text{and} \quad \operatorname{curl} \boldsymbol{\varphi} - g_2 = 0 \qquad \text{on} \quad \Gamma \times [0,T]. \tag{6.14}$$

Remark 6.2

It is interesting to notice that in the previous works concerning the case of clamped boundary conditions [17, 18], the authors assume enough regularity for both φ_Q with $Q \in \{P, S\}$, so that $\partial_{\boldsymbol{n}} \varphi_Q = \nabla \varphi_Q \cdot \boldsymbol{n}$ and $\partial_{\boldsymbol{\tau}} \varphi_Q = \nabla \varphi_Q \cdot \boldsymbol{\tau}$ are well defined (where $\boldsymbol{n} = (n_1, n_2)$ and $\boldsymbol{\tau} = (n_2, -n_1)$ denote the normal and tangential vectors represented in Figure 6.1). Under this assumption it is possible to consider normal and tangential traces in equation (6.13) to obtain the boundary conditions

$$\partial_{\boldsymbol{n}} \varphi_P = \partial_{\boldsymbol{\tau}} \varphi_S - \boldsymbol{g} \cdot \boldsymbol{n} \qquad \text{and} \qquad \partial_{\boldsymbol{n}} \varphi_S = -\partial_{\boldsymbol{\tau}} \varphi_P - \boldsymbol{g} \cdot \boldsymbol{\tau}, \tag{6.15}$$

just noticing that $\mathbf{curl}\, \varphi \cdot \boldsymbol{n} = -\partial_{\boldsymbol{\tau}} \varphi$ and $\mathbf{curl}\, \varphi \cdot \boldsymbol{\tau} = -\partial_{\boldsymbol{n}} \varphi$.

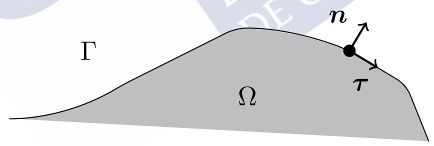

Figure 6.1: Representation of the normal an tangential vectors on $\Gamma = \partial\Omega$.

6.2 Variational formulation

In this section, our aim is to establish an adequate weak formulation for the boundary value problem ((6.6), (6.14)) that we summarize next:

$$\begin{cases} \text{Find } \boldsymbol{\varphi} = (\varphi_P, \varphi_S) : \Omega \times [0,T] \longrightarrow \mathbb{R}^2, \text{ such that} \\ \dfrac{1}{V_P^2}\, \partial_t^2 \varphi_P - \Delta \varphi_P = \operatorname{div} \boldsymbol{g}, \quad \text{in } \Omega \times [0,T], & (6.16a) \\ \dfrac{1}{V_S^2}\, \partial_t^2 \varphi_S - \Delta \varphi_S = -\operatorname{curl} \boldsymbol{g}, \quad \text{in } \Omega \times [0,T], & (6.16b) \\ \operatorname{div} \boldsymbol{\varphi} + g_1 = 0, \quad \text{on } \Gamma \times [0,T], & (6.16c) \\ \operatorname{curl} \boldsymbol{\varphi} - g_2 = 0, \quad \text{on } \Gamma \times [0,T], & (6.16d) \end{cases}$$

completed with the vanishing initial conditions (6.4) and (6.7)

$$\boldsymbol{\varphi}(t=0)=\mathbf{0} \quad \text{and} \quad \partial_t\boldsymbol{\varphi}(t=0)=\mathbf{0}, \quad \text{in } \Omega. \tag{6.17}$$

A classical approach would be to multiply (6.16a) and (6.16b) by test functions ψ_P and ψ_S in $H^1(\Omega)$, integrate by parts and use (6.15) to replace the normal derivatives of the potentials by tangential derivatives. This is the approach developed in the first works about clamped boundary conditions [17, 18]. However, to proceed in this way, we notice that we need to assume that both φ_P and φ_S are in $H^1(\Omega)$ which is not true in general (see (6.8)). Therefore, we shall proceed in a different way. For this purpose, we first notice that (6.16a) and (6.16b) can be rewritten as

$$\mathbb{D}\,\partial_t^2\boldsymbol{\varphi} - \nabla \operatorname{div}\boldsymbol{\varphi} + \mathbf{curl}\left(\operatorname{curl}\boldsymbol{\varphi}\right) = \begin{pmatrix} \operatorname{div}\boldsymbol{g} \\ -\operatorname{curl}\boldsymbol{g}\end{pmatrix}, \quad \text{where} \quad \mathbb{D} = \begin{pmatrix} \frac{1}{V_P^2} & 0 \\ 0 & \frac{1}{V_S^2}\end{pmatrix},$$

and since equality (6.9) also holds for $\boldsymbol{g}=(g_1,g_2)$, this is equivalent to

$$\mathbb{D}\,\partial_t^2\boldsymbol{\varphi} - \nabla\left(\operatorname{div}\boldsymbol{\varphi}+g_1\right) + \mathbf{curl}\left(\operatorname{curl}\boldsymbol{\varphi}-g_2\right) = \mathbf{0}.$$

Now notice that according to (6.5) and (6.9), and since $\partial_t\boldsymbol{u}(t)\in H^1(\Omega)^2$, we deduce that $(\operatorname{div}\boldsymbol{\varphi} + g_1)$ and $(\operatorname{curl}\boldsymbol{\varphi}-g_2)$ belong to $H^1(\Omega)$. Hence we have enough regularity to multiply by a test function $\boldsymbol{\psi}=(\psi_P,\psi_S)\in\boldsymbol{V}$ (defined in (6.10)) and integrate by parts. As a result we obtain

$$\begin{aligned}\int_\Omega \partial_t^2(\mathbb{D}\,\boldsymbol{\varphi})\cdot\boldsymbol{\psi}\,\mathrm{d}\boldsymbol{x} \quad &+ \quad \int_\Omega(\operatorname{div}\boldsymbol{\varphi}+g_1)\operatorname{div}\boldsymbol{\psi}\,\mathrm{d}\boldsymbol{x} \quad - \quad \int_\Gamma(\operatorname{div}\boldsymbol{\varphi}+g_1)\,\psi\cdot\boldsymbol{n}\,\mathrm{d}\boldsymbol{\gamma} \\ &+ \quad \int_\Omega(\operatorname{curl}\boldsymbol{\varphi}-g_2)\operatorname{curl}\boldsymbol{\psi}\,\mathrm{d}\boldsymbol{x} \quad + \quad \int_\Gamma(\operatorname{curl}\boldsymbol{\varphi}-g_2)\,\psi\cdot\boldsymbol{\tau}\,\mathrm{d}\boldsymbol{\gamma} \quad = \quad \mathbf{0},\end{aligned}$$

where the integrals in the boundary should be interpreted as duality products between elements in $H^{\frac{1}{2}}(\Gamma)$ and its dual $H^{-\frac{1}{2}}(\Gamma)$. In consequence, due to boundary conditions (6.16c) and (6.16d), we obtain the variational formulation

$$\left\{\begin{array}{l}\text{Find } \boldsymbol{\varphi}(t):[0,T]\longrightarrow\boldsymbol{V} \text{ such that } (\boldsymbol{\varphi},\partial_t\boldsymbol{\varphi})(t=0)=(\mathbf{0},\mathbf{0}) \text{ and} \\ \dfrac{\mathrm{d}^2}{\mathrm{d}t^2}\,m_\Omega(\boldsymbol{\varphi}(t),\boldsymbol{\psi}) + a(\boldsymbol{\varphi}(t),\boldsymbol{\psi}) = \mathrm{g}(t,\boldsymbol{\psi}), \quad \forall\,\boldsymbol{\psi}\in\boldsymbol{V},\end{array}\right. \tag{6.18}$$

where we have introduced the following linear and bilinear forms

$$m_\Omega:\boldsymbol{V}\times\boldsymbol{V}\longrightarrow\mathbb{R} \qquad \text{such that} \qquad m_\Omega(\boldsymbol{\varphi},\boldsymbol{\psi}) = \int_\Omega(\mathbb{D}\,\boldsymbol{\varphi})\cdot\boldsymbol{\psi}\,\mathrm{d}\boldsymbol{x}, \tag{6.19}$$

$$a:\boldsymbol{V}\times\boldsymbol{V}\longrightarrow\mathbb{R} \qquad \text{such that} \qquad a(\boldsymbol{\varphi},\boldsymbol{\psi}) = \int_\Omega(\operatorname{div}\boldsymbol{\varphi}\operatorname{div}\boldsymbol{\psi}+\operatorname{curl}\boldsymbol{\varphi}\operatorname{curl}\boldsymbol{\psi})\,\mathrm{d}\boldsymbol{x}, \tag{6.20}$$

$$\mathrm{g}:\boldsymbol{V}\longrightarrow\mathbb{R} \qquad \text{such that} \qquad \mathrm{g}(\boldsymbol{\psi}) = -\int_\Omega\boldsymbol{g}\cdot\begin{pmatrix}\operatorname{div}\boldsymbol{\psi}\\ -\operatorname{curl}\boldsymbol{\psi}\end{pmatrix}. \tag{6.21}$$

In next section we shall discuss the well posedness of problem (6.18), but first we pay some attention to the way the potentials are coupled, since we recall that the main interest of the method is to obtain a formulation that allows to discretize separately φ_P and φ_S. In this sense, it is interesting to notice that the mass bilinear form $m_\Omega(\cdot,\cdot)$ decouples φ_P and φ_S

$$\left\{\begin{array}{l} m_\Omega(\boldsymbol{\varphi},\boldsymbol{\psi}) = m_P(\varphi_P,\psi_P)+m_S(\varphi_S,\psi_S) \\ m_Q(\varphi_Q,\psi_Q) = \dfrac{1}{V_Q^2}\displaystyle\int_\Omega\varphi_Q\,\psi_Q\,\mathrm{d}\boldsymbol{x}, \qquad Q\in\{P,S\}.\end{array}\right. \tag{6.22}$$

However, this is not the case for the stiffness bilinear form $a(\cdot,\cdot)$ which apparently couples the potentials in all the computational domain Ω. Fortunately, we notice that in $H^1(\Omega)^2$ and therefore also for standard Lagrange finite element spaces, we can rewrite $a(\cdot,\cdot)$ as the sum of two bilinear forms, one associated to the volume that decouples the potentials as $m_\Omega(\cdot,\cdot)$ and is given by the bilinear form

$$\begin{cases} a_\Omega(\boldsymbol{\varphi},\boldsymbol{\psi}) = a_P(\varphi_P,\psi_P) + a_S(\varphi_S,\psi_S) \\ a_Q(\varphi_Q,\psi_Q) = \displaystyle\int_\Omega \nabla\varphi_Q\cdot\nabla\psi_Q\,\mathrm{d}\boldsymbol{x}, \qquad Q\in\{P,S\}, \end{cases} \tag{6.23}$$

and another part that couples the potentials but only on the surface and is given by the bilinear form

$$a_\Gamma(\boldsymbol{\varphi},\boldsymbol{\psi}) = \int_\Gamma \left(\partial_{\boldsymbol{\tau}}\varphi_P\,\psi_S + \partial_{\boldsymbol{\tau}}\psi_P\,\varphi_S\right)\mathrm{d}\boldsymbol{\gamma}, \tag{6.24}$$

where the integrals on the boundary should be interpreted as duality products between elements in $H^{\frac12}(\Gamma)$ and its dual $H^{-\frac12}(\Gamma)$. This reformulation is proven in the following lemma.

Lemma 6.3

For any $\boldsymbol{\varphi},\boldsymbol{\psi}\in H^1(\Omega)^2\times H^1(\Omega)^2$ we have the identity

$$a(\boldsymbol{\varphi},\boldsymbol{\psi}) = a_\Omega(\boldsymbol{\varphi},\boldsymbol{\psi}) + a_\Gamma(\boldsymbol{\varphi},\boldsymbol{\psi}).$$

Proof. First, we recall that for any $\boldsymbol{\varphi}\in\boldsymbol{V}$, we have that $\nabla\varphi_P + \mathbf{curl}\,\varphi_S = (\operatorname{div}\boldsymbol{\varphi}, -\operatorname{curl}\boldsymbol{\varphi})^T$, then we notice that after expansion and using $\mathbf{curl}\,\varphi_S\cdot\mathbf{curl}\,\psi_S = \nabla\varphi_S\cdot\nabla\psi_S$ and (6.23), we obtain

$$a(\boldsymbol{\varphi},\boldsymbol{\psi}) = a_\Omega(\boldsymbol{\varphi},\boldsymbol{\psi}) + \int_\Omega \nabla\varphi_P\cdot\mathbf{curl}\,\psi_S\,\mathrm{d}\boldsymbol{x} + \int_\Omega \nabla\psi_P\cdot\mathbf{curl}\,\varphi_S\,\mathrm{d}\boldsymbol{x}.$$

Next we observe that integrating by parts and noticing that $\operatorname{curl}\nabla\varphi_P = 0$,

$$\int_\Omega \nabla\varphi_P\cdot\mathbf{curl}\,\psi_S\,\mathrm{d}\boldsymbol{x} = \int_\Omega \operatorname{curl}\nabla\varphi_P\,\psi_S\,\mathrm{d}\boldsymbol{x} + \int_\Gamma \nabla\varphi_P\cdot\boldsymbol{\tau}\;\psi_S\,\mathrm{d}\boldsymbol{\gamma} = \int_\Gamma \partial_{\boldsymbol{\tau}}\varphi_P\,\psi_S\,\mathrm{d}\boldsymbol{\gamma}.$$

Analogously

$$\int_\Omega \nabla\psi_P\cdot\mathbf{curl}\,\varphi_S\,\mathrm{d}\boldsymbol{x} = \int_\Omega \operatorname{curl}\nabla\psi_P\,\varphi_S\,\mathrm{d}\boldsymbol{x} + \int_\Gamma \nabla\psi_P\cdot\boldsymbol{\tau}\,\varphi_S\,\mathrm{d}\boldsymbol{\gamma} = \int_\Gamma \partial_{\boldsymbol{\tau}}\psi_P\,\varphi_S\,\mathrm{d}\boldsymbol{\gamma}.$$

Combining the three previous equations we obtain the result. ■

6.3 Well posedness and energy considerations

In this section we discuss the well posedness of problem (6.18) which, as we shall see in the following lemmas, fits into the classical theory of second order partial differential equations (see for instance Chapter VIII in [100]). However, the analysis we develop is shorter since by construction the existence of solution of the potentials problem (6.18) is given by the existence of solution of displacements problem (6.1) (see Theorem 6.1). To begin with, we shall remark that the forms involved in problem (6.18) are all continuous.

Lemma 6.4

There exist strictly positive constants K_m, K_a and K_{g} such that

$$\begin{aligned} |m_\Omega(\boldsymbol{\varphi},\boldsymbol{\psi})| &\le K_m\|\boldsymbol{\varphi}\|_{\boldsymbol{V}}\|\boldsymbol{\psi}\|_{\boldsymbol{V}} && \text{for all}\quad \boldsymbol{\varphi},\boldsymbol{\psi}\in\boldsymbol{V}.\\ |a(\boldsymbol{\varphi},\boldsymbol{\psi})| &\le K_a\|\boldsymbol{\varphi}\|_{\boldsymbol{V}}\|\boldsymbol{\psi}\|_{\boldsymbol{V}} && \text{for all}\quad \boldsymbol{\varphi},\boldsymbol{\psi}\in\boldsymbol{V}.\\ |\mathrm{g}(\boldsymbol{\psi})| &\le K_{\mathrm{g}}\|\boldsymbol{\psi}\|_{\boldsymbol{V}} && \text{for all}\quad \boldsymbol{\psi}\in\boldsymbol{V}. \end{aligned}$$

Moreover, it is also important to notice that both bilinear forms $m_\Omega(\cdot,\cdot)$ and $a(\cdot,\cdot)$ are symmetric and positive and that the following coercivity condition holds.

Lemma 6.5

There exists a strictly positive constants α_m such that

$$m_\Omega(\boldsymbol{\psi},\boldsymbol{\psi}) \;\geq\; \alpha_m \int_\Omega |\boldsymbol{\psi}|^2 \,\mathrm{d}\boldsymbol{x} \quad \textit{for all} \quad \boldsymbol{\psi} \in \boldsymbol{V}.$$

These two lemmas are enough to obtain the following result of existence and uniqueness of solution of problem (6.18).

Theorem 6.6

Assume that $\boldsymbol{f} \in \mathcal{C}^1\big([0,T]; L^2(\Omega)^2\big)$. Then, there exists a unique strong solution of problem (6.18) *such that*

$$\boldsymbol{\varphi} \in \mathcal{C}^2([0,T]; L^2(\Omega)^2) \cap \mathcal{C}^1([0,T]; \boldsymbol{V}).$$

Proof. First of all, we notice that according to Theorem 6.1, and the posterior derivation of problem (6.18), there exists at least one solution $\boldsymbol{\varphi} = (\varphi_P, \varphi_S)$ which is given by equations (6.3) and (6.4). Moreover, as we discuss in (6.8), the vector of potentials is such that

$$\boldsymbol{\varphi} \in \mathcal{C}^2([0,T]; L^2(\Omega)^2) \cap \mathcal{C}^1([0,T]; \boldsymbol{V}).$$

In consequence, only uniqueness remains to be proved. Let us assume that there exists another solution $\boldsymbol{\varphi}^\star$ and we denote $\boldsymbol{e} = \boldsymbol{\varphi} - \boldsymbol{\varphi}^\star$. We observe that

$$\frac{\mathrm{d}^2}{\mathrm{d}t^2}\, m_\Omega(\boldsymbol{e},\boldsymbol{\psi}) + a(\boldsymbol{e},\boldsymbol{\psi}) = 0, \quad \forall\, \boldsymbol{\psi} \in \boldsymbol{V},$$

and in particular, if we consider $\boldsymbol{\psi} = \partial_t \boldsymbol{e}$ we obtain the following energy identity (subscript D holds for Dirichlet)

$$\frac{\mathrm{d}}{\mathrm{d}t}\mathcal{E}_D(\boldsymbol{e}) = 0, \quad \text{for the energy} \quad \mathcal{E}_D(\boldsymbol{e}) := \frac{1}{2}\, m_\Omega(\partial_t \boldsymbol{e}, \partial_t \boldsymbol{e}) \;+\; \frac{1}{2}\, a(\boldsymbol{e},\boldsymbol{e}). \tag{6.25}$$

Thus $\mathcal{E}_D(\boldsymbol{e}) = 0$ and we obtain $\partial_t \boldsymbol{\varphi} = \partial_t \boldsymbol{\varphi}^\star$, since considering Lemma 6.5 we have that

$$\int_\Omega |\partial_t \boldsymbol{e}|^2 \,\mathrm{d}\boldsymbol{x} \;\leq\; \frac{1}{\alpha_m} m_\Omega(\partial_t \boldsymbol{e}, \partial_t \boldsymbol{e}) \;\leq\; \frac{2}{\alpha_m}\mathcal{E}_D(\boldsymbol{e}) \;=\; 0.$$

Finally, initial conditions allow to conclude.

■

It is interesting to notice, that the energy associated to problem (6.18), which is defined by (6.25) differs from $\mathcal{E}_P(\psi_P) + \mathcal{E}_S(\psi_S)$ where $\mathcal{E}_P(\psi)$ and $\mathcal{E}_S(\psi)$ are the energies usually associated to each of the wave equations in (6.16a) and (6.16b), namely

$$\mathcal{E}_Q(\psi) = \frac{1}{2\,V_Q^2}\int_\Omega |\partial_t \psi|^2 \mathrm{d}\boldsymbol{x} + \frac{1}{2}\int_\Omega |\nabla \psi|^2 \,\mathrm{d}\boldsymbol{x}, \quad Q \in \{P, S\}. \tag{6.26}$$

More precisely, according to Lemma 6.3 the two quantities differ by a boundary term since, assuming that ψ_P and ψ_S are smooth enough, one computes that

$$\mathcal{E}_D(\boldsymbol{\psi}) = \mathcal{E}_P(\psi_P) + \mathcal{E}_S(\psi_S) + a_\Gamma(\boldsymbol{\psi},\boldsymbol{\psi}).$$

It is also interesting (and this will be important for the Neumann problem) to relate this energy to the classical elastic energy defined by

$$E_{el}(\boldsymbol{w}) = E_c(\boldsymbol{w}) + E_p(\boldsymbol{w}), \tag{6.27}$$

where the kinetic and potential energies $E_c(\boldsymbol{w})$ and $E_p(\boldsymbol{w})$ are given by

$$E_c(\boldsymbol{w}) = \frac{\rho}{2}\int_\Omega |\partial_t \boldsymbol{w}|^2 \,\mathrm{d}\boldsymbol{x}, \qquad E_p(\boldsymbol{w}) = \frac{1}{2}\int_\Omega \underline{\boldsymbol{\sigma}}(\boldsymbol{w}) : \underline{\boldsymbol{\varepsilon}}(\boldsymbol{w})\,\mathrm{d}\boldsymbol{x}, \tag{6.28}$$

where, using *Einstein's convention*, $\underline{\boldsymbol{\sigma}} : \underline{\boldsymbol{\varepsilon}} := \sigma_{ij}\varepsilon_{ij}$ is the tensor product or contraction product between two tensors. To do so, we consider $\boldsymbol{u}$ the solution in displacements and $\boldsymbol{\varphi}$ the solution in potentials and notice that in absence of source term, both are related by $\partial_t \boldsymbol{u} = \nabla\varphi_P + \mathbf{curl}\,\varphi_S$. Thus, on the one hand

$$E_c(\boldsymbol{u}) = \frac{\rho}{2}\int_\Omega |\nabla\varphi_P + \mathbf{curl}\,\varphi_S|^2 \,\mathrm{d}\boldsymbol{x} = \frac{\rho}{2}\, a\,(\boldsymbol{\varphi},\boldsymbol{\varphi})\,. \tag{6.29}$$

On the other hand, thanks to Hooke's law (5.2)

$$E_p(\boldsymbol{u}) = \frac{\lambda}{2}\int_\Omega |\mathrm{div}\,\boldsymbol{u}|^2\,\mathrm{d}\boldsymbol{x} + \mu\int_\Omega |\underline{\boldsymbol{\varepsilon}}(\boldsymbol{u})|^2\,\mathrm{d}\boldsymbol{x}. \tag{6.30}$$

Next we provide the following lemma that allows to rewrite the strain tensor $\underline{\boldsymbol{\varepsilon}}$ and which proof is provided below for completeness.

Lemma 6.7

For all $\boldsymbol{w} \in H^1(\Omega)^2$ one has

$$\int_\Omega |\underline{\boldsymbol{\varepsilon}}(\boldsymbol{w})|^2\, dx = \int_\Omega |\mathrm{div}\,\boldsymbol{w}|^2\, d\boldsymbol{x} + \frac{1}{2}\int_\Omega |\mathrm{curl}\,\boldsymbol{w}|^2\, d\boldsymbol{x} - 2\int_\Gamma w_2\,\partial_{\boldsymbol{\tau}} w_1 d\boldsymbol{\gamma}.$$

Proof. It is based on the following algebraic manipulations,

$$\begin{aligned} |\underline{\boldsymbol{\varepsilon}}(\boldsymbol{w})|^2 &= |\partial_1 w_1|^2 + |\partial_2 w_2|^2 + \tfrac{1}{2}|\partial_1 w_2 + \partial_2 w_1|^2 \\ &= |\partial_1 w_1 + \partial_2 w_2|^2 - 2\,\partial_1 w_1\,\partial_2 w_2 + \tfrac{1}{2}|\partial_1 w_2 - \partial_2 w_1|^2 + 2\,\partial_1 w_2\,\partial_2 w_1 \\ &= |\mathrm{div}\,\boldsymbol{w}|^2 + \tfrac{1}{2}|\mathrm{curl}\,\boldsymbol{w}|^2 + 2\,\mathbf{curl}\,w_1\cdot\nabla w_2. \end{aligned}$$

Finally, we obtain the result by integration of the above equality over Ω since, by an integration by parts

$$\int_\Omega \mathbf{curl}\,u_1\cdot\nabla u_2\,\mathrm{d}\boldsymbol{x} = -\int_\Gamma u_2\,\partial_{\boldsymbol{\tau}} u_1 \mathrm{d}\boldsymbol{\gamma}.$$

■

We can use this lemma to rewrite the potential energy as

$$E_p(\boldsymbol{u}) = \frac{\lambda+2\mu}{2}\int_\Omega |\mathrm{div}\,\boldsymbol{u}|^2\,\mathrm{d}\boldsymbol{x} + \frac{\mu}{2}\int_\Omega |\mathrm{curl}\,\boldsymbol{u}|^2\,\mathrm{d}\boldsymbol{x} - 2\mu\int_\Gamma u_2\;\partial_{\boldsymbol{\tau}} u_1\,\mathrm{d}\boldsymbol{\gamma}. \tag{6.31}$$

Then considering the Dirichlet boundary condition and using definition of potentials (6.3) one gets

$$E_p(\boldsymbol{u}) = \frac{\rho}{2}\, m_\Omega\,(\partial_t\boldsymbol{\varphi},\partial_t\boldsymbol{\varphi})\,. \tag{6.32}$$

Finally, joining (6.29) and (6.32) we observe that the elastic energy is related to $\mathcal{E}_D(\boldsymbol{\varphi})$ as follows

$$E_{el}(\boldsymbol{u}) = \rho\,\mathcal{E}_D(\boldsymbol{\varphi}). \tag{6.33}$$

6.4 Discrete formulation

In this section we provide a fully discrete scheme to approximate problem (6.18). First, we will present a standard Galerkin space discretization considering Lagrange finite elements spaces. As we have mentioned before, our main interest will be to allow the use of independent meshes to approximate each potential. Then, we will present a time discretization which will be close to a standard explicit leap-frog discretization of each wave equation. In that part, our main interest will be that the coupling between the potentials (which only happens on the boundary) has no influence on the resulting CFL stability condition.

6.4.1 Space discretization

The space discretization of (6.18) relies on the construction of a finite dimensional approximation of the space $\boldsymbol{V}$ that we will denote by $\boldsymbol{V}_h$. Notice that due to the density result in (6.12), standard approximation spaces of $H^1(\Omega)^2$ ensure adequate approximation properties when approximating $\boldsymbol{V}$. Moreover, in order to decouple the potentials in the volume and according to Lemma 6.3, we shall consider $\boldsymbol{V}_h \subset H^1(\Omega)^2$. Thus, let us consider $\mathcal{T}_{P,h}$ and $\mathcal{T}_{S,h}$ two triangulations of Ω, then the approximation space $\boldsymbol{V}_h$ will be naturally sought in the form

$$\boldsymbol{V}_h = V_{P,h} \times V_{S,h}, \quad \text{where} \quad V_{Q,h} = X_{p_Q}(\mathcal{T}_{Q,h}), \quad \text{for} \quad Q \in \{P, S\}, \tag{6.34}$$

where $X_p(\cdot)$ denotes the standard Lagrange finite elements spaces of order p introduced in (2.57). As mentioned, the density result in (6.12) ensures that the approximation properties in Section 2.5.1 are preserved when approximating $\boldsymbol{V}$ by $\boldsymbol{V}_h$. Furthermore, the spaces $V_{P,h}$ and $V_{S,h}$ can be constructed in different meshes and allow the use of Lemma 6.3 to evaluate $a(\cdot,\cdot)$ and that is why this method gives us the flexibility for adapting each space discretization to each type of wave. The resultant semi-discrete problem writes:

$$\left\{ \begin{array}{l} \text{Find } \boldsymbol{\varphi}_h(t) : [0,T] \longrightarrow \boldsymbol{V}_h \text{ such that } (\boldsymbol{\varphi}_h, \partial_t \boldsymbol{\varphi}_h)(t=0) = (\mathbf{0}, \mathbf{0}) \text{ and} \\ \dfrac{\mathrm{d}^2}{\mathrm{d}t^2}\, m_\Omega(\boldsymbol{\varphi}_h(t), \boldsymbol{\psi}_h) + a_\Omega(\boldsymbol{\varphi}_h(t), \boldsymbol{\psi}_h) + a_\Gamma(\boldsymbol{\varphi}_h(t), \boldsymbol{\psi}_h) = \mathrm{g}(t, \boldsymbol{\psi}_h), \quad \forall\, \boldsymbol{\psi}_h \in \boldsymbol{V}_h. \end{array} \right. \tag{6.35}$$

The associated algebraic system is obtained after introducing the vector $\mathbf{\Phi}_h^T = (\mathbf{\Phi}_{P,h}^T, \mathbf{\Phi}_{S,h}^T)$ of the Lagrange degrees of freedom of $\varphi_{P,h}$ and $\varphi_{S,h}$ (whose dimensions may be different). It takes the following form (completed with $\mathbf{\Phi}_h(0) = \frac{\mathrm{d}}{\mathrm{d}t}\mathbf{\Phi}_h(0) = \mathbf{0}$)

$$\mathbb{M}_h^\Omega \frac{\mathrm{d}^2 \mathbf{\Phi}_h}{\mathrm{d}t^2} + \mathbb{A}_h\, \mathbf{\Phi}_h = \boldsymbol{G}_h, \quad \text{where} \quad \mathbb{A}_h \coloneqq \mathbb{A}_h^\Omega + \mathbb{A}_h^\Gamma. \tag{6.36}$$

The embedding $\boldsymbol{V}_h \subset [H^1(\Omega)]^2$ authorizes the use of the exact forms to compute (note $\mathbb{O}$ refers to null matrices of the respective size)

$$\mathbb{M}_h^\Omega = \begin{pmatrix} \mathbb{M}_{P,h} & \mathbb{O} \\ \mathbb{O} & \mathbb{M}_{S,h} \end{pmatrix}, \quad \mathbb{A}_h^\Omega = \begin{pmatrix} \mathbb{A}_{P,h} & \mathbb{O} \\ \mathbb{O} & \mathbb{A}_{S,h} \end{pmatrix} \quad \text{and} \quad \mathbb{A}_h^\Gamma = \begin{pmatrix} \mathbb{O} & \mathbb{A}_{PS,h}^\Gamma \\ \left(\mathbb{A}_{PS,h}^\Gamma\right)^T & \mathbb{O} \end{pmatrix}.$$

Notice that the computation of matrices $\mathbb{M}_{Q,h}$ and $\mathbb{A}_{Q,h}$ for $Q \in \{P, S\}$ is very standard

$$(\mathbb{M}_{Q,h})_{k,l} = \frac{1}{V_Q^2} \int_\Omega \psi_Q^k\, \psi_Q^l \,\mathrm{d}\boldsymbol{x}, \quad \text{and} \quad (\mathbb{A}_{Q,h})_{k,l} = \int_\Omega \nabla \psi_Q^k, \nabla \psi_Q^l \,\mathrm{d}\boldsymbol{x},$$

where we denote by $\{\psi_Q^k\}_{k=1}^{K_Q}$ the set of Lagrange basis functions of $V_{Q,h}$ for $Q \in \{P, S\}$. However, this is not the case for the computation of the matrix $\mathbb{A}_{PS,h}$ which couples both potentials but in a very sparse way since it only couples neighbouring degrees of freedom that are located along the boundary. Notice that to compute

$$(\mathbb{A}_{PS,h}^\Gamma)_{k,l} = \int_\Gamma \partial_{\boldsymbol{\tau}} \psi_P^k\, \psi_S^l \,\mathrm{d}\gamma,$$

we require to intersect on the boundary the meshes chosen to build $V_{P,h}$ and $V_{S,h}$. A nice intersection algorithm with linear complexity to perform projections between 2d and 3d non-matching grids is presented in [41]. Following the ideas presented there, similar algorithms can be developed to perform projections between 1d non-matching grids.

Finally, we shall remark that for efficiency we can consider specific quadrature formulas that achieve mass lumping, this is to say that instead of $\mathbb{M}_h^\Omega$, we consider a different mass matrix $\widetilde{\mathbb{M}}_h^\Omega$ which is diagonal and such that the order of accuracy of the approximation is preserved. This is essential to obtain after time discretization an explicit scheme which is really computationally explicit. Many techniques can be used to achieve this goal (see [21, 22, 24, 58] and the references therein). For Lagrange finite elements, the fact that the matrix $\widetilde{\mathbb{M}}_h^\Omega$ is diagonal results from the position of the quadrature points that coincide with the Lagrange degrees of freedom. In particular when first order Lagrange finite elements are considered, it is known that the accuracy of the approximation is preserved [21] and that the diagonal elements $\widetilde{\mathbb{M}}_h^\Omega$ are nothing but the sum of the elements of the same line in the original matrix $\mathbb{M}_h^\Omega$ (which are all strictly positive since all the shape functions are positive)

$$(\widetilde{\mathbb{M}}_h^\Omega)_{i,i} = \sum_j (\mathbb{M}_h^\Omega)_{i,j} \quad \text{and} \quad (\widetilde{\mathbb{M}}_h^\Omega)_{i,j} = 0 \text{ for } j \neq i. \tag{6.37}$$

It is also worthwhile to mention that mass lumping not only simplifies the numerical computations but also adds positivity to the mass matrix. This seems to be rather specific to first order Lagrange finite elements and relies on the following lemma (that we suspect to be known but did not find in the literature):

Lemma 6.8

When first order Lagrange finite elements are considered, one has the inequality

$$\widetilde{\mathbb{M}}_h^\Omega \, \mathbf{\Psi}_h \cdot \mathbf{\Psi}_h \geq \mathbb{M}_h^\Omega \, \mathbf{\Psi}_h \cdot \mathbf{\Psi}_h.$$

Proof. Let us introduce $\mathbb{B}_h = \widetilde{\mathbb{M}}_h^\Omega - \mathbb{M}_h^\Omega$ and notice that it is enough to prove that all the eigenvalues of $\mathbb{B}_h$ are positive. Then, we use the Gershgorin circle theorem (see Theorem 7.3 in [101]) that, for real symmetric matrices, says that the spectrum $\sigma(\mathbb{B}_h)$ is included in a finite union of intervals with centre $(\mathbb{B}_h)_{i,i}$ and radius $\sum_{j\neq i} \left|(\mathbb{B}_h)_{i,j}\right|$, i.e.

$$\sigma(\mathbb{B}_h) \subset \bigcup_i \left[\, (\mathbb{B}_h)_{i,i} - \sum_{j\neq i} \left|(\mathbb{B}_h)_{i,j}\right| \, , \, (\mathbb{B}_h)_{i,i} + \sum_{j\neq i} \left|(\mathbb{B}_h)_{i,j}\right| \, \right].$$

And notice that it suffices to see that the lower bounds of the above intervals is always 0. For this, we recall that $(\mathbb{M}_h^\Omega)_{i,j} \geq 0$ and according to (6.37),

$$(\mathbb{B}_h)_{i,i} = \sum_{j\neq i} (\mathbb{M}_h^\Omega)_{i,j} \quad \text{and} \quad (\mathbb{B}_h)_{i,j} = -(\mathbb{M}_h^\Omega)_{i,j} \text{ for } j \neq i.$$

∎

6.4.2 Time discretization

In this section, as it was presented in [17], we propose a semi-implicit method that consists in treating in a explicit way the terms associated to the volume and implicitly those related to the coupling through the boundary. We expect this to provide a fully discrete scheme which on the one hand is close to standard explicit leap-frog discretization of each wave equation while on the other hand the resulting CFL stability condition is not affected by the coupling between the potentials. More precisely, let us consider a fixed time discretization step Δt and approximate the unknown

$\boldsymbol{\Phi}_h$ at each $t^n = n\,\Delta t$ by $\boldsymbol{\Phi}_h^n$, thus we choose to approximate the semi discrete problem (6.36) by the following fully discrete scheme:

$$\mathbb{M}_h^\Omega \frac{\boldsymbol{\Phi}_h^{n+1} - 2\boldsymbol{\Phi}_h^n + \boldsymbol{\Phi}_h^{n-1}}{\Delta t^2} + \mathbb{A}_h^\Omega\, \boldsymbol{\Phi}_h^n + \mathbb{A}_h^\Gamma \frac{\boldsymbol{\Phi}_h^{n+1} + 2\boldsymbol{\Phi}_h^n + \boldsymbol{\Phi}_h^{n-1}}{4} = \boldsymbol{G}_h^n, \tag{6.38}$$

completed with vanishing initial conditions $\boldsymbol{\Phi}_h^0 = \boldsymbol{\Phi}_h^1 = \mathbf{0}$. Notice, that the well-posedness of the fully-discrete problem (6.38) requires the invertibility of the matrix

$$\mathbb{M}_h^\Omega + \frac{\Delta t^2}{4}\mathbb{A}_h^\Gamma.$$

However, we postpone its verification since the stability analysis of (6.38) will provide a more restrictive condition for the admissible Δt. Thus we first analyse the stability of (6.38), which as usual relies on a discrete energy identity which can be reduced by linearity to the case of a zero right hand side (we omit details since the technique has already been presented in Section 3.4). The main lemma is the following

Lemma 6.9

Assuming $\boldsymbol{G}_h^n = 0$ for $n \geq n^*$, any solution of (6.38) *satisfies*

$$\forall\, n \geq n^*, \quad \mathcal{E}_{D,h}^{n+\frac{1}{2}} = \mathcal{E}_{D,h}^{n-\frac{1}{2}}, \tag{6.39}$$

where the discrete energy $\mathcal{E}_{D,h}^{n+\frac{1}{2}}$ is defined by

$$\begin{aligned} \mathcal{E}_{D,h}^{n+\frac{1}{2}} \;&:=\; \frac{1}{2}\left(\mathbb{M}_h^\Omega - \frac{\Delta t^2}{4}\,\mathbb{A}_h^\Omega\right)\frac{\boldsymbol{\Phi}_h^{n+1} - \boldsymbol{\Phi}_h^n}{\Delta t}\cdot\frac{\boldsymbol{\Phi}_h^{n+1} - \boldsymbol{\Phi}_h^n}{\Delta t} \\ &+\; \frac{1}{2}\,\mathbb{A}_h \frac{\boldsymbol{\Phi}_h^{n+1} + \boldsymbol{\Phi}_h^n}{2}\cdot\frac{\boldsymbol{\Phi}_h^{n+1} + \boldsymbol{\Phi}_h^n}{2}. \end{aligned} \tag{6.40}$$

Proof. (Sketch) The approach is classical. The key idea is to rewrite (6.38) considering in the term $\mathbb{A}_h^\Omega\,\boldsymbol{\Phi}_h^n$ the equality

$$\boldsymbol{\Phi}_h^n = \frac{\boldsymbol{\Phi}_h^{n+1} + 2\boldsymbol{\Phi}_h^n + \boldsymbol{\Phi}_h^{n-1}}{4} - \frac{\Delta t^2}{4}\frac{\boldsymbol{\Phi}_h^{n+1} - 2\boldsymbol{\Phi}_h^n + \boldsymbol{\Phi}_h^{n-1}}{\Delta t^2}.$$

The resultant is the modified fully implicit scheme

$$\left(\mathbb{M}_h^\Omega - \frac{\Delta t^2}{4}\mathbb{A}_h^\Omega\right)\frac{\boldsymbol{\Phi}_h^{n+1} - 2\boldsymbol{\Phi}_h^n + \boldsymbol{\Phi}_h^{n-1}}{\Delta t^2} + (\mathbb{A}_h^\Omega + \mathbb{A}_h^\Gamma)\frac{\boldsymbol{\Phi}_h^{n+1} + 2\boldsymbol{\Phi}_h^n + \boldsymbol{\Phi}_h^{n-1}}{4} = \mathbf{0}.$$

Then it suffices to multiply by

$$\frac{\boldsymbol{\Phi}_h^{n+1} - \boldsymbol{\Phi}_h^{n-1}}{2\,\Delta t}$$

and apply usual manipulations about differences of squares to obtain

$$\frac{1}{2\,\Delta t}\left[\mathcal{E}_{D,h}^{n+\frac{1}{2}} - \mathcal{E}_{D,h}^{n-\frac{1}{2}}\right] = 0,$$

which leads to the result.

■

Moreover, as we have discussed in Section 3.4, the stability of the numerical scheme (6.38) is guaranteed if $\mathcal{E}_{D,h}^{n+\frac{1}{2}}$ is positive. Thus, if we introduce the quantities

$$c_Q(h) = \sup_{\boldsymbol{\Psi}\neq\mathbf{0}} \frac{\mathbb{M}_{Q,h}^{-1}\,\mathbb{A}_{Q,h}\,\boldsymbol{\Psi}\cdot\boldsymbol{\Psi}}{\boldsymbol{\Psi}\cdot\boldsymbol{\Psi}}, \quad \text{for} \quad Q \in \{P, S\}, \tag{6.41}$$

we can write the following stability theorem.

Theorem 6.10

The numerical scheme (6.38) *is stable under the CFL stability condition*

$$\frac{\Delta t^2}{4} \max\left[c_P(h), c_S(h)\right] \ < \ 1. \tag{6.42}$$

Proof. The stability follows from the positivity of the discrete energy (6.40). Since $\mathbb{A}_h$ is positive semi-definite, this reduces to the positivity of the matrix

$$\mathbb{M}_h^\Omega - \frac{\Delta t^2}{4}\,\mathbb{A}_h^\Omega,$$

which is given by the positivity of the matrices

$$\mathbb{M}_{P,h} - \frac{\Delta t^2}{4}\,\mathbb{A}_{P,h} \quad \text{and} \quad \mathbb{M}_{S,h} - \frac{\Delta t^2}{4}\,\mathbb{A}_{S,h},$$

that is guaranteed under condition (6.42) and therefore we obtain the result. ■

Next, we show that the CFL condition (6.42) also guarantees the well posedness of the fully-discrete scheme (6.38).

Theorem 6.11

If the CFL condition (6.42) *holds, then the matrix* $\mathbb{M}_h^\Omega + \dfrac{\Delta t^2}{4}\mathbb{A}_h^\Gamma$ *is invertible.*

Proof. Notice that we are in the hypothesis of Theorem 6.10, thus $\mathbb{M}_h^\Omega - \dfrac{\Delta t^2}{4}\mathbb{A}_h^\Omega$ is positive definite. Then, recalling that $\mathbb{A}_h = \mathbb{A}_h^\Omega + \mathbb{A}_h^\Gamma$ is positive semi-definite, we obtain

$$\mathbb{M}_h^\Omega + \frac{\Delta t^2}{4}\mathbb{A}_h^\Gamma \ = \ \mathbb{M}_h^\Omega + \frac{\Delta t^2}{4}\left(\mathbb{A}_h^\Gamma + \mathbb{A}_h - \mathbb{A}_h^\Omega - \mathbb{A}_h^\Gamma\right) \ = \ \left(\mathbb{M}_h^\Omega - \frac{\Delta t^2}{4}\mathbb{A}_h^\Omega\right) + \frac{\Delta t^2}{4}\mathbb{A}_h.$$

This shows that $\mathbb{M}_h^\Omega + \frac{\Delta t^2}{4}\mathbb{A}_h^\Gamma$ is positive definite and thus invertible. ■

Remark 6.12

It can be inferred that the condition (6.42) *is also a necessary stability condition. Indeed for sources with compact support, for a certain time we simply solve two decoupled scalar wave equations (the boundary conditions do not matter) and we need to satisfy the associated CFL conditions, that are known to be necessary:*

$$\frac{\Delta t^2}{4} c_Q(h) \ < \ 1, \quad \textit{for} \quad Q \in \{P, S\}.$$

Notice that the choice of a time step that satisfies this CFL condition for both schemes is nothing but (6.42).

Remark 6.13

Let us notice that the analysis developed in this section can be easily adapted if we consider mass lumping techniques. We only need to substitute the mass matrix $\mathbb{M}_h^\Omega$ *by the approximated matrix* $\widetilde{\mathbb{M}}_h^\Omega$ *as explained in Section 6.4.1. Moreover, it is interesting to notice that in the particular case of first order Lagrange finite elements, due to Lemma 6.8, if we apply mass lumping techniques, the CFL condition is improved since the positivity of* $\mathbb{M}_h^\Omega - \Delta t^2 \mathbb{A}_h^\Omega/4$

implies the positivity of $\widetilde{\mathbb{M}}_h^\Omega - \Delta t^2 \mathbb{A}_h^\Omega/4$.

Finally, we shall recall the computations that we have developed in Section 5.2 concerning the computational gain of considering potentials formulations compared to the classical methods. There, we have shown that the gain is consequence of the two following properties for the proposed numerical scheme.

- First, the method should allow the use of independent meshes for each type of wave, in consequence we can adapt each of them to the respective wavelength, i.e., we shall consider

$$h_P = \lambda_P/N_\star \quad \text{and} \quad h_S = \lambda_S/N_\star,$$

where we recall that $N_\star$ represents the number of mesh points that we want to consider per wavelength.

- Second, recalling the introduction of the minimal time scale $T_\star$, which is such that $\lambda_Q = T_\star V_Q$ for $Q \in \{P, S\}$, we also require that the stability condition of the resultant numerical scheme is given by $\Delta t \approx T_\star/N_\star$, where the equality holds up to a positive constant only depending on the order of the finite elements considered and the quasi-uniformity factor of the meshes.

Notice that the first condition holds, since we have no restriction when considering the meshes to build $V_{P,h}$ and $V_{S,h}$. Moreover, the second condition is consequence of the CFL condition (6.42) after noticing that for quasi-uniform meshes, when h_P and h_S approaches to zero then (see (6.41) for definition of $c_Q(h)$)

$$c_P(h) \approx \frac{V_P^2}{h_P^2} \quad \text{and} \quad c_S(h) \approx \frac{V_S^2}{h_S^2},$$

where the equality holds up to a positive constant that only depends on the order of the finite elements considered and the quasi-uniformity factor of the meshes. Then, since

$$\frac{V_Q}{h_Q} = \frac{N_\star V_Q}{\lambda_Q} = \frac{N_\star}{T_\star} \quad \text{for both} \quad Q \in \{P, S\},$$

and according to (6.42) we have the expected stability condition

$$\Delta t \;\approx\; \frac{T_\star}{N_\star}.$$

Finally, we notice that for this gain, we only pay the computational price of inverting at each time step the matrix

$$\mathbb{M}_h^\Omega + \frac{\Delta t^2}{4}\mathbb{A}_h^\Gamma \quad \text{or} \quad \widetilde{\mathbb{M}}_h^\Omega + \frac{\Delta t^2}{4}\mathbb{A}_h^\Gamma.$$

Moreover, when the mass is lumped, $\widetilde{\mathbb{M}}_h^\Omega$ is diagonal and considering the sparsity pattern of $\mathbb{A}_h^\Gamma$, the evaluation of interior degrees of freedom is completely explicit while the computation of the boundary degrees of freedom amounts to invert a sparse linear system, the invertibility of which is guaranteed by the stability theorem.

6.5 Numerical results

In this section we present illustrative numerical results to exhibit the good behaviour of the method. The examples we provide correspond to the propagation of transient waves in an isotropic homogeneous domain which is bounded by a clamped boundary.

The model problem. We are interested in finding $\boldsymbol{u}(\boldsymbol{x},t)$ solution of the following elastodynamic problem (which is completed with vanishing initial data)

$$\left\{\begin{array}{rcll} \rho\,\partial_t^2\boldsymbol{u}\,-\,(\lambda+2\,\mu)\,\nabla\,\mathrm{div}\,\boldsymbol{u}\,+\,\mu\,\mathbf{curl}\,\mathrm{curl}\,\boldsymbol{u} & = & \boldsymbol{f}, & \text{in} \quad \Omega\times[0,T], \\ \boldsymbol{u} & = & \mathbf{0}, & \text{on} \quad \Gamma\times[0,T], \end{array}\right. \tag{6.43}$$

where we choose the final time to be $T=5$ and the computational domain $\Omega=[-5,5]\times[-5,5]$. We also consider the physical properties given by

$$\rho=1, \quad \lambda=56 \quad \text{and} \quad \mu=4,$$

and the medium to be excited by the following source (see Figure 6.2)

$$\boldsymbol{f}(\boldsymbol{x},t)=g(t)\,\boldsymbol{h}(\boldsymbol{x}) \quad \text{where} \quad g(t)=\partial_t\exp(-50\,(t-1)^2) \quad \text{and} \quad \boldsymbol{h}\in L^2(\Omega)^2. \tag{6.44}$$

We present three experiments depending on the value of $\boldsymbol{h}$.

First Experiment. We consider a source that generates only pressures waves up to the interaction with the boundary. In this case, $\boldsymbol{h}$ is chosen as the gradient of a smooth compactly supported function centred at $\boldsymbol{x}_0=\mathbf{0}$, i.e.

$$\boldsymbol{h}(\boldsymbol{x})=\nabla s(\boldsymbol{x}) \quad \text{where} \quad s(\boldsymbol{x})=\left\{\begin{array}{ll} \exp\left(1+\frac{1}{|2\,\boldsymbol{x}|^2-1}\right), & |\boldsymbol{x}|<0.5, \\ 0, & \text{elsewhere.} \end{array}\right.$$

Second Experiment. In a second case we consider a source that only generates shear waves up to the interaction with the boundary,

$$\boldsymbol{h}(\boldsymbol{x})=\mathbf{curl}(s(\boldsymbol{x})).$$

Third Experiment. The source we consider is localized near the boundary and generates both shear and pressure waves,

$$\boldsymbol{h}(\boldsymbol{x})=(\,\partial_2 s(\boldsymbol{x}-\boldsymbol{x}_0)\,,\,\partial_1 s(\boldsymbol{x}-\boldsymbol{x}_0)\,)^t \quad \text{where} \quad \boldsymbol{x}_0=(3.5,0)^t.$$

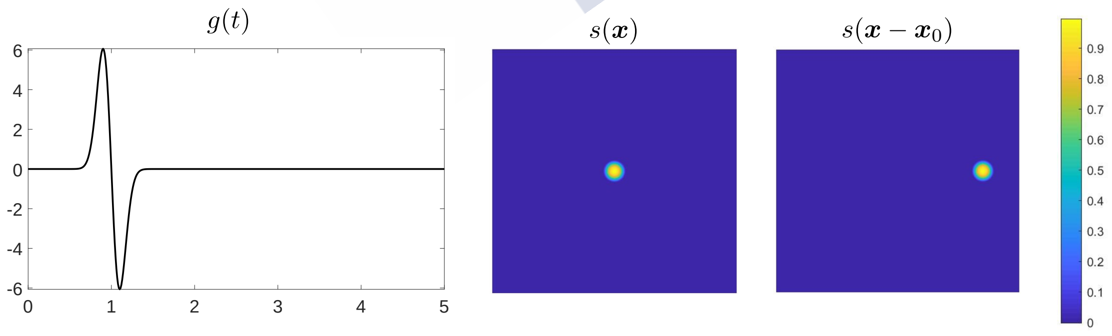

Figure 6.2: Left: time dependence of the source. Right: space dependence of the source.

Space-time discretization of the potentials formulation. According to the techniques presented in this chapter, we consider first order Lagrange finite elements spaces (defined in (6.34)). Note, that for computational reasons and since $V_P/V_S=4$, the triangulations $\mathcal{T}_{P,h}$ and $\mathcal{T}_{S,h}$ are chosen such that $h_P\simeq 4h_S$ (see Figure 6.3). Moreover, we approximate the solution of problem (6.43) by considering the semi-implicit scheme (6.38) with a time step chosen as the maximum Δt such that $0.01/\Delta t$ is an integer and $\Delta t<\Delta t^*$, where Δt^* is computed as the maximum time step allowed in (6.42).

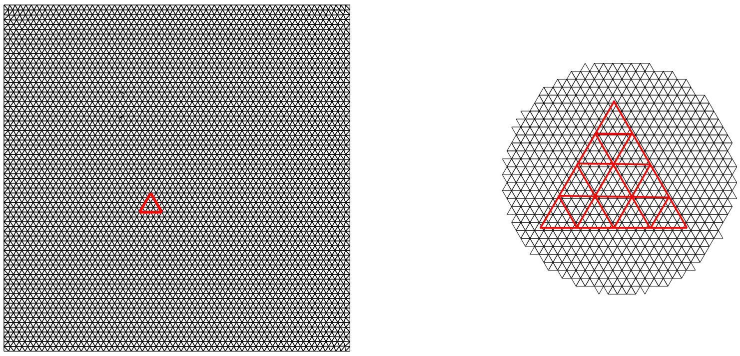

Figure 6.3: On the left we observe the triangulation $\mathcal{T}_{P,h}$ while on the right, since $\mathcal{T}_{S,h}$ is too fine to be plotted, we compare a small piece of the triangulation $\mathcal{T}_{S,h}$ with respect to the triangulation of $\mathcal{T}_{P,h}$.

Computation of a reference displacement solution. To obtain a reference solution we compute the velocity (i.e. $\boldsymbol{v} = \partial_t \boldsymbol{u}$) using a classical method. More precisely, we compute $\boldsymbol{v}_h$, a numerically approximation of $\boldsymbol{v} = \partial_t \boldsymbol{u}$, by solving a discretized version of the problem

$$\left\{ \begin{array}{rcll} \rho\, \partial_t^2 \boldsymbol{v} \,-\, (\lambda + 2\,\mu)\, \nabla \operatorname{div} \boldsymbol{v} \,+\, \mu\, \mathbf{curl}\operatorname{curl} \boldsymbol{v} & = & \partial_t \boldsymbol{f}, & \text{in} \quad \Omega \times [0,T], \\ \boldsymbol{v} & = & \mathbf{0}, & \text{on} \quad \Gamma \times [0,T]. \end{array} \right. \tag{6.45}$$

In particular we consider first order Lagrange finite elements in space (considering the triangulation $\mathcal{T}_{S,h}$) and finite differences in time, more precisely, a leap-frog scheme with the largest possible time step $\Delta\tau$ such that the scheme is stable and $0.01/\Delta\tau$ is an integer.

Procedure of comparison: Potential / Displacement. In order to validate the results we take into account the relation

$$\partial_t \boldsymbol{u} = \nabla \varphi_P + \mathbf{curl}\, \varphi_S + \boldsymbol{g} \quad \text{with} \quad \boldsymbol{g}(\boldsymbol{x},t) = \frac{\boldsymbol{h}(\boldsymbol{x})}{\rho} \int_0^t g(s)\, ds,$$

and we compare with respect to a solution obtained with the reference displacement solution (see paragraph above). The method presented provides a numerical approximation of the potentials φ_P and φ_S, thus in order to compare the obtained solution with the solution generated with the displacement formulation (6.45) we shall also introduce the orthogonal projection $\Pi_{S,h}$ from $\boldsymbol{L}^2(\Omega)$ into $V_{S,h} \times V_{S,h}$ that for every $\boldsymbol{\phi} \in \boldsymbol{L}^2(\Omega)$ assigns $\Pi_{S,h}(\boldsymbol{\phi})$ satisfying

$$\int_\Omega (\Pi_{S,h}(\boldsymbol{\phi}) - \boldsymbol{\phi}) \cdot \Psi_h \;=\; 0 \quad \forall\, \Psi_h \in V_{S,h} \times V_{S,h}.$$

In consequence, in the following, in order to validate the numerical results obtained with the potentials approach, we shall represent

$$\boldsymbol{v}_h \quad \text{compared with} \quad \widetilde{\boldsymbol{v}}_h \;:=\; \Pi_{S,h}(\nabla \varphi_{P,h}) + \Pi_{S,h}(\mathbf{curl}\, \varphi_{S,h}) + \Pi_{S,h}(\boldsymbol{g}).$$

First experiment. In this case, since the source is given by a gradient, we observe in Figures 6.4 and 6.5 that only P-waves are generated. Then the P-waves propagate in the interior of the domain and only when they reach the boundary, the S-waves are generated. It is also interesting to observe how both type of waves are continuously interacting along the boundaries of the computational domain while remain uncoupled in the interior. Finally, in Figures 6.6 and 6.7 we validate qualitatively the results obtained when using potentials formulation by comparing with respect to the solution obtained with a classical formulation.

Second experiment. Now the source is given by a curl, therefore contrary to the previous case, we observe in Figures 6.8 and 6.9 that only S-waves are generated. Then, similarly to the previous example, the S-waves propagate in the interior of the domain and only when they reach the boundary, the P-waves are generated. The results are qualitatively validated in Figures 6.10 and 6.11, where we compare the solution obtained when using potentials with respect to the solution obtained with a classical method.

Third experiment. In the last example, the source generates both types of waves as we can see in Figures 6.12 and 6.13. In this case, we still can observe how the P-waves and the S-waves propagate independently in the interior of the domain, while both type of waves continuously interact along the boundaries of the computational domain. Finally, in order to validate the results, we compare in Figures 6.14 and 6.15 the reconstructed velocity field obtained using potentials formulation with respect to the solution obtained with a classical formulation and we observe a good agreement.

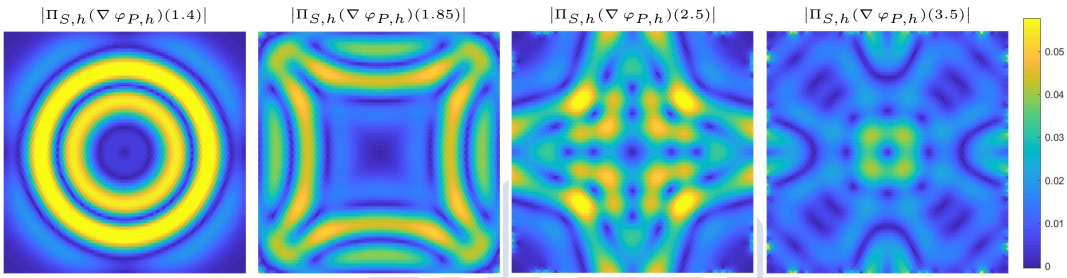

Figure 6.4: Snapshots of the reconstructed P-waves (first experiment).

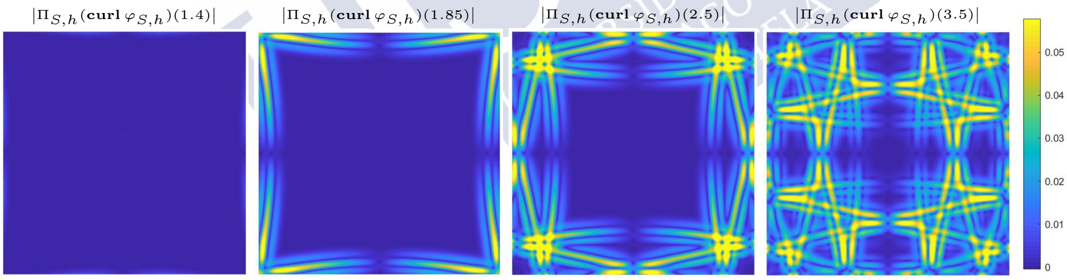

Figure 6.5: Snapshots of the reconstructed S-waves (first experiment).

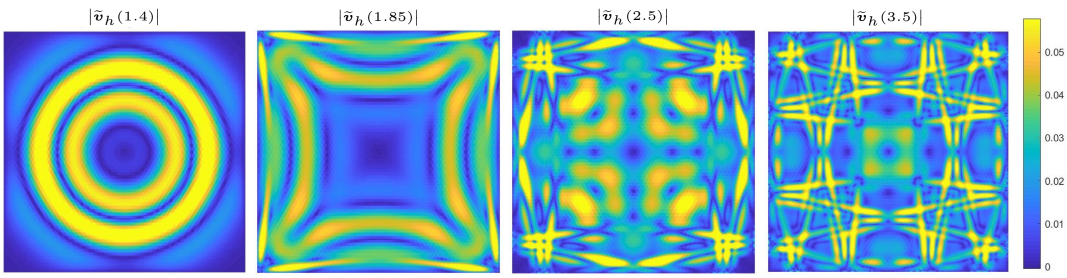

Figure 6.6: Snapshots of the reconstructed velocity field (first experiment).

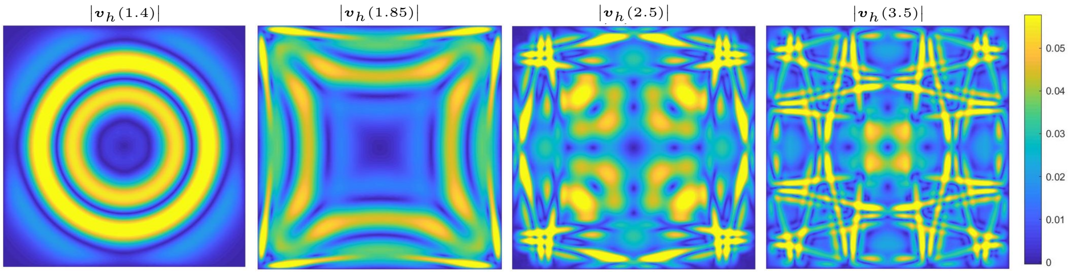

Figure 6.7: Snapshots of the velocity field (first experiment).

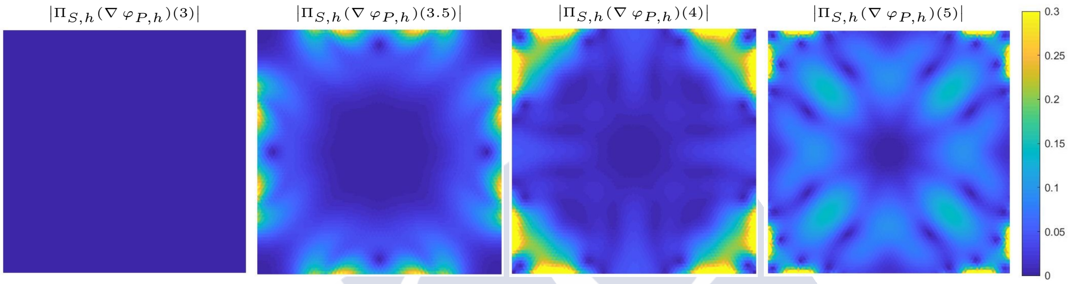

Figure 6.8: Snapshots of the reconstructed P-waves (second experiment).

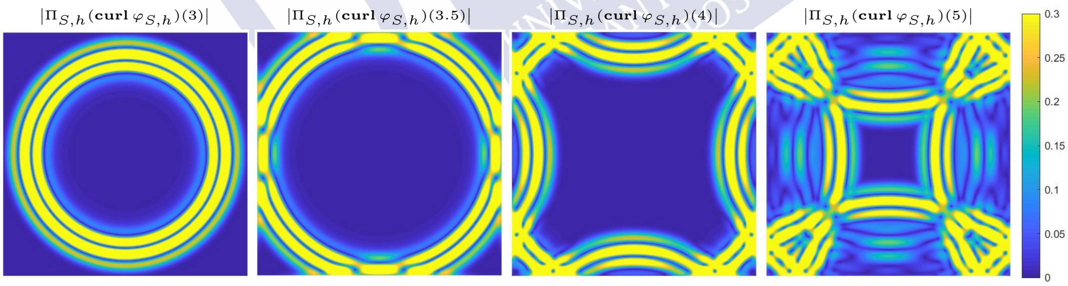

Figure 6.9: Snapshots of the reconstructed S-waves (second experiment).

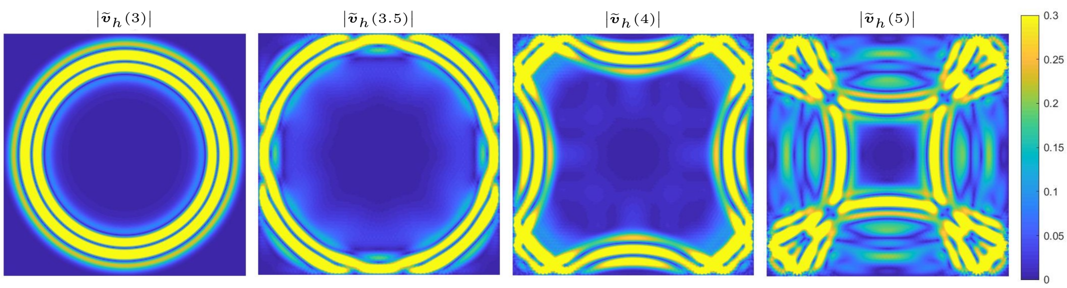

Figure 6.10: Snapshots of the reconstructed velocity field (second experiment).

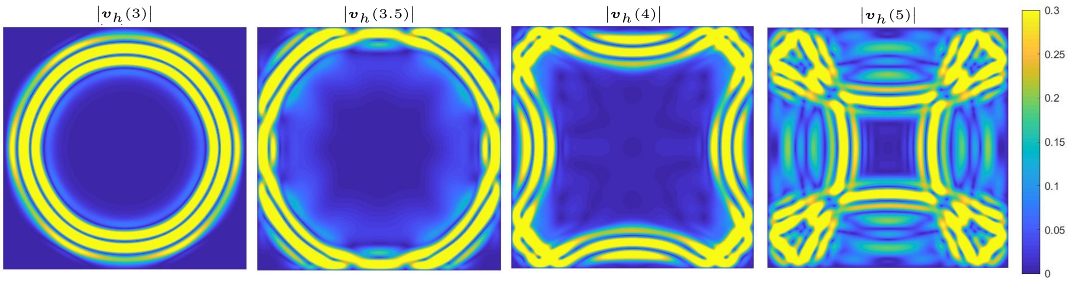

Figure 6.11: Snapshots of the velocity field (second experiment).

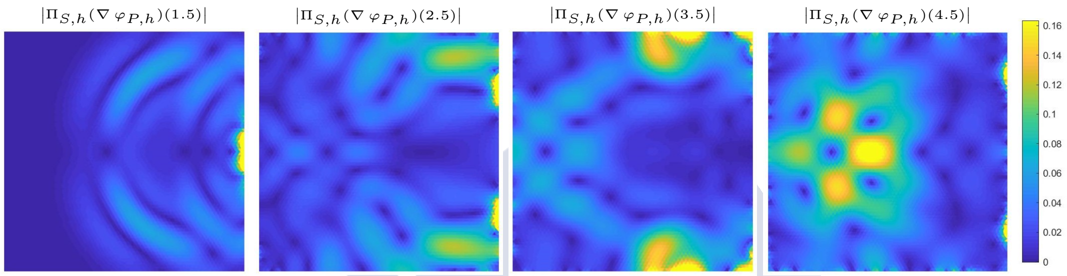

Figure 6.12: Snapshots of the reconstructed P-waves (third experiment).

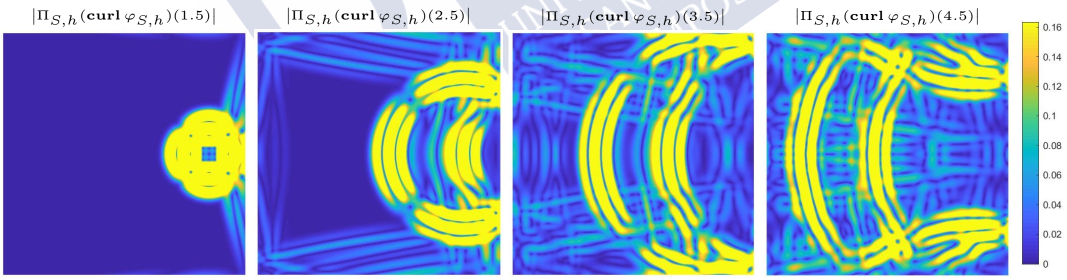

Figure 6.13: Snapshots of the reconstructed S-waves (third experiment).

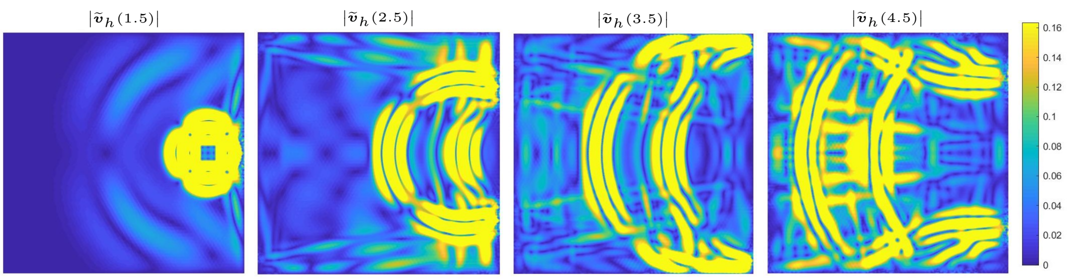

Figure 6.14: Snapshots of the reconstructed velocity field (third experiment).

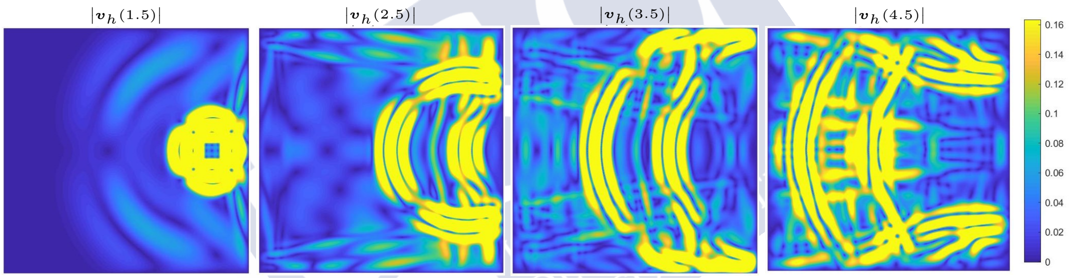

Figure 6.15: Snapshots of the velocity field (third experiment).

Chapter 7

The case of free boundary conditions

Contents

In this chapter, we address the case of an isotropic homogeneous elastic medium in 2D, which we assume to be bounded by a free boundary, that is to say, the case of Neumann boundary condition. In order to extend the technique, we follow the philosophy of the previous chapter where we have treated the case of rigid boundary conditions without finding any specific difficulty. However, we will see that the case of free boundary conditions turns out to be more challenging since severe stability issues are observed if a straightforward approach is used. In the following we first exhibit and analyse the mentioned difficulties to then propose a stabilized formulation.

7.1 Free boundary conditions for potentials

Let us consider that the 2D homogeneous isotropic elastic domain Ω is Lipschitz regular and bounded by $\Gamma = \partial\Omega$, that in the following we assume to be free. For the sake of simplicity (the reader will convince himself that this is not restrictive), we shall assume that Ω is simply connected (thus Γ is closed) and its centre of gravity is at the origin. Therefore, the displacement problem ((5.3), (5.4)) which is formulated in $\Omega \times [0,T]$, where T denotes the final computational time, is completed with the Neumann boundary condition

$$\begin{cases} \text{Find } \boldsymbol{u}(\boldsymbol{x},t) : \Omega \times [0,T] \longrightarrow \mathbb{R}^2, \text{ such that } (\boldsymbol{u}, \partial_t \boldsymbol{u})(t=0) = (0,0) \text{ and} \\ \partial_t^2 \boldsymbol{u} \,-\, V_P^2 \nabla \operatorname{div} \boldsymbol{u} \,+\, V_S^2 \,\mathbf{curl}\left(\operatorname{curl} \boldsymbol{u}\right) \,=\, \boldsymbol{f}/\rho, \quad \text{in } \Omega \times [0,T], & (7.1a) \\ \underline{\boldsymbol{\sigma}}(\boldsymbol{u})\boldsymbol{n} \,=\, \mathbf{0}, \quad \text{on } \Gamma \times [0,T], & (7.1b) \end{cases}$$

where, according to the **Hook's law** for isotropic materials (see (5.2))

$$\underline{\boldsymbol{\sigma}}(\boldsymbol{u})\boldsymbol{n} \equiv \lambda \operatorname{div} \boldsymbol{u}\, \boldsymbol{n} \,+\, 2\,\mu\, \underline{\boldsymbol{\varepsilon}}(\boldsymbol{u})\boldsymbol{n} \,=\, \mathbf{0}, \qquad \forall \boldsymbol{x} \in \Gamma \quad \text{and} \quad \forall t \in [0,T]. \tag{7.2}$$

Moreover, when solving problem (7.1), we notice that a particular role is played by the three dimensional space of the usually called *rigid displacements*

$$\begin{aligned} \boldsymbol{R}(\Omega) &= \left\{ \boldsymbol{w}_R \in L^2(\Omega)^2 \;/\; \underline{\boldsymbol{\varepsilon}}(\boldsymbol{w}_R) = \underline{\mathbf{0}} \right\} \\ &= \left\{ a(x_2, -x_1)^t + (b_1, b_2)^t,\ (a, (b_1, b_2)) \in \mathbb{R} \times \mathbb{R}^2 \right\} \end{aligned}$$

and in the following, we will assume that the source term satisfies for all times

$$\boldsymbol{f}(\cdot, t) \in \boldsymbol{L}^2_R(\Omega) := \left\{ \boldsymbol{w} \in L^2(\Omega)^2 \;/\; \int_\Omega \boldsymbol{w} \cdot \boldsymbol{w}_R \,\mathrm{d}\boldsymbol{x} = 0,\ \forall\, \boldsymbol{w}_R \in \boldsymbol{R}(\Omega) \right\}. \tag{7.3}$$

As we argue next (see Remark 7.1 Lemma 7.2 and Remark 7.3), this is not a significant restriction.

Remark 7.1

We introduce the orthogonal projection Π_R from $L^2(\Omega)^2$ into $\boldsymbol{L}^2_R(\Omega)$ that for every $\boldsymbol{w} \in L^2(\Omega)^2$

assigns $\Pi_R\, \boldsymbol{w} \in \boldsymbol{L}^2_R(\Omega)$ *satisfying*

$$\int_\Omega (\Pi_R\, \boldsymbol{w} - \boldsymbol{w})\, \widetilde{\boldsymbol{w}}\, \mathrm{d}\boldsymbol{x} = 0, \quad \forall \widetilde{\boldsymbol{w}} \in \boldsymbol{L}^2_R(\Omega). \tag{7.4}$$

We remark that, as for any projector, the space $L^2(\Omega)^2$ *can be decomposed as the direct sum*

$$L^2(\Omega)^2 = \operatorname{Ker} \Pi_R \oplus \operatorname{Im} \Pi_R = \boldsymbol{R}(\Omega) \oplus \boldsymbol{L}^2_R(\Omega).$$

The main interest of assumption (7.3) is provided in the following lemma which at the same time, as we detail in the posterior remark, guarantees that the assumption is not significantly restrictive and shows how the case $\boldsymbol{f}(\cdot,t) \in L^2(\Omega)^2$ should be treated.

Lemma 7.2

If $\boldsymbol{f}(\cdot,t) \in \boldsymbol{L}^2_R(\Omega),\ \forall\, t \geq 0$, *then*

$$\boldsymbol{u}(\cdot,t) \in \boldsymbol{L}^2_R(\Omega), \quad \forall\, t \geq 0.$$

Proof. Multiply (7.1a) by $\boldsymbol{w}_R$ and integrate over Ω. Using Green's formula,

$$\frac{\mathrm{d}^2}{\mathrm{d}t^2}\Big(\rho \int_\Omega \boldsymbol{u}(\cdot,t) \cdot \boldsymbol{w}_R\, \mathrm{d}\boldsymbol{x}\Big) \;=\; 0 \qquad \forall\, \boldsymbol{w}_R \in \boldsymbol{R}(\Omega).$$

One concludes using the initial conditions in (7.1). ■

Remark 7.3

For a source term $\boldsymbol{f}(\cdot,t) \in L^2(\Omega)^2$ *we have that* $\boldsymbol{f} = \boldsymbol{f}_R + \boldsymbol{f}^\perp_R$, *where*

$$\boldsymbol{f}_R(\cdot,t) = \Pi_R \boldsymbol{f}(\cdot,t) \in \boldsymbol{L}^2_R(\Omega) \quad \text{and} \quad \boldsymbol{f}^\perp_R(\cdot,t) = \boldsymbol{f}(\cdot,t) - \Pi_R \boldsymbol{f}(\cdot,t) \in \boldsymbol{R}(\Omega).$$

Then, it is straightforward to see that the solution $\boldsymbol{u}$ *of* (7.1) *can also be decomposed as* $\boldsymbol{u} = \boldsymbol{u}_R + \boldsymbol{u}^\perp_R$, *where* $\boldsymbol{u}_R$ *is the solution of 7.1 with the source term given by* $\boldsymbol{f}_R$ *while* $\boldsymbol{u}^\perp_R$ *is given by*

$$\boldsymbol{u}^\perp_R = \frac{1}{\rho} \int_0^t (t-s)\ \boldsymbol{f}^\perp_R(\cdot,s)\, \mathrm{d}s$$

and solves the problem $\rho\, \partial^2_t \boldsymbol{u}^\perp_R = \boldsymbol{f}^\perp_R$.

Another important property that we will require later is the following Korn's inequality in $H^1(\Omega)^2 \cap L^2_R(\Omega)$ (see [102]).

Proposition 7.4

There exists a constant $\mathcal{C}_\Omega > 0$ *such that*

$$\forall\, \boldsymbol{w} \in H^1(\Omega)^2 \cap L^2_R(\Omega), \quad \|\boldsymbol{w}\|^2_{H^1(\Omega)} \;\leq\; \mathcal{C}_\Omega \int_\Omega |\underline{\boldsymbol{\varepsilon}}(\boldsymbol{w})|^2\, \mathrm{d}\boldsymbol{x}. \tag{7.5}$$

Next, to state a result concerning the existence, uniqueness and regularity of the solution of problem (7.1), we shall first recall the definition of the Hilbert space (already introduced in (6.2))

$$\boldsymbol{D} \coloneqq \big\{\boldsymbol{w} \in H^1(\Omega)^2 \,/\, -V_P^2\, \nabla(\operatorname{div} \boldsymbol{w}) + V_S^2\, \mathbf{curl}\,(\operatorname{curl} \boldsymbol{w}) \in L^2(\Omega)^2\big\},$$

to then introduce the new functional spaces which are closed subspaces of $\boldsymbol{D}$ (subscript N holds for Neumann),

$$\boldsymbol{D}_R \coloneqq \boldsymbol{D} \cap \boldsymbol{L}^2_R(\Omega) \quad \text{and} \quad \boldsymbol{D}_N \coloneqq \big\{\boldsymbol{w} \in \boldsymbol{D}_R \,/\, \underline{\boldsymbol{\sigma}}(\boldsymbol{w})\boldsymbol{n} = 0 \text{ on } \Gamma\big\}. \tag{7.6}$$

Then, we can state the following classical theorem that results, for instance, from the application of standard Hille-Yosida's theory for evolution problems (see [78]).

Theorem 7.5

Assume that $\boldsymbol{f} \in \mathcal{C}^1\big([0,T];\boldsymbol{L}^2_R(\Omega)\big)$. *Then, problem* (7.1) *admits a unique solution:*

$$\boldsymbol{u} \in \mathcal{C}^2([0,T];L^2(\Omega)^2) \cap \mathcal{C}^1\big([0,T];H^1(\Omega)^2\big) \cap \mathcal{C}^0\big([0,T];\boldsymbol{D}_N\big).$$

Remark 7.6

We notice that according to Remark 7.1 the previous theorem can also be extended to the case $\boldsymbol{f} \in \mathcal{C}^1\big([0,T];L^2(\Omega)^2\big)$. *However, as we shall see later, the rigid displacements will have a particular role when solving the problem in potentials and that is why in the following (according to* (7.3)*) we consider only the case* $\boldsymbol{f} \in \mathcal{C}^1\big([0,T];\boldsymbol{L}^2_R(\Omega)\big)$.

Then, proceeding as in previous chapter, we introduce the scalar potentials φ_P (pressure potential) and φ_S (shear potential) via equations (5.6), i.e.

$$\rho\,\partial_t\varphi_P = (\lambda+2\mu)\,\mathrm{div}\,\boldsymbol{u} \qquad \text{and} \qquad \rho\,\partial_t\varphi_S = -\mu\,\mathrm{curl}\,\boldsymbol{u}, \tag{7.7}$$

both completed with the vanishing initial conditions (5.7)

$$\varphi_P(t=0) = 0 \qquad \text{and} \qquad \varphi_S(t=0) = 0. \tag{7.8}$$

Therefore, we can deduce again that the decomposition (5.9) holds in the interior of the computational domain Ω, so that φ_P and φ_S provide a *Helmholtz decomposition* [92] of the velocity field $\partial_t\boldsymbol{u}$ when the source vanishes

$$\partial_t\boldsymbol{u} = \nabla\,\varphi_P + \mathbf{curl}\,\varphi_S + \boldsymbol{g} \quad \text{where we recall} \quad \boldsymbol{g}(t) = \frac{1}{\rho}\int_0^t \boldsymbol{f}(s)\,ds. \tag{7.9}$$

In consequence, if we introduce the decomposition (7.9) into the equations (7.7) and differentiate in time, we obtain that the potentials satisfy the scalar wave equations in (5.10),

$$\frac{1}{V_P^2}\,\partial_t^2\varphi_P - \Delta\varphi_P = \mathrm{div}\,\boldsymbol{g} \qquad \text{and} \qquad \frac{1}{V_S^2}\,\partial_t^2\varphi_S - \Delta\varphi_S = -\mathrm{curl}\,\boldsymbol{g}, \tag{7.10}$$

which are completed with the initial condition (7.8) and also with the initial conditions for the time derivative of the potentials (as in (5.11))

$$\partial_t\varphi_P(t=0) = 0 \qquad \text{and} \qquad \partial_t\varphi_S(t=0) = 0. \tag{7.11}$$

Moreover, similarly to (6.8) and according to Theorem 7.5, we notice that the vector of potentials

$$\boldsymbol{\varphi} = (\varphi_P,\varphi_S) \quad \text{belongs to} \quad \mathcal{C}^2([0,T];L^2(\Omega)^2) \cap \mathcal{C}^1([0,T];\boldsymbol{V}), \tag{7.12}$$

where $\boldsymbol{V}$ is still defined by (6.10)

$$\boldsymbol{V} = H(\mathrm{div},\Omega) \cap H(\mathrm{curl},\Omega). \tag{7.13}$$

Next, notice that the problem must be completed with adequate boundary conditions traducing (7.1b). For this purpose and since $\partial_t\boldsymbol{u} \in H^1(\Omega)^2$, we apply the trace operator to equation (7.9) and therefore we obtain

$$\nabla\,\varphi_P + \mathbf{curl}\,\varphi_S + \boldsymbol{g} = \partial_t\boldsymbol{u}_\Gamma \qquad \text{on} \quad \Gamma\times[0,T], \tag{7.14}$$

where we have denoted by $\boldsymbol{u}_\Gamma$ the trace of the displacement field on the boundary. Moreover, notice that according to (6.9) we can rewrite the previous equation as

$$\mathrm{div}\,\boldsymbol{\varphi} + g_1 = \partial_t u_{\Gamma,1} \quad \text{and} \quad \mathrm{curl}\,\boldsymbol{\varphi} - g_2 = -\partial_t u_{\Gamma,2} \qquad \text{on} \quad \Gamma\times[0,T]. \tag{7.15}$$

Then, since $\boldsymbol{u}_\Gamma$ is not known, we would like to compute it as a function of $\boldsymbol{\varphi}$ rewriting the free boundary conditions (7.1b) in terms of the potentials defined by (7.7) and (7.8).

Remark 7.7

It is interesting to notice, that if we assume enough regularity for both φ_Q with $Q \in \{P, S\}$ so that $\partial_{\boldsymbol{n}}\varphi_Q = \nabla\varphi_Q \cdot \boldsymbol{n}$ and $\partial_{\boldsymbol{\tau}}\varphi_Q = \nabla\varphi_Q \cdot \boldsymbol{\tau}$ are well defined (where $\boldsymbol{n} = (n_1, n_2)$ and $\boldsymbol{\tau} = (n_2, -n_1)$ denote the normal and tangential vectors), we can consider normal and tangential traces in equation (7.14) to obtain the boundary conditions

$$\partial_{\boldsymbol{n}}\varphi_P = \partial_{\boldsymbol{\tau}}\varphi_S - \boldsymbol{g}\cdot\boldsymbol{n} + \partial_t \boldsymbol{u}_\Gamma \cdot \boldsymbol{n} \qquad \text{and} \qquad \partial_{\boldsymbol{n}}\varphi_S = -\partial_{\boldsymbol{\tau}}\varphi_P - \boldsymbol{g}\cdot\boldsymbol{\tau} + \partial_t \boldsymbol{u}_\Gamma \cdot \boldsymbol{\tau}, \tag{7.16}$$

just noticing that $\mathbf{curl}\,\varphi\cdot\boldsymbol{n} = -\partial_{\boldsymbol{\tau}}\varphi$ *and* $\mathbf{curl}\,\varphi\cdot\boldsymbol{\tau} = -\partial_{\boldsymbol{n}}\varphi$.

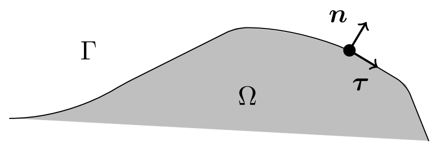

Figure 7.1: Representation of the normal an tangential vectors on $\Gamma = \partial\Omega$.

Next, in order to rewrite $\boldsymbol{u}_\Gamma$ as a function of $\boldsymbol{\varphi}$ we first remark that

$$\underline{\boldsymbol{\sigma}}(\boldsymbol{u}) \;=\; \big(\lambda + 2\mu\big)\operatorname{div}\boldsymbol{u}\,\underline{\boldsymbol{I}} \;-\; \mu\operatorname{curl}\boldsymbol{u}\,\underline{\boldsymbol{J}} \;+\; 2\,\mu\,\underline{\boldsymbol{H}}(\boldsymbol{u}),$$

$$\text{where} \quad \underline{\boldsymbol{J}} \;=\; \begin{pmatrix} 0 & 1 \\ -1 & 0 \end{pmatrix} \quad \text{and} \quad \underline{\boldsymbol{H}}(\boldsymbol{u}) \;=\; \begin{pmatrix} -\partial_2 u_2 & \partial_1 u_2 \\ \partial_2 u_1 & -\partial_1 u_1 \end{pmatrix}.$$

Then, considering the definition of the potentials (7.7) and (7.8), the free boundary condition (7.1b) can be rewritten

$$\big(\rho\,\partial_t\varphi_P\,\underline{\boldsymbol{I}} \;-\; \rho\,\partial_t\varphi_S\,\underline{\boldsymbol{J}} \;+\; 2\,\mu\,\underline{\boldsymbol{H}}(\boldsymbol{u})\big)\boldsymbol{n} \;=\; \boldsymbol{0} \quad \text{on } \Gamma.$$

Next, we notice that on the one hand

$$\big(\rho\,\partial_t\varphi_P\,\underline{\boldsymbol{I}} \;-\; \rho\,\partial_t\varphi_S\,\underline{\boldsymbol{J}}\big)\boldsymbol{n} \;=\; \rho\begin{pmatrix} \partial_t\varphi_P\; n_1 + \partial_t\varphi_S\; n_2 \\ \partial_t\varphi_P\; \tau_1 + \partial_t\varphi_S\; \tau_2 \end{pmatrix} \;=\; \rho\begin{pmatrix} \partial_t\boldsymbol{\varphi}\cdot\boldsymbol{n} \\ \partial_t\boldsymbol{\varphi}\cdot\boldsymbol{\tau} \end{pmatrix}, \quad \text{on } \Gamma,$$

while on the other hand

$$\underline{\boldsymbol{H}}(\boldsymbol{v})\,\boldsymbol{n} \;=\; \begin{pmatrix} \partial_\tau u_{2|\Gamma} \\ -\partial_\tau u_{1|\Gamma} \end{pmatrix} \;=\; \begin{pmatrix} \partial_\tau u_{\Gamma,2} \\ -\partial_\tau u_{\Gamma,1} \end{pmatrix} \quad \text{on } \Gamma.$$

Thus, recalling that $\mu = \rho\,V_S^2$, the free boundary condition (7.1b) can be rewritten as

$$\partial_\tau\, u_{\Gamma,1} \;=\; \frac{1}{2\,V_S^2}\,\partial_t\boldsymbol{\varphi}\cdot\boldsymbol{\tau}, \quad \text{and} \quad \partial_\tau\, v_{\Gamma,2} \;=\; -\frac{1}{2\,V_S^2}\,\partial_t\boldsymbol{\varphi}\cdot\boldsymbol{n}, \quad \text{on } \Gamma. \tag{7.17}$$

Now, we recall that our purpose is to get an expression for $\boldsymbol{u}_\Gamma$ in terms of the potentials, i.e., we want to get rid of the tangential derivatives in previous expression. To do so we assume that Γ is parametrized by $\boldsymbol{x}(s) \in W^{1,\infty}(0, L)$ where s is the curvilinear abscissa along Γ and L is the total length of Γ (see Figure 7.2). Notice that the choice of the point associated to $s = 0$ has no influence since the boundary is closed, however this is not the case for the direction of the parametrization that we consider to be the same that the direction of $\boldsymbol{\tau}$. In this way, we can introduce the following integral operator

$$\begin{aligned} \mathcal{I}:\quad L^2(\Gamma) &\longrightarrow L^2(\Gamma) \\ \eta \quad &\mapsto \mathcal{I}\eta(s) := \int_0^s \eta(\sigma)\,\mathrm{d}\sigma. \end{aligned} \tag{7.18}$$

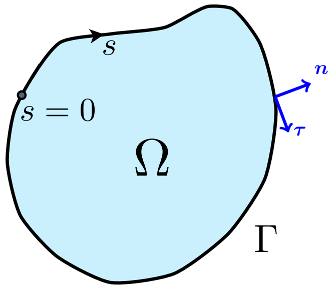

Figure 7.2: Definition of the parametrization of the boundary.

This operator maps $\{\nu \in L^2(\Gamma) \,/\, \int_\Gamma \nu \,\mathrm{d}\boldsymbol{\gamma} = 0\}$ into $H^1(\Gamma)$, then if we introduce the following subspace of $H^{-\frac{1}{2}}(\Gamma)$,

$$M := \left\{\nu \in H^{-\frac{1}{2}}(\Gamma) \,/\, \int_\Gamma \nu \,\mathrm{d}\boldsymbol{\gamma} = 0\right\}, \tag{7.19}$$

where the integral in the boundary represents the duality product between $H^{\frac{1}{2}}(\Gamma)$ and its dual $H^{-\frac{1}{2}}(\Gamma)$, we can extend the operator $\mathcal{I}$ as a linear continuous operator

$$\mathcal{I} \in \mathcal{L}(M, H^{\frac{1}{2}}(\Gamma)). \tag{7.20}$$

This operator allows, as desired, to compute $\boldsymbol{u}_\Gamma$ in terms of (φ_P, φ_S) up to an additive constant, more precisely, equations (7.17) are easily seen to be equivalent to

$$\begin{cases} u_{\Gamma,1}(\boldsymbol{x}(s)) - u_{\Gamma,1}(\boldsymbol{x}(0)) = \dfrac{1}{2\,V_S^2}\,\mathcal{I}\big(\partial_t\boldsymbol{\varphi}\cdot\boldsymbol{\tau}\big)(s), & (7.21\text{a}) \\[2ex] u_{\Gamma,2}(\boldsymbol{x}(s)) - u_{\Gamma,2}(\boldsymbol{x}(0)) = -\dfrac{1}{2\,V_S^2}\,\mathcal{I}\big(\partial_t\boldsymbol{\varphi}\cdot\boldsymbol{n}\big)(s). & (7.21\text{b}) \end{cases}$$

Notice that, since Γ is a closed boundary, $\boldsymbol{x}(0) = \boldsymbol{x}(L)$, thus the potentials satisfy

$$\mathcal{I}(\partial_t\boldsymbol{\varphi}\cdot\boldsymbol{n})(L) = \int_\Gamma \partial_t\boldsymbol{\varphi}\cdot\boldsymbol{n}\,\mathrm{d}\boldsymbol{\gamma} = 0 \quad \text{and} \quad \mathcal{I}(\partial_t\boldsymbol{\varphi}\cdot\boldsymbol{\tau})(L) = \int_\Gamma \partial_t\boldsymbol{\varphi}\cdot\boldsymbol{\tau}\,\mathrm{d}\boldsymbol{\gamma} = 0$$

Moreover, considering initial conditions (7.8) previous equation is equivalent to

$$\int_\Gamma \boldsymbol{\varphi}\cdot\boldsymbol{n}\,\mathrm{d}\boldsymbol{\gamma} = 0 \quad \text{and} \quad \int_\Gamma \boldsymbol{\varphi}\cdot\boldsymbol{\tau}\,\mathrm{d}\boldsymbol{\gamma} = 0. \tag{7.22}$$

In the sequel these two conditions are going to be crucial, we will refer to them as **gauge conditions** and they will be important in order to get rid of $\boldsymbol{u}_\Gamma(\boldsymbol{x}(0))$ in the derivation of the variational formulation.

Remark 7.8

In more general situations where the boundary has $N_c > 1$ connected components (each of them being closed) we would introduce one integral operator such as the one in (7.20) per component. In consequence, the potentials should satisfy $2N_c$ gauge conditions similar to those in (7.22).

7.2 A naive approach

In this section we follow the philosophy of previous chapter in order to tackle the boundary value problem ((7.10), (7.15), (7.21), (7.22)) that we summarize next:

$$\begin{cases} \text{Find } \boldsymbol{\varphi} = (\varphi_P, \varphi_S) : \Omega \times [0,T] \longrightarrow \mathbb{R}^2 \text{ and } \boldsymbol{u}_\Gamma : \Gamma \times [0,T] \longrightarrow \mathbb{R}^2, \text{ such that} \\ \dfrac{1}{V_P^2}\,\partial_t^2 \varphi_P - \Delta\varphi_P = \operatorname{div}\boldsymbol{g}, \quad \text{in } \Omega \times [0,T], & (7.23a) \\ \dfrac{1}{V_S^2}\,\partial_t^2 \varphi_S - \Delta\varphi_S = -\operatorname{curl}\boldsymbol{g}, \quad \text{in } \Omega \times [0,T]. & (7.23b) \\ \operatorname{div}\boldsymbol{\varphi} + g_1 = \partial_t u_{\Gamma,1}, \quad \text{on } \Gamma \times [0,T], & (7.23c) \\ \operatorname{curl}\boldsymbol{\varphi} - g_2 = -\partial_t u_{\Gamma,2}, \quad \text{on } \Gamma \times [0,T], & (7.23d) \\ u_{\Gamma,1}(\boldsymbol{x}(s)) - u_{\Gamma,1}(\boldsymbol{x}(0)) = \dfrac{1}{2\,V_S^2}\,\mathcal{I}\big(\partial_t\boldsymbol{\varphi}\cdot\boldsymbol{\tau}\big)(s), \quad \text{on } \Gamma \times [0,T], & (7.23e) \\ u_{\Gamma,2}(\boldsymbol{x}(s)) - u_{\Gamma,2}(\boldsymbol{x}(0)) = -\dfrac{1}{2\,V_S^2}\,\mathcal{I}\big(\partial_t\boldsymbol{\varphi}\cdot\boldsymbol{n}\big)(s), \quad \text{on } \Gamma \times [0,T], & (7.23f) \\ \displaystyle\int_\Gamma \boldsymbol{\varphi}\cdot\boldsymbol{n}\,\mathrm{d}\boldsymbol{\gamma} = 0 \quad \text{and} \quad \int_\Gamma \boldsymbol{\varphi}\cdot\boldsymbol{\tau}\,\mathrm{d}\boldsymbol{\gamma} = 0. & (7.23g) \end{cases}$$

completed with the vanishing initial conditions (7.8) and (7.11)

$$\boldsymbol{\varphi}(t=0) = \mathbf{0} \quad \text{and} \quad \partial_t\boldsymbol{\varphi}(t=0) = \mathbf{0}, \quad \text{in } \Omega. \tag{7.24}$$

7.2.1 Variational formulation

We provide a variational formulation which naturally eliminates $\boldsymbol{u}_\Gamma$ and provides a problem in $\boldsymbol{\varphi}$ only. To do so, we proceed as in Section 6.2 by choosing a test function $\boldsymbol{\psi} = (\psi_P, \psi_S) \in \boldsymbol{V}$ (see (7.13)) and integrating by parts. The resultant is again

$$\begin{aligned} \int_\Omega \partial_t^2(\mathbb{D}\,\boldsymbol{\varphi})\cdot\boldsymbol{\psi}\,\mathrm{d}\boldsymbol{x} \;&+\; \int_\Omega(\operatorname{div}\boldsymbol{\varphi} + g_1)\operatorname{div}\boldsymbol{\psi}\,\mathrm{d}\boldsymbol{x} \;-\; \int_\Gamma(\operatorname{div}\boldsymbol{\varphi} + g_1)\,\psi\cdot\boldsymbol{n}\,\mathrm{d}\boldsymbol{\gamma} \\ &+\; \int_\Omega(\operatorname{curl}\boldsymbol{\varphi} - g_2)\operatorname{curl}\boldsymbol{\psi}\,\mathrm{d}\boldsymbol{x} \;+\; \int_\Gamma(\operatorname{curl}\boldsymbol{\varphi} - g_2)\,\psi\cdot\boldsymbol{\tau}\,\mathrm{d}\boldsymbol{\gamma} \;=\; \mathbf{0}, \end{aligned}$$

where the integrals in the boundary should be interpreted as duality products between elements in $H^{\frac{1}{2}}(\Gamma)$ and its dual $H^{-\frac{1}{2}}(\Gamma)$. Next, using the boundary conditions (7.23c) and (7.23d) we obtain (see (6.19), (6.20) and (6.21) for the definitions of m, a and g)

$$\frac{\mathrm{d}^2}{\mathrm{d}t^2}\,m_\Omega(\boldsymbol{\varphi}(t),\boldsymbol{\psi}) - \frac{\mathrm{d}}{\mathrm{d}t}\int_\Gamma\big(u_{\Gamma,1}\,\boldsymbol{\psi}\cdot\boldsymbol{n} + u_{\Gamma,2}\,\boldsymbol{\psi}\cdot\boldsymbol{\tau}\big)\,\mathrm{d}\gamma + a(\boldsymbol{\varphi}(t),\boldsymbol{\psi}) = \mathrm{g}(t,\boldsymbol{\psi}). \tag{7.25}$$

Notice that contrary to the case of clamped boundary conditions, an additional boundary term appears due to the presence of $\boldsymbol{u}_\Gamma$. In order to rewrite the previous equation using potentials only, we make use of (7.23e) and (7.23f) to rewrite the second term as

$$\begin{aligned} -\int_\Gamma\big(u_{\Gamma,1}\,\boldsymbol{\psi}\cdot\boldsymbol{n} + u_{\Gamma,2}\,\boldsymbol{\psi}\cdot\boldsymbol{\tau}\big)\,\mathrm{d}\gamma \;&=\; \frac{1}{2\,V_S^2}\int_\Gamma\big(\mathcal{I}(\partial_t\boldsymbol{\varphi}\cdot\boldsymbol{n})\,\boldsymbol{\psi}\cdot\boldsymbol{\tau} - \mathcal{I}(\partial_t\boldsymbol{\varphi}\cdot\boldsymbol{\tau})\,\boldsymbol{\psi}\cdot\boldsymbol{n}\big)\,\mathrm{d}\boldsymbol{\gamma} \\ &\quad-\; \int_\Gamma\big(u_{\Gamma,1}(\boldsymbol{x}(0))\,\boldsymbol{\psi}\cdot\boldsymbol{n} + u_{\Gamma,2}(\boldsymbol{x}(0))\,\boldsymbol{\psi}\cdot\boldsymbol{\tau}\big)\,\mathrm{d}\gamma. \end{aligned}$$

However, the presence of $\boldsymbol{u}_\Gamma$ is not totally removed. As we have mentioned before, to totally remove $\boldsymbol{u}_\Gamma$ we shall make use of the gauge conditions (7.23g). More precisely, we are going to seek

$\boldsymbol{\varphi}(\cdot,t)$ in the space $\boldsymbol{V}_0$ which is defined by

$$\boldsymbol{V}_0 := \Big\{\boldsymbol{\varphi} \in \boldsymbol{V} \text{ s.t. } \int_\Gamma \boldsymbol{\varphi}\cdot\boldsymbol{n}\,\mathrm{d}\boldsymbol{\gamma} = \int_\Gamma \boldsymbol{\varphi}\cdot\boldsymbol{\tau}\,\mathrm{d}\boldsymbol{\gamma} = 0\Big\}. \tag{7.26}$$

In consequence, we also consider test functions satisfying the gauge conditions and notice that in that case

$$-\int_\Gamma \big(u_{\Gamma,1}\,\boldsymbol{\psi}\cdot\boldsymbol{n} + u_{\Gamma,2}\,\boldsymbol{\psi}\cdot\boldsymbol{\tau}\big)\,\mathrm{d}\gamma = \frac{\mathrm{d}}{\mathrm{d}t}\,m_\Gamma\left(\boldsymbol{\varphi},\boldsymbol{\psi}\right), \qquad \forall\boldsymbol{\psi}\in\boldsymbol{V}_0,$$

where we have introduced the bilinear form

$$m_\Gamma : \boldsymbol{V}_0\times\boldsymbol{V}_0 \longrightarrow \mathbb{R} \quad \text{s.t.} \quad m_\Gamma(\boldsymbol{\varphi},\boldsymbol{\psi}) := \frac{1}{2\,V_S^2}\int_\Gamma \big(\mathcal{I}(\boldsymbol{\varphi}\cdot\boldsymbol{n})\,\boldsymbol{\psi}\cdot\boldsymbol{\tau} - \mathcal{I}(\boldsymbol{\varphi}\cdot\boldsymbol{\tau})\,\boldsymbol{\psi}\cdot\boldsymbol{n}\big)\,\mathrm{d}\boldsymbol{\gamma}, \tag{7.27}$$

where we recall that the integral in the boundary represents the duality product between elements in $H^{\frac{1}{2}}(\Gamma)$ and its dual $H^{-\frac{1}{2}}(\Gamma)$.

Remark 7.9

Notice that $m_\Gamma(\cdot,\cdot)$ can not be defined in $\boldsymbol{V}$ since, if the gauge conditions are not satisfied, $\boldsymbol{\psi}\cdot\boldsymbol{n}$ and $\boldsymbol{\psi}\cdot\boldsymbol{\tau}$ would not belong to M (defined in (7.19)). In consequence $\mathcal{I}(\boldsymbol{\psi}\cdot\boldsymbol{n})$ and $\mathcal{I}(\boldsymbol{\psi}\cdot\boldsymbol{\tau})$ do not belong to $H^{\frac{1}{2}}(\Gamma)$ and the boundary integral in the definition of $m_\Gamma(\cdot,\cdot)$ would not be properly defined.

Finally, substituting previous equation into (7.25) we obtain the following variational formulation for the potentials:

$$\left\{\begin{array}{l} \text{Find } \boldsymbol{\varphi}(t) : [0,T] \longrightarrow \boldsymbol{V}_0 \text{ such that } (\boldsymbol{\varphi},\partial_t\boldsymbol{\varphi})(t=0) = (\boldsymbol{0},\boldsymbol{0}) \text{ and} \\ \dfrac{\mathrm{d}^2}{\mathrm{d}t^2}\,m(\boldsymbol{\varphi}(t),\boldsymbol{\psi}) + a(\boldsymbol{\varphi}(t),\boldsymbol{\psi}) = \mathrm{g}(t,\boldsymbol{\psi}), \quad \forall\,\boldsymbol{\psi}\in\boldsymbol{V}_0, \end{array}\right. \tag{7.28}$$

where the new mass bilinear form $m(\cdot,\cdot)$ is defined by

$$m\left(\boldsymbol{\varphi},\boldsymbol{\psi}\right) = m_\Omega\left(\boldsymbol{\varphi},\boldsymbol{\psi}\right) + m_\Gamma\left(\boldsymbol{\varphi},\boldsymbol{\psi}\right).$$

7.2.2 Well posedness issues

In this section we discuss the well posedness of the variational problem (7.28) which at a first glance looks like a nice hyperbolic variational problem in the sense of Lions-Magenes [103]. However, in order to fit the classical theory, continuity and some adequate coercivity (as in Lemma 6.5) for the forms $m(\cdot,\cdot)$ and $a(\cdot,\cdot)$ need to be checked. The continuity of $m_\Omega(\cdot,\cdot)$, $a(\cdot,\cdot)$ and $\mathrm{g}(\cdot)$ is provided in Lemma 6.4 while the continuity of $m_\Gamma(\cdot,\cdot)$ is given in the following result which is consequence of the the continuity of the integral operator $\mathcal{I}$ defined in (7.20).

Lemma 7.10

There exist strictly positive constant K such that

$$|m_\Gamma(\boldsymbol{\varphi},\boldsymbol{\psi})| \leq K\|\boldsymbol{\varphi}\|_{\boldsymbol{V}}\|\boldsymbol{\psi}\|_{\boldsymbol{V}} \quad \textit{for all } \boldsymbol{\varphi},\boldsymbol{\psi}\in\boldsymbol{V}_0.$$

It is also interesting to notice that all the bilinear forms are symmetric. This is clear for $m_\Omega(\cdot,\cdot)$ and $a(\cdot,\cdot)$ while for $m_\Gamma(\cdot,\cdot)$ is obtained integrating by parts along the boundary. This gives

$$m_\Gamma(\boldsymbol{\varphi},\boldsymbol{\psi}) = -\frac{1}{2\,V_S^2}\int_\Gamma \big(\mathcal{I}(\boldsymbol{\varphi}\cdot\boldsymbol{\tau})\,\boldsymbol{\psi}\cdot\boldsymbol{n} + \mathcal{I}(\boldsymbol{\psi}\cdot\boldsymbol{\tau})\,\boldsymbol{\varphi}\cdot\boldsymbol{n}\big)\,\mathrm{d}\gamma, \quad \forall(\boldsymbol{\varphi},\boldsymbol{\psi})\in\boldsymbol{V}_0\times\boldsymbol{V}_0. \tag{7.29}$$

In addition, one observes that $m(\cdot,\cdot)$ is injective.

Lemma 7.11

We have the injectivity result

$$m(\boldsymbol{\varphi},\boldsymbol{\psi})=0 \quad \forall\, \boldsymbol{\psi}\in \boldsymbol{V}_0 \quad \Longrightarrow \quad \boldsymbol{\varphi}=0.$$

Proof. Let us consider $\boldsymbol{\varphi}$ such that $m(\boldsymbol{\varphi},\boldsymbol{\psi})=0$ for all $\boldsymbol{\psi}\in\boldsymbol{V}_0$. In particular, we can choose any $\boldsymbol{\psi}\in\mathcal{D}(\Omega)^2\subset\boldsymbol{V}_0$, thus

$$m(\boldsymbol{\varphi},\boldsymbol{\psi})=m_\Omega(\boldsymbol{\varphi},\boldsymbol{\psi})=0, \quad \forall\, \boldsymbol{\psi}\in\mathcal{D}(\Omega)^2.$$

In consequence $\boldsymbol{\varphi}=0$ by density of $\mathcal{D}(\Omega)^2$ in $L^2(\Omega)^2$.

■

Concerning the coercivity of the bilinear form $m(\cdot,\cdot)$, we should verify that Lemma 6.5 still holds. However this fails to be true as we show in Theorem 7.12 under some technical assumptions on the local regularity of a part of the boundary Γ. Later in Theorem 7.41, when a better understanding of the difficulties of the problem is achieve, we will provide a more detailed result concerning the negativity of the bilinear form $m(\cdot,\cdot)$ and we will see that this assumptions are actually unnecessary, however the claimed result would be artificial at this moment, therefore for pedagogical reasons we prefer to provide the following theorem.

Theorem 7.12

Assume that there is a part of the boundary Γ that is of class $\mathcal{C}^2$. Then, there exists $\boldsymbol{\psi}\in\boldsymbol{V}_0$ such that

$$m(\boldsymbol{\psi},\boldsymbol{\psi})<0.$$

Proof. We first notice that for all $\boldsymbol{\psi}\in\boldsymbol{V}_0$

$$m_\Omega(\boldsymbol{\psi},\boldsymbol{\psi})>0 \quad \text{and} \quad m_\Gamma(\boldsymbol{\psi},\boldsymbol{\psi})=-\frac{1}{V_S^2}\int_\Gamma \mathcal{I}(\boldsymbol{\psi}_{|\Gamma}\cdot\boldsymbol{\tau})\,\boldsymbol{\psi}_{|\Gamma}\cdot\boldsymbol{n}\,\mathrm{d}\boldsymbol{\gamma}.$$

Thus, we will begin by finding $\boldsymbol{\psi}_\Gamma$ such that

$$\int_\Gamma \boldsymbol{\psi}_\Gamma\cdot\boldsymbol{n}\,\mathrm{d}\boldsymbol{\gamma}=\int_\Gamma \boldsymbol{\psi}_\Gamma\cdot\boldsymbol{\tau}\,\mathrm{d}\boldsymbol{\gamma}=0 \quad \text{and} \quad \mathcal{I}(\boldsymbol{\psi}_\Gamma\cdot\boldsymbol{\tau})=\boldsymbol{\psi}_\Gamma\cdot\boldsymbol{n}.$$

Then, by the introduction of an adequate lifting, we will define a sequence $\{\boldsymbol{\psi}_n\}_{n\in\mathbb{N}}\subset\boldsymbol{V}_0$ such that $\boldsymbol{\psi}_{n|\Gamma}=\boldsymbol{\psi}_\Gamma$ and satisfying

$$\lim_{n\to\infty} m_\Omega(\boldsymbol{\psi}_n,\boldsymbol{\psi}_n)=0 \quad \text{and} \quad m_\Gamma(\boldsymbol{\psi}_n,\boldsymbol{\psi}_n)=-\frac{1}{V_S^2}\int_\Gamma(\boldsymbol{\psi}_{|\Gamma}\cdot\boldsymbol{n})^2\,\mathrm{d}\boldsymbol{\gamma}<0.$$

In consequence, it will exists $N\in\mathbb{N}$ such that for all $n>N$ we have $m(\boldsymbol{\psi}_n,\boldsymbol{\psi}_n)<0$.
Step 1: To define an adequate $\boldsymbol{\psi}_\Gamma$, let us assume that the arc length parametrization $\boldsymbol{x}(s)$ that parametrizes Γ satisfies

$$\boldsymbol{x}(s)\in\mathcal{C}^2(a,b), \quad \text{for some } [a,b]\subset[0,L] \qquad \text{(see Figure 7.3)}.$$

Then we denote by $\boldsymbol{\tau}(s)=\boldsymbol{x}'(s)$ and $\boldsymbol{n}(s)=(-\tau_2,\tau_1)^T$ the unit tangential and normal vectors to Γ at point $\boldsymbol{x}(s)$, and for any $\theta\in\mathcal{D}(a,b)\setminus\{0\}$ such that $\int_a^b\theta(s)\mathrm{d}\boldsymbol{s}=0$, we define

$$\boldsymbol{\psi}_\Gamma(\boldsymbol{x})=\begin{cases}\theta(s)\boldsymbol{n}(s)+\theta'(s)\boldsymbol{\tau}(s), & \text{if } \boldsymbol{x}(s)\in\Gamma_{a,b}:=\{\boldsymbol{x}(s)/s\in[a,b]\},\\ \boldsymbol{0}, & \text{if } \boldsymbol{x}\in\Gamma\setminus\Gamma_{a,b}.\end{cases}$$

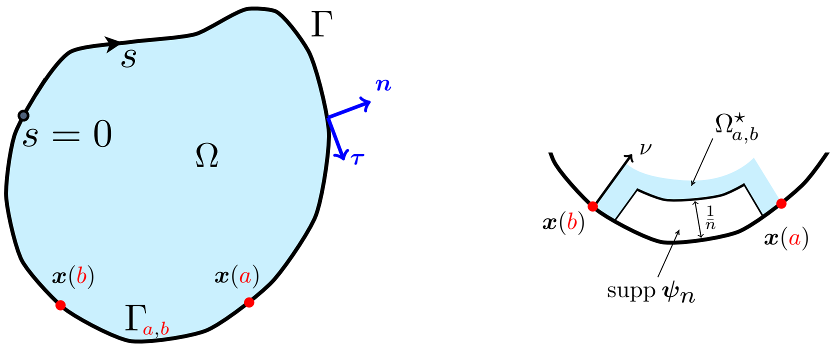

Figure 7.3: Left: Definition of the parametrization of the boundary. Right: Definition of the curvilinear coordinates and notations for the construction of the function $\boldsymbol{\psi}_\delta$ in the proof of Theorem 7.12.

In consequence, we can verify that as desired

$$\begin{aligned}
&\int_\Gamma \boldsymbol{\psi}_\Gamma \cdot \boldsymbol{n}\,\mathrm{d}\boldsymbol{\gamma} = \int_a^b \theta(s)\,\mathrm{d}\boldsymbol{s} = 0,\\
&\int_\Gamma \boldsymbol{\psi}_\Gamma \cdot \boldsymbol{\tau}\,\mathrm{d}\boldsymbol{\gamma} = \int_a^b \theta'(s)\,\mathrm{d}\boldsymbol{s} = \theta(b) - \theta(a) = 0,\\
&\mathcal{I}(\boldsymbol{\psi}_\Gamma \cdot \boldsymbol{\tau})(s) = \begin{cases} \mathcal{I}(\theta'(s)) = \theta(s)^2 = \boldsymbol{\psi}_\Gamma(\boldsymbol{x}(s)) \cdot \boldsymbol{n} & \text{if } s \in [a,b] \\ \boldsymbol{0} = \boldsymbol{\psi}_\Gamma(\boldsymbol{x}(s)) \cdot \boldsymbol{n} & \text{elsewhere} \end{cases}
\end{aligned}$$

Step 2: Now, we want to consider an adequate lifting to extend $\boldsymbol{\psi}_\Gamma$ into a fixed region

$$\Omega^\star_{a,b} := \{\boldsymbol{x}(s) - \nu\,\boldsymbol{n}(s),\ s \in (a,b),\ \nu \in (0,\nu^\star)\} \subset \Omega$$

where $\nu^\star > 0$ needs to be small enough to satisfy the inclusion. Moreover, we consider

$$\nu^\star \leq \frac{1}{2} \sup_{s\in(a,b)} \frac{1}{|c(s)|} \quad \text{where } c(s) = \boldsymbol{\tau}'(s)\cdot\boldsymbol{n}(s) \text{ is the curvature of } \Gamma \text{ on } \boldsymbol{x}(s),$$

in order to get good properties for the following change of variable

$$(s,\nu) \in (a,b) \times (0,\nu^\star) \to \boldsymbol{x}(s) - \nu\,\boldsymbol{n}(s) \in \Omega^\star_{a,b}.$$

The jacobian is given by $\mathbb{J}(s,\nu) = \big(\boldsymbol{\tau}(s) - \nu\,\boldsymbol{n}'(s), -\boldsymbol{n}(s)\big)$ and its determinant is

$$|\det\big(\mathbb{J}(s,\nu)\big)| = |-(\boldsymbol{\tau}(s) - \nu\,\boldsymbol{n}'(s))\cdot\boldsymbol{\tau}(s)| = |-1-\nu\,c(s)|,$$

which is uniformly bounded by $J^\star$ on $(a,b)\times(0,\nu^\star)$. Next, for all $n \in \mathbb{N}$ such that $1/n < \nu^\star$, we define $\psi_n \in C^1(\Omega)^2$ as

$$\boldsymbol{\psi}_n(\boldsymbol{x}) = \begin{cases} \boldsymbol{\psi}_\Gamma(\boldsymbol{x}(s))\,\chi(n\,\nu), & \text{if } \boldsymbol{x} = \boldsymbol{x}(s) - \nu\,\boldsymbol{n}(s) \in \Omega^\star_{a,b}, \\ \boldsymbol{0}, & \text{if } \boldsymbol{x} \in \Omega \setminus \Omega^\star_{a,b}, \end{cases}$$

where $\chi \in \mathcal{C}^\infty(\mathbb{R}^+)$ is such that supp $\chi \subset [0,1]$ and $\chi(0) = 1$. In consequence, on the one hand, since $\boldsymbol{\psi}_{n|\Gamma} = \boldsymbol{\psi}_\Gamma$, we have that $\boldsymbol{\psi}_n \in \boldsymbol{V}_0$ and

$$m_\Gamma(\boldsymbol{\psi}_n, \boldsymbol{\psi}_n) = -\frac{1}{V_S^2}\,\|\theta\|^2_{L^2(a,b)}.$$

While on the other hand, considering $V_P^2 > V_S^2$ and the change of variable we obtain

$$m_\Omega(\boldsymbol{\psi}_n, \boldsymbol{\psi}_n) \leq \frac{1}{V_S^2} \int_\Omega \boldsymbol{\psi}_n \cdot \boldsymbol{\psi}_n \, \mathrm{d}\boldsymbol{x} \leq \frac{J^\star}{V_S^2} \int_a^b \int_0^{\nu^\star} (\theta(s)^2 + \theta'(s)^2)\chi(n\,\nu)^2 \, \mathrm{d}s \, \mathrm{d}\nu.$$

Thus if we consider another change of variable given by $\overline{\nu} = n\,\nu$ we have that

$$m_\Omega(\boldsymbol{\psi}_n, \boldsymbol{\psi}_n) \leq \frac{J^\star}{n\,V_S^2} \int_a^b (\theta(s)^2 + \theta'(s)^2) \, \mathrm{d}s \int_0^{n\,\nu^\star} \chi(\overline{\nu})^2 \, \mathrm{d}\overline{\nu} \leq \frac{J^\star}{n\,V_S^2} \, \|\theta\|^2_{H^1(a,b)} \|\chi\|^2_{L^2(\mathbb{R})}.$$

Then it is clear that for big enough $N \in \mathbb{N}$ we have $m(\boldsymbol{\psi}_n, \boldsymbol{\psi}_n) < 0$ for all $n > N$.

■

In consequence, the variational problem (7.28) does not fit into the classical Lions-Magenes theory and an analogous to Theorem 6.6 can not be established. Moreover, as one can expect, the property of Theorem 7.12 is the cause of severe instabilities for any finite element approximation of the variational formulation (7.28). This will be exhibited in the next section.

7.2.3 Numerical instabilities of finite elements discretizations

In this section our aim is to exhibit the instabilities of a finite element approximation of the variational formulation (7.28). Then, similarly to Section 6.4.1, we first introduce a finite dimensional approximation of the space $\boldsymbol{V}_0$ given by $\boldsymbol{V}_{0h} = \boldsymbol{V}_0 \cap \boldsymbol{V}_h$, where $\boldsymbol{V}_h$ represents a finite element approximation of the space $\boldsymbol{V}$. Notice that due to the density result in (6.12), standard approximation spaces of $H^1(\Omega)^2$ ensure adequate approximation properties when approximating $\boldsymbol{V}$. Moreover, in order to decouple the potentials in the volume and according to Lemma 6.3, we shall consider $\boldsymbol{V}_{0h} \subset H^1(\Omega)^2$. Thus, let us consider $\mathcal{T}_{P,h}$ and $\mathcal{T}_{S,h}$ two triangulations of Ω, then the approximation space $\boldsymbol{V}_{0h}$ will be naturally sought in the form (see (2.57) for definition of $X_p(\cdot)$)

$$\boldsymbol{V}_{0h} = \boldsymbol{V}_0 \cap \boldsymbol{V}_h \quad \text{where} \quad \boldsymbol{V}_h = V_{P,h} \times V_{S,h} \quad \text{with} \quad V_{Q,h} = X_{p_Q}(\mathcal{T}_{Q,h}) \text{ for } Q \in \{P, S\}. \tag{7.30}$$

Then, the semi-discrete problem writes:

$$\left\{\begin{array}{l} \text{Find } \boldsymbol{\varphi}_h(t) : [0,T] \longrightarrow \boldsymbol{V}_{0h} \text{ such that } (\boldsymbol{\varphi}_h, \partial_t \boldsymbol{\varphi}_h)(t=0) = (\boldsymbol{0}, \boldsymbol{0}) \text{ and} \\ \dfrac{\mathrm{d}^2}{\mathrm{d}t^2} m(\boldsymbol{\varphi}_h(t), \boldsymbol{\psi}_h) + a(\boldsymbol{\varphi}_h(t), \boldsymbol{\psi}_h) = \mathrm{g}(t, \boldsymbol{\psi}_h), \quad \forall\, \boldsymbol{\psi}_h \in \boldsymbol{V}_{0h}. \end{array}\right. \tag{7.31}$$

Next, in order to work in the space $\boldsymbol{V}_h$ instead of $\boldsymbol{V}_{0h}$, we choose to treat the gauge conditions in the definition of $\boldsymbol{V}_0$ (see (7.26)) in weak (but exact) way by introducing two new scalar unknowns $(\eta_{\boldsymbol{n}}, \eta_{\boldsymbol{\tau}}) \in \mathbb{R}^2$ that are Lagrange multipliers. This provides the following mixed formulation which is equivalent to (7.31).

$$\left\{\begin{array}{ll} \text{Find } (\boldsymbol{\varphi}_h, \eta_{\boldsymbol{n}}, \eta_{\boldsymbol{\tau}}) : [0,T] \longrightarrow \boldsymbol{V}_h \times \mathbb{R}^2 \text{ such that } (\boldsymbol{\varphi}_h, \partial_t \boldsymbol{\varphi}_h)(t=0) = (\boldsymbol{0}, \boldsymbol{0}) \text{ and} & \\ \dfrac{\mathrm{d}^2}{\mathrm{d}t^2} m(\boldsymbol{\varphi}_h(t), \boldsymbol{\psi}_h) + a(\boldsymbol{\varphi}_h(t), \boldsymbol{\psi}_h) & \\ \qquad\qquad + \eta_{\boldsymbol{n}}(t) \displaystyle\int_\Gamma \boldsymbol{\psi}_h \cdot \boldsymbol{n} \, \mathrm{d}\boldsymbol{\gamma} + \eta_{\boldsymbol{\tau}}(t) \int_\Gamma \boldsymbol{\psi}_h \cdot \boldsymbol{\tau} \, \mathrm{d}\boldsymbol{\gamma} = \mathrm{g}(t, \boldsymbol{\psi}_h), \quad \forall\, \boldsymbol{\psi}_h \in \boldsymbol{V}_h, & (7.32a) \\ \displaystyle\int_\Gamma \boldsymbol{\varphi}_h \cdot \boldsymbol{n} \, \mathrm{d}\boldsymbol{\gamma} = 0 \quad \text{and} \quad \int_\Gamma \boldsymbol{\varphi}_h \cdot \boldsymbol{\tau} \, \mathrm{d}\boldsymbol{\gamma} = 0. & (7.32b) \end{array}\right.$$

Remark 7.13

Notice, that the introduction of Lagrange multipliers for the treatment of the gauge conditions *can not be done in the continuous problem (7.28) since $m(\cdot,\cdot)$ is not well defined in $\boldsymbol{V}\setminus\boldsymbol{V}_0$ due to the integral operator $\mathcal{I}(\cdot)$ (see Remark 7.9). However, at the discrete level the bilinear form $m(\cdot,\cdot)$ is well defined in $\boldsymbol{V}_h$, since for all $\boldsymbol{\psi}_h\in\boldsymbol{V}_h$ we have that $\boldsymbol{\psi}_h\cdot\boldsymbol{n}$ and $\boldsymbol{\psi}_h\cdot\boldsymbol{\tau}$ belong to $L^2(\Gamma)$ which is the domain of definition of the integral operator $\mathcal{I}(\cdot)$ (see (7.18)).*

In practice, this formulation is the one that adapts better for decomposition of the discrete unknowns $\varphi_{P,h}$ and $\varphi_{S,h}$ in the respective Lagrange elements. Then if we introduce the vector $\boldsymbol{\Phi}_h^T=(\boldsymbol{\Phi}_{P,h}^T,\boldsymbol{\Phi}_{S,h}^T)$ of the Lagrange degrees of freedom of $\varphi_{P,h}$ and $\varphi_{S,h}$ respectively, problem (7.32) results into the following algebraic system of ODEs (completed with $\boldsymbol{\Phi}_h(0)=\frac{\mathrm{d}}{\mathrm{d}t}\boldsymbol{\Phi}_h(0)=\boldsymbol{0}$)

$$\begin{cases} \mathbb{M}_h\,\dfrac{\mathrm{d}^2\boldsymbol{\Phi}_h}{\mathrm{d}t^2}+\mathbb{A}_h\,\boldsymbol{\Phi}_h+\eta_{\boldsymbol{n}}\boldsymbol{B}_{\boldsymbol{n}}+\eta_{\boldsymbol{\tau}}\boldsymbol{B}_{\boldsymbol{\tau}}=\boldsymbol{G}_h, & \text{(7.33a)}\\[2ex] \boldsymbol{B}_{\boldsymbol{n}}^T\boldsymbol{\Phi}_h=0 \quad\text{and}\quad \boldsymbol{B}_{\boldsymbol{\tau}}^T\boldsymbol{\Phi}_h=0, & \text{(7.33b)}\end{cases}$$

where we have introduced $\mathbb{M}_h:=\mathbb{M}_h^\Omega+\mathbb{M}_h^\Gamma$ (or $\widetilde{\mathbb{M}}_h$ and $\widetilde{\mathbb{M}}_h^\Omega$ if mass lumping is considered). Notice that $\mathbb{M}_h^\Omega$ and $\mathbb{A}_h$ are defined as in (6.36), while $\boldsymbol{B}_{\boldsymbol{n}}$, $\boldsymbol{B}_{\boldsymbol{\tau}}$ and $\mathbb{M}_h^\Gamma$ are given by

$$\boldsymbol{B}_{\boldsymbol{n}}=\begin{pmatrix}\boldsymbol{B}_{\boldsymbol{n}}^P\\ \boldsymbol{B}_{\boldsymbol{n}}^S\end{pmatrix},\quad \boldsymbol{B}_{\boldsymbol{n}}=\begin{pmatrix}\boldsymbol{B}_{\boldsymbol{\tau}}^P\\ \boldsymbol{B}_{\boldsymbol{\tau}}^S\end{pmatrix}\quad\text{and}\quad \mathbb{M}_h^\Gamma=\begin{pmatrix}\mathbb{M}_{PP,h}^\Gamma & \mathbb{M}_{PS,h}^\Gamma\\ (\mathbb{M}_{PS,h}^\Gamma)^T & \mathbb{M}_{SS,h}^\Gamma\end{pmatrix}, \tag{7.34}$$

where each matrix can be computed by exact evaluation. More precisely, if we denote by $\{\psi_Q^k\}_{k=1}^{K_Q}$ the set of Lagrange basis functions of $V_{Q,h}$ for $Q\in\{P,S\}$, we compute

$$\begin{aligned}
(\boldsymbol{B}_{\boldsymbol{n}}^P)_k &= \int_\Gamma n_1\,\psi_P^k\,\mathrm{d}\boldsymbol{\gamma}, \qquad (\boldsymbol{B}_{\boldsymbol{n}}^S)_k=\int_\Gamma n_2\,\psi_S^k\,\mathrm{d}\boldsymbol{\gamma},\\
(\boldsymbol{B}_{\boldsymbol{\tau}}^P)_k &= \int_\Gamma n_2\,\psi_P^k\,\mathrm{d}\boldsymbol{\gamma}, \qquad (\boldsymbol{B}_{\boldsymbol{\tau}}^S)_k=-\int_\Gamma n_1\,\psi_S^k\,\mathrm{d}\boldsymbol{\gamma},\\
(\mathbb{M}_{PP,h}^\Gamma)_{k,l} &= -\frac{1}{2\,V_S^2}\int_\Gamma \big(\mathcal{I}(n_2\,\psi_P^k)\,n_1\,\psi_P^l+\mathcal{I}(n_2\,\psi_P^l)\,n_1\,\psi_P^k\big)\mathrm{d}\boldsymbol{\gamma},\\
(\mathbb{M}_{SS,h}^\Gamma)_{k,l} &= \frac{1}{2\,V_S^2}\int_\Gamma \big(\mathcal{I}(n_1\,\psi_S^k)\,n_2\,\psi_S^l+\mathcal{I}(n_1\,\psi_S^l)\,n_2\,\psi_S^k\big)\mathrm{d}\boldsymbol{\gamma},\\
(\mathbb{M}_{PS,h}^\Gamma)_{k,l} &= -\frac{1}{2\,V_S^2}\int_\Gamma \big(\mathcal{I}(n_2\,\psi_P^k)\,n_2\,\psi_S^l-\mathcal{I}(n_1\,\psi_S^l)\,n_1\,\psi_P^k\big)\mathrm{d}\boldsymbol{\gamma}.
\end{aligned}$$

The computation of $\mathbb{M}_{PS,h}^\Gamma$ requires, similarly to $\mathbb{A}_{PS,h}^\Gamma$, the intersection on the boundary between the meshes chosen to build $V_{P,h}$ and $V_{S,h}$. The resultant matrix is also a very sparse matrix that in this case, due to the double integral on the boundary, couples each degree of freedom that is located along the boundary with all the other degrees of freedom on the boundary.

We shall notice that, despite of the injectivity property in Lemma 7.11, it is not clear that the matrix $\mathbb{M}_h$ is invertible (which is a necessary property if one wants to use an explicit scheme in time). Indeed, the proof was done at the continuous level using density properties of smooth compactly supported functions. At the discrete level, i.e. in finite dimensional spaces, such argument can not be used any more. However, even in the case where $\mathbb{M}_h$ is invertible, it is most likely that, because of the result of Theorem 7.12, the solution of the semi-discrete evolution problem (7.33) will blow up exponentially in time. To explain this, let us rewrite problem (7.33) as

$$\mathbb{M}_\star\frac{\mathrm{d}^2}{\mathrm{d}t^2}\begin{pmatrix}\boldsymbol{\Phi}_h\\ \widetilde{\eta}_{\boldsymbol{n}}\\ \widetilde{\eta}_{\boldsymbol{\tau}}\end{pmatrix}+\mathbb{A}_\star\begin{pmatrix}\boldsymbol{\Phi}_h\\ \widetilde{\eta}_{\boldsymbol{n}}\\ \widetilde{\eta}_{\boldsymbol{\tau}}\end{pmatrix}=\boldsymbol{G}_\star \tag{7.35}$$

where we have introduced new variables $\widetilde{\eta}_{\boldsymbol{n}}=\partial_t^2\eta_{\boldsymbol{n}}$ and $\widetilde{\eta}_{\boldsymbol{\tau}}=\partial_t^2\eta_{\boldsymbol{\tau}}$ as well as

$$\mathbb{M}_\star:=\begin{pmatrix}\mathbb{M}_h & \boldsymbol{B}_{\boldsymbol{n}} & \boldsymbol{B}_{\boldsymbol{\tau}}\\ \boldsymbol{B}_{\boldsymbol{n}}^T & 0 & 0\\ \boldsymbol{B}_{\boldsymbol{\tau}}^T & 0 & 0\end{pmatrix},\quad \mathbb{A}_\star:=\begin{pmatrix}\mathbb{A}_h & \boldsymbol{0} & \boldsymbol{0}\\ \boldsymbol{0}^T & 0 & 0\\ \boldsymbol{0}^T & 0 & 0\end{pmatrix}\quad\text{and}\quad \boldsymbol{G}_\star:=\begin{pmatrix}\boldsymbol{G}_h\\ 0\\ 0\end{pmatrix}.$$

Then, in order to use classical techniques for the solution of inhomogeneous linear systems (see Section 1.10 in [104]), we assume that $\mathbb{M}_\star$ is invertible and we rewrite the previous problem by introducing

$$\boldsymbol{\Psi} = \begin{pmatrix} \boldsymbol{\Psi}_1 \\ \boldsymbol{\Psi}_2 \end{pmatrix} \quad \text{where} \quad \boldsymbol{\Psi}_1 = -(\mathbb{M}_\star^{-1}\mathbb{A}_\star)^{\frac{1}{2}} \begin{pmatrix} \boldsymbol{\Phi}_h \\ \widetilde{\eta}_{\boldsymbol{n}} \\ \widetilde{\eta}_{\boldsymbol{\tau}} \end{pmatrix} \quad \text{and} \quad \boldsymbol{\Psi}_2 = \frac{\mathrm{d}}{\mathrm{d}t} \begin{pmatrix} \boldsymbol{\Phi}_h \\ \widetilde{\eta}_{\boldsymbol{n}} \\ \widetilde{\eta}_{\boldsymbol{\tau}} \end{pmatrix}.$$

Remark 7.14

Let us remark that $(\mathbb{M}_\star^{-1}\mathbb{A}_\star)^{\frac{1}{2}}$ exists since it is diagonalizable. First notice that $\mathbb{M}_\star^{-1}$ is symmetric, thus diagonalizable and therefore $\mathbb{M}_\star^{-\frac{1}{2}}$ exists. Moreover, since $\mathbb{A}_\star$ is symmetric, the matrix $\mathbb{M}_\star^{-\frac{1}{2}}\mathbb{A}_\star\mathbb{M}_\star^{-\frac{1}{2}}$ is also symmetric and therefore diagonalizable. Finally, we observe that $\mathbb{M}_\star^{-1}\mathbb{A}_\star = \mathbb{M}_\star^{-\frac{1}{2}}\mathbb{M}_\star^{-\frac{1}{2}}\mathbb{A}_\star\mathbb{M}_\star^{-\frac{1}{2}}\mathbb{M}_\star^{\frac{1}{2}}$, thus it is similar to a symmetric matrix, hence diagonalizable.

As a result we obtain the following problem for $\boldsymbol{\Psi}$

$$\frac{\mathrm{d}}{\mathrm{d}t}\boldsymbol{\Psi} = \begin{pmatrix} -(\mathbb{M}_\star^{-1}\mathbb{A}_\star)^{\frac{1}{2}}\boldsymbol{\Psi}_2 \\ (\mathbb{M}_\star^{-1}\mathbb{A}_\star)^{\frac{1}{2}}\boldsymbol{\Psi}_1 + \mathbb{M}_\star^{-1}\boldsymbol{G}_\star \end{pmatrix} = \begin{pmatrix} \mathbb{O} & -(\mathbb{M}_\star^{-1}\mathbb{A}_\star)^{\frac{1}{2}} \\ (\mathbb{M}_\star^{-1}\mathbb{A}_\star)^{\frac{1}{2}} & \mathbb{O} \end{pmatrix} \boldsymbol{\Psi} + \begin{pmatrix} \mathbf{0} \\ \mathbb{M}_\star^{-1}\boldsymbol{G}_\star \end{pmatrix},$$

which solution is given by

$$\boldsymbol{\Psi}(t) = \boldsymbol{\Psi}(0)e^{t\,\mathbb{D}_\star} + \int_0^t e^{(t-s)\mathbb{D}_\star} \begin{pmatrix} \mathbf{0} \\ \mathbb{M}_\star^{-1}\boldsymbol{G}_\star(s) \end{pmatrix} \mathrm{d}s, \quad \text{where} \quad \mathbb{D}_\star := \begin{pmatrix} \mathbb{O} & -(\mathbb{M}_\star^{-1}\mathbb{A}_\star)^{\frac{1}{2}} \\ (\mathbb{M}_\star^{-1}\mathbb{A}_\star)^{\frac{1}{2}} & \mathbb{O} \end{pmatrix}.$$

Next, we notice that $\boldsymbol{\Psi}(0) = \mathbf{0}$ and that

$$\begin{aligned} e^{\mathbb{D}_\star} = \sum_{k=0}^{\infty} \frac{\mathbb{D}_\star^k}{k!} &= \begin{pmatrix} \displaystyle\sum_{k=0}^{\infty} \frac{(-1)^k(\mathbb{M}_\star^{-1}\mathbb{A}_\star)^k}{(2k)!} & -\displaystyle\sum_{k=0}^{\infty} \frac{(-1)^k(\mathbb{M}_\star^{-1}\mathbb{A}_\star)^{\frac{2k+1}{2}}}{(2k+1)!} \\ \displaystyle\sum_{k=0}^{\infty} \frac{(-1)^k(\mathbb{M}_\star^{-1}\mathbb{A}_\star)^{\frac{2k+1}{2}}}{(2k+1)!} & \displaystyle\sum_{k=0}^{\infty} \frac{(-1)^k(\mathbb{M}_\star^{-1}\mathbb{A}_\star)^k}{(2k)!} \end{pmatrix} \\ &= \begin{pmatrix} \cos\left((\mathbb{M}_\star^{-1}\mathbb{A}_\star)^{\frac{1}{2}}\right) & -\sin\left((\mathbb{M}_\star^{-1}\mathbb{A}_\star)^{\frac{1}{2}}\right) \\ \sin\left((\mathbb{M}_\star^{-1}\mathbb{A}_\star)^{\frac{1}{2}}\right) & \cos\left((\mathbb{M}_\star^{-1}\mathbb{A}_\star)^{\frac{1}{2}}\right) \end{pmatrix}, \end{aligned}$$

therefore, the solution of semi-discrete problem (7.35) must satisfy

$$(\mathbb{M}_\star^{-1}\mathbb{A}_\star)^{\frac{1}{2}} \begin{pmatrix} \boldsymbol{\Phi}_h \\ \widetilde{\eta}_{\boldsymbol{n}} \\ \widetilde{\eta}_{\boldsymbol{\tau}} \end{pmatrix} = \int_0^t \sin\left((t-s)(\mathbb{M}_\star^{-1}\mathbb{A}_\star)^{\frac{1}{2}}\right)\mathbb{M}_\star^{-1}\boldsymbol{G}_\star(s)\mathrm{d}s.$$

In consequence, if $(\mathbb{M}_\star^{-1}\mathbb{A}_\star)^{-\frac{1}{2}}$ exists, the solution is given by

$$\begin{pmatrix} \boldsymbol{\Phi}_h \\ \widetilde{\eta}_{\boldsymbol{n}} \\ \widetilde{\eta}_{\boldsymbol{\tau}} \end{pmatrix} = \int_0^t (\mathbb{M}_\star^{-1}\mathbb{A}_\star)^{-\frac{1}{2}} \sin\left((t-s)(\mathbb{M}_\star^{-1}\mathbb{A}_\star)^{\frac{1}{2}}\right)\mathbb{M}_\star^{-1}\boldsymbol{G}_\star(s)\mathrm{d}s. \tag{7.36}$$

Moreover, since $\mathbb{A}_\star$ is positive and $\mathbb{M}_\star$ is most likely to be indefinite (due to the negativity result in Theorem 7.12), we expect that the matrix $\mathbb{M}_\star^{-1}\mathbb{A}_\star$ has negative eigenvalues. Therefore, there exists an eigenpair $(\boldsymbol{\Psi}_-, \lambda_-)$ with $\lambda_- < 0$, for the following symmetric generalised eigenvalue problem:

$$\text{Find } \boldsymbol{\Psi}_h \neq 0 \text{ and } \lambda \in \mathbb{R} \quad \text{such that} \quad \mathbb{A}_\star\boldsymbol{\Psi}_h = \lambda\,\mathbb{M}_\star\boldsymbol{\Psi}_h. \tag{7.37}$$

Next, we also observe that (straightforward computations considering the series expansion of the sinus)

$$(\boldsymbol{\Psi}_-, \lambda_-^{-\frac{1}{2}}\sin((t-s)\lambda_-^{\frac{1}{2}})) \quad \text{is an eigenpair of} \quad \mathbb{N}_\star := (\mathbb{M}_\star^{-1}\mathbb{A}_\star)^{-\frac{1}{2}}\sin\left((t-s)(\mathbb{M}_\star^{-1}\mathbb{A}_\star)^{\frac{1}{2}}\right).$$

In consequence (notice that ρ denotes the spectral radius)

$$\|\mathbb{N}_\star\| \;\geq\; \rho(\mathbb{N}_\star) \;\geq\; |\lambda_-|^{-\frac{1}{2}} \sinh\left((t-s)|\lambda_-|^{\frac{1}{2}}\right) \;\geq\; C\, e^{(t-s)\sqrt{|\mathcal{C}(h)|}},$$

where $\mathcal{C}(h) \in \mathbb{R}$ is such that $0 < \mathcal{C}(h) < |\lambda_-(h)|$. This would lead to a blow up with the same rate for (7.36) and in the following, we illustrate this phenomena by numerical computations.

Numerical experiments. We complete this section by providing numerical results to exhibit the instabilities of the method. We consider the computational domain

$$\Omega = [-5, 5] \times [-5, 5]$$

with the physical properties given by $\lambda = 20$, $\mu = 4$ and $\rho = 1$, and we build the space $\boldsymbol{V}_h$ using first order Lagrange finite elements on triangular meshes. Notice, that different meshes can be used for each potential, however in this section the same quasi-uniform mesh will be used for both potentials in order to ensure that the instabilities are not due to the consideration of independent meshes. The meshes we have considered (see them in Figure 7.4) were obtained using a mesh generator of the literature [69] with the following mesh size parameter h_*:

Mesh 1:$h_* = 1.44$, Mesh 2:$h_* = 0.72$, Mesh 3:$h_* = 0.36$ and Mesh 4 : $h_* = 0.18$.

For all meshes, the invertibility of $\mathbb{M}_\star$ has been observed experimentally, then problem (7.37)

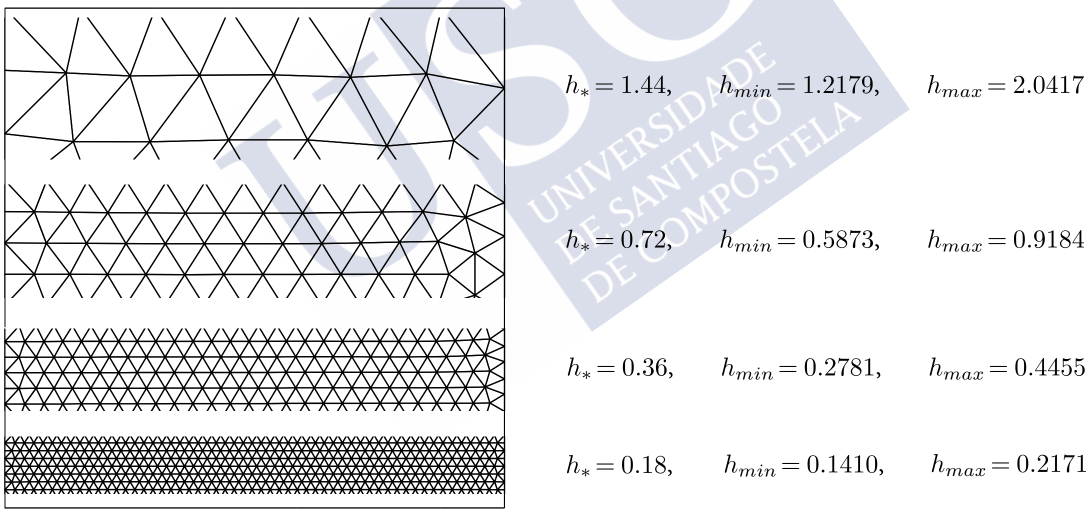

Figure 7.4: Sketch of the five different meshes considered. h_* denotes the parameters introduced to the mesh generator while h_{min} and h_{max} denote respectively the smaller and larger edge size of each resulting mesh.

can be solved numerically (we have used MATLAB code) to obtain the spectrum $\boldsymbol{\sigma}_h$. Then, in Figure 7.5 we plot the eigenvalues of problem (7.37) and we observe that

- The number of negative eigenvalues increases when h decreases.
- The smaller negative eigenvalue behaves approximately as h^{-2}.

It is also interesting to see in Figures 7.6 and 7.7 that the eigenmode corresponding to the smallest eigenvalue is concentrated close to the boundary. The finer the mesh, the more concentrated to the boundary. At the same time, we also observe that the eigenmode oscillates more and more along the boundary.

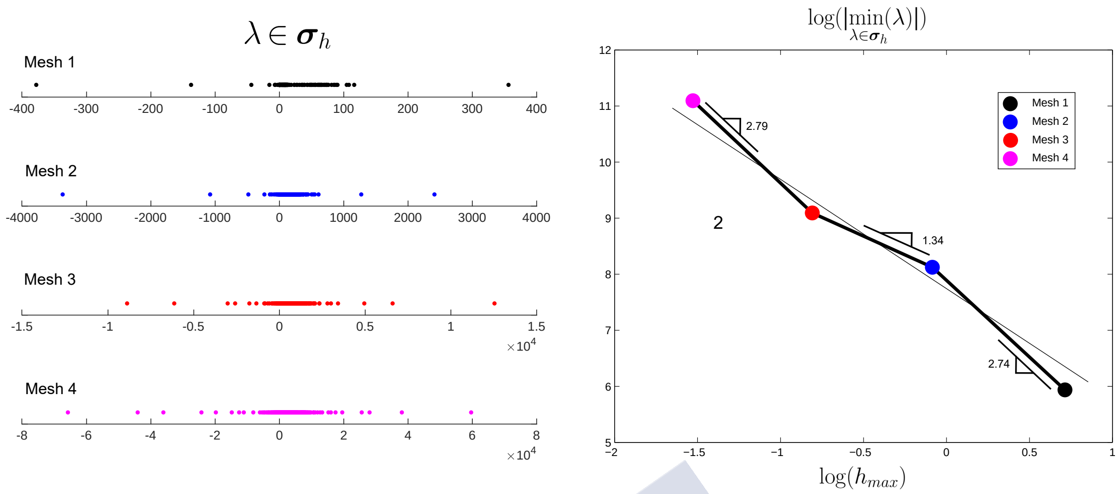

Figure 7.5: Left: Eigenvalues of problem (7.37) obtained for Meshes 1, 2, 3 and 4. Right: Evolution of the smaller eigenvalue with respect to mesh size.

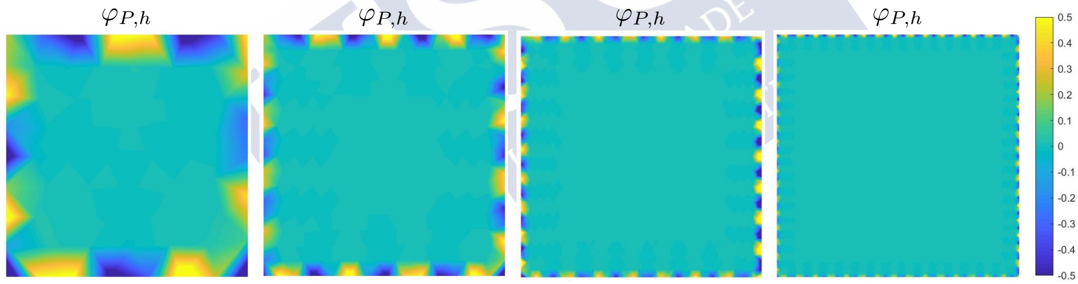

Figure 7.6: Representation of the potential $\varphi_{P,h}$ corresponding to the eigenvector related to the smaller eigenvalue of (7.37) for Meshes 1, 2, 3 and 4.

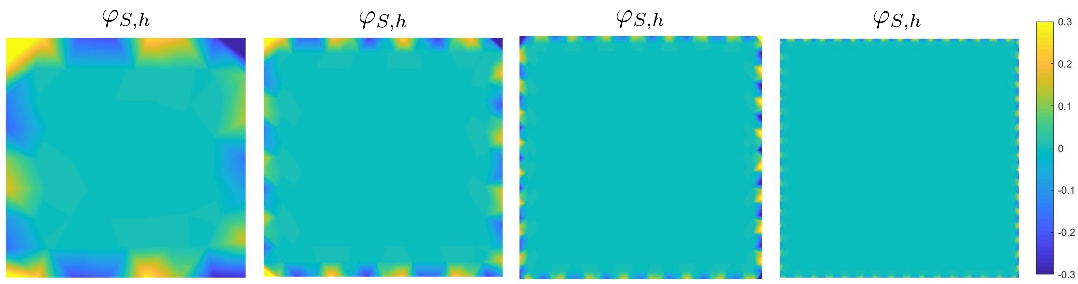

Figure 7.7: Representation of the potential $\varphi_{S,h}$ corresponding to the eigenvector related to the smaller eigenvalue of (7.37) for Meshes 1, 2, 3 and 4.

Finally, to complement these observations, we consider the same medium to be excited by a source term given by

$$\boldsymbol{f}(\boldsymbol{x},t) = \begin{pmatrix} 1 \\ 1 \end{pmatrix} \left(e^{-|\boldsymbol{x}-\boldsymbol{x}_0|^2/s_x} - e^{-|\boldsymbol{x}+\boldsymbol{x}_0|^2/s_x} \right) \partial_t \left(e^{-(t-t_0)^2/s_t} \right)$$

with $\boldsymbol{x}_0 = (1.5, 1.5)^t$ and $s_x = 0.1, t_0 = 0.8, s_t = 0.04$ (notice $\boldsymbol{f}(\cdot,t) \in \boldsymbol{L}^2_R(\Omega)$ at all times). Then, we solve problem (7.33) in order to observe the expected blow up of the solution. To dispel the idea that the observed instability could be due to the time discretization, we have used the following fully implicit scheme (completed with vanishing initial data $\boldsymbol{\Phi}_h^0 = \boldsymbol{\Phi}_h^1 = \boldsymbol{0}$)

$$\begin{cases} \mathbb{M}_h \dfrac{\boldsymbol{\Phi}_h^{n+1} - 2\boldsymbol{\Phi}_h^n + \boldsymbol{\Phi}_h^{n-1}}{\Delta t^2} + \mathbb{A}_h \dfrac{\boldsymbol{\Phi}_h^{n+1} + 2\boldsymbol{\Phi}_h^n + \boldsymbol{\Phi}_h^{n-1}}{4} + \eta_{\boldsymbol{n}}^n \boldsymbol{B}_{\boldsymbol{n}} + \eta_{\boldsymbol{\tau}}^n \boldsymbol{B}_{\boldsymbol{\tau}} = \boldsymbol{G}_h^n, & \text{(7.38a)} \\ \boldsymbol{B}_{\boldsymbol{n}}^T \boldsymbol{\Phi}_h^n = 0 \quad \text{and} \quad \boldsymbol{B}_{\boldsymbol{\tau}}^T \boldsymbol{\Phi}_h^n = 0, & \text{(7.38b)} \end{cases}$$

where $\Delta t = 0.001$ and $\boldsymbol{\Phi}_h^n$, $\eta_{\boldsymbol{n}}^n$ and $\eta_{\boldsymbol{\tau}}^n$ approximate the unknowns $\boldsymbol{\Phi}_h$, $\eta_{\boldsymbol{n}}$ and $\eta_{\boldsymbol{\tau}}$ at each $t^n = n\Delta t$. In Figures 7.8 and 7.9 we plot at three different times snapshots of the solution obtained when considering Mesh 4. These results illustrate the bad behaviour of the numerical solution since one can observe a blow-up of the solution that is initiated, as expected, close to the boundary but propagates inside the computational domain as t increases. In Figure 7.10 we quantify the

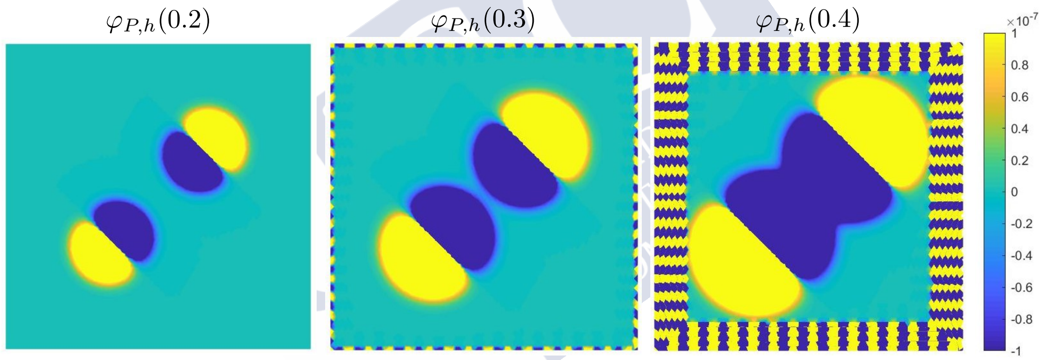

Figure 7.8: Snapshots at three different times of the potential $\varphi_{P,h}$ obtained when solving (7.38) considering Mesh 4. The colour scale is saturated on the boundary.

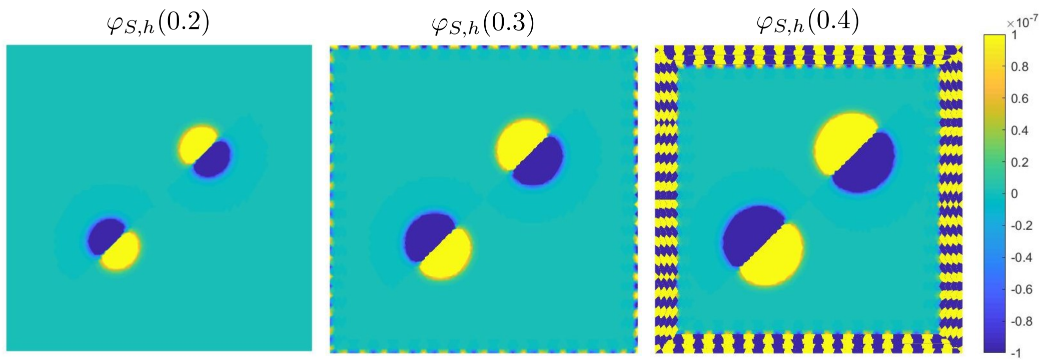

Figure 7.9: Snapshots at three different times of the potential $\varphi_{S,h}$ obtained when solving (7.38) considering Mesh 4. The colour scale is saturated on the boundary.

blow-up of the solution when considering the four meshes and we represent the variations of the

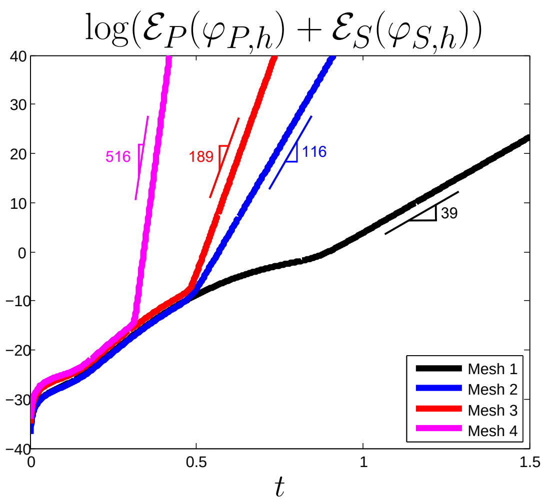

	$2\sqrt{\left\lvert \min\limits_{\lambda\in\boldsymbol{\sigma}_h}(\lambda)\right\rvert}$
Mesh 1	38.9
Mesh 2	116.1
Mesh 3	188.5
Mesh 4	513.1

Figure 7.10: We plot the evolution of $\mathcal{E}_P(\varphi_{P,h}) + \mathcal{E}_S(\varphi_{S,h})$ (where $\mathcal{E}_Q(\cdot)$ is the energy defined in (6.26) and associated to the scalar wave equation for φ_Q) for the solution of (7.38) and we compare the rate of blow-up with respect to the worst eigenvalue of problem (7.37).

sum of the energies associated to each scalar wave equation. It is interesting to notice that the rate of blow-up is approximately $2\sqrt{\left\lvert \min\limits_{\lambda\in\boldsymbol{\sigma}_h}(\lambda)\right\rvert}$.

In the following section, we come back in more details on these invertibility and stability issues. In particular, we consider a simplified toy problem associated to a simple geometry. In this case, the two issues (invertibility and lack of positivity) can be studied analytically.

7.3 A naive approach for a toy problem: The periodic half-space

In this section we analyse in a simplified configuration the nature of the instabilities exhibited in previous section in order to confirm that they are directly linked to the free boundary. The simplification comes when solving elastodynamics equations (5.3) in the cylinder

$$\Omega = (0, +\infty) \times (-\pi, \pi) \tag{7.39}$$

considering a free boundary at $x_1 = 0$ and identifying the upper and lower boundaries. In consequence, we impose periodic boundary conditions

$$\boldsymbol{u}(t, x_1, \pi) = \boldsymbol{u}(t, x_1, -\pi),\ \partial_2\boldsymbol{u}(t, x_1, \pi) = \partial_2\boldsymbol{u}(t, x_1, -\pi), \quad \forall\, x_1 \in \mathbb{R}^+, \tag{7.40}$$

in such a way that the boundary of Ω can be identified to a circle (this is a closed curve). Note that this particular example does not completely fit the assumptions made on the geometry of the domain since Ω is unbounded, however the reader will easily convince himself that this is not an essential issue.

7.3.1 Space discretization and numerical instabilities

The simple geometry we have consider, allows us to discretize the space $\boldsymbol{V}_0$ using in the direction x_2 a spectral method consisting in truncating, for each potential, the Fourier series expansion of a function in $L^2(-\pi, \pi)$ at order $L_Q > 0$ for $Q \in \{P, S\}$ (truncation parameter devoted to tend to $+\infty$). In consequence, $2\pi/L_Q$ is the minimal oscillation length allowed in the approximation of the associated Q-wave. More precisely, we choose to approximate the space $\boldsymbol{V}_0$ by the finite dimensional space $\boldsymbol{V}_h^L = V_{P,h}^L \times V_{S,h}^L$ which results from considering for $Q \in \{P, S\}$ the spaces (notice $\mathbb{i} = \sqrt{-1}$)

$$V_{Q,h}^L := \Big\{ \phi_{Q,h}^L \in H^1(\Omega, \mathbb{R}) \ \text{ s.t. } \ \phi_{Q,h}^L = \sum_{\ell=-L_Q}^{L_Q} \varphi_{Q,h}^{\ell}(x_1)\, e^{-\mathbb{i}\ell x_2} \ \text{ with } \ \varphi_{Q,h}^{\ell} \in V_{Q,h}^{1\mathrm{D}} \Big\}, \tag{7.41}$$

where $V_{Q,h}^{1\mathrm{D}}$ represents the discretization in the direction x_1 using standard finite elements. In particular we consider $V_{Q,h}^{1\mathrm{D}} \subset H^1(\mathbb{R}^+)$ the uniform discretization of $\mathbb{R}^+$ by first order Lagrange finite elements with space step h_Q, i.e.

$$V_{Q,h}^{1\mathrm{D}} := \{ \varphi_{Q,h} \in H^1(\mathbb{R}^+, \mathbb{C}) \ \text{ s.t. } \ \varphi_{Q,h}(x_1) = \sum_{j=0}^{+\infty} \varphi_Q^j\, w_{Q,j}(x_1) \} \tag{7.42}$$

where the set $\{w_{Q,j}\}$ are the piecewise affine functions that satisfy $w_{Q,j}(kh_Q) = \delta_{kj}$ (where δ is the Kronecker symbol) so that $\varphi_Q^j = \varphi_{Q,h}(jh_Q)$. Note that this space is isomorphic to the space $\ell^2(\mathbb{N})$. With this notation (analogously to (7.30)) we approximate $\boldsymbol{V}_0$ by the finite dimensional space $\boldsymbol{V}_{0h}^L := \boldsymbol{V}_h^L \cap \boldsymbol{V}_0$ which is nothing but

$$\boldsymbol{V}_{0h}^L = \Big\{ \boldsymbol{\phi}_h^L = (\phi_{P,h}^L, \phi_{S,h}^L) \in \boldsymbol{V}_h^L \ \text{ s.t. } \ \varphi_P^{0,0} = \varphi_S^{0,0} = 0 \Big\}, \tag{7.43}$$

where $\varphi_P^{0,0} := \varphi_{P,h}^0(0)$ and $\varphi_S^{0,0} := \varphi_{S,h}^0(0)$, according to the notation introduced above.

Remark 7.15

If one makes an analogy with first order quadrilateral finite elements for instance, this would correspond to discretize Ω uniformly with two different rectangular finite elements, one adapted for the P-waves and the other for the S-waves. To be more precise, we choose for $Q \in \{P, S\}$ a uniform quadrangular mesh of length $h_1 = h_Q$ in the direction x_1 and $h_2 = \pi/(2L_Q)$ in the direction x_2.

Then, we look for the solution of the semi-discrete problem (7.31) with the following expression of the bilinear forms $m(\cdot,\cdot)$ and $a(\cdot,\cdot)$ that take into account the fact that we deal with complex valued functions,

$$\begin{aligned}
m(\boldsymbol{\varphi}_h, \boldsymbol{\psi}_h) \;&=\; \frac{1}{V_P^2}\int_{-\pi}^{\pi}\int_{\mathbb{R}^+} \varphi_{P,h}\overline{\psi_{P,h}}\, dx_1\, dx_2 + \frac{1}{V_S^2}\int_{-\pi}^{\pi}\int_{\mathbb{R}^+} \varphi_{S,h}\overline{\psi_{S,h}}\, dx_1\, dx_2 \\
&\quad - \frac{1}{2\,V_S^2}\int_{-\pi}^{\pi}\Big[\Big(\int_{-\pi}^{x_2} \varphi_{P,h}\, ds\Big)\,\overline{\psi_{S,h}} + \Big(\int_{-\pi}^{x_2} \overline{\psi_{P,h}}\, ds\Big)\,\varphi_{S,h}\Big]\, \mathrm{d}x_2, \\
a(\boldsymbol{\varphi}_h, \boldsymbol{\psi}_h) \;&=\; \int_{\Omega} (\nabla \varphi_{P,h} + \mathbf{curl}\, \varphi_{S,h}) \cdot (\nabla\, \overline{\psi_{P,h}} + \mathbf{curl}\, \overline{\psi_{S,h}}\,)\, \mathrm{d}\boldsymbol{x},
\end{aligned}$$

The spectral approximation used in direction x_2 allows to decouple the semi-discrete problem (7.31) as a family of $2\max\{L_P, L_S\} + 1$ problems in 1D that can be analysed separately. First, we will show how each 1D problem reads for those frequencies such that

$$\ell \in [-L, L]\backslash\{0\}, \quad \text{where} \quad L = \min\{L_P, L_S\}.$$

Then in Remark 7.17 we will point to the simplifications that occurs for the other frequencies. Let us consider for each frequency ℓ the respective unknown $\boldsymbol{\varphi}_h^{\ell} := (\varphi_{P,h}^{\ell}, \varphi_{S,h}^{\ell})$ and we choose

$$\boldsymbol{\psi}_h = e^{-\mathbb{i}\ell x_2}\, \boldsymbol{\psi}_h^{\ell}(x_1) \quad \text{with} \quad \boldsymbol{\psi}_h^{\ell} := (\psi_{P,h}^{\ell}, \psi_{S,h}^{\ell})$$

as test functions in (7.31). Therefore, using the orthogonality properties of trigonometric functions, we get that, for each $\ell \in [-L, L]$, $\boldsymbol{\varphi}_h^{\ell}(t) : \mathbb{R}^+ \mapsto V_{P,h}^{1\mathrm{D}} \times V_{S,h}^{1\mathrm{D}}$ satisfies the following 1D semi-discrete problem (completed with vanishing initial conditions $\boldsymbol{\varphi}_h^{\ell}(0) = \frac{\mathrm{d}}{\mathrm{d}t}\boldsymbol{\varphi}_h^{\ell}(0) = \mathbf{0}$)

$$\frac{d^2}{dt^2} m_{\ell}(\boldsymbol{\varphi}_h^{\ell}, \boldsymbol{\psi}_h^{\ell}) + a_{\ell}(\boldsymbol{\varphi}_h^{\ell}, \boldsymbol{\psi}_h^{\ell}) = \mathrm{g}_{\ell}(t, \boldsymbol{\psi}_h^{\ell}), \quad \forall \boldsymbol{\psi}_h^{\ell} \in V_{P,h}^{1\mathrm{D}} \times V_{S,h}^{1\mathrm{D}} \tag{7.44}$$

where $m_\ell(\cdot,\cdot) = m_{\ell,\Omega}(\cdot,\cdot) + m_{\ell,\Gamma}(\cdot,\cdot)$, $a_\ell(\cdot,\cdot) = a_{\ell,\Omega}(\cdot,\cdot) + a_{\ell,\Gamma}(\cdot,\cdot)$ and

$$\left\{\begin{array}{rcl} m_{\ell,\Omega}(\boldsymbol{\varphi}_h^\ell,\boldsymbol{\psi}_h^\ell) &=& \dfrac{1}{V_P^2}\displaystyle\int_{\mathbb{R}^+} \varphi_{P,h}^\ell \overline{\psi_{P,h}^\ell}\,\mathrm{d}x_1 + \dfrac{1}{V_S^2}\int_{\mathbb{R}^+} \varphi_{S,h}^\ell \overline{\psi_{S,h}^\ell}\,\mathrm{d}x_1, \\ m_{\ell,\Gamma}(\boldsymbol{\varphi}_h^\ell,\boldsymbol{\psi}_h^\ell) &=& \dfrac{\mathbb{i}}{2V_S^2\ell}\,\varphi_S^{\ell,0}\overline{\psi_P^{\ell,0}} - \dfrac{\mathbb{i}}{2V_S^2\ell}\,\varphi_P^{\ell,0}\overline{\psi_S^{\ell,0}}, \quad \ell \neq 0, \\ a_{\ell,\Omega}(\boldsymbol{\varphi}_h^\ell,\boldsymbol{\psi}_h^\ell) &=& \displaystyle\int_{\mathbb{R}^+} \ell^2 \varphi_{P,h}^\ell\,\overline{\psi_{P,h}^\ell}\,\mathrm{d}x_1 + \int_{\mathbb{R}^+} \partial_1\varphi_{P,h}^\ell\,\partial_1\overline{\psi_{P,h}^\ell}\,\mathrm{d}x_1 + \\ &+& \displaystyle\int_{\mathbb{R}^+} \ell^2 \varphi_{S,h}^\ell\,\overline{\psi_{S,h}^\ell}\,\mathrm{d}x_1 + \int_{\mathbb{R}^+} \partial_1\varphi_{S,h}^\ell\,\partial_1\overline{\psi_{S,h}^\ell}\,\mathrm{d}x_1, \\ a_{\ell,\Gamma}(\boldsymbol{\varphi}_h^\ell,\boldsymbol{\psi}_h^\ell) &=& \mathbb{i}\ell\,\varphi_S^{\ell,0}\overline{\psi_P^{\ell,0}} - \mathbb{i}\ell\,\varphi_P^{\ell,0}\overline{\psi_S^{\ell,0}}. \end{array}\right. \tag{7.45}$$

Remark 7.16

Let us remark that $a_\ell(\cdot,\cdot)$ can also be expressed by

$$\begin{aligned} a_\ell(\boldsymbol{\varphi}_h^\ell,\boldsymbol{\psi}_h^\ell) &= \int_{\mathbb{R}^+} (\partial_1\varphi_{P,h}^\ell - i\ell\,\varphi_{S,h}^\ell)(\partial_1\overline{\psi_{P,h}^\ell} + i\ell\,\overline{\psi_{S,h}^\ell})\,dx_1 \\ &+ \int_{\mathbb{R}^+} (\partial_1\varphi_{S,h}^\ell + i\ell\,\varphi_{P,h}^\ell)(\partial_1\overline{\psi_{S,h}^\ell} - i\ell\,\overline{\psi_{P,h}^\ell})\,dx_1. \end{aligned}$$

Thus we notice that $a_\ell(\boldsymbol{\varphi}_h^\ell,\boldsymbol{\varphi}_h^\ell) > 0$ for all $\boldsymbol{\varphi}_h^\ell \in (V_{P,h}^{1D} \times V_{S,h}^{1D}) \setminus \{\mathbf{0}\}$ since

$$a_\ell(\boldsymbol{\varphi}_h^\ell,\boldsymbol{\varphi}_h^\ell) = 0 \;\Rightarrow\; \left\{\begin{array}{rcl} \partial_1\varphi_{P,h}^\ell = i\ell\,\varphi_{S,h}^\ell & \Rightarrow & \varphi_{S,h}^\ell = cte \\ \partial_1\varphi_{S,h}^\ell = -i\ell\,\varphi_{P,h}^\ell & \Rightarrow & \varphi_{P,h}^\ell = cte \end{array}\right\} \;\Rightarrow\; \boldsymbol{\varphi}_h^\ell = \mathbf{0}.$$

Remark 7.17

Notice that problem (7.44) is simpler when $\ell = 0$ and also when $|\ell| > L = \min L_P, L_S$ since

- $\ell = 0 \implies \varphi_P^{0,0} = \varphi_S^{0,0} = 0$ *(see (7.43)), in such a way that the bilinear forms $m_{\ell,\Gamma}(\cdot,\cdot)$ and $a_{\ell,\Gamma}(\cdot,\cdot)$ vanish. Therefore, both potentials are decoupled for this frequency.*
- $|\ell| > L \implies$ *For $Q \in \{P,S\}$ such that $L_Q = L$, we have that $\varphi_{Q,h}^\ell = 0$ and the other potentials is thus decoupled.*

In consequence, the analysis on both cases is rather standard. Then in the following, we will focus on the more complex situation which corresponds to $\ell \in [-L,L]\backslash\{0\}$.

Note that in this context, since $\boldsymbol{\phi}_h^L \in \boldsymbol{V}_{0h}^L$, the gauge conditions are satisfied and the analogous to the algebraic system (7.33) reads as (completed with $\boldsymbol{\phi}_h^L(0) = \frac{\mathrm{d}}{\mathrm{d}t}\boldsymbol{\phi}_h^L(0) = \mathbf{0}$)

$$\mathbb{M}_h^L\,\frac{\mathrm{d}^2\boldsymbol{\phi}_h^L}{\mathrm{d}t^2} + \mathbb{A}_h^L\,\boldsymbol{\phi}_h^L = \boldsymbol{G}_h^L, \tag{7.46}$$

where $\mathbb{M}_h^L$ and $\mathbb{A}_h^L$ are no longer *matrices* but *operators* that possess an orthogonal decomposition of the form

$$\mathbb{M}_h^L = \bigoplus_\ell \mathbb{M}_{h,\ell} \quad \text{and} \quad \mathbb{A}_h^L = \bigoplus_\ell \mathbb{A}_{h,\ell} \tag{7.47}$$

where for each $\ell \in [-L, L]\backslash\{0\}$ we represent $\mathbb{M}_{h,\ell}$ and $\mathbb{A}_{h,\ell}$ both in $\mathcal{L}(V^{1\mathrm{D}}_{P,h} \times V^{1\mathrm{D}}_{S,h})$, by the following infinite matrices

$$\mathbb{M}_{h,\ell} := \begin{pmatrix} \frac{h_P}{V_P^2}\mathbb{M}_\Omega & \mathbb{M}^\ell_\Gamma \\ -\mathbb{M}^\ell_\Gamma & \frac{h_S}{V_S^2}\mathbb{M}_\Omega \end{pmatrix} \quad \text{and} \quad \mathbb{A}_{h,\ell} := \begin{pmatrix} \ell^2 h_P \mathbb{M}_\Omega + h_P^{-1}\mathbb{K}_\Omega & \mathbb{A}^\ell_\Gamma \\ -\mathbb{A}^\ell_\Gamma & \ell^2 h_S \mathbb{M}_\Omega + h_S^{-1}\mathbb{K}_\Omega \end{pmatrix}, \tag{7.48}$$

where on the one hand, the boundary matrices $\mathbb{M}^\ell_\Gamma$ and $\mathbb{A}^\ell_\Gamma$ are computed exactly

$$\mathbb{M}^\ell_\Gamma := \begin{pmatrix} \frac{\mathrm{i}}{2\,V_S^2\,\ell} & 0 & \dots \\ 0 & 0 & \dots \\ \vdots & \vdots & \ddots \end{pmatrix} \quad \text{and} \quad \mathbb{A}^\ell_\Gamma := \begin{pmatrix} \mathrm{i}\,\ell & 0 & \dots \\ 0 & 0 & \dots \\ \vdots & \vdots & \ddots \end{pmatrix},$$

as well as the volume matrix $\mathbb{K}_\Omega$ which is given by

$$\mathbb{K}_\Omega := \begin{pmatrix} 1 & -1 & 0 & \dots \\ -1 & 2 & -1 & \dots \\ 0 & -1 & 2 & \dots \\ \vdots & \vdots & \vdots & \ddots \end{pmatrix}.$$

While on the other hand, the volume matrix $\mathbb{M}_\Omega$ can be computed either using exact integration or considering for each $Q \in \{P, S\}$ the following quadrature formula which provides mass lumping,

$$\oint_Q \varphi_{Q,h}\,\overline{\psi_{Q,h}}\mathrm{d}x_1 := \frac{h_Q}{2}\varphi^0_Q\,\overline{\psi^0_Q} + h_Q \sum_{j=1}^{+\infty} \varphi^j_Q\,\overline{\psi^j_Q} \quad \text{and} \quad \|\varphi_{Q,h}\|^2_{Q,h} := \oint_Q |\varphi_{Q,h}|^2 \mathrm{d}x_1. \tag{7.49}$$

In the following, when mass lumping is considered we will denote $\widetilde{\mathbb{M}}_\Omega$ instead of $\mathbb{M}_\Omega$. Moreover notice that both matrices are given by

$$\mathbb{M}_\Omega := \frac{1}{6}\begin{pmatrix} 2 & 1 & 0 & \dots \\ 1 & 4 & 1 & \dots \\ 0 & 1 & 4 & \dots \\ \vdots & \vdots & \vdots & \ddots \end{pmatrix} \quad \text{and} \quad \widetilde{\mathbb{M}}_\Omega := \frac{1}{2}\begin{pmatrix} 1 & 0 & 0 & \dots \\ 0 & 2 & 0 & \dots \\ 0 & 0 & 2 & \dots \\ \vdots & \vdots & \vdots & \ddots \end{pmatrix}.$$

Similarly, when mass lumping is considered in (7.47) and (7.48), we will also denote $\widetilde{\mathbb{M}}^L_h$, $\widetilde{\mathbb{A}}^L_h$, $\widetilde{\mathbb{M}}_{h,\ell}$ and $\widetilde{\mathbb{A}}_{h,\ell}$ instead of $\mathbb{M}^L_h$, $\mathbb{A}^L_h$, $\mathbb{M}_{h,\ell}$ and $\mathbb{A}_{h,\ell}$.

Lemma 7.18

The quadrature formulas (7.49) that allows us to compute $\widetilde{\mathbb{M}}_\Omega$ getting mass lumping, adds positivity to the matrix $\mathbb{M}_\Omega$.

Proof. First of all, for any $\varphi_{Q,h} \in V^{1\mathrm{D}}_{Q,h}$ with $Q \in \{P, S\}$ we observe that

$$\varphi^*_{Q,h}\,\widetilde{\mathbb{M}}_\Omega\,\varphi_{Q,h} = \varphi^*_{Q,h}\,\mathbb{M}_\Omega\,\varphi_{Q,h} + \varphi^*_{Q,h}\,(\widetilde{\mathbb{M}}_\Omega - \mathbb{M}_\Omega)\,\varphi_{Q,h},$$

thus it is enough to guarantee that $\varphi^*_{Q,h}\,(\widetilde{\mathbb{M}}_\Omega - \mathbb{M}_\Omega)\,\varphi_{Q,h} \geq 0$ for all $\varphi_{Q,h} \in V^{1\mathrm{D}}_{Q,h}$. To do so, we first note

$$\begin{aligned} \varphi^*_{Q,h}\,(\widetilde{\mathbb{M}}_\Omega - \mathbb{M}_\Omega)\,\varphi_{Q,h} &= \frac{1}{6}|\varphi^0_{Q,h}|^2 + \frac{1}{3}\sum_{j=1}^{\infty}|\varphi^j_{Q,h}|^2 - \frac{1}{6}\overline{\varphi^0_{Q,h}}\varphi^1_{Q,h} - \frac{1}{6}\sum_{j=1}^{\infty}\overline{\varphi^j_{Q,h}}\big(\varphi^{j+1}_{Q,h} + \varphi^{j-1}_{Q,h}\big) \\ &= \frac{1}{6}|\varphi^0_{Q,h}|^2 + \frac{1}{3}\sum_{j=1}^{\infty}|\varphi^j_{Q,h}|^2 - \frac{1}{6}\sum_{j=0}^{\infty}\big(\overline{\varphi^j_{Q,h}}\varphi^{j+1}_{Q,h} + \overline{\varphi^{j+1}_{Q,h}}\varphi^j_{Q,h}\big). \end{aligned}$$

Now, we note that by straightforward computations

$$\begin{aligned}\overline{\varphi^j_{Q,h}}\varphi^{j+1}_{Q,h}+\overline{\varphi^{j+1}_{Q,h}}\varphi^j_{Q,h} &= 2\,\mathrm{Re}(\varphi^j_{Q,h})\mathrm{Re}(\varphi^{j+1}_{Q,h})+2\,\mathrm{Im}(\varphi^j_{Q,h})\mathrm{Im}(\varphi^{j+1}_{Q,h})\\ &\leq \mathrm{Re}(\varphi^j_{Q,h})^2+\mathrm{Re}(\varphi^{j+1}_{Q,h})^2+\mathrm{Im}(\varphi^j_{Q,h})^2+\mathrm{Im}(\varphi^{j+1}_{Q,h})^2\\ &= |\varphi^j_{Q,h}|^2+|\varphi^{j+1}_{Q,h}|^2.\end{aligned}$$

Hence, we obtain that

$$\varphi^*_{Q,h}\,(\widetilde{\mathbb{M}}_\Omega-\mathbb{M}_\Omega)\,\varphi_{Q,h} \;\geq\; \frac{1}{6}|\varphi^0_{Q,h}|^2+\frac{1}{3}\sum_{j=1}^{\infty}|\varphi^j_{Q,h}|^2-\frac{1}{6}\sum_{j=0}^{\infty}\big(|\varphi^j_{Q,h}|^2+|\varphi^{j+1}_{Q,h}|^2\big).$$

Finally, the proof is concluded just noticing that the term on the right hand side is actually zero. ■

In consequence it is straightforward to verify that on the one hand, for any $\boldsymbol{\varphi}_h\in V^{1\mathrm{D}}_{P,h}\times V^{1\mathrm{D}}_{S,h}$

$$\begin{aligned}\boldsymbol{\varphi}_h^*\,\widetilde{\mathbb{M}}_{h,\ell}\,\boldsymbol{\varphi}_h &= \boldsymbol{\varphi}_h^*\,\mathbb{M}_{h,\ell}\,\boldsymbol{\varphi}_h+\boldsymbol{\varphi}_h^*\,(\widetilde{\mathbb{M}}_{h,\ell}-\mathbb{M}_{h,\ell})\,\boldsymbol{\varphi}_h\\ &= \boldsymbol{\varphi}_h^*\,\mathbb{M}_{h,\ell}\,\boldsymbol{\varphi}_h+\sum_{Q\in\{P,S\}}\frac{h_Q}{V_Q^2}\,\varphi^*_{Q,h}\,(\widetilde{\mathbb{M}}_\Omega-\mathbb{M}_\Omega)\,\varphi_{Q,h}\geq\boldsymbol{\varphi}_h^*\,\mathbb{M}_{h,\ell}\,\boldsymbol{\varphi}_h,\end{aligned}\tag{7.50}$$

while on the other hand, for any $\boldsymbol{\varphi}_h\in V^{1\mathrm{D}}_{P,h}\times V^{1\mathrm{D}}_{S,h}$

$$\begin{aligned}\boldsymbol{\varphi}_h^*\,\widetilde{\mathbb{A}}_{h,\ell}\,\boldsymbol{\varphi}_h &= \boldsymbol{\varphi}_h^*\,\mathbb{A}_{h,\ell}\,\boldsymbol{\varphi}_h+\boldsymbol{\varphi}_h^*\,(\widetilde{\mathbb{A}}_{h,\ell}-\mathbb{A}_{h,\ell})\,\boldsymbol{\varphi}_h\\ &= \boldsymbol{\varphi}_h^*\,\mathbb{A}_{h,\ell}\,\boldsymbol{\varphi}_h+\ell^2\sum_{Q\in\{P,S\}}h_Q\,\varphi^*_{Q,h}\,(\widetilde{\mathbb{M}}_\Omega-\mathbb{M}_\Omega)\,\varphi_{Q,h}\geq\boldsymbol{\varphi}_h^*\,\mathbb{A}_{h,\ell}\,\boldsymbol{\varphi}_h.\end{aligned}\tag{7.51}$$

Notice that (7.51) guarantees that $\widetilde{\mathbb{A}}_{h,\ell}$ is positive definite since $\mathbb{A}_{h,\ell}$ is positive definite according to Remark 7.16. However (7.50) is not enough to guarantee the positivity of $\widetilde{\mathbb{M}}_{h,\ell}$ (nor $\mathbb{M}_{h,\ell}$ due to (7.50)). Next, we investigate this question by analysing the sign of the eigenvalues λ of $\widetilde{\mathbb{M}}_{h,\ell}$. Note then, that any eigenpair $(\lambda,\boldsymbol{\varphi})$ with $\boldsymbol{\varphi}\neq\mathbf{0}$ must satisfy $\widetilde{\mathbb{M}}_{h,\ell}\,\boldsymbol{\varphi}=\lambda\,\boldsymbol{\varphi}$, or equivalently

$$\begin{aligned}&(\frac{h_P}{2\,V_P^2}-\lambda)\varphi^0_P+\frac{\mathbb{i}}{2\,V_S^2\,\ell}\varphi^0_S=0, &&(\frac{h_S}{2\,V_S^2}-\lambda)\varphi^0_S-\frac{\mathbb{i}}{2\,V_S^2\,\ell}\varphi^0_P=0,\\ &(\frac{h_P}{V_P}-\lambda)\varphi^j_P=0,\quad\text{for } j>0, &&(\frac{h_S}{V_S}-\lambda)\varphi^j_S=0,\quad\text{for } j>0.\end{aligned}$$

This is possible if $\varphi^0_P=\varphi^0_S=0$ and $\lambda=\frac{h_Q}{V_Q^2}>0$ for $Q\in\{P,S\}$, or if $\varphi^j_P=\varphi^j_S=0$ for all $j>0$ and

$$\begin{pmatrix}\frac{h_P}{2V_P^2}-\lambda & \frac{\mathbb{i}}{2V_S^2\ell}\\ -\frac{\mathbb{i}}{2V_S^2\ell} & \frac{h_S}{2V_S^2}-\lambda\end{pmatrix}\begin{pmatrix}\varphi^0_P\\ \varphi^0_S\end{pmatrix}=\begin{pmatrix}0\\0\end{pmatrix},\quad\text{with}\quad(\varphi^0_P,\varphi^0_S)\neq(0,0).$$

Thus λ must satisfy

$$\det\begin{pmatrix}\frac{h_P}{2V_P^2}-\lambda & \frac{\mathbb{i}}{2V_S^2\ell}\\ -\frac{\mathbb{i}}{2V_S^2\ell} & \frac{h_S}{2V_S^2}-\lambda\end{pmatrix}=\lambda^2-\frac{\lambda}{2}(\frac{h_P}{V_P^2}+\frac{h_S}{V_S^2})+\frac{h_P\,h_S}{4V_P^2V_S^2}-\frac{1}{4V_S^4\ell^2}=0.$$

This gives two different eigenvalues that we choose to denote by

$$\lambda_\pm=\frac{1}{4}(\frac{h_P}{V_P^2}+\frac{h_S}{V_S^2})\pm\frac{1}{2}\sqrt{\frac{1}{4}(\frac{h_P}{V_P^2}+\frac{h_S}{V_S^2})^2-\frac{h_P\,h_S}{V_P^2V_S^2}+\frac{1}{V_S^4\ell^2}}.$$

Consequently, as $\left(\frac{h_P}{V_P^2}+\frac{h_S}{V_S^2}\right)$ is positive, then λ_+ must be positive, while the sign of λ_- will depend on the sign$\left(\frac{h_P\,h_S}{V_P^2 V_S^2}-\frac{1}{V_S^4\ell^2}\right)$:

$$\begin{cases} \lambda_- > 0 \Longleftrightarrow \ell^2 h_P\,h_S > \dfrac{V_P^2}{V_S^2} \quad (\widetilde{\mathbb{M}}_\ell \text{ positive definite}), & (7.52a)\\ \lambda_- = 0 \Longleftrightarrow \ell^2 h_P\,h_S = \dfrac{V_P^2}{V_S^2} \quad (\widetilde{\mathbb{M}}_\ell \text{ positive but singular}), & (7.52b)\\ \lambda_- < 0 \Longleftrightarrow \ell^2 h_P\,h_S < \dfrac{V_P^2}{V_S^2} \quad (\widetilde{\mathbb{M}}_\ell \text{ negative in a 1D eigenspace}). & (7.52c) \end{cases}$$

Remark 7.19

Notice that according to (7.52b), *the operator* $\widetilde{\mathbb{M}}_h^L$ *is singular if and only if*

$$\frac{V_P}{V_S}\Big(\frac{1}{h_P\,h_S}\Big)^{\frac{1}{2}} \in \{1,\ldots,L\}.$$

Moreover, according to (7.52c), *the operator* $\widetilde{\mathbb{M}}_h^L$ *is negative in a subspace of dimension* $2\left\lfloor \frac{V_P}{V_S}\left(\frac{1}{h_P\,h_S}\right)^{\frac{1}{2}}\right\rfloor$ *and since* $V_P/V_S > \sqrt{2}$, *we observe that for reasonable values of the discretization parameters, for instance* $h_P\,h_S < 2$, *the negative subspace will always have dimension greater than one.*

This property can be understood as the analogous of Theorem 7.12 and as it was the case for problem (7.33), it is the cause of severe instabilities of semi-discrete problem (7.46).

Next, as we did in Section 7.2.3 for the general problem (7.33), we illustrate via numerical simulations, the blow-up of the solution of problem (7.46). For this simulation we use the following parameters

$$\rho = 1, \quad \lambda = 20, \quad \mu = 4, \quad L_P = L_S = 60, \quad \text{and} \quad h_P = h_S = \frac{\pi}{200}$$

and a source term located close to the boundary. Concerning the time discretization, we have considered the standard leap frog scheme, which ensures a finite propagation velocity in the direction x_1. Moreover, we have chosen a bounded domain in the direction x_1 by truncating the domain at $x_1 = x_{1,max}$ in such a way that the numerical solution does not reach the boundary $x_1 = x_{1,max}$ before the final time T of the computation. Then in Figure 7.11 we plot snapshots of the solution obtained at three different simulation times. These results illustrate the bad behaviour of the semi-discrete problem since one can observe blow-up of the solution that is initiated, as expected, close to the boundary but propagates inside the computational domain as t increases (the colour scale is saturated at the boundary). In Section 7.2.3, the instabilities of problem (7.33) were linked to the existence of strictly negative eigenvalues for the eigenvalue problem (7.37), now we make the analogous to analyse problem (7.46) by analysing problem (7.44) for each frequency ℓ (actually the associated eigenvalue problem). The advantage is that in this simplified configuration the eigenvalue problem derived for each frequency can be analysed in more detail. Thus, in next paragraph, we investigate the instabilities of problem (7.46) by looking to each specific frequency.

7.3.2 Detailed analysis of the associated eigenvalue problem

The stability of the problem (7.46) is related (as it was explained in Section 7.2.3 for problem (7.33)) to the existence of negative eigenvalues for the generalised eigenvalue problem associated to the stiffness matrix ($\mathbb{A}_h^L$ or $\widetilde{\mathbb{A}}_h^L$) and the mass matrix ($\mathbb{M}_h^L$ or $\widetilde{\mathbb{M}}_h^L$). In this section our aim is to analyse this question independently for each frequency ℓ, i.e. we investigate the existence of negative eigenvalues for the generalised eigenvalue problem associated to the stiffness matrix ($\mathbb{A}_{h,\ell}$ or $\widetilde{\mathbb{A}}_{h,\ell}$) and the mass matrix ($\mathbb{M}_{h,\ell}$ or $\widetilde{\mathbb{M}}_{h,\ell}$). In this context, the stiffness matrix is always positive

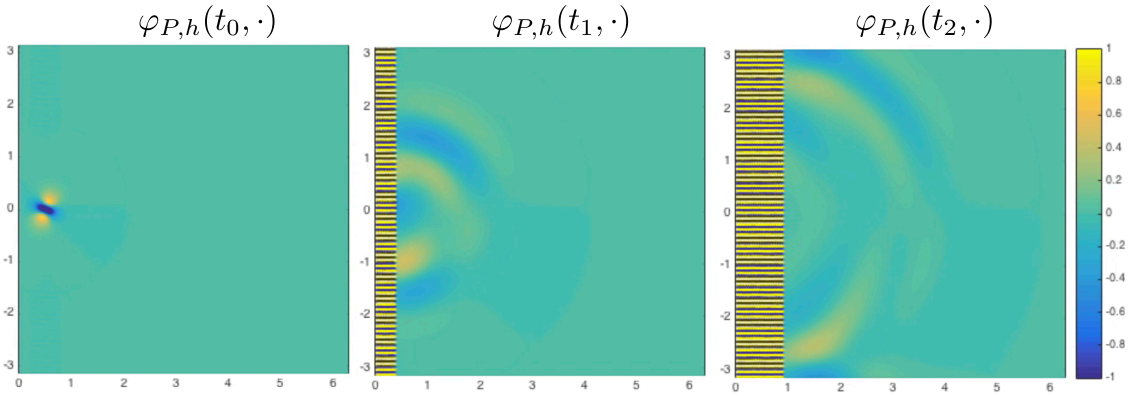

Figure 7.11: Snapshots at three different times of $\varphi_{P,h}$.

definite (see Remark 7.16 for $\mathbb{A}_{h,\ell}$ and (7.51) for $\widetilde{\mathbb{A}}_{h,\ell}$), while for reasonable space discretization such that $\ell^2 h_P\, h_S < V_P^2/V_S^2$, the mass matrix is proved to be negative in a eigenspace of dimension one (see (7.52c)).

Remark 7.20

In consequence, we expect that the mentioned generalised eigenvalue problem has one and only one negative eigenvalue. Due to the consideration of infinite dimensional matrices, the verification of this is technical and remains open. However, we conjecture that the result holds and we will use it in the forthcoming analysis.

For instance the result holds for any finite matrices, $\mathbb{A}$ positive definite, and $\mathbb{M}$ invertible and negative in an eigenspace of dimension one. On the one hand, we denote by $(\mu_j, \boldsymbol{\psi}_j)$ all the eigenpairs of the matrix $\mathbb{M}$ and let us assume that $\mu_1 < 0$ while $\mu_j > 0$ for all $j > 0$. On the other hand, we also denote by $(\lambda_j, \boldsymbol{\varphi}_j)$ all the solutions of problem:

$$\text{Find } \boldsymbol{\varphi} \neq 0 \text{ and } \lambda \in \mathbb{R} \quad \text{such that} \quad \mathbb{A}\,\boldsymbol{\varphi} = \lambda\,\mathbb{M}\,\boldsymbol{\varphi}.$$

It is known that $\{\boldsymbol{\psi}_j\}_{j=1}^N$ and $\{\boldsymbol{\varphi}_j\}_{j=1}^N$ are basis of $\mathbb{R}^N$ such that

$$\boldsymbol{\psi}_j^*\,\mathbb{M}\,\boldsymbol{\psi}_k = \delta_{jk}\mu_j \quad \text{and} \quad \boldsymbol{\varphi}_j^*\,\mathbb{M}\,\boldsymbol{\varphi}_k = \delta_{jk}/\lambda_j \quad \text{for } j,k \in \{1,\dots,N\}.$$

Therefore, there exist coefficients α_j such that

$$\boldsymbol{\psi}_1 = \sum_{j=1}^N \alpha_j \boldsymbol{\varphi}_j \quad \text{and} \quad \mu_1 = \boldsymbol{\psi}_1^*\,\mathbb{M}\,\boldsymbol{\psi}_1 = \sum_{j=1}^N \alpha_j^2\,\boldsymbol{\varphi}_j^*\,\mathbb{M}\,\boldsymbol{\varphi}_j = \sum_{j=1}^N \frac{\alpha_j^2}{\lambda_j}.$$

In consequence, since $\mu_1 < 0$, it must exist at least one eigenpair, let us say (λ_1, φ_1), such that $\lambda_1 < 0$. Next, we assume that there exist another eigenpair, let us say (λ_2, φ_2), such that $\lambda_2 < 0$. Then we notice that it is possible to write for $\beta_1 \neq 0$ and $\beta_2 \neq 0$

$$\varphi_1 = \beta_1\psi_1 + \varphi_1^\perp \quad \text{and} \quad \varphi_2 = \beta_2\psi_1 + \varphi_2^\perp \quad \text{where} \quad \varphi_1^\perp, \varphi_2^\perp \in \operatorname{span}\{\psi_2,\dots,\psi_N\}.$$

Now, we note that $\widehat{\varphi} := \beta_2\varphi_1 - \beta_1\varphi_2 = \beta_2\varphi_1^\perp - \beta_1\varphi_2^\perp \in \operatorname{span}\{\psi_2,\dots,\psi_N\}$ where $\mathbb{M}$ is positive. Therefore

$$\begin{aligned} 0 \leq \widehat{\varphi}^*\mathbb{M}\widehat{\varphi} &= (\beta_2\varphi_1 - \beta_1\varphi_2)^*\mathbb{M}(\beta_2\varphi_1 - \beta_1\varphi_2) \\ &= \beta_2^2\varphi_1^*\mathbb{M}\varphi_1 + \beta_1^2\varphi_2^*\mathbb{M}\varphi_2 \\ &= \frac{\beta_2^2}{\lambda_1} + \frac{\beta_1^2}{\lambda_2} < 0 \end{aligned}$$

which is a contradiction.

On the following we study in more detail the generalised eigenvalue problem associated to each frequency ℓ when using mass lamping. More precisely, we study the existence of negative eigenvalues for each 1D eigenvalue problem of the form

$$\text{Find } \boldsymbol{\varphi} \neq 0 \text{ and } \lambda \in \mathbb{R} \quad \text{such that} \quad \widetilde{\mathbb{A}}_{h,\ell}\, \boldsymbol{\varphi} = \lambda\, \widetilde{\mathbb{M}}_{h,\ell}\, \boldsymbol{\varphi}. \tag{7.53}$$

Note that, as $\widetilde{\mathbb{M}}_{h,\ell}$ and $\widetilde{\mathbb{A}}_{h,\ell}$ are Hermitian, every eigenvalue λ is necessarily real. Moreover, λ and its respective eigenfunction $\boldsymbol{\varphi}$ must satisfy the following system of equations

$$\left\{ \begin{aligned} &\Big(\frac{1}{h_P} + \frac{h_P}{2}(\ell^2 - \frac{\lambda}{V_P^2})\Big)\varphi_P^0 - \frac{1}{h_P}\varphi_P^1 + \mathbb{i}\big(\ell - \frac{\lambda}{2\,V_S^2\,\ell}\big)\varphi_S^0 = 0, && (7.54a)\\ &\qquad -\frac{\varphi_P^{j-1} - 2\varphi_P^j + \varphi_P^{j+1}}{h_P^2} + \ell^2\varphi_P^j = \frac{\lambda}{V_P^2}\varphi_P^j, \quad \text{for } j > 0, && (7.54b)\\ &\Big(\frac{1}{h_S} + \frac{h_S}{2}(\ell^2 - \frac{\lambda}{V_S^2})\Big)\varphi_S^0 - \frac{1}{h_S}\varphi_S^1 - \mathbb{i}\big(\ell - \frac{\lambda}{2\,V_S^2\,\ell}\big)\varphi_P^0 = 0, && (7.54c)\\ &\qquad -\frac{\varphi_S^{j-1} - 2\varphi_S^j + \varphi_S^{j+1}}{h_S^2} + \ell^2\varphi_S^j = \frac{\lambda}{V_S^2}\varphi_S^j, \quad \text{for } j > 0. && (7.54d) \end{aligned}\right.$$

It is classical that the solutions of these two coupled homogeneous linear recurrence relations with constant coefficients are expressed as

$$\varphi_P^j = C_P^+ (z_P^+)^j + C_P^- (z_P^-)^j \quad \text{and} \quad \varphi_S^j = C_S^+ (z_S^+)^j + C_S^- (z_S^-)^j,$$

where $C_Q^+, C_Q^- \in \mathbb{R}$ for $Q \in \{P,S\}$ and z_Q^+, z_Q^- for $Q \in \{P,S\}$ are the roots of the characteristic polynomials

$$-\frac{(z_Q - 1)^2}{h_Q^2} + (\ell^2 - \frac{\lambda}{V_Q^2}) z_Q = 0, \quad \text{for } Q \in \{P,S\}.$$

Therefore

$$\begin{aligned} z_Q^\pm &= 1 + \frac{h_Q^2}{2}(\ell^2 - \frac{\lambda}{V_Q^2}) \pm \frac{1}{2}\sqrt{\big(2 + h_Q^2(\ell^2 - \frac{\lambda}{V_Q^2})\big)^2 - 4}\\ &= 1 + \frac{h_Q^2}{2}(\ell^2 - \frac{\lambda}{V_Q^2}) \pm \frac{1}{2}\sqrt{\big(h_Q^2(\ell^2 - \frac{\lambda}{V_Q^2})\big)^2 + 4\,h_Q^2(\ell^2 - \frac{\lambda}{V_Q^2})}, \quad \text{for } Q \in \{P,S\}. \end{aligned}$$

Now, we divide the analysis in three cases:
- First, we consider for $Q = P$ or $Q = S$ that

$$\big(2 + h_Q^2(\ell^2 - \frac{\lambda}{V_Q^2})\big)^2 - 4 = 0,$$

or equivalently $\lambda = \ell^2\, V_Q^2$ or $\lambda = V_Q^2(\ell^2 + 4/h_Q^2)$. In this case $z_Q^+ = z_Q^-$, and as $z_Q^+ z_Q^- = 1$, we deduce that $z_Q^+ = z_Q^- = 1$. In consequence, $C_Q^+ = C_Q^- = 0$ because $\boldsymbol{\varphi} \in H^1(\mathbb{R}^+, \mathbb{C})$ and therefore, the eigenpair $(\lambda, \boldsymbol{\varphi})$ is not solution of (7.53).
- Second, we consider for $Q = P$ or $Q = S$ that

$$\big(2 + h_Q^2(\ell^2 - \frac{\lambda}{V_Q^2})\big)^2 - 4 < 0,$$

or equivalently $\ell^2\, V_Q^2 \leq \lambda \leq V_Q^2(\ell^2 + 4/h_Q^2)$. In this case $z_Q^+, z_Q^- \notin \mathbb{R}$, $z_Q^+ = \overline{z_Q^-}$ and $z_Q^+ z_Q^- = 1$. Then we deduce that $|z_Q^+| = |z_Q^-| = 1$. In consequence, $C_Q^+ = C_Q^- = 0$ because $\boldsymbol{\varphi} \in H^1(\mathbb{R}^+, \mathbb{C})$ and therefore the pair $(\lambda, \boldsymbol{\varphi})$ is not solution of (7.53).

• Finally, the remaining cases are that for $Q = P$ and $Q = S$

$$\big(2 + h_Q^2(\ell^2 - \frac{\lambda}{V_Q^2})\big)^2 - 4 > 0,$$

or equivalently $\lambda < \ell^2 V_S^2 < \ell^2 V_P^2$ or $\lambda > V_P^2(\ell^2 + 4/h_Q^2) > V_S^2(\ell^2 + 4/h_Q^2)$. In both cases $z_Q^+, z_Q^- \in \mathbb{R}$ and $z_Q^+ z_Q^- = 1$ for $Q = P$ and $Q = S$ and moreover we notice that for both $Q \in \{P, S\}$:
∘ If $\lambda < \ell^2 V_S^2$, then $z_Q^+ > 1$ and as $\boldsymbol{\varphi} \in H^1(\mathbb{R}^+, \mathbb{C})$ we can set $C_Q^+ = 0$.
∘ If $\lambda > V_P^2(\ell^2 + 4/h_Q^2)$, then $z_Q^- < -1$ and as $\boldsymbol{\varphi} \in H^1(\mathbb{R}^+, \mathbb{C})$ we can set $C_Q^- = 0$. Consequently, for both $Q = P$ and $Q = S$ we can express

$$\varphi_P^j = C_P^{\pm}(z_P^{\pm})^j \qquad \text{and} \qquad \varphi_S^j = C_S^{\pm}(z_S^{\pm})^j,$$

where the notation $\pm$ is introduce to handle the sign dependence and it is worthy to notice that this sign should be chosen equal for both φ_P and φ_S. Next, we introduce the previous expression of $\boldsymbol{\varphi}$ into the coupling conditions (7.54a) and (7.54c) to obtain the system

$$\begin{aligned}
(\frac{1}{h_P} + \frac{h_P}{2}(\ell^2 - \frac{\lambda}{V_P^2}) - \frac{z_P^{\pm}}{h_P})C_P^{\pm} + \mathbb{i}(\ell - \frac{\lambda}{2\,V_S^2\ell})C_S^{\pm} = 0,\\
(\frac{1}{h_S} + \frac{h_S}{2}(\ell^2 - \frac{\lambda}{V_S^2}) - \frac{z_S^{\pm}}{h_S})C_S^{\pm} - \mathbb{i}(\ell - \frac{\lambda}{2\,V_S^2\ell})C_P^{\pm} = 0,
\end{aligned}$$

which, by introduction of $z_P^{\pm}$, $z_S^{\pm}$ can be rewritten as:

$$\begin{aligned}
\pm\sqrt{h_P^2(\ell^2 - \frac{\lambda}{V_P^2})^2 + 4(\ell^2 - \frac{\lambda}{V_P^2})}\ \frac{C_P^{\pm}}{2} + \mathbb{i}(\ell - \frac{\lambda}{2\,V_S^2\ell})C_S^{\pm} = 0,\\
\pm\sqrt{h_S^2(\ell^2 - \frac{\lambda}{V_S^2})^2 + 4(\ell^2 - \frac{\lambda}{V_S^2})}\ \frac{C_S^{\pm}}{2} - \mathbb{i}(\ell - \frac{\lambda}{2\,V_S^2\ell})C_P^{\pm} = 0.
\end{aligned}$$

Since the system should have no trivial solution λ is such that the system is singular. Then the following equality must hold:

$$(\ell - \frac{\lambda}{2\,V_S^2\ell})^2 = \frac{1}{4}\sqrt{h_P^2(\ell^2 - \frac{\lambda}{V_P^2})^2 + 4(\ell^2 - \frac{\lambda}{V_P^2})}\sqrt{h_S^2(\ell^2 - \frac{\lambda}{V_S^2})^2 + 4(\ell^2 - \frac{\lambda}{V_S^2})}.$$

Moreover, the solutions of the previous equation, must be also solution of

$$(\ell - \frac{\lambda}{2\,V_S^2\ell})^4 = \frac{1}{16}\left(h_P^2(\ell^2 - \frac{\lambda}{V_P^2})^2 + 4(\ell^2 - \frac{\lambda}{V_P^2})\right)\left(h_S^2(\ell^2 - \frac{\lambda}{V_S^2})^2 + 4(\ell^2 - \frac{\lambda}{V_S^2})\right). \tag{7.55}$$

However, it is worthy to notice, that when solving the previous equation, we are also finding the solutions of

$$(\ell - \frac{\lambda}{2\,V_S^2\ell})^2 = -\frac{1}{4}\sqrt{h_P^2(\ell^2 - \frac{\lambda}{V_P^2})^2 + 4(\ell^2 - \frac{\lambda}{V_P^2})}\sqrt{h_S^2(\ell^2 - \frac{\lambda}{V_S^2})^2 + 4(\ell^2 - \frac{\lambda}{V_S^2})},$$

which are not of our interest. Fortunately, those solutions can be easily distinguished due to

$$(\ell - \frac{\lambda}{2\,V_S^2\ell})^2 < 0 \quad \Leftrightarrow \quad \mathrm{Im}(\ell - \frac{\lambda}{2\,V_S^2\ell}) \neq 0 \quad \Leftrightarrow \quad \mathrm{Im}(\lambda) \neq 0.$$

Therefore, we look for real solutions of equation (7.55), which by straightforward computations must be the real roots of the polynomial

$$p(\lambda) = a_4\lambda^4 + a_3\lambda^3 + a_2\lambda^2 + a_1\lambda + a_0 \tag{7.56}$$

with coefficients

$$
\begin{aligned}
a_4 &= -\frac{1}{\ell^4 V_S^8} + \frac{h_P^2\, h_S^2}{V_P^4 V_S^4} \\
a_3 &= \frac{8}{\ell^2 V_S^6} - \frac{2\,\ell^2 h_P^2\, h_S^2}{V_P^2 V_S^2}(\frac{1}{V_P^2} + \frac{1}{V_S^2}) - \frac{4}{V_P^2 V_S^2}(\frac{h_P^2}{V_P^2} + \frac{h_S^2}{V_S^2}) \\
a_2 &= -\frac{24}{V_S^4} + \frac{2\,\ell^4 h_P^2\, h_S^2 + 4\,\ell^2(h_P^2 + h_S^2) + 16}{V_P^2 V_S^2} \\
&\quad + \ell^4 h_P^2\, h_S^2(\frac{1}{V_P^2} + \frac{1}{V_S^2})^2 + 4\,\ell^2(\frac{h_P^2}{V_P^2} + \frac{h_S^2}{V_S^2})(\frac{1}{V_P^2} + \frac{1}{V_S^2}) \\
a_1 &= \frac{32\,\ell^2}{V_S^2} - (2\,\ell^6 h_P^2\, h_S^2 + 4\,\ell^4(h_P^2 + h_S^2) + 16\,\ell^2)(\frac{1}{V_P^2} + \frac{1}{V_S^2}) - 4\,\ell^4(\frac{h_P^2}{V_P^2} + \frac{h_S^2}{V_S^2}) \\
a_0 &= \ell^8 h_P^2\, h_S^2 + 4\,\ell^6(h_P^2 + h_S^2).
\end{aligned}
\tag{7.57}
$$

Now we recall that the product of the roots of a monic polynomial is related to its independent term. Therefore, we consider the two following cases to express (7.56) as a monic polynomial.

• First, we consider $a_4 = 0$ (equivalently $\ell^2 h_P\, h_S = V_P^2/V_S^2$). In that case, polynomial (7.56) has three roots, $p^{-1}(0) = \{\lambda_1, \lambda_2, \lambda_3\}$, such that

$$\lambda_1\, \lambda_2\, \lambda_3 = -\frac{a_0}{a_3}.$$

Notice now that $a_0 > 0$ while introducing $\ell^2 h_P\, h_S = V_P^2/V_S^2$ into the leading term

$$\frac{a_3}{h_P\, h_S} = \frac{8}{V_P^2 V_S^4} - \frac{2\frac{V_P^2}{V_S^2}}{V_P^2 V_S^2}(\frac{1}{V_P^2} + \frac{1}{V_S^2}) - \frac{4}{V_P^2 V_S^2}(\frac{1}{V_P^2 h_S^2} + \frac{1}{V_S^2 h_P^2}).$$

Therefore recalling that $V_P^2/V_S^2 > 2$ and considering $h_* = \max\{h_P, h_S\}$ we deduce

$$\frac{a_3}{h_P\, h_S} < \frac{8}{V_P^2 V_S^4} - \frac{4\frac{V_P^2}{V_S^2} + \frac{8}{h_*}}{V_P^4 V_S^2} < 0. \tag{7.58}$$

Then we can conclude that in this case there is **no negative eigenvalue**, because their product must be positive and we are assuming that at most there is one negative eigenvalue.

• Second, we consider $a_4 \neq 0$ (equivalently $\ell^2 h_P h_S \neq V_P^2/V_S^2$). In that case, polynomial (7.56) has four roots $p^{-1}(0) = \{\lambda_1, \lambda_2, \lambda_3, \lambda_4\}$ such that

$$\lambda_1\, \lambda_2\, \lambda_3\, \lambda_4 = \frac{a_0}{a_4}.$$

Therefore, noticing again that $a_0 > 0$, it is clear that

$$\mathrm{sign}(\lambda_1\, \lambda_2\, \lambda_3\, \lambda_4) = \mathrm{sign}(-\frac{1}{\ell^4 V_S^8} + \frac{h_P^2\, h_S^2}{V_P^4 V_S^4}) = \mathrm{sign}(\frac{\ell^4 h_P^2\, h_S^2 V_S^4 - V_P^4}{\ell^4 V_S^8 V_P^4}),$$

which implies (notice that $\ell^2 h_P\, h_S \neq V_P^2/V_S^2$)

$$
\begin{aligned}
\lambda_1\, \lambda_2\, \lambda_3\, \lambda_4 > 0 \quad &\Leftrightarrow \quad h_P^2\, h_S^2 V_S^4 \ell^4 - V_P^4 > 0 \quad \Leftrightarrow \quad \ell^2 h_P\, h_S > V_P^2/V_S^2, \\
\lambda_1\, \lambda_2\, \lambda_3\, \lambda_4 < 0 \quad &\Leftrightarrow \quad h_P^2\, h_S^2 V_S^4 \ell^4 - V_P^4 < 0 \quad \Leftrightarrow \quad \ell^2 h_P\, h_S < V_P^2/V_S^2.
\end{aligned}
$$

Therefore, due to the conjecture that there is at most one negative eigenvalue:

∘ $\ell^2 h_P\, h_S > V_P^2/V_S^2$ implies that there is **no negative eigenvalue**.

∘ $\ell^2 h_P\, h_S < V_P^2/V_S^2$ implies that there is **one negative eigenvalue**.

It is interesting to notice that this analysis of stability is totally consistent with conclusions (7.52) about the sign of $\widetilde{\mathbb{M}}_\ell$. Finally, we recall that (property of any monic polynomial of order four)

$$\lambda_1 + \lambda_2 + \lambda_3 + \lambda_4 = -\frac{a_3}{a_4}.$$

Then, taking into account (7.58) and the change of sign of a_4 is clear that

$$\lim_{\ell^2 h_P\, h_S \to \frac{V_P^2}{V_S^2}^+} (\lambda_1 + \lambda_2 + \lambda_3 + \lambda_4) = +\infty,$$
$$\lim_{\ell^2 h_P\, h_S \to \frac{V_P^2}{V_S^2}^-} (\lambda_1 + \lambda_2 + \lambda_3 + \lambda_4) = -\infty,$$

and we conclude when $\ell^2 h_P\, h_S < V_P^2/V_S^2$, that the unique negative eigenvalue tends to $-\infty$ when $\ell^2 h_P\, h_S$ tends to V_P^2/V_S^2. To illustrate this behave, we consider $V_P^2 = 28$ and $V_S^2 = 4$ and then we plot in Figure 7.12 the real roots of polynomial (7.56) with coefficients (7.57). On the left respect to $h = h_P = h_S$ for the frequency $\ell = 1$ and on the right respect to ℓ when $h = h_P = h_S = 0.1$.

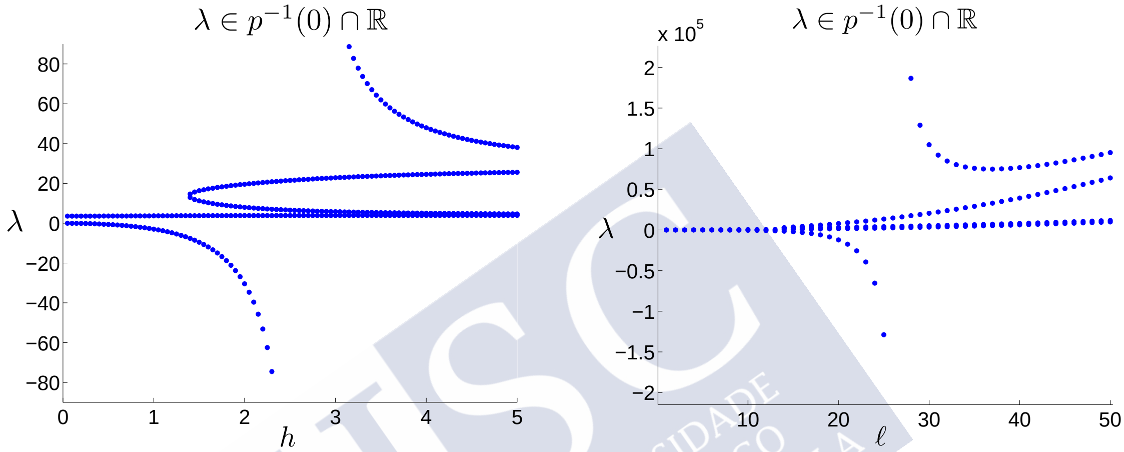

Figure 7.12: Real roots of polynomial (7.56) with coefficients (7.57), for different values of ℓ and h. On the left $\ell = 1$. On the right $h = 0.1$.

In the next section, we analyse how this analysis affects to the stability of the 2D semi-discrete problem (7.46) presented in Section 7.3.1.

7.3.3 Impact on the stability of the semi-discrete problem

When solving the 2D eigenvalue problem associated to the stiffness matrix ($\mathbb{A}_h^L$ or $\widetilde{\mathbb{A}}_h^L$) and the mass matrix ($\mathbb{M}_h^L$ or $\widetilde{\mathbb{M}}_h^L$), attending to the previous analysis, we should obtain $\min\{2L, 2\lfloor \dfrac{V_P}{h_P\, h_S V_S} \rfloor\}$ negative eigenvalues. One for each frequency we solve until we reach the "threshold" value $\ell^2 h_P\, h_S = V_P^2/V_S^2$. Moreover, we know that the most negative of those eigenvalues is the one associated to the higher $\ell^2 h_P\, h_S < V_P^2/V_S^2$. Therefore, it is worthy to consider the case when the space steps are proportional to the range of frequencies, for instance we will consider for each $Q \in \{P, S\}$ the space step $h_Q = \dfrac{C_Q}{L_Q}$ where the constants are fixed to satisfy $C_P\, C_S < \dfrac{V_P^2}{V_S^2}$. On that case,

$$L^2 h_P\, h_S \le L_P\, L_S\, h_P\, h_S = C_P\, C_S < \frac{V_P^2}{V_S^2}$$

and when L increases its value by one (consequently $h_Q = \frac{C_Q}{L+1}$ for at least one $Q \in \{P, S\}$ or possibly both if $L_P = L_S$), we accept the new frequencies $L + 1$ and $-(L + 1)$ that provide two new negative eigenvalues. We are interested on the asymptotic behaviour of those new eigenvalues when L tends to infinity (consequently h_P and h_S tend to zero), so we consider $\ell = L$ ($\ell = -L$ is analogous) and study the roots of polynomial (7.56). In the following, to simplify computations we will make two assumptions that are completely justified:

- First, based on the physics of the problem we make the natural choice of $L = L_P$. However, the case $L = L_S$ should be analogous.
- Second, to refine proportionally each type of wave, we fix the ratio between the range of frequencies that we accept for each wave, this is $L_P/L_S = C_L$.

Under such assumptions the coefficients of polynomial (7.56) reduce to:

$$
\begin{aligned}
a_4 &= -\frac{1}{L^4 V_S^8} + \frac{C_L^2\, C_P^2\, C_S^2}{L^4\, V_P^4\, V_S^4} \\
a_3 &= \frac{8}{L^2\, V_S^6} - \frac{2\, C_L^2\, C_P^2\, C_S^2}{L^2\, V_P^2\, V_S^2}(\frac{1}{V_P^2} + \frac{1}{V_S^2}) - \frac{4}{L^2\, V_P^2\, V_S^2}(\frac{C_P^2}{V_P^2} + \frac{C_L^2\, C_S^2}{V_S^2}) \\
a_2 &= -\frac{24}{V_S^4} + \frac{2\, C_L^2\, C_P^2\, C_S^2 + 4\, C_P^2 + 4\, C_L^2\, C_S^2 + 16}{V_P^2\, V_S^2} + C_L^2\, C_P^2\, C_S^2(\frac{1}{V_P^2} + \frac{1}{V_S^2})^2 \\
&\quad +4\,(\frac{C_P^2}{V_P^2} + \frac{C_L^2\, C_S^2}{V_S^2})(\frac{1}{V_P^2} + \frac{1}{V_S^2}) \\
a_1 &= \frac{32\, L^2}{V_S^2} - 2\, L^2(C_L^2\, C_P^2\, C_S^2 + 2\,(C_P^2 + C_L^2\, C_S^2) + 8)(\frac{1}{V_P^2} + \frac{1}{V_S^2}) \\
&\quad -4\, L^2(\frac{C_P^2}{V_P^2} + \frac{C_L^2\, C_S^2}{V_S^2}) \\
a_0 &= L^4\, C_L^2\, C_P^2\, C_S^2 + 4\, L^4(C_P^2 + C_L^2\, C_S^2).
\end{aligned}
\tag{7.59}
$$

Then, if we introduce the auxiliary variable $\tilde{\lambda} = \lambda/L^2$ and look for the solutions of $L^4 p(\tilde{\lambda}) = 0$, we obtain the following equation with coefficients independent of L:

$$
\begin{aligned}
&\tilde{\lambda}^4 \left(-\frac{1}{V_S^8} + \frac{C_L^2\, C_P^2\, C_S^2}{V_P^4 V_S^4} \right) + \tilde{\lambda}^3 \left(\frac{8}{V_S^6} - \frac{2\, C_L^2\, C_P^2\, C_S^2}{V_P^2 V_S^2}(\frac{1}{V_P^2} + \frac{1}{V_S^2}) \right. \\
&\left. - \frac{4}{V_P^2 V_S^2}(\frac{C_P^2}{V_P^2} + \frac{C_L^2\, C_S^2}{V_S^2}) \right) + \tilde{\lambda}^2 \left(-\frac{24}{V_S^4} + \frac{2\, C_L^2\, C_P^2\, C_S^2 + 4\, C_P^2 + 4\, C_L^2\, C_S^2 + 16}{V_P^2\, V_S^2} \right. \\
&\left. + C_L^2\, C_P^2\, C_S^2(\frac{1}{V_P^2} + \frac{1}{V_S^2})^2 + 4\,(\frac{C_P^2}{V_P^2} + \frac{C_L^2\, C_S^2}{V_S^2})(\frac{1}{V_P^2} + \frac{1}{V_S^2}) \right) + \tilde{\lambda} \left(\frac{32}{V_S^2} \right. \\
&\left. - 2\,(C_L^2\, C_P^2\, C_S^2 + 2\,(C_P^2 + C_L^2\, C_S^2) + 8)(\frac{1}{V_P^2} + \frac{1}{V_S^2}) \right) \\
&+ C_L^2\, C_P^2\, C_S^2 + 4\,(C_P^2 + C_L^2\, C_S^2) = 0.
\end{aligned}
\tag{7.60}
$$

Consequently, as the solutions of (7.60) are independent of L, we conclude that λ_1, λ_2, λ_3 and λ_4 must behave as $\mathcal{O}(L^2)$, that is, $\mathcal{O}(1/h_P^2)$ or equivalently $\mathcal{O}(C_S^2/h_S^2)$. To illustrate this behaviour, we consider again $V_P^2 = 28$ and $V_S^2 = 4$ and this time in Figure 7.13 we plot, respect to frequency $L = L_P = L_S$, the real roots of polynomial (7.56) with coefficients (7.59) when considering $h = h_P = h_S = \frac{1}{L}(\lceil \frac{V_P}{V_S} \rceil - 1)$. We observe that this conclusions are consistent with what we have observed in Figure 7.5 for the numerical instabilities of the standard finite elements discretization presented in Section 7.2.3.

7.3.4 Relation between the eigenvalues and the Rayleigh waves

On the previous section we have analysed what happens at the worst frequency when we refine together on both, the range of frequencies L and the mesh steps h_P and h_S. Now we are interested on what happens at each fixed frequency $\ell < L$ when h_P and h_S go to zero. In such case the roots of polynomial (7.56) reduce to the solutions of

$$
\frac{\lambda^4}{V_S^8 \ell^4} - \frac{8\lambda^3}{V_S^6 \ell^2} + \frac{1}{V_S^2}(\frac{24}{V_S^2} - \frac{16}{V_P^2})\lambda^2 + 16\ell^2(\frac{1}{V_P^2} - \frac{1}{V_S^2})\lambda = 0,
$$

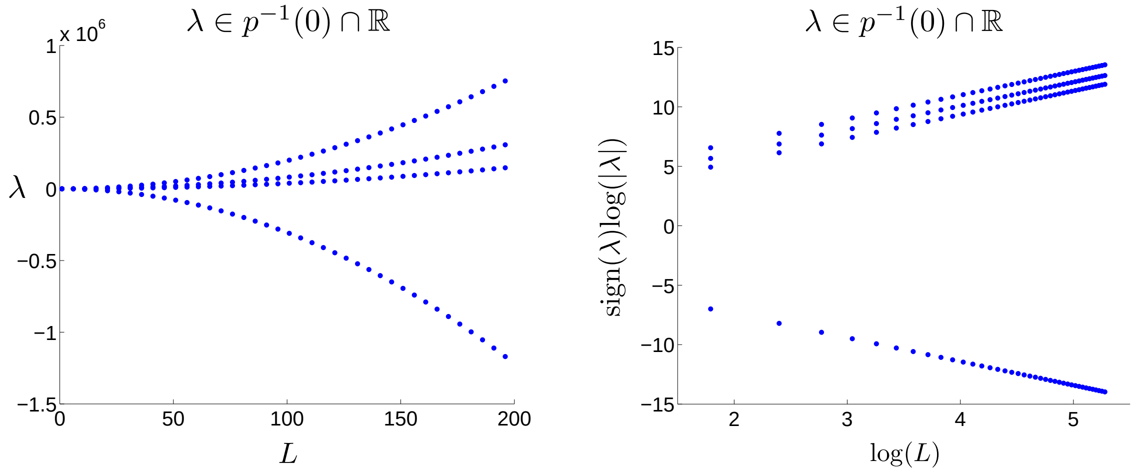

Figure 7.13: Real roots of polynomial (7.56) with coefficients (7.59).

that has a null solution (let say $\lambda_4 = 0$), plus the solutions of the following order three equation, which is actually the well known equation for the speed of Rayleigh waves:

$$\frac{\lambda^3}{\ell^6} - 8V_S^2\frac{\lambda^2}{\ell^4} + V_S^6\Big(\frac{24}{V_S^2} - \frac{16}{V_P^2}\Big)\frac{\lambda}{\ell^2} + 16V_S^8\Big(\frac{1}{V_P^2} - \frac{1}{V_S^2}\Big) = 0.$$

This equation can be rewritten as the following monic polynomial for the auxiliary variable $\tilde{\lambda} = \lambda/\ell^2$

$$\tilde{\lambda}^3 - 8V_S^2\tilde{\lambda}^2 + V_S^6\Big(\frac{24}{V_S^2} - \frac{16}{V_P^2}\Big)\tilde{\lambda} + 16V_S^8\Big(\frac{1}{V_P^2} - \frac{1}{V_S^2}\Big) = 0.$$

Then the solutions $\tilde{\lambda}_1$, $\tilde{\lambda}_2$ and $\tilde{\lambda}_3$ are independent of ℓ and satisfy

$$\tilde{\lambda}_1\,\tilde{\lambda}_2\,\tilde{\lambda}_3 = -16V_S^8\Big(\frac{1}{V_P^2} - \frac{1}{V_S^2}\Big) > 0,$$

which, due to the conjecture that there is at most one negative eigenvalue, implies that all are positive. Therefore λ_1, λ_2 and λ_3 are positive and behave as $\mathcal{O}(\ell^2)$.

7.4 The stabilized formulation

The diagnosis of the analysis in Sections 7.2.3 and 7.3 is that the space $\boldsymbol{V}_0$ is probably too large in the sense that it allows for the appearance of unstable modes after space discretization, this being linked to the non positivity of the bilinear form $m(\cdot,\cdot)$ (see Theorem 7.12). The idea for circumventing this problem is to identify an adequate subspace $\boldsymbol{V}_N$ of $\boldsymbol{V}_0$ (subscript N holds for Neumann) in such a way that:

(i) The unknown $\boldsymbol{\varphi} \equiv (\varphi_P, \varphi_S)$ defined by (7.7) and (7.8) is solution of the variational problem (7.28), but set in $\boldsymbol{V}_N$, instead of $\boldsymbol{V}_0$, i.e.

$$\left\{\begin{array}{l} \text{Find } \boldsymbol{\varphi}(t) : [0,T] \longrightarrow \boldsymbol{V}_N \text{ such that } (\boldsymbol{\varphi}, \partial_t\boldsymbol{\varphi})(t=0) = (\mathbf{0},\mathbf{0}) \text{ and} \\ \dfrac{\mathrm{d}^2}{\mathrm{d}t^2}\, m(\boldsymbol{\varphi}(t), \boldsymbol{\psi}) + a(\boldsymbol{\varphi}(t), \boldsymbol{\psi}) = \mathrm{g}(t, \boldsymbol{\psi}), \quad \forall\, \boldsymbol{\psi} \in \boldsymbol{V}_N. \end{array}\right. \tag{7.61}$$

(ii) The bilinear form $m(\cdot,\cdot)$ restricted to the space $\boldsymbol{V}_N$ satisfies a coercivity condition as in Dirichlet case (see Lemma 6.5). More precisely, we expect that there exists a strictly positive constant α_m such that

$$\forall\, \boldsymbol{\psi} \in \boldsymbol{V}_N \setminus \{0\}, \quad m(\boldsymbol{\psi}, \boldsymbol{\psi}) \geq \alpha_m \int_\Omega |\boldsymbol{\psi}|^2\,\mathrm{d}\boldsymbol{x}.$$

The item (ii) will guide the construction of $\boldsymbol{V}_N$ and it is expected to guarantee the well posedness of problem (7.61) (as in Theorem 6.6 for the Dirichlet case).

7.4.1 Construction of an adapted functional space

The construction of the new variational space is motivated by the energy naturally associated to problem (7.28). Similarly to what we observed for the Dirichlet problem (see (6.33)), we expect the energy of the Neumann problem to be related to the classical elastic energy $E_{el}(\boldsymbol{u})$ (defined in (6.27)). Let us begin by considering $\boldsymbol{\psi} = \partial_t\boldsymbol{\varphi}$ in the variational formulation (7.28), then by classical computations we obtain the following energy identity (subscript N holds for Neumann)

$$\frac{\mathrm{d}}{\mathrm{d}t}\mathcal{E}_N(\boldsymbol{\varphi}) = \mathrm{g}(t,\partial_t\boldsymbol{\varphi}), \quad \text{for the energy} \quad \mathcal{E}_N(\boldsymbol{\psi}) := \frac{1}{2}\, m(\partial_t\boldsymbol{\psi},\partial_t\boldsymbol{\psi}) \; + \; \frac{1}{2}\, a(\boldsymbol{\psi},\boldsymbol{\psi}). \tag{7.62}$$

Notice, that the energy is conserved as soon as the right hand side vanishes and that it only differs from the energy of the Dirichlet problem (defined in (6.25)) by a boundary term

$$\mathcal{E}_N(\boldsymbol{\psi}) = \mathcal{E}_D(\boldsymbol{\psi}) + \frac{1}{2}\, m_\Gamma(\partial_t\boldsymbol{\psi},\partial_t\boldsymbol{\psi}).$$

Moreover, we recall that for the Dirichlet problem, we proved that in absence of source, the energy of the solution in displacements $\boldsymbol{u}$ and the energy of the solution in potentials $\boldsymbol{\varphi}$ are related by (see (6.33))

$$E_{el}(\boldsymbol{u}) = \rho\,\mathcal{E}_D(\boldsymbol{\varphi}) \qquad \text{(in Dirichlet case).}$$

This relation was obtained in two steps (see (6.28) for the definition of potential and kinetic energies):

$$(6.29)\quad \frac{\rho}{2}\, a\,(\boldsymbol{\varphi},\boldsymbol{\varphi}) = E_c(\boldsymbol{u}) \quad \text{and} \quad (6.32)\quad \frac{\rho}{2}\, m_\Omega\,(\partial_t\boldsymbol{\varphi},\partial_t\boldsymbol{\varphi}) = E_p(\boldsymbol{u}) \qquad \text{(in Dirichlet case).}$$

We first notice that the identity (6.29) still holds for the solutions of the Neumann problem because its proof does not refer to the Dirichlet condition, it only uses $\partial_t\boldsymbol{u} = \nabla\varphi_P + \mathbf{curl}\,\varphi_S$ which is valid independently of the boundary conditions, as soon as the source term vanishes. Thus, it would be enough to obtain an equivalent to (6.32) considering $m(\cdot,\cdot)$ instead of $m_\Omega(\cdot,\cdot)$. To do so we first recall that according to Lemma 6.7 we obtain (6.31) which considering the definition of potentials (7.7) reads

$$E_p(\boldsymbol{u}) = \frac{\rho}{2}\, m_\Omega\,(\partial_t\boldsymbol{\varphi},\partial_t\boldsymbol{\varphi}) - 2\mu\int_\Gamma u_2\;\partial_{\boldsymbol{\tau}} u_1\,\mathrm{d}\boldsymbol{\gamma}. \tag{7.63}$$

Next, in order to rewrite the boundary term, we use the fact that $\boldsymbol{u}$ satisfies the free boundary conditions (7.23e), (7.23f) and (7.23g) (notice that $\boldsymbol{u}_\Gamma = \boldsymbol{u}_{|\Gamma}$ by definition). More precisely, we are going to use the fact that on Γ we have

$$\partial_{\boldsymbol{\tau}} u_1 = \frac{1}{2\,V_S^2}\,\partial_t\boldsymbol{\varphi}\cdot\boldsymbol{\tau}, \quad u_2 + \frac{1}{2\,V_S^2}\,\mathcal{I}\big(\partial_t\boldsymbol{\varphi}\cdot\boldsymbol{n}\big) = \mathrm{cte} \quad \text{and} \quad \int_\Gamma \partial_t\boldsymbol{\varphi}\cdot\boldsymbol{\tau}\,\mathrm{d}\boldsymbol{\gamma} = 0.$$

These relations allow us to obtain

$$2\mu\int_\Gamma u_2\;\partial_{\boldsymbol{\tau}} u_1\,\mathrm{d}\boldsymbol{\gamma} = -\frac{\mu}{2\,V_S^4}\int_\Gamma \mathcal{I}\big(\partial_t\boldsymbol{\varphi}\cdot\boldsymbol{n}\big)\,\partial_t\boldsymbol{\varphi}\cdot\boldsymbol{\tau}\,\mathrm{d}\boldsymbol{\gamma} = -\frac{\rho}{2} m_\Gamma(\partial_t\boldsymbol{\varphi},\partial_t\boldsymbol{\varphi}).$$

In consequence, equation (7.63) provides an equivalent to (6.32) for the Neumann case

$$E_p(\boldsymbol{u}) = \frac{\rho}{2}\, m(\partial_t\boldsymbol{\varphi},\partial_t\boldsymbol{\varphi}) \qquad \text{(in Neumann case)} \tag{7.64}$$

which proves, as desired, that in absence of source, the energy of the solution in displacements $\boldsymbol{u}$ and the energy of the solution in potentials $\boldsymbol{\varphi}$ are related by

$$E_{el}(\boldsymbol{u}) = \rho\,\mathcal{E}_N(\boldsymbol{\varphi}) \qquad \text{(in Neumann case).}$$

Moreover, according to definition (6.28) of the potential energy, the Hook's law (5.2) and applying Korn's inequality in $H^1(\Omega)^2 \cap L^2_R(\Omega)$ (see Proposition 7.4), we obtain

$$E_p(\boldsymbol{u}) = \frac{1}{2}\int_\Omega \big(\lambda\,|\operatorname{div}\boldsymbol{u}|^2 + 2\,\mu\,|\underline{\boldsymbol{\varepsilon}}(\boldsymbol{u})|^2\big)\mathrm{d}\boldsymbol{x} \geq \frac{\mu}{\mathcal{C}_\Omega}\|\boldsymbol{u}\|^2_{H^1(\Omega)}.$$

Thus, we notice that, according to the definition (7.7) of the potentials solution, noticing that $V_P > V_S$ and considering triangular inequality,

$$\int_\Omega |\partial_t\boldsymbol{\varphi}|^2\,\mathrm{d}\boldsymbol{x} = \int_\Omega \big(V_P^4\,|\operatorname{div}\boldsymbol{u}|^2 + V_S^4\,|\operatorname{curl}\boldsymbol{u}|^2\big)\,\mathrm{d}\boldsymbol{x} \leq V_P^4\int_\Omega |\nabla\boldsymbol{u}|^2\,\mathrm{d}\boldsymbol{x}. \tag{7.65}$$

Therefore, considering (7.64), we observe that

$$m(\partial_t\boldsymbol{\varphi},\partial_t\boldsymbol{\varphi}) \geq \frac{\mu}{\rho\,V_P^4\,\mathcal{C}_\Omega}\int_\Omega |\partial_t\boldsymbol{\varphi}|\,\mathrm{d}\boldsymbol{x}. \tag{7.66}$$

This relation gives the main idea for the construction of the space $\boldsymbol{V}_N$ since we are going to build it in such a way that previous inequality holds not only for $\partial_t\boldsymbol{\varphi}$ but also for any $\boldsymbol{\psi}\in\boldsymbol{V}_N$. The reader should notice that to deduce (7.66), we have made use of the definition (7.7) of the potentials solution $\boldsymbol{\varphi}$ with respect to the displacements solution $\boldsymbol{u}$, i.e.

$$\rho\,\partial_t\varphi_P = (\lambda+2\mu)\operatorname{div}\boldsymbol{u} \qquad \text{and} \qquad \rho\,\partial_t\varphi_S = -\mu\operatorname{curl}\boldsymbol{u},$$

and we have also taken into account that the displacements solution $\boldsymbol{u}$ verifies the free boundary condition (7.1b), i.e. $\boldsymbol{u}\in\boldsymbol{D}_N$ (defined in (7.6)). This motivates the introduction of the operator $\mathcal{F}\in\mathcal{L}(\boldsymbol{D},\boldsymbol{V})$ such that

$$\forall\boldsymbol{w}\in\boldsymbol{D}, \quad \text{assigns} \quad \mathcal{F}\,\boldsymbol{w} := \big(V_P^2\operatorname{div}\boldsymbol{w}, -V_S^2\operatorname{curl}\boldsymbol{w}\big)\in\boldsymbol{V}, \tag{7.67}$$

and finally the space

$$\boldsymbol{V}_N := \mathcal{F}(\boldsymbol{D}_N) \equiv \big\{\big(V_P^2\operatorname{div}\boldsymbol{w}, -V_S^2\operatorname{curl}\boldsymbol{w}\big), \quad \boldsymbol{w}\in\boldsymbol{D}_N\big\}. \tag{7.68}$$

A first remarkable property of this space is given by the following lemma.

Lemma 7.21

The space $\boldsymbol{V}_N$ is a subspace of $\boldsymbol{V}_0$.

Proof. By the definition (7.67) of the operator $\mathcal{F}$, we already know that $\boldsymbol{V}_N\subset\boldsymbol{V}$. So we only have to check that the gauge conditions in the definition (7.26) of the space $\boldsymbol{V}_0$ are also satisfied. Then we consider any $\boldsymbol{\psi}\in\boldsymbol{V}_N$, i.e.,

$$\boldsymbol{\psi} = \big(V_P^2\operatorname{div}\boldsymbol{w}, -V_S^2\operatorname{curl}\boldsymbol{w}\big), \quad \boldsymbol{w}\in\boldsymbol{D}_N. \tag{7.69}$$

The proof is essentially a matter of reproducing the computations in Section 7.1 for proving (7.17), with $\boldsymbol{\psi}$ instead of $\partial_t\boldsymbol{\varphi}$ and $\boldsymbol{w}$ instead of $\boldsymbol{u}$. Simply note that in this case, the boundary condition $\underline{\boldsymbol{\sigma}}(\boldsymbol{w})\boldsymbol{n}=\boldsymbol{0}$ on Γ follows from $\boldsymbol{w}\in\boldsymbol{D}_N$, while the equivalent of (7.7) is nothing but (7.69). Then we obtain the equivalent of (7.17), namely,

$$\partial_\tau\,w_1 = \frac{1}{2\,V_S^2}\,\boldsymbol{\psi}\cdot\boldsymbol{\tau}, \qquad \partial_\tau\,w_2 = -\frac{1}{2\,V_S^2}\,\boldsymbol{\psi}\cdot\boldsymbol{n}, \quad \text{on } \Gamma. \tag{7.70}$$

Finally, since Γ is assumed to be closed, the gauge conditions are obtained by integrating the above equalities on Γ.

■

Next, we provide another interesting property of the space $\boldsymbol{V}_N$ that we shall use later.

Lemma 7.22

For any $\boldsymbol{\psi} = (\psi_P, \psi_S) \in \boldsymbol{V}_N$, we have that $\nabla\psi_P + \mathbf{curl}\,\psi_S \in \boldsymbol{L}^2_R(\Omega)$.

Proof. Let us consider $\boldsymbol{\psi} \in \boldsymbol{V}_N$ and notice that $\boldsymbol{\psi} = (V_P^2 \operatorname{div} \boldsymbol{w}, -V_S^2 \operatorname{curl} \boldsymbol{w})$ for some $\boldsymbol{w} \in \boldsymbol{D}_N$. Then, according to Hook's law (5.2) we compute

$$\mathbf{div}\,\underline{\boldsymbol{\sigma}}(\boldsymbol{w}) = (\lambda + 2\,\mu)\nabla \operatorname{div} \boldsymbol{w} - \mu\,\mathbf{curl} \operatorname{curl} \boldsymbol{w} = \rho\big(\nabla\psi_P + \mathbf{curl}\,\psi_S\big)$$

and if we multiply by any $\boldsymbol{w}_R \in \boldsymbol{R}(\Omega)$ and integrate over Ω we obtain, using Green's formula

$$\int_\Omega \underline{\boldsymbol{\sigma}}(\boldsymbol{w}) : \underline{\boldsymbol{\varepsilon}}(\boldsymbol{w}_R)\,\mathrm{d}\boldsymbol{x} + \int_\Gamma \underline{\boldsymbol{\sigma}}(\boldsymbol{w})\boldsymbol{n} \cdot \boldsymbol{w}_R\,\mathrm{d}\gamma = -\rho \int_\Omega \big(\nabla\psi_P + \mathbf{curl}\,\psi_S\big) \cdot \boldsymbol{w}_R\,\mathrm{d}\boldsymbol{x} = 0,$$

since $\underline{\boldsymbol{\varepsilon}}(\boldsymbol{w}_R) = 0$ and $\underline{\boldsymbol{\sigma}}(\boldsymbol{w})\boldsymbol{n} = 0$ for $\boldsymbol{w} \in \boldsymbol{D}_N$.

■

Now, we remark that the solution in displacements $\boldsymbol{u}(t) \in \boldsymbol{D}_N$, for all $t \geq 0$, (due to Lemma 7.2 and the boundary conditions), then the solution in potentials, which is defined by (7.7) and (7.8), satisfies $\partial_t\boldsymbol{\varphi} = \mathcal{F}(\boldsymbol{u})$, hence $\partial_t\boldsymbol{\varphi}(t) \in \boldsymbol{V}_N$ (by definition, see (7.68)) and according to the vanishing initial conditions $\boldsymbol{\varphi}(t) \in \boldsymbol{V}_N$ for all $t \geq 0$. In consequence, the space $\boldsymbol{V}_N$ satisfies the first requirement (i). Next, we complete this section by proving that the space $\boldsymbol{V}_N$ satisfies also the second requirement (ii), i.e. the bilinear form $m(\cdot,\cdot)$ verifies the following coercivity condition in the new space $\boldsymbol{V}_N$.

Theorem 7.23

There exists a strictly positive constant α_m such that

$$\forall\, \boldsymbol{\psi} \in \boldsymbol{V}_N \setminus \{0\}, \quad m(\boldsymbol{\psi}, \boldsymbol{\psi}) \geq \alpha_m \int_\Omega |\boldsymbol{\psi}|\,\mathrm{d}\boldsymbol{x}.$$

Proof. Let $\boldsymbol{\psi} = (\psi_P, \psi_S) \in \boldsymbol{V}_N$, i.e., $\boldsymbol{\psi} = (V_P^2 \operatorname{div} \boldsymbol{w}, -V_S^2 \operatorname{curl} \boldsymbol{w})$, $\boldsymbol{w} \in \boldsymbol{D}_N$, then the proof is a mater of reproducing the computations that lead us to (7.66) but considering $\boldsymbol{\psi}$ and $\boldsymbol{w}$ instead of $\partial_t\boldsymbol{\varphi}$ and $\boldsymbol{u}$. We begin by applying Hook's law (5.2) and Lemma 6.7 to deduce that

$$\begin{aligned}\int_\Omega \underline{\boldsymbol{\sigma}}(\boldsymbol{w}) : \underline{\boldsymbol{\varepsilon}}(\boldsymbol{w})\,\mathrm{d}\boldsymbol{x} &= (\lambda + 2\mu) \int_\Omega |\operatorname{div} \boldsymbol{w}|^2\,\mathrm{d}\boldsymbol{x} + \mu \int_\Omega |\operatorname{curl} \boldsymbol{w}|^2\,\mathrm{d}\boldsymbol{x} \\ &- 4\,\mu \int_\Gamma w_2\,\partial_{\boldsymbol{\tau}} w_1 \mathrm{d}\boldsymbol{\gamma}.\end{aligned}$$

Next, since $\lambda + 2\mu = \rho\, V_P^2$ and $\mu = \rho\, V_S^2$, we compute from the definition of $\boldsymbol{\psi}$ that

$$(\lambda + 2\mu) \int_\Omega |\operatorname{div} \boldsymbol{w}|^2\,\mathrm{d}\boldsymbol{x} + \mu \int_\Omega |\operatorname{curl} \boldsymbol{w}|^2\,\mathrm{d}\boldsymbol{x} \quad = \quad \rho\, m_\Omega(\boldsymbol{\psi}, \boldsymbol{\psi}).$$

On the other hand, using (7.70) (see the proof of Lemma 7.21) we obtain

$$-\,4\,\mu \int_\Gamma w_2\,\partial_{\boldsymbol{\tau}} w_1 \mathrm{d}\boldsymbol{\gamma} \;=\; \rho\, m_\Gamma(\boldsymbol{\psi}, \boldsymbol{\psi}),$$

which combined to the two previous equalities, gives

$$m(\boldsymbol{\psi}, \boldsymbol{\psi}) = \frac{1}{\rho} \int_\Omega \underline{\boldsymbol{\varepsilon}}(\boldsymbol{w}) : \underline{\boldsymbol{\sigma}}(\boldsymbol{w})\,\mathrm{d}\boldsymbol{x} = \frac{2}{\rho} E_p(\boldsymbol{w}).$$

Therefore, considering again Hook's law (5.2) and Korn's inequality in $\boldsymbol{D}_N \subset H^1(\Omega)^2 \cap L^2_R(\Omega)$ (see Proposition 7.4), we obtain

$$m(\boldsymbol{\psi}, \boldsymbol{\psi}) = \frac{\lambda}{\rho} \int_\Omega |\operatorname{div} \boldsymbol{w}|^2 \mathrm{d}\boldsymbol{x} + \frac{2\,\mu}{\rho} \int_\Omega |\underline{\boldsymbol{\varepsilon}}(\boldsymbol{w})|^2 \mathrm{d}\boldsymbol{x} \geq \frac{2\,\mu}{\rho} \int_\Omega |\underline{\boldsymbol{\varepsilon}}(\boldsymbol{w})|^2 \mathrm{d}\boldsymbol{x} \geq \frac{2\,\mu}{\rho\, \mathcal{C}_\Omega} \int_\Omega |\nabla \boldsymbol{w}| \mathrm{d}\boldsymbol{x}$$

Finally, we notice that according to the definition of $\boldsymbol{\psi}$, noticing that $V_P > V_S$ and considering triangular inequality, we deduce

$$\int_\Omega |\boldsymbol{\psi}|^2 \,\mathrm{d}\boldsymbol{x} = \int_\Omega \left(V_P^4 \,|\mathrm{div}\, \boldsymbol{w}|^2 + V_S^4 \,|\mathrm{curl}\, \boldsymbol{w}|^2\right)|, \mathrm{d}\boldsymbol{x} \leq V_P^4 \int_\Omega |\nabla \boldsymbol{w}|^2 \,\mathrm{d}\boldsymbol{x} \leq \frac{\rho\, V_P^4\, \mathcal{C}_\Omega}{\mu} m(\boldsymbol{\psi}, \boldsymbol{\psi}).$$

■

7.4.2 Well posedness of the problem

Notice that in Section 7.4.1 we have identified, as desired, a space $\boldsymbol{V}_N$ satisfying the requirements (i) and (ii) at the beginning of Section 7.4. Next, we proceed to verify that, as expected, these properties guarantee the well posedness of problem (7.61).

Theorem 7.24

Assume that $\boldsymbol{f} \in \mathcal{C}^1\big([0,T]; \boldsymbol{L}^2_R(\Omega)\big)$. Then, there exists a unique strong solution of problem (7.61) *such that*

$$\boldsymbol{\varphi} \in \mathcal{C}^2([0,T]; L^2(\Omega)^2) \cap \mathcal{C}^1([0,T]; \boldsymbol{V}_N).$$

Proof. First, we notice that since the space $\boldsymbol{V}_N$ satisfies the first requirement (i) we have that there exists at least one solution $\boldsymbol{\varphi} \in \boldsymbol{V}_N$ which is given by equations (7.7) and (7.8). Moreover, as we have discussed in (7.12), the vector of potentials is such that

$$\boldsymbol{\varphi} \in \mathcal{C}^2([0,T]; L^2(\Omega)^2) \cap \mathcal{C}^1([0,T]; \boldsymbol{V}_N).$$

In consequence, only uniqueness remains to be proved. Let us assume that there exists another solution $\boldsymbol{\varphi}^\star \in \boldsymbol{V}_N$ and we denote $\boldsymbol{e} = \boldsymbol{\varphi} - \boldsymbol{\varphi}^\star \in \boldsymbol{V}_N$. We observe that

$$\frac{\mathrm{d}^2}{\mathrm{d}t^2} m(\boldsymbol{e}, \boldsymbol{\psi}) + a(\boldsymbol{e}, \boldsymbol{\psi}) = 0, \quad \forall\, \boldsymbol{\psi} \in \boldsymbol{V}_N,$$

and in particular, if we consider $\boldsymbol{\psi} = \partial_t \boldsymbol{e}$ we obtain the following energy identity

$$\frac{\mathrm{d}}{\mathrm{d}t} \mathcal{E}_N(\boldsymbol{e}) = 0.$$

Thus $\mathcal{E}_N(\boldsymbol{e}) = 0$ and we conclude $\boldsymbol{\varphi} = \boldsymbol{\varphi}^\star$, since due to requirement (ii) (proved in Theorem 7.23) we have that

$$\int_\Omega |\partial_t \boldsymbol{e}|^2 \,\mathrm{d}\boldsymbol{x} \;\leq\; \frac{1}{\alpha_m} m(\partial_t \boldsymbol{e}, \partial_t \boldsymbol{e}) \;\leq\; \frac{2}{\alpha_m} \mathcal{E}_N(\boldsymbol{e}) \;=\; 0.$$

■

Remark 7.25

This result can be extended for situations with a lower time regularity, however the proof is long and not central for our purposes. In consequence, for pedagogical reasons we have chosen to present Theorem 7.24 and to delay the more general result to Appendix B. In particular, we prove that $\boldsymbol{f} \in L^1([0,T]; \boldsymbol{L}^2_R(\Omega))$ guarantees the existence and uniqueness of a solution $\boldsymbol{\varphi}$ of problem (7.61) *such that*

$$\boldsymbol{\varphi} \in L^2([0,T]; \boldsymbol{V}_N), \qquad \partial_t \boldsymbol{\varphi} \in L^2([0,T]; L^2(\Omega)^2),$$

where the involved time derivatives are considered in the distributional sense.

7.5 Reformulation of the stabilized problem as a mixed problem

In Section 7.4 we have introduced a new functional space $\boldsymbol{V}_N$ where the existence and uniqueness of solution is guaranteed. However, the definition (7.68) of the space $\boldsymbol{V}_N$ is theoretical and implicit, thus it is not well adapted for discretization. In particular, it refers to displacement fields which we want to avoid. Therefore, our purpose in this section is to reformulate the stabilized problem (7.61) avoiding any reference to displacement fields.

7.5.1 Characterization of the adapted functional space

In a first step, our aim is to find a more suitable characterization of the new space $\boldsymbol{V}_N$ eluding its relation with displacement fields. We begin by recalling that the space $\boldsymbol{V}_N \subset \boldsymbol{V}$ was defined as the image of $\boldsymbol{D}_N \subset \boldsymbol{D}$ by the linear operator $\mathcal{F}$ (see (7.67) and (7.68)). Next, we will build another operator $\mathcal{S}_N \in \mathcal{L}(\boldsymbol{V};\boldsymbol{D})$ such that $\boldsymbol{D}_N = \mathcal{S}_N(\boldsymbol{V}_N)$ and that we expect to be a left inverse of $\mathcal{F}$ when restricted to $\boldsymbol{D}_N$. As we shall see later, this will imply that (see Figure 7.14 for a sketch of the images and pre-images of the operators involved)

$$\mathcal{T} := \mathcal{F} \circ \mathcal{S}_N \in \mathcal{L}(\boldsymbol{V}) \text{ is a projector from } \boldsymbol{V} \text{ into } \boldsymbol{V}_N \text{ i.e. } \operatorname{Im} \mathcal{T} = \boldsymbol{V}_N. \tag{7.71}$$

In consequence, as for any projector, we will be allowed to decompose $\boldsymbol{V}$ as the direct sum

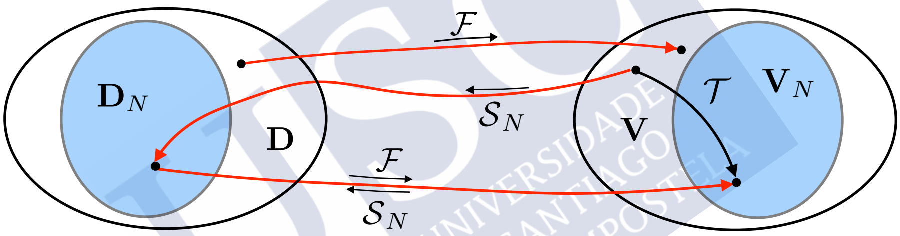

Figure 7.14: Representation of the images and pre-images of the operator $\mathcal{F}, \mathcal{S}_N$ and $\mathcal{T}$.

$$\boldsymbol{V} = \operatorname{Ker} \mathcal{T} \oplus \operatorname{Im} \mathcal{T} = \operatorname{Ker} \mathcal{T} \oplus \boldsymbol{V}_N,$$

and we expect that we can characterize $\boldsymbol{V}_N$ by orthogonality to $\operatorname{Ker} \mathcal{T}$ which, contrary to $\boldsymbol{V}$ or $\boldsymbol{V}_N$, it is completely independent of the spaces $\boldsymbol{D}$ or $\boldsymbol{D}_N$.

In order to properly define the mentioned operator $\mathcal{S}_N$, let us consider any $\boldsymbol{\psi} \in \boldsymbol{V}$ and find $\boldsymbol{w}_\star$ solution of the following elastostatic problem (whose well posedness is classic)

$$\left\{\begin{array}{ll} -\operatorname{div} \underline{\boldsymbol{\sigma}}(\boldsymbol{w}_\star) = -\rho\,\Pi_R\big(\nabla\psi_P + \mathbf{curl}\,\psi_S\big) \quad \text{in } \Omega, & (7.72a) \\ \boldsymbol{w}_\star \in H^1(\Omega)^2 \cap \boldsymbol{L}^2_R(\Omega) \quad \text{and} \quad \underline{\boldsymbol{\sigma}}(\boldsymbol{w}_\star)\boldsymbol{n} = \boldsymbol{0} \quad \text{on } \Gamma. & (7.72b) \end{array}\right.$$

Therefore we define $\mathcal{S}_N \in \mathcal{L}(\boldsymbol{V};\boldsymbol{D})$ such that

$$\forall \boldsymbol{\psi} \in \boldsymbol{V}, \quad \text{assigns} \quad \mathcal{S}_N(\boldsymbol{\psi}) := \boldsymbol{w}_\star \quad \text{solution of problem (7.72).}$$

Next, we verify the two main properties that we require for the operator $\mathcal{S}_N$.

Lemma 7.26

The image of $\mathcal{S}_N$ coincides with the space $\boldsymbol{D}_N$

$$\operatorname{Im} \mathcal{S}_N = \boldsymbol{D}_N.$$

Moreover, the operator $\mathcal{S}_N$ is a left inverse of $\mathcal{F}$ restricted to the space $\boldsymbol{D}_N$

$$\forall\, \boldsymbol{w} \in \boldsymbol{D}_N, \quad \boldsymbol{w} = \mathcal{S}_N\, \mathcal{F}\, \boldsymbol{w}.$$

Proof. First, notice that by definition of $\mathcal{S}_N$ and $\boldsymbol{D}_N$, it is straightforward to verify that $\operatorname{Im} \mathcal{S}_N \subset \boldsymbol{D}_N$. To verify the reverse inclusion we begin by considering $\boldsymbol{w} \in \boldsymbol{D}_N$ and noticing that using Green's formula

$$\int_\Omega \mathbf{div}\, \underline{\boldsymbol{\sigma}}(\boldsymbol{w}) \cdot \boldsymbol{w}_R \,\mathrm{d}\boldsymbol{x} = \int_\Omega \underline{\boldsymbol{\sigma}}(\boldsymbol{w}) : \underline{\boldsymbol{\varepsilon}}(\boldsymbol{w}_R) \,\mathrm{d}\boldsymbol{x} + \int_\Gamma \underline{\boldsymbol{\sigma}}(\boldsymbol{w})\boldsymbol{n} \cdot \boldsymbol{w}_R \,\mathrm{d}\gamma = 0,$$

since $\underline{\boldsymbol{\varepsilon}}(\boldsymbol{w}_R) = 0$ and $\underline{\boldsymbol{\sigma}}(\boldsymbol{w})\boldsymbol{n} = 0$ for $\boldsymbol{w} \in \boldsymbol{D}_N$, thus $\mathbf{div}\, \underline{\boldsymbol{\sigma}}(\boldsymbol{w}) \in \boldsymbol{L}^2_R(\Omega)$. Next, we consider $\boldsymbol{\psi} = \mathcal{F}\, \boldsymbol{w}$ which belongs to $\boldsymbol{V}_N$ by definition. Then, according to Hook's law (5.2) we compute

$$\mathbf{div}\, \underline{\boldsymbol{\sigma}}(\boldsymbol{w}) = (\lambda + 2\,\mu)\nabla \operatorname{div} \boldsymbol{w} - \mu\, \mathbf{curl} \operatorname{curl} \boldsymbol{w} = \rho\big(\nabla \psi_P + \mathbf{curl}\, \psi_S\big), \tag{7.73}$$

and since $\mathbf{div}\, \underline{\boldsymbol{\sigma}}(\boldsymbol{w})$ coincides with its own projection onto $\boldsymbol{L}^2_R(\Omega)$, we can write

$$\mathbf{div}\, \underline{\boldsymbol{\sigma}}(\boldsymbol{w}) = \rho\, \Pi_R \left(\nabla\, \psi_P + \mathbf{curl}\, \psi_S \right).$$

In consequence $\boldsymbol{w} = \mathcal{S}_N \boldsymbol{\psi}$ since $\boldsymbol{w} \in \boldsymbol{D}_N$ and thus by definition

$$\boldsymbol{w} \in H^1(\Omega)^2 \cap \boldsymbol{L}^2_R(\Omega) \quad \text{and} \quad \underline{\boldsymbol{\sigma}}(\boldsymbol{w})\boldsymbol{n} = \boldsymbol{0} \quad \text{on } \Gamma,$$

which proves that $\boldsymbol{D}_N \subset \operatorname{Im} \mathcal{S}_N$.

Finally, notice that $\boldsymbol{w} = \mathcal{S}_N \boldsymbol{\psi}$ also proves that $\mathcal{S}_N$ is a left inverse of $\mathcal{F}$ restricted to the space $\boldsymbol{D}_N$ since considering the definition of $\boldsymbol{\psi}$ we have that

$$\boldsymbol{w} = \mathcal{S}_N \boldsymbol{\psi} = \mathcal{S}_N\, \mathcal{F}\, \boldsymbol{w}.$$

■

Remark 7.27

Notice that in the previous result a particular role is played by the rigid displacements space $\boldsymbol{R}(\Omega)$. In particular the property $\boldsymbol{D}_N \subset \boldsymbol{D}_R$ is capital to prove $\boldsymbol{D}_N \subset \operatorname{Im} \mathcal{S}_N$. This and the forthcoming consequences widely justify the consideration of assumption (7.3) that leads to seek the displacement solution $\boldsymbol{u}$ directly in $\boldsymbol{D}_R$.

It is interesting to notice that, by definition of $\mathcal{F}$ and $\mathcal{S}_N$, the operator $\mathcal{T} = \mathcal{F} \circ \mathcal{S}_N$ (introduced in (7.71)) can be equivalently defined by

$$\mathcal{T}\boldsymbol{\psi} = (V_P^2 \operatorname{div} \boldsymbol{w}_\star, -V_S^2 \operatorname{curl} \boldsymbol{w}_\star) \text{ where } \boldsymbol{w}_\star \text{ is the solution of (7.72).}$$

Next, we proof an important result that confirms the conjecture made in (7.71).

Theorem 7.28

The operator $\mathcal{T}$ is a projector into $\boldsymbol{V}_N$ and consequently

$$\boldsymbol{V} = \operatorname{Ker} \mathcal{T} \oplus \operatorname{Im} \mathcal{T} = \operatorname{Ker} \mathcal{T} \oplus \boldsymbol{V}_N. \tag{7.74}$$

Proof. First of all, notice that $\mathcal{T} \in \mathcal{L}(\boldsymbol{V})$ since it is a composition of linear operators. Second, to verify that $\mathcal{T}$ is bounded we consider any $\boldsymbol{\psi} \in \boldsymbol{V}$ and according to the definition of $\mathcal{T}$, we have that $\mathcal{T}\boldsymbol{\psi} = (V_P^2 \operatorname{div} \boldsymbol{w}_\star, -V_S^2 \operatorname{curl} \boldsymbol{w}_\star)$ for some $\boldsymbol{w}_\star$, solution of problem (7.72). Thus we compute

$$\|\mathcal{T}\boldsymbol{\psi}\|^2_{\boldsymbol{V}} = V_P^4 \int_\Omega |\operatorname{div} \boldsymbol{w}_\star|^2 \,\mathrm{d}\boldsymbol{x} + V_S^4 \int_\Omega |\operatorname{curl} \boldsymbol{w}_\star|^2 \,\mathrm{d}\boldsymbol{x} + \int_\Omega |V_P^2 \nabla \operatorname{div} \boldsymbol{w}_\star + V_S^2 \mathbf{curl} \operatorname{curl} \boldsymbol{w}_\star|^2 \,\mathrm{d}\boldsymbol{x}.$$

Then, notice that the first two terms can be easily bounded by the L^2 norm of $\nabla \boldsymbol{w}_\star$ (as in (7.65)), while the last term is precisely the L^2 norm of $\frac{1}{\rho}\,\mathbf{div}\,\underline{\boldsymbol{\sigma}}(\boldsymbol{w}_\star)$ (as in (7.73)). Therefore considering problem (7.72) we obtain

$$\|\mathcal{T}\boldsymbol{\psi}\|_{\boldsymbol{V}}^2 \leq 2\,V_P^4 \int_\Omega |\nabla \boldsymbol{w}_\star|^2\,\mathrm{d}\boldsymbol{x} + \int_\Omega |\Pi_R\big(\nabla\psi_P + \mathbf{curl}\,\psi_S\big)|^2\,\mathrm{d}\boldsymbol{x}.$$

Now notice that the continuity of problem (7.72) and the projector Π_R gives as desired

$$\|\mathcal{T}\boldsymbol{\psi}\|_{\boldsymbol{V}} \leq C\|\boldsymbol{\psi}\|_{\boldsymbol{V}}, \quad \text{for some strictly positive constant } C.$$

Finally, we verify that $\mathcal{T}^2 = \mathcal{T}$. Indeed, for any $\boldsymbol{\psi} \in \boldsymbol{V}$

$$\mathcal{T}^2\boldsymbol{\psi} = \big(\mathcal{F}\,\mathcal{S}_N\big)\,\big(\mathcal{F}\,\mathcal{S}_N\big)\boldsymbol{\psi} = \mathcal{F}\,\big(\mathcal{S}_N\,\mathcal{F}\big)\,\mathcal{S}_N\boldsymbol{\psi}$$

and notice that since $\mathcal{S}_N\boldsymbol{\psi} \in \boldsymbol{D}_N$ we can consider Lemma 7.26 which gives $\big(\mathcal{S}_N\,\mathcal{F}\big)\,\mathcal{S}_N\boldsymbol{\psi} = \mathcal{S}_N\boldsymbol{\psi}$ and thus

$$\mathcal{T}^2\boldsymbol{\psi} = \mathcal{F}\mathcal{S}_N\boldsymbol{\psi} = \mathcal{T}\boldsymbol{\psi}.$$

■

Remark 7.29

The reader might notice that Theorem 7.28 is also true for $\boldsymbol{V}_0$ instead of $\boldsymbol{V}$, due to Lemma 7.21, where we proved that $\boldsymbol{V}_N \subset \boldsymbol{V}_0$. We just need to consider the operator $\mathcal{T}_0 \in \mathcal{L}(\boldsymbol{V}_0)$ defined as the restriction of $\mathcal{T}$ to $\boldsymbol{V}_0$. In consequence,

$$\boldsymbol{V}_0 = \operatorname{Ker}\mathcal{T}_0 \oplus \operatorname{Im}\mathcal{T}_0 = \operatorname{Ker}\mathcal{T}_0 \oplus \boldsymbol{V}_N. \tag{7.75}$$

We will see later that this is convenient because the property $\operatorname{Ker}\mathcal{T}_0 \subset \boldsymbol{V}_0$ will become essential for characterising $\boldsymbol{V}_N$ (in Theorem 7.32).

A first important advantage of decompositions (7.74) and (7.75) is that contrary to $\boldsymbol{V}_N$, it is possible to give an explicit description of the spaces $\operatorname{Ker}\mathcal{T}$ and $\operatorname{Ker}\mathcal{T}_0$ which are completely independent of the spaces $\boldsymbol{D}$ or $\boldsymbol{D}_N$ and thus, as it was our purpose, both elude any relation with displacement fields.

Lemma 7.30

The kernel of the operators $\mathcal{T}$ and $\mathcal{T}_0$ are characterized by

$$\operatorname{Ker}\mathcal{T} = \big\{\boldsymbol{\xi} = (\xi_P, \xi_S) \in \boldsymbol{V} \,/\, \nabla\xi_P + \mathbf{curl}\,\xi_S \in \boldsymbol{R}(\Omega)\big\}, \tag{7.76}$$

$$\operatorname{Ker}\mathcal{T}_0 = \big\{\boldsymbol{\xi} = (\xi_P, \xi_S) \in \boldsymbol{V}_0 \,/\, \nabla\xi_P + \mathbf{curl}\,\xi_S \in \boldsymbol{R}(\Omega)\big\}. \tag{7.77}$$

Proof. First notice that (7.77) is consequence of (7.76) since $\operatorname{Ker}\mathcal{T}_0 = \mathcal{T} \cap \boldsymbol{V}_0$. Thus we conclude by proving (7.76). Let us consider $\boldsymbol{\xi} \in \operatorname{Ker}\mathcal{T}$, and $\boldsymbol{w}_\star = \mathcal{S}_N\,\boldsymbol{\xi}$, solution of (7.72). Then $\mathcal{T}\boldsymbol{\xi} = 0$ means that $\operatorname{div}\boldsymbol{w}_\star = \operatorname{curl}\boldsymbol{w}_\star = 0$, and therefore $\mathbf{div}\,\underline{\boldsymbol{\sigma}}(\boldsymbol{w}_\star) = \mathbf{0}$ due to Hook's law (5.2). In consequence, since $\boldsymbol{w}_\star$ solves (7.72), we have that $\Pi_R\big(\nabla\xi_P + \operatorname{curl}\xi_S\big) = \mathbf{0}$. Reciprocally, $\nabla\psi_P + \operatorname{curl}\psi_S \in \boldsymbol{R}(\Omega)$ trivially implies that $\boldsymbol{w}_*$ is solution of (7.72).

■

Notice, that decompositions (7.74) and (7.75) are not orthogonal in the classical sense as we expected (i.e. with the scalar product in $\boldsymbol{V}$ or in $L^2(\Omega)^2$). However, for decomposition (7.75) we observe the following relation between $\operatorname{Ker}\mathcal{T}_0$ and $\boldsymbol{V}_N$ that we call m-orthogonality even though $m(\cdot,\cdot)$ is not a scalar product (indeed it is not positive in $\boldsymbol{V}_0$). We shall also remark, that the following result can not even be stated for decomposition (7.74) since $m(\cdot,\cdot)$ is not well defined for those elements not satisfying the gauge conditions (see Remark 7.9).

Lemma 7.31

For any $\boldsymbol{\varphi} \in \boldsymbol{V}_N$ and any $\boldsymbol{\xi} \in \operatorname{Ker} \mathcal{T}_0$ we have $m(\boldsymbol{\varphi}, \boldsymbol{\psi}) = 0$.

Proof. Let us consider $\boldsymbol{\varphi} \in \boldsymbol{V}_N$ and $\boldsymbol{\xi} \in \operatorname{Ker} \mathcal{T}_0$. Thus, by definition of $\boldsymbol{V}_N$, we have that $\boldsymbol{\varphi} = \mathcal{F}(\boldsymbol{w}) = \big(V_P^2 \operatorname{div} \boldsymbol{w}, -V_S^2 \operatorname{curl} \boldsymbol{w}\big)$ for some $\boldsymbol{w} \in \boldsymbol{D}_N$ and consequently

$$m_\Omega(\boldsymbol{\varphi}, \boldsymbol{\xi}) = \int_\Omega (\xi_P \operatorname{div} \boldsymbol{w} - \xi_S \operatorname{curl} \boldsymbol{\xi}) \,\mathrm{d}\boldsymbol{x} = \int_\Omega (\boldsymbol{\xi} \cdot \nabla w_1 + \boldsymbol{\xi} \cdot \mathbf{curl}\, w_2) \,\mathrm{d}\boldsymbol{x}.$$

Moreover, by Green's formulas,

$$\int_\Omega \boldsymbol{\xi} \cdot \nabla w_1 \,\mathrm{d}\boldsymbol{x} = -\int_\Omega \operatorname{div} \boldsymbol{\xi}\, w_1 \,\mathrm{d}\boldsymbol{x} + \int_\Gamma (\boldsymbol{\xi} \cdot \boldsymbol{n})\, w_1 \,\mathrm{d}\gamma,$$
$$\int_\Omega \boldsymbol{w} \cdot \mathbf{curl}\, w_2 \,\mathrm{d}\boldsymbol{x} = \int_\Omega \operatorname{curl} \boldsymbol{\xi}\, w_2 \,\mathrm{d}\boldsymbol{x} + \int_\Gamma (\boldsymbol{\xi} \cdot \boldsymbol{\tau}) w_2 \,\mathrm{d}\gamma,$$

thus we compute

$$\begin{aligned} m_\Omega(\boldsymbol{\varphi}, \boldsymbol{\xi}) \quad &= \quad -\int_\Omega (\operatorname{div} \boldsymbol{\xi}\, w_1 - \operatorname{curl} \boldsymbol{\xi}\, w_2) \,\mathrm{d}\boldsymbol{x} + \int_\Gamma \big((\boldsymbol{\xi} \cdot \boldsymbol{n})\, w_1 + (\boldsymbol{\xi} \cdot \boldsymbol{\tau})\, w_2\big) \,\mathrm{d}\gamma \\ &\quad\; -\int_\Omega (\nabla \xi_P + \mathbf{curl}\, \xi_S) \cdot \boldsymbol{w} \,\mathrm{d}\boldsymbol{x} + \int_\Gamma \big((\boldsymbol{\xi} \cdot \boldsymbol{n})\, w_1 + (\boldsymbol{\xi} \cdot \boldsymbol{\tau})\, w_2\big) \,\mathrm{d}\gamma. \end{aligned}$$

Now we recall that $\nabla \xi_P + \mathbf{curl}\ \xi_S \in \boldsymbol{R}(\Omega)$, while $\boldsymbol{w} \in \boldsymbol{D}_N \subset \boldsymbol{L}_R^2(\Omega)$, thus the volume integral vanishes and it only remains to check if

$$m_\Gamma(\boldsymbol{\varphi}, \boldsymbol{\xi}) = -\int_\Gamma \big((\boldsymbol{\xi} \cdot \boldsymbol{n})\, w_1 + (\boldsymbol{\xi} \cdot \boldsymbol{\tau})\, w_2\big) \,\mathrm{d}\gamma. \tag{7.78}$$

To do so, we need to relate $\boldsymbol{\varphi}$ and $\boldsymbol{w}$ on the boundary Γ which can be done by reproducing the computations in Section 7.1 for proving (7.21), with $\boldsymbol{\varphi}$ instead of $\partial_t \boldsymbol{\varphi}$ and $\boldsymbol{w}$ instead of $\boldsymbol{u}$. Simply note that in this case, the boundary condition $\underline{\boldsymbol{\sigma}}(\boldsymbol{w})\boldsymbol{n} = \boldsymbol{0}$ on Γ follows from $\boldsymbol{w} \in \boldsymbol{D}_N$, while the equivalent of (7.7) is nothing but $\boldsymbol{\varphi} = \mathcal{F}(\boldsymbol{w})$. Then we obtain the equivalent of (7.21), namely, (for constants c_1 and c_2)

$$w_1 + c_1 = \frac{1}{2\,V_S^2}\,\mathcal{I}\big(\boldsymbol{\varphi} \cdot \boldsymbol{\tau}\big) \text{ on } \Gamma \quad \text{and} \quad w_2 + c_2 = -\frac{1}{2\,V_S^2}\,\mathcal{I}\big(\boldsymbol{\varphi} \cdot \boldsymbol{n}\big) \text{ on } \Gamma.$$

This proves (7.78) just considering the definition of $m_\Gamma(\cdot,\cdot)$ (see (7.29)) and noticing that $\boldsymbol{\xi}$ satisfies gauge conditions.

■

Finally, as it was our purpose we provide the following result that characterizes the space $\boldsymbol{V}_N$ as the m-orthogonal to the space $\operatorname{Ker} \mathcal{T}_0$.

Theorem 7.32

We have $\boldsymbol{V}_N = \big(\operatorname{Ker} \mathcal{T}_0\big)^{\perp,m}$ where

$$\big(\operatorname{Ker} \mathcal{T}_0\big)^{\perp,m} \quad := \quad \big\{\boldsymbol{\varphi} \in \boldsymbol{V}_0 \,/\, \forall\, \boldsymbol{\xi} \in \operatorname{Ker} \mathcal{T}_0,\ m(\boldsymbol{\varphi}, \boldsymbol{\xi}) = 0\big\}.$$

Proof. Let us consider any $\boldsymbol{\varphi} \in \boldsymbol{V}_N$ and notice that according to Lemma 7.21 we have that $\boldsymbol{\varphi} \in \boldsymbol{V}_0$. Moreover, for any $\boldsymbol{\xi} \in \operatorname{Ker} \mathcal{T}_0$ we can directly apply Lemma 7.31 to obtain $m(\boldsymbol{\varphi}, \boldsymbol{\xi}) = 0$. Therefore $\boldsymbol{V}_N \subset \big(\operatorname{Ker} \mathcal{T}_0\big)^{\perp,m}$. Now, we proceed to prove the reverse inclusion $\big(\operatorname{Ker} \mathcal{T}_0\big)^{\perp,m} \subset \boldsymbol{V}_N$. To do so we consider any $\boldsymbol{\varphi} \in \big(\operatorname{Ker} \mathcal{T}_0\big)^{\perp,m}$, i.e. $\boldsymbol{\varphi} \in \boldsymbol{V}_0$ such that $m(\boldsymbol{\varphi}, \boldsymbol{\xi}) = 0$ for all $\boldsymbol{\xi} \in \operatorname{Ker} \mathcal{T}_0$. Then, for all $\boldsymbol{\psi} \in \boldsymbol{V}_0$ we can use $\boldsymbol{V}_0$ decomposition (7.75) to decompose both $\boldsymbol{\varphi}$, $\boldsymbol{\psi}$ as:

$$\boldsymbol{\varphi} = \boldsymbol{\varphi}^o + \boldsymbol{\varphi}^N, \quad \boldsymbol{\psi} = \boldsymbol{\psi}^o + \boldsymbol{\psi}^N, \quad (\boldsymbol{\varphi}^o, \boldsymbol{\psi}^o) \in (\operatorname{Ker} \mathcal{T}_0)^2, \quad (\boldsymbol{\varphi}^N, \boldsymbol{\psi}^N) \in \boldsymbol{V}_N^2.$$

And our goal is to prove that $\boldsymbol{\varphi}^o = 0$. Note that by Lemma 7.31,

$$m(\boldsymbol{\varphi}^o, \boldsymbol{\psi}^N) = 0 \qquad \text{and} \qquad m(\boldsymbol{\varphi}^N, \boldsymbol{\psi}^o) = 0. \tag{7.79}$$

Therefore, we compute

$$m(\boldsymbol{\varphi}^o, \boldsymbol{\psi}) = m(\boldsymbol{\varphi}^o, \boldsymbol{\psi}^o) + m(\boldsymbol{\varphi}^o, \boldsymbol{\psi}^N) = m(\boldsymbol{\varphi}^o, \boldsymbol{\psi}^o). \tag{7.80}$$

Next, since $\boldsymbol{\varphi}^o = \boldsymbol{\varphi} - \boldsymbol{\varphi}^N$ and $\boldsymbol{\varphi} \in \left(\operatorname{Ker} \mathcal{T}_0\right)^{\perp,m}$,

$$m(\boldsymbol{\varphi}^o, \boldsymbol{\psi}) = m(\boldsymbol{\varphi}, \boldsymbol{\psi}^o) - m(\boldsymbol{\varphi}^N, \boldsymbol{\psi}^o) \underset{(7.79)}{=} m(\boldsymbol{\varphi}, \boldsymbol{\psi}^o) = 0. \tag{7.81}$$

Thus $m(\boldsymbol{\varphi}^o, \boldsymbol{\psi}) = 0,\ \forall\, \boldsymbol{\psi} \in \boldsymbol{V}_0$. In particular, for all $\boldsymbol{\psi} \in \mathcal{D}(\Omega)^2 \subset \boldsymbol{V}_0$,

$$m_\Omega(\boldsymbol{\varphi}^o, \boldsymbol{\psi}) = m(\boldsymbol{\varphi}^o, \boldsymbol{\psi}) = 0.$$

Thus, we conclude by density of $\mathcal{D}(\Omega)^2$ in $L^2(\Omega)^2$ that $\boldsymbol{\varphi}^o = \mathbf{0}$ and therefore $\boldsymbol{\varphi} \in \boldsymbol{V}_N$. ∎

7.5.2 First stabilized mixed formulation

In this section, as it is usual for treating equality constraints (see [46, 47, 48]), we are going to introduce a Lagrange multiplier to impose the stabilization condition $\boldsymbol{\varphi} \in \boldsymbol{V}_N$, which according to Theorem 7.32 can be rephrased as

$$\boldsymbol{\varphi} \in \boldsymbol{V}_N \quad \Longleftrightarrow \quad \boldsymbol{\varphi} \in \boldsymbol{V}_0 \ \text{ and } \ m(\boldsymbol{\varphi}, \boldsymbol{\xi}) = 0, \quad \forall\, \boldsymbol{\xi} \in \operatorname{Ker} \mathcal{T}_0.$$

To do so, we introduce the new variable $\boldsymbol{\xi} \in \operatorname{Ker} \mathcal{T}_0$ to impose the solution to be in $\boldsymbol{V}_N$. This leads us to rewrite the stabilized problem (7.61) as the following mixed problem

$$\left\{\begin{array}{l} \text{Find } (\boldsymbol{\varphi}, \boldsymbol{\xi}) : [0,T] \longrightarrow \boldsymbol{V}_0 \times \operatorname{Ker} \mathcal{T}_0 \text{ such that } (\boldsymbol{\varphi}, \partial_t \boldsymbol{\varphi})(t=0) = (\mathbf{0}, \mathbf{0}) \text{ and} \\[2ex] \dfrac{\mathrm{d}^2}{\mathrm{d}t^2} m(\boldsymbol{\varphi}(t), \boldsymbol{\psi}) \ + \ a(\boldsymbol{\varphi}(t), \boldsymbol{\psi}) \ + \ m(\boldsymbol{\xi}(t), \boldsymbol{\psi}) \ = \ \mathrm{g}(t, \boldsymbol{\psi}), \qquad \forall\, \boldsymbol{\psi} \in \boldsymbol{V}_0, \qquad (7.82\text{a}) \\[2ex] \qquad\qquad\qquad\qquad\qquad\qquad m(\boldsymbol{\varphi}(t), \boldsymbol{\zeta}) \ = \ 0, \qquad\qquad \forall\, \boldsymbol{\zeta} \in \operatorname{Ker} \mathcal{T}_0. \qquad (7.82\text{b}) \end{array}\right.$$

Remark 7.33

We might be tempted to consider also Lagrange multipliers in order to impose gauge conditions (i.e. $\boldsymbol{\varphi} \in \boldsymbol{V}_0$). However, as we have already mentioned in Remark 7.13, we shall notice that in that case we would seek $\boldsymbol{\varphi}$ directly in $\boldsymbol{V}$ where the bilinear form $m(\cdot,\cdot)$ is not well defined (see Remark 7.9).

Then we have the following equivalence theorem between the above mixed problem and the stabilized variational problem (7.61) posed in the space $\boldsymbol{V}_N$.

Theorem 7.34

Assume that $\boldsymbol{f} \in \mathcal{C}^1\big([0,T]; \boldsymbol{L}^2_R(\Omega)\big)$, then problem (7.82) admits a unique solution given by $(\boldsymbol{\varphi}(t), \mathbf{0})$, where $\boldsymbol{\varphi}(t)$ is the unique solution of the problem (7.61) with regularity

$$\boldsymbol{\varphi} \in \mathcal{C}^2([0,T]; L^2(\Omega)^2) \cap \mathcal{C}^1([0,T]; \boldsymbol{V}_N) \qquad \textit{(see Theorem 7.24).}$$

Proof. Let $\boldsymbol{\varphi}(t)$ be the unique solution of problem (7.61). According to Lemma 7.21 we have that $\boldsymbol{\varphi} \in \boldsymbol{V}_0$. Moreover, it clearly satisfies (7.82b) since $\boldsymbol{V}_N = (\operatorname{Ker} \mathcal{T}_0)^{\perp,m}$ (Theorem 7.32) and thus it only remains to check (7.82a). To do so, we consider the decomposition (7.75) of $\boldsymbol{V}_0$, and we proceed first for the $\boldsymbol{\psi} \in \boldsymbol{V}_N$ and then for the $\boldsymbol{\psi} \in \operatorname{Ker} \mathcal{T}_0$. Notice that for $\boldsymbol{\psi} \in \boldsymbol{V}_N$ the equation (7.82a) becomes exactly the equation in problem (7.61). On the other hand, for $\boldsymbol{\psi} \in \operatorname{Ker} \mathcal{T}_0$ we have by (7.77) that $\nabla \psi_P + \mathbf{curl}\, \psi_S \in \boldsymbol{R}(\Omega)$ and according to the definition of $\mathrm{g}(t, \cdot)$, which is given by (6.21) and (7.9), we have that (since by hypothesis $\boldsymbol{f} \in \boldsymbol{L}^2_R(\Omega)$)

$$\mathrm{g}(t, \boldsymbol{\psi}) = \frac{1}{\rho} \int_0^t \int_\Omega \boldsymbol{f}(\boldsymbol{x}, s) \big(\nabla \psi_P(\boldsymbol{x}) + \mathbf{curl}\, \psi_S(\boldsymbol{x})\big)\, \mathrm{d}\boldsymbol{x}\, \mathrm{d}s = 0, \quad \forall \boldsymbol{\psi} \in \operatorname{Ker} \mathcal{T}_0.$$

Moreover, we also notice that according to Lemma 7.22 we have that $\nabla \varphi_P + \mathbf{curl}\, \varphi_S \in \boldsymbol{L}^2_R(\Omega)$. Then, considering definition of $a(\cdot, \cdot)$, which is given by (6.20), we have that

$$\begin{aligned} a(\boldsymbol{\varphi}(t), \boldsymbol{\psi}) &= \int_\Omega (\operatorname{div} \boldsymbol{\varphi} \operatorname{div} \boldsymbol{\psi} + \operatorname{curl} \boldsymbol{\varphi} \operatorname{curl} \boldsymbol{\psi})\, \mathrm{d}\boldsymbol{x} \\ &= \int_\Omega \big(\nabla \varphi_P + \mathbf{curl}\, \varphi_S\big) \cdot \big(\nabla \psi_P + \mathbf{curl}\, \psi_S\big)\, \mathrm{d}\boldsymbol{x} = 0, \quad \forall \boldsymbol{\psi} \in \operatorname{Ker} \mathcal{T}_0. \end{aligned}$$

Thus, equation (7.82a) reduces to

$$\frac{\mathrm{d}^2}{\mathrm{d}t^2} m(\boldsymbol{\varphi}(t), \boldsymbol{\psi}) = 0, \quad \forall \boldsymbol{\psi} \in \operatorname{Ker} \mathcal{T}_0,$$

which clearly holds from second equation and in consequence, $(\boldsymbol{\varphi}(t), \mathbf{0})$ is solution of (7.82).

It only remains to prove the uniqueness of solutions of (7.82). Let $(\boldsymbol{\varphi}, \boldsymbol{\xi})$ be a solution of (7.82) with $\mathrm{g}(\cdot, \cdot) = 0$. Then, on the one hand (7.82b) implies $\boldsymbol{\varphi} \in \boldsymbol{V}_N$ while on the other hand, by restricting the test function $\boldsymbol{\psi}$ in (7.82a) to $\boldsymbol{\psi} \in \boldsymbol{V}_N$, we deduce that $\boldsymbol{\varphi}$ is the solution of (7.61) with $\mathrm{g}(\cdot, \cdot) = 0$. Thus, by uniqueness of solution of problem (7.61) (see Theorem 7.24) we have that $\boldsymbol{\varphi} = \mathbf{0}$. Finally, we then deduce that

$$m(\boldsymbol{\xi}(t), \boldsymbol{\psi}) = 0, \quad \forall \boldsymbol{\psi} \in \boldsymbol{V}_0,$$

which leads to $\boldsymbol{\xi} = \mathbf{0}$ due to the injectivity property in Lemma 7.11.

■

The reader could be surprised that we introduce an additional unknown that we know is $\mathbf{0}$, however, we remark that in the context of mixed variational formulations this is standard (see for instance sections 9.3 and 9.4 in [47] for other examples). In fact, what is important in problems like (7.82) is not the role of the Lagrange multiplier but the introduction of equation (7.82b). Moreover, it is also interesting to point that after discretization, we can eventually obtain a stable discrete problem in which the approximation of the unknown $\boldsymbol{\xi}$ is no longer $\mathbf{0}$.

7.5.3 Characterization of the multipliers space

Let us begin this section by recalling that the mixed variational problem (7.82) is not only equivalent to problem (7.61), as we show in Theorem 7.34, but it also happens to be nicer in the sense that any reference to displacement fields has been completely removed. However, we shall also notice that the mixed problem (7.82) is still not well adapted for finite element discretization since we need a priori to construct a Galerkin approximation of the space $\operatorname{Ker} \mathcal{T}_0$. In order to work around this problem, we are going to provide a characterization of the space $\operatorname{Ker} \mathcal{T}_0$, which on the one hand is better adapted for discretization, while on the other hand emphasizes the fact that $\operatorname{Ker} \mathcal{T}_0$ is small compared to $\boldsymbol{V}_0$. A first result in this direction is presented in the following lemma.

Lemma 7.35

The space $\ker \mathcal{T}_0$ *can be decomposed as the direct sum*

$$\operatorname{Ker} \mathcal{T}_0 = \boldsymbol{K}_0 \oplus \boldsymbol{K}_R,$$

where

$$\begin{aligned} \boldsymbol{K}_0 &= \left\{\boldsymbol{\xi} \in \boldsymbol{V}_0 \,/\, \nabla\xi_P + \mathbf{curl}\,\xi_S = \mathbf{0}\right\} \\ &= \left\{\boldsymbol{\xi} \in \boldsymbol{V}_0 \,/\, \mathrm{div}\,\boldsymbol{\xi} = \mathrm{curl}\,\boldsymbol{\xi} = 0\right\} \\ \textit{and} \quad \boldsymbol{K}_R &= \mathrm{span}\{\boldsymbol{\xi}_R\} \quad \textit{where} \quad \boldsymbol{\xi}_R = (0, |\boldsymbol{x}|^2)^T. \end{aligned}$$

Proof. Let us consider any $\boldsymbol{\xi} \in \mathrm{Ker}\,\mathcal{T}_0$ and we begin by noticing that

$$\xi \in \boldsymbol{V}_0 \iff \xi \in \boldsymbol{V} \quad \text{and} \quad \int_\Omega \mathrm{div}\,\xi\,\mathrm{d}\boldsymbol{x} = \int_\Omega \mathrm{curl}\,\xi\,\mathrm{d}\boldsymbol{x} = 0. \tag{7.83}$$

Thus, according to the definition (7.77) of $\mathrm{Ker}\,\mathcal{T}_0$, we have that

$$(\mathrm{div}\,\boldsymbol{\xi}, -\mathrm{curl}\,\boldsymbol{\xi})^T \in \left\{\boldsymbol{w} \in \boldsymbol{R}(\Omega) \,/\, \int_\Omega \boldsymbol{w}\,\mathrm{d}\boldsymbol{x} = 0\right\} = \mathrm{span}\{(x_2, -x_1)^T\}$$

and therefore, there exists $a \in \mathbb{R}$ such that $(\mathrm{div}\,\boldsymbol{\xi}, -\mathrm{curl}\,\boldsymbol{\xi})^T = a\,(x_2, -x_1)^T$. Now, notice that this actually gives $(\mathrm{div}\,\boldsymbol{\xi}, -\mathrm{curl}\,\boldsymbol{\xi})^T = (\mathrm{div}\,\boldsymbol{\xi}_{\boldsymbol{R}}, -\mathrm{curl}\,\boldsymbol{\xi}_{\boldsymbol{R}})^T$, or equivalently $\boldsymbol{\xi} - a\,\boldsymbol{\xi}_R \in \boldsymbol{K}_0$ which concludes the prove since $\boldsymbol{\xi} = a\,\boldsymbol{\xi}_R + \boldsymbol{\xi}_0$ for some $\boldsymbol{\xi}_0 \in \boldsymbol{K}_0$.

■

Remark 7.36

In Lemma 7.35 we have characterized $\mathrm{Ker}\,\mathcal{T}_0$ *by distinguishing between the elements in* $\boldsymbol{K}_0$ *that came from the rigid displacement* $\mathbf{0}$ *and the elements in* $\boldsymbol{K}_R$ *that came from the other rigid displacements. The reader might be surprised that* $\boldsymbol{K}_R$ *has dimension one since* $\boldsymbol{R}(\Omega)$ *has dimension three, but this is only due to the intersection with* $\boldsymbol{V}_0$ *which includes two linear constraints.*

Remark 7.37

It is interesting to remark, that $\boldsymbol{\xi}_R$ *will be slightly different if the centre of gravity of* Ω *is not at the origin (assumption made for simplicity at the beginning of Section 7.1).*

Remark 7.38

We also remark, that the characterization (7.83) of $\boldsymbol{V}_0$ *is only valid when* Ω *is simply connected and bounded by* $\Gamma = \partial\Omega$.

A very surprising consequence of Lemma 7.35 is given in Theorem 7.39 that proves the existence and uniqueness of solution in $(\boldsymbol{K}_R)^{\perp,m}$, i.e. of the mixed variational problem

$$\left\{\begin{aligned} &\text{Find } (\boldsymbol{\varphi}, c_R) : [0,T] \longrightarrow \boldsymbol{V}_0 \times \mathbb{R} \text{ such that } (\boldsymbol{\varphi}, \partial_t\boldsymbol{\varphi})(t=0) = (\mathbf{0},\mathbf{0}) \text{ and} \\ &\frac{\mathrm{d}^2}{\mathrm{d}t^2}\, m(\boldsymbol{\varphi}(t), \boldsymbol{\psi}) \;+\; a(\boldsymbol{\varphi}(t), \boldsymbol{\psi}) \;+\; c_R(t)\, m(\boldsymbol{\xi}_R, \boldsymbol{\psi}) \;=\; \mathrm{g}(t, \boldsymbol{\psi}), \qquad \forall\, \boldsymbol{\psi} \in \boldsymbol{V}_0, \qquad (7.84\mathrm{a}) \\ &\qquad\qquad m(\boldsymbol{\varphi}(t), \boldsymbol{\xi}_R) \;=\; 0. \qquad (7.84\mathrm{b}) \end{aligned}\right.$$

Theorem 7.39

Assume that $\boldsymbol{f} \in \mathcal{C}^1\big(0,T; \boldsymbol{L}^2_R(\Omega)\big)$, *then problem (7.84) admits a unique solution given by* $(\boldsymbol{\varphi}(t), 0)$, *where* $\boldsymbol{\varphi}(t)$ *is the unique solution of the problem (7.61) with regularity*

$$\boldsymbol{\varphi} \in \mathcal{C}^2(0,T; L^2(\Omega)^2) \cap \mathcal{C}^1(0,T; \boldsymbol{V}_N) \qquad \textit{(see Theorem 7.24).}$$

Proof. The proof is consequence of Theorem 7.34 and Lemma 7.35. Let us notice that the only difference between problem (7.82) and problem (7.84) seems to be that in (7.84) we do not impose

$$m(\boldsymbol{\varphi}, \boldsymbol{\xi}_0) = 0 \quad \forall \boldsymbol{\xi}_0 \in \boldsymbol{K}_0.$$

However, according to the definitions of $a(\cdot,\cdot)$ and $\mathrm{g}(\cdot)$ (given in (6.20) and (6.21)), when we consider in (7.84a) test functions $\boldsymbol{\psi} \in \boldsymbol{K}_0$, we obtain

$$\frac{\mathrm{d}^2}{\mathrm{d}\, t^2} m(\boldsymbol{\varphi}, \boldsymbol{\xi}_0) = 0 \quad \forall \boldsymbol{\xi}_0 \in \boldsymbol{K}_0.$$

Thus, integrating twice in time and considering the initial condition we complete the proof. ■

Even though problem (7.84) is well posed, it would be naive to believe that the bilinear form $m(\cdot,\cdot)$ is positive in $(\boldsymbol{K}_R)^{\perp,m}$. In fact, according to the negativity result in Theorem 7.12 and the analysis of numerical instabilities developed in Sections 7.2.3 and 7.3, we expect $m(\cdot,\cdot)$ to be negative in a space related to the boundary and infinite dimensional (note that in (7.84) we are m-orthogonal to a space of dimension one). In consequence, any Galerkin discretization of problem (7.84) is expected to be unstable since a reasoning like in Theorem 7.39 is probably not possible at the discrete level. Thus, we still believe that the mixed problem (7.82) is nicer and that an adequate characterization of $\operatorname{Ker} \mathcal{T}_0$ would lead us to an equivalent formulation which is well adapted for discretization. Therefore, as it already was the purpose of this section, we provide a characterization for the space $\operatorname{Ker} \mathcal{T}_0$ which is well adapted for discretization. To do so, and taking into account Lemma 7.35, we need to characterize the space $\boldsymbol{K}_0$. Thus, as a first step, we note that the space $\boldsymbol{K}_0$ is closely related to the space of harmonic functions

$$\mathcal{H}(\Omega) \;:=\; \{q \in H^1(\Omega) \,/\, \Delta q = 0 \text{ in } \Omega\}.$$

This space is known to be such that $\mathcal{H}(\Omega)/\mathbb{R}$ is isomorphic to the space M of boundary functions (defined in (7.19)), so we expect to find also an isomorphism $\mathcal{E}$ between $\boldsymbol{K}_0$ and M. That, would allow us to replace the Lagrange multiplier $\boldsymbol{\xi} \in \operatorname{Ker} \mathcal{T}_0$ by another Lagrange multiplier $\eta \in M$ and obtain an alternative reformulation of the mixed variational problem (7.82) which will be given in Section 7.5.4. We expect this alternative formulation to be satisfactory from the numerical point of view, because it is easy to approximate the space M with finite elements (defined on the boundary Γ). However, we notice that this will depend on the isomorphism $\mathcal{E}$ and how easy is to approximate it numerically.

Lemma 7.40

The space $\boldsymbol{K}_0$ can be alternatively characterized as

$$\boldsymbol{K}_0 \;=\; \nabla\mathcal{H}(\Omega) \;:=\; \{\nabla q \,/\, q \in \mathcal{H}(\Omega)\}.$$

Proof. Let us begin by considering $q \in \mathcal{H}(\Omega)$. On the one hand, $\operatorname{curl} \nabla q = 0$ in Ω since the curl of a gradient is always zero. On the other hand, $\operatorname{div} \nabla q = \Delta q = 0$ in Ω since $q \in \mathcal{H}(\Omega)$. Thus $\nabla\mathcal{H}(\Omega) \subset \boldsymbol{K}_0$. Now, for the reverse inclusion, let us consider $\boldsymbol{\xi} \in \boldsymbol{K}_0$. Then, since $\operatorname{curl} \boldsymbol{\xi} = 0$ in Ω which is simply connected, by Theorem 2.9 in [49], we deduce that $\boldsymbol{\xi} = \nabla q$ with $q \in H^1(\Omega)/\mathbb{R}$. Moreover, since $\operatorname{div} \boldsymbol{\xi} = 0$ in Ω, we have $\Delta q = 0$ in Ω, i.e. $q \in \mathcal{H}(\Omega)$ and thus $\boldsymbol{K}_0 \subset \nabla\mathcal{H}(\Omega)$. ■

An interesting consequence of this characterization is given in the following result that generalizes Theorem 7.12 bringing a new light on the absence of positivity of the bilinear form $m(\cdot,\cdot)$ and emphasizing the “bad role” of $\boldsymbol{K}_0$ and the need for removing this space in the construction of the “good” space $\boldsymbol{V}_N$.

Theorem 7.41

In the space $\boldsymbol{K}_0$, we have the formula

$$\forall \boldsymbol{\xi} \in \boldsymbol{K}_0, \qquad m_\Gamma(\boldsymbol{\xi}, \boldsymbol{\xi}) = -\frac{1}{V_S^2} \int_\Omega |\boldsymbol{\xi}|^2 \, \mathrm{d}\boldsymbol{x}.$$

As a consequence, the quadratic form $m(\boldsymbol{\xi}, \boldsymbol{\xi})$ is negative semi-definite in $\boldsymbol{K}_0$:

$$\forall \boldsymbol{\xi} \in \boldsymbol{K}_0, \qquad m(\boldsymbol{\xi}, \boldsymbol{\xi}) = -\frac{1}{V_*^2} \int_\Omega |\xi_P|^2 \, \mathrm{d}\boldsymbol{x} \quad \textit{where} \quad \frac{1}{V_*^2} := \frac{1}{V_S^2} - \frac{1}{V_P^2} > 0.$$

Proof. According to Lemma 7.40, for any $\boldsymbol{\xi} \in \boldsymbol{K}_0$ there exists $q \in \mathcal{H}(\Omega)$ such that $\boldsymbol{\xi} = \nabla q$. Thus, by definition (7.29) of $m_\Gamma(\cdot, \cdot)$

$$m_\Gamma(\boldsymbol{\varphi}, \boldsymbol{\varphi}) = -\frac{1}{V_S^2} \int_\Gamma \mathcal{I}(\boldsymbol{\xi} \cdot \boldsymbol{\tau}) \, \boldsymbol{\xi} \cdot \boldsymbol{n} \, \mathrm{d}\boldsymbol{\gamma} = -\frac{1}{V_S^2} \int_\Gamma \mathcal{I}(\partial_{\boldsymbol{\tau}} q) \, \partial_{\boldsymbol{n}} q \, \mathrm{d}\boldsymbol{\gamma}.$$

Next, we shall notice that $\mathcal{I}(\partial_{\boldsymbol{\tau}} q) = q + c$ for a constant $c \in \mathbb{R}$ and since q is harmonic $\int_\Gamma \partial_{\boldsymbol{n}} q \, \mathrm{d}\gamma = 0$, thus we compute

$$m_\Gamma(\boldsymbol{\varphi}, \boldsymbol{\varphi}) \, \mathrm{d}\boldsymbol{\gamma} = -\frac{1}{V_S^2} \int_\Gamma q \, \partial_{\boldsymbol{n}} q \, \mathrm{d}\boldsymbol{\gamma} = -\frac{1}{V_S^2} \int_\Omega |\nabla q|^2 \, \mathrm{d}\boldsymbol{x} = -\frac{1}{V_S^2} \int_\Omega |\boldsymbol{\xi}|^2 \, \mathrm{d}\boldsymbol{x}.$$

■

Now, we provide a specific isomorphism between the space M (defined in (7.19)) and a subspace of $\mathcal{H}(\Omega)$ that will be useful later in order to define the isomorphism $\mathcal{E}$ between $\boldsymbol{K}_0$ and M. We introduce the lifting operator $p(\cdot)$ from M into $\mathcal{H}(\Omega)$ that for every $\nu \in M$ assigns the unique $p(\nu) \in \mathcal{H}(\Omega)$ solution of (see Remark 7.42)

$$-\Delta p(\nu) = 0 \text{ in } \Omega, \quad \partial_{\boldsymbol{n}} p(\nu) = \nu \text{ on } \Gamma \quad \text{and} \quad p = \mathcal{I}(\nabla p \cdot \boldsymbol{\tau}) \text{ on } \Gamma. \tag{7.85}$$

It is immediate to see that the lifting operator $p(\cdot)$ is an isomorphism from M into

$$\{p \in \mathcal{H}(\Omega) \,/\, \mathcal{I}(\nabla p \cdot \boldsymbol{\tau}) = p\}.$$

Remark 7.42

It is well known that the first and second equations in (7.85) *define* p *up to an additive constant* b. *Moreover, since the function $d := \mathcal{I}(\nabla p \cdot \boldsymbol{\tau}) - p$ is a constant for any p ($\partial_{\boldsymbol{\tau}} d = 0$), we can adjust the constant b in such a way that the third equation in* (7.85) *is also satisfied.*

Finally, we relate $\boldsymbol{K}_0$ with the space M by introducing the operator $\mathcal{E}$ that we prove next to be an isomorphism

$$\begin{aligned} \mathcal{E} : M \quad &\longrightarrow \quad \boldsymbol{K}_0 \\ \nu \quad &\mapsto \quad \mathcal{E}(\nu) = \nabla p(\nu). \end{aligned} \tag{7.86}$$

Note that $\mathcal{E}(\nu) \in \boldsymbol{K}_0$ since on the one hand $\mathcal{E}(\nu)$ is curl free as any gradient does, while on the other hand the fact that it is divergence free follows from the first equation in (7.85).

Theorem 7.43

The operator $\mathcal{E}$ is an isomorphism from M into $\boldsymbol{K}_0$.

Proof. Let us consider ν such that $\mathcal{E}(\nu) = 0$, thus $\nabla p(\nu) = 0$ and by continuity of the normal trace operator, $\nu = 0$. Therefore $\mathcal{E}$ is injective. Now, let us consider $\boldsymbol{\xi} \in \boldsymbol{K}_0$ and notice that according to Lemma 7.40 there exists $q \in \mathcal{H}(\Omega)$ such that $\boldsymbol{\xi} = \nabla q$. In consequence $\nu = \boldsymbol{\xi} \cdot \boldsymbol{n}$ is such that $\mathcal{E}(\nu) = \boldsymbol{\xi}$. Therefore $\mathcal{E}$ is also surjective which concludes the proof.

■

Finally, before we reformulate the mixed variational problem (7.82) by using Theorem 7.43, we complete this section with a result that confirms the importance of being m-orthogonal to the space $\boldsymbol{K}_0$. Therefore, let us introduce the space

$$\boldsymbol{W}_N := (\boldsymbol{K}_0)^{\perp,m} \qquad \big(\text{notice that } \boldsymbol{W}_N \supset \boldsymbol{V}_N = (\boldsymbol{K}_0 \oplus \boldsymbol{K}_R)^{\perp,m}\big). \tag{7.87}$$

Then, we prove the following result that represents the positive counterpart of Theorem 7.41.

Theorem 7.44

In the space $\boldsymbol{W}_N$, the quadratic form $m(\boldsymbol{\varphi},\boldsymbol{\varphi})$ takes the form (note $\frac{1}{V_*^2} := \frac{1}{V_S^2} - \frac{1}{V_P^2} > 0$)

$$m(\boldsymbol{\varphi},\boldsymbol{\varphi}) = \frac{1}{V_*^2}\int_\Omega |\xi_P|^2\,\mathrm{d}\boldsymbol{x} + m_\Omega(\boldsymbol{\varphi}-\boldsymbol{\xi},\boldsymbol{\varphi}-\boldsymbol{\xi}) \quad \text{where} \quad \boldsymbol{\xi} = \mathcal{E}(\boldsymbol{\varphi}\cdot\boldsymbol{n}) = \nabla p(\boldsymbol{\varphi}\cdot\boldsymbol{n}). \tag{7.88}$$

In consequence, we notice that $m(\boldsymbol{\varphi},\boldsymbol{\varphi}) \geq 0$ for all $\boldsymbol{\varphi} \in \boldsymbol{W}_N$. Moreover, we also prove that

$$m(\boldsymbol{\varphi},\boldsymbol{\varphi}) > 0, \qquad \forall \boldsymbol{\varphi} \in \boldsymbol{V}_N \setminus \{\boldsymbol{0}\}. \tag{7.89}$$

Proof. *Step 1: Proof of* (7.88).
For any $\boldsymbol{\varphi} \in \boldsymbol{W}_N = (\boldsymbol{K}_0)^{\perp,m}$, we know that $\boldsymbol{\xi} = \mathcal{E}(\boldsymbol{\varphi}\cdot\boldsymbol{n}) = \nabla p(\boldsymbol{\varphi}\cdot\boldsymbol{n})$ belongs to $\boldsymbol{K}_0$, so that $m(\boldsymbol{\varphi},\boldsymbol{\xi}) = 0$. Then, if we denote $p_{\boldsymbol{\varphi}} = p(\boldsymbol{\varphi}\cdot\boldsymbol{n})$ we have that

$$\begin{aligned}\frac{1}{V_P^2}\int_\Omega \varphi_P\,\partial_1 p_{\boldsymbol{\varphi}}\,\mathrm{d}\boldsymbol{x} &+ \frac{1}{V_S^2}\int_\Omega \varphi_S\,\partial_2 p_{\boldsymbol{\varphi}}\,\mathrm{d}\boldsymbol{x}\\ &- \frac{1}{2V_S^2}\int_\Gamma \mathcal{I}(\boldsymbol{\varphi}\cdot\boldsymbol{\tau})\,\partial_{\boldsymbol{n}} p_{\boldsymbol{\varphi}}\,\mathrm{d}\gamma - \frac{1}{2V_S^2}\int_\Gamma \mathcal{I}\big(\partial_{\boldsymbol{\tau}} p_{\boldsymbol{\varphi}}\big)\,\boldsymbol{\varphi}\cdot\boldsymbol{n}\,\mathrm{d}\gamma = 0.\end{aligned} \tag{7.90}$$

Now, considering the definition of $p_{\boldsymbol{\varphi}} = p(\boldsymbol{\varphi}\cdot\boldsymbol{n})$ which is given by (7.85), we rewrite the last two terms as

$$-\frac{1}{2V_S^2}\int_\Gamma \mathcal{I}(\boldsymbol{\varphi}\cdot\boldsymbol{\tau})\,\partial_{\boldsymbol{n}} p_{\boldsymbol{\varphi}}\,\mathrm{d}\gamma = -\frac{1}{2V_S^2}\int_\Gamma \mathcal{I}(\boldsymbol{\varphi}\cdot\boldsymbol{\tau})\,\boldsymbol{\varphi}\cdot\boldsymbol{\tau}\,\mathrm{d}\gamma = \frac{1}{2}\,m_\Gamma(\boldsymbol{\varphi},\boldsymbol{\varphi})$$

$$\text{and} \quad -\frac{1}{2V_S^2}\int_\Gamma \mathcal{I}\big(\partial_{\boldsymbol{\tau}} p_{\boldsymbol{\varphi}}\big)\,\boldsymbol{\varphi}\cdot\boldsymbol{n}\,\mathrm{d}\gamma = -\frac{1}{2V_S^2}\int_\Gamma p_{\boldsymbol{\varphi}}\,\partial_{\boldsymbol{n}} p_{\boldsymbol{\varphi}}\,\mathrm{d}\gamma = -\frac{1}{2V_S^2}\int_\Omega |\nabla p_{\boldsymbol{\varphi}}|^2\,\mathrm{d}\boldsymbol{x}.$$

In consequence, if we introduce this into equation (7.90) we deduce that

$$m_\Gamma(\boldsymbol{\varphi},\boldsymbol{\varphi}) = \frac{1}{V_S^2}\int_\Omega |\nabla p_{\boldsymbol{\varphi}}|^2\,\mathrm{d}\boldsymbol{x} - \frac{2}{V_P^2}\int_\Omega \varphi_P\,\partial_1 p_{\boldsymbol{\varphi}}\,\mathrm{d}\boldsymbol{x} - \frac{2}{V_S^2}\int_\Omega \varphi_S\,\partial_2 p_{\boldsymbol{\varphi}}\,\mathrm{d}\boldsymbol{x},$$

and therefore, adding $m_\Omega(\boldsymbol{\varphi},\boldsymbol{\varphi})$,

$$\begin{aligned} m(\boldsymbol{\varphi},\boldsymbol{\varphi}) &= \frac{1}{V_P^2}\int_\Omega |\varphi_P|^2\,\mathrm{d}\boldsymbol{x} - \frac{2}{V_P^2}\int_\Omega \varphi_P\,\partial_1 p_{\boldsymbol{\varphi}}\,\mathrm{d}\boldsymbol{x} + \frac{1}{V_S^2}\int_\Omega |\partial_1 p_{\boldsymbol{\varphi}}|^2\,\mathrm{d}\boldsymbol{x}\\ &+ \frac{1}{V_S^2}\int_\Omega |\varphi_S|^2\,\mathrm{d}\boldsymbol{x} - \frac{2}{V_S^2}\int_\Omega \varphi_S\,\partial_2 p_{\boldsymbol{\varphi}}\,\mathrm{d}\boldsymbol{x} + \frac{1}{V_S^2}\int_\Omega |\partial_2 p_{\boldsymbol{\varphi}}|^2\,\mathrm{d}\boldsymbol{x}.\end{aligned}$$

Notice that we can rearrange the above expression as a sum of squares and thus considering $\boldsymbol{\xi} = \nabla p_{\boldsymbol{\varphi}}$, we obtain (7.88).

Step 2: $m(\boldsymbol{\varphi},\boldsymbol{\varphi}) = 0$ and $\boldsymbol{\varphi} \in \boldsymbol{V}_N = (\boldsymbol{K}_0 \oplus \boldsymbol{K}_R)^{\perp,m}$ implies $\boldsymbol{\varphi} = 0$.

Since $\boldsymbol{\varphi} \in \boldsymbol{V}_N \subset (\boldsymbol{K}_0)^{\perp,m}$, we can use (7.88). Therefore, the condition $m(\boldsymbol{\varphi},\boldsymbol{\varphi}) = 0$ implies $\partial_1 p_{\boldsymbol{\varphi}} = 0$ as well as $\boldsymbol{\varphi} = \nabla p_{\boldsymbol{\varphi}}$. In consequence $\varphi_P = 0$ and $p_{\boldsymbol{\varphi}}(x_1,x_2) \equiv p_{\boldsymbol{\varphi}}(x_2)$. Moreover, since $p_{\boldsymbol{\varphi}}$ is harmonic (i.e. $\partial_2^2 p_{\boldsymbol{\varphi}} = 0$), we deduce that $\varphi_S = \partial_2 p_{\boldsymbol{\varphi}} = a$ for some constant $a \in \mathbb{R}$. Written differently, we thus have

$$\boldsymbol{\varphi} = a\,\boldsymbol{\varphi}_* \quad \text{where} \quad \boldsymbol{\varphi}_* := (0,1)^T. \tag{7.91}$$

It remains to show that $a = 0$ and this is where we are going to use the m-orthogonality to the space $\boldsymbol{K}_R = \operatorname{span}\{\boldsymbol{\xi}_R\}$ (where $\boldsymbol{\xi}_R = \frac{1}{2}(0, |\boldsymbol{x}|^2)^t$ according to Lemma 7.35). To do so, we first notice that, since $m(\boldsymbol{\varphi}, \boldsymbol{\xi}_R) = a\, m(\boldsymbol{\varphi}_*, \boldsymbol{\xi}_R)$, it suffices to check that $m(\boldsymbol{\varphi}_*, \boldsymbol{\xi}_R) \neq 0$. Thus we first compute

$$m_\Omega(\boldsymbol{\varphi}_*, \boldsymbol{\xi}_R) = \frac{J}{2V_S^2}, \quad \text{where} \quad J := \int_\Omega |\boldsymbol{x}|^2 \,\mathrm{d}\boldsymbol{x} > 0 \quad (\text{inertia momentum of } \Omega).$$

Next, in order to compute $m_\Gamma(\boldsymbol{\varphi}_*, \boldsymbol{\xi}_R)$, we notice that $\boldsymbol{\varphi}_* = -\mathbf{curl}\, q_1 = \nabla q_2$ with $q_1(\boldsymbol{x}) = x_1$ and $q_2(\boldsymbol{x}) = x_2$. Thus, according to definition (7.27) of $m_\Gamma(\cdot,\cdot)$, we have (since $\mathbf{curl}\, q_1 \cdot \boldsymbol{n} = -\partial_{\boldsymbol{\tau}} q_1$ and $\nabla q_2 \cdot \boldsymbol{\tau} = \partial_{\boldsymbol{\tau}} q_2$)

$$m_\Gamma(\boldsymbol{\varphi}_*, \boldsymbol{\xi}_R) = \frac{1}{2\,V_S^2} \int_\Gamma \mathcal{I}(\partial_\tau q_1)\, \boldsymbol{\xi}_R \cdot \boldsymbol{\tau} \,\mathrm{d}\boldsymbol{\gamma} - \frac{1}{2\,V_S^2} \int_\Gamma \mathcal{I}(\partial_\tau q_2)\, \boldsymbol{\xi}_R \cdot \boldsymbol{n} \,\mathrm{d}\boldsymbol{\gamma}. \tag{7.92}$$

Moreover, for $j \in \{1, 2\}$ we have that $\mathcal{I}(\partial_{\boldsymbol{\tau}} q_j) = q_j + c_j$ for a constant $c_j \in \mathbb{R}$ and since $\boldsymbol{\xi}_R \in \boldsymbol{V}_0$ (thus satisfies gauge conditions) we compute

$$\begin{aligned} &\int_\Gamma \mathcal{I}(\partial_\tau q_1)\, \boldsymbol{\xi}_R \cdot \boldsymbol{\tau} \,\mathrm{d}\boldsymbol{\gamma} = \int_\Gamma q_1\, \boldsymbol{\xi}_R \cdot \boldsymbol{\tau} \,\mathrm{d}\boldsymbol{\gamma} = -\frac{1}{2} \int_\Gamma x_1 |\boldsymbol{x}|^2\, n_1 \mathrm{d}\boldsymbol{\gamma}, \\ \text{and} \quad &\int_\Gamma \mathcal{I}(\partial_\tau q_2)\, \boldsymbol{\xi}_R \cdot \boldsymbol{n} \,\mathrm{d}\boldsymbol{\gamma} = \int_\Gamma q_2\, \boldsymbol{\xi}_R \cdot \boldsymbol{n} \,\mathrm{d}\boldsymbol{\gamma} = -\frac{1}{2} \int_\Gamma x_2 |\boldsymbol{x}|^2\, n_2 \,\mathrm{d}\boldsymbol{\gamma}. \end{aligned}$$

In consequence, if we introduce this into equation (7.92) we deduce that

$$m_\Gamma(\boldsymbol{\varphi}_*, \boldsymbol{\xi}_R) = \frac{-1}{4V_S^2} \int_\Gamma \boldsymbol{x} \cdot \boldsymbol{n}\, |\boldsymbol{x}|^2 \,\mathrm{d}\boldsymbol{\gamma} = \frac{-1}{4V_S^2} \int_\Omega \left(\operatorname{div}(\boldsymbol{x}) |\boldsymbol{x}|^2 + \boldsymbol{x}\, \nabla |\boldsymbol{x}|^2\right) \mathrm{d}\boldsymbol{x} \;=\; -\frac{\mathbf{J}}{V_S^2}.$$

Finally, we notice that

$$m(\boldsymbol{\varphi}_*, \boldsymbol{\xi}_R) = m_\Omega(\boldsymbol{\varphi}_*, \boldsymbol{\xi}_R) + m_\Gamma(\boldsymbol{\varphi}_*, \boldsymbol{\xi}_R) = -\frac{\mathbf{J}}{2V_S^2} \neq 0, \tag{7.93}$$

which concludes the proof.

■

The reader might notice that in Theorem 7.23 we have proved a stronger result, namely,

$$m(\boldsymbol{\varphi}, \boldsymbol{\varphi}) \geq \alpha_m \int_\Omega |\varphi|^2 \,\mathrm{d}\boldsymbol{x}, \qquad \forall\, \boldsymbol{\varphi} \in \boldsymbol{V}_N, \quad \text{for some} \quad \alpha_m > 0. \tag{7.94}$$

However, the proof of Theorem 7.23 refers to displacement fields since it uses the characterization (7.68) of the space $\boldsymbol{V}_N$ as well as the Korn's inequality in $\boldsymbol{D}_R$ (see Proposition 7.4). In consequence, it seems difficult to extend to the discrete setting. On the other hand, the proof of Theorem 7.44 avoids any reference to displacement fields and as it will be shown later, it can be extended to the discrete setting.

Finally, even though it is not clear how to deduce (7.94) from (7.88) and (7.89), we note that (7.88) yields the following "partial" L^2 coercivity result, namely

$$m(\boldsymbol{\varphi}, \boldsymbol{\varphi}) \geq \alpha_* \int_\Omega |\varphi_P|^2 \,\mathrm{d}\boldsymbol{x}, \qquad \forall\, \boldsymbol{\varphi} \in \boldsymbol{V}_N, \quad \text{for some } \alpha_* > 0.$$

7.5.4 Second stabilized mixed formulation

The variational mixed problem (7.82) can now be reformulated taking into account Lemma 7.35 and Theorem 7.43. Thus we obtain a new variational problem in which the Lagrange multiplier

$\boldsymbol{\xi} \in \operatorname{Ker} \mathcal{T}_0$ is replaced by two new Lagrange multipliers that we denote $(\eta, \eta_R) \in M \times \mathbb{R}$.

$$\left\{\begin{array}{l}\text{Find } (\boldsymbol{\varphi}, \eta, \eta_R) : [0,T] \longrightarrow \boldsymbol{V}_0 \times M \times \mathbb{R} \text{ such that } (\boldsymbol{\varphi}, \partial_t \boldsymbol{\varphi})(t=0) = (\mathbf{0}, \mathbf{0}) \text{ and} \\[2mm] \dfrac{\mathrm{d}^2}{\mathrm{d}t^2} m(\boldsymbol{\varphi}, \boldsymbol{\psi}) \; + \; a(\boldsymbol{\varphi}, \boldsymbol{\psi}) \; + \; b(\eta, \boldsymbol{\psi}) \; + \; \eta_R \, m(\boldsymbol{\xi}_R, \boldsymbol{\psi}) \; = \; \mathrm{g}(t, \boldsymbol{\psi}), \qquad \forall \, \boldsymbol{\psi} \in \boldsymbol{V}_0, \quad (7.95\mathrm{a}) \\[2mm] \hfill b(\nu, \boldsymbol{\varphi}) \; = \; 0, \qquad \forall \, \nu \in M, \quad (7.95\mathrm{b}) \\[2mm] \hfill m(\boldsymbol{\xi}_R, \boldsymbol{\varphi}) \; = \; 0, \qquad (7.95\mathrm{c}) \end{array}\right.$$

where the bilinear form $b(\cdot,\cdot)$ is defined by (see (7.86) for the definition of $\mathcal{E}$)

$$b : M \times \boldsymbol{V}_0 \longrightarrow \mathbb{R} \quad \text{such that} \quad b(\nu, \boldsymbol{\psi}) \coloneqq m(\mathcal{E}(\nu), \boldsymbol{\psi}). \tag{7.96}$$

Finally we conclude this section with the following result that provides the well posedness of the mixed variational problem (7.95) as well as its equivalence to previous formulations.

Theorem 7.45

Assume that $\boldsymbol{f} \in \mathcal{C}^1\big([0,T]; \boldsymbol{L}^2_R(\Omega)\big)$, then problem (7.95) admits a unique solution given by $(\boldsymbol{\varphi}(t), \mathbf{0})$, where $\boldsymbol{\varphi}(t)$ is the unique solution of the problem (7.61) with regularity

$$\boldsymbol{\varphi} \in \mathcal{C}^2([0,T]; L^2(\Omega)^2) \cap \mathcal{C}^1([0,T]; \boldsymbol{V}_N) \qquad \textit{(see Theorem 7.24).}$$

Proof. Notice that according to Theorem 7.43 and the definition (7.96) of the bilinear form $b(\cdot,\cdot)$, the problem (7.95) is equivalent to problem (7.82). Thus the proof is direct consequence of Theorem 7.34. ■

7.6 The stabilized approach for the toy problem

In this section, in order to analyse the stabilized mixed formulation (7.95) in a simplified configuration, we go back to the particular case of the toy problem described in Section 7.3. We shall recall that in this context, since we assume Ω to be unbounded, there is no rigid motion in $L^2(\Omega)$. Moreover, the major advantage of this simplified configuration is that the operator $\mathcal{E}$ can be exactly evaluated as we show next. First, let us notice that in this configuration the functional space M (defined in (7.19)) reduces to

$$M = \left\{ \nu \in H^{-\frac{1}{2}}(-\pi, \pi) \, / \, \int_{-\pi}^{\pi} \nu(x_2) \, \mathrm{d}x_2 = 0 \right\}.$$

Then, the isomorphism $\mathcal{E}$ defined in (7.86) between M and $\boldsymbol{K}_0$, reduces to $\mathcal{E}\,\nu = \nabla p(\nu)$ where $p(\nu) = p_\nu$ is the unique solution of (according to definition (7.85)) that we provide next (see (7.97))

$$\text{Find } p_\nu \in H^1_{per}(\Omega) \coloneqq \left\{ \, q \in H^1(\Omega) \text{ s.t. } q(x_1, -\pi) = q(x_1, \pi), \, x_1 \in \mathbb{R}^+ \right\} \text{ such that}$$

$$\int_\Omega \nabla p_\nu \cdot \nabla q \, \mathrm{d}\boldsymbol{x} = \int_{-\pi}^{\pi} \nu(x_2) \, q(x_2, 0) \, \mathrm{d}x_2, \quad \forall q \in H^1_{per}(\Omega).$$

Remark 7.46

Notice that the uniqueness of solution of previous problem is simple since $\nabla p_\nu = 0$ implies $p_\nu = cte$ but since Ω is unbounded then the constants do not belong to $H^1(\Omega)$. On the other hand, the existence of solution is complicated to ensure and requires technical results (see for *instance [105]). However we avoid these difficulties by providing an explicit expression for the solution that of course guarantees the existence.*

Both p_ν and $\mathcal{E}\nu$ can be computed explicitly using separation of variables and Fourier series in x_2. More precisely, writing that

$$\nu := \sum_{\ell\neq 0} \nu_\ell \, e^{-\mathbb{i}\ell x_2},$$

one can easily show that

$$p_\nu = \sum_{\ell\neq 0} \nu_\ell \, p^\ell(x_1)\, e^{-\mathbb{i}\ell x_2} \quad \text{with} \quad p^\ell(x_1) := \frac{1}{|\ell|}\, e^{-|\ell| x_1}, \quad \forall\, \ell \neq 0, \tag{7.97}$$

and in consequence

$$\mathcal{E}\nu = \sum_{\ell\neq 0} \nu_\ell \, \mathcal{E}^\ell(x_1)\, e^{-\mathbb{i}\ell x_2} \quad \text{with} \quad \mathcal{E}^\ell(x_1) := -\big(\, e^{-|\ell| x_1}, \mathbb{i}\,\mathrm{sign}(\ell)\, e^{-|\ell| x_1}\,\big)^T, \quad \forall\, \ell \neq 0. \tag{7.98}$$

7.6.1 Space discretization

For the discretization, we keep the same notation as in Section 7.3.1 and we only need to provide an approximation space for M. Thus we introduce the new finite dimensional space

$$M_h^L \equiv M_L := \Big\{ \eta_L(x_2) = \sum_{\ell=-L_M}^{L} \eta^\ell e^{-\mathbb{i}\ell x_2} \;\text{ with }\; \eta^0 = 0 \Big\}.$$

First, notice that this space is independent of the discretization in the direction x_1, while on the direction x_2 we truncate the spectral approximation at order L (we recall $L = \min\{L_P, L_S\}$). In this context, we have already mentioned that no rigid motion exists in $L^2(\Omega)$. Moreover, as we have already pointed in Section 7.3.1, the gauge conditions are trivially satisfied. Thus, a semi-discrete approximation of problem (7.95) reads:

$$\left\{\begin{array}{l}
\text{Find } (\boldsymbol{\phi}_h^L, \eta_L) : [0,T] \longrightarrow \boldsymbol{V}_{0h}^L \times M_L \text{ such that } (\boldsymbol{\phi}_h^L, \partial_t \boldsymbol{\phi}_h^L)(t=0) = (\mathbf{0},\mathbf{0}) \text{ and} \\[2ex]
\dfrac{\mathrm{d}^2}{\mathrm{d}t^2}\, m(\boldsymbol{\phi}_h^L, \boldsymbol{\psi}_h^L) \;+\; a(\boldsymbol{\phi}_h^L, \boldsymbol{\psi}_h^L) \;+\; b(\eta_L, \boldsymbol{\psi}_h^L) \;=\; \mathrm{g}(t, \boldsymbol{\psi}_h^L), \qquad \forall\, \boldsymbol{\psi}_h^L \in \boldsymbol{V}_{0h}^L, \qquad (7.99\text{a}) \\[2ex]
\qquad\qquad\qquad\qquad\qquad\qquad b(\nu_L, \boldsymbol{\phi}_h^L) \;=\; 0, \qquad\qquad \forall\, \nu_L \in M_L. \qquad (7.99\text{b})
\end{array}\right.$$

Moreover, we can proceed as in Section 7.3.1 and rewrite the semi-discrete problem (7.99) as a family of $2\max\{L_P, L_S\}+1$ problems in 1D that are parametrized by ℓ and can be analysed separately. More precisely, for each frequency $\ell \in [-L, L] \setminus \{0\}$ we have to solve the following semi-discrete problem (notice the Lagrange multiplier is simply a scalar and the spaces $V_{Q,h}^{1\mathrm{D}}$ for $Q \in \{P, S\}$ are defined in (7.42))

$$\left\{\begin{array}{l}
\text{Find } \big(\boldsymbol{\varphi}_h^\ell, \eta^\ell\big) : \mathbb{R}^+ \longrightarrow V_{P,h}^{1\mathrm{D}} \times V_{S,h}^{1\mathrm{D}} \times \mathbb{R} \text{ such that } (\boldsymbol{\varphi}_h^\ell, \partial_t \boldsymbol{\varphi}_h^\ell)(t=0) = (\mathbf{0},\mathbf{0}) \text{ and} \\[2ex]
\dfrac{\mathrm{d}^2}{\mathrm{d}t^2}\, m_\ell(\boldsymbol{\varphi}_h^\ell(t), \boldsymbol{\psi}_h^\ell) + a_\ell(\boldsymbol{\varphi}_h^\ell(t), \boldsymbol{\psi}_h^\ell) + \eta^\ell(t)\, b_\ell(\boldsymbol{\psi}_h^\ell) = \mathrm{g}_\ell(t, \boldsymbol{\psi}_h^\ell), \quad \forall\, \boldsymbol{\psi}_h^\ell \in V_{P,h}^{1\mathrm{D}} \times V_{S,h}^{1\mathrm{D}} \quad (7.100\text{a}) \\[2ex]
b_\ell(\boldsymbol{\varphi}_h^\ell(t)) = 0, \qquad\qquad\qquad\qquad\qquad\qquad\qquad\qquad\qquad\qquad\qquad\qquad (7.100\text{b})
\end{array}\right.$$

where the linear form $b_\ell(\boldsymbol{\psi}_h^\ell) := m_\ell\big(\boldsymbol{\psi}_h^\ell, \mathcal{E}^\ell\big)$ can be exactly evaluated since according to (7.45) and (7.98),

$$\begin{aligned}
b_\ell(\boldsymbol{\psi}_h^\ell) \;=\; & -\frac{1}{V_P^2}\int_{\mathbb{R}^+} \psi_{P,h}^\ell\, e^{-|\ell| x_1}\,\mathrm{d}x_1 + \frac{\mathbb{i}\,\mathrm{sign}(\ell)}{V_S^2}\int_{\mathbb{R}^+} \psi_{S,h}^\ell\, e^{-|\ell| x_1}\,\mathrm{d}x_1 \\
& -\frac{\mathbb{i}}{2\,\ell\, V_S^2}\,\psi_{S,h}^\ell(0) + \frac{1}{2\,|\ell|\, V_S^2}\,\psi_{P,h}^\ell(0).
\end{aligned} \tag{7.101}$$

Remark 7.47

Similarly to Remark 7.17, we notice that problem (7.100) is simpler when $\ell = 0$ and also when $|\ell| > L$ since

- $\ell = 0 \implies \varphi_P^{0,0} = \varphi_S^{0,0} = 0$, *thus the bilinear forms $m_{\ell,\Gamma}(\cdot,\cdot)$ and $a_{\ell,\Gamma}(\cdot,\cdot)$ vanish and we just introduce $\mathcal{E}^0(\cdot) = 0$.*
- $|\ell| > L \implies$ *For $Q \in \{P, S\}$ such that $L_Q = L$, we have that $\varphi_{Q,h}^{\ell} = 0$ while the other potential is decoupled. Then, we also consider $\mathcal{E}^{\ell}(\cdot) = 0$.*

In consequence, the analysis on both cases is rather standard. Then, in the following, we will focus on the more complex situation which corresponds to $\ell \in [-L, L] \setminus \{0\}$.

Notice that in this context the algebraic system associated to (7.99) reads as (completed with vanishing initial conditions $\boldsymbol{\phi}_h^L(0) = \frac{\mathrm{d}}{\mathrm{d}t}\boldsymbol{\phi}_h^L(0) = \mathbf{0}$)

$$\begin{cases} \mathbb{M}_h^L \dfrac{\mathrm{d}^2\boldsymbol{\phi}_h^L}{\mathrm{d}t^2} + \mathbb{A}_h^L\,\boldsymbol{\phi}_h^L + \eta_L \mathbb{B}_h^L = \boldsymbol{G}_h^L, & (7.102a) \\ (\mathbb{B}_h^L)^T\,\boldsymbol{\phi}_h^L = 0, & (7.102b) \end{cases}$$

where $\mathbb{M}_h^L$ and $\mathbb{A}_h^L$ are still the operators defined in (7.47), while $\mathbb{B}_h^L$ is defined as the operator

$$\mathbb{B}_h^L = \bigoplus_{\ell} \boldsymbol{B}_{h,\ell},$$

where for each $\ell \in [-L, L]\backslash\{0\}$ we represent $\boldsymbol{B}_{h,\ell}$ by the infinite vector $\boldsymbol{B}_{h,\ell} \coloneqq (\boldsymbol{B}_{P,h}^{\ell}, \boldsymbol{B}_{S,h}^{\ell})^T$ that can be computed exactly and is given by

$$\begin{aligned} (\boldsymbol{B}_{P,h}^{\ell})_1 &= \frac{1}{|\ell|^2 h_P V_P^2} - \frac{1}{|\ell| V_P^2} + \frac{1}{2V_S^2|\ell|} - \frac{e^{-|\ell| h_P}}{|\ell|^2 h_P V_P^2}, \\ (\boldsymbol{B}_{P,h}^{\ell})_j &= \frac{2\,e^{-jh_P|\ell|}\big(1 - \cosh(|\ell| h_P)\big)}{|\ell|^2 h_P V_P^2}, \quad \text{for } j \geq 2 \\ (\boldsymbol{B}_{S,h}^{\ell})_1 &= -\frac{\mathrm{i}}{\ell|\ell| h_S V_S^2} + \frac{\mathrm{i}}{2\,\ell\, V_S^2} + \frac{\mathrm{i}\,e^{-|\ell| h_S}}{\ell|\ell| h_S V_S^2}, \\ (\boldsymbol{B}_{S,h}^{\ell})_j &= -\frac{2\,e^{-jh_S|\ell|}\big(1 - \cosh(|\ell| h_S)\big)}{\ell|\ell| h_S V_S^2}, \quad \text{for } j \geq 2. \end{aligned}$$

Remark 7.48

We remark that we can use quadrature formula (7.49) for the computation of the stabilization term (7.101). In that case we denote $\widetilde{\boldsymbol{B}}_{h,\ell}$ instead of $\boldsymbol{B}_{h,\ell}$ (and in consequence $\widetilde{\mathbb{B}}_h^L$ instead of $\mathbb{B}_h^L$) which is represented by the infinite vector $\widetilde{\boldsymbol{B}}_{h,\ell} \coloneqq (\widetilde{\boldsymbol{B}}_{P,h}^{\ell}, \widetilde{\boldsymbol{B}}_{S,h}^{\ell})^T$ where

$$(\widetilde{\boldsymbol{B}}_{P,h}^{\ell})_1 = -\frac{h_P}{2\,V_P^2} + \frac{1}{2\,|\ell| V_S^2}, \qquad \text{and} \quad (\widetilde{\boldsymbol{B}}_{P,h}^{\ell})_j = -\frac{h_P\,e^{-jh_P|\ell|}}{V_P^2}, \quad \text{for } j \geq 2,$$

$$(\widetilde{\boldsymbol{B}}_{S,h}^{\ell})_1 = \frac{\mathrm{i}\,h_S\,\mathrm{sign}(\ell)}{2\,V_S^2} - \frac{\mathrm{i}\,\mathrm{sign}(\ell)}{2\,V_S^2|\ell|}, \quad \text{and} \quad (\widetilde{\boldsymbol{B}}_{S,h}^{\ell})_j = \frac{\mathrm{i}\,h_S\,\mathrm{sign}(\ell)\,e^{-jh_S|\ell|}}{V_S^2}, \quad \text{for } j \geq 2.$$

7.6.2 Well-posedness and stability analysis

It is well known that the well-posedness and stability analysis of the semi-discrete problem (7.100) is linked to the two following properties:

i) The uniform coercivity of the bilinear form $m_\ell(\cdot,\cdot)$ in the kernel of $b_\ell(\cdot)$.

ii) The verification of an adequate *uniform Inf-Sup condition.*

Let us begin by verifying *ii*) which is simpler since in our context reduces to the following result.

Proposition 7.49

For any fixed $h_\star > 0$ we prove for $h \in (0, h_\star]$, that there exists a constant $\delta > 0$ independent of h such that

$$\exists\, \boldsymbol{\varphi}_h \in V^{1D}_{P,h} \times V^{1D}_{S,h} \quad \textit{such that} \quad \boldsymbol{B}_{h,\ell}\, \boldsymbol{\varphi}_h \geq \delta \|\boldsymbol{\varphi}_h\|_{L^2(\mathbb{R}^+,\mathbb{C})^2}.$$

Proof. Let us consider $\boldsymbol{\varphi}_h = (w_0, 0)$ where w_0 is the piecewise affine function that satisfies $w_0(0) = 1$ and $w_0(j\, h_P) = 0$ for all $j > 1$. Then, by straightforward computations we obtain

$$\|\boldsymbol{\varphi}_h\|^2_{L^2(\mathbb{R}^+,\mathbb{C})^2} = \frac{h_P}{3} \quad \text{and} \quad \boldsymbol{B}_{h,\ell}\, \boldsymbol{\varphi}_h = \frac{1 - e^{-|\ell| h_P}}{V_P^2\, h_P\, |\ell|^2} + \frac{1}{|\ell|}\Big(\frac{1}{2\, V_S^2} - \frac{1}{V_P^2}\Big).$$

In consequence, since $e^{-|\ell| h_P} < 1$ and $2V_S^2 < V_P^2$ we can conclude that

$$\frac{\boldsymbol{B}_{h,\ell}\, \boldsymbol{\varphi}_h}{\|\boldsymbol{\varphi}_h\|_{L^2(\mathbb{R}^+,\mathbb{C})^2}} = \frac{3^{\frac12}\,(1 - e^{-|\ell| h_P})}{V_P^2\, h_P^{\frac32}\, |\ell|^2} + \frac{3^{\frac12}}{h_P^{\frac12}\, |\ell|}\big(\frac{1}{2\, V_S^2} - \frac{1}{V_P^2}\big) > \frac{3^{\frac12}}{h_\star^{\frac12}\, |\ell|}\big(\frac{1}{2\, V_S^2} - \frac{1}{V_P^2}\big) =: \delta > 0.$$

■

Next, we focus on the verification of the property *i*) which can be seen as the discrete equivalent of Theorem 7.23.

Proposition 7.50

There exists $K_e > 0$ independent of h such that

$$\boldsymbol{B}_{h,\ell}\, \boldsymbol{\varphi}_h = 0 \quad \Longrightarrow \quad \boldsymbol{\varphi}_h^* \mathbb{M}_{h,\ell} \boldsymbol{\varphi}_h > K_e \|\boldsymbol{\varphi}_h\|^2_{L^2(\mathbb{R}^+,\mathbb{C})^2}.$$

Proof. We first recall that according to the definition of $m_\ell(\cdot,\cdot)$ (see (7.48)), we obtain

$$\begin{aligned} \boldsymbol{\varphi}_h^* \mathbb{M}_{h,\ell} \boldsymbol{\varphi}_h &= \frac{h_P}{V_P^2} \varphi_{P,h}^* \mathbb{M}_\Omega \varphi_{P,h} + \frac{h_S}{V_S^2} \varphi_{S,h}^* \mathbb{M}_\Omega \varphi_{S,h} + \frac{\mathbb{i}}{2V_S^2 \ell}\, \varphi^0_{S,h} \overline{\varphi^0_{P,h}} - \frac{\mathbb{i}}{2V_S^2 \ell}\, \varphi^0_{P,h} \overline{\varphi^0_{S,h}} \\ &= \frac{\|\varphi_{P,h}\|^2_{L^2(\mathbb{R}^+,\mathbb{C})}}{V_P^2} + \frac{\|\varphi_{S,h}\|^2_{L^2(\mathbb{R}^+,\mathbb{C})}}{V_S^2} - \frac{1}{\ell\, V_S^2} \mathrm{Im}\big(\overline{\varphi^0_{P,h}} \varphi^0_{S,h}\big). \end{aligned} \tag{7.103}$$

Next we obtain bounds for the last term on the right hand side. From the assumption $\boldsymbol{B}_{h,\ell}\, \boldsymbol{\varphi}_h = 0$ we know that $\mathbb{i}\, \overline{\varphi^0_{P,h}}\, \boldsymbol{B}_{h,\ell}\, \boldsymbol{\varphi}_h = 0$, i.e.,

$$-\frac{\overline{\varphi^0_{P,h}} \varphi^0_{S,h}}{\ell\, V_S^2} = \mathbb{i}\, \frac{|\varphi^0_{P,h}|^2}{|\ell| V_S^2} - 2\, \overline{\varphi^0_{P,h}} \int_{\mathbb{R}^+} \Big(\mathbb{i}\, \frac{\varphi_{P,h}}{V_P^2} + \mathrm{sign}(\ell) \frac{\varphi_{S,h}}{V_S^2}\Big) e^{-|\ell| x_1} \mathrm{d}x_1$$

which implies

$$-\frac{\mathrm{Im}\, \big(\overline{\varphi^0_{P,h}} \varphi^0_{S,h}\big)}{\ell\, V_S^2} = \frac{|\varphi^0_{P,h}|^2}{|\ell| V_S^2} - 2\, \mathrm{Im}\, \Big(\overline{\varphi^0_{P,h}} \int_{\mathbb{R}^+} \Big(\mathbb{i}\, \frac{\varphi_{P,h}}{V_P^2} + \mathrm{sign}(\ell) \frac{\varphi_{S,h}}{V_S^2}\Big) e^{-|\ell| x_1}\, \mathrm{d}x_1\Big).$$

Thus, using Cauchy-Schwarz inequality, we get

$$\begin{aligned} -\frac{\operatorname{Im}\left(\overline{\varphi^0_{P,h}}\varphi^0_{S,h}\right)}{\ell\, V_S^2} &\geq \frac{|\varphi^0_{P,h}|^2}{|\ell| V_S^2} \\ &- 2\,|\varphi^0_{P,h}| \Big(\frac{\|\varphi_{P,h}\|_{L^2(\mathbb{R}^+,\mathbb{C})}}{V_P^2} + \frac{\|\varphi_{S,h}\|_{L^2(\mathbb{R}^+,\mathbb{C})}}{V_S^2} \Big) \|e^{-|\ell| x_1}\|_{L^2(\mathbb{R}^+,\mathbb{C})}. \end{aligned} \tag{7.104}$$

Then by Young's inequality, we get that for any $\eta > 0$ ($Q \in \{P, S\}$)

$$2\,|\varphi^0_{P,h}| \|\varphi_{Q,h}\|_{L^2(\mathbb{R}^+,\mathbb{C})} \|e^{-|\ell| x_1}\|_{L^2(\mathbb{R}^+,\mathbb{C})} \leq \eta |\varphi^0_{P,h}|^2 \|e^{-|\ell| x_1}\|^2_{L^2(\mathbb{R}^+,\mathbb{C})} + \frac{1}{\eta} \|\varphi_{Q,h}\|^2_{L^2(\mathbb{R}^+,\mathbb{C})}.$$

Using this inequality into (7.104) one gets

$$\begin{aligned} -\frac{1}{\ell\, V_S^2} \operatorname{Im}\left(\overline{\varphi^0_{P,h}}\varphi^0_{S,h}\right) &\geq |\varphi^0_{P,h}|^2 \Big(\frac{1}{|\ell| V_S^2} - \eta \big(\frac{1}{V_P^2} + \frac{1}{V_S^2} \big) \|e^{-|\ell| x_1}\|^2_{L^2(\mathbb{R}^+,\mathbb{C})} \Big) \\ &\quad - \frac{1}{\eta} \Big(\frac{1}{V_P^2} \|\varphi_{P,h}\|^2_{L^2(\mathbb{R}^+,\mathbb{C})} + \frac{1}{V_S^2} \|\varphi_{S,h}\|^2_{L^2(\mathbb{R}^+,\mathbb{C})} \Big). \end{aligned} \tag{7.105}$$

In consequence, introducing (7.105) into (7.103) we finally get

$$\begin{aligned} \boldsymbol{\varphi}_h^* \mathbb{M}_{h,\ell} \boldsymbol{\varphi}_h &\geq |\varphi^0_{P,h}|^2 \Big(\frac{1}{|\ell| V_S^2} - \eta \big(\frac{1}{V_P^2} + \frac{1}{V_S^2} \big) \|e^{-|\ell| x_1}\|^2_{L^2(\mathbb{R}^+,\mathbb{C})} \Big) \\ &+ \big(1 - \frac{1}{\eta}\big) \Big(\frac{1}{V_P^2} \|\varphi_{P,h}\|^2_{L^2(\mathbb{R}^+,\mathbb{C})} + \frac{1}{V_S^2} \|\varphi_{S,h}\|^2_{L^2(\mathbb{R}^+,\mathbb{C})} \Big). \end{aligned}$$

Then notice that, to be able to conclude, it is sufficient to show that we can find η such that

$$\eta > 1 \quad \text{and} \quad 1 \geq \eta \left(\frac{V_S^2}{V_P^2} + 1 \right) |\ell|\, \|e^{-|\ell| x_1}\|^2_{L^2(\mathbb{R}^+,\mathbb{C})}, \tag{7.106}$$

which amounts to check $\left(V_S^2/V_P^2 + 1\right)\, |\ell|\, \|e^{-|\ell| x_1}\|^2_{L^2(\mathbb{R}^+,\mathbb{C})} < 1$, that is always true since $V_S^2 < V_P^2$ and

$$\|e^{-|\ell| x_1}\|^2_{L^2(\mathbb{R}^+,\mathbb{C})} = \int_{\mathbb{R}^+} e^{-2\,|\ell| x_1}\, \mathrm{d}x_1 = \frac{1}{2\,|\ell|}.$$

In consequence, we can choose η such that (7.106) holds for $0 < \ell \leq L$ and therefore the proof is concluded.

■

Let us recall that in Section 7.3.2, the stability of the 1D problem (7.44) was linked to the existence of negative eigenvalues of the 1D eigenvalue problem (7.53). Then, we can make the analogous to relate the stability of problem (7.100) to the existence of strictly negative eigenvalues of the 1D eigenvalue problem

$$\text{Find } (\boldsymbol{\varphi}, \eta) \neq (\mathbf{0}, 0) \text{ and } \lambda \in \mathbb{R} \text{ such that } \quad \begin{pmatrix} \mathbb{A}_{h,\ell} & \mathbf{0} \\ \mathbf{0} & 0 \end{pmatrix} \begin{pmatrix} \boldsymbol{\varphi} \\ \eta \end{pmatrix} = \lambda \begin{pmatrix} \mathbb{M}_{h,\ell} & \boldsymbol{B}_\ell \\ \boldsymbol{B}_\ell^T & 0 \end{pmatrix} \begin{pmatrix} \boldsymbol{\varphi} \\ \eta \end{pmatrix}. \tag{7.107}$$

Notice, that we can analysis this problem in a similar way to what was done in Section 7.3.2 for the unstable case. For this approach, we need to rewrite (7.107) as non homogeneous linear recurrence relation which resolution becomes rather cumbersome. Fortunately, this can be avoided noticing that $\mathbb{A}_{h,\ell}$ is positive definite (see Remark 7.16) and thus the positivity of all the eigenvalues is related to the positivity of $\mathbb{M}_{h,\ell}$ in the Ker $\boldsymbol{B}_\ell$, which is guaranteed by Proposition 7.50.

7.6.3 About mass lumping

First of all, we recall that according to (7.50), when the mass is lumped we have that for any $\boldsymbol{\varphi}_h \in V^{1\mathrm{D}}_{P,h} \times V^{1\mathrm{D}}_{S,h}$

$$\boldsymbol{\varphi}_h^* \widetilde{\mathbb{M}}_{h,\ell}\, \boldsymbol{\varphi}_h \geq \boldsymbol{\varphi}_h^* \mathbb{M}_{h,\ell}\, \boldsymbol{\varphi}_h.$$

Then, in the case we consider exact integration for the computation of $\boldsymbol{B}_{h,\ell}$, the analysis in previous section guarantees also the well-posedness and stability. However, when we also consider quadrature formula (7.49) for the computation of the stabilization term $\widetilde{\boldsymbol{B}}_{h,\ell}$, the analysis has to be repeated and to do so we assume that $L\, h_Q < 1$ for both $Q \in \{P, S\}$.

Proposition 7.51

If $|\ell|\, h_P < 1$, then there exists $\delta > 0$ independent of h such that

$$\exists\, \boldsymbol{\varphi}_h \in V^{1D}_{P,h} \times V^{1D}_{S,h} \quad \textit{such that} \quad \widetilde{\boldsymbol{B}}_{h,\ell}\, \boldsymbol{\varphi}_h \geq \delta(\|\varphi_{P,h}\|^2_{P,h} + \|\varphi_{S,h}\|^2_{S,h})^{\frac{1}{2}}.$$

Proof. Let us consider $\boldsymbol{\varphi}_h = (w_0, 0)$ where w_0 is the piecewise affine function that satisfies $w_0(0) = 1$ and $w_0(j\, h_P) = 0$ for all $j > 1$. Then, by straightforward computations we obtain

$$\|w_0\|^2_{P,h} = \frac{h_P}{2} < \frac{1}{2|\ell|} \qquad \text{and} \qquad \widetilde{\boldsymbol{B}}_{h,\ell}\, \boldsymbol{\varphi}_h = \frac{1}{2|\ell| V_S^2} - \frac{h_P}{2\, V_P^2} > \frac{1}{2|\ell|}\left(\frac{1}{V_S^2} - \frac{1}{V_P^2}\right)$$

In consequence, since $V_S^2 < V_P^2$ we can conclude that

$$\frac{\boldsymbol{B}_{h,\ell}\, \boldsymbol{\varphi}_h}{(\|\varphi_{P,h}\|^2_{P,h} + \|\varphi_{S,h}\|^2_{S,h})^{\frac{1}{2}}} > \frac{1}{\sqrt{2|\ell|}}\left(\frac{1}{V_S^2} - \frac{1}{V_P^2}\right) > 0.$$

■

Proposition 7.52

If $|\ell|\, h_Q < 1$ for both $Q \in \{P, S\}$, then there exists $K_e > 0$ independent of h such that

$$\widetilde{\boldsymbol{B}}_{h,\ell}\, \boldsymbol{\varphi}_h = 0 \quad \Longrightarrow \quad \boldsymbol{\varphi}_h^* \widetilde{\mathbb{M}}_{h,\ell} \boldsymbol{\varphi}_h > K_e \|\boldsymbol{\varphi}_h\|^2_{L^2(\mathbb{R}^+,\mathbb{C})^2}.$$

Proof. The computations in Proposition 7.50 can be developed analogously here with the only difference that, instead of (7.106), we need to verify

$$\eta > 1 \quad \text{and} \quad 1 \geq \eta\, |\ell| \left(\frac{V_S^2}{V_P^2} \|e^{-|\ell| x_1}\|^2_{P,h} + \|e^{-|\ell| x_1}\|^2_{S,h}\right).$$

Then we need to check if $|\ell| \left(\|e^{-|\ell| x_1}\|^2_{P,h} + \|e^{-|\ell| x_1}\|^2_{S,h}\, V_S^2/V_P^2\right) < 1$. To do so, we compute

$$|\ell|\, \|e^{-|\ell| x_1}\|^2_{Q,h} \;=\; \frac{|\ell| h_Q}{2} + |\ell| h_Q \sum_{j\geq 1}^{+\infty} e^{-2|\ell| j h_Q} = \frac{|\ell| h_Q}{2} + |\ell| h_Q\, (e^{2|\ell| h_Q} - 1)^{-1} =: g(|\ell| h_Q),$$

which, as a function of $|\ell| h_Q$, can be proven to be positive and monotonically increasing in $\mathbb{R}^+$. Finally, considering the assumption $L\, h_Q \leq 1$, we have

$$\begin{aligned} |\ell| \left(\frac{V_S^2}{V_P^2} \|e^{-|\ell| x_1}\|^2_{P,h} + \|e^{-|\ell| x_1}\|^2_{S,h}\right) \quad &\leq \quad \left(\frac{V_S^2}{V_P^2} + 1\right) g(1) \\ &= \quad \left(\frac{V_S^2}{V_P^2} + 1\right) \underbrace{\left(\frac{1}{2} + (e^2 - 1)^{-1}\right)}_{\approx 0.6565} < 1, \end{aligned}$$

where we have used that $V_S^2/V_P^2 + 1 < 3/2$. In consequence, we can choose η such that (7.106) holds for $0 < \ell \leq L$ and therefore the proof is concluded.

■

7.6.4 Numerical test

Now, to illustrate the stabilization, we solve the stable semi-discrete problem (7.102) after applying in time a standard leap frog scheme, which ensures a finite propagation velocity in the direction x_1. Moreover, we have chosen a bounded domain in the direction x_1 by truncating the domain at $x_1 = x_{1,max}$ in such a way that the numerical solution does not reach the boundary $x_1 = x_{1,max}$ before the final time T of the computation. The choice of physical data and discretization parameters is the same as for unstable case

$$\rho = 1, \quad \lambda = 20, \quad \mu = 4, \quad L_P = L_S = 60, \quad \text{and} \quad h_P = h_S = \frac{\pi}{200}$$

as well as for the source term which is located close to the boundary. Then in Figure 7.15 we plot snapshots of the solution obtained at two different simulation times. These results illustrate the stabilization of the method since no instability has been observed in time as predicted by our analysis.

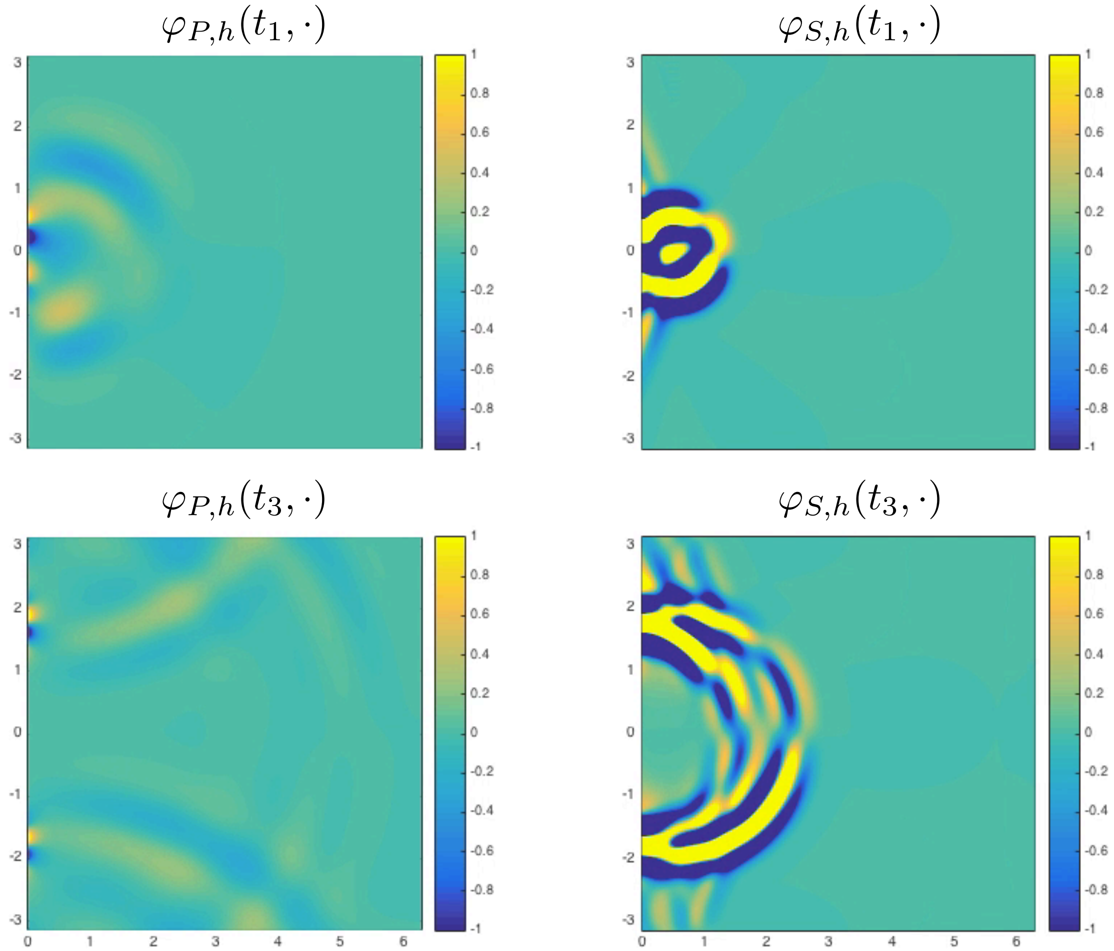

Figure 7.15: Snapshots at two different times $t_1 < t_3$ of the solution of (7.102) using a spectral approximation in x_2 and first order Lagrange finite elements in x_1.

7.6.5 A remark on the efficiency of the method

Let us begin by noticing that for the efficiency of the method, the sparsity of the matrix $\mathbb{B}_h^L$ (or $\widetilde{\mathbb{B}}_h^L$ if we consider mass lumping) is crucial. Unfortunately, we observe that for each frequency

$\ell \in [-L, L]\backslash\{0\}$ the vectors $\boldsymbol{B}_{h,\ell}$ are full (the same happens for $\widetilde{\boldsymbol{B}}_{h,\ell}$) since $\mathcal{E}^\ell$ is not locally supported (see (7.98)). Off course, in this toy problem, for the 1D problem associated to each frequency, this is not a significant drawback concerning efficiency. However, we expect a similar property in the general case when approximating the isomorphism $\mathcal{E}$ defined in (7.86) and thus a penalisation of the resultant numerical scheme. In this sense, we conjecture that the approximation of $\mathcal{E}$ can be localised and thus the efficiency of the method improved. This conjecture is motivated by the observation of the vectors $\boldsymbol{B}_{h,\ell} = (\boldsymbol{B}^\ell_{P,h}, \boldsymbol{B}^\ell_{S,h})^T$ (and $\widetilde{\boldsymbol{B}}_{h,\ell}$) in the particular case of the toy problem that we are analysing in this section. More precisely, we exhibit in Figure 7.16 the decaying behaviour of the coefficients $(\boldsymbol{B}^\ell_{Q,h})_j$ for $j > 1$ and $Q \in \{P, S\}$ (and also $(\widetilde{\boldsymbol{B}}^\ell_{Q,h})_j$) when considering different values of ℓ and h (with $h_P = h_S = h$). Attending to these considerations,

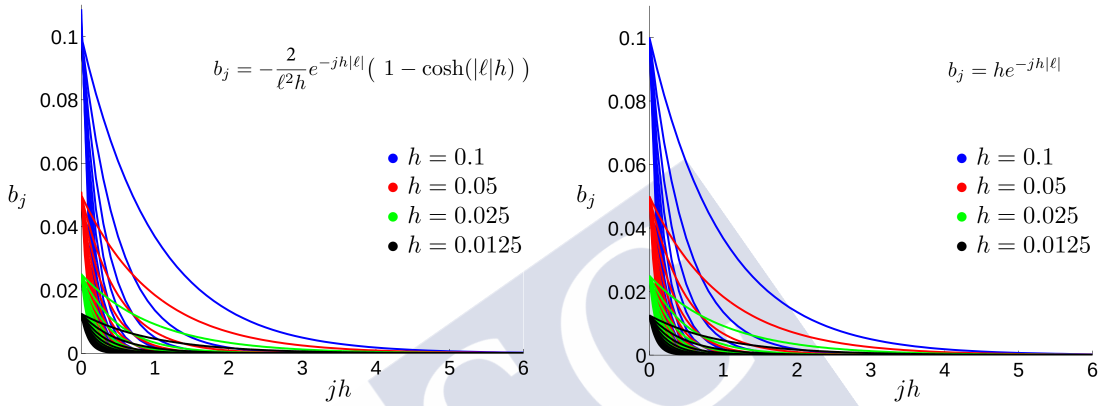

Figure 7.16: Decaying behave of the coefficients of $\boldsymbol{B}^\ell_{Q,h}$ and $\widetilde{\boldsymbol{B}}^\ell_{Q,h}$ for $Q \in \{P, S\}$ when considering an increasing frequency $\ell \in \{1, \ldots, 10\}$ and different values of h.

when frequency increases and the space step is small, it seems reasonable to approximate the stabilizing equation $\boldsymbol{B}_{h,\ell}\,\boldsymbol{\varphi}_h = 0$ (or $\widetilde{\boldsymbol{B}}_{h,\ell}\,\boldsymbol{\varphi}_h = 0$) by

$$\sum_{Q\in\{P,S\}} \sum_{j=1}^{J^\ell_Q} (\boldsymbol{B}^\ell_{Q,h})_j (\varphi_{Q,h})_j = 0 \quad \Big(\text{or} \quad \sum_{Q\in\{P,S\}} \sum_{j=1}^{J^\ell_Q} (\widetilde{\boldsymbol{B}}^\ell_{Q,h})_j (\varphi_{Q,h})_j = 0\Big), \tag{7.108}$$

where the $J^\ell_Q \in \mathbb{N}$ should be chosen carefully for each frequency and each potential and represents a truncation parameter which can essentially be seen as the cut off $1_{[0,J^\ell_Q h_Q]}$ which is used to localize $\mathcal{E}^\ell$. As we have already mentioned, a similar property is expected in the general case and would be of interest concerning the efficiency of the method, however we remark that the analysis of this approach is complicated, not standard and has not been carried out in the forthcoming sections.

7.7 Galerkin space discretization

This section is devoted to the development of an adequate space discretization of the stabilized mixed variational formulation (7.95). With this purpose, we begin by providing an abstract Galerkin approximation of the problem. Notice that for pedagogical reasons, we delay the details in the particular choice of the finite dimensional spaces involved.

7.7.1 Discrete functional spaces

The consideration of an adequate Galerkin approximation of the mixed problem (7.95) relies first on the introduction of finite dimensional approximations of the spaces $\boldsymbol{V}_0$ and M that will be denoted by $\boldsymbol{V}_{0h}$ and M_h. On the one hand, we will consider $\boldsymbol{V}_{0h} = \boldsymbol{V}_0 \cap \boldsymbol{V}_h$, where $\boldsymbol{V}_h$ represents a finite dimensional approximation of the space $\boldsymbol{V}$. Notice that according to the density result in (6.12), standard approximation spaces of $H^1(\Omega)^2$ ensure adequate approximation properties when approximating $\boldsymbol{V}$. Thus, in order to decouple the potentials in the volume and according to Lemma 6.3, we consider

$$\boldsymbol{V}_{0h} = \boldsymbol{V}_0 \cap \boldsymbol{V}_h \quad \text{where} \quad \boldsymbol{V}_h = V_{P,h} \times V_{S,h} \subset \boldsymbol{V} \quad \text{with} \quad V_{Q,h} \subset H^1(\Omega) \text{ for } Q \in \{P, S\}.$$

At this moment, $V_{Q,h}$ are abstract spaces that we only assume to satisfy the following approximation property

$$\lim_{h\to 0} \inf_{\psi_{Q,h}\in V_{Q,h}} \|\psi_{Q,h} - \psi_Q\|_{H^1(\Omega)} = 0, \quad \forall \psi_Q \in H^1(\Omega). \tag{7.109}$$

Remark 7.53

We remark that due to the density of $H^1(\Omega)^2$ in $\boldsymbol{V}$ (see (6.12)) and the continuous embedding of $\boldsymbol{V}$ in $H^1(\Omega)^2$, the approximation property (7.109) implies

$$\lim_{h\to 0} \inf_{\boldsymbol{\psi}_h\in \boldsymbol{V}_h} \|\boldsymbol{\psi}_h - \boldsymbol{\psi}\|_{\boldsymbol{V}} = 0, \quad \forall\, \boldsymbol{\psi} \in \boldsymbol{V},$$

which is a standard consistency condition for Galerkin approximation.

On the other hand, for the approximation of the functional space M we consider

$$M_h \subset L^2(\Gamma) \cap M \subset M.$$

Notice that the space M_h is also an abstract space which we assume to satisfy the respective approximation property

$$\lim_{h\to 0} \inf_{\nu_h\in M_h} \|\nu_h - \nu\|_M = 0, \quad \forall\, \nu \in M. \tag{7.110}$$

7.7.2 Non-conforming approximation of $m(\cdot,\cdot)$ and $b(\cdot,\cdot)$

First of all, let us recall that according to the definition (7.96), we have that $b(\nu, \boldsymbol{\psi}) = m(\mathcal{E}(\nu), \boldsymbol{\psi})$ where $\mathcal{E}(\nu) = \nabla p(\nu)$ can not be computed exactly in general since $p(\nu)$ is given by (7.85). In consequence, we need to make a non-conforming approximation of the bilinear form $b(\cdot,\cdot)$ which is based in replacing the operator $\mathcal{E}(\cdot)$ by a discrete version $\mathcal{E}_h(\cdot)$ which is defined by the Galerkin approximation of problem (7.85).

Moreover, for stability reasons, we would like to obtain an analogous to Theorem 7.23 at the discrete level. Unfortunately, as we mentioned before, the proof of Theorem 7.23 refers to displacement fields and seems to be difficult to extend to the discrete setting. Instead, as we will show later, it is going to be enough to provide at the discrete level an analogous to Theorem 7.44 which avoids any reference to displacement fields. To do so, we first notice that in the proof of Theorem 7.44, we use that $\boldsymbol{\varphi} \cdot \boldsymbol{n} \in M$ for all $\boldsymbol{\varphi} \in \boldsymbol{V}_0$, which at the discrete level is not true in general. To circumvent this issue and in order to be able to mimic the proof of Theorem 7.44, it will be useful to make a non-conforming approximation of the bilinear forms $m(\cdot,\cdot)$ and $b(\cdot,\cdot)$ where we project into M_h the terms related to normal traces of elements in $\boldsymbol{V}_{0h}$.

In the following, and taking into account the previous considerations, we proceed to describe the non-conforming approximation of the bilinear forms $m(\cdot,\cdot)$ and $b(\cdot,\cdot)$.

A discrete bilinear form $m_h(\cdot,\cdot)$. The modification of the bilinear form $m(\cdot,\cdot)$ only affects to $m_\Gamma(\cdot,\cdot)$ and requires the introduction of the orthogonal projection operator Π_h from $L^2(\Gamma)$ into M_h, that for every $\nu \in L^2(\Gamma)$, assigns $\Pi_h\nu \in M_h$ such that

$$\int_\Gamma (\Pi_h \nu)\, \widetilde{\nu}_h \, d\boldsymbol{\gamma} = \int_\Gamma \nu\, \widetilde{\nu}_h \, d\boldsymbol{\gamma}, \quad \forall\, \widetilde{\nu}_h \in M_h. \tag{7.111}$$

Then, we set for all $(\boldsymbol{\varphi}_h, \boldsymbol{\psi}_h) \in \boldsymbol{V}_h \times \boldsymbol{V}_h$

$$m_h(\boldsymbol{\varphi}_h, \boldsymbol{\psi}_h) \coloneqq m_\Omega(\boldsymbol{\varphi}_h, \boldsymbol{\psi}_h) + m_{\Gamma,h}(\boldsymbol{\varphi}_h, \boldsymbol{\psi}_h), \tag{7.112}$$

where the symmetric bilinear form $m_{\Gamma,h}(\cdot,\cdot)$ is defined consistently with the expression (7.29) for $m_\Gamma(\cdot,\cdot)$, with a clever use the projection operator Π_h, the interest of which will appear later,

$$\begin{aligned} m_{\Gamma,h}(\boldsymbol{\varphi}_h, \boldsymbol{\psi}_h) \quad \coloneqq \quad & -\frac{1}{2\,V_S^2} \int_\Gamma \mathcal{I}(\boldsymbol{\varphi}_h \cdot \boldsymbol{\tau})\, \Pi_h(\boldsymbol{\psi}_h \cdot \boldsymbol{n})\, \mathrm{d}\boldsymbol{\gamma} \\ & -\frac{1}{2\,V_S^2} \int_\Gamma \mathcal{I}(\boldsymbol{\psi}_h \cdot \boldsymbol{\tau})\, \Pi_h(\boldsymbol{\varphi}_h \cdot \boldsymbol{n})\, \mathrm{d}\boldsymbol{\gamma}. \end{aligned} \tag{7.113}$$

Remark 7.54

Note that if the space of normal traces of functions in $\boldsymbol{V}_h$, namely

$$\boldsymbol{V}_{\boldsymbol{n},h}(\Gamma) = \{\boldsymbol{\psi}_{h|\Gamma} \cdot \boldsymbol{n},\ \boldsymbol{\psi}_h \in \boldsymbol{V}_h\} \subset L^2(\Gamma),$$

is included in M_h then $m_{\Gamma,h}(\cdot,\cdot) = m_\Gamma(\cdot,\cdot)$ since then, $\Pi_h \boldsymbol{\nu}_h = \boldsymbol{\nu}_h,\ \forall\, \boldsymbol{\nu}_h \in \boldsymbol{V}_{\boldsymbol{n},h}(\Gamma)$.

A discrete bilinear form $b_h(\cdot,\cdot)$. Next, let us recall that according to the definition (7.96) of the bilinear form $b(\cdot,\cdot)$ we have $b(\nu, \boldsymbol{\psi}) = m(\mathcal{E}(\nu), \boldsymbol{\psi})$. Moreover, according to the definition (7.86) of $\mathcal{E}$ we have that $\mathcal{E}(\nu) = \nabla p(\nu)$ with $p(\nu)$ given by (7.85). Thus we have

$$\begin{aligned} b(\nu, \boldsymbol{\psi}) \quad = \quad & \frac{1}{V_P^2} \int_\Omega \partial_1 p(\nu)\, \psi_P\, \mathrm{d}\boldsymbol{x} \ + \ \frac{1}{V_S^2} \int_\Omega \partial_2 p(\nu)\, \psi_S\, \mathrm{d}\boldsymbol{x} \\ - \quad & \frac{1}{2V_S^2} \int_\Gamma \mathcal{I}(\boldsymbol{\psi} \cdot \boldsymbol{\tau})\, \nabla p(\nu) \cdot \boldsymbol{n}\, \mathrm{d}\boldsymbol{\gamma} \ - \ \frac{1}{2V_S^2} \int_\Gamma \mathcal{I}(\nabla p(\nu) \cdot \boldsymbol{\tau})\, \boldsymbol{\psi} \cdot \boldsymbol{n}\, \mathrm{d}\boldsymbol{\gamma}. \end{aligned} \tag{7.114}$$

As we mentioned before, $p(\nu)$ can not be computed exactly in general and needs to be approximated, therefore the same happens for $\mathcal{E}(\nu)$ and $b(\nu, \boldsymbol{\psi})$. In consequence, we need to make a non-conforming approximation of the bilinear form $b(\cdot,\cdot)$ which is based in replacing the operator $\mathcal{E}(\cdot)$ by a discrete version $\mathcal{E}_h(\cdot)$ which is defined by the Galerkin approximation of problem (7.85). For this purpose, let us first introduce another finite dimensional subspace of $H^1(\Omega)$ satisfying the same approximation property than (7.109) and that must contain the constant functions. More precisely, we introduce

$$P_h \subset H^1(\Omega) \quad \text{such that} \quad \lim_{h \to 0} \inf_{p_h \in P_h} \|p_h - p\|_{H^1(\Omega)} = 0, \quad \forall p \in H^1(\Omega). \tag{7.115}$$

Then, we define $\mathcal{E}_h \in \mathcal{L}(M_h, \boldsymbol{L}^2(\Omega))$ such that $\mathcal{E}_h(\nu_h) = \nabla p_h$ where $p_h \equiv p_h(\nu_h)$ is defined as the unique solution of (Galerkin approximation of problem (7.85))

$$\left\{ \begin{array}{l} \text{Find } p_h \in P_h \text{ such that} \\ \displaystyle\int_\Omega \nabla p_h \cdot \nabla q_h \, \mathrm{d}\boldsymbol{x} = \int_\Gamma \nu_h q_h \, \mathrm{d}\boldsymbol{\gamma}, \quad \forall q_h \in P_h, \\ \mathcal{I}(\nabla p_h \cdot \boldsymbol{\tau}) = p_h. \end{array} \right. \tag{7.116}$$

Now, according to Rham diagrams [106], note that ∇p_h belongs to $H(\mathrm{curl}, \Omega)$, thus the term $\nabla p_h \cdot \boldsymbol{\tau}$ is well defined. However, ∇p_h does not belong to $H(\mathrm{div}, \Omega)$ in general, therefore the term $\nabla p_h \cdot \boldsymbol{n}$ might not be well defined. In consequence, we can not consider $m(\cdot,\cdot)$ nor $m_h(\cdot,\cdot)$ for the approximation of $b(\cdot,\cdot)$. Instead, we recall that at the continuous level $\nabla p(\nu) \cdot \boldsymbol{n} = \nu$ and we consider according to (7.114) and (7.116)

$$\begin{aligned} b_h(\nu_h, \boldsymbol{\psi}_h) \quad \coloneqq \quad & \frac{1}{V_P^2} \int_\Omega \partial_1 p_h\, \psi_{P,h}\, \mathrm{d}\boldsymbol{x} \ + \ \frac{1}{V_S^2} \int_\Omega \partial_2 p_h\, \psi_{S,h}\, \mathrm{d}\boldsymbol{x} \\ - \quad & \frac{1}{2V_S^2} \int_\Gamma \mathcal{I}(\boldsymbol{\psi}_h \cdot \boldsymbol{\tau})\, \nu_h\, \mathrm{d}\boldsymbol{\gamma} \ - \ \frac{1}{2V_S^2} \int_\Gamma p_h\, \Pi_h(\boldsymbol{\psi}_h \cdot \boldsymbol{n})\, \mathrm{d}\boldsymbol{\gamma}. \end{aligned} \tag{7.117}$$

Note that we have also considered the operator Π_h as in the definition of $m_h(\cdot,\cdot)$ since it will be required in order to be able to mimic at the discrete level the proof of Theorem 7.44.

Remark 7.55

Let us remark that p_h, *defined by* (7.116), *is a discrete harmonic function in the sense that*

$$\int_\Omega \nabla p_h \cdot \nabla q_h \,\mathrm{d}\boldsymbol{x} = 0, \quad \forall q_h \in P_h \cap H_0^1(\Omega),$$

which is discrete equivalent of the property

$$\int_\Omega \nabla p \cdot \nabla q \,\mathrm{d}\boldsymbol{x} = 0, \quad \forall q \in H_0^1(\Omega),$$

that characterizes harmonic functions that belongs to $H^1(\Omega)$.

7.7.3 Semi-discrete approximation of the mixed problem

In accordance with the previous sections, we consider the following non-conforming Galerkin approximation of the mixed problem (7.95):

$$\left\{\begin{array}{ll} \text{Find } (\boldsymbol{\varphi}_h, \eta_h, \eta_R) : [0,T] \longrightarrow \boldsymbol{V}_{0h} \times M_h \times \mathbb{R} \text{ such that } (\boldsymbol{\varphi}_h, \partial_t \boldsymbol{\varphi}_h)(t=0) = (\boldsymbol{0},\boldsymbol{0}) \text{ and} & \\ \dfrac{\mathrm{d}^2}{\mathrm{d}t^2} m_h(\boldsymbol{\varphi}_h, \boldsymbol{\psi}_h) \;+\; a(\boldsymbol{\varphi}_h, \boldsymbol{\psi}_h) \;+\; b_h(\eta_h, \boldsymbol{\psi}_h) & \\ \qquad\qquad + \eta_R\, m(\boldsymbol{\xi}_R, \boldsymbol{\psi}_h) \;=\; \mathrm{g}(t, \boldsymbol{\psi}_h), \quad \forall\, \boldsymbol{\psi}_h \in \boldsymbol{V}_{0h}, & (7.118a) \\ \qquad\qquad b_h(\nu_h, \boldsymbol{\varphi}_h) \;=\; 0, \quad \forall\, \nu_h \in M_h, & (7.118b) \\ \qquad\qquad m(\boldsymbol{\xi}_R, \boldsymbol{\varphi}_h) \;=\; 0. & (7.118c) \end{array}\right.$$

Next, in order to work in the space $\boldsymbol{V}_h$ instead of $\boldsymbol{V}_{0h}$, we choose to treat the gauge conditions in the definition of $\boldsymbol{V}_0$ (see (7.26)) in weak (but exact) way by introducing two new scalar unknowns $(\eta_{\boldsymbol{n}}, \eta_{\boldsymbol{\tau}}) \in \mathbb{R}^2$ that are Lagrange multipliers associated to the gauge conditions in the definition of $\boldsymbol{V}_0$. This provides the following mixed formulation (the equivalence with (7.118) will be straightforward after existence and uniqueness)

$$\left\{\begin{array}{ll} \text{Find } (\boldsymbol{\varphi}_h, \eta_h, \eta_R, \eta_{\boldsymbol{n}}, \eta_{\boldsymbol{\tau}}) : [0,T] \longrightarrow \boldsymbol{V}_h \times M_h \times \mathbb{R}^3 \text{ such that } (\boldsymbol{\varphi}_h, \partial_t \boldsymbol{\varphi}_h)(t=0) = (\boldsymbol{0},\boldsymbol{0}) \text{ and} & \\ \dfrac{\mathrm{d}^2}{\mathrm{d}t^2} m_h(\boldsymbol{\varphi}_h, \boldsymbol{\psi}_h) \;+\; a(\boldsymbol{\varphi}_h, \boldsymbol{\psi}_h) \;+\; b_h(\eta_h, \boldsymbol{\psi}_h) \;+\; \eta_R\, m(\boldsymbol{\xi}_R, \boldsymbol{\psi}_h) & \\ \qquad + \eta_{\boldsymbol{n}} \displaystyle\int_\Gamma \boldsymbol{\psi}_h \cdot \boldsymbol{n} \,\mathrm{d}\boldsymbol{\gamma} \;+\; \eta_{\boldsymbol{\tau}} \int_\Gamma \boldsymbol{\psi}_h \cdot \boldsymbol{\tau} \,\mathrm{d}\boldsymbol{\gamma} \;=\; \mathrm{g}(t, \boldsymbol{\psi}_h), \quad \forall\, \boldsymbol{\psi}_h \in \boldsymbol{V}_h, & (7.119a) \\ \qquad\qquad b_h(\nu_h, \boldsymbol{\varphi}_h) \;=\; 0, \quad \forall\, \nu_h \in M_h, & (7.119b) \\ \displaystyle\int_\Gamma \boldsymbol{\psi}_h \cdot \boldsymbol{n} \,\mathrm{d}\boldsymbol{\gamma} = 0, \quad \int_\Gamma \boldsymbol{\psi}_h \cdot \boldsymbol{\tau} \,\mathrm{d}\boldsymbol{\gamma} = 0 \quad \text{and} \quad m(\boldsymbol{\xi}_R, \boldsymbol{\varphi}_h) \;=\; 0. & (7.119c) \end{array}\right.$$

Moreover, we can consider appropriate basis $\{\psi_Q^k\}_{k=1}^{K_Q}$ for the spaces $V_{Q,h}$ for $Q \in \{P, S\}$, as well as $\{\nu^k\}_{k=1}^{K_M}$ for the spaces M_h. Then, if we denote by $\boldsymbol{\Phi}_h^T = (\boldsymbol{\Phi}_{P,h}^T, \boldsymbol{\Phi}_{S,h}^T)$ and $\boldsymbol{E}_h$ the vectors of degrees of freedom of $\boldsymbol{\varphi}_h$ and η_h in these basis, the problem (7.119) results into the following algebraic system of ODEs (completed with $\mathbf{\Phi}_h(0) = \frac{\mathrm{d}}{\mathrm{d}t}\mathbf{\Phi}_h(0) = \mathbf{0}$)

$$
\begin{cases}
\mathbb{M}_h \dfrac{\mathrm{d}^2\mathbf{\Phi}_h}{\mathrm{d}t^2} + \mathbb{A}_h\mathbf{\Phi}_h + \mathbb{B}_h\boldsymbol{E}_h + \eta_R\,\boldsymbol{B}_R + \eta_{\boldsymbol{n}}\,\boldsymbol{B}_{\boldsymbol{n}} + \eta_{\boldsymbol{\tau}}\,\boldsymbol{B}_{\boldsymbol{\tau}} = \boldsymbol{G}_h, & (7.120\text{a})\\
\mathbb{B}_h^T\mathbf{\Phi}_h = \mathbf{0}, & (7.120\text{b})\\
\boldsymbol{B}_R^T\mathbf{\Phi}_h = 0, \quad \boldsymbol{B}_{\boldsymbol{n}}^T\mathbf{\Phi}_h = 0, \quad \boldsymbol{B}_{\boldsymbol{\tau}}^T\mathbf{\Phi}_h = 0, & (7.120\text{c})
\end{cases}
$$

where $\mathbb{M}_h$, $\mathbb{A}_h$, $\boldsymbol{B}_{\boldsymbol{n}}$, $\boldsymbol{B}_{\boldsymbol{\tau}}$ and $\boldsymbol{G}_h$ are computed as in (7.33) with the only modification that now

$$
\begin{aligned}
(\mathbb{M}^\Gamma_{PP,h})_{k,l} &= -\frac{1}{2\,V_S^2}\int_\Gamma \big(\mathcal{I}(n_2\,\psi_P^k)\,\Pi_h(n_1\,\psi_P^l) + \mathcal{I}(n_2\,\psi_P^l)\,\Pi_h(n_1\,\psi_P^k)\big)\mathrm{d}\boldsymbol{\gamma},\\
(\mathbb{M}^\Gamma_{SS,h})_{k,l} &= \frac{1}{2\,V_S^2}\int_\Gamma \big(\mathcal{I}(n_1\,\psi_S^k)\,\Pi_h(n_2\,\psi_S^l) + \mathcal{I}(n_1\,\psi_S^l)\,\Pi_h(n_2\,\psi_S^k)\big)\mathrm{d}\boldsymbol{\gamma},\\
(\mathbb{M}^\Gamma_{PS,h})_{k,l} &= -\frac{1}{2\,V_S^2}\int_\Gamma \big(\mathcal{I}(n_2\,\psi_P^k)\,\Pi_h(n_2\,\psi_S^l) - \mathcal{I}(n_1\,\psi_S^l)\,\Pi_h(n_1\,\psi_P^k)\big)\mathrm{d}\boldsymbol{\gamma}.
\end{aligned}
$$

While for the new terms $\boldsymbol{B}_R$ and $\mathbb{B}_h \coloneqq \mathbb{B}_h^\Omega + \mathbb{B}_h^\Gamma$ we consider

$$
\boldsymbol{B}_R = \begin{pmatrix}\boldsymbol{B}_R^P\\ \boldsymbol{B}_R^S\end{pmatrix}, \quad \mathbb{B}_h^\Omega = \begin{pmatrix}\mathbb{B}^\Omega_{P,h}\\ \mathbb{B}^\Omega_{S,h}\end{pmatrix} \quad \text{and} \quad \mathbb{B}_h^\Gamma = \begin{pmatrix}\mathbb{B}^\Gamma_{P,h}\\ \mathbb{B}^\Gamma_{S,h}\end{pmatrix},
$$

where we have to compute

$$
\begin{aligned}
&(\boldsymbol{B}_R^P)_k = m\big(\boldsymbol{\xi}_R, (\psi_P^k, 0)\big), && (\boldsymbol{B}_R^S)_k = m\big(\boldsymbol{\xi}_R, (0, \psi_S^k)\big),\\
&(\mathbb{B}^\Omega_{P,h})_{k,l} = \frac{1}{V_P^2}\int_\Omega \psi_P^k\,\partial_1 p_h(\nu^l)\,\mathrm{d}\boldsymbol{x}, && (\mathbb{B}^\Omega_{S,h})_{k,l} = \frac{1}{V_S^2}\int_\Omega \psi_S^k\,\partial_2 p_h(\nu^l)\,\mathrm{d}\boldsymbol{x},\\
&(\mathbb{B}^\Gamma_{P,h})_{k,l} = -\frac{1}{2\,V_S^2}\int_\Gamma \big(\mathcal{I}(n_2\,\psi_P^k)\,\nu^l + p_h(\nu^l)\,\Pi_h(n_1\,\psi_P^k)\big)\mathrm{d}\boldsymbol{\gamma},\\
&(\mathbb{B}^\Gamma_{S,h})_{k,l} = -\frac{1}{2\,V_S^2}\int_\Gamma \big(\mathcal{I}(-n_1\,\psi_S^k)\,\nu^l + p_h(\nu^l)\,\Pi_h(n_2\,\psi_S^k)\big)\mathrm{d}\boldsymbol{\gamma}.
\end{aligned}
$$

Remark 7.56

Let us remark that the matrix $\mathbb{B}_h^\Omega$ is full (then also $\mathbb{B}_h$) since $p_h(\nu^l)$ for $l \in \{1,\dots,K_M\}$ are not locally supported (see (7.116)). However, notice that $\mathbb{B}_h$ is small compared to $\mathbb{M}_h$ and $\mathbb{A}_h$ which dimensions are $(K_P+K_S)\times(K_P+K_S)$ while the dimensions of $\mathbb{B}_h$ are $(K_P+K_S)\times K_M$.

We also remark that the computation of $\mathbb{B}_h$ is cumbersome. First we need to compute $p_h(\nu^l)$, for each $l \in \{1,\dots,K_M\}$ and notice that this requires the intersection on the boundary between the meshes chosen to build P_h and M_h. Second, in order to compute $\mathbb{B}_h^\Omega$, notice that we also require the intersection in the volume between the meshes chosen to build each $V_{Q,h}$ and P_h. Finally, for the computation of $\mathbb{B}_h^\Gamma$ we make use of the previous intersection between the meshes used for P_h and M_h, but we also require the intersection between the meshes chosen to build each $V_{Q,h}$ and M_h. Of course, many of this computations can be lightened by choosing conforming meshes for the different spaces involved.

Note that formulation (7.119) has the advantage of well separating the role of the Lagrange multiplier η_h from $(\eta_R, \eta_{\boldsymbol{n}}, \eta_{\boldsymbol{\tau}})$. However, for the sequel, it will be useful to have a more compact writing of (7.119) by introducing a generalized Lagrange multiplier

$$
\widehat{\eta}_h \coloneqq (\eta_h, \eta_R, \eta_{\boldsymbol{\tau}}, \eta_{\boldsymbol{n}}) \in \widehat{M}_h = M_h \times \mathbb{R}^3.
$$

Then the semi-discrete problem (7.119) rewrites

$$\left\{\begin{array}{ll} \text{Find } (\boldsymbol{\varphi}_h, \widehat{\eta}_h) : [0,T] \longrightarrow \boldsymbol{V}_h \times \widehat{M}_h \text{ such that } (\boldsymbol{\varphi}_h, \partial_t \boldsymbol{\varphi}_h)(t=0) = (\mathbf{0},\mathbf{0}) \text{ and} & \\ \dfrac{\mathrm{d}^2}{\mathrm{d}t^2}\, m_h(\boldsymbol{\varphi}_h, \boldsymbol{\psi}_h) \;+\; a(\boldsymbol{\varphi}_h, \boldsymbol{\psi}_h) \;+\; \widehat{b}_h(\widehat{\eta}_h, \boldsymbol{\psi}_h) \;=\; \mathrm{g}(t, \boldsymbol{\psi}_h), \quad \forall\, \boldsymbol{\psi}_h \in \boldsymbol{V}_h, & \text{(7.121a)} \\ \widehat{b}_h(\widehat{\nu}_h, \boldsymbol{\varphi}_h) \;=\; 0, \quad \forall\, \widehat{\nu}_h \in \widehat{M}_h. & \text{(7.121b)} \end{array}\right.$$

where the bilinear form $\widehat{b}(\cdot,\cdot) : \widehat{M}_h \times \boldsymbol{V}_h \to \mathbb{R}$ is defined for $\big(\widehat{\nu}_h, \boldsymbol{\psi}_h\big) \in \widehat{M}_h \times \boldsymbol{V}_h$ by

$$\widehat{b}_h(\widehat{\nu}_h, \boldsymbol{\psi}_h) = b_h(\nu_h, \boldsymbol{\psi}_h) + \nu_R\, m(\boldsymbol{\xi}_R, \boldsymbol{\psi}_h) + \nu_{\boldsymbol{n}} \int_\Gamma \boldsymbol{\psi}_h \cdot \boldsymbol{n}\, \mathrm{d}\boldsymbol{\gamma} + \nu_{\boldsymbol{\tau}} \int_\Gamma \boldsymbol{\psi}_h \cdot \boldsymbol{\tau}\, \mathrm{d}\boldsymbol{\gamma}. \tag{7.122}$$

Similarly, we also introduce $\widehat{\boldsymbol{E}}_h^T = (\boldsymbol{E}_h^T, \eta_R, \eta_{\boldsymbol{n}}, \eta_{\boldsymbol{\tau}})$ and $\widehat{\mathbb{B}}_h = \big(\mathbb{B}_h, \boldsymbol{B}_R, \boldsymbol{B}_{\boldsymbol{n}}, \boldsymbol{B}_{\boldsymbol{\tau}}\big)$. Then the algebraic system (7.120) can be rewritten as (completed with $\boldsymbol{\Phi}_h(0) = \frac{\mathrm{d}}{\mathrm{d}t}\boldsymbol{\Phi}_h(0) = \mathbf{0}$)

$$\left\{\begin{array}{ll} \mathbb{M}_h \dfrac{\mathrm{d}^2 \boldsymbol{\Phi}_h}{\mathrm{d}t^2} + \mathbb{A}_h \boldsymbol{\Phi}_h + \widehat{\mathbb{B}}_h\, \widehat{\boldsymbol{E}}_h = \boldsymbol{G}_h, & \text{(7.123a)} \\ \widehat{\mathbb{B}}_h^T \boldsymbol{\Phi}_h = \mathbf{0}. & \text{(7.123b)} \end{array}\right.$$

Finally, let us remark that according to Theorem 7.45 we will look for solutions of (7.123) with the regularity

$$\boldsymbol{\Phi}_h \in \mathcal{C}^2([0,T]; \mathbb{R}^{K_P+K_S}) \quad \text{and} \quad \widehat{\boldsymbol{E}}_h \in \mathcal{C}^0([0,T]; \mathbb{R}^{K_M+3}),$$

which going back to (7.119), corresponds to

$$\boldsymbol{\varphi}_h \in \mathcal{C}^2([0,T]; \boldsymbol{V}_h), \quad \eta_h \in \mathcal{C}^0([0,T]; M_h) \quad \text{and} \quad (\eta_R, \eta_{\boldsymbol{n}}, \eta_{\boldsymbol{\tau}}) \in \mathcal{C}^0([0,T]; \mathbb{R}^3).$$

7.7.4 Well-posedness and stability of the semi-discrete problem

The well-posedness and stability analysis of the semi-discrete problem (7.121) (or equivalently the algebraic system (7.123)), are classically linked to the uniform coercivity of $m_h(\cdot,\cdot)$ in the space

$$\boldsymbol{V}_{N,h} := \{\boldsymbol{\psi}_h \in \boldsymbol{V}_h,\ \widehat{b}_h(\widehat{\nu}_h, \boldsymbol{\psi}_h) = 0,\ \forall\, \widehat{\nu}_h \in \widehat{M}_h\}, \qquad (\text{discrete equivalent of } \boldsymbol{V}_N) \tag{7.124}$$

as well as the verification of an adequate *uniform Inf-Sup condition*. More precisely, we would like to find two constants, $\alpha > 0$ and $\delta > 0$, independent of h and such that

$$m_h(\boldsymbol{\psi}_h, \boldsymbol{\psi}_h) \geq \alpha \int_\Omega |\boldsymbol{\psi}_h|\, \mathrm{d}\boldsymbol{x}, \quad \forall\, \boldsymbol{\psi}_h \in \boldsymbol{V}_{N,h}, \tag{7.125}$$

$$\forall\, \widehat{\nu}_h \in \widehat{M}_h,\ \exists\, \boldsymbol{\psi}_h \in \boldsymbol{V}_h \quad \text{such that} \quad \widehat{b}_h(\widehat{\nu}_h, \boldsymbol{\psi}_h) \geq \delta\, \|\widehat{\nu}_h\|_{\widehat{M}} \|\boldsymbol{\psi}_h\|_{\boldsymbol{V}}. \tag{7.126}$$

Unfortunately, the verification of both properties remains open and appears to be challenging. On the one hand, condition (7.125) represents a discrete equivalent to Theorem 7.23, but $\boldsymbol{V}_{N,h} \not\subseteq \boldsymbol{V}_N$ and as we have mentioned before, the proof of Theorem 7.23 refers to displacement fields and seems difficult to be extended to the discrete setting. On the other hand, for condition (7.126) we even do not know if there exists an equivalent at the continuous level.

In consequence, in this section, our aim is to develop an alternative approach based in the weaker conditions (which we verify under reasonable assumptions):

(B.1) The positivity of the bilinear form $m_h(\cdot,\cdot)$ in the space $\boldsymbol{V}_{N,h}$:

$$m_h(\boldsymbol{\psi}_h, \boldsymbol{\psi}_h) > 0, \quad \forall\, \boldsymbol{\psi}_h \in \boldsymbol{V}_{N,h} \setminus \{\mathbf{0}\},$$

$$\text{equivalently} \quad \mathbb{M}_h \boldsymbol{\Psi}_h \cdot \boldsymbol{\Psi}_h > 0, \quad \forall\, \boldsymbol{\Psi}_h \neq \mathbf{0} \quad \text{such that} \quad \widehat{\mathbb{B}}_h^T \boldsymbol{\Psi}_h = \mathbf{0}.$$

(**B.2**) The non-uniform *Inf-Sup condition*:

$$\widehat{b}_h(\widehat{\nu}_h, \boldsymbol{\psi}_h) = 0, \quad \forall\, \boldsymbol{\psi}_h \in \boldsymbol{V}_h \quad \Longrightarrow \quad \widehat{\nu}_h = \boldsymbol{0},$$

$$\text{equivalently} \quad \mathbb{B}_h \widehat{\boldsymbol{E}}_h \;\Longrightarrow\; \widehat{\boldsymbol{E}}_h = \boldsymbol{0} \quad \big(\text{i.e. } \operatorname{Ker} \widehat{\mathbb{B}}_h = \{\boldsymbol{0}\}\big).$$

Remark 7.57

*Since the spaces $\boldsymbol{V}_{N,h}$ and $\widehat{M}_h$ are finite dimensional spaces, the conditions (**B.1**) and (**B.2**) are equivalent to the existence of constants $\alpha_h > 0$ and $\delta_h > 0$ such that*

$$m_h(\boldsymbol{\psi}_h, \boldsymbol{\psi}_h) \geq \alpha_h \int_\Omega |\boldsymbol{\psi}_h| \, \mathrm{d}\boldsymbol{x}, \quad \forall\, \boldsymbol{\psi}_h \in \boldsymbol{V}_{N,h},$$

$$\forall\, \widehat{\nu}_h \in \widehat{M}_h, \; \exists\, \boldsymbol{\psi}_h \in \boldsymbol{V}_h \quad \textit{such that} \quad \widehat{b}_h(\widehat{\nu}_h, \boldsymbol{\psi}_h) \geq \delta_h \, \|\widehat{\nu}_h\|_{\widehat{M}} \|\boldsymbol{\psi}_h\|_{\boldsymbol{V}}.$$

As we have mentioned before, we do not know if α_h and δ_h can be made independent of h. Of course, we conjecture that this is the case for any "reasonable" choice of the approximation spaces and we remark that this question is fundamental for the development of a convergence analysis of the method.

As we shall see later, condition (**B.1**) is a sufficient condition for ensuring the existence of solution of problem (7.121), as well as a necessary condition for time stability. Moreover, we shall also see that condition (**B.1**) implies that the Lagrange multiplier $\widehat{\eta}_h(t)$ is uniquely defined up to any function of time with values in

$$\widehat{M}_{N,h} := \{\nu_h \in \widehat{M}_h, \; \widehat{b}_h(\nu_h, \boldsymbol{\psi}_h) = 0, \; \forall\, \boldsymbol{\psi}_h \in \boldsymbol{V}_h\}.$$

Therefore, it is going to be condition (**B.2**) the one that ensures that $\widehat{\eta}_h(t)$ is uniquely defined, since it implies that $\widehat{M}_{N,h} = \{\boldsymbol{0}\}$. In consequence, it is clear that condition (**B.1**) is of fundamental importance, while condition (**B.2**) is much less crucial since we are essentially interested in $\boldsymbol{\varphi}_h$. Moreover in practice, the failure of (**B.2**) can be circumvented by selecting the solution $\widehat{\eta}_h$ of minimal norm (e.g. in $L^2(\Gamma) \times \mathbb{R}^3$) via pseudo-inverse procedure that we shall describe in Section 7.7.4.1. Therefore, the rest of this section is devoted to:

- Provide an adequate compatibility condition between P_h and $V_{S,h}$ in order to ensure (**B.1**).
- Show that (**B.1**) implies the well-posedness of problem (7.121) in the sense explained above.
- Show that (**B.1**) guarantees the time stability of the semi-discrete mixed problem (7.121).

Let us remark that the verification of the compatibility condition between P_h and $V_{S,h}$ (which implies (**B.1**)) and the condition (**B.2**) is postponed to Section 7.7.5 where we discuss both conditions for the particular case of Lagrange finite elements.

On the positivity condition (B.1). As we shall see next, the verification of the positivity condition (**B.1**) relies in the extension of Theorem 7.44 to the discrete case. Then, we will see that according to the construction of the discrete bilinear forms $m_h(\cdot,\cdot)$ and $b_h(\cdot,\cdot)$, we are able to obtain a discrete equivalent of (7.88). However, we shall notice that this is not enough to obtain also (7.89) (which is actually (**B.1**)) since we have used in (7.91) the following trivial property of the harmonic functions

$$\Delta p = 0, \quad \partial_1 p = 0 \quad \Longrightarrow \quad \exists\,(a,b) \in \mathbb{R}^2 \text{ s.t. } p = a\,x_2 + b. \tag{7.127}$$

Thus, in order to obtain also a discrete equivalent of (7.89), we will require the following compatibility assumption between the spaces P_h and $V_{S,h}$.

Assumption II.1

For any $p_h \in P_h$ such that $\partial_1 p_h = 0$ and $\partial_2 p_h \in V_{S,h}$ then

$$\int_\Omega \partial_2 p_h \partial_2 q_h \, \mathrm{d}\boldsymbol{x} = 0, \quad \forall q_h \in P_h \cap H_0^1(\Omega) \quad \Longrightarrow \quad \exists\, (a,b) \in \mathbb{R}^2 \text{ s.t. } p_h = a\, x_2 + b.$$

Therefore, let us introduce the space (discrete equivalent of $\boldsymbol{W}_N$ defined in (7.87))

$$\boldsymbol{W}_{N,h} := \big\{\boldsymbol{\psi}_h \in \boldsymbol{V}_{0h},\ b_h(\nu_h, \boldsymbol{\psi}_h) = 0,\ \forall\, \nu_h \in M_h\big\} \qquad \big(\text{notice that } \boldsymbol{W}_{N,h} \supset \boldsymbol{V}_{N,h}\big). \tag{7.128}$$

Then, we prove the following result that represent the discrete equivalent of Theorem 7.44.

Theorem 7.58

In the space $\boldsymbol{W}_{N,h}$, the quadratic form $m_h(\boldsymbol{\psi}_h, \boldsymbol{\psi}_h)$ takes the form (note $\frac{1}{V_*^2} := \frac{1}{V_S^2} - \frac{1}{V_P^2} > 0$)

$$m_h(\boldsymbol{\psi}_h, \boldsymbol{\psi}_h) = \frac{1}{V_*^2} \int_\Omega |\partial_1 p_h(\nu_h)|^2 \, d\boldsymbol{x} + m_\Omega\big(\boldsymbol{\psi}_h - \nabla p_h(\nu_h), \boldsymbol{\psi}_h - \nabla p_h(\nu_h)\big), \tag{7.129}$$

*where $\nu_h = \Pi_h(\boldsymbol{\psi}_h \cdot \boldsymbol{n}) \in M_h$. In consequence, we notice that $m_h(\boldsymbol{\psi}_h, \boldsymbol{\psi}_h) \geq 0$ for all $\boldsymbol{\varphi} \in \boldsymbol{W}_{N,h}$. Moreover, if Assumption II.1 is satisfied, we also prove that (**B.1**) holds true:*

$$m_h(\boldsymbol{\psi}_h, \boldsymbol{\psi}_h) > 0, \qquad \forall \boldsymbol{\varphi} \in \boldsymbol{V}_{N,h} \setminus \{\boldsymbol{0}\}.$$

Proof. The proof is done by mimicking the proof of Theorem 7.44 at the semi-discrete level.
Step 1: Proof of (7.129)
For any $\boldsymbol{\psi} \in \boldsymbol{W}_{N,h}$ and according to the definition of $\boldsymbol{W}_{N,h}$ and $b_h(\cdot,\cdot)$ (which are given in (7.128) and (7.117)), we have that for any function ν_h in M_h,

$$\begin{aligned} \frac{1}{V_P^2} \int_\Omega \partial_1 p_h(\nu_h)\, \psi_{P,h} \, \mathrm{d}\boldsymbol{x} &+ \frac{1}{V_S^2} \int_\Omega \partial_2 p_h(\nu_h)\, \psi_{S,h} \, \mathrm{d}\boldsymbol{x} \\ -\frac{1}{2V_S^2} \int_\Gamma \mathcal{I}(\boldsymbol{\psi}_h \cdot \boldsymbol{\tau})\, \nu_h \, \mathrm{d}\boldsymbol{\gamma} &- \frac{1}{2V_S^2} \int_\Gamma p_h(\nu_h)\, \Pi_h(\boldsymbol{\psi}_h \cdot \boldsymbol{n}) \, \mathrm{d}\boldsymbol{\gamma} = 0, \end{aligned} \tag{7.130}$$

where we recall that $p_h(\nu_h)$ is the discrete harmonic function defined as the solution of (7.116). Next, we choose $\nu_h = \Pi_h(\boldsymbol{\psi}_h \cdot \boldsymbol{n}) \in M_h$ (this is where Π_h is needed) and we compute from the definition (7.113) of the discrete bilinear form $m_{\Gamma,h}(\cdot,\cdot)$:

$$-\frac{1}{2\,V_S^2} \int_\Gamma \mathcal{I}(\boldsymbol{\psi}_h \cdot \boldsymbol{\tau})\, \nu_h \, \mathrm{d}\boldsymbol{\gamma} = -\frac{1}{2\,V_S^2} \int_\Gamma \mathcal{I}(\boldsymbol{\psi}_h \cdot \boldsymbol{\tau})\, \Pi_h(\boldsymbol{\psi}_h \cdot \boldsymbol{n}) \, \mathrm{d}\boldsymbol{\gamma} = \frac{1}{2} m_{\Gamma,h}(\boldsymbol{\psi}_h, \boldsymbol{\psi}_h).$$

Then, since $p_h(\nu_h)$ is the solution of (7.116), we have that (considering $q_h = p_h(\nu_h)$ in (7.116))

$$\frac{1}{2V_S^2} \int_\Gamma p_h(\nu_h)\, \Pi_h(\boldsymbol{\psi}_h \cdot \boldsymbol{n}) \, \mathrm{d}\boldsymbol{\gamma} = \frac{1}{2V_S^2} \int_\Gamma p_h(\nu_h)\, \nu_h \, \mathrm{d}\boldsymbol{\gamma} = \frac{1}{2V_S^2} \int_\Omega |\nabla p_h(\nu_h)|^2 \, \mathrm{d}\boldsymbol{x}.$$

In consequence, if we introduce the last two equalities into (7.130), we obtain

$$m_{\Gamma,h}(\boldsymbol{\psi}_h, \boldsymbol{\psi}_h) = \frac{1}{V_S^2} \int_\Omega |\nabla p_h(\nu_h)|^2 \, \mathrm{d}\boldsymbol{x} - \frac{2}{V_P^2} \int_\Omega \psi_{P,h}\, \partial_1 p_h(\nu_h) \, \mathrm{d}\boldsymbol{x} - \frac{2}{V_S^2} \int_\Omega \psi_{S,h}\, \partial_2 p_h(\nu_h) \, \mathrm{d}\boldsymbol{x},$$

and therefore, adding $m_\Omega(\boldsymbol{\psi}_h, \boldsymbol{\psi}_h)$,

$$\begin{aligned} m(\boldsymbol{\psi}_h, \boldsymbol{\psi}_h) \;=\; & \frac{1}{V_P^2} \int_\Omega |\psi_{P,h}|^2 \, \mathrm{d}\boldsymbol{x} - \frac{2}{V_P^2} \int_\Omega \psi_{P,h}\, \partial_1 p_h(\nu_h) \, \mathrm{d}\boldsymbol{x} + \frac{1}{V_S^2} \int_\Omega |\partial_1 p_h(\nu_h)|^2 \, \mathrm{d}\boldsymbol{x} \\ + \; & \frac{1}{V_S^2} \int_\Omega |\psi_{S,h}|^2 \, \mathrm{d}\boldsymbol{x} - \frac{2}{V_S^2} \int_\Omega \psi_{S,h}\, \partial_2 p_h(\nu_h) \, \mathrm{d}\boldsymbol{x} + \frac{1}{V_S^2} \int_\Omega |\partial_2 p_h(\nu_h)|^2 \, \mathrm{d}\boldsymbol{x}. \end{aligned}$$

Notice that we can rearrange the above expression as a sum of squares and we obtain (7.88).

Step 2: $m_h(\boldsymbol{\psi}_h, \boldsymbol{\psi}_h) = 0$ *and* $\boldsymbol{\psi}_h \in \boldsymbol{V}_{N,h}$ *imply* $\boldsymbol{\psi}_h = 0$.

This is where Assumption II.1 is needed. Indeed, using (7.129) (notice that we have the inclusion $\boldsymbol{V}_{N,h} \subset \boldsymbol{W}_{N,h}$), $m_h(\boldsymbol{\psi}_h, \boldsymbol{\psi}_h) = 0$ implies $\partial_1 p_h = 0$ and $\boldsymbol{\psi}_h = \nabla p_h$. Then, we immediately deduce that, $\psi_{P,h} = 0$ and $\partial_2 p_h \in V_{S,h}$. Moreover since, p_h is a discrete harmonic function, i.e.,

$$\int_\Omega \partial_2 p_h \, \partial_2 q_h = 0, \quad \forall\, q_h \in P_h \cap H_0^1(\Omega),$$

we can use Assumption II.1 to state that p_h is an affine function of x_2 and that $\psi_{S,h}$ is constant. Finally, we use the orthogonality of $\boldsymbol{\psi}_h$ to $\mathbf{K}_R$ to conclude that $\boldsymbol{\psi}_h = \mathbf{0}$ as in the proof of Theorem 7.44.

■

Notice that Assumption II.1, which appears as a compatibility condition between the spaces P_h and $V_{S,h}$, is implied by the following assumption that only involves the space P_h (since $V_{S,h} \subset H^1(\Omega)$).

Assumption II.2

For any $p_h \in P_h$ *such that* $\partial_1 p_h = 0$ *and* $\partial_2 p_h \in H^1(\Omega)$ *then*

$$\int_\Omega \partial_2 p_h \, \partial_2 q_h = 0, \quad \forall\, q_h \in P_h \cap H_0^1(\Omega) \quad \Longrightarrow \quad \exists\,(a,b) \in \mathbb{R}^2 \text{ s.t. } p_h = a\, x_2 + b$$

This assumption is a more natural discrete equivalent to property (7.127) and can be interpreted as follows: "*Every discrete harmonic function of P_h (see Remark 7.55 for definition of discrete harmonic), which derivative $\partial_2 p_h$ has $H^1(\Omega)$-regularity and that is independent of x_1 is an affine function of x_2*".

Remark 7.59

It is interesting to remark that, whatever is the choice of the spaces $V_{P,h}$ and $V_{S,h}$, the Assumption II.2 which only involves P_h is enough to guarantee Assumption II.1 and therefore (according to Theorem 7.58) the positivity property ((**B.1**)). *This may seem surprising since $\mathbb{M}_h$ does not depend in the choice P_h however, the reader should notice that $\widehat{\mathbb{B}}_h$ does.*

7.7.4.1 Well-posedness of the semi-discrete problem

In this section, we assume that condition (**B.1**) is satisfied and we analyse the well-posedness of the semi-discrete problem (7.121) in its algebraic form which is given in (7.123). As it was mentioned before, the major difficulty for the analysis of problem (7.123) is that the matrix $\mathbb{M}_h$ is not positive. Therefore, in order to circumvent this problem, we propose an exact penalized version of (7.123). The basic ingredient is the following result in linear algebra.

Lemma 7.60

Let $\mathbb{M} \in \mathbb{R}^{n,n}$ be a symmetric matrix and $\mathbb{B} \in \mathbb{R}^{n,m}$ a rectangular matrix such that

$$\mathbb{M}\,\boldsymbol{\Psi} \cdot \boldsymbol{\Psi} > 0, \quad \forall\, \boldsymbol{\Psi} \neq \mathbf{0} \quad \text{such that} \quad \mathbb{B}^T \boldsymbol{\Psi} = \mathbf{0}.$$

Then, there exists a sufficiently small $\varepsilon > 0$ such that

$$\big(\mathbb{M} + \frac{1}{\varepsilon}\mathbb{B}\,\mathbb{B}^T\big)\boldsymbol{\Psi} \cdot \boldsymbol{\Psi} > 0, \quad \forall\, \boldsymbol{\Psi} \in \mathbb{R}^n \setminus \{\mathbf{0}\}. \tag{7.131}$$

Proof. Let us begin by introducing the notation $\mathbf{\Phi}\cdot\mathbf{\Psi}$ for the usual inner product in $\mathbb{R}^n$, as well as $\|\cdot\|_2$ for the corresponding euclidean norm. Then, notice that we proceed by contradiction. Thus we assume that (7.131) is not true, which implies that there exists a sequence $(\mathbf{\Psi}_k)_{k\in\mathbb{N}}$ such that $\|\mathbf{\Psi}_k\|_2 = 1$ and

$$\big(\mathbb{M} + k\,\mathbb{B}\,\mathbb{B}^T\big)\mathbf{\Psi}_k\cdot\mathbf{\Psi}_k \le 0. \tag{7.132}$$

Since $(\mathbf{\Psi}_k)_{k\in\mathbb{N}}$ is a bounded sequence in a finite dimensional space, we can assume that it converges towards $\mathbf{\Psi}$ with $\|\mathbf{\Psi}\|_2 = 1$. Therefore, dividing by k equation (7.132), we obtain

$$\mathbb{B}\,\mathbb{B}^T\mathbf{\Psi}\cdot\mathbf{\Psi} = \lim_{k\to\infty}\big(\frac{1}{k}\mathbb{M} + \mathbb{B}\,\mathbb{B}^T\big)\mathbf{\Psi}_k\cdot\mathbf{\Psi}_k \le 0.$$

In consequence, we have that $(\mathbb{B}^T\mathbf{\Psi})\cdot(\mathbb{B}^T\mathbf{\Psi}) \le \mathbf{0}$, which implies $\mathbb{B}^T\mathbf{\Psi} = \mathbf{0}$ and by hypothesis $\mathbb{M}\,\mathbf{\Psi}\cdot\mathbf{\Psi} > 0$. Finally, we notice that (since $\mathbb{B}\,\mathbb{B}^T$ is positive)

$$\mathbb{M}\,\mathbf{\Psi}_k\cdot\mathbf{\Psi}_k \le \big(\mathbb{M} + k\,\mathbb{B}\,\mathbb{B}^T\big)\mathbf{\Psi}_k\cdot\mathbf{\Psi}_k \le 0 \quad\Longrightarrow\quad \mathbb{M}\,\mathbf{\Psi}\cdot\mathbf{\Psi} \le 0,$$

which is a contradiction.

■

Now, we notice that thanks to (**B.1**), we can apply Lemma 7.60 to $\mathbb{M} = \mathbb{M}_h$ and $\mathbb{B} = \widehat{\mathbb{B}}_h$. Thus, there exists ε sufficiently small such that

$$\mathbb{M}_h^\varepsilon := \mathbb{M}_h + \frac{1}{\varepsilon}\,\widehat{\mathbb{B}}_h\,\widehat{\mathbb{B}}_h^T \quad \text{is positive definite.} \tag{7.133}$$

Thus, we introduce the penalised system (completed with $\mathbf{\Phi}_h^\varepsilon(0) = \dfrac{\mathrm{d}}{\mathrm{d}t}\mathbf{\Phi}_h^\varepsilon(0) = \mathbf{0}$)

$$\left\{\begin{aligned} &\mathbb{M}_h^\varepsilon\frac{\mathrm{d}^2\mathbf{\Phi}_h^\varepsilon}{\mathrm{d}t^2} + \mathbb{A}_h\mathbf{\Phi}_h^\varepsilon + \widehat{\mathbb{B}}_h\,\widehat{\boldsymbol{E}}_h^\varepsilon = \boldsymbol{G}_h, && (7.134a)\\ &\widehat{\mathbb{B}}_h^T\mathbf{\Phi}_h^\varepsilon = \mathbf{0}. && (7.134b)\end{aligned}\right.$$

Remark 7.61

A priori, the solution of problem (7.134) *depends on the parameter* ε*. However, we notice that* $\widehat{\mathbb{B}}_h^T\mathbf{\Phi}_h^\varepsilon = \mathbf{0}$ *implies that* $\mathbb{M}_h^\varepsilon = \mathbb{M}_h$*. In consequence, the penalisation does not change the problem and therefore:*

Any solution of (7.123) *is a solution of* (7.134) *and reciprocally.*

Indeed, in the literature, this technique is usually known as "exact penalisation".

Thanks to the penalization, we enter the more standard framework (see [79] for the case of static problems) and as a consequence we can state the following result.

Theorem 7.62

Assume that condition (**B.1**) *holds and that* $\boldsymbol{G}_h \in \mathcal{C}^0([0,T];\mathbb{R}^{K_P+K_S})$*. Then, problem* (7.123) *admits a unique solution*

$$(\mathbf{\Phi}_h, \overline{\boldsymbol{E}}_h) \in \mathcal{C}^2([0,T];\mathbb{R}^{K_P+K_S}) \times \mathcal{C}^0([0,T];(\mathrm{Ker}\,\widehat{\mathbb{B}}_h)^\perp).$$

Any other solution is of the form $(\mathbf{\Phi}_h, \overline{\boldsymbol{E}}_h + \boldsymbol{E}_h^0)$ *where* $\boldsymbol{E}_h^0 \in \mathcal{C}^0([0,T];\mathrm{Ker}\,\widehat{\mathbb{B}}_h)$ *is arbitrary.*

Proof. Let us first notice that according to Remark 7.61, problem (7.123) is equivalent to the penalised problem (7.134), thus in the following we denote by $(\mathbf{\Phi}_h, \overline{\boldsymbol{E}}_h)$ the solution of both systems. The way we proceed to prove existence (and uniqueness) of the solution $(\mathbf{\Phi}_h, \overline{\boldsymbol{E}}_h)$ is as

follows.
In a first step, we assume that a solution $(\boldsymbol{\Phi}_h, \widehat{\boldsymbol{E}}_h)$ exists and we eliminate $\widehat{\boldsymbol{E}}_h$ to construct a well-posed problem in $\boldsymbol{\Phi}_h$ alone (see (7.139)). In a second step, with the solution $\boldsymbol{\Phi}_h$ of this problem, we construct a particular $\overline{\boldsymbol{E}}_h \in C^0(0,T;(\operatorname{Ker}\widehat{\mathbb{B}}_h)^\perp)$ (see (7.137)) and prove that $(\boldsymbol{\Phi}_h, \overline{\boldsymbol{E}}_h)$ solves (7.134). Note that this process proves in particular the uniqueness of $\boldsymbol{\Phi}_h$.
Step 1: We first obtain obtain an equation for $\widehat{\boldsymbol{E}}_h$ only. For this, we multiply (7.134a) by $\widehat{\mathbb{B}}_h^T(\mathbb{M}_h^\varepsilon)^{-1}$, which exists thanks to condition **(B.1)** which implies (7.133). Thus we obtain

$$\mathbb{C}_h^\varepsilon\,\widehat{\boldsymbol{E}}_h = \widehat{\mathbb{B}}_h^T\,\widehat{\boldsymbol{G}}_h \tag{7.135}$$

where we have set

$$\mathbb{C}_h^\varepsilon \coloneqq \widehat{\mathbb{B}}_h^T(\mathbb{M}_h^\varepsilon)^{-1}\widehat{\mathbb{B}}_h \quad\text{and}\quad \widehat{\boldsymbol{G}}_h \coloneqq (\mathbb{M}_h^\varepsilon)^{-1}(\boldsymbol{G}_h - \mathbb{A}_h\boldsymbol{\Phi}_h) \in \mathcal{C}^0([0,T];\mathbb{R}^N). \tag{7.136}$$

Moreover, from a classical result in linear algebra (see [107], Section 8.1 for instance) we have

$$\operatorname{Im}(\widehat{\mathbb{B}}_h^T) = \operatorname{Im}(\mathbb{C}_h^\varepsilon).$$

Therefore, there exists a solution $\widehat{\boldsymbol{E}}_h$ of (7.135), which is unique up to an element of $\operatorname{Ker}\widehat{\mathbb{B}}_h$. Next, we restore uniqueness by the so-called pseudo-inverse procedure that selects the (unique) particular solution $\overline{\boldsymbol{E}}_h$ of minimum euclidean norm. This is equivalent to impose that $\overline{\boldsymbol{E}}_h$ is orthogonal to $\operatorname{Ker}\widehat{\mathbb{B}}_h$ or equivalently, to impose that $\mathbb{P}_h\,\overline{\boldsymbol{E}}_h = \boldsymbol{0}$ where $\mathbb{P}_h$ is the orthogonal projection operator from $\mathbb{R}^{K_M+3}$ into $\operatorname{Ker}\widehat{\mathbb{B}}_h$. It is well known (see [108] for instance) that this solution is given by

$$\overline{\boldsymbol{E}}_h = (\widehat{\mathbb{C}}_h^\varepsilon)^{-1}\widehat{\mathbb{B}}_h^T\,\widehat{\boldsymbol{G}}_h, \quad\text{where}\quad \widehat{\mathbb{C}}_h^\varepsilon \coloneqq \big(\mathbb{C}_h^\varepsilon + (\mathbb{P}_h)^T\mathbb{P}_h\big). \tag{7.137}$$

Now, since $\widehat{\mathbb{B}}_h\,\widehat{\boldsymbol{E}}_h = \widehat{\mathbb{B}}_h\,\overline{\boldsymbol{E}}_h$, we see from (7.134a), that $\boldsymbol{\Phi}_h$ must satisfy

$$\mathbb{M}_h^\varepsilon\frac{\mathrm{d}^2\boldsymbol{\Phi}_h}{\mathrm{d}t^2} + \mathbb{A}_h\boldsymbol{\Phi}_h + \widehat{\mathbb{B}}_h\,(\widehat{\mathbb{C}}_h^\varepsilon)^{-1}\widehat{\mathbb{B}}_h^T\,\widehat{\boldsymbol{G}}_h = \boldsymbol{G}_h. \tag{7.138}$$

Thus considering the definition of $\widehat{\boldsymbol{G}}_h$ (see (7.136)), we obtain that

$$\begin{aligned}\mathbb{M}_h^\varepsilon\frac{\mathrm{d}^2\boldsymbol{\Phi}_h}{\mathrm{d}t^2} + \mathbb{A}_h\boldsymbol{\Phi}_h - \widehat{\mathbb{B}}_h\,(\widehat{\mathbb{C}}_h^\varepsilon)^{-1}\widehat{\mathbb{B}}_h^T\big(\mathbb{M}_h^\varepsilon\big)^{-1}\mathbb{A}_h\boldsymbol{\Phi}_h \\ = \boldsymbol{G}_h - \widehat{\mathbb{B}}_h\,(\widehat{\mathbb{C}}_h^\varepsilon)^{-1}\widehat{\mathbb{B}}_h^T\big(\mathbb{M}_h^\varepsilon\big)^{-1}\boldsymbol{G}_h.\end{aligned} \tag{7.139}$$

Notice that problem (7.139) has a unique solution $\boldsymbol{\Phi}_h \in \mathcal{C}^2([0,T];\mathbb{R}^{K_P+K_S})$ since $\mathbb{M}_h^\varepsilon$ is positive.

Step 2: Now we prove that the couple $(\boldsymbol{\Phi}_h, \overline{\boldsymbol{E}}_h)$ is solution of (7.134), where $\boldsymbol{\Phi}_h$ is solution of (7.139) and $\overline{\boldsymbol{E}}_h$ is given by (7.137). First, by definition of $\overline{\boldsymbol{E}}_h$ we have $\overline{\boldsymbol{E}}_h \in \mathcal{C}^0([0,T];\mathbb{R}^{M+3})$ and, from (7.138) we have that

$$\mathbb{M}_h^\varepsilon\frac{\mathrm{d}^2\boldsymbol{\Phi}_h}{\mathrm{d}t^2} + \mathbb{A}_h\boldsymbol{\Phi}_h + \widehat{\mathbb{B}}_h\,\overline{\boldsymbol{E}}_h = \boldsymbol{G}_h.$$

Then, it only remains to check that $\widehat{\mathbb{B}}_h^T\boldsymbol{\Phi}_h \;= \boldsymbol{0}$. To do so, we multiply the equation above by $\widehat{\mathbb{B}}_h^T\big(\mathbb{M}_h^\varepsilon\big)^{-1}$, thus we get

$$\begin{aligned}\widehat{\mathbb{B}}_h^T\frac{\mathrm{d}^2\boldsymbol{\Phi}_h}{\mathrm{d}t^2} &= \widehat{\mathbb{B}}_h^T\big(\mathbb{M}_h^\varepsilon\big)^{-1}\big(\boldsymbol{G}_h - \mathbb{A}_h\boldsymbol{\Phi}_h\big) - \widehat{\mathbb{B}}_h^T\big(\mathbb{M}_h^\varepsilon\big)^{-1}\widehat{\mathbb{B}}_h\,\overline{\boldsymbol{E}}_h \\ &= \widehat{\mathbb{B}}_h^T\,\widehat{\boldsymbol{F}}_h - \mathbb{C}_h^\varepsilon\,\overline{\boldsymbol{E}}_h = \boldsymbol{0}.\end{aligned}$$

Finally, we conclude using the initial conditions $\boldsymbol{\Phi}_h(0) = \dfrac{\mathrm{d}}{\mathrm{d}t}\boldsymbol{\Phi}_h(0) = \boldsymbol{0}$.

■

Remark 7.63

Notice that $\boldsymbol{f} \in L^1([0,T];\boldsymbol{V}_{N,h})$ is enough to have that $\boldsymbol{G}_h \in \mathcal{C}^0([0,T];\mathbb{R}^{K_P+K_S})$ thanks to (6.21) and (5.8).

7.7.4.2 Time stability analysis

In this section, we analyse the time stability of the semi-discrete problem (7.121) under the assumption that condition (**B.1**) is satisfied. Notice, that the time stability of semi-discrete problem (7.121) is classically analysed considering energy techniques. Thus, we begin by considering $\boldsymbol{\psi}_h = \partial_t \boldsymbol{\varphi}_h(t)$ in (7.121a), then by classical computations we obtain the following energy identity (which represents a semi-discrete equivalent to (7.62))

$$\frac{\mathrm{d}}{\mathrm{d}t}\mathcal{E}_{N,h}(\boldsymbol{\varphi}_h) = \mathrm{g}(t, \partial_t \boldsymbol{\varphi}_h), \quad \text{where} \quad \mathcal{E}_{N,h}(\boldsymbol{\psi}) := \frac{1}{2}\, m_h(\partial_t \boldsymbol{\psi}_h, \partial_t \boldsymbol{\psi}_h) + \frac{1}{2}\, a(\boldsymbol{\psi}_h, \boldsymbol{\psi}_h). \tag{7.140}$$

Then, the semi-discrete energy of the solution $\mathcal{E}_{N,h}(\boldsymbol{\varphi}_h)$ is conserved as soon as the right hand side vanishes. Moreover, as long as condition (**B.1**) is satisfied, we also have that $\mathcal{E}_{N,h}(\boldsymbol{\psi}) > 0$ for all $\boldsymbol{\psi} \in \boldsymbol{V}_{N,h} \setminus \{\mathbf{0}\}$ (notice that $\boldsymbol{\varphi}_h(t) \in \boldsymbol{V}_{N,h}$ due to (7.121b)). In the following result, we prove that the positivity of the semi-discrete energy of the solution actually implies the stability of the semi-discrete problem (7.121).

Theorem 7.64

Assume that condition (**B.1**) *holds and that* $\boldsymbol{f} \in L^1([0,T]; \boldsymbol{V}_{N,h})$*. Then there exists a constant* $C > 0$*, independent of* T *and* h*, such that the unique solution* $\boldsymbol{\varphi}_h \in \mathcal{C}^2([0,T]; \boldsymbol{V}_{N,h})$ *of the semi-discrete problem* (7.121) *satisfies*

$$\sup_{t\in[0,T]} \mathcal{E}^{\frac{1}{2}}_{N,h}(\boldsymbol{\varphi}_h(t)) \leq C \|\boldsymbol{f}\|_{L^1([0,T];L^2(\Omega)^2)}. \tag{7.141}$$

Proof. Let us first remark that integrating in time the energy identity in (7.140) and using the initial condition we obtain

$$\mathcal{E}_{N,h}(\boldsymbol{\varphi}_h(t)) = \int_0^t \mathrm{g}(s, \partial_t \boldsymbol{\varphi}_h(s))\,\mathrm{d}s. \tag{7.142}$$

Next, we considering (6.21) and integrate by parts to rewrite the contribution of the right hand side as follows

$$\begin{aligned}
\int_0^t \mathrm{g}(s, \partial_t \boldsymbol{\varphi}_h(s))\,\mathrm{d}s &= -\int_0^t \int_\Omega \boldsymbol{g}(s) \cdot \left(\mathrm{div}\left(\partial_t \boldsymbol{\varphi}_h(s)\right), -\mathrm{curl}\left(\partial_t \boldsymbol{\varphi}_h(s)\right)\right)^T \mathrm{d}\boldsymbol{x}\,\mathrm{d}s \\
&= \int_0^t \int_\Omega \partial_t \boldsymbol{g}(s) \cdot \left(\mathrm{div}\left(\boldsymbol{\varphi}_h(s)\right), -\mathrm{curl}\left(\boldsymbol{\varphi}_h(s)\right)\right)^T \mathrm{d}\boldsymbol{x}\,\mathrm{d}s \\
&- \int_\Omega \boldsymbol{g}(t) \cdot \left(\mathrm{div}\left(\boldsymbol{\varphi}_h(t)\right), -\mathrm{curl}\left(\boldsymbol{\varphi}_h(t)\right)\right)^T \mathrm{d}\boldsymbol{x}.
\end{aligned}$$

In consequence, according to (5.8) we deduce

$$\begin{aligned}
\int_0^t \mathrm{g}(s, \partial_t \boldsymbol{\varphi}_h(s))\,\mathrm{d}s &= \frac{1}{\rho} \int_0^t \int_\Omega \boldsymbol{f}(s) \cdot \left(\mathrm{div}\left(\boldsymbol{\varphi}_h(s)\right), -\mathrm{curl}\left(\boldsymbol{\varphi}_h(s)\right)\right)^T \mathrm{d}\boldsymbol{x}\,\mathrm{d}s \\
&- \frac{1}{\rho} \int_\Omega \int_0^t \boldsymbol{f}(s)\,\mathrm{d}s \cdot \left(\mathrm{div}\left(\boldsymbol{\varphi}_h(t)\right), -\mathrm{curl}\left(\boldsymbol{\varphi}_h(t)\right)\right)^T \mathrm{d}\boldsymbol{x}.
\end{aligned}$$

Hence, using Cauchy-Schwartz inequality, as well as the definition (6.20) of the bilinear form $a(\cdot,\cdot)$, we have that

$$\begin{aligned}
\left|\int_0^t \mathrm{g}(s, \partial_t \boldsymbol{\varphi}_h(s))\,\mathrm{d}s\right| &\leq \frac{1}{\rho} \int_0^t \|\boldsymbol{f}(s)\|_{L^2(\Omega)^2}\ \left\|\left(\mathrm{div}\left(\boldsymbol{\varphi}_h(s)\right), -\mathrm{curl}\left(\boldsymbol{\varphi}_h(s)\right)\right)^T\right\|_{L^2(\Omega)^2}\,\mathrm{d}s \\
&+ \frac{1}{\rho} \int_0^t \|\boldsymbol{f}(s)\|_{L^2(\Omega)^2}\,\mathrm{d}s\ \left\|\left(\mathrm{div}\left(\boldsymbol{\varphi}_h(t)\right), -\mathrm{curl}\left(\boldsymbol{\varphi}_h(t)\right)\right)^T\right\|_{L^2(\Omega)^2} \\
&\leq \frac{2}{\rho}\ \|\boldsymbol{f}\|_{L^1([0,t];L^2(\Omega)^2)}\ \sup_{s\in[0,t]} \sqrt{a(\boldsymbol{\varphi}_h(s), \boldsymbol{\varphi}_h(s))}.
\end{aligned}$$

Now, we make use of condition (**B.1**) to point that $a(\boldsymbol{\varphi}_h(s), \boldsymbol{\varphi}_h(s)) \leq 2\,\mathcal{E}_{N,h}(\boldsymbol{\varphi}_h(s))$ and therefore, combining previous inequality with (7.142) we obtain

$$\sup_{t\in[0,T]} \mathcal{E}_{N,h}(\boldsymbol{\varphi}_h(t)) \leq \frac{2\sqrt{2}}{\rho}\, \|\boldsymbol{f}\|_{L^1([0,T];L^2(\Omega)^2)} \sup_{s\in[0,T]} \sqrt{\mathcal{E}_{N,h}(\boldsymbol{\varphi}_h(s))},$$

which directly gives the result of the theorem.

■

Corollary 7.65

Assume that condition (**B.1**) *holds and that* $\boldsymbol{f} \in L^1([0,T];\boldsymbol{V}_{N,h})$. *Then there exists a constant* $C > 0$, *independent of* T *and* h, *such that the unique solution* $\boldsymbol{\varphi}_h \in \mathcal{C}^2([0,T];\boldsymbol{V}_{N,h})$ *of the semi-discrete problem* (7.121) *satisfies*

$$\sqrt{a(\boldsymbol{\varphi}_h(t), \boldsymbol{\varphi}_h(t))} \leq C\,\|\boldsymbol{f}\|_{L^1([0,T];L^2(\Omega)^2)}, \tag{7.143}$$

$$\sqrt{m_h(\boldsymbol{\varphi}_h(t), \boldsymbol{\varphi}_h(t))} \leq C\,T\,\|\boldsymbol{f}\|_{L^1([0,T];L^2(\Omega)^2)}. \tag{7.144}$$

Proof. First of all, we notice that according to the positivity condition (**B.1**), we have that $a(\boldsymbol{\varphi}_h(t), \boldsymbol{\varphi}_h(t)) \leq 2\,\mathcal{E}_{N,h}(\boldsymbol{\varphi}_h(t))$. Then, since we are in the hypothesis of Theorem 7.64 we have that (7.143) holds

$$\sqrt{a(\boldsymbol{\varphi}_h(t), \boldsymbol{\varphi}_h(t))} \leq \sqrt{2} \sup_{t\in[0,T]} \sqrt{\mathcal{E}_{N,h}(\boldsymbol{\varphi}_h)(t)} \leq C\,\|\boldsymbol{f}\|_{L^1([0,T];L^2(\Omega)^2)}.$$

Moreover, thanks to the vanishing initial condition we can write

$$\boldsymbol{\varphi}_h(t) = \int_0^t \partial_t \boldsymbol{\varphi}_h(s)\,\mathrm{d}s.$$

Then, since $\sqrt{m_h(\cdot,\cdot)}$ is a norm on $\boldsymbol{V}_{N,h}$ and taking into account Jensen's inequality (a continuous version of the triangular inequality), we obtain

$$\sqrt{m_h(\boldsymbol{\varphi}_h(t), \boldsymbol{\varphi}_h(t))} \leq \int_0^t \sqrt{m_h(\partial_t\boldsymbol{\varphi}_h(s), \partial_t\boldsymbol{\varphi}_h(s))}\,\mathrm{d}s \leq \sqrt{2}\; t \sup_{t\in[0,T]} \mathcal{E}^{\frac{1}{2}}_{N,h}(\boldsymbol{\varphi}_h(t)).$$

Finally we use again Theorem 7.64 to obtain (7.144).

■

The relative weakness of the above result is that it is not clear whether estimations (7.143) and (7.144) guarantee an uniform (in h) estimate of $\boldsymbol{\varphi}_h(t)$ in $\boldsymbol{V} = H(\mathrm{div},\Omega) \cap H(\mathrm{curl},\Omega)$. Notice that (7.143) provides control of the L^2-norm of the divergence and the curl of $\boldsymbol{\psi}_h$ (by definition of $a(\cdot,\cdot)$). Moreover, thanks to the expression (7.129) of $m_h(\cdot,\cdot)$ in $\boldsymbol{V}_{N,h}$), we also control the L^2-norm of $\varphi_{P,h}(t)$. However, the reader should notice that we do not have any control of L^2-norm of $\varphi_{S,h}(t)$.

7.7.5 Application to first order Lagrange finite elements

In this section, we restrict our analysis to the case of a polygonal domain Ω and first order Lagrange finite elements. Under this assumption, we provide a particular choice for the finite dimensional spaces $V_{P,h}$, $V_{S,h}$, P_h and M_h such that the following properties are automatically guaranteed:

- The approximation properties (7.109), (7.110) and (7.115).
- The compatibility condition presented in Assumption II.2, in order to satisfy the positivity property (**B.1**) (see Remark 7.59 and Theorem 7.58).

- The non-uniform discrete *Inf-Sup condition* (**B.2**).

On the one hand, we notice that $V_{P,h}$, $V_{S,h}$ and P_h are subsets of $H^1(\Omega)$. Thus, as it is standard, we consider (see (2.57) for definition of $X_p(\cdot)$)

$$V_{P,h} \coloneqq X_1(\mathcal{T}_{P,h}), \quad V_{S,h} \coloneqq X_1(\mathcal{T}_{S,h}) \quad \text{and} \quad P_h \coloneqq X_1(\mathcal{T}_h), \tag{7.145}$$

where $\mathcal{T}_{P,h}$, $\mathcal{T}_{S,h}$ and $\mathcal{T}_h$ are quasi-uniform triangulations of Ω. On the other hand, we notice that $M_h \subset H^{-\frac{1}{2}}(\Gamma)$ and that Γ has corners since we are assuming that Ω is a polygon. Moreover, we will require later that the components of the outward normal vector $\boldsymbol{n} = (n_1, n_2)^T$ belong to M_h, since it implies that (Π_h is the projection from $L^2(\Gamma)$ into M_h defined in (7.111)),

$$\Pi_h(n_1) = n_1 \quad \text{and} \quad \Pi_h(n_2) = n_2. \tag{7.146}$$

Thus we propose an approximation space which allows discontinuities on the corners of Γ (as it is usual in mortar element methods [56] and we have detailed in Section 2.7.1). Therefore, let us denote by χ the set of corners that separate Γ into a family of edges

$$\{\gamma_k\}_{k=1}^s \quad \text{such that} \quad \Gamma = \bigcup_{k=1}^s \gamma_k \quad \text{and} \quad \gamma_k \cap \gamma_j \in \chi \quad \text{if} \quad k \neq j.$$

Then, for each $k \in \{1, \ldots, s\}$, we introduce a quasi-uniform 1D mesh $\mathcal{G}_{k,h}$ of the respective edge γ_k and we consider (see (2.85) for definition of $Y_p(\cdot)$)

$$M_h = \{\nu_h \in M \ / \ \nu_{h|\gamma_k} \in Y_1(\mathcal{G}_k), \ 1 \leq k \leq s\}.$$

Notice that according to Proposition 2.44 and Corollary 2.67, this particular choice of the spaces $V_{P,h}$, $V_{S,h}$, P_h and M_h satisfies the approximation properties (7.109), (7.110) and (7.115).

7.7.5.1 Non-uniform coercivity

In the following result, we prove that the space P_h actually verifies the compatibility condition presented in Assumption II.2 and therefore the positivity property (**B.1**) is automatically guaranteed due to Remark 7.59 and Theorem 7.58.

Theorem 7.66

With the choice of the space P_h given by (7.145), *the compatibility presented in Assumption II.2 holds.*

Proof. For any $p_h \in P_h$ we have that $p_{h|\kappa} \in \mathcal{P}_1$ for all $\kappa \in \mathcal{T}_h$ and therefore $\partial_2 p_h$ is constant in κ. In consequence, since Ω is connected, the condition $\partial_2 p_h \in H^1(\Omega)$ is enough to conclude that this constant is the same in all the triangles, i.e. $\partial_2 p_h = a$ for some $a \in \mathbb{R}$.

■

7.7.5.2 Non-uniform discrete Inf-Sup condition

Now, we discuss the non-uniform discrete *Inf-Sup condition* (**B.2**) which, as we have mentioned before, is less important but nevertheless desirable. It appears that proving this property is slightly more difficult than proving the positivity property (**B.1**) and moreover, in the process we will require the consideration of the following assumptions:

Assumption II.3

For each $k \in \{1, \ldots, s\}$, the quasi-uniform 1D mesh $\mathcal{G}_{k,h}$ of the edge γ_k is the restriction of $\mathcal{T}_h$ to the edge γ_k, i.e.

$$\mathcal{G}_{k,h} \coloneqq \{\partial\kappa \cap \gamma_k \ / \ \kappa \in \mathcal{T}_h\}.$$

Assumption II.4

The triangulation $\mathcal{T}_h$ of Ω is such that all the edges parallel to the x_2 axis not belonging to the boundary have at least one extremity inside Ω.

Assumption II.5

The triangulation $\mathcal{T}_h$ of Ω is such that for all $\kappa \in \mathcal{T}_h$ there exists a function $\psi_{S,\kappa} \in V_{S,h}$ which support is included in κ and such that $\int_\kappa \psi_{S,K}\,\mathrm{d}\boldsymbol{x} \neq 0$.

The purpose of Assumption II.3 is to obtain the following compatibility condition between the spaces M_h and P_h that can be seen as a weaker Inf-Sup condition (which is classical in mortar element methods, see [56] for instance)

$$\nu_h \in M_h, \quad \int_\Gamma \nu_h\, q_h\, \mathrm{d}\boldsymbol{\gamma} = 0 \quad \forall\, q_h \in P_h \quad \Longrightarrow \quad \nu_h = 0. \tag{7.147}$$

Moreover, note that Assumption II.4 is not very restrictive since, even when it fails, a small modification of $\mathcal{T}_h$ allows to recover it (see for instance Figure 7.17). Notice also that Assumption II.5 is a compatibility condition between the space $V_{S,h}$ and P_h. The reader will easily verify that this assumption holds if $\mathcal{T}_{S,h}$ is a sub-mesh of $\mathcal{T}_h$ so that any open triangle κ of $\mathcal{T}_h$ contains a node of $\mathcal{T}_{S,h}$, as illustrated by Figure 7.17b.

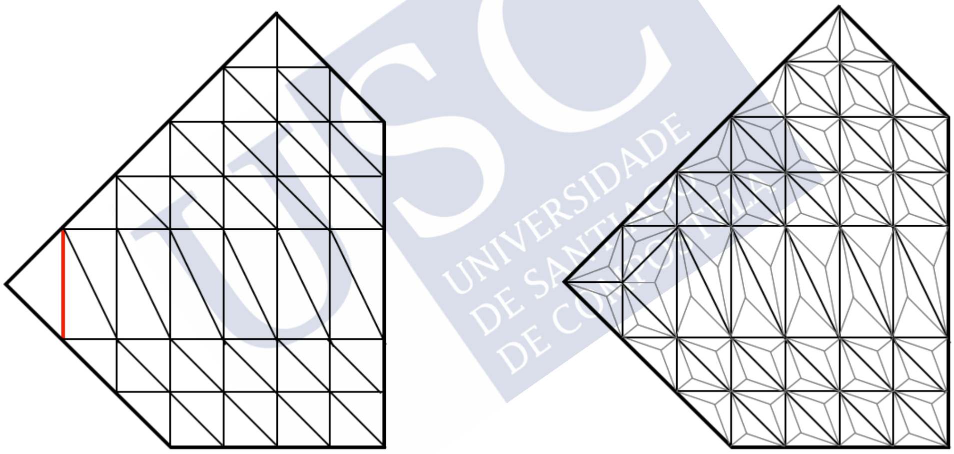

(a) Sketch of a triangulation $\mathcal{T}_h$ that does not satisfy Assumption II.4 because of the leftmost interior edge (in red).

(b) Sketch of a triangulation $\mathcal{T}_h = \mathcal{T}_{P,h}$ (in black) and $\mathcal{T}_{S,h}$ (in grey) satisfying both assumptions II.4 and II.5.

Figure 7.17: Graphic representation of assumptions II.4 and II.5.

Next, considering previous assumptions, we proceed to verify the non-uniform discrete *Inf-Sup condition* (**B.2**) in two steps. First, we prove an intermediate *Inf-Sup condition* for the bilinear form $b_h(\cdot,\cdot)$ and then we extend the result for the augmented bilinear form $\widehat{b}_h(\cdot,\cdot)$.

Lemma 7.67

If the assumptions II.3, II.4 and II.5 hold, then

$$b_h(\nu_h, \boldsymbol{\psi}_h) = 0, \quad \forall\, \boldsymbol{\psi}_h \in \boldsymbol{V}_h \cap H_0^1(\Omega)^2 \quad \Longrightarrow \quad \nu_h = 0. \tag{7.148}$$

Proof. Let us assume that $b_h(\nu_h, \boldsymbol{\psi}_h) = 0$ for all $\boldsymbol{\psi}_h \in \boldsymbol{V}_h \cap H_0^1(\Omega)^2$. Thus, considering the definition (7.117) of the bilinear form $b_h(\cdot,\cdot)$, we have

$$b_h(\nu_h, \boldsymbol{\psi}_h) = \frac{1}{V_P^2} \int_\Omega \partial_1 p_h(\nu_h)\, \psi_{P,h}\, \mathrm{d}\boldsymbol{x} + \frac{1}{V_S^2} \int_\Omega \partial_2 p_h(\nu_h)\, \psi_{S,h}\, \mathrm{d}\boldsymbol{x}, \tag{7.149}$$

where $p_h \equiv p_h(\nu_h)$ is defined by (7.116). Then, the rest of the proof is dedicated to prove that $\nabla p_h = 0$ since according to definition (7.116) of $p_h(\nu_h)$, it implies

$$\int_\Gamma \nu_h\, q_h \,\mathrm{d}\boldsymbol{\gamma} = 0, \quad \forall\, q_h \in P_h,$$

and according to the weaker *Inf-Sup condition* (7.147) (which is in part due to Assumption II.3) we conclude $\nu_h = 0$. Therefore, let κ be any triangle of $\mathcal{T}_h$ and notice that $\partial_2 p_h$ is constant on κ. Thus, considering Assumption II.5, we take $\boldsymbol{\psi}_h = (0, \psi_{S,\kappa})$ in (7.148) and get

$$\int_\kappa \partial_2 p_h\, \psi_{S,\kappa}\,\mathrm{d}x \;=\; \partial_2 p_{h|\kappa} \int_\kappa \psi_{S,\kappa}\,\mathrm{d}x \;=\; 0.$$

In consequence, $\partial_2 p_{h|\kappa} = 0$ and therefore

$$p_h(\boldsymbol{x}) = a_\kappa\, x_1 + b_\kappa, \quad \forall\, \boldsymbol{x} \in \kappa.$$

Moreover, let κ' be a triangle of $\mathcal{T}_h$ that share an edge with κ and notice that with the same arguments we also have

$$p_h(\boldsymbol{x}) = a_{\kappa'}\, x_1 + b_{\kappa'}, \quad \forall\, \boldsymbol{x} \in \kappa'.$$

Next, to prove that $a_\kappa = a_{\kappa'}$ and $b_\kappa = b_{\kappa'}$ we consider the two following cases that depend on the orientation of the edge $e = \kappa \cap \kappa'$ (notice that both cases are mutually exclusive).

A If e is **not parallel** to the x_2 axis: We can consider $\boldsymbol{x} \in e$ and $\boldsymbol{x}' \in e$ such that $x_1 \neq x_1'$. Then, thanks to the continuity of p_h across e, we have that

$$\left.\begin{aligned} (a_\kappa - a_{\kappa'})\, x_1 + (b_\kappa - b_{\kappa'}) = 0 \\ (a_\kappa - a_{\kappa'})\, x_1' + (b_\kappa - b_{\kappa'}) = 0 \end{aligned}\right\} \text{ and therefore } \quad a_\kappa = a_{\kappa'} \quad \text{and} \quad b_\kappa = b_{\kappa'}.$$

B If e is **parallel** to the x_2 axis: This is where the admissibility condition in Assumption II.4 comes into play. Notice, that it implies that there exists an extremity v of e which is in the interior of Ω. Therefore, the corresponding Lagrange basis function q_v belongs to $P_h \cap H_0^1(\Omega)$. Then, as illustrated in Figure 7.18, two cases arise:

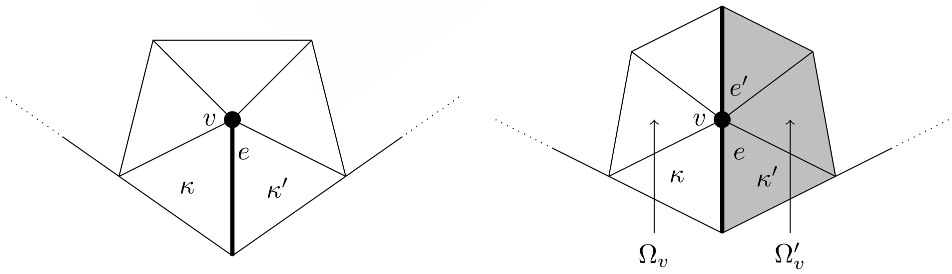

Figure 7.18: Left: sketch of the configuration **B1**. Right: sketch of the configuration **B2**. Each time the element κ is chosen adjacent to the boundary Γ.

B1 There is not any other edge parallel to the x_2 axis that has v as a vertex: In this case, we can argue several times as in case **A** turning around v without crossing e (see Figure 7.18). Then, we conclude again that $a_\kappa = a_{\kappa'}$ and $b_\kappa = b_{\kappa'}$.

B2 There is another edge e' parallel to the x_2 axis that has v as a vertex: Then, the vertical segment $\overline{e \cup e'}$ splits the support of q_v into two parts (see Figure 7.18 right)

$$\operatorname{supp}\, q_v = \overline{\Omega_v} \cup \overline{\Omega_v'}, \quad \text{where} \quad \kappa \subset \Omega_v \quad \text{and} \quad \kappa' \subset \Omega_v'.$$

In this case, we first argue as in case **A** to obtain that $\partial_1 p_h = a_\kappa$ in Ω_v and $\partial_1 p_h = a_{\kappa'}$ in Ω'_v. Next, since p_h is a discrete harmonic function we choose $q_h = q_v$ in (7.116) to obtain

$$\int_\Omega \partial_1 p_h\, \partial_1 q_v \,\mathrm{d}\boldsymbol{x} = 0 \quad\Longrightarrow\quad a_\kappa \int_{\Omega_v} \partial_1 q_v \,\mathrm{d}\boldsymbol{x} + a_{\kappa'} \int_{\Omega'_v} \partial_1 q_v \,\mathrm{d}\boldsymbol{x} = 0.$$

Thus, using Green's formula we obtain $(a_\kappa - a_{\kappa'}) \int_{e\cup e'} q_v \,\mathrm{d}\boldsymbol{\gamma} = 0$ which implies $a_\kappa = a_{\kappa'}$. Moreover, the continuity of p_h across e also implies $b_\kappa = b_{\kappa'}$.

Now notice that by connexity of Ω, the above arguments can be repeated in order to deduce that p_h is an affine function in all Ω, i.e.

$$p_h(\boldsymbol{x}) = a\, x_1 + b, \quad \forall\, \boldsymbol{x} \in \Omega.$$

Finally, we consider in (7.149) the test function $\boldsymbol{\psi}_h = (\psi_{P,h}, 0) \in \boldsymbol{V}_h \cap H_0^1(\Omega)^2$ where $\psi_{P,h} \in V_{P,h}$ is such that $\int_\Omega \psi_{P,h} \,\mathrm{d}\boldsymbol{x}$, thus

$$b_h(\nu_h, \boldsymbol{\psi}_h) = \frac{1}{V_P^2} \int_\Omega \partial_1 p_h\, \psi_{P,\Omega} \,\mathrm{d}\boldsymbol{x} = a \int_\Omega \psi_{P,\Omega} \,\mathrm{d}\boldsymbol{x} = 0 \quad \text{which implies} \quad a = 0.$$

Therefore $\nabla p_h = 0$ and the proof is completed. ■

Theorem 7.68

If the assumptions II.3, II.4 and II.5 hold, then (**B.2**) *holds, i.e.*

$$\widehat{b}_h(\widehat{\nu}_h, \boldsymbol{\psi}_h) = 0, \quad \forall\, \boldsymbol{\psi}_h \in \boldsymbol{V}_h \quad\Longrightarrow\quad \widehat{\nu}_h = \boldsymbol{0}. \tag{7.150}$$

Proof. We begin by noticing that according to the definition (7.122) of the augmented bilinear form $\widehat{b}_h(\cdot,\cdot)$, the left hand side of (7.150) becomes

$$b_h(\nu_h, \boldsymbol{\psi}_h) + \nu_R\, m(\boldsymbol{\xi}_R, \boldsymbol{\psi}_h) + \nu_{\boldsymbol{n}} \int_\Gamma \boldsymbol{\psi}_h \cdot \boldsymbol{n} \,\mathrm{d}\gamma + \nu_{\boldsymbol{\tau}} \int_\Gamma \boldsymbol{\psi}_h \cdot \boldsymbol{\tau} \,\mathrm{d}\gamma = 0, \quad \forall\, \boldsymbol{\psi}_h \in \boldsymbol{V}_h. \tag{7.151}$$

Then, we will proceed in different steps where we first show that $\nu_R = 0$, then that $\nu_h = 0$ and finally that $\nu_{\boldsymbol{n}} = \nu_{\boldsymbol{\tau}} = 0$.
Step 1: Notice, that to prove $\nu_R = 0$, it is enough to find $\boldsymbol{\varphi}_* \in \boldsymbol{V}_{0h}$ such that

$$m(\boldsymbol{\xi}_R, \boldsymbol{\varphi}_*) \neq 0 \quad \text{and} \quad b_h(\nu_h, \boldsymbol{\varphi}_*) = 0 \quad \forall\, \nu_h \in M_h.$$

Then, we consider $\boldsymbol{\varphi}_* = (0,1)^T$ since according to (7.93) is such that $m(\boldsymbol{\xi}_R, \boldsymbol{\varphi}_*) \neq 0$. Moreover, we easily verify that $\boldsymbol{\varphi}_* \in \boldsymbol{V}_{0h}$ since

$$\int_\Gamma \boldsymbol{\varphi}_* \cdot \boldsymbol{n} \,\mathrm{d}\boldsymbol{\gamma} = \int_\Omega \operatorname{div} \boldsymbol{\varphi}_* = 0 \quad \text{and} \quad \int_\Gamma \boldsymbol{\varphi}_* \cdot \boldsymbol{\tau} \,\mathrm{d}\boldsymbol{\gamma} = -\int_\Omega \operatorname{curl} \boldsymbol{\varphi}_* = 0.$$

And to complete this step we consider definition (7.117) of the bilinear form $b_h(\cdot,\cdot)$ to obtain (notice $p_h = p_h(\nu_h)$)

$$\begin{aligned} b_h(\nu_h, \boldsymbol{\varphi}_*) &= \frac{1}{V_S^2} \int_\Omega \partial_2 p_h \mathrm{d}\boldsymbol{x} - \frac{1}{2V_S^2} \int_\Gamma \mathcal{I}(\boldsymbol{\varphi}_* \cdot \boldsymbol{\tau})\, \nu_h \,\mathrm{d}\boldsymbol{\gamma} - \frac{1}{2V_S^2} \int_\Gamma p_h\, \Pi_h(\boldsymbol{\varphi}_* \cdot \boldsymbol{n}) \,\mathrm{d}\boldsymbol{\gamma}, \\ &= \frac{1}{V_S^2} \int_\Gamma p_h\, n_2 \mathrm{d}\boldsymbol{\gamma} - \frac{1}{2V_S^2} \int_\Gamma \mathcal{I}(\boldsymbol{\varphi}_* \cdot \boldsymbol{\tau})\, \nu_h \,\mathrm{d}\boldsymbol{\gamma} - \frac{1}{2V_S^2} \int_\Gamma p_h\, \Pi_h(n_2) \,\mathrm{d}\boldsymbol{\gamma}, \end{aligned}$$

where we have used Green's formula to obtain the second line. Then, notice that according to (7.146) we have that $\Pi_h(\boldsymbol{\varphi} \cdot \boldsymbol{n}) = n_2$ and moreover we can rewrite $\boldsymbol{\varphi}_* = \nabla x_2$ which implies $\mathcal{I}(\boldsymbol{\varphi}_* \cdot \boldsymbol{\tau}) = \mathcal{I}(\partial_{\boldsymbol{\tau}} x_2) = x_2$. In consequence

$$b_h(\nu_h, \boldsymbol{\varphi}) = \frac{1}{2\,V_S^2} \int_\Gamma p_h\, n_2 \,\mathrm{d}\boldsymbol{\gamma} - \frac{1}{2V_S^2} \int_\Gamma x_2\, \nu_h \,\mathrm{d}\boldsymbol{\gamma}. \tag{7.152}$$

To complete this step, we recall that p_h is a discrete harmonic function, thus we consider $q_h = x_2$ in (7.116) to obtain

$$\int_\Omega \partial_2 p_h \,\mathrm{d}\boldsymbol{x} = \int_\Gamma \nu_h\, x_2 \,\mathrm{d}\boldsymbol{\gamma} \quad \text{thus} \quad \int_\Gamma p_h\, n_2 \,\mathrm{d}\boldsymbol{x} = \int_\Gamma \nu_h\, x_2 \,\mathrm{d}\boldsymbol{\gamma}.$$

This equality, combined with (7.152), gives $b_h(\nu_h, \boldsymbol{\varphi}_*) = 0$ and completes the first step.

Step 2: To prove $\nu_h = 0$ we use Lemma 7.67. Notice, that we have already proved that $\nu_R = 0$, thus we simply consider in (7.151) test functions $\boldsymbol{\psi}_h$ in $\boldsymbol{V}_h \cap H_0^1(\Omega)^2$ and we obtain

$$b_h(\nu_h, \boldsymbol{\psi}_h) = 0, \quad \forall\, \boldsymbol{\psi}_h \in \boldsymbol{V}_h \cap H_0^1(\Omega)^2,$$

which is precisely the hypothesis in Lemma 7.67 and therefore allows us to conclude that $\nu_h = 0$.

Step 3: Notice that, to prove $\nu_{\boldsymbol{n}} = 0$, it is enough to consider in (7.151) the test function $\boldsymbol{\psi}_{\boldsymbol{n}} = (x_1, x_2)^T \in \boldsymbol{V}_h$ which satisfies

$$\int_\Gamma \boldsymbol{\psi}_{\boldsymbol{n}} \cdot \boldsymbol{n} \,\mathrm{d}\boldsymbol{\gamma} = \int_\Omega \operatorname{div} \boldsymbol{\psi}_{\boldsymbol{n}} \,\mathrm{d}\boldsymbol{x} = \int_\Omega 2 \,\mathrm{d}\boldsymbol{x} > 0 \quad \text{and} \quad \int_\Gamma \boldsymbol{\psi}_{\boldsymbol{n}} \cdot \boldsymbol{\tau} \,\mathrm{d}\boldsymbol{\gamma} = \int_\Omega \operatorname{curl} \boldsymbol{\psi}_{\boldsymbol{n}} \,\mathrm{d}\boldsymbol{x} = 0.$$

Step 4: Similarly, to prove $\nu_{\boldsymbol{\tau}} = 0$, it is enough to consider in (7.151) the test function $\boldsymbol{\psi}_{\boldsymbol{\tau}} = (x_2, -x_1)^T \in \boldsymbol{V}_h$ which satisfies

$$\int_\Gamma \boldsymbol{\psi}_{\boldsymbol{\tau}} \cdot \boldsymbol{n} \,\mathrm{d}\boldsymbol{\gamma} = \int_\Omega \operatorname{div} \boldsymbol{\psi}_{\boldsymbol{\tau}} \,\mathrm{d}\boldsymbol{x} = 0 \quad \text{and} \quad \int_\Gamma \boldsymbol{\psi}_{\boldsymbol{\tau}} \cdot \boldsymbol{\tau} \,\mathrm{d}\boldsymbol{\gamma} = \int_\Omega \operatorname{curl} \boldsymbol{\psi}_{\boldsymbol{\tau}} \,\mathrm{d}\boldsymbol{x} = \int_\Omega 2 \,\mathrm{d}\boldsymbol{x} > 0.$$

■

7.7.5.3 About mass lumping

For efficiency, we can consider specific quadrature formulas that achieve mass lumping as we have already explained in Section 6.4.1 for the Dirichlet case. This technique, usually provides an approximated mass matrix that is diagonal and preserves the order of accuracy as it was the case for the Dirichlet problem. However, in the Neumann case, since the mass is given by $\mathbb{M}_h = \mathbb{M}_h^\Omega + \mathbb{M}_h^\Gamma$ this seems not possible. Instead, the approximation concerns only the volume part of the mass matrix and we consider

$$\widetilde{\mathbb{M}}_h := \widetilde{\mathbb{M}}_h^\Omega + \mathbb{M}_h^\Gamma$$

where $\widetilde{\mathbb{M}}_h^\Omega$ is a diagonal matrix. In the particular case of first order Lagrange finite elements, this matrix is given by (6.37) and it is known to add positivity to the mass as we have proved in Lemma 6.8, i.e.

$$\widetilde{\mathbb{M}}_h^\Omega\, \boldsymbol{\Psi}_h \cdot \boldsymbol{\Psi}_h \geq \mathbb{M}_h^\Omega\, \boldsymbol{\Psi}_h \cdot \boldsymbol{\Psi}_h.$$

An important consequence of this property is that if $\mathbb{M}_h$ satisfies the positivity condition (**B.1**), then $\widetilde{\mathbb{M}}_h$ also does and therefore the semi-discrete problem (7.123) is well-posed and stable when mass lumping is considered for the computation of $\widetilde{\mathbb{M}}_h^\Omega$.

7.8 Time discretization

In this section, we investigate the well-known theta-schemes (Section 7.8.1) and a semi-implicit scheme (Section 7.8.2). The theta-scheme will be considered as the reference scheme and the semi-implicit scheme as an improvement and an extension of the scheme that was already proposed for the case of the Dirichlet condition in Section 6.4.2. Its advantages will be outlined in terms of the CFL condition. Throughout this section, Δt will denote a time step such that $N\Delta t = T$, the vectors $\boldsymbol{\Phi}_h^n$ and $\widehat{\boldsymbol{E}}_h^n$ will respectively denote the approximation of $\boldsymbol{\Phi}_h(n\Delta t)$ and $\widehat{\boldsymbol{E}}_h(n\Delta t)$, where $(\boldsymbol{\Phi}_h, \widehat{\boldsymbol{E}}_h)$ is the solution of (7.123) and $\boldsymbol{G}_h^n = \boldsymbol{G}_h(n\Delta t)$.

7.8.1 Theta-schemes.

The schemes we propose in this section are a family of conservative centered integrators, parameterized by $\theta \in \mathbb{R}$ and that belong to the class of Newmark schemes. When applied to (7.123), these schemes lead to (completed with $\boldsymbol{\Phi}_h^0 = \boldsymbol{\Phi}_h^1 = \mathbf{0}$)

$$\begin{cases} \mathbb{M}_h \dfrac{\boldsymbol{\Phi}_h^{n+1} - 2\,\boldsymbol{\Phi}_h^n + \boldsymbol{\Phi}_h^{n-1}}{\Delta t^2} + \mathbb{A}_h \{\boldsymbol{\Phi}_h^n\}_\theta + \widehat{\mathbb{B}}_h\, \widehat{\boldsymbol{E}}_h^n = \boldsymbol{G}_h^n, & (7.153a) \\ \widehat{\mathbb{B}}_h^T \boldsymbol{\Phi}_h^n = \mathbf{0}, & (7.153b) \end{cases}$$

where we have used the notation $\{\boldsymbol{\Phi}_h^n\}_\theta := \theta\,\boldsymbol{\Phi}_h^{n+1} + (1 - 2\,\theta)\boldsymbol{\Phi}_h^n + \theta\,\boldsymbol{\Phi}_h^{n-1}$. Unfortunately, it is not clear if the matrix $\mathbb{M}_h + \theta \Delta t^2 \mathbb{A}_h$ is invertible, which is a necessary property to use a Schur complement strategy, as we presented in Section 3.4.1. In consequence, at each iteration, since $\boldsymbol{\Phi}_h^{n-1}$ and $\boldsymbol{\Phi}_h^n$ are known, we compute $\boldsymbol{\Phi}_h^{n+1}$ and $\widehat{\boldsymbol{E}}_h^n$ by solving the linear problem

$$\mathbb{L}_{\theta,h} \big(\boldsymbol{\Phi}_h^{n+1}, \widehat{\boldsymbol{E}}_h^n\big)^T = \Big(\boldsymbol{G}_h^n + \mathbb{M}_h \frac{2\,\boldsymbol{\Phi}_h^n - \boldsymbol{\Phi}_h^{n-1}}{\Delta t^2} - (1-2\theta)\mathbb{A}_h \boldsymbol{\Phi}_h^n - \theta\,\mathbb{A}_h \boldsymbol{\Phi}_h^{n-1}, \mathbf{0}\Big)^T \tag{7.154}$$

where we have introduced the following matrix

$$\mathbb{L}_{\theta,h} = \begin{pmatrix} \dfrac{\mathbb{M}_h}{\Delta t^2} + \theta \mathbb{A}_h & \widehat{\mathbb{B}}_h \\ \widehat{\mathbb{B}}_h^T & \mathbb{O} \end{pmatrix}. \tag{7.155}$$

The invertibility of this matrix and therefore the well-posedness of the fully-discrete problem (7.153) is given in the following result.

Theorem 7.69

*If properties (**B.1**) and (**B.2**) are satisfied, then the matrix $\mathbb{L}_{\theta,h}$ is invertible.*

Proof. This can be done along the same lines of the analysis of the semi-discrete problem (7.123), thus we refer to Theorem 7.62 for details and here we only provide a sketch of the proof. First we note that the invertibility of the matrix $\mathbb{L}_{\theta,h}$ is equivalent (this is exact penalization) to the invertibility of the matrix

$$\mathbb{L}_{\theta,h}^{\varepsilon} = \begin{pmatrix} \dfrac{\mathbb{M}_h}{\Delta t^2} + \dfrac{\widehat{\mathbb{B}}_h \widehat{\mathbb{B}}_h^T}{\varepsilon} + \theta \mathbb{A}_h & \widehat{\mathbb{B}}_h \\ \widehat{\mathbb{B}}_h^T & \mathbb{O} \end{pmatrix},$$

where ε is chosen small enough so that (this is possible thanks to Lemma 7.60)

$$\frac{\mathbb{M}_h}{\Delta t^2} + \frac{\widehat{\mathbb{B}}_h \widehat{\mathbb{B}}_h^T}{\varepsilon} \quad \text{is positive definite.}$$

Then, since $\mathbb{A}_h$ is non negative, the first block of $\mathbb{L}_{\theta,h}^{\varepsilon}$ is also positive definite. Finally, a standard Schur complement procedure yields the invertibility of $\mathbb{L}_{\theta,h}^{\varepsilon}$. ■

Remark 7.70

*If only (**B.1**) holds, but not (**B.2**), we have*

$$\operatorname{Ker} \mathbb{L}_{\theta,h} = \big\{(\mathbf{0}, \widehat{\boldsymbol{E}}_h)^T \ / \ \widehat{\boldsymbol{E}}_h \in \operatorname{Ker} \widehat{\mathbb{B}}_h\big\}.$$

Next, as it is classical (see Section 3.4 for details), we analyse the stability of the fully-discrete problem (7.153) considering energy techniques. Thus we introduce the notation $\boldsymbol{\Phi}_h^{n+\frac{1}{2}} := \frac{1}{2}\big(\boldsymbol{\Phi}_h^{n+1}+\boldsymbol{\Phi}_h^{n}\big)$ and define the following discrete energy

$$\mathcal{E}_{h,\theta}^{n+\frac{1}{2}} := \frac{1}{2}\,\mathbb{M}_{h,\Delta t}\frac{\boldsymbol{\Phi}_h^{n+1}-\boldsymbol{\Phi}_h^{n}}{\Delta t}\cdot\frac{\boldsymbol{\Phi}_h^{n+1}-\boldsymbol{\Phi}_h^{n}}{\Delta t}+\frac{1}{2}\,\mathbb{A}_h\boldsymbol{\Phi}_h^{n+\frac{1}{2}}\cdot\boldsymbol{\Phi}_h^{n+\frac{1}{2}}, \tag{7.156}$$

where $\mathbb{M}_{h,\Delta t} := \mathbb{M}_h - \Delta t^2\Big(\frac{1-4\theta}{4}\Big)\mathbb{A}_h$ is a modified mass matrix. Then, we show below that the fully-discrete problem (7.153) is stable if this energy is a positive quadratic functional on $\operatorname{Ker}\widehat{\mathbb{B}}_h^T$. In consequence, since $\mathbb{A}_h$ is a positive semi-definite matrix, it is enough to have that

$$\widehat{\mathbb{B}}_h^T\boldsymbol{\Psi}_h = 0 \quad\Longrightarrow\quad \mathbb{M}_{h,\Delta t}\boldsymbol{\Psi}_h\cdot\boldsymbol{\Psi}_h \geq 0.$$

This condition is usually called CFL condition and notice that for $\theta \geq 1/4$, it is directly satisfied when **(B.1)** holds, while for $\theta < 1/4$ it requires the verification of the following assumption.

Assumption II.6

When $\theta < 1/4$, we assume that Δt is such that

$$\alpha < 1 \quad \textit{where} \quad \alpha = \Delta t^2\Big(\frac{1-4\theta}{4}\Big)\max_{\boldsymbol{\psi}_h\in\boldsymbol{V}_{N,h}\setminus\{\mathbf{0}\}}\frac{a(\boldsymbol{\psi}_h,\boldsymbol{\psi}_h)}{m_h(\boldsymbol{\psi}_h,\boldsymbol{\psi}_h)}. \tag{7.157}$$

In the following result, we prove that the positivity of the discrete energy actually implies the stability of the fully-discrete problem (7.153).

Theorem 7.71

If **(B.1)**, **(B.2)** *and Assumption II.6 hold, there exists $C > 0$, independent of T and h, such that the unique solution $\boldsymbol{\Phi}_h^n$ of the fully-discrete problem (7.153) satisfies*

$$\max_{n\in\{0,\dots,N\}}\big(\mathcal{E}_{h,\theta}^{n+\frac{1}{2}}\big)^{\frac{1}{2}} \leq C\|\boldsymbol{f}\|_{L^1([0,T];L^2(\Omega)^2)}. \tag{7.158}$$

Proof. The first part of the proof is standard and has already been presented in this manuscript (see Section 3.4), thus we skip some of the details. We first rewrite (7.153a) as

$$\Big(\mathbb{M}_h - \frac{1-4\,\theta}{4}\Delta t^2\mathbb{A}_h\Big)\frac{\boldsymbol{\Phi}_h^{n+1}-2\,\boldsymbol{\Phi}_h^{n}+\boldsymbol{\Phi}_h^{n-1}}{\Delta t^2}+\mathbb{A}_h\frac{\boldsymbol{\Phi}_h^{n+1}+2\,\boldsymbol{\Phi}_h^{n}+\boldsymbol{\Phi}_h^{n-1}}{4}+\widehat{\mathbb{B}}_h\,\widehat{\boldsymbol{E}}_h^n = \boldsymbol{G}_h^n.$$

Then, we multiply by $(\boldsymbol{\Phi}_h^{n+1}-\boldsymbol{\Phi}_h^{n-1})/2\Delta t$ and we obtain the following discrete energy identity

$$\frac{\mathcal{E}_{h,\theta}^{n+\frac{1}{2}}-\mathcal{E}_{h,\theta}^{n-\frac{1}{2}}}{\Delta t} = \boldsymbol{G}_h^n\cdot\frac{\boldsymbol{\Phi}_h^{n+1}-\boldsymbol{\Phi}_h^{n-1}}{2\Delta t}.$$

In consequence, after summation over discrete times, we deduce that

$$\begin{aligned}\mathcal{E}_{h,\theta}^{n+\frac{1}{2}} &= \Delta t\sum_{m=1}^{n}\boldsymbol{G}_h^m\cdot\frac{\boldsymbol{\Phi}_h^{m+1}-\boldsymbol{\Phi}_h^{m-1}}{2\Delta t}\\ &= -\Delta t\sum_{m=1}^{n-1}\frac{\boldsymbol{G}_h^{m+1}-\boldsymbol{G}_h^{m}}{\Delta t}\cdot\boldsymbol{\Phi}_h^{m+\frac{1}{2}}+\boldsymbol{G}_h^n\cdot\boldsymbol{\Phi}_h^{n+\frac{1}{2}},\end{aligned} \tag{7.159}$$

which is nothing but a discrete equivalent of the identity (7.142) for the semi-discrete case. Now, in order to rewrite the terms on the right hand side, we first introduce $\boldsymbol{\varphi}_h^m$ for the approximation of $\boldsymbol{\varphi}_h(m\Delta t)$ (analogously to the introduction of $\boldsymbol{\Phi}_h^m$ for the approximation of $\boldsymbol{\Phi}_h(m\Delta t)$). Then, taking into account the definition (6.21) we have that

$$\begin{aligned}\boldsymbol{G}_h^n \cdot \boldsymbol{\Phi}_h^m &= \boldsymbol{G}_h(n\Delta t) \cdot \boldsymbol{\Phi}_h^m = \mathrm{g}(n\Delta t, \boldsymbol{\varphi}_h^m) \\ &= -\int_\Omega \boldsymbol{g}(n\Delta t) \cdot \left(\operatorname{div} \boldsymbol{\varphi}_h^m, -\operatorname{curl} \boldsymbol{\varphi}_h^m\right)^T \mathrm{d}\boldsymbol{x}.\end{aligned}$$

Moreover, according to (5.8) we also have that

$$\boldsymbol{g}(n\Delta t) = \sum_{k=0}^{n-1} \frac{1}{\rho} \int_{k\Delta t}^{(k+1)\Delta t} \boldsymbol{f}(s)\, \mathrm{d}s,$$

and combining the two previous equations

$$\left(\boldsymbol{G}_h^{m+1} - \boldsymbol{G}_h^m\right) \cdot \boldsymbol{\Phi}_h^{m+\frac{1}{2}} = -\frac{1}{\rho} \int_\Omega \int_{m\Delta t}^{(m+1)\Delta t} \boldsymbol{f}(s)\, \mathrm{d}s \cdot \left(\operatorname{div} \boldsymbol{\varphi}_h^{m+\frac{1}{2}}, -\operatorname{curl} \boldsymbol{\varphi}_h^{m+\frac{1}{2}}\right)^T \mathrm{d}\boldsymbol{x}.$$

In consequence, (7.159) becomes

$$\begin{aligned}\mathcal{E}_{h,\theta}^{n+\frac{1}{2}} &= \frac{1}{\rho} \sum_{m=1}^{n-1} \int_\Omega \int_{m\Delta t}^{(m+1)\Delta t} \boldsymbol{f}(s)\, \mathrm{d}s \cdot \left(\operatorname{div} \boldsymbol{\varphi}_h^{m+\frac{1}{2}}, -\operatorname{curl} \boldsymbol{\varphi}_h^{m+\frac{1}{2}}\right)^T \mathrm{d}\boldsymbol{x} \\ &- \frac{\Delta t}{\rho} \int_\Omega \sum_{k=0}^{n-1} \int_{k\Delta t}^{(k+1)\Delta t} \boldsymbol{f}(s)\, \mathrm{d}s \cdot \left(\operatorname{div} \boldsymbol{\varphi}_h^{n+\frac{1}{2}}, -\operatorname{curl} \boldsymbol{\varphi}_h^{n+\frac{1}{2}}\right)^T \mathrm{d}\boldsymbol{x}.\end{aligned}$$

Hence, using Cauchy-Schwartz inequality, as well as the definition (6.20) of the bilinear form $a(\cdot,\cdot)$, we have that

$$\begin{aligned}\mathcal{E}_{h,\theta}^{n+\frac{1}{2}} &\leq \frac{1}{\rho} \sum_{m=1}^{n-1} \int_{m\Delta t}^{(m+1)\Delta t} \|\boldsymbol{f}(s)\|_{L^2(\Omega)^2}\, \mathrm{d}s \left\| \left(\operatorname{div} \boldsymbol{\varphi}_h^{m+\frac{1}{2}}, -\operatorname{curl} \boldsymbol{\varphi}_h^{m+\frac{1}{2}}\right)^T \right\|_{L^2(\Omega)^2} \\ &+ \frac{\Delta t}{\rho} \sum_{k=0}^{n-1} \int_{k\Delta t}^{(k+1)\Delta t} \|\boldsymbol{f}(s)\|_{L^2(\Omega)^2}\, \mathrm{d}s \left\| \left(\operatorname{div} \boldsymbol{\varphi}_h^{n+\frac{1}{2}}, -\operatorname{curl} \boldsymbol{\varphi}_h^{n+\frac{1}{2}}\right)^T \right\|_{L^2(\Omega)^2} \\ &\leq \frac{1+\Delta t}{\rho} \|\boldsymbol{f}(s)\|_{L^1([0,t^n],L^2(\Omega)^2)} \max_{m \in \{0,\ldots,n\}} \sqrt{a(\boldsymbol{\varphi}_h^{m+\frac{1}{2}}, \boldsymbol{\varphi}_h^{m+\frac{1}{2}})}.\end{aligned}$$

Now, we make use of condition **(B.1)** and Assumption II.6, to point that $a(\boldsymbol{\varphi}_h^{m+\frac{1}{2}}, \boldsymbol{\varphi}_h^{m+\frac{1}{2}}) \leq 2\,\mathcal{E}_{h,\theta}^{m+\frac{1}{2}}$ and therefore

$$\max_{n \in \{0,\ldots,N\}} \mathcal{E}_{h,\theta}^{n+\frac{1}{2}} \leq \sqrt{2}\, \frac{1+\Delta t}{\rho} \|\boldsymbol{f}(s)\|_{L^1([0,t^n],L^2(\Omega)^2)} \max_{m \in \{0,\ldots,N\}} \sqrt{\mathcal{E}_{h,\theta}^{m+\frac{1}{2}}},$$

which directly gives the result of the theorem.

■

Corollary 7.72

If **(B.1)**, **(B.2)** *and Assumption II.6 hold, there exists* $C > 0$, *independent of* T *and* h, *such that the unique solution* $\boldsymbol{\Phi}_h^n$ *of the fully-discrete problem* (7.153) *satisfies, for all* $n \in \{0, \ldots, N\}$,

$$\left(\mathbb{A}_h \boldsymbol{\Phi}_h^{n+\frac{1}{2}} \cdot \boldsymbol{\Phi}_h^{n+\frac{1}{2}}\right)^{\frac{1}{2}} \leq C \|\boldsymbol{f}\|_{L^1([0,T];L^2(\Omega)^2)}, \tag{7.160}$$

$$\left(\mathbb{M}_h \boldsymbol{\Phi}_h^{n+1} \cdot \boldsymbol{\Phi}_h^{n+1}\right)^{\frac{1}{2}} \leq C_\alpha\, T \|\boldsymbol{f}\|_{L^1([0,T];L^2(\Omega)^2)}, \tag{7.161}$$

where $C_\alpha = 1$ *if* $\theta \geq 1/4$ *or* $C_\alpha = C/\sqrt{1-\alpha}$ *if* $\theta < 1/4$.

Proof. First, of all, we notice that according to the positivity condition (**B.1**), we have that $\mathbb{A}_h \boldsymbol{\Phi}_h^{n+\frac{1}{2}} \cdot \boldsymbol{\Phi}_h^{n+\frac{1}{2}} \leq 2\, \mathcal{E}_{h,\theta}^{n+\frac{1}{2}}$. Then, since we are in the hypothesis of Theorem 7.71 we have that (7.160) holds

$$\left(\mathbb{A}_h \boldsymbol{\Phi}_h^{n+\frac{1}{2}} \cdot \boldsymbol{\Phi}_h^{n+\frac{1}{2}}\right)^{\frac{1}{2}} \leq \sqrt{2} \max_{n\in\{0,\dots,N\}} \sqrt{\mathcal{E}_{h,\theta}^{n+\frac{1}{2}}} \leq C\, \|\boldsymbol{f}\|_{L^1([0,T];L^2(\Omega)^2)}.$$

Now we notice that $\sqrt{\mathbb{M}_h \boldsymbol{\Phi}\cdot\boldsymbol{\Phi}}$ defines a norm in $\boldsymbol{V}_{N,h}$ (due to (**B.1**)) and considering Assumption II.6, we can bound (α is defined in (7.157))

$$\begin{aligned}
\text{If } \theta \geq 1/4 \quad \mathbb{M}_h \boldsymbol{\Phi}\cdot\boldsymbol{\Phi} \quad &\leq \quad \mathbb{M}_{h,\Delta t} \boldsymbol{\Phi}\cdot\boldsymbol{\Phi},\\
\text{If } \theta < 1/4 \quad \mathbb{M}_h \boldsymbol{\Phi}\cdot\boldsymbol{\Phi} \quad &= \quad \left(\mathbb{M}_h - \frac{1-4\,\theta}{4}\Delta t^2 \mathbb{A}\right)\boldsymbol{\Phi}\cdot\boldsymbol{\Phi} + \frac{1-4\,\theta}{4}\Delta t^2 \mathbb{A}\boldsymbol{\Phi}\cdot\boldsymbol{\Phi}\\
&\leq \quad \mathbb{M}_{h,\Delta t}\boldsymbol{\Phi}\cdot\boldsymbol{\Phi} + \alpha\, \mathbb{M}_h \boldsymbol{\Phi}\cdot\boldsymbol{\Phi}.
\end{aligned}$$

Thus, $\sqrt{\mathbb{M}_h \boldsymbol{\Phi}\cdot\boldsymbol{\Phi}} \leq C_\alpha \sqrt{\mathbb{M}_{h,\Delta t} \boldsymbol{\Phi}\cdot\boldsymbol{\Phi}}$ where $C_\alpha = 1$ if $\theta \geq 1/4$ or $C_\alpha = 1/\sqrt{1-\alpha}$ if $\theta < 1/4$. Moreover, according to (7.153b), $\boldsymbol{\Phi}^n \in \boldsymbol{V}_{N,h}$ for all $n \in \{0,\dots,N\}$ and thanks to the vanishing initial conditions, we can write

$$\boldsymbol{\Phi}_h^{n+1} = \sum_{m=1}^{n} \left(\boldsymbol{\Phi}_h^{m+1} - \boldsymbol{\Phi}_h^{m}\right).$$

In consequence, considering triangular inequality we compute

$$\begin{aligned}
\left(\mathbb{M}_h \boldsymbol{\Phi}_h^{n+1}\cdot\boldsymbol{\Phi}_h^{n+1}\right)^{\frac{1}{2}} \quad &\leq \quad C_\alpha \sum_{m=1}^{n} \left(\mathbb{M}_{h,\Delta t}\left(\boldsymbol{\Phi}_h^{m+1} - \boldsymbol{\Phi}_h^{m}\right)\cdot\left(\boldsymbol{\Phi}_h^{m+1} - \boldsymbol{\Phi}_h^{m}\right)\right)^{\frac{1}{2}}\\
&\leq \quad \sqrt{2}\, C_\alpha \Delta t \sum_{m=1}^{n} \left(\mathcal{E}_{h,\theta}^{m+\frac{1}{2}}\right)^{\frac{1}{2}} = \sqrt{2}\, C_\alpha\, \Delta t\, n \max_{m\in\{1,\dots,n\}} \left(\mathcal{E}_{h,\theta}^{m+\frac{1}{2}}\right)^{\frac{1}{2}}
\end{aligned}$$

Finally, we notice $N\,\Delta t = T$, take the maximum in $\{0,\dots,N\}$ and use again Theorem 7.71, thus we obtain (7.161).

■

7.8.2 Semi-implicit scheme

In this section, we follow the ideas presented in Section 6.4.2 for the Dirichlet case and firstly introduced in [17], in order to introduce a semi-implicit time discretization where we treat implicitly only the part of the bilinear form $a(\cdot,\cdot)$ which is related to the boundary Γ. More precisely, the semi-implicit scheme for (7.123) is obtained by treating implicitly with $\theta = \frac{1}{4}$ the "boundary part" $\mathbb{A}_h^\Gamma$ of $\mathbb{A}_h$, and explicitly the remaining part:

$$\left\{\begin{array}{l}
\mathbb{M}_h \dfrac{\boldsymbol{\Phi}_h^{n+1} - 2\,\boldsymbol{\Phi}_h^{n} + \boldsymbol{\Phi}_h^{n-1}}{\Delta t^2} + \mathbb{A}_h^\Omega \boldsymbol{\Phi}_h^n + \mathbb{A}_h^\Gamma \{\boldsymbol{\Phi}_h^n\}_{\frac{1}{4}} + \widehat{\mathbb{B}}_h\, \widehat{\boldsymbol{E}}_h^n = \boldsymbol{G}_h^n,\\
\widehat{\mathbb{B}}_h^T \boldsymbol{\Phi}_h^n = 0,
\end{array}\right. \tag{7.162}$$

completed with $\boldsymbol{\Phi}_h^0 = \boldsymbol{\Phi}_h^1 = \boldsymbol{0}$. Unfortunately, as for theta-schemes presented in Section 7.8.1, it is not clear if the matrix $\mathbb{M}_h + \theta \Delta t^2 \mathbb{A}_h^\Gamma$ is invertible, which is a necessary property to use a Schur complement strategy, as we presented in Section 3.4.1. In consequence, at each iteration, since $\boldsymbol{\Phi}_h^{n-1}$ and $\boldsymbol{\Phi}_h^n$ are known, we compute $\boldsymbol{\Phi}_h^{n+1}$ and $\widehat{\boldsymbol{E}}_h^n$ by solving the linear problem

$$\mathbb{L}_{\Gamma,h}\left(\boldsymbol{\Phi}_h^{n+1}, \widehat{\boldsymbol{E}}_h^n\right)^T = \left(\boldsymbol{G}_h^n + \mathbb{M}_h \frac{2\,\boldsymbol{\Phi}_h^n - \boldsymbol{\Phi}_h^{n-1}}{\Delta t^2} - \mathbb{A}_h^\Omega \boldsymbol{\Phi}_h^n - \frac{1}{2}\mathbb{A}_h^\Gamma \boldsymbol{\Phi}_h^n - \frac{1}{4}\,\mathbb{A}_h \boldsymbol{\Phi}_h^{n-1}, \boldsymbol{0}\right)^T \tag{7.163}$$

where we have introduced the following matrix

$$\mathbb{L}_{\Gamma,h} = \begin{pmatrix} \dfrac{\mathbb{M}_h}{\Delta t^2} + \dfrac{\mathbb{A}_h^\Gamma}{4} & \widehat{\mathbb{B}}_h \\ \widehat{\mathbb{B}}_h^T & \mathbb{O} \end{pmatrix}.$$

In this case, contrary to the case of theta-schemes presented in Section 7.8.1, the well posedness of the fully-discrete problem (7.162) is not given only by (**B.1**) and (**B.2**) since $\mathbb{A}_h^\Gamma$ has no sign in $\boldsymbol{V}_{N,h}$. We had the same situation in Section 6.4.2 for the Dirichlet case and we proceed here similarly, i.e. we find first an adequate stability condition and then we show that it also provides well-posedness. Thus we proceed again by energy techniques, therefore we define the following discrete energy

$$\mathcal{E}_{N,h}^{n+\frac{1}{2}} = \frac{1}{2}\Big(\mathbb{M}_h - \frac{\Delta t^2}{4}\mathbb{A}_h^\Omega\Big)\frac{\boldsymbol{\Phi}_h^{n+1} - \boldsymbol{\Phi}_h^n}{\Delta t} \cdot \frac{\boldsymbol{\Phi}_h^{n+1} - \boldsymbol{\Phi}_h^n}{\Delta t} + \frac{1}{2}\,\mathbb{A}_h \boldsymbol{\Phi}_h^{n+\frac{1}{2}} \cdot \boldsymbol{\Phi}_h^{n+\frac{1}{2}}. \tag{7.164}$$

Note that an important difference between (7.156) and (7.164), is that, in the first term of the sum, $\mathbb{A}_h$ has been replaced by $\mathbb{A}_h^\Omega$ (and, less important, $1-4\theta$ by 1). Then, the fully-discrete problem (7.162) is stable if this energy is a positive quadratic functional on $\operatorname{Ker}\widehat{\mathbb{B}}_h^T$. In consequence, since $\mathbb{A}_h$ is a positive semi-definite matrix, it is enough to have that

$$\widehat{\mathbb{B}}_h^T \boldsymbol{\Psi}_h = 0 \quad \Longrightarrow \quad \Big(\mathbb{M}_h - \frac{\Delta t^2}{4}\mathbb{A}_h^\Omega\Big)\boldsymbol{\Psi}_h \cdot \boldsymbol{\Psi}_h \geq 0.$$

The verification of this CFL condition requires the consideration of the following assumption.

Assumption II.7

We assume that Δt is such that

$$\alpha < 1 \quad \textit{where} \quad \alpha = \frac{\Delta t^2}{4} \max_{\boldsymbol{\psi}_h \in \boldsymbol{V}_{N,h}\setminus\{\boldsymbol{0}\}} \frac{a_\Omega(\boldsymbol{\psi}_h, \boldsymbol{\psi}_h)}{m_h(\boldsymbol{\psi}_h, \boldsymbol{\psi}_h)}. \tag{7.165}$$

Therefore, the well-posedness of the fully discrete problem (7.162) is given by the following result.

Theorem 7.73

If (**B.1**), (**B.2**) *and Assumption II.7 hold, then the matrix $\mathbb{L}_{\Gamma,h}$ is invertible.*

Proof. This is similar to Theorem 7.69, thus we refer again to Theorem 7.62 for details and here we only provide a sketch of the proof. First, and this is the main difference with respect to Theorem 7.69, we notice that

$$\mathbb{L}_{\Gamma,h} = \begin{pmatrix} \dfrac{\mathbb{M}_h}{\Delta t^2} + \dfrac{\mathbb{A}_h^\Gamma}{4} & \widehat{\mathbb{B}}_h \\ \widehat{\mathbb{B}}_h^T & \mathbb{O} \end{pmatrix} = \begin{pmatrix} \dfrac{\mathbb{M}_h}{\Delta t^2} - \dfrac{\mathbb{A}_h^\Omega}{4} & \widehat{\mathbb{B}}_h \\ \widehat{\mathbb{B}}_h^T & \mathbb{O} \end{pmatrix} + \begin{pmatrix} \dfrac{\mathbb{A}_h}{4} & \mathbb{O} \\ \mathbb{O} & \mathbb{O} \end{pmatrix}.$$

Then, since $\mathbb{A}_h$ is a positive semi-definite matrix we are only concern about the first term. Moreover, according to Assumption II.7, $\frac{\mathbb{M}_h}{\Delta t^2} - \frac{\mathbb{A}_h^\Omega}{4}$ is positive in $\operatorname{Ker}\widehat{\mathbb{B}}_h^T$, thus we are in the hypothesis of Lemma 7.60, i.e. there exists a sufficiently small $\varepsilon > 0$ such that

$$\frac{\mathbb{M}_h}{\Delta t^2} - \frac{\mathbb{A}_h^\Omega}{4} + \frac{\widehat{\mathbb{B}}_h \widehat{\mathbb{B}}_h^T}{\varepsilon} \quad \text{is positive definite.}$$

Finally, we note that the invertibility of the matrix $\mathbb{L}_{\Gamma,h}$ is equivalent (this is exact penalization) to the invertibility of the matrix

$$\mathbb{L}_{\Gamma,h}^\varepsilon = \begin{pmatrix} \dfrac{\mathbb{M}_h}{\Delta t^2} + \dfrac{\widehat{\mathbb{B}}_h \widehat{\mathbb{B}}_h^T}{\varepsilon} + \dfrac{\mathbb{A}_h^\Gamma}{4} & \widehat{\mathbb{B}}_h \\ \widehat{\mathbb{B}}_h^T & \mathbb{O} \end{pmatrix}.$$

Then, since the first block of $\mathbb{L}^{\varepsilon}_{\Gamma,h}$ is positive definite, a standard Schur complement procedure yields the invertibility of $\mathbb{L}^{\varepsilon}_{\Gamma,h}$.

■

Next, we provide also a stability result which is obtained by the same approach as in Theorem 7.71 and Corollary 7.72 (thus the proof is omitted).

Theorem 7.74

If (**B.1**), (**B.2**) *and Assumption II.7 hold, there exists a constant $C > 0$, independent of T and h, such that the unique solution $\boldsymbol{\Phi}_h^n$ of the fully-discrete problem* (7.162) *satisfies*

$$\max_{n\in\{0,\dots,N\}} \left(\mathcal{E}_h^{n+\frac{1}{2}}\right)^{\frac{1}{2}} \leq C\|\boldsymbol{f}\|_{L^1([0,T];L^2(\Omega)^2)}. \tag{7.166}$$

As a consequence, the a priori estimates (7.160) *and* (7.161) *hold true.*

7.8.3 Analysis of the CFL conditions for first order Lagrange finite elements

In this section, our aim is to recall the computations that we have developed in Section 5.2 concerning the computational gain of considering potentials formulations compared to the classical methods. There, we have shown that the gain is consequence of the two following properties for the proposed numerical scheme.

- First, the method should allow the use of independent meshes for each type of wave, in consequence we can adapt each of them to the respective wavelength, i.e., we shall consider

$$h_P = \lambda_P/N_\star \quad \text{and} \quad h_S = \lambda_S/N_\star,$$

  where we recall that $N_\star$ represents the number of mesh points that we want to consider per wavelength.

- Second, recalling the introduction of the minimal time scale $T_\star$, which is such that $\lambda_Q = T_\star V_Q$ for $Q \in \{P, S\}$, we also require that the stability condition of the resultant numerical scheme is given by $\Delta t < C\,T_\star/N_\star$ where C is a positive constant only depending on the order of the finite elements considered.

Notice that the first condition holds, since the only restriction when considering the meshes to build $V_{P,h}$ and $V_{S,h}$ is given by Assumption II.5 which is a compatibility condition between the spaces P_h and $V_{S,h}$. However, the verification of the second condition is more involved and requires the consideration of other assumptions (that we detail later) and that should also be compatible with Assumption II.5.

Before going into more details, let us first explain why it is difficult to obtain a sufficient stability condition of the form $\Delta t < C\,T_\star/N_\star$, for example for the semi-implicit scheme (7.162). A natural approach, that we recall for completeness, would consist in starting from the following classical local inequality to get corresponding global inequalities.

Lemma 7.75

For all $v \in \mathcal{P}_1(\kappa)$, we have that

$$\int_\kappa |\nabla v|^2 \,\mathrm{d}\boldsymbol{x} \;\leq\; \frac{72}{\varrho_\kappa^2} \int_\kappa |v|^2 \,\mathrm{d}\boldsymbol{x},$$

where ϱ_κ is the radius of the largest disk included in κ.

Proof. We give a short proof for the sake of completeness. Following the notation of [109], let $\boldsymbol{F}_\kappa(\widehat{\boldsymbol{x}}) = \mathbb{B}_\kappa \widehat{\boldsymbol{x}} + \boldsymbol{b}_\kappa$ denote the affine mapping from the reference element $\widehat{\kappa}$ (the triangle with vertices $(0,0)^T, (0,1)^T$ and $(1,0)^T$) to the element κ. Then (as in Theorem 3.12 in [109]) we can deduce

$$\begin{aligned}\int_\kappa |\nabla v|^2 \,\mathrm{d}\boldsymbol{x} &\leq \|\mathbb{B}_\kappa^{-1}\|_2^2 \,|\det \mathbb{B}_\kappa| \int_{\widehat{\kappa}} |\nabla_{\widehat{\boldsymbol{x}}}(v \circ \boldsymbol{F}_\kappa)|^2 \,\mathrm{d}\widehat{\boldsymbol{x}},\\ \int_\kappa |v|^2 \,\mathrm{d}\boldsymbol{x} &= |\det \mathbb{B}_\kappa| \int_{\widehat{\kappa}} |v \circ \boldsymbol{F}_\kappa|^2 \,\mathrm{d}\widehat{\boldsymbol{x}},\end{aligned}$$

where $\nabla_{\widehat{\boldsymbol{x}}}$ is the gradient operator in the local coordinates $\widehat{\boldsymbol{x}}$ and $\|\cdot\|_2$ denotes the matrix norm induced by the euclidean norm. Moreover, we can solve the eigenvalue problem

$$\int_{\widehat{\kappa}} \nabla \widehat{w} \cdot \nabla \widehat{v} \,\mathrm{d}\widehat{\boldsymbol{x}} = \lambda \int_{\widehat{\kappa}} \widehat{w}\,\widehat{v} \,\mathrm{d}\widehat{\boldsymbol{x}}, \quad \forall\, \widehat{v} \in \mathcal{P}_1(\widehat{\kappa}).$$

and obtain the eigenpairs $(\lambda = 0, \widehat{w} = 1)$, $(\lambda = 12, \widehat{w} = \widehat{x}_1 - \widehat{x}_2)$ and $(\lambda = 36, \widehat{w} = -2 + 3\,\widehat{x}_1 + 3\,\widehat{x}_2)$. In consequence, we have that

$$\int_{\widehat{\kappa}} |\nabla_{\widehat{\boldsymbol{x}}}(v \circ \boldsymbol{F}_\kappa)|^2 \,\mathrm{d}\widehat{\boldsymbol{x}} \;\leq\; 36 \int_{\widehat{\kappa}} |v \circ \boldsymbol{F}_\kappa|^2 \,\mathrm{d}\widehat{\boldsymbol{x}}.$$

Finally, since $\|\mathbb{B}_\kappa^{-1}\|_2 \leq \sqrt{2}/\varrho_\kappa$ (see Theorem 3.1.3 in [109]), we can combine the previous equations to obtain the result

$$\int_\kappa |\nabla v|^2 \,\mathrm{d}\boldsymbol{x} \;\leq\; 36\, \|\mathbb{B}_\kappa^{-1}\|_2^2 \,|\det \mathbb{B}_\kappa| \int_{\widehat{\kappa}} |v \circ \boldsymbol{F}_\kappa|^2 \,\mathrm{d}\widehat{\boldsymbol{x}} \;=\; \frac{72}{\varrho_\kappa^2} \int_\kappa |v|^2 \,\mathrm{d}\boldsymbol{x}.$$

■

Remark 7.76

A family of triangulations $\mathcal{T}_h$ is said to be quasi-uniform, if there exists a constant $\varrho > 0$ (usually called the quasi-uniformity factor) independent of h and such that $\forall \kappa \in \mathcal{T}_h$ we have that $\varrho_\kappa \geq \varrho\, h$ where ϱ_κ is the radius of the largest disk included in κ.

In consequence, since we are considering quasi-uniform triangulations $\mathcal{T}_{P,h}$ and $\mathcal{T}_{S,h}$, we obtain the following result which is straightforward.

Theorem 7.77

For any $Q \in \{P, S\}$, let us denote by ϱ_Q the quasi-uniformity factor of the family of triangulations $\mathcal{T}_{Q,h}$. Then, for any $\psi_{Q,h} \in V_{Q,h}$, we have that

$$\int_\Omega |\nabla \psi_{Q,h}|^2 \,\mathrm{d}\boldsymbol{x} \;\leq\; \frac{72}{h_Q^2\, \varrho_Q^2} \int_\Omega |\psi_{Q,h}|^2 \,\mathrm{d}\boldsymbol{x}.$$

Therefore, we deduce immediately that for all $\boldsymbol{\psi}_h \in \boldsymbol{V}_h$ we have (notice $V_Q/h_Q = N_\star/T_\star$)

$$\begin{aligned} a_\Omega(\boldsymbol{\psi}_h, \boldsymbol{\psi}_h) &\leq \frac{72}{\min\{\varrho_P, \varrho_S\}^2} \Big(\frac{1}{h_P^2} \int_\Omega |\psi_{P,h}|^2 \,\mathrm{d}\boldsymbol{x} + \frac{1}{h_S^2} \int_\Omega |\psi_{S,h}|^2 \,\mathrm{d}\boldsymbol{x} \Big) \\ &\leq \frac{72}{\min\{\varrho_P, \varrho_S\}^2} \, \frac{N_\star^2}{T_\star^2} \, m_\Omega(\boldsymbol{\psi}_h, \boldsymbol{\psi}_h). \end{aligned} \tag{7.167}$$

However, the CFL condition (7.165) is given by

$$\Delta t^2 \;<\; 4 \Big(\max_{\boldsymbol{\psi}_h \in \boldsymbol{V}_{N,h} \setminus \{\boldsymbol{0}\}} \frac{a_\Omega(\boldsymbol{\psi}_h, \boldsymbol{\psi}_h)}{m_h(\boldsymbol{\psi}_h, \boldsymbol{\psi}_h)} \Big)^{-1}.$$

Moreover, according to the discrete coercivity **(B.1)** (see Remark 7.57), we have that

$$m_h(\boldsymbol{\psi}_h, \boldsymbol{\psi}_h) \;\geq\; \alpha_h \|\boldsymbol{\psi}_h\|_{L^2(\Omega)^2}^2 \;\geq\; \alpha_h\, V_S^2\, m_\Omega(\boldsymbol{\psi}_h, \boldsymbol{\psi}_h).$$

Thus, according to (7.167) we obtain

$$\max_{\boldsymbol{\psi}_h \in \mathbf{V}_{N,h}\setminus\{\mathbf{0}\}} \frac{a_\Omega(\boldsymbol{\psi}_h,\boldsymbol{\psi}_h)}{m_h(\boldsymbol{\psi}_h,\boldsymbol{\psi}_h)} \;\leq\; \frac{1}{\alpha_h\, V_S^2} \max_{\boldsymbol{\psi}_h \in \mathbf{V}_{N,h}\setminus\{\mathbf{0}\}} \frac{a_\Omega(\boldsymbol{\psi}_h,\boldsymbol{\psi}_h)}{m_\Omega(\boldsymbol{\psi}_h,\boldsymbol{\psi}_h)}.$$

Then, we notice that a sufficient stability condition for the scheme is given by

$$\Delta t^2 \;<\; \alpha_h\, V_S^2\, \frac{\min\{\varrho_P,\varrho_S\}^2}{18}\, \frac{T_\star^2}{N_\star^2}.$$

Unfortunately, we are not able to prove that $(\alpha_h\, V_S^2)$ is bounded from below by a quantity independent of (h_P, h_S), as well as (V_P, V_S). This is why we need to proceed differently, and to do so, we consider the following technical assumption for the triangulations $\mathcal{T}_{P,h}$, $\mathcal{T}_{S,h}$ and $\mathcal{T}_h$.

Assumption II.8

We assume that the triangulations $\mathcal{T}_{P,h}$ and $\mathcal{T}_{S,h}$ are subtriangulations of $\mathcal{T}_h$, hence the approximation spaces satisfy $P_h \subset V_{P,h}$ and $P_h \subset V_{S,h}$ (by saying $\mathcal{T}_h'$ is a subtriangulation of $\mathcal{T}_h$, we mean that any triangle of $\mathcal{T}_h$ is a finite union of triangles of $\mathcal{T}_h'$).

Remark 7.78

Notice that under Assumption II.8, it is not always possible to consider $h_P = \lambda_P/N_\star$ and $h_S = \lambda_S/N_\star$ which provides the important property $h_Q/V_Q = T_\star/N_\star$ for $Q \in \{P,S\}$. However, this is not so constraining, since in practice we can consider $\mathcal{T}_{P,h} = \mathcal{T}_h$ and $\mathcal{T}_{S,h}$ a subtriangulation of $\mathcal{T}_h$ such that

$$h_P = \frac{\lambda_P}{N_\star} \quad \text{and} \quad h_S = \frac{h_P}{R} \quad \textit{where} \quad R = \left\lceil \frac{V_P}{V_S} \right\rceil = \alpha_R \frac{V_P}{V_S} \quad \textit{with} \quad \alpha_R \gtrsim 1.$$

This choice, slightly improves the approximation of the shear waves, since (note $V_Q = \lambda_Q T_\star$)

$$h_S = \frac{h_P}{R} = \frac{\lambda_P}{R\, N_\star} = \frac{\lambda_P}{\alpha_R\, N_\star} \frac{V_S}{V_P} = \frac{\lambda_S}{\alpha_R\, N_\star} \lesssim \frac{\lambda_S}{N_\star}.$$

And moreover, it provides only a small penalisation for the ratio (note $h_P/V_P = T_\star/N_\star$)

$$\frac{h_S}{V_S} = \frac{h_P}{R\, V_S} = \frac{h_P}{\alpha_R\, V_P} = \frac{T_\star}{\alpha_R\, N_\star} \lesssim \frac{T_\star}{N_\star}.$$

It is also interesting to notice that we can also consider $R = \lfloor V_P/V_S \rfloor$ which, contrary to the previous case, leads to a small loss of accuracy for the shear waves and a slightly improvement for the ratio h_S/V_S.

Theorem 7.79

Let us consider a family of quasi-uniform triangulations $\mathcal{T}_h$ with quasi-uniformity factor ϱ and the families of subtriangulations $\mathcal{T}_{P,h}$ and $\mathcal{T}_{S,h}$ such that Assumption II.8 holds. Then:

(i) A sufficient stability condition for the semi-implicit scheme (7.162) is

$$\Delta t \;< \Delta t_{EI} \quad \textit{with} \quad \Delta t_{EI} = \frac{\varrho}{3\sqrt{2}} \min\left\{\frac{h_P}{V_P}, \frac{h_S}{V_S}\right\}. \tag{7.168}$$

(ii) A sufficient stability condition for the theta-scheme (7.153) is

$$\Delta t < \frac{\Delta t_{LF}}{(1-4\,\theta)^{\frac{1}{2}}} \;\textit{with}\; \Delta t_{LF} = \Delta t_{EI}/\sqrt{2}. \tag{7.169}$$

Proof. We restrict ourselves to prove the point (i), however at the end of this proof, we make some comments concerning the verification of the point (ii), which is quite similar.
The idea is to obtain a global bound in the whole domain Ω from local bounds in each triangle κ. This leads us to introduce the "broken" discrete spaces

$$\begin{aligned} V^\flat_{P,h} &:= \big\{\varphi_{P,h} \in L^2(\Omega) \;/\; \forall\,\kappa \in \mathcal{T}_{P,h},\ \varphi_{P,h|\kappa} \in \mathcal{P}_1(\kappa)\big\}, \\ V^\flat_{S,h} &:= \big\{\varphi_{S,h} \in L^2(\Omega) \;/\; \forall\,\kappa \in \mathcal{T}_{S,h},\ \varphi_{S,h|\kappa} \in \mathcal{P}_1(\kappa)\big\}, \\ \boldsymbol{V}^\flat_h &:= V^\flat_{P,h} \times V^\flat_{S,h}, \end{aligned} \tag{7.170}$$

as well as the "broken" bilinear form $a^\flat_\Omega(\cdot,\cdot)$ defined by

$$a^\flat_\Omega(\boldsymbol{\varphi}_h,\boldsymbol{\psi}_h) := \sum_{\kappa\in\mathcal{T}_h} a_{\Omega,\kappa}(\boldsymbol{\varphi}_h,\boldsymbol{\psi}_h), \quad \forall\,(\boldsymbol{\varphi}_h,\boldsymbol{\psi}_h) \in \boldsymbol{V}^\flat_h \times \boldsymbol{V}^\flat_h.$$

where we have defined

$$a_{\Omega,\kappa}(\boldsymbol{\varphi}_h,\boldsymbol{\psi}_h) := \int_\kappa \big(\nabla\varphi_{P,h}\cdot\nabla\psi_{P,h} + \nabla\varphi_{S,h}\cdot\nabla\psi_{S,h}\big)\,\mathrm{d}\boldsymbol{x}.$$

Let us remark that $\boldsymbol{V}_h \subset \boldsymbol{V}^\flat_h$ and that $a_\Omega(\cdot,\cdot)$ and $a^\flat_\Omega(\cdot,\cdot)$ coincide in $\boldsymbol{V}_h$. Then, we proceed in two steps, we first prove that the stability condition (7.165) for the semi-implicit scheme (7.162) holds if

$$m_\Omega(\boldsymbol{\psi}_h,\boldsymbol{\psi}_h) - \frac{\Delta t^2}{4}\, a^\flat_\Omega(\boldsymbol{\psi}_h,\boldsymbol{\psi}_h) \geq 0, \quad \forall\,\boldsymbol{\psi}_h \in \boldsymbol{V}^\flat_h. \tag{7.171}$$

Then we prove that (7.171) holds under the new stability condition (7.168).
Step 1: (7.171) *implies* (7.165).
For all $q_h \in P_h$ we have according to Assumption II.8 that $\nabla q_h \subset \boldsymbol{V}^\flat_h$. Moreover, since $q_{h|\kappa} \in \mathcal{P}_1(\kappa)$ for all $\kappa \in \mathcal{T}_h$, we also have that $\partial^2_{i,j} q_{h|\kappa} = 0$ for all $i,j \in \{1,2\}$. In consequence, for any $q_h \in P_h$ and $\boldsymbol{\varphi}_h \in \boldsymbol{V}^\flat_h$, we have that

$$a^\flat_\Omega(\boldsymbol{\varphi}_h - \nabla q_h, \boldsymbol{\varphi}_h - \nabla q_h) = a^\flat_\Omega(\boldsymbol{\varphi}_h,\boldsymbol{\varphi}_h).$$

Thus if we consider $\boldsymbol{\psi}_h = \boldsymbol{\varphi}_h - \nabla q_h$ in (7.171), we obtain

$$m_\Omega(\boldsymbol{\varphi}_h - \nabla q_h, \boldsymbol{\varphi}_h - \nabla q_h) \;-\; \frac{\Delta t^2}{4}\, a^\flat_\Omega(\boldsymbol{\varphi}_h,\boldsymbol{\varphi}_h) \;\geq\; 0, \quad \forall\,(\boldsymbol{\varphi}_h, q_h) \in \boldsymbol{V}^\flat_h \times P_h. \tag{7.172}$$

Now, we recall (7.129) (see Theorem 7.58), which for any $\boldsymbol{\varphi}_h \in \boldsymbol{V}_{N,h}$ proves that

$$m_h(\boldsymbol{\varphi}_h,\boldsymbol{\varphi}_h) \;\geq\; m_\Omega(\boldsymbol{\varphi}_h - \nabla p_h(\nu_h), \boldsymbol{\varphi}_h - \nabla p_h(\nu_h)), \quad \text{with} \quad \nu_h = \Pi_h(\boldsymbol{\varphi}_h\cdot\boldsymbol{n}).$$

Therefore, if we consider $q_h = p_h(\nu_h)$ in (7.172), we obtain

$$m_h(\boldsymbol{\varphi}_h,\boldsymbol{\varphi}_h) \;-\; \frac{\Delta t^2}{4}\, a^\flat_\Omega(\boldsymbol{\varphi}_h,\boldsymbol{\varphi}_h) \;\geq\; 0, \quad \forall\,\boldsymbol{\varphi}_h \in \boldsymbol{V}_{N,h},$$

which is nothing but (7.165) since the bilinear forms $a^\flat_\Omega(\cdot,\cdot)$ and $a_\Omega(\cdot,\cdot)$ coincide in $\boldsymbol{V}_{N,h} \subset \boldsymbol{V}_h$.
Step 2: (7.168) *implies* (7.171).
Let us first notice that, similarly to the computations in (7.167), we can now show for all $\boldsymbol{\psi}_h$, that (notice now $\varrho_P = \varrho_S = \varrho$ and we do not assume $V_Q/h_Q = N_\star/T_\star$)

$$a^\flat_\Omega(\boldsymbol{\psi}_h,\boldsymbol{\psi}_h) \;\leq\; \frac{72}{\varrho^2}\ \max\Big\{\frac{V_P^2}{h_P^2}, \frac{V_S^2}{h_S^2}\Big\}\ m_\Omega(\boldsymbol{\psi}_h,\boldsymbol{\psi}_h).$$

In consequence, the hypothesis gives

$$\Delta t^2 \;<\; \frac{\varrho^2}{18}\min\Big\{\frac{h_P^2}{V_P^2}, \frac{h_S^2}{V_S^2}\Big\} \;=\; 4\Big(\frac{72}{\varrho^2}\max\Big\{\frac{V_P^2}{h_P^2}, \frac{V_S^2}{h_S^2}\Big\}\Big)^{-1} \;\leq\; 4\Big(\max_{\boldsymbol{\psi}_h\in\boldsymbol{V}^\flat_h\setminus\{\boldsymbol{0}\}} \frac{a^\flat_\Omega(\boldsymbol{\psi}_h,\boldsymbol{\psi}_h)}{m_\Omega(\boldsymbol{\psi}_h,\boldsymbol{\psi}_h)}\Big)^{-1}.$$

Notice this directly implies (7.171) and concludes the proof of point (i).
Remarks concerning point (ii)*:*
The proof for the theta-scheme is done along the same lines, introducing the broken version $a^\flat(\cdot,\cdot)$ of the bilinear form $a(\cdot,\cdot)$ and establishing the equivalent to (7.171). Let us simply mention that the $\sqrt{2}$ factor appearing in the right hand side is a consequence of the obvious (but sharp) inequality between the quadratic forms associated to $a(\cdot,\cdot)$ and $a_\Omega(\cdot,\cdot)$ (and the same holds for the broken versions)

$$\forall\, \boldsymbol{\varphi} \in \boldsymbol{V}, \quad a(\boldsymbol{\varphi},\boldsymbol{\varphi}) \leq 2\, a_\Omega(\boldsymbol{\varphi},\boldsymbol{\varphi}).$$

■

Remark 7.80

It may be possible that Assumption II.8 made on the triangulations is not really needed for guaranteeing sufficient stability conditions similar to those of Theorem 7.79. Note however, that we use it in the proof and that it is not so constraining in practice (see Remark 7.78).

Remark 7.81

If we compare the sufficient CFL condition (7.168) *for the semi-implicit scheme* (7.162)*, with respect to the CFL condition* (7.169) *of the explicit theta-scheme* (7.153) *with* $\theta = 0$ *(standard Leap-Frog scheme), we see that the obtained CFL for the Leap-Frog scheme is* $\sqrt{2}$ *more restrictive (which is not surprising).*

Finally, we conclude this section by noticing that in practice, we consider the meshes as it was explained in Remark 7.78, thus in Theorem 7.79 we have that

$$\Delta t < \frac{\varrho}{3\sqrt{2}}\,\frac{T_\star}{N_\star} \quad \text{or} \quad \Delta t < \frac{\varrho}{6(1-4\theta)^{\frac{1}{2}}}\,\frac{T_\star}{N_\star},$$

which in both cases is independent of the ratio V_P/V_S.

7.9 Numerical results for the stabilized formulation

Similarly to Section 6.5 where we have presented illustrative numerical results for the case of clamped boundary conditions, in this section we present numerical results to exhibit the good behaviour of the method for the case of free boundary conditions. The examples we provide correspond to the propagation of transient waves in an isotropic homogeneous domain which is bounded by a free boundary.

The model problem. We are interested in finding $\boldsymbol{u}(\boldsymbol{x},t)$ solution of the following elastodynamic problem (which is completed with vanishing initial data)

$$\left\{\begin{aligned} \rho\,\partial_t^2\boldsymbol{u} - (\lambda+2\,\mu)\,\nabla\operatorname{div}\boldsymbol{u} + \mu\,\mathbf{curl}\operatorname{curl}\boldsymbol{u} &= \boldsymbol{f}, \quad \text{in} \quad \Omega\times[0,T], \\ \underline{\boldsymbol{\sigma}}(\boldsymbol{u})\boldsymbol{n} &= \mathbf{0}, \quad \text{on} \quad \Gamma\times[0,T], \end{aligned}\right. \tag{7.173}$$

where we choose the final time to be $T = 5$ and the computational domain $\Omega = [-5,5]\times[-5,5]$, which centre of gravity is at the origin. We also consider the physical properties given by

$$\rho = 1, \quad \lambda = 56 \quad \text{and} \quad \mu = 4,$$

and the medium to be excited by the following source (see Figure 7.19)

$$\boldsymbol{f}(\boldsymbol{x},t) = g(t)\,\boldsymbol{h}(\boldsymbol{x}) \quad \text{where} \quad g(t) = \partial_t \exp(-50\,(t-1)^2) \quad \text{and} \quad \boldsymbol{h} \in \boldsymbol{L}^2_R(\Omega). \tag{7.174}$$

We present three experiments depending on the value of $\boldsymbol{h}$.

First Experiment. We consider a source that generates only pressures waves up to the interaction with the boundary. In this case, $\boldsymbol{h}$ is chosen as the gradient of a smooth compactly supported function centred at $\boldsymbol{x}_0 = \boldsymbol{0}$, i.e.

$$\boldsymbol{h}(\boldsymbol{x}) = \nabla s(\boldsymbol{x}) \quad \text{where} \quad s(\boldsymbol{x}) = \exp\left(1 + \frac{1}{|2\,\boldsymbol{x}|^2 - 1}\right), \quad \text{if} \quad |\boldsymbol{x}| < 0.5,$$

and zero elsewhere. We shall remark that $\boldsymbol{h} \in \boldsymbol{L}^2_R(\Omega)$ since s is compactly supported and

$$\int_\Omega \nabla s \cdot \boldsymbol{w}_R \,\mathrm{d}\boldsymbol{x} \;=\; -\int_\Omega s\;\operatorname{div}(\boldsymbol{w}_R)\,\mathrm{d}\boldsymbol{x} \;=\; 0, \quad \forall \boldsymbol{w}_R \in \boldsymbol{R}(\Omega).$$

Second Experiment. In a second case we consider a source that only generates shear waves up to the interaction with the boundary,

$$\boldsymbol{h}(\boldsymbol{x}) = \mathbf{curl}(x_2\, s(\boldsymbol{x})).$$

We remark that $\boldsymbol{h} \in \boldsymbol{L}^2_R(\Omega)$ since,

$$\int_\Omega \mathbf{curl}(x_2\, s) \cdot \boldsymbol{w}_R \,\mathrm{d}\boldsymbol{x} \;=\; \int_\Omega x_2\, s\;\operatorname{curl}(\boldsymbol{w}_R)\,\mathrm{d}\boldsymbol{x} = 0 \quad \forall \boldsymbol{w}_R \in \boldsymbol{R}(\Omega),$$

because $\operatorname{curl}(\boldsymbol{w}_R)$ is constant and $x_2\, s(\boldsymbol{x})$ has zero average in Ω.

Third Experiment. The source we consider is localized near the boundary and generates both shear and pressure waves,

$$\boldsymbol{h}(\boldsymbol{x}) = (\,\partial_2 s(\boldsymbol{x}-\boldsymbol{x}_0)\,,\,\partial_1 s(\boldsymbol{x}-\boldsymbol{x}_0)\,)^t \quad \text{where} \quad \boldsymbol{x}_0 = (3.5, 0)^t.$$

Notice that $\boldsymbol{h} \in \boldsymbol{L}^2_R(\Omega)$ since

$$\int_\Omega \begin{pmatrix}\partial_2 s\\ \partial_1 s\end{pmatrix} \cdot \boldsymbol{w}_R \,\mathrm{d}\boldsymbol{x} = \int_\Omega \mathbf{curl}\, s \cdot \begin{pmatrix} w_{R,1}\\ -w_{R,2}\end{pmatrix} \mathrm{d}\boldsymbol{x} = \int_\Omega s\;\operatorname{curl}\begin{pmatrix} w_{R,1}\\ -w_{R,2}\end{pmatrix} \mathrm{d}\boldsymbol{x} = 0, \quad \forall \boldsymbol{w}_R \in \boldsymbol{R}(\Omega).$$

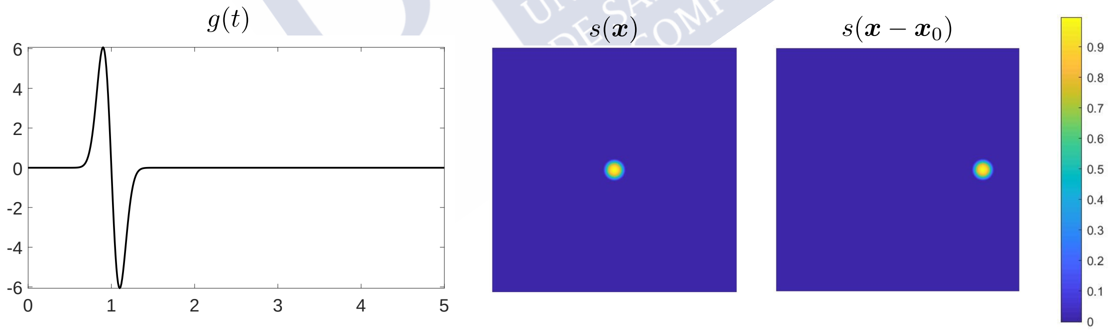

Figure 7.19: Left: time dependence of the source. Right: space dependence of the source.

Space discretization of the potential formulation. According to the technique we have presented in this chapter, the finite elements spaces $V_{P,h}$, $V_{S,h}$, P_h and M_h must be adequately chosen. In Section 7.7.5 we have detailed a particular choice in order to automatically guarantee the good properties of the method. Therefore, we consider the first order Lagrange finite elements spaces defined in (7.145) and (7.6.1) where the triangulations involved ($\mathcal{T}_{P,h}$, $\mathcal{T}_{S,h}$ and $\mathcal{T}_h$) will satisfy assumptions II.4 and II.5. Moreover, we shall also notice that $V_P/V_S = 4$, thus for computational reasons we would like to consider $h_P \simeq 4h_S$. In consequence, we first introduce the triangulation $\mathcal{T}_h$ given in Figure 7.20 (Left) which satisfies Assumption II.4. Then, on the one hand we choose $\mathcal{T}_{P,h} = \mathcal{T}_h$, while on the other hand we choose $\mathcal{T}_{S,h}$ given by the second refinement of $\mathcal{T}_h$ (see Figure 7.20 Right) in order to verify Assumption II.5 and the property $h_P \simeq 4h_S$.

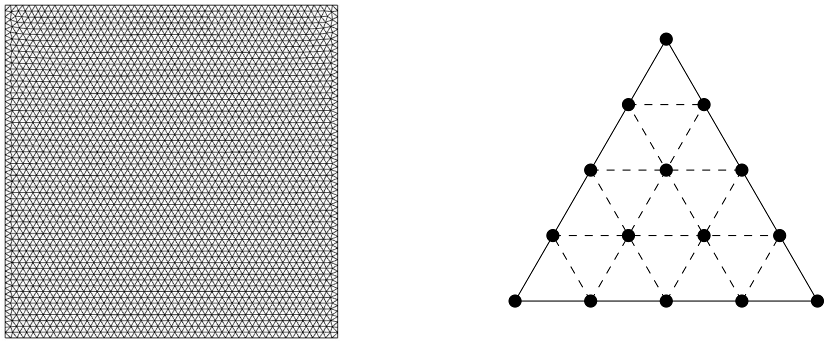

Figure 7.20: On the left we observe the triangulation $\mathcal{T}_h$ (which is equal to $\mathcal{T}_{P,h}$). On the right we plot how each element is divided in order to compute $\mathcal{T}_{S,h}$ as the second refinement of $\mathcal{T}_h$.

Time discretization. We approximate the solution of problem (7.173) by considering the semi-implicit scheme (7.162). The maximum time step allowed Δt^* is computed as in (6.42) and then the time step Δt for the simulations is chosen as the maximum time step such that $\Delta t < \Delta t^*$ and $0.01/\Delta t$ is an integer.

Computation of a reference displacement solution. To obtain a reference solution we compute the velocity (i.e. $\boldsymbol{v} = \partial_t \boldsymbol{u}$) using a classical method. More precisely, we compute $\boldsymbol{v}_h$, a numerically approximation of $\boldsymbol{v} = \partial_t \boldsymbol{u}$, by solving a discretized version of the problem

$$\left\{ \begin{array}{rcll} \rho\,\partial_t^2 \boldsymbol{v} \,-\, (\lambda + 2\,\mu)\,\nabla\,\mathrm{div}\,\boldsymbol{v} \,+\, \mu\,\mathbf{curl}\,\mathrm{curl}\,\boldsymbol{v} &=& \partial_t \boldsymbol{f}, & \text{in} \quad \Omega \times [0,T], \\ \underline{\boldsymbol{\sigma}}(\boldsymbol{v})\boldsymbol{n} &=& \mathbf{0}, & \text{on} \quad \Gamma \times [0,T]. \end{array} \right. \tag{7.175}$$

In particular we consider first order Lagrange finite elements in space (considering the triangulation $\mathcal{T}_{S,h}$) and finite differences in time, more precisely, a leap-frog scheme with the largest possible time step $\Delta\tau$ such that the scheme is stable and $0.01/\Delta\tau$ is an integer.

Procedure of comparison: Potential / Displacement. In order to validate the results we take into account the relation

$$\partial_t \boldsymbol{u} = \nabla\varphi_P + \mathbf{curl}\,\varphi_S + \boldsymbol{g} \quad \text{with} \quad \boldsymbol{g}(\boldsymbol{x},t) = \frac{\boldsymbol{h}(\boldsymbol{x})}{\rho} \int_0^t g(s)\,ds,$$

and we compare with respect to a solution obtained by a classical method in displacement. The method presented provides a numerical approximation of the potentials φ_P and φ_S, thus in order to compare the obtained solution with the solution generated with the displacement formulation (7.175) we shall also introduce the orthogonal projection $\Pi_{S,h}$ from $\boldsymbol{L}^2(\Omega)$ into $V_{S,h} \times V_{S,h}$ that for every $\boldsymbol{\phi} \in \boldsymbol{L}^2(\Omega)$ assigns $\Pi_{S,h}(\boldsymbol{\phi})$ satisfying

$$\int_\Omega (\Pi_{S,h}(\boldsymbol{\phi}) - \boldsymbol{\phi}) \cdot \Psi_h \;=\; 0 \quad \forall \Psi_h \in V_{S,h} \times V_{S,h}.$$

In consequence, in the following, in order to validate the numerical results obtained with the potentials approach, we shall represent

$$\boldsymbol{v}_h \quad \text{compared with respect to} \quad \widetilde{\boldsymbol{v}}_h \;:=\; \Pi_{S,h}(\nabla\varphi_{P,h}) + \Pi_{S,h}(\mathbf{curl}\,\varphi_{S,h}) + \Pi_{S,h}(\boldsymbol{g}).$$

First experiment. Since the source is given by a gradient, we observe in Figures 7.21 and 7.22 that the source only generates P-waves that propagate in the interior of the domain. Then, when the P-waves reach the boundary, S-waves are generated and propagate in the interior of the domain. It is interesting to observe how both type of waves are continuously interacting along the boundary. Finally, in Figures 7.23 and 7.24 we validate qualitatively the results obtained when using potentials formulation by comparing with respect to the solution obtained with a classical formulation.

Second experiment. Contrary to the previous example, now the source is given by a rotational and therefore, as we observe in Figures 7.25 and 7.26, only S-waves are generated by the source. Similarly to the previous case, we now observe that S-waves propagate in the interior of the domain and only when they reach the boundary we observe that P-waves are generated. In order to validate qualitatively the results, we compare in Figures 7.27 and 7.28 the results obtained when using potentials with respect to the solution obtained with a classical method.

Third experiment. In this case, both types of waves are generated by the source as we can see in Figures 7.29 and 7.30. Then we observe again that both types of waves propagate independently in the interior of the domain while on the boundary the interaction of both waves is stronger than in the previous cases. In consequence, the well known Rayleigh waves are observed (specially) in Figure 7.29. Finally, as in the previous case, we compare in Figures 7.31 and 7.32 the reconstructed velocity field obtained using potentials formulation with respect to the solution obtained with a classical formulation.

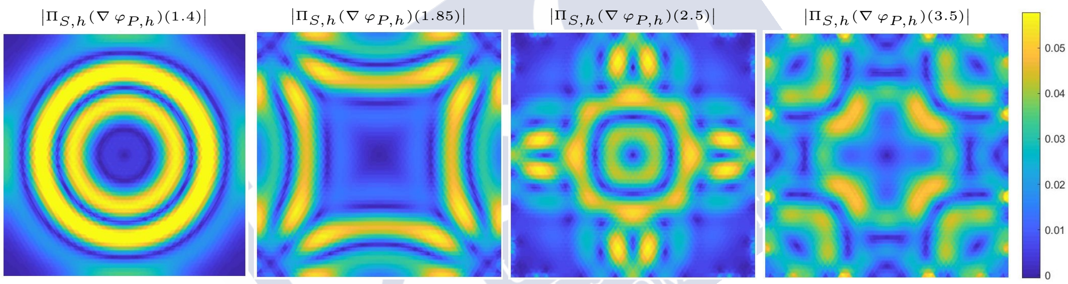

Figure 7.21: Snapshots of the reconstructed P-waves (first experiment).

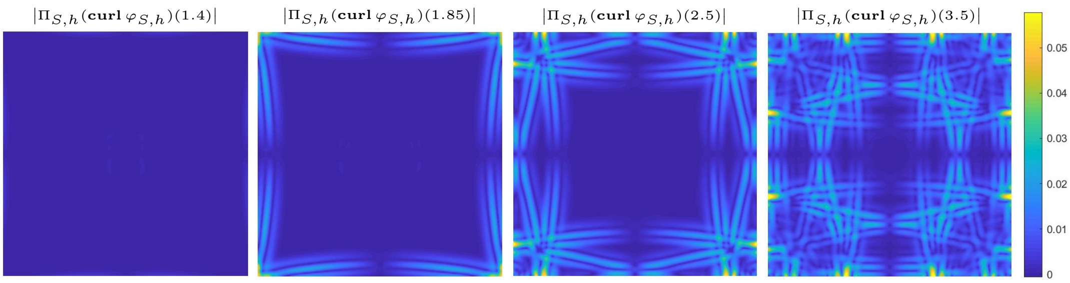

Figure 7.22: Snapshots of the reconstructed S-waves (first experiment).

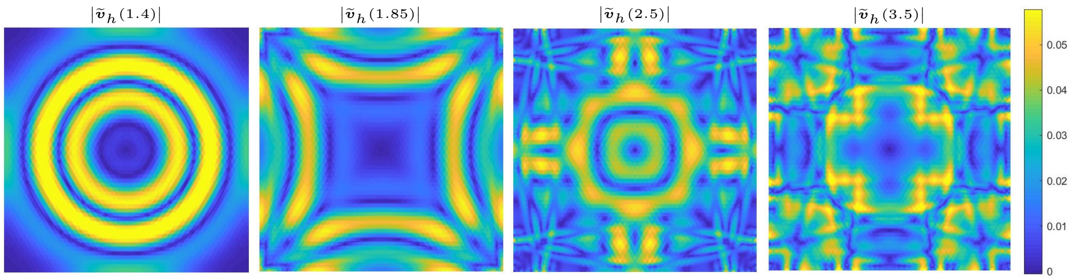

Figure 7.23: Snapshots of the reconstructed velocity field (first experiment).

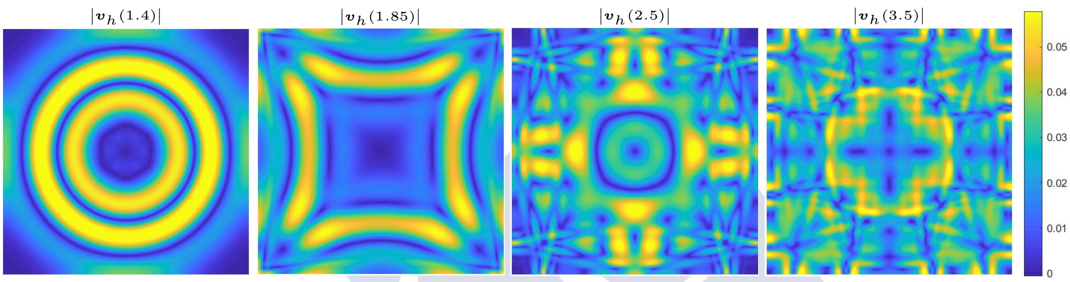

Figure 7.24: Snapshots of the velocity field (first experiment).

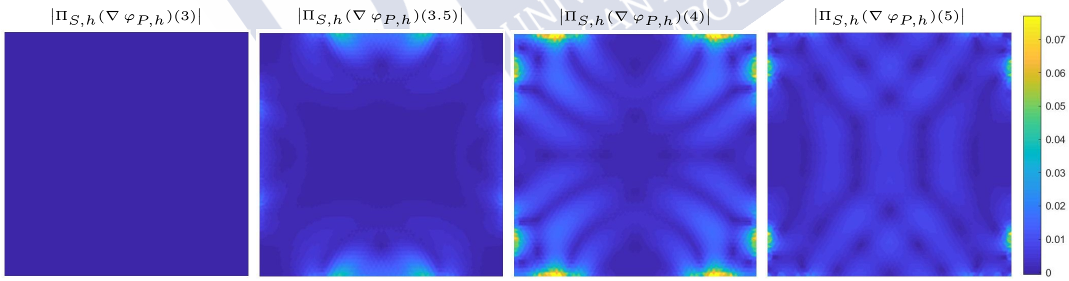

Figure 7.25: Snapshots of the reconstructed P-waves (second experiment).

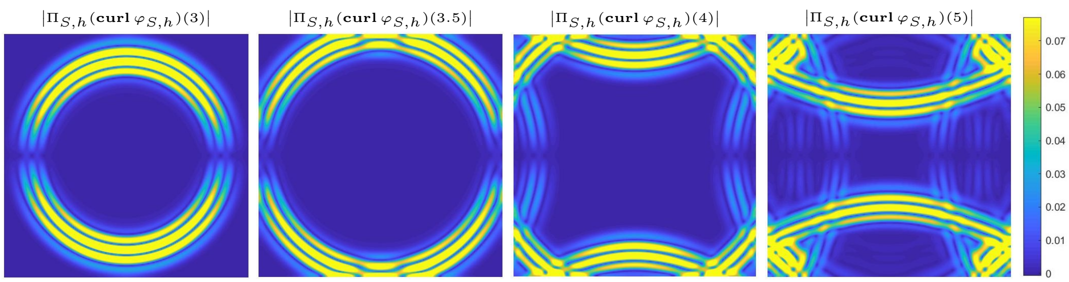

Figure 7.26: Snapshots of the reconstructed S-waves (second experiment).

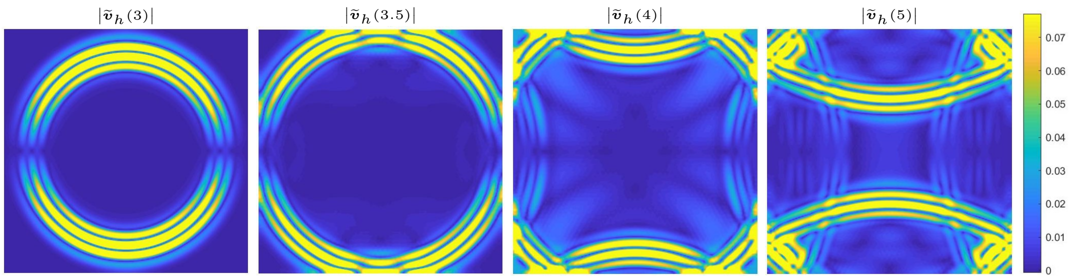

Figure 7.27: Snapshots of the reconstructed velocity field (second experiment).

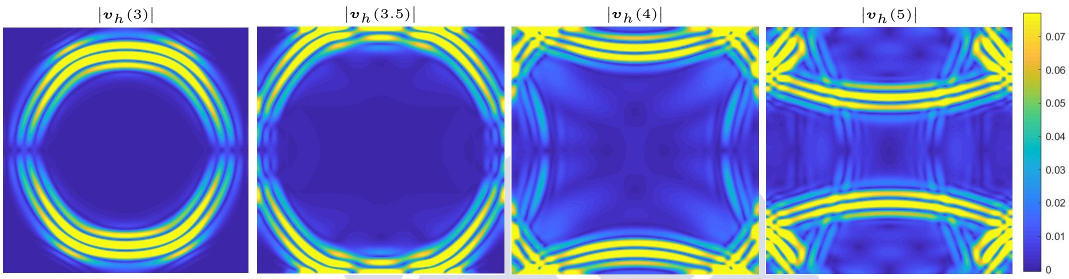

Figure 7.28: Snapshots of the velocity field (second experiment).

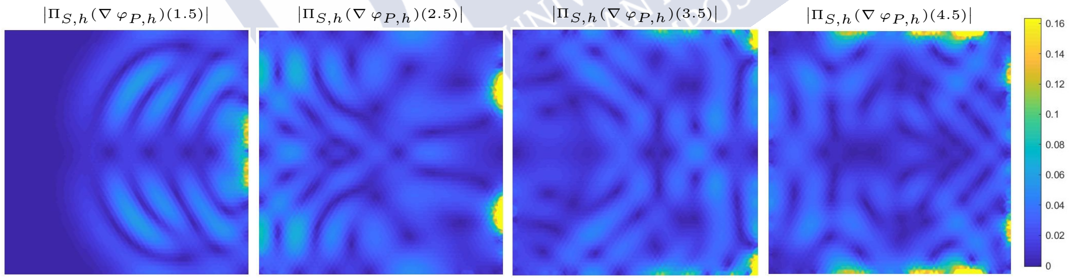

Figure 7.29: Snapshots of the reconstructed P-waves (third experiment).

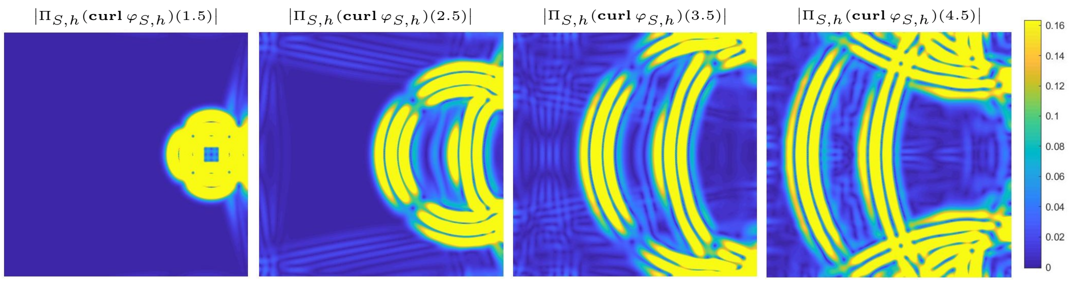

Figure 7.30: Snapshots of the reconstructed S-waves (third experiment).

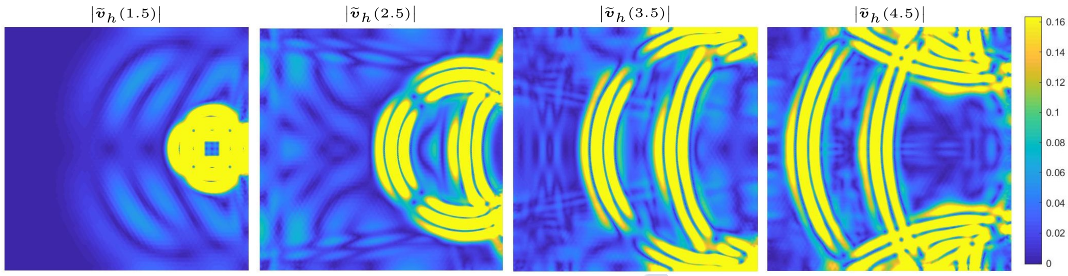

Figure 7.31: Snapshots of the reconstructed velocity field (third experiment).

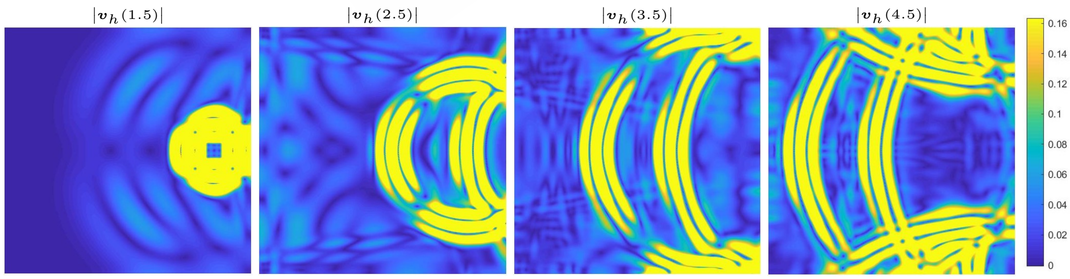

Figure 7.32: Snapshots of the velocity field (third experiment).

Chapter 8

Conclusions and perspectives

In this second part of the thesis, we have revisited the numerical resolution of 2D linear isotropic elastodynamics equations, which govern the propagation of waves in elastic isotropic solids. In this context, it is well-known that there are two different types of waves, usually called pressure waves and shear waves, that in the free space are known to propagate independently with different velocities V_P and V_S respectively (notice $V_P > V_S$). In consequence, as we have detailed in Section 5.2, classical space-time discretization techniques based in Lagrange finite elements in space and explicit finite differences in time are not efficient when $V_P >> V_S$. The cause of this being that, for accuracy, the space step must be adapted to the smaller wavelength (which is proportional to the minimal velocity V_S), while the time step is constrained by a stability condition that involves the maximal velocity V_P. Thus, to circumvents this issue, we have presented a technique which is base in the Helmholtz decomposition of the displacement field using scalar potentials and that allows to discretize separately the pressure waves and the shear waves.

In Chapter 6 we have revisited the treatment of the **clamped boundary conditions** and presented a detailed analysis of well-posedness and stability for the fully-discrete scheme. Moreover, a special attention has been devoted to guarantee the efficiency of the method compared to the standard space-time discretization methods for the displacements formulation. Let us also remark that the derivation of a detailed error analysis of the methodology is still an **open** question although numerical results are encouraging.

In Chapter 7, we have addressed the case of the **free boundary conditions**, which is the main contribution of this part of the thesis. In this sense, we have first presented the natural extension of the method in order to exhibit the instabilities that arise after space discretization. In particular, we have detected that the mass bilinear form associated to the resultant variational formulation is not positive. We have proved that this is linked to an additional boundary term which is related to the free boundary. So we have developed a new approach where the key idea is to find a smaller space (but still sufficiently large to contain the solution of the original problem) in which the mass bilinear form is coercive and thus the problem is stable. The definition of the new space is quite implicit, but fortunately, we have been able to characterize it as the *orthogonal* (with respect to the mass bilinear form) of another subspace which is itself isomorphic to a space of scalar functions defined on the boundary. Then, we have exploited this characterization by proposing a mixed variational formulation in which the solution is imposed to be in the new space by treating the mentioned *orthogonality* relation as a constraint, leading to the introduction of a Lagrange multiplier that is defined along the boundary.

The resultant mixed formulation is proved to be well-posed and stable. The next step was to proof a similar result at the discrete level. In this sense, we have shown, for Galerkin space discretizations satisfying a non-uniform coercivity property and a non-uniform discrete Inf-Sup condition that the semi-discrete problem is also well-posed and stable. Then we have proved under reasonable assumptions, that the first order Lagrange finite elements automatically satisfy both conditions and therefore the resultant semi-discrete numerical scheme is well-posed and stable.

The reader should notice that the verification of a uniform discrete coercivity condition and a uniform *Inf-Sup* condition remains as an **open** question which is fundamental for the development of a convergence analysis of the method which has not been carried out in this work.

Moreover, two different time discretizations of the semi-discrete problem have been presented and proved to be well-posed an stable. A special attention has been devoted to obtain reasonable assumptions that guarantee that the CFL stability condition of the fully-discrete scheme is independent of the ratio V_P/V_S. The chapter is concluded with numerical experiments that confirm the good properties of the method.

In conclusion, we have succeed in the extension of the potentials decomposition to the case of free boundary condition. However, this work has raised numerous open questions that could not be addressed yet and that we would like to treat in future works:

- Of course, we would like to tackle the full convergence analysis of the method, which is also an **open** question for the case of clamped boundary conditions. Moreover we note that for the case of free boundary conditions, as we have already mentioned, this question requires the verification of a uniform discrete coercivity condition and a uniform discrete *Inf-Sup* condition, which appears to be a challenging task.

- Another important question concerns the efficiency of the overall method in the case of free boundary conditions. More precisely, we recall that the method we have proposed requires the inversion of one of the following matrices, depending on the time discretization we consider (see problems (7.154) and (7.163)):

$$\mathbb{L}_{\theta,h} = \begin{pmatrix} \dfrac{\mathbb{M}_h}{\Delta t^2} + \theta \mathbb{A}_h & \widehat{\mathbb{B}}_h \\ \widehat{\mathbb{B}}_h^T & \mathbb{O} \end{pmatrix} \quad \text{or} \quad \mathbb{L}_{\Gamma,h} = \begin{pmatrix} \dfrac{\mathbb{M}_h}{\Delta t^2} + \dfrac{\mathbb{A}_h^\Gamma}{4} & \widehat{\mathbb{B}}_h \\ \widehat{\mathbb{B}}_h^T & \mathbb{O} \end{pmatrix}.$$

  Then, the sparsity of these matrices is crucial for the efficiency of the method, however, as we have justified in Remark 7.56, the matrix $\widehat{\mathbb{B}}_h$ is dense and penalises the overall numerical scheme. In this sense, we expect that the stabilization procedure can be modified in such a way that the sparsity of the corresponding matrix $\widehat{\mathbb{B}}_h$ can be improved (keeping the stability). This conjecture is partially motivated by the observation of this matrix in the particular case of the stabilised toy problem (see Section 7.6.5). However we remark that the analysis of this approach is complicated, not standard and remains as an **open** question.

- We would also like to address the case of transmission boundary conditions between two isotropic media. A first look into this question has shown that the difficulties that arise in this context are similar to those found in the case of free boundary conditions. Indeed no special difficulties arise at the continuous level, however the extension of the technique to the discrete case is not trivial and certain difficulties appear. In consequence, this question remains **open** although we are optimistic since numerical results are encouraging (see Figure 8.1).

- Concerning transmission problems, it would also be interesting to develop a technique that allows to consider a displacements formulation in one region and the potentials formulation in the other.

- Finally, also the 3D case could be addressed, however the approach may be very different. Note, that in this context, the potential corresponding to the shear waves in the Helmholtz decomposition is no longer scalar but vector valued and moreover, it is associated with a gauge condition (i.e. a divergence free condition) that should be taken into account.

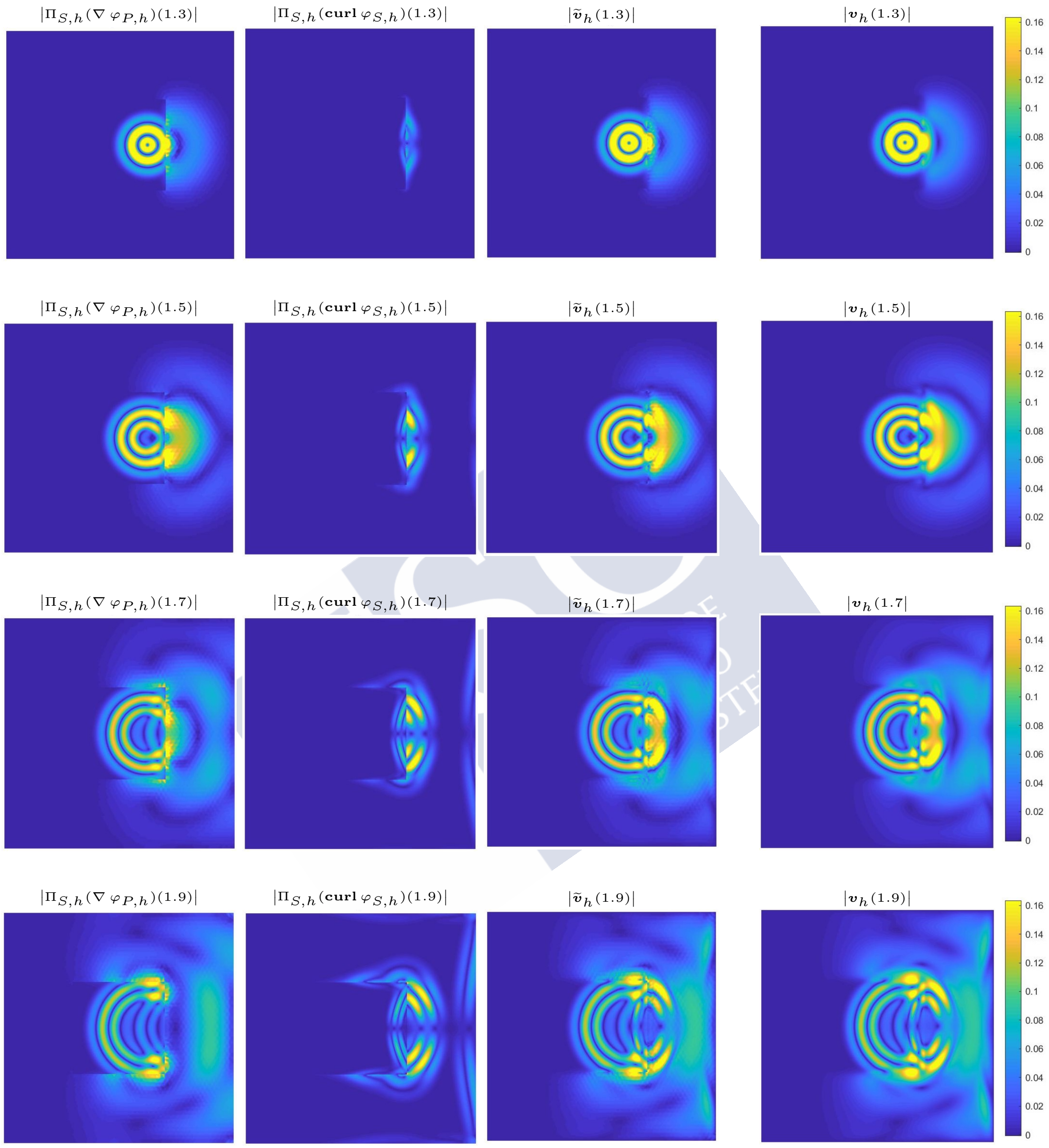

Figure 8.1: Encouraging numerical results for a transmission problem where we consider a piecewise homogeneous domain $\Omega = \Omega_1 \cup \Omega_2$ with a clamped boundary. In Ω_1 (a square centred in Ω) the density and Lame coefficients are given by $\rho_1 = 8$, $\lambda_1 = 16$ and $\mu_1 = 8$, while in the region Ω_2 are given by $\rho_2 = 1$, $\lambda_2 = 56$ and $\mu_2 = 4$. We plot snapshots at different times of the velocity field computed with a displacements formulations (Right) and the reconstructed P-waves, S-waves and velocity field computed with a formulation using potentials.

Appendices

Appendix A

About the Arlequin formulation with L^2-coupling

Let us assume that problem (2.17) has a unique solution $(\boldsymbol{u}, \lambda) \in W \times M$. We wonder if the coupling can be done considering the scalar product $(\cdot,\cdot)_{L^2(\omega)}$ in the definition of the bilinear form $b(\cdot,\cdot)$. Then in the following we denote

$$b^*(\cdot,\cdot) : W \times L^2(\omega) \longrightarrow \mathbb{R} \quad \text{such that} \quad b^*(\boldsymbol{v}, m) = (v_1 - v_2, m)_{L^2(\omega)}. \tag{A.1}$$

First, it is clear that given a solution $(\boldsymbol{u}, \lambda)$ of (2.17) we also have

$$b^*(\boldsymbol{u}, m) = 0, \quad \forall m \in L^2(\omega).$$

The difficulty comes when searching $\lambda^* \in L^2(\omega)$ such that

$$(\lambda^*, w)_{L^2(\omega)} = (\lambda, w)_{H^1(\omega)}, \quad \forall w \in H^1(\omega). \tag{A.2}$$

The existence and uniqueness of solution of this problem, similarly to the existence and uniqueness of solution of problem (2.17), is given by the following *Inf-Sup condition* (see Theorem 2.6 in [64]):

$$\inf_{m \in L^2(\omega)} \sup_{w \in H^1(\omega)} \frac{|(w,m)|_{L^2(\omega)}}{\|m\|_{L^2(\omega)} \, \|w\|_{H^1(\omega)}} \geq \delta > 0. \tag{A.3}$$

Thus in any case, the question seems to be related to either the previous *Inf-Sup condition* or the one associated to problem (2.17).

$$\inf_{m \in L^2(\omega)} \sup_{\boldsymbol{v} \in W} \frac{|b^*(\boldsymbol{v}, m)|}{\|m\|_{L^2(\omega)} \, \|\boldsymbol{v}\|_1} \geq \delta > 0. \tag{A.4}$$

In the following, we investigate the provability of (A.4), but notice that with small modifications we can easily extend the result for (A.3).

The Inf-Sup does not hold. First, let us notice that to prove the failure of the *Inf-Sup condition* (A.4), it is enough to find a sequence $\{m_n\}_{n\in\mathbb{N}} \subset L^2(\omega)$ such that for all $\boldsymbol{v} \in W$

$$\lim_{n\to\infty} \frac{|(m_n, v_1 - v_2)_{L^2(\omega)}|}{\|m_n\|_{L^2(\omega)} \|\boldsymbol{v}\|_1} = 0.$$

This would allow to conclude since for all $\delta > 0$ would exist $N > 0$ such that

$$\inf_{m \in M} \sup_{\boldsymbol{v} \in W} \frac{|b^*(\boldsymbol{v}, m)|}{\|m\|_{L^2(\omega)} \, \|\boldsymbol{v}\|_1} \leq \frac{|(m_N, v_1 - v_2)_{L^2(\omega)}|}{\|m_N\|_{L^2(\omega)} \|\boldsymbol{v}\|_1} < \delta.$$

Next, in order to find an upper bound easier to handle, we want to consider Holder inequality

$$(m_n, v_1 - v_2)_{L^2(\omega)} \leq \|m_n\|_{L^a(\omega)} \|v_1 - v_2\|_{L^b(\omega)}, \quad \text{with} \quad a, b \in [1, \infty) \quad \text{such that} \quad \frac{1}{a} + \frac{1}{b} = 1.$$

But we need to be careful in the choice of a and b. First, notice that $v_1 - v_2 \in H^1(\omega)$, then we need to chose b such that $H^1(\omega) \subset L^b(\omega)$. Second, we need to chose a such that $L^2(\omega) \subset L^a(\omega)$ since this guarantees $\|\cdot\|_{L^2(\omega)} \geq \|\cdot\|_{L^a(\omega)}$. Notice that otherwise, it would not be possible to finding an adequate sequence $\{m_n\}_{n\in\mathbb{N}} \subset L^2(\omega)$ such that

$$\lim_{n\to\infty} \frac{\|m_n\|_{L^a(\omega)}}{\|m_n\|_{L^2(\omega)}} = 0.$$

Thus to chose a and b such that both requirements are satisfied, we recall the Morrey-Sobolev embedding theorem (Corollary B.43 in [64])

$$W^{s,p}(\Omega) \subset \begin{cases} L^q(\Omega), & \text{if} \quad 1 \leq p < \frac{d}{s} \quad \text{and} \quad p \leq q \leq \frac{pd}{d-p}, \\ L^q(\Omega), & \text{if} \quad p = \frac{d}{s} \quad \text{and} \quad p \leq q < \infty, \\ L^\infty(\Omega) \cap \mathcal{C}^{0,\alpha}(\overline{\Omega}), & \text{if} \quad p > \frac{d}{s} \quad \text{and} \quad \alpha = 1 - \frac{d}{sp}. \end{cases}$$

In our context, $s = 1$, $p = 2$ and d the dimension of our problem. Thus, in any case, we can chose for example $a = 3/2$ and $b = 3$. This choice allows to reduce our problem to find adequate sequence $\{m_n\}_{n\in\mathbb{N}} \subset L^2(\omega)$ such that for all $\boldsymbol{v} \in W$

$$\lim_{n\to\infty} \frac{|(m_n, v_1 - v_2)_{L^2(\omega)}|}{\|m_n\|_{L^2(\omega)} \|\boldsymbol{v}\|_1} \leq \frac{\|v_1 - v_2\|_{H^1(\omega)}}{\|\boldsymbol{v}\|_1} \lim_{n\to\infty} \frac{\|m_n\|_{L^{\frac{3}{2}}(\omega)}}{\|m_n\|_{L^2(\omega)}}.$$

Moreover, we easily verify that (using Cauchy-Schwarz and Young's inequality)

$$\begin{aligned} \|v_1 - v_2\|^2_{H^1(\omega)} &= \|v_1\|^2_{H^1(\omega)} + \|v_2\|^2_{H^1(\omega)} - 2(v_1, v_2)_{H^1(\omega)} \\ &\leq \|v_1\|^2_{H^1(\omega)} + \|v_2\|^2_{H^1(\omega)} + \|v_1\|_{H^1(\omega)} \|v_2\|^2_{H^1(\omega)} \leq 2(\|v_1\|^2_{H^1(\omega)} + \|v_2\|^2_{H^1(\omega)}) \leq 2\|\boldsymbol{v}\|_1^2. \end{aligned}$$

Thus the problem is finally reduced to find $\{m_n\}_{n\in\mathbb{N}} \subset L^2(\omega)$ such that

$$\lim_{n\to\infty} \frac{\|m_n\|_{L^{\frac{2}{3}}(\omega)}}{\|m_n\|_{L^2(\omega)}} = 0.$$

But still there is one last difficulty before we give the adequate choice for the sequence. This is related to the position of the domain ω. We shall assume in the following, without any loss of generality that the origin is inside of ω. Therefore, exists $\varepsilon > 0$ such that

$$\omega_\varepsilon = [0, \varepsilon]^d \ \subset \ \omega.$$

Then we choose $\{m_n\}_{n\in\mathbb{N}} \subset L^2(\omega)$ such that for all $n \in \mathbb{N}$ we define

$$m_n = \begin{cases} x_1^n & \text{if} \quad \boldsymbol{x} \in \omega_\varepsilon, \\ 0 & \text{if} \quad \boldsymbol{x} \in \omega \setminus \omega_\varepsilon. \end{cases}$$

Thus we proceed to compute

$$\|m_n\|_{L^{\frac{3}{2}}(\omega)} = \|m_n\|_{L^{\frac{3}{2}}(\omega_\varepsilon)} = \varepsilon^{\frac{2(d-1)}{3}} \Big(\int_0^\varepsilon x_1^{\frac{3n}{2}} \mathrm{d}x \Big)^{\frac{2}{3}} = \varepsilon^{\frac{2(d-1)}{3}} \Big(\frac{\varepsilon^{\frac{3n}{2}+1}}{\frac{3n}{2}+1} \Big)^{\frac{2}{3}} = \frac{\varepsilon^{n+\frac{2d}{3}}}{(\frac{3n}{2}+1)^{\frac{2}{3}}},$$

$$\|m_n\|_{L^2(\omega)} = \|m_n\|_{L^2(\omega_\varepsilon)} = \varepsilon^{\frac{d-1}{2}} \Big(\int_0^\varepsilon x_1^{2n} \mathrm{d}x \Big)^{\frac{1}{2}} = \varepsilon^{\frac{d-1}{2}} \Big(\frac{\varepsilon^{2n+1}}{2n+1} \Big)^{\frac{1}{2}} = \frac{\varepsilon^{n+\frac{d}{2}}}{(2n+1)^{\frac{1}{2}}}.$$

Finally, combining the previous equalities and noting that $2/3 > 1/2$, we conclude

$$\lim_{n\to\infty} \frac{\|m_n\|_{L^{\frac{3}{2}}(\omega)}}{\|m_n\|_{L^2(\omega)}} = \varepsilon^{\frac{d}{6}} \lim_{n\to\infty} \frac{(2n+1)^{\frac{1}{2}}}{(\frac{3n}{2}+1)^{\frac{2}{3}}} = 0.$$

Appendix B

Generalized well-posedness of the stabilized potentials formulation in the case of free boundary conditions.

In this appendix we generalise Theorem 7.24 and prove the existence and uniqueness of solution of problem (7.61) considering a lower time regularity, in particular we assume that the source term is given by $\boldsymbol{f} \in L^1([0,T]; \boldsymbol{L}^2_R(\Omega))$. The approach is not standard since problem (7.61) does not fit the classical theory for second order hyperbolic problems, see [80] for instance. This is due to the fact that $\sqrt{m(\boldsymbol{\varphi},\boldsymbol{\varphi})}$ is a norm in the space $\boldsymbol{V}_N$ which satisfies

$$K_1 \|\boldsymbol{\varphi}\|^2_{L^2(\Omega)^2} \;\leq\; m(\boldsymbol{\varphi},\boldsymbol{\varphi}) \;\leq\; K_2 \|\boldsymbol{\varphi}\|^2_{\boldsymbol{V}}, \tag{B.1}$$

but it is not equivalent to the norm in $\boldsymbol{V}_N$ that is $\|\cdot\|_{\boldsymbol{V}}$ and is given by (6.11).

Theorem B.1

Assume that $\boldsymbol{f} \in L^1([0,T]; \boldsymbol{L}^2_R(\Omega))$. Then, there exists a unique solution $\boldsymbol{\varphi}$ of problem (7.61) such that

$$\boldsymbol{\varphi} \in L^2([0,T]; \boldsymbol{V}_N), \qquad \partial_t \boldsymbol{\varphi} \in L^2([0,T]; L^2(\Omega)^2), \tag{B.2}$$

where the involved time derivatives are considered in the distributional sense.

Proof. *Step 1: Existence of solution of a regularized problem.*
We start by introducing the regularized ε-dependent problem

$$\left\{\begin{array}{l} \text{Find } \boldsymbol{\varphi}_\varepsilon(t) : [0,T] \longrightarrow \boldsymbol{V}_N \subset L^2(\Omega)^2 \text{ such that } (\boldsymbol{\varphi}_\varepsilon, \partial_t \boldsymbol{\varphi}_\varepsilon)(t=0) = (\mathbf{0},\mathbf{0}) \text{ and} \\ \dfrac{\mathrm{d}^2}{\mathrm{d}t^2}\, m_\varepsilon(\boldsymbol{\varphi}_\varepsilon(t), \boldsymbol{\psi}) + a(\boldsymbol{\varphi}_\varepsilon(t), \boldsymbol{\psi}) = \mathrm{g}(t, \boldsymbol{\psi}), \quad \forall\, \boldsymbol{\psi} \in \boldsymbol{V}_N, \end{array}\right. \tag{B.3}$$

where we have introduced the bilinear form

$$m_\varepsilon(\boldsymbol{\varphi},\boldsymbol{\psi}) \;:=\; m(\boldsymbol{\varphi},\boldsymbol{\psi}) \;+\; \varepsilon\, a(\boldsymbol{\varphi},\boldsymbol{\psi}). \tag{B.4}$$

Notice that now, the mapping $\boldsymbol{\varphi} \mapsto \sqrt{m_\varepsilon(\boldsymbol{\varphi},\boldsymbol{\varphi})}$ is a norm in $\boldsymbol{V}_N$ equivalent to the norm in $\boldsymbol{V}$. Moreover, we recall that

$$\mathrm{g}(t,\boldsymbol{\psi}) = -\int_\Omega \boldsymbol{g} \cdot (\operatorname{div} \boldsymbol{\psi}, -\operatorname{curl} \boldsymbol{\psi})^t \,\mathrm{d}\boldsymbol{x} \quad \text{where} \quad \boldsymbol{g}(t) = \frac{1}{\rho} \int_0^t \boldsymbol{f}(s)\,\mathrm{d}s.$$

Thus, since we are assuming that $\boldsymbol{f}$ belongs to $L^1([0,T];\boldsymbol{L}^2_R(\Omega))$, we deduce that there exists a unique solution of the regularized problem (B.3)

$$\boldsymbol{\varphi}_\varepsilon \in \mathcal{C}^2([0,T];\boldsymbol{V}_N).$$

Step 2: Convergence to a solution of problem (7.61).
We begin by estimating $\boldsymbol{\varphi}_\varepsilon$. To do so, we choose in (B.3) the test function $\boldsymbol{\psi} = \partial_t\boldsymbol{\varphi}_\varepsilon \in \boldsymbol{V}_N$ and after time integration we obtain (due to vanishing initial conditions)

$$\begin{aligned} m(\partial_t\boldsymbol{\varphi}_\varepsilon(t),\partial_t\boldsymbol{\varphi}_\varepsilon(t)) \;+\; \varepsilon\, a(\partial_t\boldsymbol{\varphi}_\varepsilon(t),\partial_t\boldsymbol{\varphi}_\varepsilon(t)) \;+\; a(\boldsymbol{\varphi}_\varepsilon(t),\boldsymbol{\varphi}_\varepsilon(t))& \\ = \; 2\int_0^t \mathrm{g}(s,\partial_t\boldsymbol{\varphi}_\varepsilon(s))\,\mathrm{d}s,& \end{aligned} \tag{B.5}$$

where we have used the vanishing initial conditions. Next we rewrite the contribution of the right hand side as follows, (integrating by parts)

$$\begin{aligned} \int_0^t \mathrm{g}(s,\partial_t\boldsymbol{\varphi}_\varepsilon(s))\,\mathrm{d}s \;&=\; -\int_0^t\int_\Omega \boldsymbol{g}(s)\cdot\big(\mathrm{div}\,(\partial_t\boldsymbol{\varphi}_\varepsilon(s)),-\mathrm{curl}\,(\partial_t\boldsymbol{\varphi}_\varepsilon(s))\big)^T\mathrm{d}\boldsymbol{x}\,\mathrm{d}s \\ &=\; \int_0^t\int_\Omega \partial_t\boldsymbol{g}(s)\cdot\big(\mathrm{div}\,(\boldsymbol{\varphi}_\varepsilon(s)),-\mathrm{curl}\,(\boldsymbol{\varphi}_\varepsilon(s))\big)^T\mathrm{d}\boldsymbol{x}\,\mathrm{d}s \\ &\quad -\int_\Omega \boldsymbol{g}(t)\cdot\big(\mathrm{div}\,(\boldsymbol{\varphi}_\varepsilon(t)),-\mathrm{curl}\,(\boldsymbol{\varphi}_\varepsilon(t))\big)^t\mathrm{d}\boldsymbol{x}. \end{aligned}$$

In consequence, if we consider the definition of $\boldsymbol{g}(\cdot)$ we obtain

$$\begin{aligned} \int_0^t \mathrm{g}(s,\partial_t\boldsymbol{\varphi}_\varepsilon(s))\,\mathrm{d}s \;&=\; \frac{1}{\rho}\int_0^t\int_\Omega \boldsymbol{f}(s)\cdot\big(\mathrm{div}\,(\boldsymbol{\varphi}_\varepsilon(s)),-\mathrm{curl}\,(\boldsymbol{\varphi}_\varepsilon(s))\big)^T\mathrm{d}\boldsymbol{x}\,\mathrm{d}s \\ &\quad -\; \frac{1}{\rho}\int_\Omega\int_0^t \boldsymbol{f}(s)\,\mathrm{d}s\cdot\big(\mathrm{div}\,(\boldsymbol{\varphi}_\varepsilon(t)),-\mathrm{curl}\,(\boldsymbol{\varphi}_\varepsilon(t))\big)^T\mathrm{d}\boldsymbol{x}. \end{aligned}$$

Therefore, we obtain the following bound

$$\begin{aligned} \Big|\int_0^t \mathrm{g}(s,\partial_t\boldsymbol{\varphi}_\varepsilon(s))\,\mathrm{d}s\Big| \;&\leq\; \frac{1}{\rho}\int_0^t \|\boldsymbol{f}(s)\|_{L^2(\Omega)^2}\;\|\big(\mathrm{div}\,(\boldsymbol{\varphi}_\varepsilon(s)),-\mathrm{curl}\,(\boldsymbol{\varphi}_\varepsilon(s))\big)^T\|_{L^2(\Omega)^2}\,\mathrm{d}s \\ &\quad +\; \frac{1}{\rho}\int_0^t \|\boldsymbol{f}(s)\|_{L^2(\Omega)^2}\,\mathrm{d}s\;\|\big(\mathrm{div}\,(\boldsymbol{\varphi}_\varepsilon(t)),-\mathrm{curl}\,(\boldsymbol{\varphi}_\varepsilon(t))\big)^T\|_{L^2(\Omega)^2} \\ &\leq\; \frac{2}{\rho}\;\|\boldsymbol{f}\|_{L^1([0,t];L^2(\Omega)^2)}\;\sup_{s\in[0,t]}\sqrt{a(\boldsymbol{\varphi}_\varepsilon(s),\boldsymbol{\varphi}_\varepsilon(s))}. \end{aligned}$$

and by Young's inequality

$$\Big|\int_0^t \mathrm{g}(s,\partial_t\boldsymbol{\varphi}_\varepsilon(s))\,\mathrm{d}s\Big| \;\leq\; \big(\frac{2}{\rho^2}\;\|\boldsymbol{f}\|^2_{L^1([0,t];L^2(\Omega)^2)} \;+\; \frac{1}{2}\sup_{s\in[0,t]} a(\boldsymbol{\varphi}_\varepsilon(s),\boldsymbol{\varphi}_\varepsilon(s))\big).$$

Then, if we apply in (B.5) the norm inequalities (B.1), we obtain that

$$\begin{aligned} \sup_{0\leq t\leq T}\Big(\|\partial_t\boldsymbol{\varphi}_\varepsilon(t)\|^2_{L^2(\Omega)^2} \;+\; \varepsilon\, a(\partial_t\boldsymbol{\varphi}_\varepsilon(t),\partial_t\boldsymbol{\varphi}_\varepsilon(t)) \;+\; a(\boldsymbol{\varphi}_\varepsilon(t),\boldsymbol{\varphi}_\varepsilon(t))\Big)& \\ \leq\; K_0\,\|\boldsymbol{f}\|^2_{L^1([0,T];L^2(\Omega)^2)},& \end{aligned} \tag{B.6}$$

where $K_0 > 0$ is a constant independent of ε. We conclude that the sequence $\partial_t\boldsymbol{\varphi}_\varepsilon$ is bounded in $L^2([0,T];L^2(\Omega)^2)$. Therefore the same holds true for $\boldsymbol{\varphi}_\varepsilon$, and as a consequence $\boldsymbol{\varphi}_\varepsilon$ is also bounded in $L^2([0,T];\boldsymbol{V}_N)$. Next, since $\boldsymbol{V}_N$ is a closed subspace of $\boldsymbol{V}$, we can extract a subsequence (that we still denote by $\boldsymbol{\varphi}_\varepsilon$) such that

$$\boldsymbol{\varphi}_\varepsilon \rightharpoonup \boldsymbol{\varphi} \in L^2([0,T];\boldsymbol{V}_N), \quad \boldsymbol{\varphi}_\varepsilon \rightharpoonup \boldsymbol{\varphi} \in L^2([0,T];L^2(\Omega)^2),$$
$$\partial_t\boldsymbol{\varphi}_\varepsilon \rightharpoonup \boldsymbol{d\varphi} \in L^2([0,T];L^2(\Omega)^2),$$

where the convergence holds in the weak topology. Furthermore, it can be easily proven that $\partial_t\boldsymbol{\varphi} = \boldsymbol{d\varphi}$ where the time derivative is considered in the distributional sense. Finally we prove that

$$\frac{\mathrm{d}^2}{\mathrm{d}t^2}\, m(\boldsymbol{\varphi}(t),\boldsymbol{\psi}) + a(\boldsymbol{\varphi}(t),\boldsymbol{\psi}) = \mathrm{g}(t,\boldsymbol{\psi}), \quad \forall\, \boldsymbol{\psi} \in \boldsymbol{V}_N,$$

where the time derivative are, once again, considered in the distributional sense. Let $\Theta \in \mathcal{D}(-\infty,T)$, we have from (B.3)

$$\int_0^T \big(m(\boldsymbol{\varphi}_\varepsilon(t),\boldsymbol{\psi}) + \varepsilon\, a(\boldsymbol{\varphi}_\varepsilon(t),\boldsymbol{\psi})\big)\ \Theta''(t)\ \mathrm{d}t \ + \int_0^T a(\boldsymbol{\varphi}_\varepsilon(t),\boldsymbol{\psi})\ \Theta(t)\ \mathrm{d}t \ = \int_0^T \mathrm{g}(t,\boldsymbol{\psi})\ \Theta(t)\ \mathrm{d}t.$$

The above-mentioned weak convergence, together with (B.6), allows to easily pass to the limit in each term and prove that

$$\int_0^T m(\boldsymbol{\varphi}(t),\boldsymbol{\psi})\ \Theta''(t)\ \mathrm{d}t \ + \int_0^T a(\boldsymbol{\varphi}(t),\boldsymbol{\psi})\ \Theta(t)\ \mathrm{d}t \ = \int_0^T \mathrm{g}(t,\boldsymbol{\psi})\ \Theta(t)\ \mathrm{d}t.$$

Step 3: Uniqueness.
Let us first prove uniqueness in

$$\mathcal{C}^2([0,T];L^2(\Omega)^2) \cap \mathcal{C}^1([0,T];\boldsymbol{V}_N). \tag{B.7}$$

Assume that $\boldsymbol{\varphi}_1$ and $\boldsymbol{\varphi}_2$ are solution of problem (7.61) both belonging to this space. In consequence, $\boldsymbol{\varphi} := \boldsymbol{\varphi}_1 - \boldsymbol{\varphi}_2$ satisfies (7.61) with vanishing data. Then if we consider the test function $\boldsymbol{\psi} = \partial_t\boldsymbol{\varphi}$ in the variational formulation, we deduce

$$0 \ = \ m(\partial_t^2\boldsymbol{\varphi},\partial_t\boldsymbol{\varphi}) + a(\boldsymbol{\varphi},\partial_t\boldsymbol{\varphi}) \ = \ \frac{\mathrm{d}}{\mathrm{d}\,t}\Big\{\frac{1}{2}\, m(\partial_t\boldsymbol{\varphi},\partial_t\boldsymbol{\varphi}) + \frac{1}{2}\, a(\boldsymbol{\varphi},\boldsymbol{\varphi})\Big\}.$$

Next, we integrate in time to obtain

$$m(\partial_t\boldsymbol{\varphi}(t),\partial_t\boldsymbol{\varphi}(t)) \ + \ a(\boldsymbol{\varphi}(t),\boldsymbol{\varphi}(t)) \ = \ 0.$$

Thus $\partial_t\boldsymbol{\varphi}(t) = 0$ and therefore $\boldsymbol{\varphi}(t) = \boldsymbol{\varphi}(0) = 0$ leading to the uniqueness. Finally, let us assume that we have two solutions $\boldsymbol{\varphi}_i$, $i \in \{1,2\}$ such that

$$\boldsymbol{\varphi}_i \in L^2([0,T];\boldsymbol{V}_N) \quad \text{and} \quad \partial_t\boldsymbol{\varphi}_i \in L^2([0,T];L^2(\Omega)^2).$$

Then $\boldsymbol{\Phi}$ defined as the second anti-derivative of $\boldsymbol{\varphi} = \boldsymbol{\varphi}_1 - \boldsymbol{\varphi}_2$ belongs to the space in (B.7) and, by linearity, satisfies (7.61) with vanishing data. In consequence, $\boldsymbol{\Phi} = \boldsymbol{0}$ which leads to $\boldsymbol{\varphi}_1 = \boldsymbol{\varphi}_2$.

■

Resumen en castellano

La tesis está dividida en **dos partes diferentes** donde nos interesamos por cuestiones independientes, que nos han llevado al desarrollo de dos técnicas distintas, pero que en la práctica se espera que puedan ser combinadas. En ambas partes, además de la curiosidad intelectual, nos guiamos también por un objetivo común, el desarrollo de métodos eficientes para la resolución numérica de problemas de propagación de ondas.

El método Arlequin

En la **primera parte** de la tesis, nos interesamos por el desarrollo de una técnica de descomposición de dominios que esté bien adaptada para la consideración de fenómenos locales en problemas de acústica y prestamos especial atención a la eficiencia del método en presencia de defectos tales como fisuras, agujeros y/o inclusiones, que además pueden estar rodeados por una región dañada. La principal dificultad en este tipo de problemas viene dada por la discrepancia entre la escala del defecto y la estructura, esto requiere el uso de mallados finos en torno al defecto y que necesitan ser generados para cada nuevo defecto, lo cual en la práctica resulta computacionalmente caro (ver Figura .1).

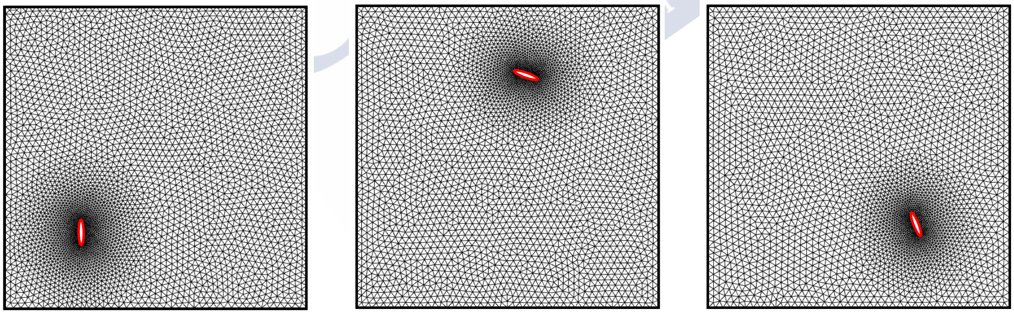

Figura .1: Mallados adaptados a diferentes posiciones de un obstáculo.

En muchas aplicaciones nos interesa resolver el mismo problema para muchas configuraciones diferentes, como ocurre en problemas de optimización donde el dominio cambia de una iteración a la siguiente. Un ejemplo son los problemas de detección de obstáculos, donde el mismo problema debe ser resuelto para cada nueva posición del obstáculo que es dada por un proceso de optimización, de modo que el coste computacional de remallar el dominio para cada nueva posición del obstáculo es muy elevado. En este sentido, los métodos de descomposición de dominios con superposición ofrecen una interesante alternativa, dado que permiten considerar un parche que puede ser fácilmente adaptado a distintas posiciones del mismo defecto (ver Figura .2).

Entre los métodos de descomposición de dominios, nosotros consideramos el método Arlequin (ver [8, 9]) como punto de partida. Esta técnica permite dividir el problema en cada región y acoplar la solución en las zonas de intersección de manera débil. De este modo se obtienen distintos problemas variacionales que a su vez deben ser corregidos mediante la introducción de un

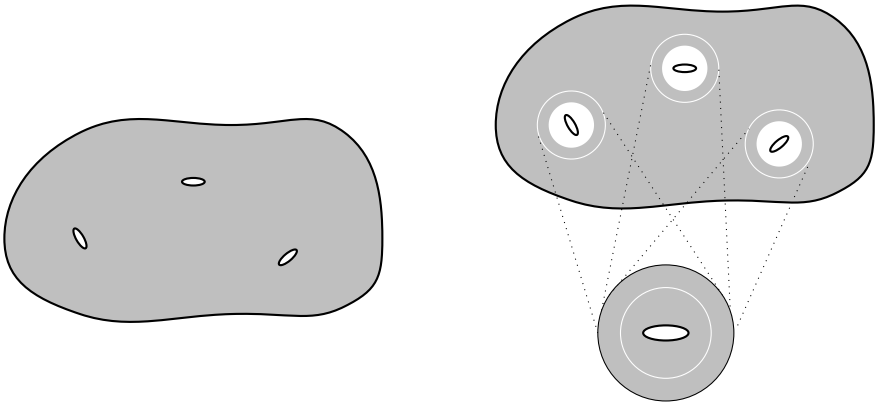

Figura .2: Ejemplo de descomposición de dominios que nos gustaría considerar para tratar cada posición del obstáculo con el mismo parche.

multiplicador de Lagrange que es definido en cada región de intersección. La técnica es presentada en el contexto de la ecuación de Helmholtz y la ecuación de ondas, aunque en principio podría extenderse a otros campos.

Preliminares: Consideremos $\Theta \subset \mathbb{R}^2$, un dominio abierto, acotado, simplemente conexo y con frontera Lipschitz y denotemos por $\mathcal{O} \subset \Theta$ el defecto (posiblemente vacío), el cual asumimos que es compacto. Entonces, introducimos el domino defectuoso $\Omega := \Theta \setminus \mathcal{O}$, con coeficientes físicos $(\rho, \mu) \in L^\infty(\Omega)^2$ tales que $\rho(\boldsymbol{x}) \geq \rho_0 > 0$ y $\mu(\boldsymbol{x}) \geq \mu_0 > 0$ y planteamos los siguientes problemas:

- Ecuación de Helmholtz: Dada la fuente $f \in L^2(\Omega)$ y supongamos que ℓ no es una frecuencia natural de Ω, encontrar $u \in H^1(\Omega)$ tal que

$$\left\{ \begin{array}{rcll} -\,\ell^2\,\rho\,u\,-\,\mathrm{div}(\mu\,\nabla u) &=& f, & \text{en} \quad \Omega, \\ \nabla u \cdot \mathbf{n} &=& 0, & \text{en} \quad \partial\Omega. \end{array} \right.$$

- Ecuación de ondas: Dada la fuente $f \in \mathcal{C}^1([0,T]; L^2(\Omega))$ y las condiciones iniciales $(u, \partial_t u, f)(t = 0) = (0,0,0)$, encontrar $u(t) \in H^1(\Omega)$ tal que

$$\left\{ \begin{array}{rll} \rho\,\partial_t^2 u\,-\,\mathrm{div}(\mu\,\nabla u) = f, & \text{en } \Omega, & t \in [0,T], \\ \nabla u \cdot \mathbf{n} = 0, & \text{en } \partial\Omega, & t \in [0,T]. \end{array} \right.$$

Arlequin clásico: Consideramos el dominio Ω descompuesto en dos nuevos dominios Ω_1 y Ω_2 tales que $\Omega_1 \cup \Omega_2 = \Omega$ y $\partial\Omega_1 \cap \partial\Omega_2 = \emptyset$. Además, con el propósito de distribuir entre Ω_1 y Ω_2 los términos correspondientes a la región $\omega = \Omega_1 \cap \Omega_2$, introducimos los coeficientes $(\alpha_j, \beta_j) \in L^\infty(\Omega_j)^2$ para $j \in \{1, 2\}$, tales que

$$\begin{array}{lllll} \alpha_1 + \alpha_2 = 1 \;\text{ en }\; \omega, & \alpha_j = 1 \;\text{ en }\; \Omega_j \setminus \omega & \text{y} & \displaystyle\inf_{\boldsymbol{x}\in\Omega_j} \alpha_j(\boldsymbol{x}) \geq \alpha_0 > 0 & \text{para} \quad j \in \{1,2\}, \\ \beta_1 + \beta_2 = 1 \;\text{ en }\; \omega, & \beta_j = 1 \;\text{ en }\; \Omega_j \setminus \omega & \text{y} & \displaystyle\inf_{\boldsymbol{x}\in\Omega_j} \beta_j(\boldsymbol{x}) \geq \beta_0 > 0 & \text{para} \quad j \in \{1,2\}. \end{array}$$

De este modo podemos introducir las formas bilineales en $W := H^1(\Omega_1) \times H^1(\Omega_2)$ dadas por

$$m : W \times W \longrightarrow \mathbb{R} \qquad \text{tal que} \qquad m(\boldsymbol{u}, \boldsymbol{v}) = \sum_{j=1}^{2} (\alpha_j\,\rho\,u_j, v_j)_{L^2(\Omega_j)},$$

$$a : W \times W \longrightarrow \mathbb{R} \qquad \text{tal que} \qquad a(\boldsymbol{u}, \boldsymbol{v}) = \sum_{j=1}^{2} (\beta_j\,\mu\,\nabla u_j, \nabla v_j)_{L^2(\Omega_j)},$$

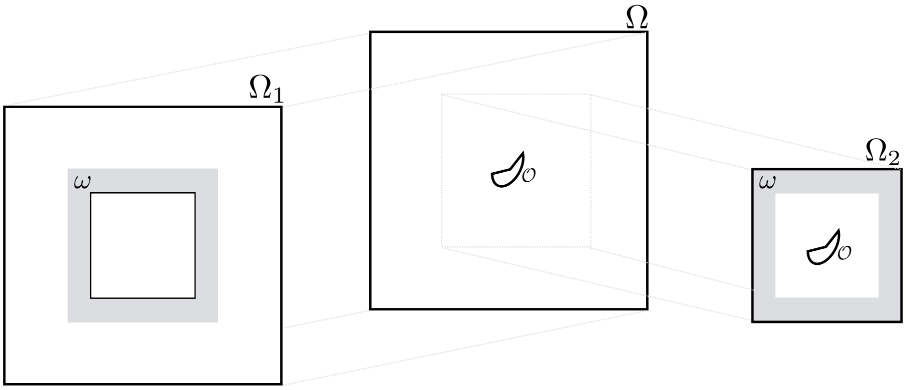

Figura .3: Descomposición típica de un dominio que incluye un defecto. La región de acople ω is la intersección entre Ω_1 y Ω_2.

que nos permiten dividir el problema en cada región. Además, ambos problemas deben ser corregidos mediante un multiplicador de Lagrange que a su vez nos permite acoplar ambas soluciones en la región de intersección de manera débil. Para esto introducimos el espacio $M := H^1(\omega)$ y la forma bilineal

$$b : W \times M \longrightarrow \mathbb{R} \quad \text{tal que} \quad b(\boldsymbol{v}, m) = (v_1 - v_2, m)_{H^1(\omega)}.$$

Finalmente buscamos la solución dada por $\boldsymbol{u} = (u_{|\Omega_1}, u_{|\Omega_2})$ resolviendo:

- Ecuación de Helmholtz: Dada la fuente $f \in L^2(\Omega)$ tal que (por simplicidad) $\mathrm{sop}\{f\} \subset \Omega_1 \setminus \omega$ y supongamos que ℓ no es una frecuencia natural de Ω,

$$\left\{\begin{array}{l} \text{Encontrar } (\boldsymbol{u}, \boldsymbol{\lambda}) \in W \times M \text{ tal que} \\ -\,\ell^2\, m(\boldsymbol{u}, \boldsymbol{v}) \;+\; a(\boldsymbol{u}, \boldsymbol{v}) \;+\; b(\boldsymbol{v}, \lambda) \;=\; (f, \boldsymbol{v})_{L^2(\Omega_1)}, \quad \forall \boldsymbol{v} \in W, \\ \qquad\qquad\qquad\qquad\qquad\quad b(\boldsymbol{u}, m) \;=\; 0, \qquad\qquad\quad \forall m \in M. \end{array}\right.$$

- Ecuación de ondas: Dada la fuente $f \in \mathcal{C}^1([0,T]; L^2(\Omega))$ tal que (por simplicidad) $\mathrm{sop}\{f(t)\} \subset \Omega_1 \setminus \omega$ para todo $t \geq 0$ y las condiciones iniciales $(u, \partial_t u, f)(t = 0) = (0, 0, 0)$,

$$\left\{\begin{array}{l} \text{Encontrar } (\boldsymbol{u}(t), \boldsymbol{\lambda}(t)) : [0,T] \longrightarrow W \times M \text{ tal que } (\boldsymbol{u}, \partial_t \boldsymbol{u})(t=0) = (\boldsymbol{0}, \boldsymbol{0}) \text{ y} \\ \dfrac{\mathrm{d}^2}{\mathrm{d}t^2}\, m(\boldsymbol{u}, \boldsymbol{v}) \;+\; a(\boldsymbol{u}, \boldsymbol{v}) \;+\; b(\boldsymbol{v}, \boldsymbol{\lambda}) \;=\; (f, \boldsymbol{v})_{L^2(\Omega_1)}, \qquad \forall \boldsymbol{v} \in W, \\ \qquad\qquad\qquad\qquad\qquad b(\boldsymbol{u}, \boldsymbol{m}) \;=\; 0, \qquad\qquad\quad \forall \boldsymbol{m} \in M. \end{array}\right.$$

En la práctica, esta metodología nos permite considerar un mallado $\mathcal{T}_{1,h}$ de Θ y otro mallado $\mathcal{T}_{2,h}$ de un entorno de $\mathcal{O}$, de modo que para cada posición de $\mathcal{O}$, podemos escoger Ω_1 como el dominio resultante de eliminar en $\mathcal{T}_{1,h}$ los elementos que interactúan con $\mathcal{O}$ y Ω_2 como el dominio resultante de adaptar $\mathcal{T}_{2,h}$ a la posición real del obstáculo (ver Figura .4). De este modo, tenemos mallas adecuadas para discretizar W, sin embargo también es necesario discretizar M, lo cual requiere considerar una malla conforme con ω que no sería válida para una nueva posición del obstáculo.

Arlequin modificado: Con el objetivo de eludir esta dificultad, presentamos una versión modificada del método que evita acoplar en $\omega_c \subset \omega$, asumiendo que existe una constante $C \in (0, 1)$ tal que

$$\alpha_1 = \beta_1 = C \quad \text{y} \quad \alpha_2 = \beta_2 = 1 - C \quad \text{en} \quad \omega_c.$$

Entonces, distinguimos entre cuatro tipos de acoples diferentes en función de la elección de ω_c. Cada tipo de acople, implica la introducción de diferentes multiplicadores de Lagrange que estarán

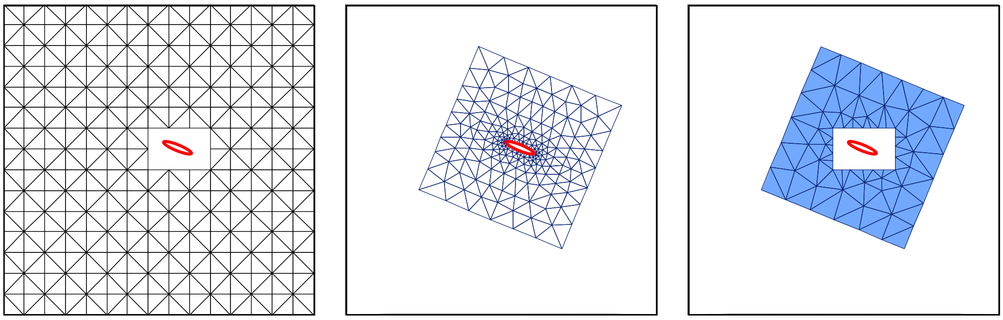

(a) Reducción del mallado de Θ para una posicón dada de $\mathcal{O}$. (b) Mallado fino $\mathcal{T}_{2,h}$ adaptado a la posición de $\mathcal{O}$. (c) Malla requerida para la zona de itnersección ω.

Figura .4: Mallados adaptados para una descomposición de Arlequin estándar.

asociados a las diferentes partes de ω que se describen en la Figura .5. Como resultado, sustituyendo M y $b(\cdot,\cdot)$ por alguna de las siguientes parejas

$$M_{BB} = [H^{\frac{1}{2}}(\gamma_i)]' \times [H^{\frac{1}{2}}(\gamma_e)]', \qquad b_{BB}(\boldsymbol{v},\boldsymbol{m}) = \langle v_1 - v_2, m_i\rangle_{\gamma_i} + \langle v_1 - v_2, m_e\rangle_{\gamma_e},$$

$$M_{BV} = [H^{\frac{1}{2}}(\gamma_i)]' \times H^1(\omega_e), \qquad b_{BV}(\boldsymbol{v},\boldsymbol{m}) = \langle v_1 - v_2, m_i\rangle_{\gamma_i} + (v_1 - v_2, m_e)_{H^1(\omega_e)},$$

$$M_{VB} = H^1(\omega_i) \times [H^{\frac{1}{2}}(\gamma_e)]', \qquad b_{VB}(\boldsymbol{v},\boldsymbol{m}) = (v_1 - v_2, m_i)_{H^1(\omega_i)} + \langle v_1 - v_2, m_e\rangle_{\gamma_e},$$

$$M_{VV} = H^1(\omega_i) \times H^1(\omega_e), \qquad b_{VV}(\boldsymbol{v},\boldsymbol{m}) = (v_1 - v_2, m_i)_{H^1(\omega_i)} + (v_1 - v_2, m_e)_{H^1(\omega_e)},$$

se obtienen las nuevas formulaciones que se pueden enmarcar en las siguientes formulaciones abstractas:

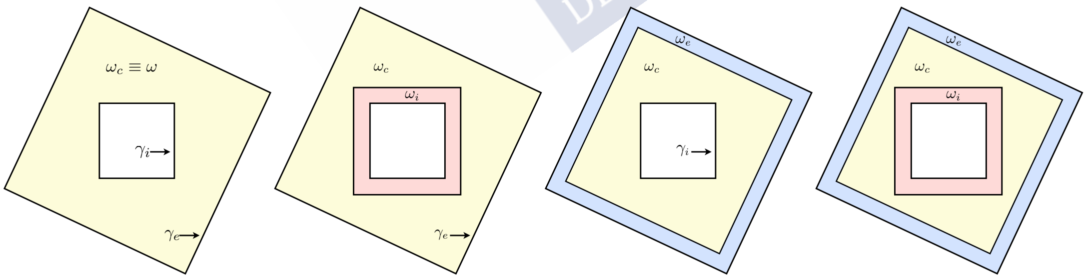

BB Boundary-Boundary: El acople se efectúa en γ_i y γ_e.

BV Boundary-Volume: El acople se efectúa en ω_i y γ_e.

VB Volume-Boundary: El acople se efectúa en γ_i y ω_e.

VV Volume-Volume: El acople se efectúa en ω_i y ω_e.

Figura .5: Representación de las regiones de $\omega = \Omega_1 \cap \Omega_2$ donde las nuevas formulaciones efectúa el acople.

- Ecuación de Helmholtz: Dada la fuente $f \in L^2(\Omega)$ tal que (por simplicidad) $\text{sop}\{f\} \subset \Omega_1 \setminus \omega$ y supongamos que ℓ no es una frecuencia natural de Ω ni de ω_c,

$$\left\{\begin{array}{l} \text{Encontrar } (\boldsymbol{u},\boldsymbol{\lambda}) \in W \times M_C \text{ tal que} \\ -\,\ell^2\, m(\boldsymbol{u},\boldsymbol{v}) \;+\; a(\boldsymbol{u},\boldsymbol{v}) \;+\; b_C(\boldsymbol{v},\lambda) \;=\; (f,\boldsymbol{v})_{L^2(\Omega_1)}, \quad \forall \boldsymbol{v} \in W, \\ \qquad\qquad\qquad\qquad\qquad\quad b_C(\boldsymbol{u},m) \;=\; 0, \qquad\qquad \forall m \in M_C. \end{array}\right.$$

- Ecuación de ondas: Dada la fuente $f \in \mathcal{C}^1([0,T]; L^2(\Omega))$ tal que (por simplicidad) $\mathrm{sop}\{f(t)\} \subset \Omega_1 \setminus \omega$ para todo $t \geq 0$ y las condiciones iniciales $(u, \partial_t u, f)(t=0) = (0,0,0)$,

$$\left\{\begin{array}{l} \text{Encontrar } (\boldsymbol{u}(t), \boldsymbol{\lambda}(t)) : [0,T] \longrightarrow W \times M_C \text{ tal que } (\boldsymbol{u}, \partial_t \boldsymbol{u})(t=0) = (\mathbf{0}, \mathbf{0}) \text{ y} \\ \dfrac{\mathrm{d}^2}{\mathrm{d}t^2} m(\boldsymbol{u}, \boldsymbol{v}) \; + \; a(\boldsymbol{u}, \boldsymbol{v}) \; + \; b_C(\boldsymbol{v}, \boldsymbol{\lambda}) \; = \; (f, \boldsymbol{v})_{L^2(\Omega_1)}, \qquad \forall \boldsymbol{v} \in W, \\ \qquad\qquad\qquad\qquad\qquad b_C(\boldsymbol{u}, \boldsymbol{m}) \; = \; 0, \qquad\qquad\qquad \forall \boldsymbol{m} \in M_C. \end{array}\right.$$

Cabe destacar que estas nuevas formulaciones no requieren el uso de un mallado específico de la región de intersección ω. En su lugar, para discretizar el problema es suficiente disponer de mallados $\mathcal{G}_{i,h}$ (de ω_i o γ_i) y $\mathcal{G}_{e,h}$ (de ω_e o γ_e) de cada una de las regiones de acople (dependiendo de si son acoples de volumen o de frontera), pero esto siempre es posible dado que en la práctica escogeremos estas regiones conformes con los mallados de Ω_1 y Ω_2 (ver Figura .6).

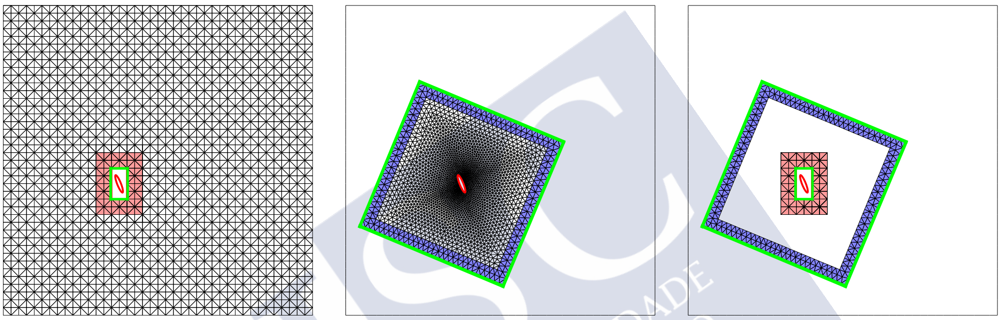

(a) Mallado de Ω_1 y submallado de las posibles zonas de acople γ_i (en verde) y ω_i (en rojo)

(b) Mallado de Ω_2 y submallado de las posibles zonas de acople γ_e (en verde) y ω_e (in azul)

(c) Mallados necesarios para cada uno de los nuevos acoples.

Figura .6: Ejemplo de mallados necesarios para utilizar las nuevas variantes del método Arlequin.

Para la discretización espacial del método utilizamos los espacios de elementos finitos de Lagrange de orden p

$$X_p(\mathcal{T}_h) = \Big\{ v_h \in \mathcal{C}^0\big(\bigcup_{\kappa \in \mathcal{T}_h} \kappa \big) \text{ tal que } \forall \kappa \in \mathcal{T}_h,\, v_{h|\kappa} \in \mathcal{P}_p \Big\}$$

y consideramos

$$W_h = X_p(\mathcal{T}_{1,h}) \times X_p(\mathcal{T}_{2,h}) \subset W \quad \text{y} \quad M_{C,h} = X_p(\mathcal{G}_{i,h}) \times X_p(\mathcal{G}_{e,h}) \subset M_C,$$

donde $\mathcal{G}_{i,h}$ (resp. $\mathcal{G}_{e,h}$) es la restricción a ω_i o γ_i (resp. ω_e o γ_e) del mallado $\mathcal{T}_{1,h}$ (resp. $\mathcal{T}_{2,h}$). Por otra parte, para la discretización en tiempo utilizamos un esquema de diferencia finitas de orden dos que es explícito en Ω_1 (que evita el obstáculo y posee una malla regular, ver Figura .6a) mientras que en Ω_2 (que captura el obstáculo y posee una malla refinada, ver Figura .6b) es implícito e incondicionalmente estable garantizando así la eficiencia del esquema numérico resultante.

Como resultado, se obtienen formulaciones discretas de ambos problemas (con cualquiera de los acoples) las cuales bajo ciertas hipótesis se demuestra que están bien planteadas, son estables y garantizan la optimalidad de los esquemas numéricos propuestos cuando la solución sea suficientemente regular. Sin embargo, en problemas 2D nos restringimos al caso de dominios poligonales (a menos que se consideren elementos finitos isoparamétricos, lo cual se abordará en trabajos futuros) y por tanto, regiones de intersección con esquinas. Como consecuencia, la regularidad del multiplicador de Lagrange puede ser baja y esto repercute en la convergencia del método la cual se ve penalizada.

Arlequin modificado para dominios poligonales: Para mejorar la convergencia del método cuando la región de intersección es poligonal se procede de forma diferente si el acople es de frontera o de volumen. A continuación detallamos los cambios para los acoples **BB** y **VV**, mientras que para los casos **BV** y **VB** el procedimiento se deduce fácilmente de estos.

- En el caso de acoples de frontera, es suficiente introducir nuevos espacios de discretización que introducen discontinuidades en las esquinas (de forma similar al método mortar, ver [56]). En particular consideramos como espacio de aproximación (notar que *op* se refiere a la opción, *cl* de *clásico* o *du* de *dual*)

$$M_{BB,h} = M_{B_i,h} \times M_{B_e,h} \subset M_{BB} = [H^{\frac{1}{2}}(\gamma_i)]' \times [H^{\frac{1}{2}}(\gamma_e)]',$$

$$\text{con} \quad M_{B_j,h} = \{m_{j,h} \ / \ m_{j,h|\gamma_{j,k}} \in Y_p^{op}(\mathcal{G}_{j,k}), \ 1 \leq k \leq s_j\}, \quad \text{para } j \in \{i,e\} \text{ y } op \in \{cl, du\},$$

  donde denotamos por $\mathcal{G}_{j,k}$ las restricciones a $\gamma_{j,k}$ de los mallados $\mathcal{T}_{1,h}$ y $\mathcal{T}_{2,h}$, y donde se introducen los espacios $Y_p^{op}(\mathcal{G}_{j,k})$ definidos en la sección 2.7.1.1

- En el caso de acoples de volumen, es necesario modificar la formulación de modo que se obtengan multiplicadores que sean más regulares. Para esto, descomponemos las regiones de acople ω_j con $j \in \{i,e\}$ en distintas regiones de modo que se reduzca los ángulos en las esquinas. Más concretamente, consideramos descomposiciones como la que se presenta en la Figura .7, es decir

$$\{\omega_{j,k}\}_{k=1}^{N_j} \quad \text{donde los } \omega_{j,k} \text{ son abiertos disjuntos de } \omega_j \text{ tales que} \quad \bigcup_{k=1}^{N_j} \overline{\omega_{j,k}} = \overline{\omega_j},$$

$$\text{y el esqueleto} \quad \mathcal{S}_j = \bigcup_{k=1}^{N_j} \partial\omega_{j,k} \quad \text{verifica} \quad \mathcal{S}_j = \bigcup_{k=1}^{N_j} \gamma_{j,k} \quad \text{con } \gamma_{j,k} \text{ segmentos rectos.}$$

  Esto nos permite considerar una nueva formulación del método Arlequin donde el acople se realiza por separado en cada una de las nuevas regiones introducidas. Para ello consideramos

$$M_{VV} = [H^{\frac{1}{2}}(\mathcal{S}_i)]' \times \prod_{k=1}^{N_i} H_0^1(\omega_{i,k}) \times [H^{\frac{1}{2}}(\mathcal{S}_e)]' \times \prod_{k=1}^{N_e} H_0^1(\omega_{e,k}),$$

$$\begin{aligned} b_{VV}(\boldsymbol{v}, \boldsymbol{m}) \;\; = \;\; & \langle v_1 - v_2, m_{\mathcal{S}_i} \rangle_{\mathcal{S}_i} \;\; + \;\; \sum_{k=1}^{N_i} (v_1 - v_2, m_{i,k})_{H^1(\omega_{i,k})} \\ + \;\; & \langle v_1 - v_2, m_{\mathcal{S}_e} \rangle_{\mathcal{S}_e} \;\; + \;\; \sum_{k=1}^{N_e} (v_1 - v_2, m_{e,k})_{H^1(\omega_{e,k})}. \end{aligned}$$

  Cabe destacar que la discretización del problema resultante, requiere el uso de mallas específicas para las regiones $\omega_{j,k}$ y $\gamma_{j,k}$, de forma que podamos considerar el espacio de elementos finitos dado por

$$M_{VV,h} = M_{\mathcal{S}_i,h} \times \prod_{k=1}^{N_i} M_{V_{i,k},h} \times M_{\mathcal{S}_e,h} \times \prod_{k=1}^{N_e} M_{V_{e,k},h} \subset M_{VV},$$

  donde se introducen para $j \in \{i,e\}$

$$\begin{aligned} M_{\mathcal{S}_j,h} \;\; &= \;\; \{m_{\mathcal{S}_j,h} \ / \ m_{\mathcal{S}_j,h|\gamma_{j,k}} \in Y_p^{op}(\mathcal{F}_{j,k}), \ 1 \leq k \leq s_j\}, \\ \text{y} \quad M_{V_{j,k},h} \;\; &= \;\; X_p(\mathcal{G}_{j,k}) \cap H_0^1(\omega_{j,k}) \quad \text{for} \quad k \in \{1, \ldots, N_j\}. \end{aligned}$$

  En la práctica los mallados $\mathcal{F}_{j,k}$ y $\mathcal{G}_{j,k}$ se obtienen restringiendo a $\gamma_{j,k}$ y ω_{jk} los mallados $\mathcal{T}_{1,h}$ y $\mathcal{T}_{2,h}$, de modo que estos deberán de ser construidos considerando esta restricción.

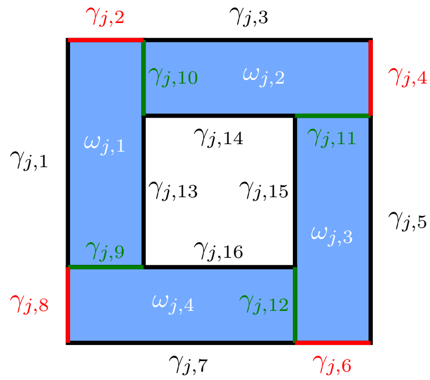

Figura .7: Descomposición de ω_j en los respectivos $\omega_{j,k}$ y descomposición del esqueleto resultante $\mathcal{S}_j$ en los segmentos rectos $\gamma_{j,k}$. Notar que en la práctica necesitaremos mallas de cada $\gamma_{j,k}$ y $\omega_{j,k}$.

Con la metodología presentada, se obtienen esquemas numéricos bien planteados, estables y que en el caso de acoples de frontera son óptimos si la solución es suficientemente regular, sin embargo, en el caso de acoples de volumen, el resultado es un esquema numérico compatible con elementos finitos de hasta segundo orden.

Finalmente, cabe destacar que a lo largo del documento, se presentan resultados numéricos que respaldan los resultados teóricos demostrados. Así mismo, también se abordan ejemplos académicos que exhiben las ventajas de la metodología presentada.

Formulación en potenciales para la elastodinámica

En la **segunda parte** de la tesis, nos interesamos por una cuestión clásica, la resolución numérica de las ecuaciones de la elastodinámica lineal en medios isótropos, que modelan la propagación de ondas en sólidos elásticos e isótropos. En este contexto es conocido que existen dos tipos diferentes de ondas que se propagan al mismo tiempo (ondas de presión y ondas de corte) y que en el espacio libre viajan de forma independiente con diferentes velocidades que denotamos V_P y V_S (notar que $V_P > V_S$) y en consecuencia con diferente longitud de onda que viene dada por $\lambda_P = T_\star V_P$ y $\lambda_S = T_\star V_S$, donde $T_\star$ representa la escala temporal del problema (notar que $\lambda_P > \lambda_S$). En la práctica, cuando ambos tipos de ondas no viajan a velocidades similares, los métodos clásicos de discretización espacio-temporal basados en elementos finitos (EF) en espacio y diferencias finitas (DF) en tiempo no son eficientes. Esto es debido a la combinación de dos factores, por un lado elegimos por precisión una discretización espacial adaptada a la longitud de onda más pequeña, es decir, proporcional a λ_S,

$$h = \frac{\lambda_S}{N_\star}, \tag{.12}$$

donde $N_\star$ denota el número de grados de libertad que queremos considerar por longitud de onda. Por otro lado, si consideramos un esquema de diferencias finitas explícito en tiempo, debemos elegir un paso de tiempo que está restringido por una condición de estabilidad que implica la velocidad máxima V_P, es decir

$$\Delta t \approx \frac{h}{V_P} \approx \frac{T_\star}{N_\star}\frac{V_S}{V_P}.$$

Por tanto, los métodos explícitos clásicos solo se recomiendan cuando las ondas de presión y las ondas de corte se propagan con velocidades similares, es decir, cuando V_P/V_S es pequeño (ver Figura .8) dado que los valores grandes de V_P/V_S penalizan la eficiencia del esquema numérico resultante. Entonces, surge una pregunta natural: ¿Cómo procedemos para valores altos de V_P/V_S? En la literatura, se pueden encontrar trabajos donde se consideran modelos aproximados para el caso en que la diferencia entre ambas velocidades es muy grande, sin embargo estas técnicas no son precisas cuando la diferencia entre las velocidades es moderada.

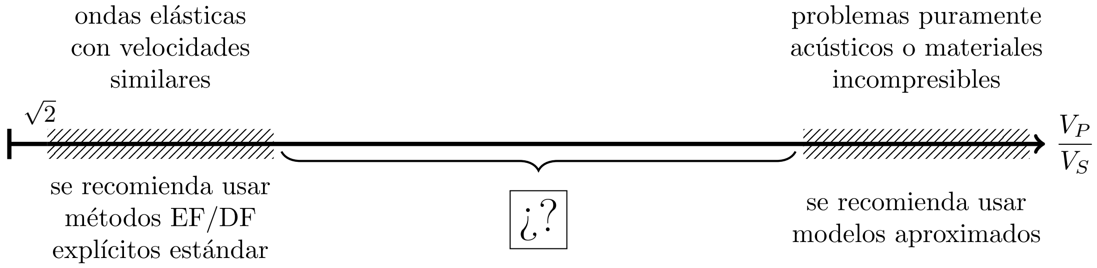

Figura .8: Diagrama de los diferentes regímenes dependiendo del valor de V_P/V_S y la correspondiente elección del método de discretización más eficiente.

En este trabajo, presentamos una metodología que nos permita tratar valores intermedios de V_P/V_S de forma eficiente sin penalizar la precisión del método. Esta técnica está motivada por los métodos clásicos que consideran la descomposición de Helmholtz de un campo vectorial para escribir el vector de desplazamientos como la suma de las ondas de presión y ondas de corte. De este modo, las ecuaciones de la elastodinámica se relacionan con dos ecuaciones de ondas escalares que son relativas a cada tipo de onda. El resultado es un sistema de ecuaciones que en el espacio libre está totalmente desacoplado y mejor adaptado para su discretización por elementos finitos, dado que permite discretizar por separado cada tipo de onda. Sin embargo, la dificultades surgen al considerar dominios acotados o localmente homogéneos, dado que ambos tipos de ondas están acopladas en las fronteras.

Preliminares: Por simplicidad, nos restringimos al análisis del caso 2D, mientras que la extensión a dimensiones superiores será el objetivo de futuros trabajos. Entonces, denotamos por $\boldsymbol{u} = (u_1, u_2)$ el vector desplazamientos que, en el caso de un medio elástico, isótropo y homogéneo, es conocido que viene determinado por las siguientes ecuaciones:

$$\rho\, \partial_t^2 \boldsymbol{u} \;-\; (\lambda + 2\mu)\, \nabla \operatorname{div} \boldsymbol{u} + \mu\, \mathbf{curl}\big(\operatorname{curl} \boldsymbol{u}\big) \;=\; \boldsymbol{f},$$

donde $\lambda > 0$ y $\mu > 0$ son los coeficientes de Lamé, $\rho > 0$ es la densidad y la fuente $\boldsymbol{f}$ es dada. De este modo, las velocidades de ambos tipos de ondas vienen dadas por

$$V_P \;=\; \sqrt{\frac{\lambda + 2\,\mu}{\rho}} \qquad \text{y} \qquad V_S \;=\; \sqrt{\frac{\mu}{\rho}}.$$

Además, este problema debe ser completado con condiciones iniciales, que por simplicidad consideramos nulas,

$$\boldsymbol{u}(t = 0) = \mathbf{0} \qquad \text{y} \qquad \partial_t \boldsymbol{u}(t = 0) = \mathbf{0}.$$

Así mismo, en presencia de fronteras, debemos introducir condiciones de contorno adecuadas. En este trabajo se estudian dos casos:

Frontera **rígida** Γ :	Frontera **libre** Γ :
$\boldsymbol{u} = \mathbf{0}$ en Γ.	$\boldsymbol{\sigma}(\boldsymbol{u})\boldsymbol{n} = 0$ en Γ.

Formulación en potenciales en el espacio libre: Con el objetivo de relacionar las ecuaciones de la elastodinámica con un sistema equivalente que distinga entre ambos tipos de ondas, introducimos los potenciales de presión y de corte como los campos escalares obtenidos al resolver las siguientes ecuaciones diferenciales ordinarias:

$$\left\{ \begin{array}{rcl} \rho\, \partial_t \varphi_P &=& (\lambda + 2\mu) \operatorname{div} \boldsymbol{u}, \\ \varphi_P(t = 0) &=& 0, \end{array} \right. \qquad \left\{ \begin{array}{rcl} \rho\, \partial_t \varphi_S &=& -\mu \operatorname{curl} \boldsymbol{u}, \\ \varphi_S(t = 0) &=& 0. \end{array} \right.$$

Esto, nos permite obtener de las ecuaciones de la elastodinámica, la siguiente relación entre los potenciales y el campo de desplazamientos:

$$\partial_t \boldsymbol{u} = \nabla \varphi_P + \mathbf{curl}\, \varphi_S + \boldsymbol{g}, \quad \text{donde} \quad \boldsymbol{g}(t) = \frac{1}{\rho}\int_0^t \boldsymbol{f}(s)\, ds.$$

Si introducimos esta expresión en la definición de cada potencial, obtenemos que cada uno por separado ha de satisfacer las siguientes ecuaciones de ondas escalares:

$$\begin{cases} \dfrac{1}{V_P^2}\,\partial_t^2 \varphi_P - \Delta\varphi_P = \operatorname{div} \boldsymbol{g}, \\ (\varphi_P, \partial_t\varphi_P)(t=0) = (0,0), \end{cases} \qquad \begin{cases} \dfrac{1}{V_S^2}\,\partial_t^2 \varphi_S - \Delta\varphi_S = -\operatorname{curl} \boldsymbol{g}, \\ (\varphi_S, \partial_t\varphi_S)(t=0) = (0,0). \end{cases}$$

Notar que ambos problemas están totalmente desacoplados y por tanto nos podemos beneficiar de los métodos conocidos para el tratamiento numérico de la ecuación de ondas. Por tanto, por un lado podemos considerar mallas diferentes para cada tipo de onda y adaptar cada una de ellas a su respectiva longitud de onda, es decir

$$h_P \;=\; \frac{\lambda_P}{N_\star} \quad \text{y} \quad h_S \;=\; \frac{\lambda_S}{N_\star}.$$

Por otro lado, si en ambos problemas consideramos el mismo esquema de diferencias finitas explícito en tiempo, cada paso de tiempo estará restringido por una condición de estabilidad del tipo

$$\Delta t_P \;\approx\; \frac{h_P}{V_P} \;=\; \frac{T_\star}{N_\star} \quad \text{y} \quad \Delta t_S \;\approx\; \frac{h_S}{V_S} \;=\; \frac{T_\star}{N_\star}.$$

Por tanto, la estabilidad del esquema numérico resultante evita el factor de penalización V_P/V_S obteniendo así un método más eficiente. Sin embargo, cabe destacar que en dominios acotados, ambos tipos de ondas, que se propagan independientemente dentro del dominio, están acopladas en las fronteras. Esta es la principal fuente de complejidad, dado que las condiciones de contorno en desplazamientos no son fáciles de expresar en términos de potenciales.

Formulación en potenciales en dominios con frontera rígida: Este caso ha sido tratado originalmente en [17, 18] aunque en este trabajo se revisa esta cuestión por motivos pedagógicos. Entonces consideramos el medio elástico, homogéneo e isótropo $\Omega \subset \mathbb{R}^2$ que asumimos conexo, Lipschitz y acotado por una frontera $\Gamma = \partial\Omega$, la cual suponemos rígida. En consecuencia el problema en desplazamientos se formula ahora como,

$$\begin{cases} \text{Encontrar } \boldsymbol{u}(\boldsymbol{x},t) : \Omega \times [0,T] \longrightarrow \mathbb{R}^2, \text{ tal que } (\boldsymbol{u}, \partial_t \boldsymbol{u})(t=0) = (0,0) \text{ y} \\ \partial_t^2 \boldsymbol{u} \;-\; V_P^2\, \nabla \operatorname{div} \boldsymbol{u} \;+\; V_S^2\, \mathbf{curl}\big(\operatorname{curl} \boldsymbol{u}\big) \;=\; \boldsymbol{f}/\rho, \quad \text{en } \Omega \times [0,T], \\ \boldsymbol{u}(\boldsymbol{x},t) \;=\; \mathbf{0}, \quad \text{en } \Gamma \times [0,T]. \end{cases}$$

En este contexto, se obtiene para los potenciales φ_P y φ_S el siguiente sistema de ecuaciones (notar que $\boldsymbol{g} = (g_1, g_2)$):

$$\begin{cases} \text{Encontrar } \boldsymbol{\varphi} = (\varphi_P, \varphi_S) : \Omega \times [0,T] \longrightarrow \mathbb{R}^2, \text{ tal que } (\boldsymbol{\varphi}, \partial_t \boldsymbol{\varphi})(t=0) = (0,0) \text{ y} \\ \dfrac{1}{V_P^2}\,\partial_t^2 \varphi_P - \Delta\varphi_P = \operatorname{div} \boldsymbol{g}, \quad \text{en } \Omega \times [0,T], \\ \dfrac{1}{V_S^2}\,\partial_t^2 \varphi_S - \Delta\varphi_S = -\operatorname{curl} \boldsymbol{g}, \quad \text{en } \Omega \times [0,T], \\ \operatorname{div} \boldsymbol{\varphi} + g_1 = 0, \quad \text{en } \Gamma \times [0,T], \\ \operatorname{curl} \boldsymbol{\varphi} - g_2 = 0, \quad \text{en } \Gamma \times [0,T]. \end{cases}$$

Para establecer una formulación variacional de este problema, cabe primero destacar que en general $\boldsymbol{u}(t) \in H^1(\Omega)^2$, de modo que teniendo en cuenta la definición de los potenciales φ_P y φ_S, vamos a buscar la solución $\boldsymbol{\varphi}$ en el espacio

$$\boldsymbol{V} \coloneqq H(\mathrm{div}, \Omega) \cap H(\mathrm{curl}, \Omega).$$

Por tanto, considerando este espacio se obtiene la siguiente formulación variacional:

$$\left\{ \begin{array}{l} \text{Encontrar } \boldsymbol{\varphi}(t) : [0,T] \longrightarrow \boldsymbol{V} \text{ tal que } (\boldsymbol{\varphi}, \partial_t \boldsymbol{\varphi})(t=0) = (\mathbf{0}, \mathbf{0}) \text{ y} \\ \dfrac{\mathrm{d}^2}{\mathrm{d}t^2}\, m_\Omega(\boldsymbol{\varphi}(t), \boldsymbol{\psi}) + a(\boldsymbol{\varphi}(t), \boldsymbol{\psi}) = \mathrm{g}(t, \boldsymbol{\psi}), \quad \forall\, \boldsymbol{\psi} \in \boldsymbol{V}, \end{array} \right.$$

donde se introducen las siguientes formas

$$m_\Omega : \boldsymbol{V} \times \boldsymbol{V} \longrightarrow \mathbb{R} \qquad \text{tal que} \qquad m_\Omega(\boldsymbol{\varphi}, \boldsymbol{\psi}) = \frac{1}{V_P^2} \int_\Omega \varphi_P\, \psi_P \,\mathrm{d}\boldsymbol{x} + \frac{1}{V_S^2} \int_\Omega \varphi_S\, \psi_S \,\mathrm{d}\boldsymbol{x},$$

$$a : \boldsymbol{V} \times \boldsymbol{V} \longrightarrow \mathbb{R} \qquad \text{tal que} \qquad a(\boldsymbol{\varphi}, \boldsymbol{\psi}) = \int_\Omega (\mathrm{div}\, \boldsymbol{\varphi}\, \mathrm{div}\, \boldsymbol{\psi} + \mathrm{curl}\, \boldsymbol{\varphi}\, \mathrm{curl}\, \boldsymbol{\psi}) \,\mathrm{d}\boldsymbol{x},$$

$$\mathrm{g} : \boldsymbol{V} \longrightarrow \mathbb{R} \qquad \text{tal que} \qquad \mathrm{g}(\boldsymbol{\psi}) = -\int_\Omega \boldsymbol{g} \cdot \begin{pmatrix} \mathrm{div}\, \boldsymbol{\psi} \\ -\mathrm{curl}\, \boldsymbol{\psi} \end{pmatrix}.$$

Atendiendo a la definición de la forma bilineal $a(\cdot,\cdot)$ se observa que ambos potenciales estarían acoplados en todo Ω, sin embargo en la práctica no será así. Esto es debido a dos factores, por un lado construiremos el espacio de aproximación $\boldsymbol{V}_h$ considerando elementos finitos de Lagrange, por lo tanto $\boldsymbol{V}_h \coloneqq V_{P,h} \times V_{S,h} \subset H^1(\Omega)^2 \subset \boldsymbol{V}$ (esto es posible gracias a que $H^1(\Omega)^2$ es denso en $\boldsymbol{V}$). Y por otro lado, se demuestra que

$$a(\boldsymbol{\varphi}, \boldsymbol{\psi}) = a_\Omega(\boldsymbol{\varphi}, \boldsymbol{\psi}) + a_\Gamma(\boldsymbol{\varphi}, \boldsymbol{\psi}), \quad \forall \boldsymbol{\varphi}, \boldsymbol{\psi} \in H^1(\Omega)^2 \times H^1(\Omega)^2,$$

donde se introducen las nuevas formas bilineales

$$a_\Omega : H^1(\Omega) \times H^1(\Omega) \longrightarrow \mathbb{R} \qquad \text{tal que} \qquad a_\Omega(\boldsymbol{\varphi}, \boldsymbol{\psi}) = \int_\Omega \nabla\varphi_P\, \nabla\psi_P \,\mathrm{d}\boldsymbol{x} + \int_\Omega \nabla\varphi_S\, \nabla\psi_S \,\mathrm{d}\boldsymbol{x},$$

$$a_\Gamma : H^1(\Omega) \times H^1(\Omega) \longrightarrow \mathbb{R} \qquad \text{tal que} \qquad a_\Gamma(\boldsymbol{\varphi}, \boldsymbol{\psi}) = \int_\Gamma \left(\partial_{\boldsymbol{\tau}} \varphi_P\, \psi_S + \partial_{\boldsymbol{\tau}} \psi_P\, \varphi_S \right) \mathrm{d}\boldsymbol{\gamma},$$

donde las integrales en la frontera representan productos de dualidad entre $H^{\frac{1}{2}}(\Gamma)$ y su dual $H^{-\frac{1}{2}}(\Gamma)$. Por tanto, el problema discreto planteado en el espacio $\boldsymbol{V}_h$ estará acoplado únicamente a lo largo de la frontera Γ tal y como se detalla en la siguiente formulación:

$$\left\{ \begin{array}{l} \text{Encontrar } \boldsymbol{\varphi}_h(t) : [0,T] \longrightarrow \boldsymbol{V}_h \text{ tal que } (\boldsymbol{\varphi}_h, \partial_t \boldsymbol{\varphi}_h)(t=0) = (\mathbf{0}, \mathbf{0}) \text{ y} \\ \dfrac{\mathrm{d}^2}{\mathrm{d}t^2}\, m_\Omega(\boldsymbol{\varphi}_h(t), \boldsymbol{\psi}_h) + a_\Omega(\boldsymbol{\varphi}_h(t), \boldsymbol{\psi}_h) + a_\Gamma(\boldsymbol{\varphi}_h(t), \boldsymbol{\psi}_h) = \mathrm{g}(t, \boldsymbol{\psi}_h), \quad \forall\, \boldsymbol{\psi}_h \in \boldsymbol{V}_h. \end{array} \right.$$

Por otra parte, para la discretización en tiempo utilizamos un esquema de diferencias finitas semi-implícito de orden dos que consiste en tratar de forma explícita los términos asociados al volumen y de forma implícita los términos asociados al acople de ambos potenciales a través de la frontera. Como resultado se obtiene un esquema numérico que permite escoger mallados adaptados a cada tipo de onda (es decir $h_P = \lambda_P / N_\star$ y $h_S = \lambda_S / N_\star$) y que al mismo tiempo tiene como condición de estabilidad

$$\Delta t \approx \frac{T_\star}{N_\star},$$

evitando así el factor de penalización V_P/V_S y garantizando la eficiencia del método.

Formulación en potenciales en dominios con frontera libre: En este caso, consideramos que el medio elástico, homogéneo e isótropo $\Omega \subset \mathbb{R}^2$ es Lipschitz y está acotado por una frontera $\Gamma = \partial\Omega$, la cual suponemos libre. Además, por simplicidad, suponemos que Ω es simplemente conexo y que su centro de gravedad está en el origen. En consecuencia, el problema en desplazamientos se formula ahora como

$$\left\{\begin{array}{l} \text{Encontrar } \boldsymbol{u}(\boldsymbol{x},t) : \Omega \times [0,T] \longrightarrow \mathbb{R}^2, \text{ tal que } (\boldsymbol{u}, \partial_t \boldsymbol{u})(t=0) = (0,0) \text{ y} \\ \partial_t^2 \boldsymbol{u} \,-\, V_P^2 \nabla \operatorname{div} \boldsymbol{u} \,+\, V_S^2 \,\mathbf{curl}\left(\operatorname{curl} \boldsymbol{u}\right) \,=\, \boldsymbol{f}/\rho, \quad \text{in } \Omega \times [0,T], \\ \underline{\boldsymbol{\sigma}}(\boldsymbol{u})\boldsymbol{n} \,=\, \mathbf{0}, \quad \text{on } \Gamma \times [0,T], \end{array}\right.$$

En este contexto, se obtiene para los potenciales φ_P y φ_S el siguiente sistema de ecuaciones:

$$\left\{\begin{array}{l} \text{Encontrar } \boldsymbol{\varphi} = (\varphi_P, \varphi_S) : \Omega \times [0,T] \longrightarrow \mathbb{R}^2, \text{ tal que } (\boldsymbol{\varphi}, \partial_t \boldsymbol{\varphi})(t=0) = (0,0) \text{ y} \\ \dfrac{1}{V_P^2}\, \partial_t^2 \varphi_P - \Delta \varphi_P = \operatorname{div} \boldsymbol{g}, \quad \text{en } \Omega \times [0,T], \\ \dfrac{1}{V_S^2}\, \partial_t^2 \varphi_S - \Delta \varphi_S = -\operatorname{curl} \boldsymbol{g}, \quad \text{en } \Omega \times [0,T]. \\ \operatorname{div} \boldsymbol{\varphi} + g_1 - \dfrac{1}{2\,V_S^2}\, \mathcal{I}\left(\partial_t^2 \boldsymbol{\varphi} \cdot \boldsymbol{\tau}\right) \in \mathbb{P}_0, \quad \text{en } \Gamma \times [0,T], \\ \operatorname{curl} \boldsymbol{\varphi} - g_2 - \dfrac{1}{2\,V_S^2}\, \mathcal{I}\left(\partial_t \boldsymbol{\varphi} \cdot \boldsymbol{n}\right) \in \mathbb{P}_0, \quad \text{en } \Gamma \times [0,T], \\ \displaystyle\int_\Gamma \boldsymbol{\varphi} \cdot \boldsymbol{n} \,\mathrm{d}\boldsymbol{\gamma} = 0 \quad \text{and} \quad \int_\Gamma \boldsymbol{\varphi} \cdot \boldsymbol{\tau} \,\mathrm{d}\boldsymbol{\gamma} = 0, \end{array}\right.$$

donde $\mathcal{I}(\cdot)$ es el operador integral definido por

$$\begin{array}{rccl} \mathcal{I} : & M & \longrightarrow & H^{\frac{1}{2}}(\Gamma), \\ & \eta & \mapsto & \mathcal{I}\eta(s) := \displaystyle\int_0^s \eta(\sigma)\,\mathrm{d}\sigma, \end{array} \quad \text{con} \quad M := \left\{\eta \in H^{-\frac{1}{2}}(\Gamma) \,/\, \int_\Gamma \eta \,\mathrm{d}\boldsymbol{\gamma} = 0\right\}.$$

La dificultad añadida en este caso surge al tratar de obtener una formulación variacional adecuada para el problema anterior. Para ello, en un inicio procedemos de manera análoga al caso de frontera rígida, buscando ahora la solución en potenciales en el espacio

$$\boldsymbol{V}_0 := \left\{\boldsymbol{\varphi} \in \boldsymbol{V} \text{ tal que } \int_\Gamma \boldsymbol{\varphi} \cdot \boldsymbol{n} \,\mathrm{d}\boldsymbol{\gamma} = \int_\Gamma \boldsymbol{\varphi} \cdot \boldsymbol{\tau} \,\mathrm{d}\boldsymbol{\gamma} = 0\right\}.$$

Con esta elección obtenemos la siguiente formulación variacional:

$$\left\{\begin{array}{l} \text{Encontrar } \boldsymbol{\varphi}(t) : [0,T] \longrightarrow \boldsymbol{V}_0 \text{ tal que } (\boldsymbol{\varphi}, \partial_t \boldsymbol{\varphi})(t=0) = (\mathbf{0},\mathbf{0}) \text{ y} \\ \dfrac{\mathrm{d}^2}{\mathrm{d}t^2}\, m(\boldsymbol{\varphi}(t), \boldsymbol{\psi}) + a(\boldsymbol{\varphi}(t), \boldsymbol{\psi}) = \mathrm{g}(t, \boldsymbol{\psi}), \quad \forall\, \boldsymbol{\psi} \in \boldsymbol{V}, \end{array}\right.$$

donde se introduce la nueva forma bilineal dada por

$$m : \boldsymbol{V}_0 \times \boldsymbol{V}_0 \longrightarrow \mathbb{R} \quad \text{tal que} \quad m(\boldsymbol{\varphi}, \boldsymbol{\psi}) = m_\Omega(\boldsymbol{\varphi}, \boldsymbol{\psi}) + m_\Gamma(\boldsymbol{\varphi}, \boldsymbol{\psi}),$$

$$m_\Gamma : \boldsymbol{V}_0 \times \boldsymbol{V}_0 \longrightarrow \mathbb{R} \quad \text{tal que} \quad m_\Gamma(\boldsymbol{\varphi}, \boldsymbol{\psi}) = \frac{1}{2\,V_S^2} \int_\Gamma \left(\mathcal{I}(\boldsymbol{\varphi} \cdot \boldsymbol{n})\, \boldsymbol{\psi} \cdot \boldsymbol{\tau} - \mathcal{I}(\boldsymbol{\varphi} \cdot \boldsymbol{\tau})\, \boldsymbol{\psi} \cdot \boldsymbol{n}\right) \mathrm{d}\boldsymbol{\gamma}.$$

El inconveniente de esta formulación es que en el espacio $\boldsymbol{K}_0 := \left\{\boldsymbol{\xi} \in \boldsymbol{V}_0 \,/\, \operatorname{div} \boldsymbol{\xi} = \operatorname{curl} \boldsymbol{\xi} = 0\right\}$, se cumple que

$$\forall\, \boldsymbol{\xi} \in \boldsymbol{K}_0, \qquad m(\boldsymbol{\xi}, \boldsymbol{\xi}) = -\frac{1}{V_*^2} \int_\Omega |\xi_P|^2 \,\mathrm{d}\boldsymbol{x} \quad \text{donde} \quad \frac{1}{V_*^2} := \frac{1}{V_S^2} - \frac{1}{V_P^2} > 0.$$

En consecuencia, el problema variacional anterior no se puede analizar utilizando las herramientas clásicas. Y de hecho se demuestra que esta propiedad es la causa de la aparición de inestabilidades cuando el problema es aproximado utilizando elementos finitos. Por tanto, el diagnóstico es que el espacio $\boldsymbol{V}_0$ es en realidad un espacio demasiado grande en el sentido de que permite la aparición de modos inestables tras su discretización. La idea para resolver este problema es buscar la solución en un subespacio $\boldsymbol{V}_N$ de $\boldsymbol{V}_0$, de modo que el nuevo espacio sea lo suficientemente grande para contener la solución en potenciales y que al mismo tiempo $m(\cdot,\cdot)$ sea coerciva en $\boldsymbol{V}_N$. En consecuencia, se puede utilizar la teoría clásica para analizar el siguiente problema:

$$\begin{cases} \text{Encontrar } \boldsymbol{\varphi}(t) : [0,T] \longrightarrow \boldsymbol{V}_N \text{ tal que } (\boldsymbol{\varphi}, \partial_t \boldsymbol{\varphi})(t=0) = (\mathbf{0},\mathbf{0}) \text{ y} \\ \dfrac{\mathrm{d}^2}{\mathrm{d}t^2} m(\boldsymbol{\varphi}(t), \boldsymbol{\psi}) + a(\boldsymbol{\varphi}(t), \boldsymbol{\psi}) = \mathrm{g}(t, \boldsymbol{\psi}), \quad \forall\, \boldsymbol{\psi} \in \boldsymbol{V}_N. \end{cases}$$

El inconveniente de esta nueva formulación es que la definición de este nuevo espacio $\boldsymbol{V}_N$ es compleja y no está bien adaptada para su discretización, sin embargo, es posible caracterizar este espacio como el *m-ortogonal* (ortogonal con respecto a la forma bilineal $m(\cdot,\cdot)$) de otro subespacio de $\boldsymbol{V}_0$. En particular se demuestra que

$$\boldsymbol{\varphi} \in \boldsymbol{V}_N \quad \Longleftrightarrow \quad \boldsymbol{\varphi} \in \boldsymbol{V}_0 \ \text{ y } \ m(\boldsymbol{\varphi}, \boldsymbol{\xi}) = 0, \quad \forall\, \boldsymbol{\xi} \in \boldsymbol{K}_0 \oplus \boldsymbol{K}_R,$$

donde $\boldsymbol{K}_R = \operatorname{span}\{\boldsymbol{\xi}_R\}$ con $\boldsymbol{\xi}_R = (0, |\boldsymbol{x}|^2)$ viene determinado por los movimientos rígidos en desplazamientos. Además el espacio $\boldsymbol{K}_0$ resulta ser a su vez isomorfo al espacio M de funciones definidas sobre la frontera y dicho isomorfismo viene dado por

$$\begin{aligned} \mathcal{E} : M \quad &\longrightarrow \quad \boldsymbol{K}_0 \\ \eta \quad &\mapsto \quad \mathcal{E}(\eta) = \nabla p(\eta), \end{aligned} \qquad \text{donde} \quad \begin{cases} -\Delta p = 0 & \text{en } \Omega, \\ \partial_{\boldsymbol{n}} p = \eta & \text{en } \Gamma, \\ p = \mathcal{I}(\nabla p \cdot \boldsymbol{\tau}) & \text{en } \Gamma. \end{cases}$$

Esto nos permite reescribir la anterior caracterización del espacio $\boldsymbol{V}_N$ de la siguiente forma

$$\boldsymbol{\varphi} \in \boldsymbol{V}_N \quad \Longleftrightarrow \quad \begin{cases} \boldsymbol{\varphi} \in \boldsymbol{V}_0, \\ m(\boldsymbol{\varphi}, \boldsymbol{\xi}_R) = 0, \\ m(\boldsymbol{\varphi}, \mathcal{E}(\eta)) = 0, \quad \forall\, \eta \in M. \end{cases}$$

Entonces, esta caracterización se puede explotar para proponer una formulación variacional mixta donde se impone que la solución pertenezca al nuevo espacio $\boldsymbol{V}_N$ tratando la mencionada *ortogonalidad* como una restricción, lo que lleva a la introducción de dos multiplicadores de Lagrange, es decir

$$\begin{cases} \text{Encontrar } (\boldsymbol{\varphi}, \eta, \eta_R) : [0,T] \longrightarrow \boldsymbol{V}_0 \times M \times \mathbb{R} \text{ tales que } (\boldsymbol{\varphi}, \partial_t \boldsymbol{\varphi})(t=0) = (\mathbf{0},\mathbf{0}) \text{ y} \\ \dfrac{\mathrm{d}^2}{\mathrm{d}t^2} m(\boldsymbol{\varphi}, \boldsymbol{\psi}) + a(\boldsymbol{\varphi}, \boldsymbol{\psi}) + b(\eta, \boldsymbol{\psi}) + \eta_R\, m(\boldsymbol{\xi}_R, \boldsymbol{\psi}) = \mathrm{g}(t, \boldsymbol{\psi}), \quad \forall\, \boldsymbol{\psi} \in \boldsymbol{V}_0, \\ b(\nu, \boldsymbol{\varphi}) = 0, \quad \forall\, \nu \in M, \\ m(\boldsymbol{\xi}_R, \boldsymbol{\varphi}) = 0, \end{cases}$$

donde la forma bilineal $b(\cdot,\cdot)$ está definida como

$$b : M \times \boldsymbol{V}_0 \longrightarrow \mathbb{R} \quad \text{tal que} \quad b(\nu, \boldsymbol{\psi}) := m(\mathcal{E}(\nu), \boldsymbol{\psi}).$$

La ventaja de esta nueva formulación es que tras su discretización por elementos finitos en espacio (lo cual no es trivial debido a la definición de $b(\cdot,\cdot)$) y diferencias finitas en tiempo, se obtiene un esquema numérico el cual demostramos que bajo ciertas hipótesis está bien planteado, es estable y su condición de estabilidad no está penalizada por el factor V_P/V_S.

Finalmente cabe destacar que no se ha llevado a cabo un análisis detallado del error, cuestión que será abordada en trabajos futuros, sin embargo se han presentado resultados numéricos que respaldan los resultados teóricos obtenidos, mostrando las ventajas del método y que han sido validados comparándolos con los resultados numéricos obtenidos a través de métodos clásicos para la resolución de las ecuaciones de la elastodinámica lineal en su formulación en desplazamientos.

Bibliography

[1] E. Bécache, J. Rodríguez, C. Tsogka. A fictitious domain method with mixed finite elements for elastodynamics. *SIAM Journal on Scientific Computing* **2007**, *Vol. 29*, pp. 1244–1267.

[2] E. Bécache, J. Rodríguez, C. Tsogka. Convergence results of the fictitious domain method for a mixed formulation of the wave equation with a Neumann boundary condition. *ESAIM: Mathematical Modelling and Numerical Analysis - Modélisation Mathématique et Analyse Numérique* **2009**, *Vol. 43*, pp. 377–398.

[3] E. Burman, S. Claus, P. Hansbo, M. G. Larson, A. Massing. CutFEM: Discretizing geometry and partial differential equations. *International Journal for Numerical Methods in Engineering* **2015**, *Vol. 104*, pp. 472–501.

[4] S. Sticko, G. Kreiss. A stabilized Nitsche cut element method for the wave equation. *Computer Methods in Applied Mechanics and Engineering* **2016**, *Vol. 309*, pp. 364 – 387.

[5] Y. Maday, C. Mavriplis, A. Patera. Nonconforming mortar element methods: Application to spectral discretizations. *Second International Congerence on Domain Decomposition Methods for Partial Differential Equations* **1988**.

[6] C. Bernardi, Y. Maday, A. T. Patera. A new nonconforming approach to domain decomposition: The mortar element method. *Nonlinear Partial Differential Equations and Their Applications* **1992**, pp. 13–51.

[7] C. Bernardi, Y. Maday, A. T. Patera. Domain decomposition by the mortar element method. *Asymptotic and numerical methods for partial differential equations with critical parameters* **1993**, pp. 269–286.

[8] H. B. Dhia. Problèmes mécaniques multi-échelles: la méthode Arlequin. *Comptes Rendus de l'Académie des Sciences-Series IIB-Mechanics-Physics-Astronomy* **1998**, *Vol. 326*, pp. 899–904.

[9] H. B. Dhia, G. Rateau. Mathematical analysis of the mixed Arlequin method. *Numerical Analyis* **2001**, *Vol. 332*, pp. 649–654.

[10] P. Joly, *Numerical methods for elastic wave propagation* in *Waves in nonlinear pre-stressed materials*, Springer, **2007**, pp. 181–281.

[11] E. Bécache, P. Joly, C. Tsogka. A new family of mixed finite elements for the linear elastodynamic problem. *SIAM Journal on Numerical Analysis* **2002**, *Vol. 39*, pp. 2109–2132.

[12] S. K. Lahiri, J. Bonet, J. Peraire, L. Casals. A variationally consistent fractional timestep integration method for incompressible and nearly incompressible Lagrangian dynamics. *International journal for numerical methods in engineering* **2005**, *Vol. 63*, pp. 1371–1395.

[13] G. Scovazzi, B. Carnes, X. Zeng, S. Rossi. A simple, stable, and accurate linear tetrahedral finite element for transient, nearly, and fully incompressible solid dynamics: a dynamic variational multiscale approach. *International Journal for Numerical Methods in Engineering* **2016**, *Vol. 106*, pp. 799–839.

[14] S. Rossi, N. Abboud, G. Scovazzi. Implicit finite incompressible elastodynamics with linear finite elements: A stabilized method in rate form. *Computer Methods in Applied Mechanics and Engineering* **2016**, *Vol. 311*, pp. 208–249.

[15] G. Scovazzi, T. Song, X. Zeng. A velocity/stress mixed stabilized nodal finite element for elastodynamics: Analysis and computations with strongly and weakly enforced boundary conditions. *Computer Methods in Applied Mechanics and Engineering* **2017**, *Vol. 325*, pp. 532–576.

[16] F. Caforio, S. Imperiale. A conservative penalisation strategy for the semi-implicit time discretisation of the incompressible elastodynamics equation. *Advanced Modeling and Simulation in Engineering Sciences* **2018**, *Vol. 5*, p. 30.

[17] A. Burel, S. Imperiale, P. Joly. Solving the homogeneous isotropic linear elastodynamics equations using potentials and finite elements. The case of the rigid boundary condition. *Numerical Analysis and Applications* **2012**, *Vol. 5*, pp. 136–143.

[18] A. Burel, *Contributions à la simulation numérique en élastodynamique: découplage des ondes P et S, modèles asymptotiques pour la traversée de couches minces*, Ph.D. thesis, Université Paris Sud-Paris XI, **2014**.

[19] J. Albella, S. Imperiale, P. Joly, J. Rodríguez. Solving 2D linear isotropic elastodynamics by means of scalar potentials: a new challenge for finite elements. *Journal of Scientific Computing* **2018**.

[20] J. Albella Martínez, S. Imperiale, P. Joly, J. Rodríguez. Numerical Analysis of a Method for Solving 2D Linear Isotropic Elastodynamics with Free Boundary Condition using Potentials and Finite Elements. **2019**, preprint: https://hal.inria.fr/hal-02345808.

[21] G. Cohen, P. Joly, J. E. Roberts, N. Tordjman. Higher order triangular finite elements with mass lumping for the wave equation. *SIAM Journal on Numerical Analysis* **2001**, *Vol. 38*, pp. 2047–2078.

[22] G. Cohen, *Higher-Order Numerical Methods for Transient Wave Equations*, Springer, **2002**.

[23] Y. Maday, A. T. Patera. Spectral element methods for the incompressible Navier-Stokes equations. *State-of-the-art surveys on computational mechanics (A90-47176 21-64). New York, American Society of Mechanical Engineers.* **1989**, pp. 71–143.

[24] D. Komatitsch, J. Tromp. Introduction to the spectral element method for three-dimensional seismic wave propagation. *Geophysical journal international* **1999**, *Vol. 139*, pp. 806–822.

[25] V. Dolean, H. Fahs, L. Fezoui, S. Lanteri. Locally implicit discontinuous Galerkin method for time domain electromagnetics. *Journal of Computational Physics* **2010**, *Vol. 229*, pp. 512–526.

[26] S. Descombes, S. Lanteri, L. Moya. Locally implicit time integration strategies in a discontinuous Galerkin method for Maxwell's equations. *Journal of Scientific Computing* **2013**, *Vol. 56*, pp. 190–218.

[27] E. Bécache, P. Joly, J. Rodríguez. Space–time mesh refinement for elastodynamics. Numerical results. *Computer methods in applied mechanics and engineering* **2005**, *Vol. 194*, pp. 355–366.

[28] G. Derveaux, P. Joly, J. Rodriguez, *Chap 13: Space time mesh refinement methods* in *Effective computational methods for wave propagation*, Chapman and Hall/CRC, **2008**.

[29] T. P. Fries, T. Belytschko. The extended/generalized finite element method: An overview of the method and its applications. *International Journal for Numerical Methods in Engineering* **2010**, *Vol. 84*, pp. 253–304.

[30] M. T. Cao-Rial, C. Moreno, P. Quintela. A new methodology for element partition and integration procedures for XFEM. *Finite Elements in Analysis and Design* **2016**, *Vol. 113*, pp. 1–13.

[31] M. Komijani, R. Gracie. An enriched finite element model for wave propagation in fractured media. *Finite Elements in Analysis and Design* **2017**, *Vol. 125*, pp. 14 – 23.

[32] H. B. Dhia, O. Jamond. On the use of XFEM within the Arlequin framework for the simulation of crack propagation. *Computer methods in applied mechanics and engineering* **2010**, *Vol. 199*, pp. 1403–1414.

[33] S. Sticko, G. Kreiss. Higher order cut finite elements for the wave equation. *Journal of Scientific Computing* **2019**, *Vol. 80*, pp. 1867–1887.

[34] H. B. Dhia, C. Zammali. Level-Sets and Arlequin framework for dynamic contact problems. *Revue Europeenne des Elements* **2004**, *Vol. 13*, pp. 403–414.

[35] H. B. Dhia, C. Zammali. Level-Sets fields, placement and velocity based formulations of contact-impact problems. *International journal for numerical methods in engineering* **2007**, *Vol. 69*, pp. 2711–2735.

[36] H. Qiao, Q. D. Yang, W. Q. Chen, C. Z. Zhang. Implementation of the Arlequin method into ABAQUS: Basic formulations and applications. *Advances in Engineering Software* **2011**, *Vol. 42*, pp. 197–207.

[37] A. Ghanem, M. Torkhani, N. Mahjoubi, T. N. Baranger, A. Combescure. Arlequin framework for multi-model, multi-time scale and heterogeneous time integrators for structural transient dynamics. *Computer methods in applied mechanics and engineering* **2013**, *Vol. 254*, pp. 292–308.

[38] H. B. Dhia, G. Rateau. Application of the Arlequin method to some structures with defects. *Revue Européenne des Éléments* **2002**, *Vol. 11*, pp. 291–304.

[39] H. B. Dhia, G. Rateau. The Arlequin method as a flexible engineering design tool. *International journal for numerical methods in engineering* **2005**, *Vol. 62*, pp. 1442–1462.

[40] J. Albella, H. B. Dhia, S. Imperiale, J. Rodríguez. Mathematical and Numerical Study of Transient Wave Scattering by Obstacles with a New Class of Arlequin Coupling. *SIAM Journal on Numerical Analysis* **2019**, *Vol. 57*, pp. 2436–2468.

[41] M. J. Gander, C. Japhet. Algorithm 932: PANG: software for nonmatching grid projections in 2D and 3D with linear complexity. *ACM Transactions on Mathematical Software (TOMS)* **2013**, *Vol. 40*, p. 6.

[42] H. B. Dhia. Further insights by theoretical investigations of the multiscale Arlequin method. *International Journal for Multiscale Computational Engineering* **2008**, *Vol. 6*.

[43] W. A. Strauss, *Partial differential equations: An introduction*, Wiley, **2007**.

[44] P. Grisvard. Problemes aux limites dans les polygones. Mode d'emploi. *Bulletin de la Direction des Etudes et Recherches Series C Mathematiques, Informatique* **1986**, *Vol. 1*, pp. 21–59.

[45] P. Grisvard, *Elliptic problems in nonsmooth domains. Monographs and Studies in Mathematics*, *Vol. 24*, Pitman, **1985**.

[46] P. Bochev, R. B. Lehoucq. On the finite element solution of the pure Neumann problem. *SIAM review* **2005**, *Vol. 47*, pp. 50–66.

[47] A. B. de Castro, D. Gómez, P. Salgado, *Mathematical models and numerical simulation in electromagnetism*, *Vol. 74*, Springer, **2014**.

[48] W. Jiang, N. Liu, Y. Tang, Q. H. Liu. Mixed finite element method for 2D vector Maxwell's eigenvalue problem in anisotropic media. *Progress In Electromagnetics Research* **2014**, *Vol. 148*, pp. 159–170.

[49] V. Girault, P. A. Raviart, *Finite element methods for Navier-Stokes equations: theory and algorithms*, *Vol. 5*, Springer Science & Business Media, **2012**.

[50] H. Brezis, *Functional analysis, Sobolev spaces and partial differential equations*, Springer Science & Business Media, **2010**.

[51] I. Babuška. Error bounds for finite element methods. *Numerische Mathematik* **1971**, *Vol. 16*, pp. 322–333.

[52] F. Brezzi. On the existence, uniqueness and approximation of saddle-point problems arising from Lagrangian multipliers. *Publications mathématiques et informatique de Rennes* **1974**, pp. 1–26.

[53] E. Bécache, P. Ciarlet, C. Hazard, E. Luneville, *La méthode des éléments finis: de la théorie à la pratique. Compléments. II*, Les Presses de l'ENSTA, **2010**.

[54] W. Rudin, *Functional Analysis*, McGraw-Hill, Inc., **1991**.

[55] F. B. Belgacem. The mortar finite element method with Lagrange multipliers. *Numerische Mathematik* **1999**, *Vol. 84*, pp. 173–197.

[56] B. I. Wohlmuth, *Discretization Methods and Iterative Solvers Based on Domain Decomposition*, *Vol. 17*, Springer-Verlag, Heidelberg, **2001**.

[57] P. Grisvard. Espaces intermédiaires entre espaces de Sobolev avec poids. *Annali della Scuola Normale Superiore di Pisa-Classe di Scienze* **1963**, *Vol. 17*, pp. 255–296.

[58] J.-L. Guermond, R. Pasquetti. A correction technique for the dispersive effects of mass lumping for transport problems. *Computer Methods in Applied Mechanics and Engineering* **2013**, *Vol. 253*, pp. 186–198.

[59] J. Céa. Approximation variationnelle des problèmes aux limites. *Annales de l'institut Fourier* **1964**, *Vol. 14*, pp. 345–444.

[60] R. A. Adams, J. J. F. Fourier, *Sobolev spaces*, *Vol. 140*, Elsevier, **2003**.

[61] P. Clément. Approximation by finite element functions using local regularization. *Revue française d'automatique, informatique, recherche opérationnelle. Analyse numérique* **1975**, *Vol. 9, R2*, pp. 77–84.

[62] C. Bernardi. Optimal finite-element interpolation on curved domains. *SIAM Journal on Numerical Analysis* **1989**, *Vol. 26*, pp. 1212–1240.

[63] C. Bernardi, V. Girault. A local regularization operator for triangular and quadrilateral finite elements. *SIAM Journal on Numerical Analysis* **1998**, *Vol. 35*, pp. 1893–1916.

[64] A. Ern, J.-L. Guermond, *Theory and Practice of Finite Elements*, *Vol. 159*, Springer Science & Business Media, **2013**.

[65] W. McLean, W. C. H. McLean, *Strongly elliptic systems and boundary integral equations*, Cambridge university press, **2000**.

[66] O. Steinbach. On the stability of the L_2 projection in fractional Sobolev spaces. *Numerische Mathematik* **2001**, *Vol. 88*, pp. 367–379.

[67] M. Abramowitz, I. A. Stegun, *Handbook of mathematical functions with formulas, graphs, and mathematical table* in *US Department of Commerce*, National Bureau of Standards Applied Mathematics series 55, **1965**.

[68] D. H. Baffet, M. J. Grote, S. Imperiale, M. Kachanovska. Energy Decay and Stability of a Perfectly Matched Layer For the Wave Equation. **2018**, preprint: https://hal.archives-ouvertes.fr/hal-01865484.

[69] P. O. Persson, G. Strang. A simple mesh generator in MATLAB. *SIAM review* **2004**, *Vol. 46*, pp. 329–345.

[70] B. I. Wohlmuth. A mortar finite element method using dual spaces for the Lagrange multiplier. *SIAM journal on numerical analysis* **2000**, *Vol. 38*, pp. 989–1012.

[71] P. Oswald, B. Wohlmuth. On polynomial reproduction of dual FE bases. *Thirteenth international conference on domain decomposition methods* **2001**, pp. 85–96.

[72] B. I. Wohlmuth, R. H. Krause. A multigrid method based on the unconstrained product space for mortar finite element discretizations. *SIAM journal on numerical analysis* **2001**, *Vol. 39*, pp. 192–213.

[73] B. P. Lamichhane, B. I. Wohlmuth. Higher order dual Lagrange multiplier spaces for mortar finite element discretizations. *Calcolo* **2002**, *Vol. 39*, pp. 219–237.

[74] C. Wieners, B. I. Wohlmuth. Duality estimates and multigrid analysis for saddle point problems arising from mortar discretizations. *SIAM Journal on Scientific Computing* **2003**, *Vol. 24*, pp. 2163–2184.

[75] B. I. Wohlmuth, B. P. Lamichhane. Mortar finite elements for interface problems. *Computing* **2004**, *Vol. 72*, pp. 333–348.

[76] B. I. Wohlmuth. Hierarchical a posteriori error estimators for mortar finite element methods with Lagrange multipliers. *SIAM journal on numerical analysis* **1999**, *Vol. 36*, pp. 1636–1658.

[77] D. Braess, *Finite elements: Theory, fast solvers, and applications in solid mechanics*, Cambridge University Press, **2007**.

[78] P. Joly. Analyse et approximation de modèles de propagation d'ondes. *Cours de l'Ecole polytechnique, Paris* **2001**.

[79] F. Brezzi, M. Fortin, *Mixed and hybrid finite element methods*, *Vol. 15*, Springer Science & Business Media, **2012**.

[80] R. Dautray, J. L. Lions, *Mathematical Analysis and Numerical Methods for Science and Technology*, Springer-Verlag Berlin, **1992**.

[81] G. A. Baker. Error Estimates for Finite Element Methods for Second Order Hyperbolic Equations. *Siam Journal on Numerical Analysis* **1976**, *Vol. 13*, pp. 564–576.

[82] J. Chabassier, S. Imperiale. Stability and dispersion analysis of improved time discretization for simply supported prestressed Timoshenko systems. Application to the stiff piano string. *Wave Motion* **2013**, *Vol. 50*, pp. 456–480.

[83] Y. Saad, *Iterative methods for sparse linear systems*, *Vol. 82*, siam, **2003**.

[84] A. J. Wathen. An analysis of some element-by-element techniques. *Computer Methods in Applied Mechanics and Engineering* **1989**, *Vol. 74*, pp. 271–287.

[85] R. Cottereau, R. Sevilla. Stability of an explicit high-order spectral element method for acoustics in heterogeneous media based on local element stability criteria. *International Journal for Numerical Methods in Engineering* **2018**, *Vol. 116*, pp. 223–245.

[86] T. Rylander, A. Bondeson. Stability of explicit–implicit hybrid time-stepping schemes for Maxwell's equations. *Journal of Computational Physics* **2002**, *Vol. 179*, pp. 426–438.

[87] M. E. Gurtin, *An introduction to continuum mechanics*, *Vol. 158*, Academic press, **1982**.

[88] P. G. Ciarlet, *Elasticité tridimensionnelle*, *Vol. 1*, Masson, **1986**.

[89] K. Aki, P. G. Richards, *Quantitative seismology*, **2002**.

[90] J. Bercoff, M. Tanter, M. Muller, M. Fink. The role of viscosity in the impulse diffraction field of elastic waves induced by the acoustic radiation force. *IEEE transactions on ultrasonics, ferroelectrics, and frequency control* **2004**, *Vol. 51*, pp. 1523–1536.

[91] E. Bretin, L. G. Bustos, A. Wahab. On the Green function in visco-elastic media obeying a frequency power-law. *Mathematical Methods in the Applied Sciences* **2011**, *Vol. 34*, pp. 819–830.

[92] A. A. Rodríguez, A. Valli, *Eddy Current Approximation of Maxwell Equations: Theory, Algorithms and Applications*, *Vol. 4*, Springer Science & Business Media, **2010**.

[93] D. Komatitsch, R. Martin. An unsplit convolutional perfectly matched layer improved at grazing incidence for the seismic wave equation. *Geophysics* **2007**, *Vol. 72*, pp. 155–167.

[94] J. Virieux. P-SV wave propagation in heterogeneous media: Velocity-stress finite-difference method. *Geophysics* **1986**, *Vol. 51*, pp. 889–901.

[95] R. Glowinski, O. Pironneau. Numerical methods for the first biharmonic equation and for the two-dimensional Stokes problem. *SIAM Review* **1979**, *Vol. 21*, pp. 167–212.

[96] I. Babuška, J. Osborn, J. Pitkäranta. Analysis of mixed methods using mesh dependent norms. *Mathematics of Computation* **1980**, *Vol. 35*, pp. 1039–1062.

[97] J.-L. Guermond, L. Quartapelle. Uncoupled ω–Ψ formulation for plane flows in multiply connected domains. *Mathematical Models and Methods in Applied Sciences* **1997**, *Vol. 7*, pp. 731–767.

[98] P. Monk, *Finite element methods for Maxwell's equations*, Oxford University Press, **2003**.

[99] C. Amrouche, C. Bernardi, M. Dauge, V. Girault. Vector potentials in three-dimensional non-smooth domains. *Mathematical Methods in the Applied Sciences* **1998**, *Vol. 21*, pp. 823–864.

[100] J. L. Lions, *Equations differentielles operationnelles: et problémes aux limites*, Springer-Verlag, **1961**.

[101] W. Gander, M. J. Gander, F. Kwok, *Scientific computing - An introduction using Maple and MATLAB*, *Vol. 11*, Springer Science & Business, **2014**.

[102] P. G. Ciarlet. On Korn's inequality. *Chinese Annals of Mathematics, Series B* **2010**, *Vol. 31*, pp. 607–618.

[103] E. Magenes, J. L. Lions, *Non-homogeneous boundary value problems and applications*, Springer Berlin Heidelberg, **1972**.

[104] L. Perko, *Differential equations and dynamical systems*, *Vol. 7*, Springer Science & Business Media, **2013**.

[105] V. Milisic, U. Razafison. Weighted Sobolev spaces for the Laplace equation in periodic infinite strips. *preprint arXiv:1302.4253* **2013**.

[106] L. Demkowicz, P. Monk, L. Vardapetyan, W. Rachowicz. De Rham diagram for hp finite element spaces. *Computers & Mathematics with Applications* **2000**, *Vol. 39*, pp. 29–38.

[107] P. G. Ciarlet, *Introduction à l'analyse numérique matricielle et à l'optimisation*, Dunod, **1998**.

[108] A. Ben-Israel, T. N. E. Greville, *Generalized Inverses: Theory and Applications*, Springer-Verlag New York, **2003**.

[109] P. G. Ciarlet, *The finite element method for elliptic problems*, *Vol. 40*, SIAM, **2002**.